Revista Internacional de Contaminación Ambiental ISSN: 0188-4999 VOLUMEN 34

6th International Symposium on Sediment Management San Cristóbal de Las Casas

I2SM México 2018

Chiapas, Mexico
June 19-23, 2018

SEMARNAT Secretaría de Medio Ambiente y Recursos Naturales
IMTA Instituto Mexicano de Tecnología del Agua
IMT Lille Douai École Mines-Télécom IMT-Université de Lille
ASIMS
CONAGUA Comisión Nacional del Agua
UNICACH
UNACH Universidad Autónoma de Chiapas
ECOSUR

Revista Internacional de Contaminación Ambiental **Volumen 34**

Proceedings

6th International Symposium on Sediment Management
San Cristóbal de Las Casas, Chiapas, Mexico
June 19-23, 2018

Anne M. Hansen
Chair, 6th International Symposium on Sediment Management (I2SM 2018)
Mexican Institute of Water Technology, Mexico

Nor-Edine Abriak
I2SM 2018 Scientific Chair
President, Association of the International Symposium on Sediment Management
IMT Lille Douai, France

Published by: Revista Internacional de Contaminación Ambiental Sección Editorial del Centro de Ciencias de la Atmósfera de la Universidad Nacional Autónoma de México
Circuito de la Investigación s/n, Ciudad Universitaria, Delegación Coyoacán, C.P. 04510, Ciudad de México, México.
Teléfono (+52 55) 5622-4240 ext. 81888,
http://www.revistascca.unam.mx/rica, editora.rica@atmosfera.unam.mx .

ISSN: 0188-4999

Table of contents

Preface vii

Organization ix

Plenary lecture 1

New advances in passive sampling to measure freely dissolved concentrations and linking with bioaccumulation models for sediment risk assessment 3
Fadaei Hilda and Ghosh Upal

Session topics

1. Geochemistry at the sediment-water interface 9

Trace metals geochemistry in the sediments of a natural wetland 11
Alfaro-De la Torre M. Catalina, Pérez-Castillo F. Virginia1 and Briones-Gallardo Roberto

Use of oxygenation to repress release of redox-sensitive compounds from profundal sediment in the Valle de Bravo reservoir, Mexico 17
Beutel Marc W., García-Gallardo Teresa , Falcón-Rojas Axel, Furhmann Byran and Hansen Anne M.

Evaluation of two methods for the control of phosphorus in water-sediment systems 21
García-Gallardo María Teresa, Hansen Anne M., Falcón-Rojas Axel, and Beutel Marc

2. Remediation of contaminated sites: natural attenuation, processing and reuse 27

Approaches for eutrophication control in a mexican reservoir 29
Hansen Anne M.

Effects of GGBS on the solidification/stabilization of port sediments contaminated with heavy metals 35
Gutsalenko T., Bourdot A., Chaouche M., Seymour P. and Frouin L.

Design of two permeable barriers for nitrate removal in groundwater 41
Sandoval Dangelo, Silva Ana Elisa, Hansen Anne M. and García Rolando

Influence of vegetation on water balance of engineered cover systems for reclaimed mine sites: literature review and outlooks 45
Botula Yves-Dady, Guittonny Marie, Bussière Bruno and Maqsoud Abdelkabir

3. Characterization and monitoring of sediments and porous media 51

Lack of correlation between mercury in sediments and fish muscle, lake Chapala, Mexico 53
Alvarado Claudia, Ramírez Gerardo, Diaz José J. and Cortez Diego

Mineralogy and geochemistry of stream sediments, from La Purísima basin dam, Guanajuato-Mexico 57
Rueda Luisa, Miranda-Avilés Raúl, Puy-Alquiza María Jesús and Zanor Gabriela A.

Water quality in mexican caribbean: Analysis of benthic bioindicators and physicochemical parameters of water 65
Camacho-Cruz Karla, Ortiz-Hernández Ma. Concepción, Sánchez-González Alberto, Carrillo-Bibriezca Laura and -Navarrete Alberto de Jesús

Identification of environmental covariables that influence gully formation in the mixteca region 71
Toledo-Medrano María Lorenza, Fernández-Reynoso Demetrio S., Martínez-Menez Mario R., Rubio-Granados Erasmo and García-Rodríguez José Luis

Sediment characteristics of 18 tropical, karst lakes in Chiapas, Mexico 77
Alcocer Javier, Oseguera Luis A., Ardiles Vilma S., Mora Lucy and Prado Blanca

Effect of thickness and sediment type on seismic amplification in the urban area of Chiapa de Corzo, Chiapas 83
Moreno Ceballo Roberto, González Herrera Raúl, Paz Tenorio Jorge Antonio, Aguilar Carboney Jorge Alfredo and del Carpio Penagos Carlos Uriel

Assessment of methods for extraction of metagenomic DNA from sediments of lakes of the national park “Lagunas de Montebello”, Chiapas, Mexico 91
García-Rodríguez Jorge Arturo, Castañón-González José Humberto, Gutiérrez-Miceli Federico Antonio, Peña-Ocaña Betsy Anaid, Trejo-Valencia Radames and Ruíz-Valdiviezo, Víctor Manuel

Quantification of pesticides and heavy metals in sediments of the "Enchanted" lake of the national park ponds of Montebello, Chiapas, Mexico 99
Díaz-Cancino Carolina Elizabeth, Castañón-González José Humberto, Villalobos-Maldonado Juan José, Ruíz-Valdiviezo Víctor Manuel, Báez-Sañudo Reginaldo, Adrián Gómez-De Jesús and Trejo-Valencia Radames

Physicochemical characterization, elemental speciation and hydrogeochemical modeling of Santa Lucía peloid used for therapeutic uses 105
Suárez Muñoz Margaret, Martínez-Villegas Nadia, González-Hernández Patricia, Melián Rodríguez Clara, Barrios Cossio Josiel, Hernández Rebeca, Fagundo Juan R., Díaz Rizo Oscar, Gelen Rudnicas Alina, Díaz López Cristina and Pérez-Gramatges Aurora

Valorization of waterways sediments in Wallonia (Belgium): study of a landscaped mound 111
Florian Liénard and Laurence Haouche

Phospholipid ester fatty acids (PLFA) in bottom trawling fishing areas in the gulf of California
Aguíñiga-García Sergio, Sánchez-González Alberto, Torres-Rojas Yassir Edén, Carreón-Palau Laura, Marmolejo-Rodríguez Ana Judith, Dorantes-Hernández J. Manuel, Pérez-Falls Zenia, Olivares-Rodríguez Elsy Alejandra, LLadó-Cabrera Dayli and Camacho-Cruz Karla Andrea 117

Identification of organic compounds in cajío peloid (Cuba)
Suárez Muñoz Margaret, Martinez-Villegas Nadia, González-Hernández Patricia, Melián Rodríguez Clara, Barrios Cossio Josiel, Hernández Díaz Rebeca, Fagundo Castillo Juan R, Díaz Rizo Oscar, Díaz López Cristina and Pérez-Gramatges Aurora 121

Determination of arsenic in sediment samples from a well in the Comarca Lagunera, Mexico
Mejía Miguel, González Luis, Briones Roberto, Ojeda María del Carmen, Cardona Antonio and Soto Pedro 129

4. Sediment-driven reactions and transport of pollutants in rivers and groundwater 135

Cohesive suspended sediment transport model for the Grijalva and Usumacinta rivers, Mexico
García-Aragón J. A., Izquierdo-Ayala K., Castillo-Uzcanga M.M., Carrillo, L. and Salinas Tapia H. 137

Numerical modeling of sediment transport with leveles of hydrocarbons in a shallow lagoon
Herrera-Díaz Israel E., Gutierrez-Vaca Cesar and Saldaña-Robles Adriana 143

Evaluation of surface and groundwater quality related with the discharges composition and water-sediment interactions, with agriwater software
Bautista Francisco and Pacheco Aristeo 149

Role of sediment and suspended matter in the fate of flagrances from WWTP-effluent
Alary Claire, Belles Angel and Franke Christine 151

5. Water-sediment interactions in rivers and hydraulic works 155

Experimental estimation of structures impact pressure of a granular debris flow
Mendoza-López Francisco Alonso, García-Aragón Juan Antonio, Salinas-Tapia Humberto and Díaz-Delgado Carlos 157

Erosion distribution in the Djorf-Torba dam area (southwest of Algeria: Bechar)
Belaout Fateh, Mekerta Belkacem, Kalloum Slimane and Semcha Abdelaziz 163

Scour estimation of a bridge pier, a case of study
González V. José Alfredo, Espinoza A. Joselina and Bonola A. Isaac 169

Volumetric measuring of sediments in a transportable prismatic channel
Mundo-Molina Martin 173

Importance of the an analysis of the alterations in the floodplain of the proposed Las Cruces dam
Gracia Jesús and Ramos Judith 177

Application of empirical methods to determine the change in the curve elevations areas-capacities to three reservoirs located in the mexican republic 183
Morales-Saldivar Jorge Antonio, González Verdugo José Alfredo and Espinoza Ayala Joselina

Suspended sediments content along the Usumacinta river, the mexican tropics 193
Oseguera Luis A., Alcocer Javier, Cuevas Daniel and Cortés Guzmán Daniela

Sediment modeling to develop a deposition prediction model at la Gavia river, Mexico 199
Tejeda Samuel, Bernal-Banda Rodolfo, Flores-Gutiérrez Leonarda María, Salinas Tapia Humberto, López- Rebollar Boris Miguel, Zarazúa-Ortega Graciela

6. Sediments and environmental regulation 205

Quality of sediments in two rivers impacted by industrial activities 207
Saldaña Fabela Pilar y Gómez Balandra María Antonieta

Sediments as part of the environmental flow regulations 211
Gómez-Balandra María Antonieta, Saldaña-Fabela María del Pilar and Llerandi-Juárez Rosa Dina

Growing media manufacturing from fluvial sediments and green wastes following E.U ecolabel framework 217
Mamindy-Pajany Yannick, Scribot Cyril and Abriak Nor-Edine

7. Reuse and management of sludge from water treatment 221

Estimating H_2S concentration in biogas produced by anaerobic sludge from sulfur-rich wastewaters 223
Quijano Guillermo, Figueroa-González Ivonne, Moreno Gloria and Moreno-Andrade Iván

Characterizing the evolution of sediment-like wastes exposed to ambient conditions in open reservoirs 227
Hernández D., Astudillo C.A., Fernández-Palacios, E., Cataldo, F., Tenreiro, C. and Gabriel D.

Trace metals stimulation of biochemical methane potential from pretreated waste activated sludge 233
Peralta E. D., Noyola A., Barrios J. A. and Durán U.

Sludge wastewater treatment plants a raw mater to produce a green-cement 239
Djafari Driss, Zentar Rachid, Mekerta Belkacem and Semcha Abdelaziz

8. Perspectives of the industry 243

Levels of Mn, Zn, Pb and Hg in sediments of the Zamora river, Ecuador 245
Mora Abrahan, Jumbo-Flores Diana and Mahlknecht Jürgen

Chemical and mineralogical characterization of sediments formed by mine wastes leachates
Valdez-Bernal Fátima, Ramos-Arroyo Yann, Escot-Espinoza Victor and Briones-Gallardo Roberto 251

Evaluation of manganese insolubility on bodies of water on a mining region in Mexico
Scheel-Hinojosa Patrick 255

Geochemical trends of arsenic and iron in a small reservoir that receives mine drainage
Bravo América, Ramos Yann, Torres Esther, and Ayora Carlos 261

Diatoms in marine sediments contaminated by potentially toxic elements from mining activities
Martínez Yuriko Jocselin, Marmolejo-Rodríguez Ana J. and Siqueiros Beltrones David A. 265

Monitored natural attenuation of heavy metals in the Sonora river: the water quality
Ceniceros-Gómez Agueda E., Gutiérrez Ruiz Margarita E., Romero Francisco M. and Martínez-Jardines L. 267

Retention of metals in secondary minerals in sediments of a mine drainage
Ramos Yann and Ayora Carlos 271

Evolution of the quality of the sediments of the Todos Os Santos bay: role of biogeochemical conditions and actions of main stakeholders
Tavares, Tania M., Silva, Sonilda, M.T., Oliva, Sergio T., Sant'Anna Jr, Nilson Lockwood David, Gutierrez-Ruiz Margarita, Queiróz-Vivanco Daniel and Aguirre-Gomes Arturo 275

Migration of potentially toxic elements in creek sediments from a semiarid coastal system influenced by the abandoned gold mining district at San Antonio - El Triunfo
Romero Francisco, Gutiérrez-Ruiz Margarita, Martínez-Jardines Gerardo, Magdaleno-Rico Carlos, Espino-Ortega Violeta and Hernández Cruz Griselda 281

Soil clay components and trace metal stabilization
Bobadilla Ballesteros Martha Daniela, Tapia Sánchez Xóchitl, Millán Malo Beatriz Marcela, Fuentes Romero Elizabeth, García Calderón Norma Eugenia and Altuzar Coello Patricia Eugenia 285

Spatial distribution of arsenic and lead in stream sediments in a micro-basin with ancient mining activities
Montes-Avila I., Cardona-Benavides A., Lázaro-Báez I., Razo-Soto I. and Hernández-Ruiz S. 289

9. Advances in sediment management 297

Preventing land subsidence: using sediment as a resource (USAR)
Verweij G.H. 299

The effect of treated sediments on self-compacting mortars properties using design of experiments
Safhi Amine el Mahdi, Rivard Patrice, Benzerzour Mahfoud and Abriak Nor-Edine 301

Environmental assessment of two sediments reused in road engineering: feedback after one year of monitoring through the sedimed project
Ustache Aurélien, Rebischung Flore, Tessier Erwan and Pieters Alain 307

Some reasons to valorize dredged sediments 313
Semcha Abdélaziz, Marouf Hafida, Abbou Mohamed

Valorisation of fine dune sand in asphalt concrete 317
Akacem Mustapha, Mekerta Belkacem, Zester Rachid, Moulay Omar Hassan and Abbou Mohamed

The relationship between organic matter content and the immediate bearing index of dredged sediments 323
Hamouche Fawzi and Zentar Rachid

10. Radioisotope dating and chronological characterization of sediments 327

Chronological study of metals in a sediment core from the Alvarado Lagoon System (SLA), Veracruz, Mexico 329
Velandia A.L., Villanueva F.S. and Botello A.V.

Anthropogenic influence on the sediment chemistry of balamtetik lake, Chiapas, Mexico 335
Caballero Margarita, Mora Lucy, Muñoz Esperanza, Escolero Oscar, Bonifaz Roberto and Prado Blanca

Importance of surface sediments for reliable 210Pb dating 341
Yang Handong, Lencioni Lucia and Patmore Ian

Temporal variation of metal enrichment in coastal marine sediments off Baja California, Mexico 347
Macías-Zamora J.V., Ramírez-Álvarez N., Álvarez-Aguilar A. and Hernández-Guzmán F.A.

11. Contamination of sediments by oil spills: current situation, management strategies and regulations 351

Aquifer and agricultural soil contamination originating from clandestine drilling in pipelines transporting hydrocarbons 353
Suárez-Arriaga Mario-César

Metals in sediments of the NW of the gulf of Mexico, lithogenic vs anthropogenic. possible geochemical disturbance due to the spill of the deepwater horizon 361
Reyes-Yedra Claudia , Ponce-Vélez Guadalupe and Vázquez-Botello Alfonso

Evaluation of an hydrocarbon polluted soil after being remediated 367
Lara Guzmán Uriel, Castillo Román José, Sánchez Hernández Andrés, and Teutli León Margarita

Preface

The city of San Cristóbal de Las Casas, located in central highlands of Mexico, was founded in 1528 by Diego de Mazariegos. Two thirds of the municipality is made up of mountainous terrain with the rest valley floor. The city is located at 2,200 meters above sea level in a small valley surrounded by hills. Although it is located in a tropical area, its climate is temperate due to the altitude. The natural vegetation of the area is a forest of pine and oak trees. However, most of the surrounding hills have lost their native trees due to high deforestation. Reasons for this include cutting for firewood, urban development, poor resource management, fires and agriculture. The deforestation has led to erosion problems blocking rivers and streams and affecting groundwater recharge of the area's freshwater springs.

The 6th International Symposium on Sediment Management (I2SM 2018) is also the 10th anniversary of the I2SM symposia and is being held in San Cristóbal de Las Casas, Chiapas, Mexico, from June 19 to 23, 2018. This symposium addresses main aspects of sediment research, management, and regulation, including recent advances in understanding of geochemical processes at the sediment-water interface, remediation of contaminated sites, monitoring and characterization, reactive transport of pollutants, environmental regulation, and reuse and management of sediments and sludge.

The symposium is being organized by participants from the Instituto Mexicano de Tecnología del Agua (IMTA), Universidad de Ciencias y Artes de Chiapas (UNICACH), Universidad Autónoma de Chiapas (UNACH), Comisión Nacional del Agua (CONAGUA), Colegio de la Frontera Sur (ECOSUR), and Association for the International Symposium on Sediment Management (ASIMS). Sponsors of I2SM 2018 include IMTA, UNICACH, UNACH, Servicios de Recuperación en Agua (SERAGUA), Perkin Elmer de México, Agilent Technologies México, Centro de Mexicano de Innovación en Energía Geotérmica (CeMIE-GEO), and Beta Analytic, FL, USA.

Ninety abstracts are presented in both oral and poster sessions of this symposium from which 65 papers are included in this proceeding. The articles were submitted by scientists, engineers, specialists, professionals, decision-makers, and students from 16 countries (Argelia, Belgium, Brazil, Canada, Chile, Colombia, Cuba, Ecuador, France, Ireland, Marruecos, Mexico, Netherlands, Spain, UK, and USA). According to the topics, papers are divided into 11 session topics although many of them represent multi-disciplinary studies, which incorporate a variety of advanced methodologies. This special issue of the journal Revista Internacional de Contaminación Ambiental (RICA) begins with the Plenary Lectures, followed by contributed papers for the specific session topics as follows:

- Geochemistry at the sediment-water interface
- Remediation of contaminated sites: natural attenuation, processing, and reuse
- Characterization and monitoring of sediments and porous media
- Sediment-driven reactions and transport of pollutants in rivers and groundwater

- Water-sediment interactions in rivers and hydraulic works
- Sediments and environmental regulation
- Reuse and management of sludge from water treatment
- Perspectives of the industry
- Advances in sediment management
- Radioisotope dating and chronological characterization of sediments
- Contamination of sediments by oil spills: current situation, management strategies and regulations

We would like to thank the editors of the journal Revista Internacional de Contaminación Ambiental (RICA) for the opportunity to publish this special issue, the session chairs for organizing the different topics of the symposium, the scientific committee for selecting and classifying the abstracts, Carlos E. Corzo, Abel A. Ruiz, and Axel Falcón for the editorial assistance, and Gema Alín Martínez for the graphical design of the cover page.

Anne M. Hansen
Mexican Institute of Water Technology
Chair, I2SM 2018

Organization

ASSOCIATION OF THE INTERNATIONAL SYMPOSIUM ON SEDIMENT MANAGEMENT (ASIMS)

- Nor-Edine Abriak – Chairman, IMT Lille Douai
- Mahfoud Benzerzour – Co-Chairman, IMT Lille Douai
- Rachid Zentar – Co-Chairman, IMT Lille Douai

I2SM 2018 ORGANIZING COMMITTEE

- Mario López – Coordinator of Hydrology, IMTA
- Ernesto Castellanos – Director of the Faculty of Engineering, UNACH
- Raúl Saavedra Horita – Coordinator of Hydraulics, IMTA
- Carlos Gutiérrez – Head of Groundwater Hydrology, IMTA
- José Alfredo González – Head of the Hydraulics Laboratory, IMTA
- Marco A. Sánchez – Head of Marketing and Editorial Services, IMTA
- José Luis Arellano – Mexican National Water Commission, CONAGUA
- Martín Mundo Molina – Faculty of Engineering, UNACH
- Roel Simuta Champo – School of Topography and Hydrology, UNICACH
- Jesús Carmona - Institutional Laboratories Area, ECOSUR
- Anne M. Hansen –Hydrogeochemistry Laboratory, IMTA (*Chairman*)

Plenary lecture

New advances in passive sampling to measure freely dissolved concentrations and linking with bioaccumulation models for sediment risk assessment

Hilda Fadaei[1] and Upal Ghosh[2]
[1]Department of Chemical, Biochemical, and Environmental Engineering,
[2]University of Maryland Baltimore County, Baltimore, Maryland, USA

ABSTRACT

While hydrophobic pollutants like polychlorinated biphenyls (PCBs) bind strongly to sediments, the process of uptake in aquatic organisms is controlled by an aqueous pathway. Measuring the freely dissolved concentrations of PCBs is challenging due to the very low concentrations and association with suspended particles. Recent advances in passive sampling have made it possible to accurately measure freely dissolved concentrations of bioaccumulative pollutants in water. This presentation provides an overview of the science behind passive sampling and new guidance documents that have been published recently. The criterial for selection of a passive sampling approach is discussed and include clear delineation of measurement goals, whether laboratory-based "ex situ" and/or field-based "in situ" application is desired, and ultimately which sampling method is best suited to fulfill the measurement objectives. Guidelines are provided for proper calibration and validation, including use of provisional values for polymer–water partition coefficients, determination of equilibrium status, and confirmation of nondepletive measurement conditions. Finally, results of the application of passive sampling in a case study involving the prediction of bioaccumulation in fish before and after sediment remediation is presented.

Keywords: Sediment, Passive Sampling, Polychlorinated Biphenyls, Polyaromatic Hydrocarbons

INTRODUCTION

Aquatic sediments form the final repositories of past and ongoing discharges of hydrophobic organic compounds (HOCs) such as polychlorinated biphenyls (PCBs), many pesticides, dioxins, as well as mercury (Hg) and methylmercury (MeHg). These sediment-associated pollutants serve as long-term exposure sources to aquatic ecosystems. Cleanup of contaminated sediments remains a major technological challenge. Traditional approaches do not always achieve the risk reduction goals for human health and ecosystem protection and can even be destructive for natural resources. Sediment HOCs can be accumulated by aquatic or benthic organisms through ingestion and dermal absorption, and subsequently passed up to higher organisms and humans. Assessments of pollutant fate, transport, bioaccumulation, and toxicity of impacted sediments have historically been based on total pollutant concentrations and geochemical properties (e.g., total organic carbon) of bulk sediment (U.S. EPA 2012a).

Such assessments have been challenged by a gradually evolving understanding of the complexity of chemical sequestration in sediments and the contribution of various geochemical phases such as black carbon which are often difficult to quantify and accurately characterize (NRC 2003; Ghosh and Hawthorne, 2010). Researchers have therefore focused on developing measures that account for bioavailability and better reflect the potential of chemicals to cause adverse impact, be mobilized from, or be degraded in a given sediment. Freely dissolved porewater concentrations in sediment have been used to assess bioavailability of bioaccumulative chemicals and to assess site-specific risk of PAHs to benthic invertebrates. Direct measurement of sparingly soluble chemicals like PCBs in the pore water phase is challenging due to the interference with colloidal particles. Passive sampling of the porewater phase has emerged as an alternative technique to assess freely dissolved concentrations of hydrophobic chemicals without interference from colloidal particles. A recently published guidance document on passive sampling (Ghosh et al. 2014) provides a detailed description of the approach and can be used to measure native equilibrium partitioning constants for PCBs and PAHs in sediments.

METHODS

Passive sampling. In this research, the guidance document on passive sampling (Ghosh et al. 2014) was followed to measure native equilibrium partitioning constants for PCBs and PAHs in sediments. Briefly, the method involves contacting the wet sediment or water phase in the field with a passive sampler for a period of about 1 month. For field deployment, the samplers were enclosed in a frame and stainless steel mesh and placed in the field.

For the laboratory in-situ measurement, the samplers were placed into the sediments used for the bioaccumulation experiment described below. The polyethylene passive samplers were pre-loaded with performance reference compounds to allow correction for any non-equilibrium, especially for the strongly hydrophobic compounds. After the period of contact, the passive samplers were removed from the sediment, cleaned to remove any attached sediment particles, and extracted in hexane and acetone to measure PCBs and PAHs accumulated into the passive sampler. Consensus values of passive sampler partition constants were used as described in Ghosh et al. (2014) to calculate the aqueous concentration in equilibrium with the sediment. Site-specific partition constants for the compounds were then calculated by dividing the sediment phase concentration with the equilibrium aqueous phase concentration. The loss of performance reference compounds during the deployment period was used to correct for non-equilibrium as described in Fernandez et al. (2009).

Bioaccumulation measurement. PCB uptake in the freshwater oligochaetes (*L. variegatus*) was measured in laboratory beaker exposures based on USEPA (2000). PCB accumulation in fish was measured in laboratory aquaria under controlled experimental conditions as described in Fadaei et al. (2015).

Analytical measurements. PCB and pesticide analysis were performed on an Agilent 6890N gas chromatograph (Restek, Bellefonte, PA, USA) with an electron capture detector and a fused silica capillary column (Rtx-5MS, 60 m x 0.25 mm i.d, 0.25 µm film thickness). PCB standards for calibration were purchased as hexane solutions from Ultra Scientific (NorthKingstown, RI, USA). Internal standards, 2,4,6- trichlorobiphenyl (PCB 30) and 2,2',3,4,4',5,6,6'- octachlorobiphenyl (PCB 204) was added to all samples. A total of about 90 PCB congeners were measured using this method. In some cases peaks coelute which are identified and reported as the sum of congeners.

RESULTS AND DISCUSSION

The advantage provided by passive samplers lies in their ability to sample target chemicals, which typically exist in extremely low aqueous concentrations, to analytically detectable levels, and to do so in a time-integrative fashion. During sampler deployment, contaminants diffuse into the polymer approaching a thermodynamic equilibrium with the external water phase. This can be modeled as a diffusion process with rate kinetics controlled by the sampler's geometry, the concentration gradient between sampler and water, and an overall mass transfer coefficient representing the resistances to transfer in the sampling polymer and the external, aqueous boundary layer (Fernandez and others 2009).

The relative importance of each source of mass transfer resistance can be described in terms of the target compound's octanol-water partitioning coefficient. When passive samplers are deployed in static sediments, mass transfer is limited by the sediment side (i.e., the aqueous boundary layer) for most hydrophobic compounds (Booij et al. 2003). In practice, this means that samplers in stagnant sediments may be kinetically inhibited from reaching equilibrium with highly hydrophobic contaminants during a typical deployment time of one month. To account for this nonequilibrium, performance reference compounds (PRCs) can be loaded into samplers prior to deployment. PRCs are compounds with chemical characteristics similar to those of the target contaminants but not present in the field at detectable levels. Loss of PRCs from samplers is used to characterize sampler equilibration during the period of deployment, and to adjust measured contaminant concentrations accordingly. The depletion rate of a PRC during sampler deployment reflects the uptake rates of a target analyte, assuming isotropic exchange kinetics occur (Figure 1).

Because of the differences in the compound properties for the PRC and the target analyte, correction is needed to calculate the fractional approach to equilibrium for the target analyte from the fractional PRC dissipation at time t. In addition, PRC correction becomes difficult if sorption in the surrounding media is concentration dependent.

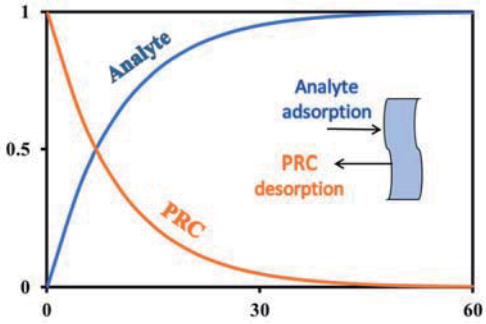

Fig. 1 PRC dissipation and compound uptake kinetics generally assumed for the performance reference compound (PRC) approach. (Ghosh et al. 2014).

As part of the risk assessment of contaminated sediment sites, sediment samples are typically analyzed to determine the likelihood that contamination will result in adverse effects to benthic invertebrates and higher trophic level organisms. The results of these analyses can be used to develop site-specific measures of exposure as well as measures of

biological effects. Resultant exposure-effect relationships can ultimately form the basis for risk estimates and management/remediation plans.

However, considerable uncertainty in these relationships can result from an incomplete understanding of bioavailability, which can be highly variable among sites. The use of PSMs to determine and compare freely dissolved concentration in pore water to observed effects can reduce uncertainty in sediment assessments and management decisions.

An example of a tiered assessment that uses passive sampling is presented in the USEPA guidance document on Equilibrium Partitioning Sediment Benchmarks (ESBs) (U.S. EPA, 2012). The first tier of this approach uses ESBs to evaluate the likelihood of toxicity to the benthos using an additive toxic unit (TU) model (Figure 2). In the second tier, passive samplers can be used to measure concentrations of freely dissolved contaminants in pore water. As in the first tier, concentrations in pore water that do not exceed the benchmark are considered protective of benthic aquatic organisms, but concentrations that exceed the benchmark may pose a risk and may require further consideration. Sediment toxicity testing can be conducted in the third tier to verify the findings of the first two tiers. However, it should be recognized that if a whole sediment toxicity test finds significant toxicity, the cause or causes may be toxic chemicals other than those measured in Tiers 1 and 2 (e.g., specific pesticides or ammonium) or by confounding factors such as inappropriate oxygen levels or pH.

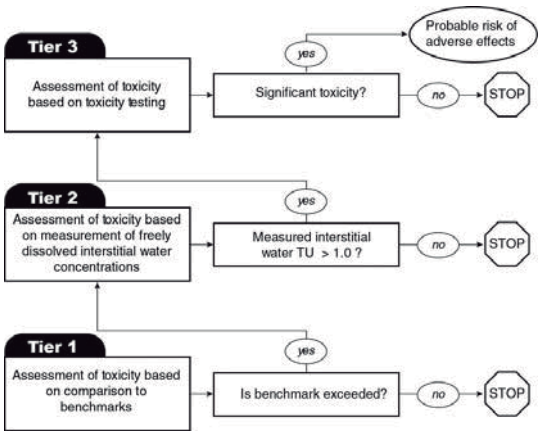

Fig. 2. Schematic of a tiered assessment that uses passive sampling to measure C_{free} for organic chemicals (based on U.S. EPA 2012).

Case study of passive sampling in predicting uptake in fish. The biological uptake of hydrophobic organic chemicals such as PCBs in fish is controlled by the bioavailability in sediments. In-situ sediment amendment with sorbents such as activated carbon (AC) can effectively reduce the bioavailability of PCBs. However, there is limited experimental or modeling assessment of how bioavailability changes in sediments impact bioaccumulation in fish – the primary risk driver for exposure to humans and top predators in the aquatic ecosystem. In this case study we performed laboratory aquarium experiments and modeling to explore how PCB sorption in sediments impacted exposure pathways and bioaccumulation in fish (Fadaei et al. 2015). Results showed that freely dissolved PCBs in porewater and overlying water measured by passive sampling were reduced by more than 95% upon amendment with 4.5% fine granular AC. The amendment also reduced the PCB uptake in fish by 87% after 90 days of exposure. Measured freely dissolved concentrations of PCBs were incorporated in equilibrium and kinetic models for predicting uptake by fish. Predicted uptake using the kinetic model was generally within a factor of 2 for total PCBs measured in fish (Figure 3). The kinetic model output was most sensitive to overlying water PCBs, lipid fraction, and dissolved oxygen concentration (regulating gill ventilation). Our results indicate that by incorporating changes in freely dissolved PCB concentrations in bioaccumulation models it is possible to predict effectiveness of sediment remediation in reducing PCB uptake in fish.

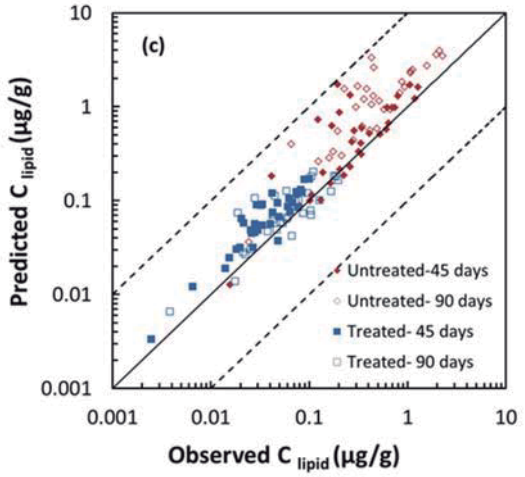

Fig. 3. Observed and predicted PCB concentrations in zebrafish using the Arnot and Gobas bioaccumulation model with ingestion. Closed symbols refer to 45 days results and open symbols refer to 90 days (Fadaei et al., 2015).

CONCLUSIONS

Measurement of freely dissolved concentrations of hydrophobic pollutants is sufficiently mature and scientifically accepted that relatively specific guidance can be provided for their routine use in contaminated sediment site assessments. The use and

interpretation of passive sampling presents a departure from conventional methods of site assessments and therefore requires the involvement of trained personnel familiar with the science. The use of passive sampling will result in the collection of better quality and more robust data, solidifying the scientific basis for environmental management decisions.

ACKNOWLEDGEMENTS

Research support is acknowledged from the National Institutes of Environmental Health Sciences and The Department of Defense, Strategic Environmental Research and Development Program.

REFERENCES

[1].Booij K, Smedes F, van Weerlee EM. 2002. Spiking of performance reference compounds in low density polyethylene and silicone passive water samplers. *Chemosphere*. 46(8):1157-1161.

[2]. Fernandez, L.A., J.K. MacFarlane, A.P. Tcaciuc, and P.M. Gschwend. 2009. Using performance reference compounds in polyethylene passive samplers to deduce sediment porewater concentrations for numerous target chemicals. *Environ. Sci. Technol.* 43:8888-8894.

[3].Ghosh U, Hawthorne S. 2010. Particle-Scale measurement of PAH aqueous equilibrium partitioning in Impacted Sediments. *Environ. Sci. Technol.* 44: 1204-1210.

[4] [NRC]. The National Research Council. 2003. Bioavailability of Contaminants in Soils and Sediments; National Academies Press: Washington, DC.

[5]. Ghosh U, Kane Driscoll S, Burgess RM, Jonker MTO, Reible D, Gobas F, Choi Y, Apitz SE, Maruya KA, Gala WR et al. . 2014. Passive sampling methods for contaminated sediments: practical guidance for selection, calibration, and implementation. *Integr. Environ. Assess. Manag.* 10(2):210-223.

[6] U.S. EPA. 2012. Equilibrium Partitioning Sediment Benchmarks (ESBs) for the Protection of Benthic Organisms: Procedures for the Determination of the Freely Dissolved Interstitial Water Concentrations of Nonionic Organics. EPA-600-R-02-012. Office of Research and Development, Washington, DC 20460.

[7].Fadaei, H.; Watson, A.; Place, A.; Connolly, J.; Ghosh, U., 2015. Effect of PCB Bioavailability Changes in Sediments on Bioaccumulation in Fish. *Environ. Sci. Technol.* 49, (20), 12405-12413.

Session topics

1. Geochemistry at the sediment-water interface

Session chairs: Ma. Catalina Alfaro[1] and Mario Villalobos[2]
[1]Facultad de Ciencias Químicas, Universidad Autónoma de San Luis Potosí, México
[2]Laboratorio de Geoquímica Ambiental, Instituto de Geología de la UNAM, México

Exchange of solutes and particles between the water and sediments, and prevailing geochemical conditions at the sediment-water interface, affect the diffusion of dissolved oxygen and internal cycling of nutrients, the chemical stabilization of organic and inorganic pollutants, AND the fate and availability of substances for the benthic organisms and plants. Before being effectively stabilized and accumulated, pollutants entering surface waters participate in several bio-geochemical processes. Even after pollutants are controlled at the sources, sediments may act as secondary sources, releasing substances upon changing biogeochemical conditions through molecular diffusion, particles resuspension, bioturbation and/or bioirrigation. Among these processes, diffusion fluxes at the sediment-water interface may control the magnitude and direction of geochemical processes, affecting the nutrient and pollutant cycle, and their environmental fate, which are crucial to evaluate the implementation of remediation actions and their effectivity. Works in this thematic are welcome, of particular interest are those related to the containment of polluted sediments or dredged materials.

TRACE METALS GEOCHEMISTRY IN THE SEDIMENTS OF A NATURAL WETLAND

Alfaro-De la Torre M. Catalina[1], Pérez-Castillo F. Virginia[1] and Briones-Gallardo Roberto[2]
[1]Facultad de Ciencias Químicas, UASLP, México; [2]Instituto de Metalurgia, UASLP, México

ABSTRACT

Bottom sediments were collected in natural wetland to evaluate the concentrations of Fe, Mn, other metals, sulfides, sulfate and pH with depth in the sediments and in the porewater. Our results suggest a geochemical control of Fe from sulfides which varies within season. At the end of spring (May), the metals mobilization occurs probably related to a major productivity of this ecosystem in contrast with the shape of profiles observed in fall (November). This interaction between Fe and sulfides are probably controlling other metals and the availability of nutrients like P, to the plants in the wetland. Diffusion fluxes at the sediment-water interface suggested a contribution of Fe from the sediments to the water column particularly; the concentration profiles suggest the diffusion of Mn from the sediment to the water column and a contribution of Cd, Hg, As and Ni to the sediments from the water column. The sediments in the wetland are reduced and characterized for a high production of sulfides.

Keywords: Iron, Sulfides, Sediment-water interface, Diffusion fluxes

INTRODUCTION

Sediments act as the sink and the source on many pollutants entering the aquatic ecosystems through wastewater discharges and atmospheric deposition. In this context, understanding the contributions of trace elements from external sources and the factors affecting their effective deposition in the sediments is critical. Some important processes and factors affect the elements mobility in sediments like the adsorption/desorption processes, salinity and particularly, changes in the redox conditions, sulfur and carbonate availability, pH and organic matter in wetlands. The effective accumulation of trace elements in the sediments is subjected to those processes. The mobility of some elements as Cd, As, Ni, Hg at sediment-water interface is related to the oxic-anoxic conditions of the sediments, to the Fe and Mn reduction and to the oxidation of the organic matter reported as the main carrier phases of some toxics in the water column. The mobility and availability of metals in wetland sediments can be significantly reduced by the formation of metal sulfide precipitates under anoxic conditions and be affected by oxidizing conditions at the rhizosphere of plants [1]. Few studies are reported about these processes in continental wetlands, the majority refers to coastal systems.

In this work, we elucidate some of these processes in the freshwater wetland "Ciénega de Tamasopo" located in the limits of the Nearctic-Neotropical region, Central Mexico.

METHODS

The study was done in the tropical wetland "Ciénega Tamasopo" located in Central Mexico (Figure 1) [2]. The wetland supplies water for agriculture (sugar cane) and for ~3000 inhabitants and has been impacted by residues from the fields and settlements around; also, agriculture contributes with air pollution caused by particles from the burning of sugar cane field at harvest (from October until January, each year). Water column depth is shallow, until 0.3m during the dry seasons (May to August) and increase during the raining period (September; ~1.5m or more).

Vegetation is dominated by hydrophyte plants (*Nymphaea goudotiana*, *Elodea* sp., *Typha* sp., *Cladium* sp). Vegetation acts as a filter of sediments at the wetland shore, however, air pollution is probably contributing with inorganic and organic substances.

Sampling

On May 2009, two sediment cores were collected with a gravity sampler (Wildco 2404-A14) at deepest site (SS-W, Figure 1) at an area not covered by plants. Sediments were cut in 0.5, 1 and 2 cm slices, preserved at 4 °C and oven dried (60 °C, 12 h) in the laboratory. Acrylic porewater samplers (1 cm vertical resolution peepers; comprising two columns of 4 mL cell) were deployed (3 peepers; left in place for two week) on May 2009 and November 2011 to collect porewater and overlying water.

Peepers were deaerated with N_2 for a minimum of 15 days prior to filling the cells with deionized water and covering them with a hydrophilic cellulose acetate membrane (0.2 µm). Upon retrieval, peepers were sampled immediately for the measurement of pH and total dissolved concentrations of sulfides (Σ [HS^-]), metals (Fe, Mn, trace elements) and major anions (results not shown).

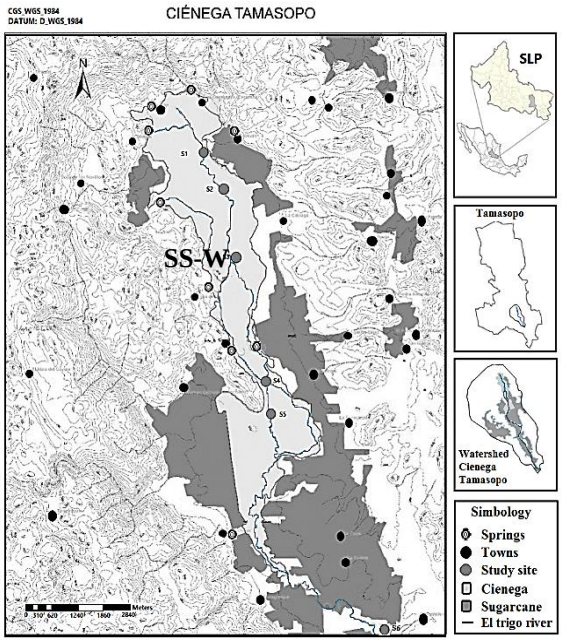

Fig. 1. Location of the wetland "Ciénega de Tamasopo" SLP. Mexico and the sampling site SS-W. Processed with data from INEGI (1999).

Analyses

Sub-samples (0.1 - 0.5 g) of homogenized sediments were acid digested (HNO_3, $HClO_4$ and HF; [3]) to determine metals by Atomic Absorption Spectrophotometry (SpectrAA Varian 220Z or 220FS). Reference sediment sample (TH-2, National Water Research Institute) was used for metals; the recovery was between 85-110%, and a laboratory control sample was analyzed for the water measurements.

In water, sulfides were determined by the Cline method [4] and sulfates by ion chromatography (Dionex HPLC-IC 2500) and metals by Atomic Absorption Spectrophotometry (SpectrAA Varian 220Z). All pH were measured within 10 - 30 min in the field with an electrode (IQ 150 pH meter). Samples and field blanks were stored to 4 °C in dark during their transportation to the laboratory.

RESULTS AND DISCUSSION

Oxidation and reduction reactions are of fundamental importance in wetland ecosystems. The fluctuating water table between the dry season and post-raining may affect the redox state because a shallow water column could promote changes from anaerobic to aerobic conditions at the sediment surface. In the wetland, the water column varies from 0.3m to ~1.5m depth, and this could expose the reduced sediments. In this work, concentration profiles of Fe, Mn, Cd, As, Ni, Hg, sulfates (SO_4^{2-}), total dissolved sulfides ($\Sigma[HS^-]$) and pH were determined using dyalisis sampler at two occasions: the dry period (May 2009) and after the raining period (Novembrer 2011). Total metals concentration profiles in the sediments were obtained in May 2009. Figure 2, 3 and 4 show the profiles of total Fe and Mn in the sediments, and pH, ORP, sulfates, sulfides, Fe and Mn in porewater determined in May 2009 and November 2011 respectively. Concentration profiles of metals in the sediments and ORP profiles were only determined in May 2009. ORP values (<-150mV) are characteristics of conditions where the sulfates reduction occurs [1].

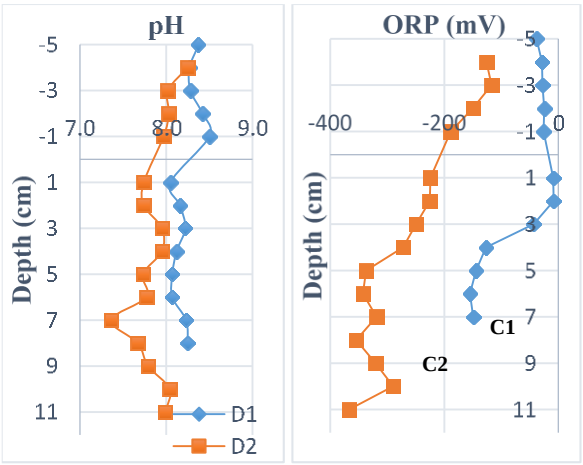

Fig. 2. pH and Redox Potential (ORP) with depth determined in porewater (D1, D2) and in sediment cores (C1, C2; May 2009).

Water pH in the wetland corresponds to slight alkaline system; the geology of this region is of the karstic type. The oxidation-reduction potentials (ORP; Fig 2) show the heterogeneity of the sediments, the reducing conditions prevailing in the sediments even at the sediment – water interface and the rapid decrease of the redox potential with depth. The sulfate and sulfide concentration profiles (Figs. 3 and 4) proved that sulfate reduction is an important process occurring in the sediments of this wetland [5,6]. Sulfide concentration between profiles varied more significantly when the water column was shallow as occurring during the dry period (May 2009; Fig. 3).

Metals respond to changes in the ORP [1]. Their mobility could be significantly affected if those changes affect the metal-binding capacity of organic matter, induce reductive-dissolution of Fe/Mn-oxyhydroxides or sulfides oxidations. In reducing

conditions, metals adsorbed on the Fe/Mn-hydroxides are desorbed and could precipitate as sulfides in the sulfate reduction zone. In contrast, changes from a reduced to an oxidizing environment oxidize sulfides; in these conditions some metals as Fe can be mobilized and re-precipitated at the oxic – anoxic interface. This is probably the process affecting the chemical behavior of Fe and Mn [6].

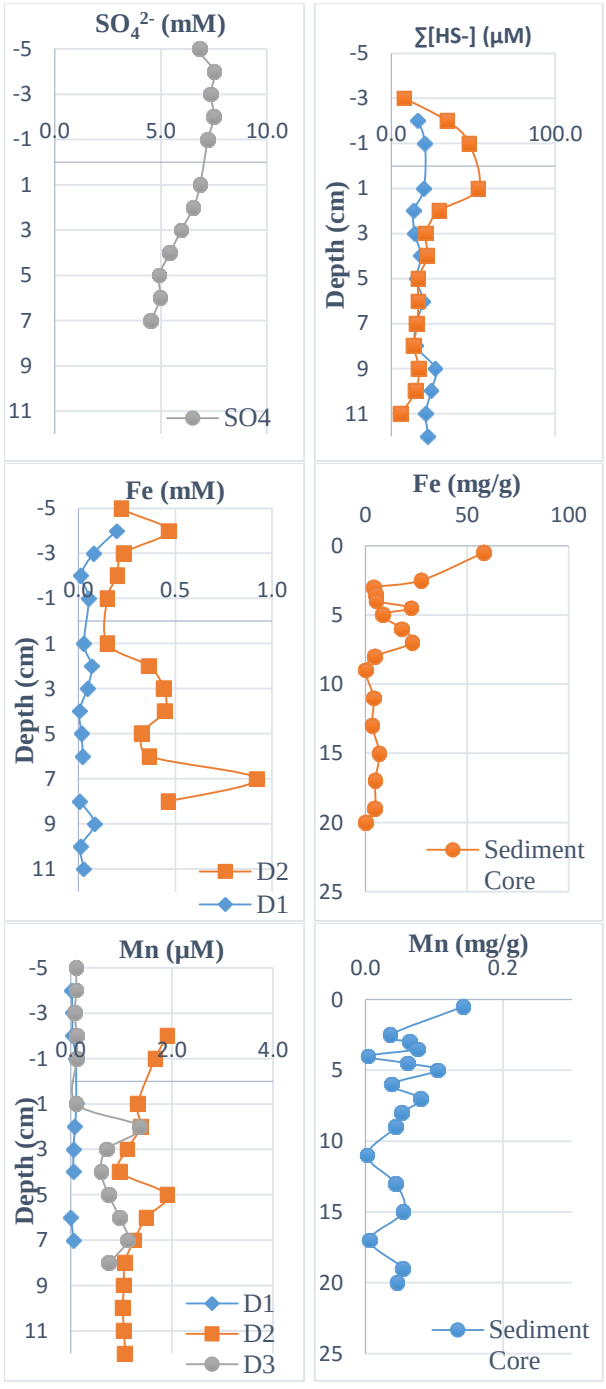

Fig. 3. Concentration profiles of sulfates, sulfides, Fe and Mn in the porewater (D1, D2, D3) and sediments of the "Ciénega de Tamasopo" determined on May 2009.

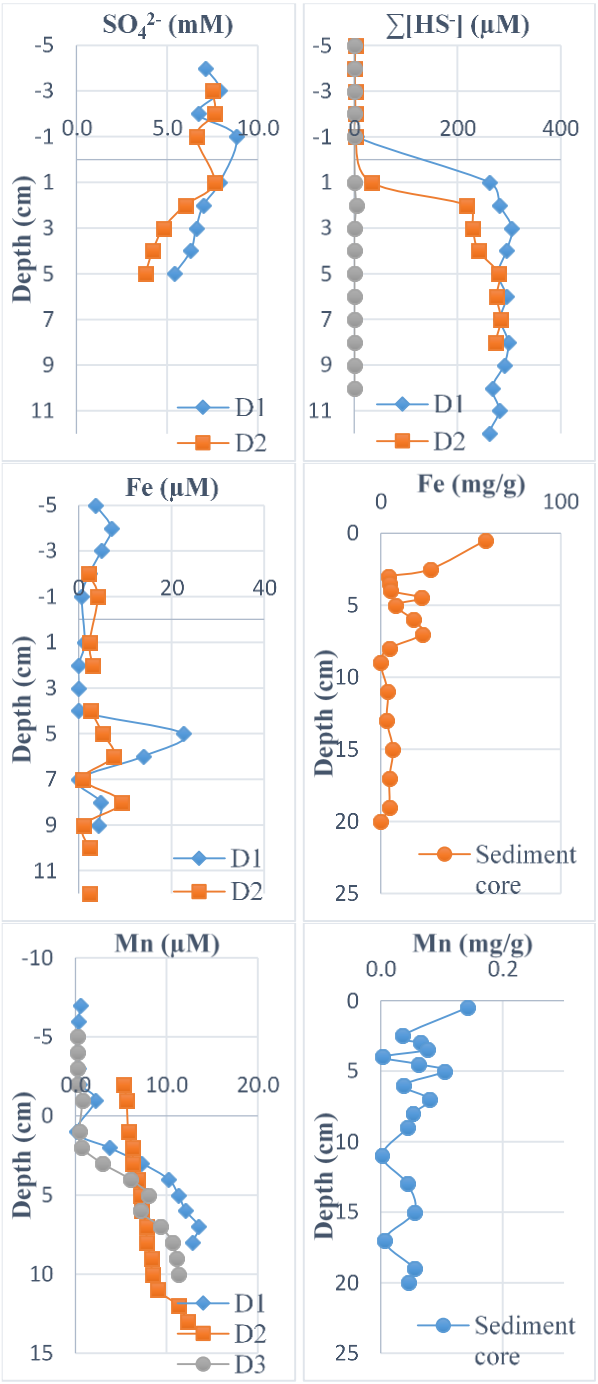

Fig. 4. Concentration profiles of sulfates, sulfides, Fe and Mn in the porewater (D1, D2, D3) and sediments of the "Ciénega de Tamasopo" determined on November 2011.

Figures 3 and 4 show a mobilization of Fe and Mn at depth where sulfides are produced and diffusion to the sediment – water interface probably conducing to an internal recycling that could explain the surficial enrichment of the sediment with these elements. Similar results have been reported in lake sediment [7].

Iron fluxes at the sediment-water interface (0.33±0.35 µmol/cm^2.d; determined in November

2011) suggest the diffusion of this metal from the sediment to the water column).

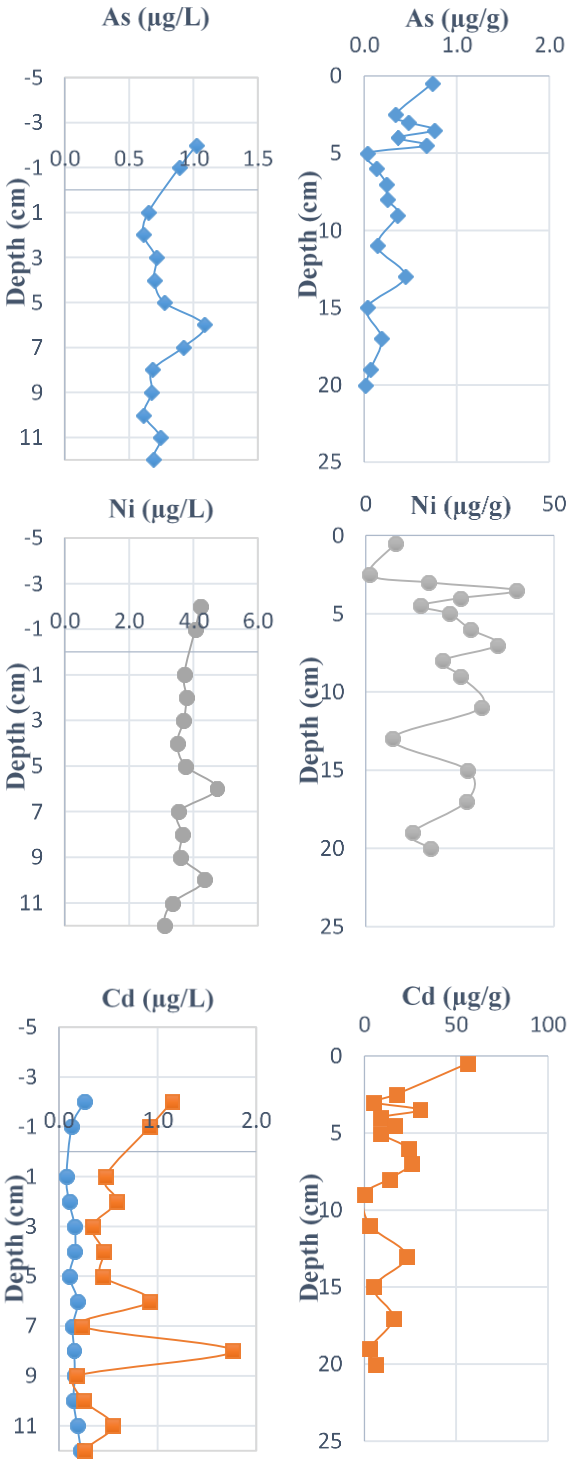

Fig. 5. Concentration profiles of As, Cd, Ni and Hg in the porewater and sediments of the "Ciénega de Tamasopo" determined on May 9.

Sediments in the wetland are rich in Fe as shown in Fig. 3. The redox behavior of this element probably control the stable accumulation of toxic elements (As, Cd, Hg, Ni) in the sediments and their mobilization at the sediment-water interface; also, their accumulation by plants in the wetland. The sediment cores and porewater sampling were done at a site without direct influence of plants; however, the oxidizing conditions at the rhizosphere in the wetland could induce the mobilization of metals and their accumulation by the plants as suggested by Vandecasteele et al. [8].

Fig. 5 shows the concentration profiles of As, Cd, Ni and Hg in porewater and As, Cd and Ni in the sediments. Some important information can be highlighted. Firstly, the enrichment of As and Cd in the surficial sediments that seems to be related to a contribution of the water column, a decreased concentration where sulfate are reduced probably related to a precipitation as Me-sulfides (concentration of As and Cd increase in the sediment at this depth) and a mobilization in deeper sediments. The same behavior was observed for Hg; unfortunately we could not determine Hg in the sediments. In contrast, there is a slight contribution of Ni from the water-column and lower concentration at 0-5cm depth contrasting with increased concentrations in the sediments.

CONCLUSIONS

Sulfate reduction (and sulfide production) is a main process occurring at the sediment-water interface. This major redox process affects the mobilization of Fe, Mn and toxic elements as As, Cd, Hg. Mobilization of Fe and Mn and a re-precipitation as metal sulfides suggest a recycling of these elements and enrichment at sediment surface. The cycle of the trace elements is probably related to this Fe/Mn behavior. Concentration profiles of Cd, As, and Hg also suggest a contribution from the water column. Ni seems to be a very mobile element and thus it is unclear the main contribution.

ACKNOWLEDGEMENTS

This work was carried out with financial support from CONACYT project 90228 and the PROMEP-RED for the UASLP-CA-37. FVPC was awarded a graduate fellowship from CONACYT No 240468. We thank the support from the Tamasopo municipality (Eladio Ruiz Sánchez), the Ejido Cabezas, and the fieldwork support of Rebeca Y. Pérez Rodríguez, Claudio M. Padilla González, Isidro Montes Ávila, Fortunato and Virgilio Landa Verde.

REFERENCES

[1] Du Laing G., Rinklebe J., Vandecasteele B., Meers E., Tack F.M.G., "Trace metal behavior in estuarine and riverine floodplain soils and sediments: A review", Science of the Total Environment, Vol. 407, 2009, pp. 3972-3985.

[2] FIR: Ficha Informativa de los Humedales de Ramsar – Versión 2006-2008.
[3] Fortin D., Leppard G.G., Tessier A., "Characteristics of lacustrine diagenetic iron oxyhydroxides", Geochimica et Cosmochimica Acta, Vol. 57(18), Sept. 1993, pp. 4391-4404.
[4] Cline, J.D., "Spectrophotometric determination of hydrogen sulfide in natural waters", Limnology and Oceanography, Vol. 14, 1969, pp. 454-458.
[5] Pérez Castillo F.V., "Dinámica de C, N, P y Fe en agua y sedimentos del humedal Ciénega de Tamasopo, S.L.P.", PhD Thesis, 2017, 209p.
[6] Pérez-Castillo F.V., Alfaro-De la Torre M.C, Pérez-Rodríguez R.Y., Comín-Sebastián F.S., "Tracing anthropogenic disturbances of a wetland through carbon and nitrogen isotope analyses in sediments", J. of Natural Resources and Development, Vol. 7, 2017, pp. 22-29.
[7] Alfaro-De la Torre M.C., Tessier A., "Cadmium deposition and mobility in the sediments of an acidic oligotrophic lake", Geochimica et Cosmochimica Acta, Vol. 66(20), Oct. 2002, pp. 3549-3562.
[8] Vandecasteele B., Du Laing G., Tack F.M.G., "Effect of submergence-emergence sequence of organic matter or aluminosilicate amendment on metal uptake by woody wetland plant species from contaminated sediments", Environmental Pollution, Vol. 145, 2007, pp. 329-338.

USE OF OXYGENATION TO REPRESS RELEASE OF REDOX-SENSITIVE COMPOUNDS FROM PROFUNDAL SEDIMENT IN THE VALLE DE BRAVO RESERVOIR, MEXICO

Beutel Marc W.[1], García-Gallardo Teresa [2], Falcón-Rojas Axel [2], Furhmann Byran [1] and Hansen Anne M. [2]
[1]University of California, Merced, USA; [2]Mexican Institute of Water Technology (IMTA), Mexico

ABSTRACT

Valle de Bravo is a mesotrophic water supply reservoir located in the highlands west of Mexico City. Reservoir bottom water goes anaerobic in the summer, resulting in the release of redox-sensitive compounds from profundal sediment that degrade water quality. This study used experimental sediment-water interface chambers to assess the flux of redox-sensitive nutrients (ammonia and phosphate) and metals (manganese and iron) from profundal sediment under aerobic and anaerobic conditions. Results showed that maintenance of well-oxygenated conditions at the sediment-water interface resulted in a significant decrease in the sediment flux of phosphate (-0.1 vs 2.5 mg-P/m^2·d) and manganese (-1.0 vs 2.4 mg/m^2·d) compared to anaerobic conditions. Aerobic conditions also enhanced microbial ammonia oxidation to nitrate. Results indicate that hypolimnetic oxygenation, the engineered addition of dissolved oxygen to the bottom of lakes and reservoirs using pure oxygen gas, could be effective in lowering internal nutrient loading and enhancing water quality in the reservoir.

Keywords: Internal Nutrient Loading, Phosphorus, Ammonia, Hypolimnetic Oxygenation

INTRODUCTION

Surface water reservoirs are vulnerable to nutrient pollution from human activity in their watersheds. In a process known as cultural eutrophication, external nutrient loading can lead to excessive algal growth in surface waters. When algae sink into bottom water, they are biodegraded by respiring bacteria resulting in deoxygenation of the profundal zone. Under anaerobic low-redox conditions, profundal sediment tends to release ammonia via mineralization [1] and phosphate via reductive dissolution of phosphate-rich iron oxides [2]. Internal nutrient loading exacerbates external nutrient loading and reinforces the eutrophication process [3], [4].

Anaerobic sediment also releases redox-sensitive compounds that are toxic to biota (e.g., ammonia and sulfide) and complicate potable water treatment (e.g., manganese and iron). Anaerobic conditions in bottom water also degrade habitat for aerobic biota including cold-water fish that need cool, oxygenated water in the summertime, and zooplankton that use dark oxygenated bottom water to avoid fish predation.

The general topic of this research project – water quality management in reservoirs – is an especially significant topic in California and Mexico, where population growth coupled with water scarcity and changing hydrology related to climate change are threatening water sustainability [5]. Coastal areas of southern California and much of central Mexico have high incident threat to human water security, where incident threat accounts for a cumulative array of diverse stressors to water security at a given geographical location [6]. As one of the largest and fastest growing megacities in the world, the populace of the Mexico City metropolitan region needs improvements in water management to ensure a stable and sustainable water supply [7]. In California, a number of studies suggest that climate change will lead to more severe droughts, with a higher frequency of hot and dry conditions challenging the State's future water security and threatening to "turn the Golden State brown" [8].

The objective of this study was to assess sediment release rates of nutrients (phosphate, ammonia and nitrate) and metals (iron and manganese) under aerobic and anaerobic conditions. The working hypothesis was that maintenance of an oxygenated sediment-water interface would repress nutrient and metal release. These results inform plans to potentially install a hypolimnetic oxygenation system in the Valle de Bravo reservoir.

Hypolimnetic oxygenation is the engineered addition of dissolved oxygen, using pure oxygen gas, to the bottom of lakes and reservoirs [9]. By using pure oxygen instead of air as an oxygen source, the size and energy needs of engineered systems to supply large amounts of oxygen to reservoir bottom water is relatively small. Hypolimnetic oxygenation systems typically include an on-shore liquid oxygen storage tank, piping down to the lake bottom, and either a submerged contact cone with water pump [10] or linear bubble plume diffuser [11]. Systems are capable of economically injecting large amounts of dissolved oxygen (1-100 metric tons per day) into reservoirs and other surface waters (lakes, rivers, estuaries, harbors) in need of oxygen enhancement.

STUDY SITE

The Valle de Bravo reservoir is a high-elevation, tropical water body located in the highlands of Mexico 150 km west of Mexico City. The lake thermally stratifies with a warm layer of water overlaying cooler bottom water for most of the year, except in the winter when surface water cools and windy conditions keep the water column fully mixed. The reservoir has a maximum depth of 38.6 m, a surface area of 18.6 km^2, and a maximum volume of 391 million m^3. The reservoir is a critical component of the water supply for Mexico City metropolitan area and Toluca. With over 20 million residents, the region requires almost 7 million m^3 of water per day [12]. Local groundwater supplies half of this demand and the rest is transported from outside the Mexico City Basin. The Valle de Bravo reservoir accounts for a quarter of this outside supply. The reservoir is also a popular recreational site.

Over the past 20 years, water quality in the Valle de Bravo reservoir has degraded due to nutrient pollution that has stimulated the growth of toxic cyanobacteria [13]. The decay of excessive phytoplankton has led to anaerobic conditions in bottom waters and sediment release of phosphate and ammonia, both of which can enhance phytoplankton production in surface waters. Several factors unique to the Valle de Bravo reservoir make it especially susceptible to oxygen depletion in bottom waters and internal loading of nutrients [14]. Being at higher elevation (~1,800 m above sea level), the reservoir has a lower dissolved oxygen saturation concentration, so water can hold less oxygen than a reservoir near sea level. In addition, the duration of thermal stratification in the warm tropical reservoir is long, typically from March through September [2], meaning that there is plenty of time for bottom water to accumulate pollutants released from sediment. Finally, strong winds oriented across the length of the reservoir promote intermittent mixing of nutrient-rich bottom water into surface water throughout the summer and fall.

METHODS

To assess our hypothesis, we incubated lab-scale sediment-water chambers under aerobic conditions followed by anaerobic conditions and monitored water quality overlaying sediment with time. A total of 4 chambers were collected in the deep zone of the reservoir near the dam in September 2017. The polycarbonate chambers are 25 cm high and 9.5 cm in diameter and contain 5-8 cm of sediment and ~1.5 L of overlaying water (Fig. 1). To collect samples, first a minimally disturbed sediment-water interface was collected using an Ekman dredge. The dredge was brought to the surface and a subsample of the sediment-water interface was collected by pushing a chamber cylinder into overlaying water and sediment and capping the bottom by hand. Chambers were then topped up with bottom water prior to transport.

Fig. 1 Photo of sediment-water interface chamber

Chambers were incubated at the Hydrogeochemistry Laboratory of the Mexican Institute of Water Technology (IMTA), in the dark at *in situ* temperature (~14 ^oC). Chambers were first incubated under aerobic conditions by bubbling with air for 18 days and water samples were collected at days 0, 4, 7, 11, 14 and 18. Chambers were topped up with bottom water and incubated under anaerobic conditions by bubbling with nitrogen gas for 14 days and water samples were collected at days 0, 4, 7, 11, 14. Water samples were analyzed for phosphate, ammonia, nitrate, total manganese and total iron using standard colorimetric methods. Based on water quality data, flux rates ($g/m^2 \cdot d$) for compounds of interest were estimated as the change in concentration over time, multiplied by the chamber water volume and divided by the area of the sediment. Flux rates were compared statistically between aerobic and anaerobic treatments using a paired (by chamber) student t-test.

RESULTS AND DISCUSSION

Table 1 summarizes results in terms of average chemical fluxes under aerobic versus anaerobic conditions for phosphate, ammonia, nitrate, manganese and iron. Mean fluxes of phosphate and manganese were significantly higher under anaerobic conditions. Mean iron fluxes were also higher under anaerobic conditions, but high variability in flux values led to a lack of statistical significance between treatments. Metals release from aquatic sediment is generally attributed to

microbial reductive dissolution of metal oxides in surfacial sediment [15]. Phosphate adsorbed to iron oxides is also released in this process [16]. Manganese oxides are especially sensitive to moderate drops in redox at the sediment-water interface and readily dissolve and flux out of profundal sediments into overlaying water primarily as Mn(II). Iron release from sediment occurs at lower redox than manganese and tends to be more sustained than manganese release. Iron release is also more complex than manganese release because sediment and water can be a sink for Fe(II) via precipitation with S^{2-} to form FeS (solid). In addition, sulfide in sediment can enhance iron release from sediment at low redox by abiotically reducing iron oxides that were resistant to microbial reductive dissolution.

Table 1 Summary of flux results for replicate experimental sediment-water interface chambers under aerobic and anaerobic conditions

	Chambers				
Chemical	**1**	**2**	**3**	**4**	**Mean**
Phosphate					
aerobic	-0.0	-0.1	0.0	-0.2	-0.1*
anaerobic	3.0	0.2	2.7	3.9	2.5*
Ammonia					
aerobic	19.1	8.3	11.1	9.6	12.0
anaerobic	15.3	15.8	1.1	13.4	11.4
Nitrate					
aerobic	-0.5	0.8	2.3	1.1	0.9*
anaerobic	-1.9	0.0	-0.9	-1.8	-1.1*
Manganese					
aerobic	-0.9	-1.8	-1.0	-0.5	-1.0*
anaerobic	2.3	3.2	1.9	2.2	2.4*
Iron					
aerobic	-1.3	-3.8	-0.6	-1.7	-1.8
anaerobic	1.4	0.5	-0.2	8.4	2.5

Note: all units in mg/m^2·d. * significant difference ($p < 0.05$) between aerobic and anaerobic treatments.

Figure 2 shows the entire data set for phosphate flux with time in all experimental chambers. All chambers except chamber 2 showed clear patterns of phosphate release under anaerobic conditions. Phosphate fluxes ranged from 1.5-6 mg-P/m^2·d and averaged 2.5 mg-P/m^2·d (Table 1). Note that phosphate fluxes did not start until after 4 days into the anaerobic phase of the chamber experiment. This is likely because it took some time for redox to drop to the level that supported microbial reductive dissolution of iron oxides in surfacial sediments. The magnitude of phosphate fluxes from anaerobic sediment measured in this study are typical of moderately eutrophic lakes like the Valle de Bravo reservoir. Typical release rates range from 2-10, 7-13, and 15-27 mg-P/m^2·d for mesotrophic, eutrophic and hypereutrophic systems, respectively [17].

With regards to the nitrogen cycle, nitrate fluxes were significantly different between treatments, being negative (uptake) under aerobic conditions and positive (release) under anaerobic conditions. The presence of oxygen at the sediment-water interface enhances microbial nitrification, converting ammonia to nitrate [1]. In contrast, a lack of oxygen promotes biological denitrification, the conversion of nitrate to nitrogen gas. These dynamics explain the nitrate accumulation observed at the end of the aerobic phase and the rapid loss of nitrate at the beginning of the anaerobic phase. Ammonia flux was positive under both aerobic and anaerobic conditions, suggesting that aeration had a limited effect on repressing ammonia release from sediment. Anaerobic ammonia release rates measured in the Valle de Bravo reservoir (mean of 11.4 mg-N/m^2·d; Table 1) were similar to other sites, which generally range from 5-10 mg-N/m^2·d in mesotrophic lakes and 10-20 mg-N/m^2·d in eutrophic lakes [1]. The observed aerobic ammonia release indicates that surficial sediment in the Valle de Bravo reservoir has a rich store of organic matter that undergoes mineralization under both aerobic and anaerobic conditions. This is a consequence of eutrophication and the buildup of organic matter in sediment which has little chance of undergoing oxidation since summertime bottom water is void of oxygen.

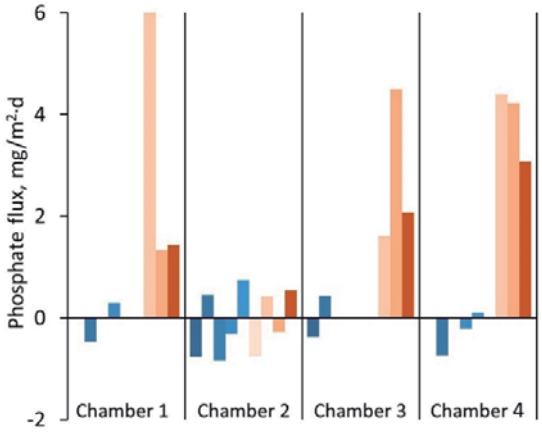

Fig. 2 Patterns of phosphate fluxes in experimental sediment-water interface chambers under aerobic (blue on left) and anaerobic (orange on right) conditions. All chambers except chamber 2 showed clear patterns of phosphate release under anaerobic conditions

FINAL CONSIDERATIONS

The Valle de Bravo reservoir is a critical water supply and recreational resource for central Mexico. Like many reservoirs throughout the world, water quality in the reservoir has degraded over time due to elevated external nutrient loadings. This has resulted in hypolimnetic anoxia and enhanced internal nutrient loading, which is likely exacerbating eutrophication and its negative ecological consequences. Experimental results confirmed that maintenance of an oxygenated sediment-water interface resulted in significant decreases in sediment release rates of phosphate and manganese under aerobic versus anaerobic conditions. Aerobic conditions also appeared to lower sediment release of iron and promote conversion of ammonia to nitrate.

Results support the contention that engineered oxygen addition to bottom waters would repress internal phosphorus loading. Further analysis is needed to confirm that internal loading, in addition to external loading, is a significant factor in controlling algal production in the reservoir. One advantage of oxygenation is that improvements in water quality are immediate (DO in bottom water, enhanced cold-water habitat) or near term on the time scale of years (lower internal nutrient loading, lower algal productivity). This contrasts with watershed management which is institutionally and socially complex and may take many years to decades to successfully implement. While both internal and external nutrient loading control is needed to ultimately improve water quality in the Valle de Bravo reservoir, in-lake management efforts like hypolimnetic oxygen that target redox-sensitive compounds at the profundal sediment-water interface could be a meaningful start on the path to ecological and water quality restoration of the reservoir.

ACKNOWLEDGEMENTS

This work was funded in part by a UCMEXUS-CONACYT 2016 Collaborate Grants Program.

REFERENCES

[1] Beutel MW, Inhibition of ammonia release from anoxic profundal sediments in lakes using hypolimnetic oxygenation. Ecol Eng, Vol. 28, 2006, pp. 271–279.

[2] Hansen AM, Márquez-Pacheco H, Internal phosphorus load in a Mexican reservoir: Forecast and validation. Environ Toxicol Chem, Vol. 34, 2015, pp. 2583–2589.

[3] Marsden MW, Lake restoration by reducing external phosphorus loading: the influence of sediment phosphorus release. Freshwater Biology, Vol. 21, 1989, pp. 139–162.

[4] Welch, EB, Cooke GB, Internal phosphorus loading in shallow lakes: importance and control. Lake Reserv Manage, Vol. 11, 1995, pp. 273–281.

[5] Grant SB, Taking the "waste" out of "wastewater" for human water security and ecosystem sustainability. Science, Vol. 337, 2012, pp. 681–686.

[6] Vörösmarty CJ, Global threats to human water security and river biodiversity. Nature, Vol. 467, 2010, 555–561.

[7] Tortajada C, Water management for a megacity: Mexico City metropolitan area. Ambio, Vol. 32, 2003, pp. 124–129.

[8] Mann ME, Gleick PH, Climate change and California drought in the 21st century. Proceed Nat Academy Sci, Vol. 112, 2015, pp. 3858–3859.

[9] Beutel MW, AJ Horne, A review of the effects of hypolimnetic oxygenation on lake and reservoir water quality. Lake Reserv Manage, Vol. 15, 1999, pp. 285–297.

[10] Speece RE, Lateral thinking solves stratification problems. Water Qual Int, Vol. 3, 1994, pp. 12–5.

[11] Mobley MH, Brock WG, Widespread oxygen bubbles to improve reservoir releases. Lake Reserv Manage, Vol. 11, 1995, pp. 231–234.

[12] Jordán R, Rehner J & Samaniego J. Regional Panorama Latin America, Megacities and Sustainability. Economic Commission for Latin America and the Caribbean, 2010, 202 p. Available at http://www.giz-cepal.cl/files/megacities_and_sustainability.pdf (Consulted on March 2018).

[13] Valeriano-Riveros ME, Vilaclara G, Castillo-Sandoval FS, Merino-Ibarra M, Phytoplankton composition changes during water level fluctuations in a high-altitude, tropical reservoir. Inland Waters, Vol. 4, 2014, pp. 337–348.

[14] Merino-Ibarra M, Monroy-Ríos E, Vilaclara G, Castillo FS, Gallegos ME, Ramírez-Zierold J, Physical and chemical limnology of a wind-swept tropical highland reservoir. Aquatic Ecol, Vol. 42, 2008, pp. 335–345.

[15] Davison W, Iron and manganese in lakes. Earth-Science Reviews, Vol. 34, 1993, pp. 119–163.

[16] Boström B, Jansson M, Forsberg C. Phosphorus release from lake sediments. Arch Hydrobiol Beih Ergebn Limnol, Vol. 18, 1982, pp. 5–59.

[17] Nurnberg GK, Phosphorus release from anoxic sediments: What we know and how we can deal with it. Limnetica, Vol. 10, 1994, pp. 1–4.

EVALUATION OF TWO METHODS FOR THE CONTROL OF PHOSPHORUS IN WATER-SEDIMENT SYSTEMS

García-Gallardo María Teresa[1], Hansen Anne M.[1], Falcón-Rojas Axel[1], and Beutel Marc[2]
Mexican Institute of Water Technology (IMTA), Jiutepec, Mor., Mexico[1], University of California, Merced, USA[2]

ABSTRACT

Enrichment of phosphorus (P) in water is known as eutrophication. It has been reported that even controlling external load of P, it is necessary limit the internal load of this nutrient. In this work were experimentally evaluate hypolimnetic oxygenation and Phoslock® to control internal phosphorus load. Evaluation was developed in reactors with water and sediment from a Mexican reservoir as follows: i) No treatment, ii) Treatment with oxygenation, and iii) Treatment with Phoslock®. Evaluation was performed by 65 d, at room temperature in dark and using mechanical agitation. The results show that oxygenation and Phoslock® allows the reduction of phosphorus concentration in water, but they did not reached the desired concentration (0.035 mg/L). The analysis of TP in sediment showed that the oxygenation treatment allowed a greater retention of this nutrient in the sediment. It is concluded under these experimental conditions that oxygenation controls P in water and sediment better than the adsorbent. But it is recommended to evaluate both methods in the same incubation in order to know if the combination provides better results.

Keywords: Eutrophication, Internal load of P, Phosphorus control, Oxygenation, Phoslock®.

INTRODUCTION

The enrichment of phosphorus (P) in water bodies causes a problem known as eutrophication, which represents one of the most frequent and severe water pollution problems worldwide [1], [2]. If the P comes from the outside of a water body, from the watershed, it is known as external phosphorus load (EPL) for example: deposition from atmosphere, P from erosion of watershed and P from industrial and domestic discharges [3],[4]. On the other hand, the internal phosphorus load (IPL) includes P released by the decomposition of organic matter (OM), by lysis of microbial cells and the P released from the sediment by the dissolution of metal oxides of iron (Fe), manganese (Mn) and aluminium (Al) [5], which normally occurs at low oxygen concentration and Eh ≤ 50 mV [6] due to dissolution and redox reactions at sediment-water interface.

For many years the efforts to control the process of eutrophication have focused on the control of the EPL, which is the most important measure for the reduction of P in water bodies, but even this, the IPL represents an important contribution of this nutrient [7], mainly in lakes with thermal stratification. In these cases it is common employ complementary techniques to EPL limitation, for decrease internal release of P, for example: inactivation of nutrients, dilution, hypolimnetic oxygenation, increase of circulation water, removal of hypolimnetic waters and the dredging of sediments [8], all of them meanly aim to reduce the concentration of orthophosphate (a form assimilated by photosynthetic organisms). It is important mention that sometimes will be necessary more than one method to reach the desired conditions in the water.

Hypolimetic oxygenation and the application of the Phoslock® adsorbent are two of the most used methods for IPL control and have shown acceptable results in laboratory, mesocosm and field tests [9]-[13]. Hypolimnetic oxygenation consists in the injection of pure O_2 to the deep zones, where the solubility is greater and without altering the thermal stratification of water [9],[13], reverting hypolimnetic anoxia, when dissolved oxygen is below 2 mg/L [14] and promoting the adsorption of P by oxides and hydroxides of Fe and Mn. In this sense, it has reported a removal of total phosphorus (TP) concentration in water of 30-80% with respect to pre-treatment concentrations. Other benefits of this technique is the reduction of reduce compounds like Fe(II), Mn(II), S^{2-} and NH_4 as well control of mercury (Hg) and methyl mercury (M-Hg) in water [15], [16].

Phoslock® is an adsorbent consisting of bentonite modified with lanthanum (La) ions (5%), which is used to chemically and permanently bind the water soluble P, forming a mineral called rabdofan [10], [17]- [19]. The adsorbent reacts with a molar ratio of 1: 1 (La: PO_4) and presents optimal results at pH= 5-7 [10], [20]. According to [21] and [12] Phoslock® remove between 60 y 80% of TP. Additionally to remove dissolved P, Phoslock® form a barrier in sediment and prevents the release of P from deeper layers [10], And it presents a low ecotoxicological effect for aquatic organisms.

In this work were experimentally compared hypolimnetic oxygenation and Phoslock® for the control of IPL to reach a total phosphorus (TP)

concentration of mesotrophic state (0.035 mg/L) according to OCDE [21] with water and sediment from the Valle de Bravo reservoir, Mexico; which has been determined as eutrophic and it is relevant because it provides water to be treated and send to Mexico city and localities around and due to the recreational activities performed in the reservoir.

METHODS

Sampling of water and sediment

On August 2016 was carried out a sampling of water and sediment at the Valle de Bravo reservoir, State of Mexico. The sampling sites 1, 2 and 3 (Figure 1) were selected because they showed high concentrations of TP and OM in sediment according to [22]. At these points, water was collected from the midpoints of the epilimnium (~6 m) and hypolimnium (~20 m).

The water samples were obtained with a horizontal van Dorn bottle (Wildco Instruments) of 2L capacity. The sediment samples were obtained with a van Veen dredge, taking only the first five superficial centimetres of each sample and store them in hermetic plastic bags. Both, water and sediment were ice stored and in dark.

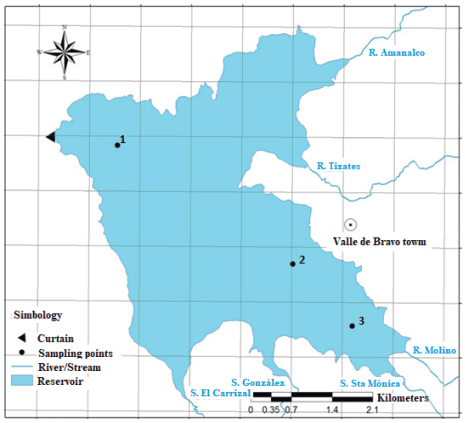

Figure 1. Sampling points in Valle de Bravo reservoir [22].

In laboratory was determined in sediment the moisture according to [23], % OM with methodology of [24], TP with HCl_4 method reported in [25], this measurement was performed before and after the treatments [25] and total iron (TFe) with method 6020 A [26] was analysed only the initial sediment. In water TP and Fe(II) were measured with colorimetric kits of Merck® in photometer Pharo 300 of the same brand. Water was enrichment with KH_2PO_4 (J. T. Baker, 99%) to obtain 0.28 mg/L of TP. Then it was made a compound sample of water and sediment by separate, mixing the same volume from each sampling point.

Evaluation of phosphorus control

The evaluation of the control of P was carried out in three experimental reactors (Figure 2) with water and sediment in a ratio of 15: 1 (w/w): i) No treatment, in which water and sediment were incubated with a continue flux of N_2(g) (purity 98%), ii) Treatment with oxygenation, where water and sediment were maintain with a flux of O_2 (g) (98%) and iii) Treatment with Phoslock®, using the relation 100:1 (Phoslock:TP) and with a flux of N_2(g). The relation of adsorbent was calculated considering the concentration of TP in water and sediment and the percentage of P potentially releasable [30]. Experiment was performed for 65 d at room temperature of 26.5 ± 0.2 °C, and with mechanic agitation (80 rpm) in the bottom of reactors. Reactors were covered of light with a lining.

Figure 2. Reactors for evaluation of treatments.

During the evaluation time, Eh and pH were monitored and samples of the water-sediment suspension were taken on days 0, 1, 2, 3, 4, 7, 10, 16, 22, 29 and 65; the samples were centrifuged for 10 minutes at 12,000 rpm, then the supernatant was separated and used for analyse the TP and Fe(II) with Merck colorimetric methods. The differences in control of phosphorus were compared statistically with two ways ANOVA test with α=0.05.

RESULTS AND DISCUSSION

Table 1 shows the results of OM and TP obtained in sediment after the treatments. It is observed that three methods presented degradation of OM showing that under reduced and oxidized condition OM may be degraded. But oxygenation presented greater reduction of OM in sediment, due to aerobic environments promote a greater proliferation of microorganisms responsible of this process [27]. On the other hand, the TP was retained mainly reactor with oxygenation treatment as it was expected by the oxidation of Fe and Mn [28]. Although, the second place to retention was experiment without treatment instead of Phoslock, what means that even the reduced conditions in the reactor without treatment, other oxidized compounds could be retained by adsorption soluble P in the solid phase, for example:

NO_3 and SO_4 [29]. Also it is important mentioned that concentration of TP in sediment in the reactor with no treatment, did not get decreased 35% as was expected and according to [30] who reports this release from P attached with oxides of Al/Fe and OM. This event could be because the employed sediment was collected in the stratification phase of reservoir and the potentially releasable P could have been liberated. In the case of Phoslock, less P was retained with Phoslock showing less capacity to absorb despite the great affinity of P.

The content of TFe of initial sediment was useful to know the capacity of retention P in the case of oxygenation treatment. According to [31] a relation by weight of TFe:TP≥15 shows a good capacity of sediment to retain P and prevent a release of this nutrient; in this work considering initial concentration of TP and TFe (Table 1) this relation was 13.46, lower of the relation of a good retention, but higher than the relation to unable to retain P, which is 10.

Table 1. Organic matter and total phosphorus and iron in sediment after treatments.

Treatment	% OM	TP (mg/g)	TFe (mg/g)
Initial sediment	16.8	1.56	21
No treatment	15.0	1.64	ND
Oxygenation	14.4	1.71	ND
Phoslock®	14.6	1.46	ND

ND= Not determined

Eh and pH behaviour observed during the evaluation P control, shows in Figure 3 and 4, respectively. It was clearly reduced and acid condition for no treatment and Phoslock®. The incubation with no treatment showed an Eh = -98.81 ± 43.31 and pH = 5.7 ± 0.4, whereas the reactor of Phoslock® remained with Eh = -117.30 ± 30.81 and pH = 5.7 ± 0.4. On the other hand, the oxygenation treatment was maintained also in acid conditions but with an Eh = 244.36 ± 247.86 and pH = 4.0 ± 0.6.

The results of TP are observed in Figure 5, the P concentration was variable the first 3 days. In the reactor without treatment, TP increase the first day, then drastically get down, this fall may be happened due to the initial oxygen in the system caused the retention of P in the sediment. However, after the third day, P increased as it was expected in a reduced system [6] until reach 0.22 mg/L in day 65. Considering the experimental conditions of this reactor, it was expected more liberation of P from sediment, nearly of 35% of TP which could be released to water under this reduced conditions as was reported by [30]. One possibility to no observe more dissolution is the absence of soluble P in reduced conditions, which can be explained due to the behaviour of Fe(II) (Figure 6) it can be noted the concentration of Fe(II) was almost constant the all-time of evaluation, indicating there was no more dissolution of oxides and hydroxides of Fe.

While in oxygenation evaluation, after variations presented in the first days, it is possible observe in the third day the highest concentration of P under oxidized conditions which could be released with P liberation from OM degradation as it was mentioned before. After this time, P was constant until the final of experiment, when it was 0.14 mg/L, higher than desired concentration. Considering the relation observed TFe:TP, could be possible iron in sediment was not enough to precipitate P, because as [31] reported in his work, only relations of 15or above and pH<8 were favourable to retain P. In this evaluation, behaviour of Fe(II) denoted its absent since the third day which reinforce that the oxidized environment of this incubation favoured the change from Fe (II) to Fe (III) which is precisely the form that precipitates P and promotes its retention in the sediment [12]; also Mn and Al could participate in this retention [28]. As the desired concentration was not obtained, we suggest the content of Fe and possibly mechanic agitation was responsible of this. Similar situation was reported by [32] whom observed that resuspension of sediment promote liberation of this nutrient in short time test because of reactions of equilibrium.

On the other hand, Phoslock® showed the lowest concentration on the fourth day of incubation, slower than oxygenation results and this confirm the fast results that it is possible obtain with this method [33]. Nonetheless, in the following days P increased and reached a final concentration of 0.16 mg/L, slightly higher than P concentration reached with oxygenation. It should be noted that with the same dose of Phoslock®, higher percentages of TP removal have been reported [11], [20]. The low reduction in TP removal observed in this work could be related with the relation 100:1 (Phoslock:P) could be underestimated for this sediment and water maintained with mechanical agitation. Second reason, could be the presence of humic substances because of OM degradation, according with [17] the humic substances induce interferences of lanthanum and bentonite [33]. And also an experimental consideration could affect the results, because in each sampling was extracted a part of adsorbent and consequently it causes to leaving less active clay in the system. Regarding the behaviour of Fe(II) (Figure 6) the initial concentration was remained for almost the entire incubation as initial concentration Fe(II)>130 mg/L. In fact, this behaviour looks similar to P performance, showing a positive relation as in no treatment evaluation. It is important observe that none of the treatments reached the desired concentration of 0.035 mg/L TP that indicates a mesotrophic state [21]. According with statistical analyses the differences of TP are different statically significant.

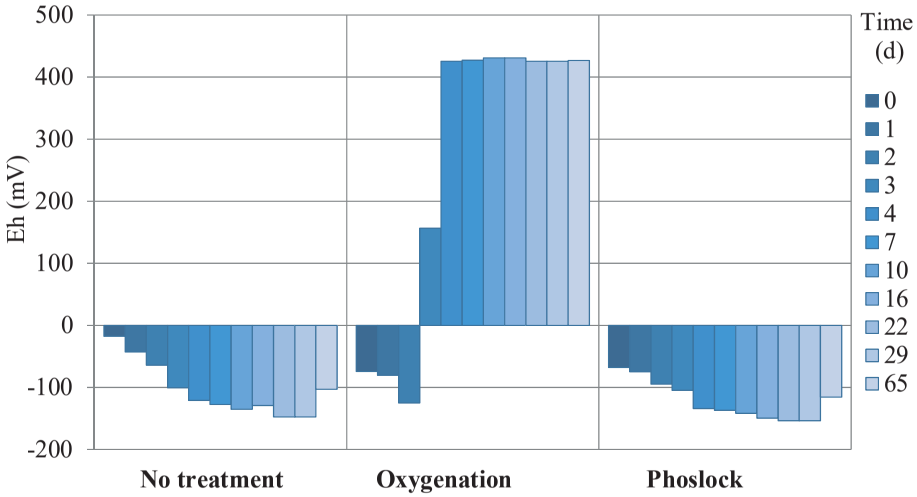

Figure 3. Behaviour of redox potential during evaluation of control of phosphorus.

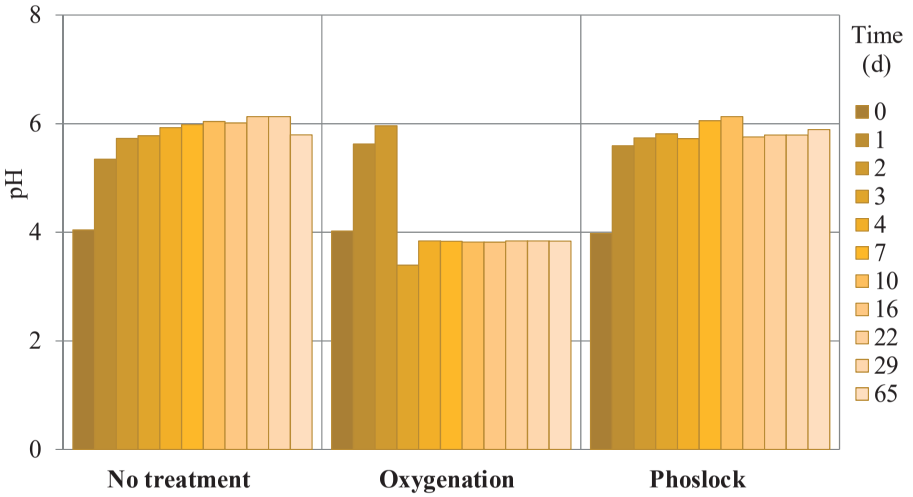

Figure 4. Behaviour of pH during evaluation of control of phosphorus.

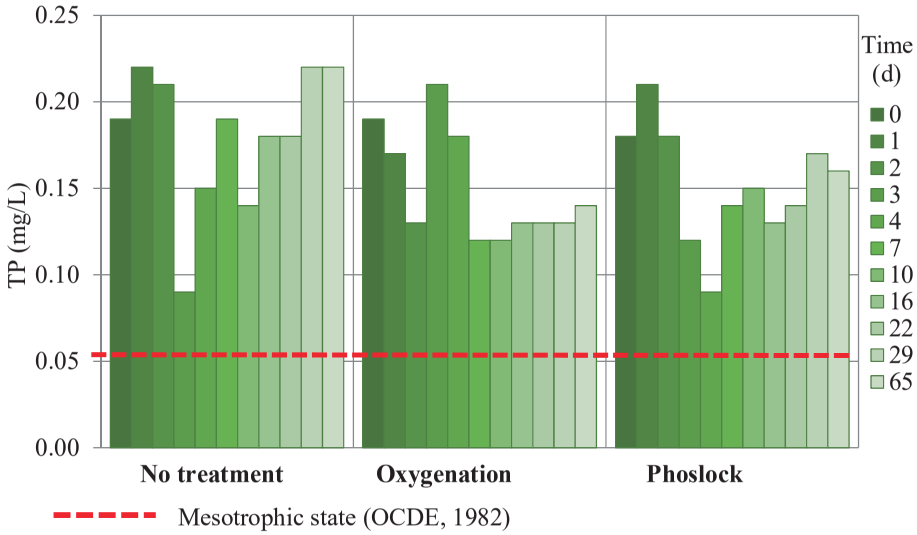

Figure 5. Behaviour of TP during evaluation of control of phosphorus.

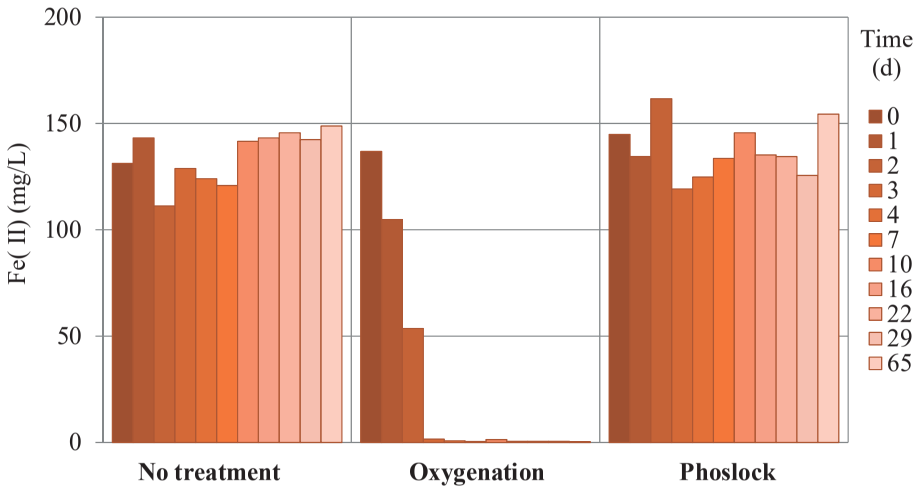

Figure 6. Behaviour of Fe(II) in incubations during evaluation of control of phosphorus

Under these experimental conditions, oxygenation is slightly more efficient than Phoslock® to control P concentration in water and sediment. But it is important mentioned that oxygenation is considered as a temporary method [34] for that it is proposed to combine both methods to evaluate the control of P; since oxygenation controls P and reduced compounds and Phoslock® has the advantage of retaining this nutrient permanently in the solid phase.

CONCLUSIONS AND RECOMMENDATIONS

It was observed that the oxygenation presented better control of P through its reduction in water and retention on sediment, due to formation of oxides and hydroxides of Fe, demonstrated by totally reduction of this reduced metal in water. Nevertheless, the relation TFe:TP was lower than 15 which has been observed as ideal to retain P in solid phase. Also mechanical agitation could induce resuspension and maintaining of P and consequently it did not allow higher P control and its reduction from water to sediment.

The application of Phoslock® caused the greatest decreasing of dissolved P, although this increased in the rest of evaluation and the final concentration was higher than oxygenation, possibly because under this experimental conditions the quantity of adsorb result underestimated, also humic substances from OM degradation could affect the process. Other reason could be that in each sampling event during evaluation, adsorbent was extracted from the system leaving less active clay.

In the experiment without treatment, variable P concentrations were observed that finally reached the same order of magnitude as the initial concentrations. Also, the concentration of Fe (II) remains practically constant as for the Phoslock® application. It did not present release of P as was expected, possibly because the absence of potentially releasable P.

Based on the results, it is recommended to evaluate the effect of the agitation in experiments of phosphorus control in water and sediment. And also evaluate both methods at the same reactor in order to know if the combination result better.

ACKNOWLEDGMENTS

This work was funded by the Scientific Research and Technological Development Fund of the Mexican Institute of Water Technology. We acknowledge to MEng. Carlos Corzo and MSc. Adriana Villa for the facilities to develop this work.

REFERENCIAS

[1] Smith V y Schindler D, “Eutrophication science: where do we go from here?” Trends Ecol Evol, Vol. 24, Apr. 2009, pp. 201-207.

[2] Lürling M, Mackay E, Reitzel K. y Spears B, “A critical perspective on geo-engineering for eutrophication management in lakes”, Water Res., Vol. 97, Jun. 2016, pp. 1-10.

[3] Guildford S, Hecky R, “Total nitrogen, total phosphorus, and nutrient limitation in lakes and oceans: Is there a common relationship?”. Limnol Oceanogr, Vol. 45, Sep. 2000, pp. 1213-1223.

[4] Holdren C, Jones W. y Taggart J, “Managing lakes and reservoirs”, Madlson, WI: North American Lake Magament Society and Terrene Institute, in cooperation with U. S. Environmental Protection Agency, 2001, ch 7.

[5] Wetzel R, “Limnology: lake and river ecosystems”, London, UK: Academic Press, 2001, ch 13.

[6] Hansen AM y Márquez-Pacheco H, “Internal phosphorus load in a mexican reservoir: forecast and validation”, Environ Toxicol Chem, Vol. 34, Nov. 2015, pp. 2583-2589.

[7] Penn M, Auer M, Doerr S, Driscoll C, Brooks C y Effler S, “Seasonality in phosphorus release rates from sediments of a hypereutropic lake under a matrix of pH and redox conditions”, Can J Fish Aquat Sci., Vol. 57, Apr. 2000, pp. 1033-1041.

[8] UNESCO (Organización de las Naciones Unidas para la Educación, la Ciencia y la Cultura). “El control de la eutroficación en lagos y pantanos.”, España, Pirámide, 1992.

[9] Beutel M y Horne A, “A review of the effects of hypolimnetic oxygenation on lake and reservoir water quality”, Lake Reservoir Manag, Vol. 15, Jan. 1999, pp. 285-297.

[10] Haghseresht F, Wang S y Do D, “A novel lanthanum modified bentonite, Phoslock®, for phosphate removal from wastewaters”, Appl Clay Sci, Vol. 46, Dec. 2009, pp. 369-375.

[11] Bishop W, McNabb T, Cormican I, Willis B y Hyde S, “Operational evaluation of Phoslock phosphorus locking technology in Laguna Niguel Lake, California”, Water Air Soil Pollut, Vol. 225, Jun. 2014, pp. 1-11.

[12] Gerling A, Browne R, Gantzer P, Moblye M, Little J y Carey A, “First report of the successful operation of a side stream supersaturation hypolimnetic oxygenation system in a eutrophic, shallow reservoir”, Water Res. Vol. 67, Dec. 2014, pp. 129-143.

[13] Gantzer P, Bryan L y Little J, “Effect of hypolimnetic oxygenation on oxygen depletion rates in two water-supply reservoirs”, Water Res., Apr. 2009, Vol. 43, pp. 1700-1710.

[14] Diaz R. “Overview of hypoxia around the world”, J Environ Qual., Vol. 30, May. 2001, pp. 275-281.

[15] Moore B, Croos B, Beutel M, Dent S, Preece E, Swanson M, “Newman Lake restoration: A case

study Part. III Hypolimnetic oxygenation", Lake Reserv Manage. Vol. 28, Sep. 2012, pp. 311-327.
[16] Beutel M, Dent S, Reed B, Marshall P, Gebremariam S, Moore B, Cross B, Gantzar P, y Shallenberger E, "Effects of hypolimnetic oxygen addition on mercury bioaccumulation in Twin Lakes, Washington, USA", Sci Total Environ , Vol. 496, Dec. 2014, pp. 688–700.
[17] Meis S, Spears B, Maberly C y Perkins R, "Assessing the mode of actions of Phoslock in the control of phosphorus release from the bed sediments in a shallow lake (Loch Flemington, UK)", Water Res., Vol. 47, Sep. 2013, pp. 4460-4473.
[18] Zamparas M, Gavriil G, Coutelieris F y Zacharias I, "A theorical and experimental study on the P-adsorption of Phoslock", Appl Surf Sci., Vol. 335, Apr. 2015, pp. 174-152.
[19] Ross G, Haghseresht F y Cloete T, "The effect of pH and anoxia on the performance of Phoslock®, a phosphorus binding clay", Harmful Algae, Vol. 7, Jun. 2008, pp. 545-550.
[20] Waajen G, van Oosterhout F, Douglas G y Lürling M, "Management of eutrophication in Lake De Kuil (The Netherlands) using a combined flocculant", Water Res., Vol. 97, Jun. 2016, pp. 1-13.
[21] OECD (Organization for Economic Co-Operation and Economic Development). "Eutrophication of Waters. Monitoring, Assessment and Control. Paris, 1982.
[22] CONAGUA-IMTA (Comisión Nacional de Agua-Instituto Mexicano de Tecnología del Agua), "Caracterización de sedimentos en la presa Valle de Bravo, Estado de México y evaluación de diferentes técnicas de control de nutrientes. 1ª Etapa. Convenio de colaboración OAVM-DT-MEX-09-453-RF-CC. Informe final", 2009.
[23] ASTM (American Society for Testing and Materials), "Standard Test Methods for Moisture, Ash, and Organic Matter of Peat and Other Organic Soils", 2000.
[24] Zagal E y Sadzawka R, "Protocolo de métodos de análisis para suelos y lodos", Chile, Universidad de Concepción, Facultad de Agronomía Chillán, Chile, 2007, pp. 28-30.
[25] Kou S, "Phosphorus" In: Sparks, D. L. (ed). Methods of soil analysis: part 3-chemical methods. American Society of Agronomy, Soil Science Society of America, 1996.
[26] EPA (Environmental Protection Agency), "Test Methods For Evaluating Solid Waste, Physical/Chemical Methods" USA, Third Edition, 1986.
[27] Cooke D, Welch E, Peterson S, y Nicholson S, "Restoration and management of lakes and reservoirs", 3rd Edition. Florida, USA, CRC Press Taylor and Francis Group, 2005, pp. 161.
[28] Canfield D, Kristensen E y Thamdrup B, "The phosphorus cycle" In: Advances in Marine Biology. Elsevier Inc. Vol. 48, 2005, pp. 419-440.
[29] Beutel M, Horne A, Taylor W, Losee R y Whitney R, "Effects of oxygen and nitrate on nutrient release from profundal sediments of a large, oligo-mesotrophic reservoir, Lake Mathews, California", Lake Reserv Manage, Vol. 24, Jan. 2008, pp. 18-29.
[30] Márquez-Pacheco H, Hansen A y Falcón-Rojas A, "Phosphorus control in a eutrophied reservoir", Environ Sci Pollut Res, Vol. 20, Dec. 2013, pp. 8446-8456.
[31] Jensen H, Kristensen P, Jeppesen E, y Skytthe A, "Iron:phosphorus ratio in surface sediment as an indicator of phosphate release from aerobic sediment in shallow lakes", Hydrobiologia, Vol. 235, Jul. 1992, pp. 731-743.
[32] Sondergaard M, Kristensen P y Jeppesen E, "Phosphorus release from resuspended sediment in the shallow and wind-exposed Laka Arreso, Denmark" Hydrobiologia, Vol. 228, Jan. 1992, pp. 91-99.
[33] Lürling M, Van Oosterhout F y Waajen G, "Humic substances interfere with phosphate removal by lanthanum modified clay in controlling eutrophication", Water Res., Vol. 54, May. 2014, pp. 78-88.
[34] Liboriussen L, Sondergaard M, Jeppesen E, Thorsgaard I, Grünfeld S, Jakobsen T, Hansen K, "Effect of hypolimnetic oxygenation on water quality: results from five Danish lakes", Hydrobiologia, Vol. 625, Jun. 2009, pp. 157-172.

2. Remediation of contaminated sites: natural attenuation, processing, and reuse

Session chairs: Teresa Alarcón-Herrera[1] and Víctor Luna-Pabello[2]
[1]Centro de Investigación en Materiales Avanzados, México
[2]Laboratorio de Microbiología Experimental, Facultad de Química, México

Advanced practices based on new technologies, improved processes, and evolving science allows to clean up contaminated sites in a more efficient and sustainable manner while achieving one of our challenges of protecting human health and the environment. The goal of remediation is to restore the site to its pollution-free state. Natural attenuation, is rapidly becoming a widely used approach to manage soil contamination by hazardous substances in product releases by different accidents or leaks and leachate from many different sites including among others, mining waste sites, industrial and hazardous waste sites and landfills. In this session, the idea is to bring together parties from all aspects of the remediation of contaminated sites community, to exchange ideas and experiences on the management of soil, groundwater, and sediment. Including the current methodologies needed by groundwater scientists and engineers in their efforts to evaluate subsurface contamination problems, to estimate risk to human health and ecosystems through mathematical models, and remediation strategies approached. Works in these thematic are welcome.

APPROACHES FOR EUTROPHICATION CONTROL IN A MEXICAN RESERVOIR

Hansen Anne M.
Coordination of Hydrology, Mexican Institute of Water Technology, Mexico

ABSTRACT

Changes in land uses in hydrological river basins due to population growth and productive activities cause deterioration of water bodies, making lakes and reservoirs increasingly vulnerable to accelerated eutrophication processes [1]. Such processes are caused by internal nutrient loads from water and sediments and by external loads from wastewater discharges and runoff from the watershed [2]. These loads may stimulate growth of plants in water bodies, producing organic matter in water and sediment, where bacteria require oxygen for its degradation. This oxygen demand eventually causes anoxic conditions that promote internal nutrient loads [3]. Temperature differences as well as wind-driven mixing of water in lakes and reservoirs, distribute these nutrients, stimulating further plant growth, and reinforcing anoxic conditions and additional release of nutrients. It is therefore urgent to develop and apply methods for eutrophication control in lakes and reservoirs. In this paper, two different eutrophication control technologies were evaluated and compared: Application of the adsorbent Phoslock, and Hypolimnetic oxygenation. Although these technologies have been applied in lakes and reservoirs around the World [4], design parameters must be obtained for each case due to varying climatic, biogeographic, and anthropogenic characteristics of the lakes and reservoirs and their watersheds. Mass-balance models are required to describe remediation requirements for water bodies. In this study, mass balances were performed for target contaminants, remediation design parameters obtained, control scenarios evaluated, and a technical and economic analyses of the different solution options were carried out.

Keywords: Eutrophication control, Phoslock, Hypolimnetic oxygenation, Mass balance, Technical and economic analyses

INTRODUCTION

Phosphorus (P) and oxygen demand (OD) are among the main nutrients that control eutrophication (accumulation of nutrients) of water in lakes and reservoirs. Sediments act as sinks as well as sources of P and OD in lakes and reservoirs. The accumulation of P in sediments and the release to the water column, known as internal P load (IPL), is the result of different physical, chemical and biological processes.

Phosphorus in sediments is associated with organic matter and minerals and its release to the water column is result of the desorption and dissolution of P from the sediments and the diffusion to the water column. Under oxidized conditions, iron (Fe) and manganese (Mn) occur in oxidized forms with high affinity for P, while part of these Fe and Mn oxides are dissolved under reduced conditions, implying that adsorbed P may be released.

Several studies report the accumulation and release of P under oxidized and reduced conditions in laboratory experiments and in water bodies and point out that there is increased release of P under reduced conditions, mainly related to the reduction of Fe and Mn (Fig. 1).

With the aim of defining eutrophication control strategies in a Mexican reservoir used as a drinking water supply, in this work two different eutrophication control strategies were assessed:

(1) Application of the adsorbent Phoslock
(2) Hypolimnetic oxygenation.

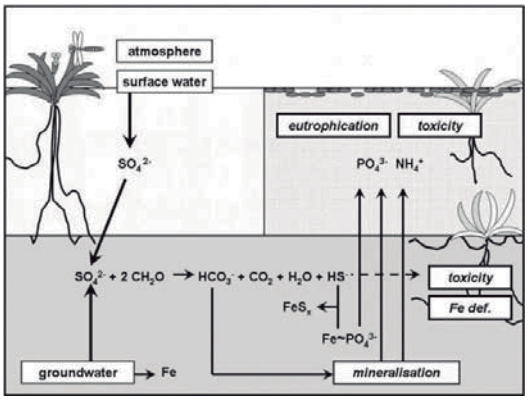

Fig. 1 Sulfate and iron-reducing bacteria in sediment convert Fe(III) to Fe(II) and S(VI) to S(-II), releasing Fe-associated PO_4^{3-}. As a result, water becomes eutrophied. Simultaneously, sulphide and ammonium toxicity and iron deficiency may occur [5].

The study area is the eutrophied reservoir of the Valle de Bravo dam that is part of the Cutzamala

system, which supplies 15 m^3/s of water to Mexico City.

METHODS

For both strategies, mass-balance models were applied that take into account both external and internal contaminant loads, pollutant concentrations in water, concentrations in sediment susceptible to be released (in case of P) or degraded (in case of oxygen demand), export of contaminants through water extraction, fisheries or removal of water hyacinth.

Assessment of application of adsorbent

To determine the amount of adsorbent and the duration of the P control in the Valle de Bravo reservoir, Hansen and Márquez-Pacheco [6] developed and applied a model that considers the external and the internal P loads, P concentrations in water and sediment, extracted P, and P susceptible to be released from the sediment (Fig. 2).

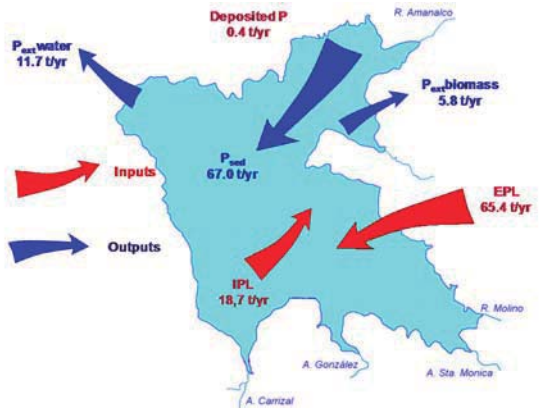

Fig. 2 Mass balance for P in the Valle de Bravo reservoir [6]

This model considers that, once applied, the adsorbent is distributed uniformly by physical and biological processes in "x" cm of sediment and the adsorbent reacts with potentially available P (P_{pa}) to be released over time from this sediment layer. Each year, the sediment thickness increases by a new annual layer caused by the sedimentation of "y" cm. Since a layer of the same thickness is being buried, the thickness of "x" is considered to remain constant.

The amount of adsorbent necessary to control $\underline{P_{pa}}$ in the sediment is 100%. When excess adsorbent (Ads_{exc}) is added, the P_{pa} control occurs for future sediment layers as well and the Ads_{exc} distribution in each annual layer (Ads_{lay}) can be calculated as follows:

$$Ads_{lay} = [Ads_{exc} - \frac{100\ y}{x}]\frac{1}{(x+y)/y} \quad (1)$$

Where:

Ads_{lay} = amount of adsorbent in the sediment layer (%)

Ads_{exc} = excess adsorbent in the sediment layer, allowing P to be controlled in future layers (%)

x = thickness of sediment mixed by physical and / or biological processes (m)

y = layer of new sediment that accumulates every year (m)

$\frac{100\ y}{x}$ = amount of adsorbent to control P en y (%)

$(x+y)/y$ = number of annual layers in x+y

As long as Ads_{lay} is positive, the ability to immobilize P_{pa} in the sediment persists so that the time duration of P control in the sediment is equal to the period that meets the following condition:

$$t = t\ (Ads_{lay} \geq 0) \quad (2)$$

The amount of adsorbent required for control of P in the first annual application ($Ads_{1.yr}$), is calculated with Eq. 3. For this, the concentration of P_{pa} and the average density of sediment, "ρ", in the layer "x" were taken into account, as well as the area, "A", where IPL occurs, as well as the dosis (amount of adsorbent per unit P to be removed), ($dAds$).

$$Ads_{1.yr} = x \cdot \rho \cdot A \cdot [P_{pa}] \cdot dAds \cdot 10^{-4} \quad (3)$$

Where $x \cdot \rho \cdot A \cdot [P_{pa}]$ is the mass of P_{pa} in the layer "x" of the area where IPL occurs, and 10^{-4} is the conversion factor for "cm g ha mg/cm^3 kg" to metric tons (t). Eq. 4 determines the amount of adsorbent to be applied annually (Ads_{ann}) after the first application of adsorbent:

$$Ads_{ann} = Ads_{1.yr} \cdot y/(x+y) \quad (4)$$

The amount of adsorbent required to control P_{pa} in the first multiannul application ($Ads_{1.man}$), is calculated by Eq. 5, while Eq. 6 calculates the amount of adsorbent necessary in the following multiannual application (Ads_{mul}).

$$Ads_{1.man} = Ads_{1.yr}\ (1 + Ads_{exc}) \quad (5)$$

$$Ads_{mul} = Ads_{1.yr} \cdot Ads_{exc} \quad (6)$$

The amount of adsorbent necessary to maintain P concentrations that classify water as mesotrophic (*MW*), (Ads_{wat}), is calculated with Eq. 7.

$$Ads_{wat} = ([P] - MW)\, V \cdot dAds \tag{7}$$

Where V is the water volume in the reservoir, and ([*P*]-*MW*)*V* is the amount of P to be removed. To determine the variation of P in water (ΔP), the mass balance of P was applied (Eq. 8), where *EPL* and *IPL* are the external and internal P loads, P_{ext} is P extracted by the effluent and by extracted biomass, P_{sed} is sedimented P and *([P]-MW)V*, the amount of P to be controlled:

$$\Delta P = EPL + IPL - P_{ext} - P_{sed} - ([P] - MW)\, V \tag{8}$$

To calculate the P concentration in water the year after application of the adsorbent ($[P]_{n+1}$), ΔP is divided by V and added to the initial concentration of P (Eq. 9).

$$[P]_{n+1} = [P]_n + \frac{\Delta P}{V} \tag{9}$$

Before $[P]_{n+1}$ exceeds *MW*, a new application of adsorbent is required. The control of P in water occurs as long as concentrations of P are lower than MW (Eq. 10):

$$t = t\,([P] < MW) \tag{10}$$

The model was applied to determine the duration of P control, using parameters as determined for the Valle de Bravo reservoir (Table 1).

Assessment of hypolimnetic oxygenation

To predict the accumulation of dissolved oxygen (DO) in water of lakes and reservoirs, where installation and operation of hypolimnetic oxygenation systems (HOS) is being planned, Hansen et al. [7] developed a mass balance model, which considers the inputs and outputs of OD as well as natural contributions of DO, and DO supplied by the HOS (Eq. 11, Fig. 3).

$$OD_{fin} = OD_{wat} + OD_{sed} + OD_{EL} - OD_{ext} - DO_{nat} - DO_{HOS} \tag{11}$$

Where:

OD_{fin} = OD in bottom water after a definite period (e.g. one year)
OD_{wat} = OD in the bottom water at the beginning of the period
OD_{ext} = OD been extracted during the period
OD_{sed} = OD of sediment during the period
OD_{EL} = External load of OD during the period
DO_{nat} = DO provided during the period by external sources, photosynthesis and interaction with the atmosphere
DO_{HOS} = DO provided by the HOS during the period

Table 1 Parameters used for the P mass-balance

Parameter	Symbol	Unit
Mixed sediment layer	*x*	cm
Yearly accumulated sediment layer	*y*	cm
Potentially available P	P_{pa}	mg/kg
Sediment density in the "*x*" layer	ρ	g/cm^3
Area where IPL occurs	*A*	ha
Dosis of adsorbent per unit P	*dAds*	kg/kg
Initial concentra-tion of P in water	[*P*]	mg/L
Range of P for mesotrophic water (MW)	*0.015<MW<0.025*	mg/L
Water volume	*V*	Mm^3
External P load	*EPL*	t/yr
Extracted P	P_{ext}	t/yr
Sedimented P	P_{sed}	t/yr
Internal P load	*IPL*	t/yr

The OD of water and sediment were determined through respirometry of water and sediment samples from the reservoir in experimental reactors as described by Hansen et al. [8].

To determine OD_{wat} before initiating the operation of HOS, the average Chemical Oxygen Demand (COD) observed for the Valle de Bravo reservoir, was multiplied with the volume of the hypolimnion (water below the thermocline). For subsequent periods, OD_{wat} was the OD_{fin}, for each previous period.

To determine OD_{sed}, the results obtained for experimental reactors [8] were multiplied by the area of the reservoir.

The OD_{EL} was estimated through an inventory of emissions, considering diffuse and point sources in the watershed. These include discharges from both untreated municipal wastewater and effluents from wastewater treatment plants. Diffuse sources include

discharges from fish farming and runoff from soils with different land uses.

For the first simulation period, OD_{ext} was determined as the product of COD and the volume of water extracted in the period. For subsequent periods, the reduction in COD was obtained by weighting the previous COD with the average OD_{wat} in the previous and subsequent periods.

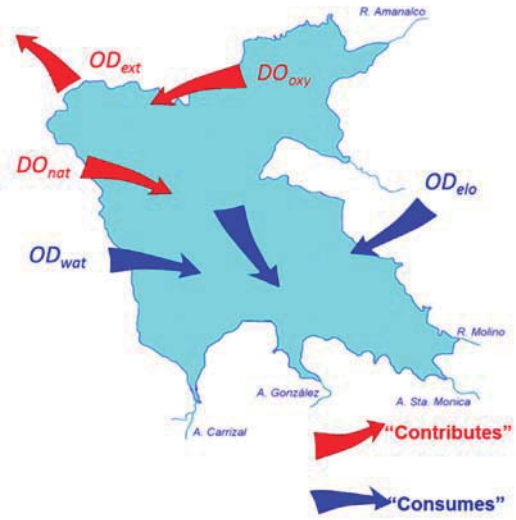

Fig. 3 Conceptual model for the OD mass balance in the Valle de Bravo reservoir [8]

DO_{nat} is DO contributed by photosynthesis and interaction with atmosphere. The reservoir is in steady state with respect to COD, therefore OD_{fin} - $OD_{wat} \cong 0$, and DO_{nat} was obtained by reorganizing Eq. 11.

Finally, according to the HOS manufacturers [9], an HOS operating under the temperature and pressure conditions at the deepest part of the Valle de Bravo reservoir, would supply ≈ 6 t/d of DO, i.e. 2.190 t/yr [ECO_2 Technology, personal communication, 2016).

Comparison of Phoslock and HOS assessments for the Valle de Bravo reservoir

The two technologies were assessed and classified for possible application in the Valle de Bravo dam, considering the following criteria:

- Performance/Effectiveness Degree to which the technology is expected to cause improved conditions in the reservoir. Based on results published in [8] and [10]-
- Initial cost Expenses for preliminary studies as well as acquisition, transport, import, installation, and application costs
- Reliability Capacity of the technology to keep operating continuously and efficiently. Includes operation and maintenance costs
- Logistics Location of equipment/operation.

RESULTS AND DISCUSSION

The results for the assessment of eutrophication control by application of the adsorbent Phoslock are presented in Table 2 and those for the assessment of eutrophication control by hypolimnetic oxygenation, in Table 3. It is observed that especially for the application of Phoslock, the reduction of external loads is crucial to reduce amounts of adsorbent and consequent costs.

Table 2 Estimated amounts and frequencies of Phoslock applications for P control in the Valle de Bravo reservoir [10]

Scenario	Application: Water (t)	Sediment (t)	Total (t)
100% EPL			
Annual application in sediment			
Year 1	1,998	9,288	11,286
Future 1-yr applications	431/yr	1,592/yr	2,023
Five-yearly application in sediment			
Year 1	1,998	19,968	21,966
Future 5-yr applications	431/yr	10,681/5 yr	11,112
64% EPL			
Annual application in sediment			
Year 1	1,480	5,944	7,424
Future 1-yr applications	0	1,019/yr	1,019
Five-yearly application in sediment			
Year 1	1,480	12,780	14,260
Future 5-yr applications	0	6,836/5 yr	6,836

The application of Phoslock would allow to immobilize P in the reservoir, however, it is not expected to reverse the anoxic condition in the bottom of the dam in a shorter time period. In addition, it would be necessary to carry out subsequent applications on a regular basis to control P that enters the reservoir through both EPL and IPL.

In the case of HOS it is observed that if only one HOS is installed, the 36% reduction of OD_{EL} implies half of the time to obtain excess OD_{fin} as compared to no reduction of OD_{EL} (Table 3). For two or three HOS, this difference is only one year.

Table 3 Time to obtain year-round excess dissolved oxygen in bottom water of the Valle de Bravo reservoir for different scenarios [8]

Number of HOS	OD_{EL} (%)	Time to obtain excess OD_{fin} (yr)
1	100	20
1	64	10
2	**100**	**6**
2	**64**	**5**
3	100	4
3	64	3

To obtain excess DO in the bottom water of the reservoir after five to six years of operation, two HOS should be installed and operated full-time followed by part-time operation in following years. Since results do not improve significantly with three HOS instead of two, this option is not recommended.

The assessment and classification of the two eutrophication control technologies are presented in Table 4 and evaluated according to the following criteria:

Evaluation	Score	Significance
Good/high	*3*	*Year-round DO_{exc} and low P; low initial or maintenance costs*
Reasonable/ Regular	*2*	*Slow establishment of DO_{exc}; high initial or maintenance costs*
Poor/Low	*1*	*Anoxic conditions in the reservoir; very high initial or maintenance costs*

The results suggest that the HOS may offer the overall best solution for remediation of the Valle de Bravo reservoir as long as external contaminant loads are not being sufficiently controlled.

Considering the actual OD_{EL}, this technology is expected to provide excess oxygen to the bottom water after six years of operation of two HOS. Besides, the cost for installation and operation of HOS is substantially lower than for applications of the adsorbent Phoslock.

Table 4 Technical and economic analyses of the application of two eutrophication control technologies in the Valle de Bravo reservoir

Assessment criteria	Remediation technology	
	Phoslock	***HOS***
Performance /Effectiveness	*Reduction of P expected to occur in two weeks [10]); OD_{sed} would persist*	*Decrease in P and increase in DO expected to occur in 5-6 yr [8]*
Score	2	2
Initial cost (USD)	*Relatively high (18 M)*	*Relatively low (9.5M)*
Score	1	3
Reliability	*High-cost reapplications when EPL not controlled (3.5 M USD/yr)*	*Relatively low maintenance cost (0.5 M USD/yr)*
Score	1	3
Logistics	*Applied all over most of the reservoir; settles out in few days*	*On-shore O_2 generators piping to submerged contact cones/diffusers in deepest sites of the reservoir*
Score	3	2
Total score	**7**	**10**

CONCLUSIONS

Mass-balance modeling approaches were applied to evaluate performances of two different remediation strategies for the Valle de Bravo reservoir, Mexico. Model input parameters were determined by experimental evaluation, analysis of information on water quality, precipitation and land uses in the watershed.

Different scenarios for external loads were evaluated, and a technical and economic analysis of the different solution options was performed. These results suggest that HOS may offer the overall best solution for remediation of the Valle de Bravo reservoir as long as external contaminant loads are not sufficiently controlled.

ACKNOWLEDGEMENTS

The author thanks the Organismo de Cuencas Aguas del Valle de México (OCAVM), Mexican National Water Commission (CONAGUA) for financial support (Projects no. 224 OAVM-DT-MEX-09-453-RF-CC, OAVM-DT-MEX-10-441-RF-CC, and OAVM-DT-225 MEX-11-479-RF-CC); Carlos Corzo and Axel Falcón from IMTA for their technical assistance.

REFERENCES

[1] Cooke GD, Welch EB, Peterson S & Nichols SA. Restoration and management of lakes and reservoirs. CRC press. 2016

[2] Zamparas M & Zacharias I. Restoration of eutrophic freshwater by managing internal nutrient loads. A review. Science of the Total Environment, Vol. 496, 2014, 551-562.

[3] Giles CD, Isles PD, Manley T, Xu Y, Druschel GK & Schroth, AW. The mobility of phosphorus, iron, and manganese through the sediment–water continuum of a shallow eutrophic freshwater lake under stratified and mixed water-column conditions. Biogeochemistry, Vol. 127 (1), 2016, 15-34.

[4] Beutel MW & Horne AJ. A review of the effects of hypolimnetic oxygenation on lake and reservoir water quality. Lake and Reservoir Management, Vol. 15 (4), 1999, 285-297.

[5] Smolders AJ P, Lamers LPM, Lucassen ECHET, Van der Velde G & Roelofs JGM. Internal eutrophication: how it works and what to do about it—a review. Chemistry and Ecology, Vol. 22 (2), 2004, 93-111.

[6] Hansen AM & Márquez-Pacheco H. MOCONPAI Model that determines the duration of phosphorus control in water bodies through immobilization with and insoluble adsorbent (In Spanish). Mathematical model registered by the Mexican Institute of Water Technology. Public Record of Copyright no. 03-2012-092610424400-01, Mexico City, 2012.

[7] Afsar A & Groves S. Comparison of P-inactivation efficacy and ecotoxicity of alum and Phoslock. PWS Report Number IR 015/09, 2009. Phoslock Water Solutions Limited. Available at http://www.phoslock.eu/media/7401/Comparison_of_P-inactivation_efficacy_and_ecotoxicity_of_Alum_and_Phoslock,July_2009.pdf (Accessed March 2018).

[8] Hansen AM, Hernández-Martínez C & Falcón-Rojas A (2016) Evaluation of eutrophication control through hypolimnetic oxygenation, Procedia Earth and Planetary Science, 17, 598-601.

[9] ECO_2 Technology. Hypolimnetic oxygenation system for water quality improvements. Available on http://www.eco2tech.com/ (Accessed March 2018).

[10] Márquez-Pacheco H, Hansen AM & Falcón-Rojas A (2013) Phosphorous control in a eutrophied reservoir. Environ Sci Pollut Res, DOI 10.1007/s11356-013-1701-2, December 2013, 20 (12), pp 8446-8456

EFFECTS OF GGBS ON THE SOLIDIFICATION/STABILIZATION OF PORT SEDIMENTS CONTAMINATED WITH HEAVY METALS

Gutsalenko T. [1], Bourdot A. [1], Chaouche M. [1] and Seymour P. [2] Frouin L. [2]
[1]LMT, CNRS/ENS-Cachan/Paris-Saclay University, France; [2] Ecocem Ltd. F1, Ireland

ABSTRACT

The stability of heavy metal (HM) compounds contained in the Dublin port sediments solidified in different hydraulic binders was considered through leaching tests. Four different binders were considered: Portland cement (OPC), Portland cement-Granulated ground blast furnace slag (GGBS) (at two different GGBS contents), and a supersulfated mix. The leaching test results under initially neutral pH conditions indicated that the HM compounds were rather stable in the sediment. Surprisingly, addition of the binder led in general to the destabilization of the HM compounds. The OPC binder was found to be the most destabilizing binder. Increasing the amount of GGBS in the binder led to the decrease of the destabilization effect. This was correlated with the XAS (Synchrotron X-ray Absorption Spectroscopy) results, which showed that the chemical environment of Cu and Zn was not modified in the case of binders with high GGBS content. The time evolution of the compressive strength of the binder-sediment samples was also considered. Is was found that the strength of the GGBS-based samples increased with time, while those with plain OPC decreases significantly beyond 28 days.

Keywords: GGBS, Heavy metals, Port sediments, Leaching tests, XAS, Speciation

INTRODUCTION

Marine basins are polluted due to mining, chemical, mechanical industry, agriculture industry emissions, port activities (paintings used for boats).

Dredged sediments present a serious harmful ecological impact by discharge into the marine environment. Some sediments are so heavily polluted that they are considered as a hazardous waste and are regulated in Europe by the Decree of August 9, 2006 which defines threshold values N1 and N2 for heavy metals, PCB, HAP, TBT.

In this study the Solidification/Stabilization method using an hydraulic binder for sediments valorization is considered because of technical, environmental and economic benefits.

Granulated ground blast furnace slag (GGBS) based binders have been shown to be highly effective in immobilizing various heavy metals [1]. GGBS is expected to impact immobilization through several mechanisms: the porosity of the binder is finer (due in particular to its pozzolanic activity), presence of hydrotalcite like phases that are characterized by high immobilization capacity, etc. In the present study the impact of GGBS on the stabilization of port sediments is considered. Using XAS, the origin of the positive effects of GGBS is investigated by considering the evolution of the speciation of some of heavy metals when the sediment is embedded in the binder.

MATERIALS

Sediment

Sediment sampling took place at Alexandra basin (Dublin Port) at around 1.5 m depth. According to the laser granulometric analysis, the sediment comprises mainly very fine fractions with the average diameter of about 40 μm (Fig. 1).

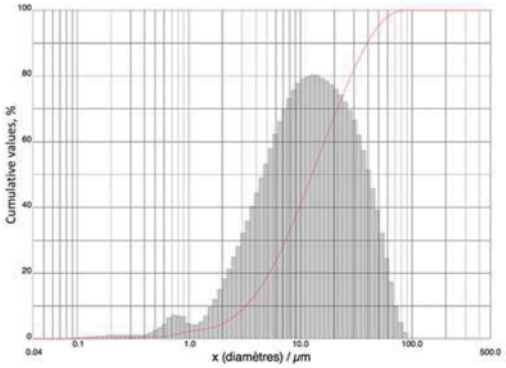

Fig. 1 Granulometric analysis of Dublin sediment

The cation exchange capacity for the exchangeable ions Al^{3+}, Ca^{2+}, Fe^{2+}, K^{+}, Mg^{2+}, Mn^{2+}, Na^{+} is determined using a solution of hexaamminecobalt (III) chloride, which is used as extraction reagent. The obtained value is 21.3 cmol/kg. This characteristic is important for the

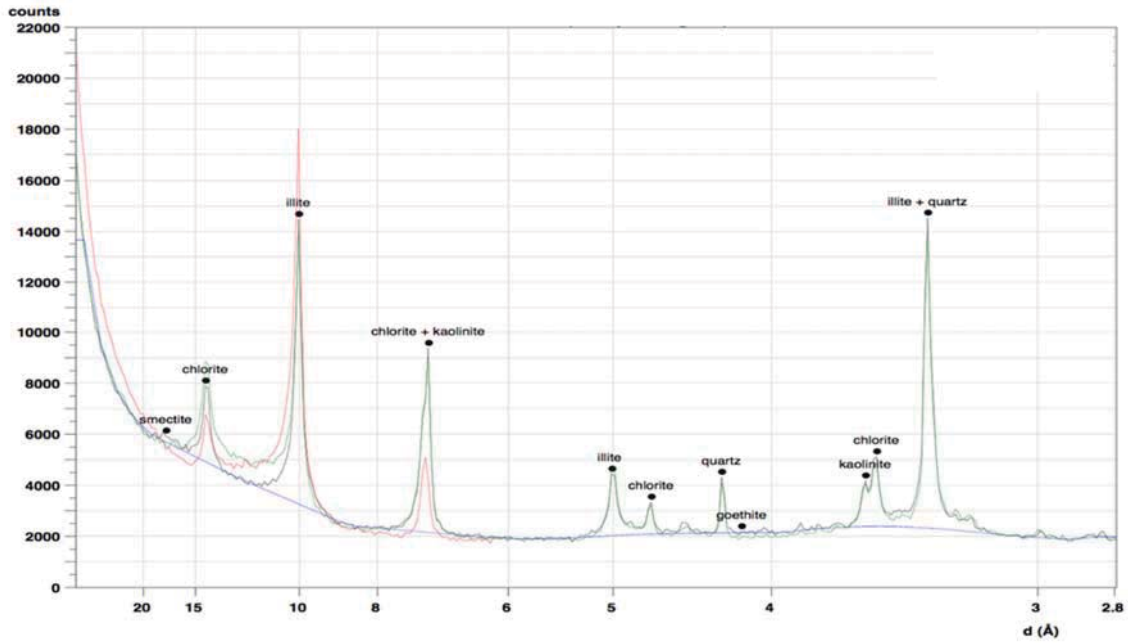

Fig. 2 XRD of the clay fraction of the Dublin sediment

sediment treatment with hydraulic binders, when the sediment-binder interaction is accompanied by ions consumption by clays and an organic matter that can delay hydration process.

The sediment consisted of both organic and inorganic components. The average value of the organic carbon in the Dublin sediment was 35,3 g/kg. The main inorganic crystalline components observed by X-ray diffraction (Co Kα, λ = 1.79°) were mainly Quartz, Calcite, Muscovite, and several clays as Illite. The XRD analysis for only clay fraction was also carried out (Fig. 2). The samples are composed mainly of Illite (59 and 58% respectively) associated with chlorite (25 and 23%) and kaolinite (14 and 13%). Smectite is present in trace amounts <2%. Microanalysis by ICP-MS indicated the presence of several heavy metals as Zn, Cu, Ni, Cr, Pb and As.

Binders

The hydraulic binders considered consisted of mixtures of Portland cement and slag (GGBS) from ECOCEM Ireland. The binder corresponding to F4 (Table 1) is composed of GGBS and anhydrous calcium sulfate Ca_2SO_4 (99% of purity from Alfa Aesar) with a very low amount of cement. F4 is a supersulfated type mix.

METHODS

The sediments were first sieved to remove the aggregates larger than 4 mm. Before being mixed with the binder, the sediment sample was let to settle over 24h and the bleeding water was removed. This led to water content of 45%±1.5% by weight and density of 1400±70 kg/m^3. The sediment-binder mixes considered are reported Table 1.

Table 1 Sediment-binder mixes considered

	Binder content in kg per m^3 of sediment		
Formulation	Cement	GGBS	$CaSO_4$
F0	-	-	-
F1	150	-	-
F2	75	75	-
F3	22.5	127.5	-
F4	1.5	127.5	21

The compressive strength of the sediment–binder samples (prismatic molds 40x40x160 mm) was determined at both 28 and 90 days. Shrinkage measurements (at 24°C±1°C, 91%±1.5% RH) and 3-D X-R microtomography imaging (voxel size 7.5x7.5x7.5 microns) were also performed to compare F1 (low GGBS content) and F3 (high GGBS content) samples.

The leaching tests were performed according to [2]. This consisted in dispersing 90±5g of solid particles of sediment-binder in 900 ml of demineralized water (pH=5-7.5 and conductivity <0.5 mS/m) for 24 hours at 10 rpm (horizontal rotation) in a room at controlled temperature 24°C±1°C. For each formulation three samples were prepared and analyzed using ICP-MS technique.

K-edge XAS measurements were performed at the Synchrotron SOLEIL (FRANCE) at the

beamline SAMBA. In the present study speciation of Zn and Cu were investigated. Three months aged sediment-binder samples were considered.

RESULTS

The compressive strength of the samples is reported in Table 2. F4 samples strength was too low to be measured. At 28 days the strength is not modified when replacing 50% of OPC with GGBS. Increasing the replacement level of OPC with GGBS leads to a significant decrease of the strength at 28 days. On the other hand, at longer term (90 days) the strength of the samples with GGBS exceeds that of cement-based mixes. In addition, the strength of the GGBS-based materials increases between 28 and 90 days while that of the OPC-based samples decreases.

It is well known that long term performances of GGBS-based materials are superior to those of OPC-based materials, in particular in such harsh medium [3, 4].

Table 2 Compressive strength of the mixes after 28 and 90 days

Formulation	$R_{c,28days}$ (MPa)	$R_{c,90days}$ (MPa)
F1	1.90±0.14	0.77±0.08
F2	1.90±0.14	2.53±0.22
F3	1.10±0.07	2.00±0.13
F4	-	-

The degradation of the strength of the OPC-based samples is correlated with shrinkage results. Between 60 and 90 days the shrinkage deformation of F1 is higher and goes with a greater loss of mass (Fig. 3).

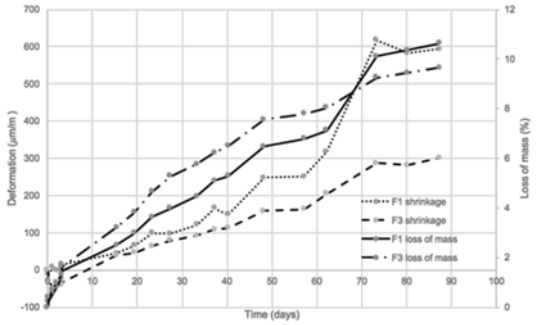

Fig. 3 Shrinkage and loss of mass with time (F1 versus F3)

This phenomenon can be explained by changes in the microstructure of F1 over time. To follow the hydration phases evolution, the XRD analysis (Fig. 4) was carried out only for F1 formulation due to the presence of mostly amorphous phases in GGBS-mixes.

The greatest amount of Portlandite is formed between 7 and 30 days, but then the peaks decreased significantly. The Ettringite phase completely disappeared after 60 days of storage. C_4AHx phase reached its maximum at 45 days and then decreased. The decrease of the amount of these hydration products may be attributed to internal carbonation resulting from eventual decomposition of organic matter at high pH. This led then porosity increase and degradation of the strength. Yet, this have to be investigated in more details.

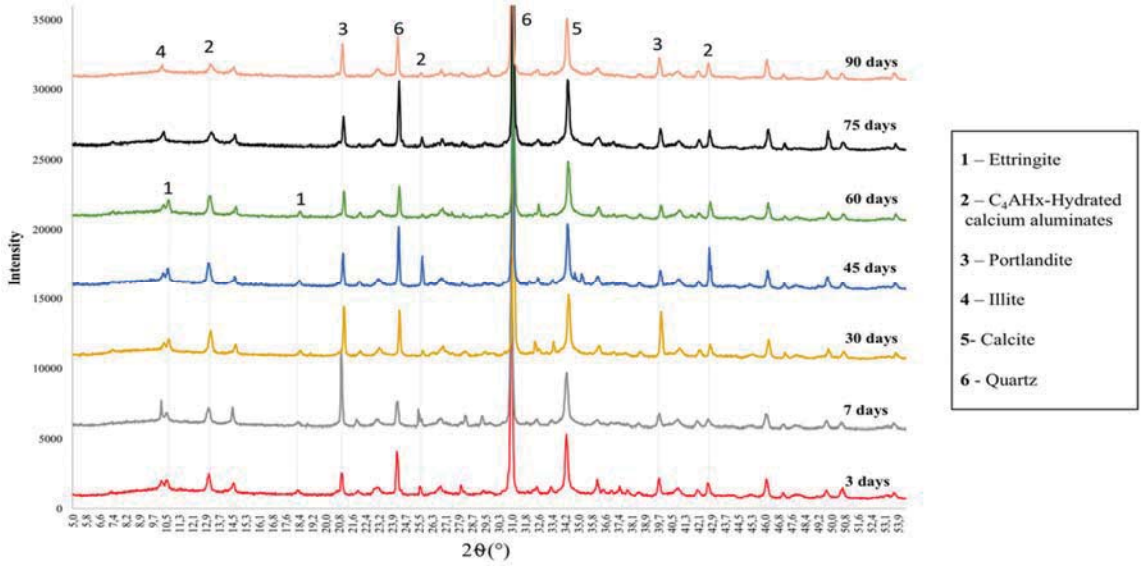

Fig. 4 XRD of F1 formulation over time

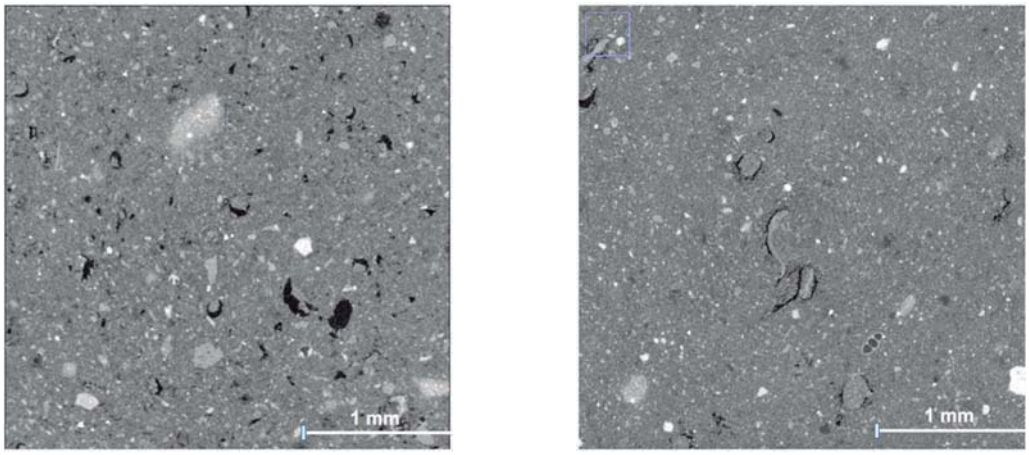

Fig. 5 X-ray tomography images of F1 (left) (OPC-sediment) and F3 (right) (OPC/GGBS-sediment) samples

The microtomographic images (Fig. 5) show the presence of a significant amount of pores for F1 sample in comparison to the F3 (GGBS-based binder), which microstructure is denser. These results are correlated with strength evolution.

Leaching test

The leaching test results for the HMs are reported in Fig. 6. Surprisingly the leachability of the HMs from the sediment (F0) is rather low. This suggests that they should be present in rather stable compounds (see XAS results). The effect of the binder depends on the HM considered. For instance As, Cr, Pb and Zn are quite efficiently immobilized with all the binders. On the other hand, Cu and Ni are rather destabilized in the presence of the binder. It can be noticed that the destabilizing effect decreases when the level of OPC substitution with GBBS increases. The supersulfated mix (F4) has the least destabilization effect, although its strength is low. The primary parameter that may have an impact on leachability is the pH value [5] since dissolution of metal species is highly dependent upon this parameter. Most metal species are soluble at low and very high pH and stable around neutral pH. The highest pH is obtained with the OPC-based samples (around 12.5). Overall the pH decreases when increasing the fraction of GGBS. The lowest pH is obtained with the supersulfated binder. There seems to be then a correlation between pH level and destabilization of the heavy metal compounds. Actually, solubility of metals such as Cu significantly increases at high pH [6]. This may be a primary explanation for the significant increase of leachability of this metal in a cementitious environment (Fig. 6).

XAS measurements

The evolution of the speciation of Cu and Zn when the sediment is solidified with a binder was considered using the XAS technique. Zn K-edge XAS signals of the samples are reported in Fig. 7.

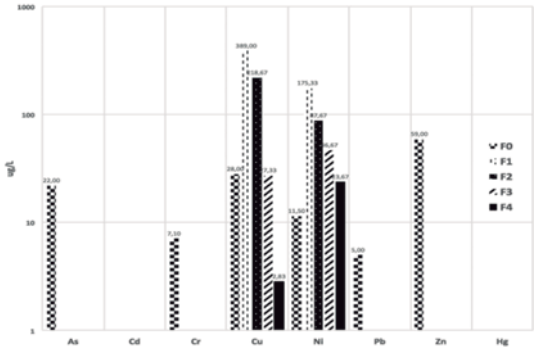

Fig. 6 Amount of leached heavy metals for the different formulations

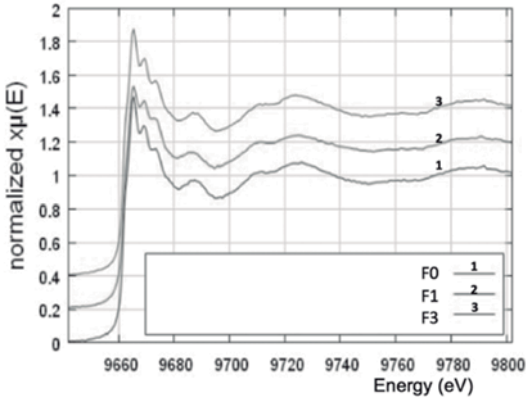

Fig. 7 Zn K-edge XAS spectra of the three different samples considered

The Zn XAS of the sediment (F0) and that of the F3 (OPC/GGBS-sediment) are identical. This indicates that there is no modification of the chemical environment of Zn in the presence of the high content GGBS binder. In the OPC-sediment sample (F1) the XANES part (X-ray Absorption Near Edge Structure) is modified, although very slightly, but this suggests an actual change of the chemical environment of Zn when the sediment is embedded in this binder. Indeed the ratio between the first peak corresponding to the white line and the second peak is smaller compared to the case of the two other samples.

In Fig. 8 the Zn K-edge XANES part of the three samples are reported. These results are very similar to those of zinc chromate spinels at different Zn/Cr molar ratios and annealing temperatures reported in [7]. Note that the XANES of the sediment and that of the sediment embedded in the 85%GGBS binder are indistinguishable. The signals are very similar, suggesting that Zn in the sediments are very likely to be mainly in zinc chromate form.

The pre-edge shoulder corresponds to the transition 1s3d. The shoulder almost disappears in the presence of Portland cement. This suggests a transition from tetrahedral to octahedral coordination type of Zn [7]. The presence of Portland cement impacts also the pro-edge features similarly to the value of the Zn/Cr molar ratio [7].

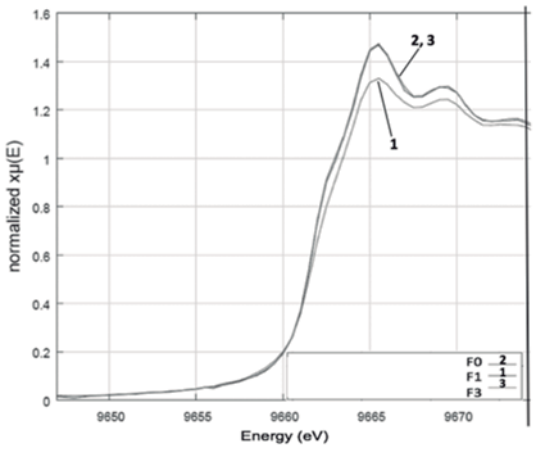

Fig. 8 Zn K-edge XANES spectra of the samples considered

The probable presence of Zn-chromate in the sediment may explain in particular the high level of chromium found in the sediment as determined with XRF. Zn-chromate has been largely used as primer in boat paints. This compound is highly stable and may accumulate over time in port sediments.

Figure 9 represents the Cu K-edge XANES spectra for the four different samples considered (F0 to F4).

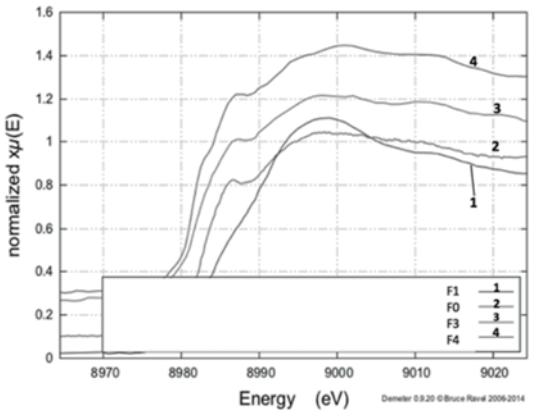

Fig. 9 Cu K-edge XANES spectra for the different mixes considered

It can be noticed that the chemical environment of Cu is not modified when the sediment is embedded in the high amount GGBS binder. On the other hand, there is a significant change of the speciation of Cu in the presence of Portland cement. In particular, the pre-peak, assigned to the transition from 1s to 3d shell [8], disappears in the presence of Portland cement. This pre-peak indicates the presence of Cu(II). Therefore, in the OPC embedded sediment one has mainly Cu (I).

Figure 10 shows XANES spectra of typical Cu-compound references (data kindly supplied by Søren Kristiansen from Aarhus university, Denmark). Comparison of Cu K-edge XANES of the sediment with the different reference signals indicates indeed that the oxidation state of cupper is mainly (II) (similar pre edge), while in the OPC blended sediment it is rather in (I).

Our available reference data do not match the whole XANES spectra. The closest XANES reference signals found in the literature are those reported in [8]. The XANES signal of the supersulfated based sample is very close to that of cuprous sulfide (Cu_2S) [8]. The XANES of the sediment and that of the 85%GGBS-15%OPC blended sediment may be a combination of those of cuprous sulfide and cupric sulfide (CuS).

At first glance the presence of these sulfide compounds is rather intriguing. Yet a possible explanation may be put forward. Indeed, cupper sulfate was largely used as antifouling agent in boat paints for a long time. Under anaerobic conditions the eventual presence of sulfate-reducing bacteria (SRB), which breath sulfates reducing them to sulfides, may actually lead to the transformation of cupper sulfates to cuprous (or cupric) sulfides. This phenomenon should take place in the similar manner

than reported in [9] regarding the issue of corrosion of cupper in seawater due to SRB, leading to the formation of a biofilm, which is mainly composed of cuprous sulfide.

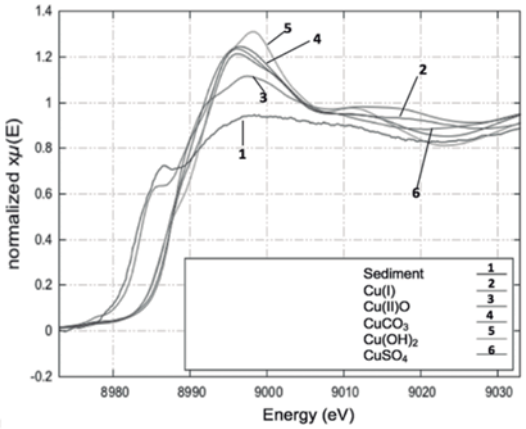

Fig. 10 Cu K-edge XANES spectra of various Cu-compound references

CONCLUSIONS

Leaching tests were performed on Dublin port sediments embedded in binders with different contents of GGBS. It was found that the leachability of most of heavy metals contained in the sediment under initially neutral pH conditions is quite low. This indicated that the heavy metals within the sediment are embedded in stable compounds. This was confirmed with XAS in the case of Cu and Zn. In some cases addition of the binder led unexpectedly to the destabilization of the heavy metal compounds increasing their leachability. The Portland cement binder was found to be the most destabilizing binder. Increasing the amount of GGBS led to a decrease of the destabilization effect. This was correlated with the XAS results, which showed that the chemical environment of Cu and Zn was not modified in the case of binders with high GGBS content.

REFERENCES

[1] Deja, J. (2002). Immobilization of Cr6+, Cd2+, Zn2+ and Pb2+ in alkali-activated slag binders. *Cement and Concrete Research*, *32*(12), 1971-1979.

[2] NF EN 12457-2 Indice de classement : X30-402-2. Titre: Caractérisation des déchets - Lixiviation - Essai de conformité pour lixiviation des déchets fragmentés et des boues.

[3] C. Shi and J. Qian “High performance cementing materials from industrial slags — a review” Ressources, Conservation and Recycling (2000) 29, 195–207.

[4] M. Rondeux, L. Courard, F. Michel “Durability of slag-based cements towards sulphatic attacks”. [5] Spence RD, Shi C, editors. “Stabilization and solidification of hazardous, radioactive and mixed wastes”. Boca Raton, FL: CRC Press; 2005

[6] V. Chatain, D. Blan, D. Borschneck & C. Delorme. Environ Sci Pollut Res (2013) 20:66–74.

[7] Tian, S., Wang, S., Wu, Y., Gao, J., Xie, H., Li, X., ... & Tan, Y. (2015). The real active sites over Zn–Cr catalysts for direct synthesis of isobutanol from syngas: structure-activity relationship. *RSC Advances*, *5*(108),89273-89281.

[8] Kumar, P., Nagarajan, R., & Sarangi, R. (2013). Quantitative X-ray absorption and emission spectroscopies: electronic structure elucidation of Cu_2S and CuS.*Journal of Materials Chemistry C*, *1*(13), 2448-2454.

[9] Chen, S., Wang, P., & Zhang, D. (2014). Corrosion behavior of copper under biofilm of sulfate-reducing bacteria. Corrosion science, 87, 407-415.

DESIGN OF TWO PERMEABLE BARRIERS FOR NITRATE REMOVAL IN GROUNDWATER

Sandoval Dangelo[1], Silva Ana Elisa[2] Hansen Anne M.[3] and García Rolando [4]
[1]Masters and Doctorate Program in Environmental Engineering, Mexican National Autonomous University (UNAM), Mexico [2]School of Engineering, UNAM, [3]Mexican Institute of Water Technology. [4]School of Chemistry, UNAM[4]

ABSTRACT

The main issue with nitrate relies in the mobile nature of the compound, which in groundwater, is not adsorbed, allowing it to be dissolved in great amounts. Additionally, ingestion above 50 mg⁄L NO_3^- by infants under three months old could cause methemoglobinemia. The aim of the present investigation was to select a microbial consortium to grow on size 2-6 mm tezontle for the biologic denitrification, and the chemical conditioning of size 2-4 mm zeolite, to form permeable barriers for nitrate removal in groundwater. The experimental phase consisted of several activities for the development of a biological barrier and a zeolite anionic exchange barrier. In this investigation, four possible sources of microbial consortia were evaluated for the development of the definite microbial consortium for biological denitrification: *i).* Upflow Anaerobic Sludge Blanket (UASB), *ii).* Anaerobic-Anoxic-Aerobic sludge (A-A-A), and two depths of soil samples from the Xochimilco chinampas *iii).* From 20 to 30 cm, and *iv).* From 30 to 40 cm. The zeolite was physically and chemically conditioned in order to obtain a particle size of 4-6 mm, and an anion exchange capacity of 0.94 meq/g. From the performance in growth curves of the consortia and the nitrate removal, the UASB sludge was selected as the best of the four evaluated. This consortium was multiplied and fixed as a biofilm in a porous material locally knowns as "tezontle", from volcanic origin. Considering a retention time of 20.5 h, the size of the barrier for biological denitrification was dimensioned 0.20 m high and 10.2 cm diameter. As for the design of the zeolite barrier, it was considered a removal in groundwater of 100 mg⁄L NO_3^-, dimensions of the barrier were 0.1 m high and 10.2 cm diameter.

Keywords: Nitrate, Permeable barrier, Groundwater, Biofilm, Zeolite

INTRODUCTION

Pollution of groundwater caused by inorganic forms of nitrogen (NO_3^-, NO_2^- and NH_4^+) is a big concern around the world [1]. Nitrates (NO_3^-) are related with the nitrogen cycle in the soil due to the processes that depend of microbial degradation, likewise nitrate is an indicator of pollution in natural waters [2].

According to [3], the issue with nitrate relies in its nature as a mobile compound, which is not adsorbed in groundwater or any other material in the aquifer, nor precipitated as a mineral; this allows nitrate to dissolve in great amounts in groundwater and may be mobilized in the subsurface as a sediment and through fractured rocks as well.

Nitrates are not considered to be toxic, in general the ingestion of concentrations higher than 10 mg/L $N - NO_3^-$) represents a health risk and a potential hazard of developing the disease methemoglobinemia, which mainly affects infants under 3 months old [4].

Regular processes like coagulation, flocculation, sedimentation, filtration and adsorption are not efficient for NO_3^- removal; biological processes are relatively more efficient and therefore more commonly used. Other methods are available such as chemical, photochemical and electrochemical methods for nitrate reduction in water [5].

An alternative to mitigate nitrate pollution in groundwater could be the construction of reactive barriers (RB), which consist in subsoil systems that generate a natural water gradient in which water passes through and the pollutant is either retained, immobilized or transformed into a non-toxic species [6].

This investigation intends to design and condition a biological permeable barrier on size 2-6 mm tezontle and a size 2-4 mm zeolite anion exchange barrier for nitrate removal in groundwater.

MATERIALS AND METHODS

The experiment was conducted in the Environmental and Sanitary Engineering Laboratory (LISA) of the Engineering Faculty, UNAM, Mexico. It consisted in two parallel activities for the development and designing of the biological barrier based on a microbiological consortium, obtained from four potential sources of biological denitrifying

microorganisms; the second activity consisted in the development of the physical-chemical anionic exchange barrier of zeolite

Considering sites where microbiological consortia for denitrification might develop, four samples were evaluated: *i).* An AAA (Anaerobic-Anoxic-Aerobic) type sludge from a residual domestic water treatment plant of the UNAM campus, *ii).* An UASB (Upflow Anaerobic Sludge Blanket Reactor) granular sludge from a brewery plant, and of soil samples obtained close to the root area *iii).* From 20 to 30 cm, and *iv).* From 30 to 40 cm, both from the Xochimilco chinampas which are irrigated with wastewater.

Each sludge sample of 150 mL or 50 g of soil sample, was inoculated with 250 mL synthetic water solution with 164 mg/L KNO_3^-, 31 mg/L $KH_2PO_4^-$, 26 mg/L $CaCl_4^-$, 0.68 mg/L $MgSO_4^-$ and 198 mL/m^3 C_2H_5OH, and kept in agitation at 50 r.p.m and room temperature of 18.1±1.4 °C.

For the microbial growth curve, a sample was obtained every five days in order to determine total volatile solids (TVS mg/L) according to Mexican regulation [7], as well as pH, redox potential (Eh) and NO_3^- concentration with a colorimetric method [8] and dissolved oxygen according to [9].

The microbial consortium that denitrified more readily NO_3^- was selected and added to a column reactor of tezontle (a porous igneous rock commonly available in volcanic areas of Mexico), conditioned with the above-mentioned synthetic water and stabilized during a period of 30 d for development of the biofilm.

For the design of the biological barrier the hydraulic retention time (**θ**) was determined by using NO_3^- concentration (mg/L) in the influent (***S*****o**) and effluent (***S***); the volatile suspended solids [7] (***X*** mg/L); the average temperature (**T** °C); a rate of specific denitrification (**U**$_{DN}$), and the dissolved oxygen (**DO**) of the synthetic groundwater, as shown in Eqs. 1 and 2 [10].

$$U_{DN}^{'} = U_{DN} \times 1.09^{(T-20)}(1 - DO) \quad (1)$$

$$\theta[d^{-1}] = S_o - S/U_{DN}^{'} \times X \quad (2)$$

Based on Darcy's Law, a theoretical value of permeability of the materials of the aquifer was used in order to determine the longitude of the biological barrier; stablishing a 10.6 cm diameter, a flow rate was calculated for the columns to operate.

In parallel, clinoptilolite zeolite was activated to form an anionic exchanger. This process consisted in the separation of the material with a No.16 mesh, followed by separation and washing of the coarse fraction with distilled water and drying during 24 h at 103 °C. Subsequently, 50 g of activated zeolite were added to an Erlenmeyer flask with 1L 0.1 M NaOH and agitated during 24 h at 40°C.

The zeolite-NaOH suspension was decanted and washed with deionized water and finally dried during 24 h at 103°C. Batch tests were performed to determine the anion exchange capacity of the processed zeolite, as well as 12 h tests with a 100 mg/L NO_3^- solution to determine its efficiency.

The concentration of anions in the UNAM Campus groundwater was determined using a liquid chromatograph with a conductivity detector (Water 432) with a stationary phase column (Metrohm); the groundwater samples were taken every 8 h in a 24 h period.

The same flow rate as the one used in the biological barrier was used for the ion exchange barrier, in addition other parameters were considered such as: the anionic exchange capacity of the zeolite, the concentration of ions in the solution (meq/L), the flow rate (L/d), the mass flow (meq/d), and the amount of zeolite needed.

RESULTS AND DISCUSSION

Growth curves of the microbial consortia are shown in (Fig. 1). From the Xochimilco chinampa sources, values under 20 mg/L TVS were obtained; meanwhile the sludge from the wastewater plant samples showed values over 110 mg/L de TVS.

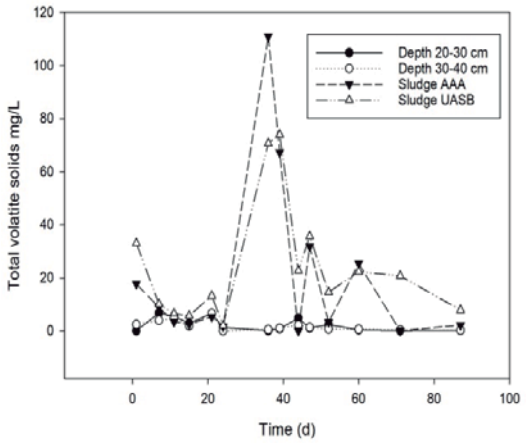

Fig. 1 Growth curves of microbial consortia measured as TVS (mg/L)

In general, all samples analyzed showed conditions that are suitable for biological denitrification, such as pH close to seven and Eh around zero [11], as well as dissolved oxygen concentrations around zero [12].

As for the final concentrations of NO_3^-, these were 3.83 mg/L in the UASB reactor; 12,7 mg/L in the 20 to 30 cm depth soil sample reactor, and 36.7 mg/L in the 30 to 40 cm depth soil sample reactor. Due to its faster growth, the microbial consortia from the UASB reactor was chosen for the

fixation stage of the biofilm over the tezontle substrate.

Equations (1) and (2) were used to determine the hydraulic retention time (THR) in the columns; the parameters are detailed in Table 1.

Table 1 Parameters for the biological barrier on tezontle

Parameters	Value
S_o	100 mg/L $\boldsymbol{NO_3^-}$
S	40 mg/L $\boldsymbol{NO_3^-}$
X	120 mg/L $\boldsymbol{NO_3^-}$
T	23 °C
U_{DN}	0.45
DO	0.4 mg/L
Θ	20.5 h^{-1}
Flow	1894.27 mL/d
barrier height	20 cm

As for the anion exchange barrier, it was determined that the exchange rate was 0.94 meq/g zeolite. Figure 2 shows the results of the batch removal test; in which it is observed that close to 10 h the highest removal efficiency is reached.

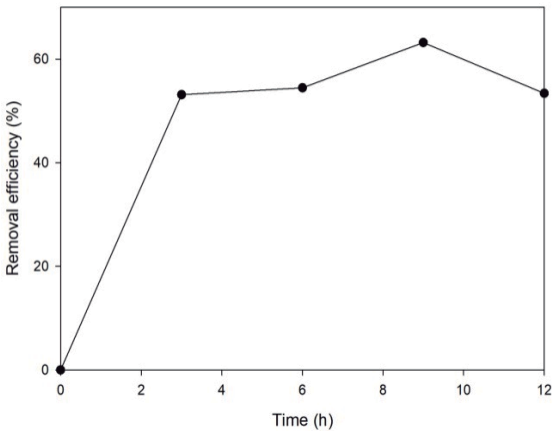

Fig. 2 Removal efficiency in different NO_3^- concentrations in activated zeolite

The ion concentration of the groundwater (mg/L) and additional criteria for the design of the anion exchange barrier are shown in the Table 2 and 3. Zeolite has a negative decompensated charge which causes a low affinity for anion exchange, so when changing the superficial charge of the zeolite, a good performance of the barrier is expected [13].

Table 2 Anion concentration of the groundwater

Anion	mg/L
$\boldsymbol{F^-}$	< LOD
$\boldsymbol{HCO_3^-}$	144.6
$\boldsymbol{Cl^-}$	40.3
$\boldsymbol{Br^-}$	< LOD
$\boldsymbol{PO_4^-}$	< LOD
$\boldsymbol{SO_4^{-2}}$	42.5
$\boldsymbol{NO_3^-}$	36.0
TOC	0.7

LOD: Limit of detection

Table 3 Parameters for the zeolite anion exchange barrier

Parameters	Value
Anions in groundwater	5.52 meq/L
Flow	1894.27 mL/d
Massflow	10.43 mg/L
Amount of zeolite	333 g
Density of zeolite	0.76 g/cm^3
Barrier height	10 cm
θ	20.5 h^{-1}

Considering the parameters in Tables 1 and 2, the commercial sand with particle size 0.18 mm and a hydraulic conductivity of $3.97x10^{-5}$ m/s, the final result is two reactors with the following dimensions: a) A biological barrier (BB) with 30 cm sand in the bottom, 20 cm tezontle covered with the biofilm, and 30 cm sand in the top of the column and b) An anion exchange barrier (AEB) made of 30 cm of sand in the bottom, 10 cm of activated zeolite and 30 cm of sand in the top of the column (Fig. 3).

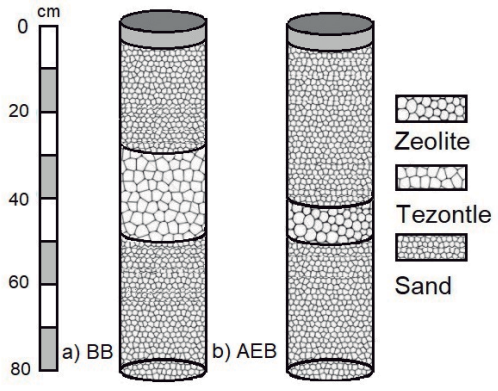

Fig. 3 Diagram of the two permeable barriers for nitrate removal in groundwater as designed in this study

CONCLUSIONS

The microbial consortia from the UASB reactor, grown on tezontle showed potential for biological denitrification of water. It was also documented that when the surface charge of the zeolite is modified, anions from groundwater can be removed; the highest efficiency for $\boldsymbol{NO_3^-}$, removal was observed at 4 days of operation of the column; however, the ion exchange barrier became saturated after 7 days.

A cost analysis was made for the construction of the barriers. In terms of the laboratory reagents, the biological barrier has a lower cost than the anion exchange barrier. As for the operation of each barrier, the development of the biological consortia requires 6 months for its development meanwhile the activation of the zeolite only requires 48 hours.

ACKNOWLEDGEMENTS

For the support given by the National Council of Science and Technology (CONACYT-SENER CVU 780094) and the Office of International Affairs and External Cooperation of the University of Costa Rica. Special thanks to the National Laboratory of Geochemistry and Mineralogy of the Institute of Geology- UNAM, and to Arabela Vega for assisting with the translation.

REFERENCES

[1] Gilbert O., Pomierny S., Rowe I., Kalin R. 2008. Selection of organic substrates as potential reactive materials for use in a denitrification permeable reactive barrier (PRB). Bioresource Technology (1): 7587 – 7596.

[2] Cabrera A., Pacheco J., Pérez R. 2004. Diagnóstico de la calidad del agua subterránea en los sistemas municipales de abastecimiento en el Estado de Yucatán, México. Ingeniería 8 (2) 165- 179.

[3] Pacheco J., Marín L., Cabrera A., Steinich B., Escolero O. 2001. Nitrate temporal and spatial patterns in 12 water-supply Wells, Yucatan, Mexico. Environmental Geology. 40 (6) 708 – 715.

[4] Fewtrell L. Drinking water nitrate, methamoglobinemia and global burden of disease: a discussion. Environmental Health Perspect. 112 (14) 1371-1374.

[5] Moussavi G., Shekoohiyan S. 2016. Simultaneous nitrate reduction and acetaminophen oxidation using the continuous-flow chemical-less VUV process as an integrated advanced oxidation and reduction process. Journal of Hazardous Materials. 318 (1) 329-338.

[6] Powell R., Blowes D., Gillham R., Schultz D., Sivavec T., Puls R., Vogan J., Powell P. 1998. Permeable reactive barrier technologies for contaminant remediation. United States Environmental Protection Agency. Washington DC, United State. 102 p.

[7] NMX-AA-0340SCFI-2015. 2015. Análisis de Agua, medición de sólidos y sales disueltas en aguas naturales, residuales y residuales tratadas-Métodos de Prueba. Secretaría de Economía. México. Estados Unidos Mexicanos 20 p.

[8] Fernández G. 2014. Manual de laboratorio de química del agua. Facultad de Ingeniería. Universidad Nacional Autónoma de México. 171 p.

[9] NMX-AA-012-SCFI-2001. 2001. Análisis de agua: Determinación de oxígeno disuelto en aguas naturales, residuales y residuales tratadas-Método de Prueba. Secretaría de Economía. Estados Unidos Mexicanos. México. 20 p.

[10] Eckenfelder W. 1989. Industrial Water Pollution Control. McGraw Hill Book Company. United State. 400 p.

[11] Metcalf y Eddy INC. 1996. Ingeniería de Aguas Residuales. Tratamiento, vertido y reutilización. Tomo II. McGraw Hill. Mexico.1485 p

[12] Gerardi MH. 2006. Wasterwater Bacteria. Ed John Wiley & Sons Inc. 256 p.

[13] Barczyk K., Mozgawa W., Krol M. 2014. Studies of anions sorption on natural zeolites. Spectrochemica Acta Part A: Molecular and Biomolecular Spectroscopy. 133 (2014) 876 – 882.

INFLUENCE OF VEGETATION ON WATER BALANCE OF ENGINEERED COVER SYSTEMS FOR RECLAIMED MINE SITES: LITERATURE REVIEW AND OUTLOOKS

Botula Yves-Dady [1], Guittonny Marie [1], Bussière Bruno [1,2], Maqsoud Abdelkabir [1]
[1]Research Institute on Mines and Environment, Université du Québec en Abitibi-Témiscamingue, Canada
[2]NSERC-UQAT Industrial Chair on Mine Site Reclamation, Université du Québec en Abitibi-Témiscamingue, Canada

ABSTRACT

Engineered cover systems made of various fine and coarse soil materials are often used for the reclamation of mine tailings facilities and are expected to perform from long period of time to perpetuity. This performance can be assessed using the water balance components, particularly water percolation, storage and evapotranspiration. Establishment of vegetation that can thrive on rehabilitated mine sites is a legal requirement that mining companies should fulfill after mine closure. Plant communities can influence the performance of engineered covers by acting on different components of their water balance and by modifying their hydrogeological properties. However, the influence of vegetation and other ecological processes are often neglected by engineers and modelers when designing and evaluating the performance of mine engineered covers. Moreover, the approach used to integrate vegetation parameters in numerical water balance models is often simplistic. The objective of our paper is to demonstrate through a literature review of practical case studies how vegetation can influence different components of the water balance of engineered cover systems. Interception of precipitations, reduction of runoff, increase of infiltration, increase of transpiration and modification of the soil albedo are the main effects of vegetation on water balance of cover systems and should be considered during modelling. The main conclusion of our literature review is that an approach exclusively based on engineering aspects is not appropriate to design a sustainable system that achieves objectives of mine closure in the long term. Therefore, a multidisciplinary and dynamic approach that integrates both engineering and ecological aspects is needed.

Keywords: Engineered Covers, Vegetation, Water Balance, Mine Reclamation, Numerical models

INTRODUCTION

All over the world, the mining sector faces important environmental challenges due to the impacts of mining activities on the local environment ([1]; [2]). Mine wastes often contain sulfide minerals that can react with oxygen and water and result in the production of acid mine drainage (AMD). The AMD process results in an increase in metals concentrations (e.g. Fe, Cu, Zn, As, Cd, Pb) and a sharp decrease of pH in the mine effluents ([3]; [2]). Long-term control and remediation measures need to be implemented in mine tailings storage facilities (TSF) in order to prevent AMD generation ([4]; [5]). This is possible through reclamation of mine sites ([2]).

The objective of mine engineered cover systems is to exclude water and/or oxygen that are responsible of the AMD production process when they are brought into contact with sulfide minerals ([2], [6]). Engineered covers made of various fine and coarse soil materials are often used for the reclamation of mine tailings facilities and are expected to perform from long period of time to perpetuity.

Establishment of vegetation that can thrive on rehabilitated mine sites is a legal requirement that mining companies should fulfill after mine closure (e.g. [7]; [8]). Plant communities can influence the performance of engineered cover systems by acting on different components of their water balance and by modifying their hydrogeological properties. However, the influence of vegetation and other ecological processes are often neglected by engineers and modelers when designing and evaluating the performance of cover systems ([9]; [10]; [11]).

The objective of this paper is to show how vegetation can influence the components of the water balance of engineered cover systems on reclaimed mine sites through a review of different case studies.

BRIEF OVERVIEW ON MINE ENGINEERED COVER SYSTEMS

To prevent oxidation of reactive mine wastes on the storage facilities, covers are generally used ([12]; [2]). Configurations of these covers are very similar to engineered covers that have been used for many years for landfill sites (e.g. [13]; [14]; [15]). These

covers belong to a large group of "engineered covers".

In this paper, we will focus on two types of engineered cover systems used to prevent AMD on mine waste storage facilities: (1) oxygen barriers and (2) water infiltration barriers.

Oxygen Barrier Systems

Under humid climates, oxygen flux control is usually considered as the most efficient way to limit AMD in the long term ([16]; [17]; [18]). Three types of oxygen barriers are found: water covers, monolayer covers with an elevated water table (EWT) and covers with capillary barrier effects (CCBE).

Water covers

Deposition of mine tailings beneath a water cover is considered technically efficient to prevent AMD due to the limited availability of dissolved oxygen and its low diffusion coefficient in water ([19]; [20]). However, many mine operators are reluctant with the prospect of maintaining a large volume of water over the mine wastes for perpetuity ([18]). Moreover, the benefits of implementing a water cover greatly vary from one site to the other ([19]). Therefore, engineered soil covers have been found to be an attracting alternative to water covers with rivalling performance ([18]). They are described in the subsequent sections.

Monolayer cover with an elevated water table

The principle of a monolayer cover with an EWT is based on maintaining a high degree of saturation within the reactive mine tailings above the water table. This technique is based on the low level of oxygen diffusion in quasi-saturated conditions to inhibit oxidation of sulfide-bearing wastes ([21]; [22]; [23]).

An additional layer made of coarse- or fine-grained materials is placed above the reactive mine wastes. A layer with coarse-grained materials will limit water loss through evaporation and maximize infiltration ([22]) whereas a layer with fine-grained materials will increase water retention and restrain oxygen diffusion across the cover system ([24]; [25]).

Cover with capillary barrier effects

In temperate climate, CCBEs constitute a practical and efficient solution to limit AMD generation ([26], [27]). This technique consists in covering waste storage facilities of several (two to five) layers of materials with distinct textural and hydrogeological properties. In a CCBE, these layers are assembled in order to create capillary barrier effects ([2], [28]; [29]).

The layer made of fine-grained materials, placed on top of a coarse-grained layer that easily desaturates, tends to store moisture coming from the soil surface as water does not easily move downward into the underlying material that shows a low hydraulic conductivity under unsaturated conditions ([2]; [28]; [26]; [27]). An additional layer of coarse-grained materials is placed above the fine-grained layer to limit loss of water through evaporation ([27]).

Water Infiltration Barrier Systems

Store-and-release cover systems

In semi-arid and arid climates, limiting water infiltration through "store-and-release" or evapotranspiration covers has been presented by various authors as an efficient mean to prevent AMD (e.g. [30]; [31]; [32]; [33]). Their functioning is based on the physical process of evaporation or evapotranspiration. The moisture-retaining layers of store-and-release covers are generally made of materials that store water during rainy periods and release it rapidly to the atmosphere during dry spells ([31]; [32]). Moreover, the evapotranspiration layer should be thick enough to hold all infiltrated water until its removal by soil evaporation and/or plant transpiration ([34]).

Low saturated hydraulic conductivity cover systems

Low saturated hydraulic conductivity cover systems are applied in the reclamation of TSF to exclude or limit water flowing from the soil surface to the sulfide-bearing mine wastes in order to limit the production of AMD. This type of engineered cover is composed of one or several layers of natural and/or geosynthetic materials of low saturated hydraulic conductivity ([35]). They can be made of natural fine material (e.g. silt, clay or till), modified geomaterials (e.g. soil-bentonite mixtures), geomembranes or geocomposites ([36]). Saturated hydraulic conductivity values required for these materials should be lower than 10^{-6}–10^{-8} cm/s ([37]) to assure an optimum performance of these cover systems.

INFLUENCE OF VEGETATION ON THE WATER BALANCE OF MINE ENGINEERED COVER SYSTEMS: CASE STUDIES

The general water balance can be described by the following equation (e.g. [38]):

$$P = Ic + E + T + I + R + \Delta S \quad (1)$$

where: P is precipitation, Ic is interception, E is evaporation, T is transpiration, I is infiltration, R is runoff, and ΔS is the change in soil water storage. The components of the water balance are generally expressed in mm and are illustrated in Fig. 1.

The influence of vegetation on water balance of soil cover systems is known to be complex ([39]) and these processes are non-linear and varies with time ([7]; [11]; [40]). As stated earlier, vegetation may modify the performance of a mine engineered cover system by acting on one or more components of its water balance. Some case studies in Canada, Australia, New Zealand and China are presented below to highlight the importance of vegetation on the functioning of engineered covers on different mine sites (see Table 1). Specifically, the influence of different vegetation types on interception, runoff, infiltration and (evapo) transpiration on reclamation covers were investigated in these case studies. Most of the reclaimed mine sites are covered with a mixture of grass and tree species with the exception of the Syncrude Canada Ltd. mine site in the Alberta province that is covered exclusively with grasses (Table 1).

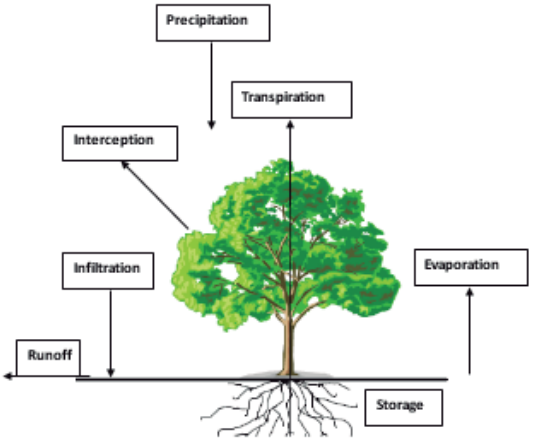

Fig. 1 Schematic representation of the components of the soil-plant water balance (modified from Norbert Móricz, 2010)

Interception

At Syncrude Canada Ltd. mine site in Alberta (Canada), grass species were found to be quite efficient in limiting the effects of erosion on engineered covers notably through intercepting rainwater ([39]). In New Zealand, [41] reported that vegetation that grows on mine reclamation covers intercepts a part of rainwater.

Runoff

Reference [42] studied the effects of vegetation on runoff and erosion on reclaimed land at the Antaibao opencast coal mine dump in Shanxi province (China). Vegetation reduced the quantity, intensity and speed of runoff ([43]; [44]; [45]) particularly on sloped surfaces [42].

Infiltration

Various studies were conducted to analyze the effect of vegetation on water infiltration through engineered covers on reclaimed mine sites. In the Québec region (Canada), the penetration of plant roots through layers of CCBEs was studied on Les Terrains Aurifères (LTA) site and on the Lorraine mine site by [46] and [47], respectively. References [46] and [47] found that deep-rooted woody species reached the fine-grained layer that is the moisture-retaining layer of a CCBE aiming at limiting the diffusion of oxygen to reactive tailings.

After closure of a bauxite mine in the Northern Territory of Australia, [48] observed that water infiltration rate increased by several orders of magnitude in 25 years. The reclaimed mine sites had a vegetation cover increasingly dominated by eucalypt, where acacia trees were declining and grasses were sparsely growing. However, [48] attributed the changes of the infiltration rate to the joint action of physical (micro-aggregation) and biological processes.

Transpiration

Vegetation was found to have a strong influence on evapotranspiration rates (10–20 mm increase of cumulative actual evapotranspiration during the summer period) and on water storage of covers at the Syncrude Canada Ltd mine site in Alberta, Canada ([49]).

Reference [50] indicated that a good choice of the vegetation type is important to increase the efficiency of a store-and-release cover on the Kidston mine site in North Queensland (Australia). Reference [51] showed that establishment of vegetation (trees and grasses) on the waste rock pile led to increased evapotranspiration compared to the bare waste rock surface in the Elk Valley coal mine in British Columbia (Canada).

Table 1 Influence of vegetation on water balance components of mine-engineered covers in Canada, Australia, New Zealand and China

Mining site	Localisation	Vegetation type	Water balance component	Cover systems	References
Syncrude Canada Ltd. Mine	North McMurray (Alberta, Canada)	Grasses	Interception	Peat/till	[39]
Not specified	New Zealand	Not specified	Interception	Not specified	[41]
Antaibao opencast coal mine dump	Shanxi Province (China)	Grasses, legumes shrubs, trees	Runoff	Not specified	[42]
Alcan Gove mine	Northern Territory (Australia)	Grasses, shrubs, trees	Infiltration	Natural soil	[48]
Syncrude Canada Ltd. Mine	North McMurray (Alberta, Canada)	Grasses	(Evapo)transpiration	Peat/till	[49]
Kidston Gold mines	North Queensland (Australia)	Grasses, trees	(Evapo)transpiration	Store-and-release	[50]
Teck Coal Ltd. coal mines	Elk Valley (British Columbia, Canada)	Grasses, trees	(Evapo)transpiration	Store-and-release	[51]

Modification of the soil albedo

Vegetation plays a role in the evaporative power of the atmosphere through the albedo effect ([52]). The fraction of radiation that is not intercepted by the vegetation depends on the vegetation cover ([53]) and this has a direct influence on soil evaporation. To the limit of our knowledge, the influence of vegetation cover on the modification of the soil albedo has not been investigated for mine engineered covers.

CONCLUSION

From the case studies described above, we demonstrated that vegetation could affect the functioning of mine engineered cover systems by acting on different components of their water balance. However, only a limited number of studies on mine engineering covers took into account the aspect of vegetation.

Specifically, in assessing the performance of engineered covers as oxygen and/or water barriers on reclaimed mine sites, interception of water by vegetation, contribution of vegetation to runoff or in modifying the soil albedo are not considered. Moreover, in most studies, quantification of the effect of vegetation on the performance of mine cover systems is generally limited to one or rarely two components of the water balance equation. Numerical models used to assess the performance of mine reclamation covers can integrate the effect of vegetation but only to a limited extent. Thus, most engineers and modelers often neglect the influence of vegetation and other ecological processes when designing and assessing the performance of engineered cover systems.

From this review, we can conclude that an approach exclusively based on engineering aspects is not appropriate to design a sustainable system that achieves objectives of mine closure in the long term. Therefore, a multidisciplinary and dynamic approach that integrates both engineering and ecological aspects is needed.

ACKNOWLEDGEMENTS

The authors acknowledge the “Fonds de recherche du Québec – Nature et technologies” (FRQNT) for funding the study under the project number 2015-MI-192695.

REFERENCES

[1] Bussière B, Lelièvre J, Ouellet J, Bois D, “Utilisation de résidus miniers désulfurés comme recouvrement pour prévenir le DMA: analyse technico-économique sur deux cas réels”, in Proc. Conf. on Mining and the Environment, Sudbury, Ontario, Canada, Vol. 1, 1995, pp. 59-68.

[2] Aubertin M, Bussière B, Bernier L, Environnement et gestion des rejets miniers. Manual on CD-Rom, Presses Int. Polytechnique, 2002, Montréal., QC, Canada.

[3] Ritchie AIM, "The waste-rock environment", in Short course handbook on environmental geochemistry of sulfide mine-wastes, Ed. Blowes & Jambor, Mineralogical Association of Canada, 1994, pp. 133-161.
[4] Ritcey GM, Tailings management, problems and solutions in the mining industries. New York: Elsevier, 1989.
[5] Bussière B, "Acid mine drainage from abandoned mine sites: problematic and reclamation approaches", in Proc. Int. Symp. on Geoenvironmental Engineering, Advances in Environmental Geotechnics, Hangzhou, China, 2009, pp. 111-125.
[6] Aubertin M, Bussière B, Pabst T, James M, Mbonimpa M, "Review of the reclamation techniques for acid-generating mine wastes upon closure of disposal sites" in Proc. Geo-Chicago 2016, Chicago, USA, 2016, pp. 343-358.
[7] MEND (Mine Environment Neutral Drainage Program), Modelling the critical interactions between cover systems and vegetation. Natural Resources Canada, Mine Environmental Neutral Drainage Program, MEND Report 2.21.6, 2014.
[8] MERN (Ministre de l'Énergie et des Ressources Naturelles), Guide de préparation du plan de réaménagement et de restauration des sites miniers au Québec. Ministère de l'Énergie et des Ressources naturelles. Gouvernement du Québec, 2016.
[9] Traynham B, "Monitoring the long-term performance of engineered containment systems: the role of ecological processes", PhD Thesis, Vanderbilt University, USA, 2010.
[10] Traynham B, Clarke J., Burger J, Waugh, J, "Engineered containment systems: Identification of dominant ecological processes for long-term performance assessment and monitoring", Remediation Journal, Vol. 22, 2012, pp. 93-103.
[11] Dejong J, Tibbett M, Fourie A, "Geotechnical systems that evolve with ecological processes", Environ. Earth Sci., Vol. 73, 2015, pp. 1067-1082.
[12] Aubertin M, Bussière B, "Étude préliminaire - Évaluation des barrières sèches construites à partir de résidus miniers alcalins". Rapport soumis au Centre de recherches minérales. Projet C.D.T. P1610, École Polytechnique de Montréal, 1991.
[13] Tchobanoglous G, Theisen H, Eliassen R, Solid wastes: Engineering principles and management issues. New York: Mc-Graw-Hill, 1977.
[14] Daniel DE, Geotechnical practice for waste disposal. London: Chapman & Hall, 1993.
[15] Rowe RK, Quigley RM, Brachman RWI, Booker JR, Barrier systems for waste disposal facilities. London: Taylor & Francis, 2004.
[16] SRK (Steffens, Robertson and Kirsten, Inc.), Draft acid rock drainage technical guide, Vol. l., SRK, 1989.
[17] MEND (Mine Environment Neutral Drainage Program), MEND Manual, Report 5.4.2. MEND Program, CANMET, Natural Resources Canada, Ottawa, Ontario, 2001.
[18] Demers I, Bussière B, Mbonimpa M, Benzaazoua M, "Oxygen diffusion and consumption in low-sulphide tailings covers", Can. Geotech. J., Vol. 46, 2009, pp. 454-469.
[19] St-Arnaud L, "Water covers for the decommissioning of sulfidic mine tailings impoundments", in Proc. 3rd Int. Conf. on the Abatement of Acidic Drainage, Pittsburgh, Pa., 25–29. Special Publication SP 06A-94, Bureau of Mines, US Department of the Interior, Washington, DC, Vol. 1, 1994, pp. 279-287.
[20] Davé NK, Lim TP, Horne D, Boucher Y, Stuparyk R, "Water cover on reactive tailings and wasterock: Laboratory studies of oxidation and metal release characteristics", in Proc. 4th Int. Conf. on Acid Rock Drainage (ICARD), Vancouver, British Columbia, Canada, 1997, pp. 779-794.
[21] Aubertin M, Bussière B, Monzon M, Joanes A-M, Gagnon D, Barbera J-M, Aachib M, Bedard C, Chapuis RP, Bernier L, "Étude sur les barrières sèches construites à partir des résidus miniers. – Phase II: Essais en place". Rapport de recherche Projet CDT P1899, NEDEM/MEND 2.22.2c, 1999.
[22] Dagenais AM, Aubertin M, Bussière B, "Parametric study on the water content profiles and oxidation rates in nearly saturated tailings above the water table", in Proc. 7th Int. Conf. on Acid Rock Drainage (ICARD), St. Louis, Missouri, USA, 2006, pp. 405-420.
[23] Ouangrawa M, Aubertin M, Molson J, Bussière B, Zagury GJ, "Preventing acid mine drainage with an elevated water table: Long-term column experiments and parameter analysis", Water Air Soil Poll., Vol. 213, 2010, pp. 437-458.
[24] Demers I, Bussière B, Aachib M, Aubertin M, "Repeatability evaluation of instrumented column tests in cover efficiency evaluation for the prevention of acid mine drainage", Water Air Soil Poll., Vol. 219, 2011, pp. 113-128.
[25] Ethier MP, Bussière B, Aubertin M, Maqsoud A, Demers I, Lacroix R, "In situ evaluation of the elevated water table technique combined with a monolayer cover on reactive tailings: monitoring strategy and preliminary results", in Proc. 66th CGS Conf., GeoMontreal 2013, Montreal, Canada, 2013.
[26] Bussière B, Maqsoud A, Aubertin M, Martschuk J, McMullen J, Julien M, "Performance of the oxygen limiting cover at the LTA site, Malartic, Québec", CIM Bulletin, 99 (1096): pp. 1-11, 2006.
[27] Bussière B, Aubertin M, Mbonimpa M, Molson JW, Chapuis RP, "Field experimental cells to evaluate the hydrogeological behaviour of oxygen

barriers made of silty materials", Can. Geotech. J., Vol. 44, 2007, pp. 245-265.
[28] Aubertin M, Molson J, Bussière B, Dagenais AM, "Investigations of layered cover systems acting as oxygen barriers to limit acid mine drainage", in Proc. 5th Int. Conf. Environmental Geotechnics, Cardiff, UK., Vol. 2, 2006, pp. 827-835.
[29] Kalonji-Kabambi A, Bussière B, Demers I, "Hydrogeological behaviour of covers with capillary barrier effects made of mining materials", Geotech. Geol. Eng., Vol. 35, 2017, pp. 1199-1220.
[30] Albright WH, Benson CH, Gee GW, Roesler AC, Abichou T, Apiwantragoon P, Lyles BF, Rock SA, "Field water balance of landfill final covers", J. Environ. Qual., Vol. 33, 2004, pp. 2317-2332.
[31] Bossé B, Bussière B, Hakkou R, Maqsoud A, Benzaazoua M, "Field experimental cells to assess hydrogeological behaviour of store-and-release covers made with phosphate mine waste", Can. Geotech. J., Vol. 52, 2015, pp. 1255-1269.
[32] Hauser VL, Evapotranspiration covers for landfills and waste sites. Boca Raton: CRC Press, 2008.
[33] Knidiri J, Bussière B, Hakkou R, Bossé B, Maqsoud A, Benzaazouaa M, "Hydrogeological behaviour of an inclined store-and-release cover experimental cell made with phosphate mine wastes", Can. Geotech. J., Vol. 54, 2017, pp. 102-116.
[34] Lamoureux S, Straker J, Barbour L, O'Kane M, "Enhancing the understanding for the influence of vegetation on cover system performance in a Canadian mining context", in Proc. 9th Int. Conf. on Acid Rock Drainage (ICARD), Ottawa, Canada, 2012.
[35] Aubertin M, Chapuis RP, Aachib M, Bussière B, Ricard JF, Tremblay L, "Évaluation en laboratoire de barrières sèches construites à partir de résidus miniers". École Polytechnique de Montréal, NEDEM/MEND Projet 2.22.2a, 1995.
[36] Boulanger-Martel V, "Performance d'une couverture avec effets de barrière capillaire faite de mélanges gravier-bentonite pour contrôler la migration d'oxygène en conditions nordiques", MSc Thesis, Université de Montréal, Canada, 2015.
[37] Chapuis RP, "Sand-bentonite liners: predicting permeability from laboratory tests", Can. Geotech. J., Vol. 27, 1990, pp. 47-57.
[38] Hillel D, Environmental Soil Physics: Fundamentals, applications, and environmental considerations. San Diego: Academic Press, 1998.
[39] Shurniak R, "Predictive modeling of moisture movement within soil cover systems for saline/sodic overburden piles", MSc Thesis, University of Saskatchewan, Canada, 2003.
[40] Fourie A, Tibbett M, "Post-mining landforms — Engineering a biological system", Mine Closure 2007. Australian Centre for Geomechanics, Perth, Australia, 2007.
[41] Ayres B, O'Kane M, Mine waste cover systems: an international perspective and applications for mine closure in New Zealand, in Proc. AusIMM New Zealand Branch Annual Conf., Nelson, New Zealand, 2013.
[42] Zhang L, Wang J, Bai Z, Lv C, "Effects of vegetation on runoff and soil erosion on reclaimed land in an opencast coal-mine dump in a loess area", Catena, Vol. 128, 2015, pp. 44-53.
[43] Gutierrez J, Hernandez I, "Runoff and interrill erosion as affected by grass cover in a semi-arid rangeland of northern Mexico", J. Arid Environ., Vol. 34, 1996, pp. 287-295.
[44] Le Bissonnais Y, Lecomte V, Cerdan O, "Grass strip effects on runoff and soil loss", Agronomie, Vol. 24, 2004, pp. 129-136.
[45] Zuazo VHD, Pleguezuelo CRR, "Soil-erosion and runoff prevention by plant covers: a review", Agron. Sustain. Dev., Vol. 28, 2008, pp. 65-86.
[46] Trépanier S, Étude sur des barrières visant à limiter l'impact de l'infiltration des racines sur la performance des recouvrements multicouches, MSc Thesis, Université du Québec en Abitibi-Témiscamingue, Canada, 2005.
[47] Smirnova E, Bussière B, Tremblay F, Cyr J, "Vegetation succession and root penetration on the Lorraine cover used to limit acid mine drainage", in Proc. 34th Annual meeting and conf. of the CLRA, Québec, Canada [on CD-ROM], 2009.
[48] Spain AV, Hinz DA, Ludwig J, Tibbett M, Tongway D, "Mine closure and ecosystem development: Alcan Gove bauxite mine, NT, Australia", Mine Closure, Perth, Australia, 2006.
[49] Shurniak RE, Barbour SL, "Modeling of water movement within reclamation covers on oilsands mining overburden piles" in Proc. National Meeting of the American Society of Mining and Reclamation, Lexington, Kentucky, 2002, pp. 622-644.
[50] Williams DJ, Stolberg DJ, Currey NA, "Long-term monitoring of Kidston's "Store/Release" cover system over potentially acid forming waste rock piles", in Proc. 7th Int. Conf. on Acid Rock Drainage (ICARD), St Louis, Missouri, USA, 2006, pp. 2385-2396.
[51] Fraser S, "Evaluating the influence of vegetation on evapotranspiration from waste rock surfaces in the Elk Valley, British Columbia", MSc Thesis, McMaster University, Canada, 2014.
[52] Cosandey C, Robinson M, Hydrologie continentale. Paris: Armand Colin, 2012.
[53] Firman D, Allen E, "Relationship between light interception, ground cover and leaf area index in potatoes", J. Agr. Sci.-Cambridge, Vol. 113, 1989, pp. 355-359.

3. Characterization and monitoring of sediments and porous media

Session chairs: Nadia Martínez Villegas[1] and Perla Alonso EguíaLis[2]
[1]Departamento de Geociencia Aplicada, Instituto Potosino de Investigación Científica y Tecnológica, México
[2]Laboratorio de Bioindicadores, Instituto Mexicano de Tecnología del Agua, México

Sediment monitoring and characterization are activities of major importance for the comprehension of concentrations of contaminants, and biogeochemical and ecological processes that occur in the water-sediment interface in both spatial and temporal scales. The availability and behavior of organic and inorganic contaminants, the physical, chemical, and microbiological interactions, and their effects on benthic biota will heavily depend on the composition and structure of these matrices. The theme of this session is intended to attract papers that help to understand the importance of sediment monitoring and characterization in a multidisciplinary perspective in order to provide new insight in this topic as well as methodological and application bases.

LACK OF CORRELATION BETWEEN MERCURY IN SEDIMENTS AND FISH MUSCLE, LAKE CHAPALA MEXICO

Alvarado Claudia [1], Ramírez Gerardo [2], Diaz José J. [3] and Cortez Diego [1]
[1]Food Technology Unit, [2]Analytical Services Lab, [3]Technological Prospecting Lab, Centro de Investigación y Asistencia en Tecnología y Diseño del Estado de Jalisco, Mexico.

ABSTRACT

The aim of this study was to evaluate the relation between mercury concentrations in wild carps and sediments at the same points from Lake Chapala, México. Total mercury (HgT) concentration were analyzed in the edible part of 142 carps (*Cyprinus carpio*), in 14 sediments and in water sites where the fish were caught. Correlation test between HgT from fish muscle and HgT sediments in each site were evaluated. Graphic representation of global trend of HgT in fish flesh into Lake Chapala is shown. The overall mean HgT in edible muscle of carp was 0.39 mg kg^{-1}, below the Mexican and International mercury limits for fish flesh. HgT in sediments were higher than reported from sediments in USA and Canada. The correlation coefficient test (r) between sediment and fish HgT concentration was 0.394. Two Lake Chapala areas were detected with significant high HgT in sediments but La Palma point at soutest close to Lerma River mouth was positive correlated with high fish HgT concentration. The pH of the Lake Chapala water (8.1-9.5) was maybe the key factor that influences the low concentration of HgT in water, and therefore in HgT carp concentration.

Keywords: Lake Chapala, Heavy Metals, Mercury, Carp

INTRODUCTION

Lake Chapala is the largest natural lake in Mexico, with total surface of 114,659 ha, it is located 42 km south of the Metropolitan Area of Guadalajara. Sediments from Lake Chapala has been reported to contain heavy metals and also fish from the lake has been found with mercury, cadmium and other heavy metals in high concentration [1]. On the other hand, fish have specific mechanism for metal uptake and bioaccumulation, and chemical factors such as alkalinity, buffer capacity, hardness and the pH influence the metal bioavailability an for instance their accumulation in fish [2]. The aim of this study was to evaluate the relation between mercury concentrations in wild carps from 14 points in Lake Chapala and mercury concentration from sediment and water in the same regions.

MATERIALS AND METODS

Total mercury (HgT) concentration were analyzed in the edible part of 142 carps (*Cyprinus carpio*) and in the 14 sediments and water sites where the fish were caught, in Lake Chapala, Mexico. Figure 1 shows location of fish capture, in every site at least 10 carps between 800 to 1200 g of weight were collected. Samples were analyzed by atomic absorption spectrometry coupled with cold vapor (CV-AAS) in a Perkin Elmer AAnalyst 200 (Waltham, MA) spectrophotometer coupled with flow injection system FIAS 100. Analyses for fish were conducted by method AOAC 977.15, AOAC 977.22 was used to analyze water and method EPA 990.08 was used for sediment. Correlation test between HgT from fish muscle and HgT sediments in each site, fish weight, size, and distance between the fishing site and Lerma River mouth were evaluated. An interpolation of the average values of the fish concentrations were conducted to represent the spatial distribution of the mercury concentrations in the lake. The interpolation was carried out by spatial analysis using the tools offered by the geostatistical analysis module of ArcGIS software.

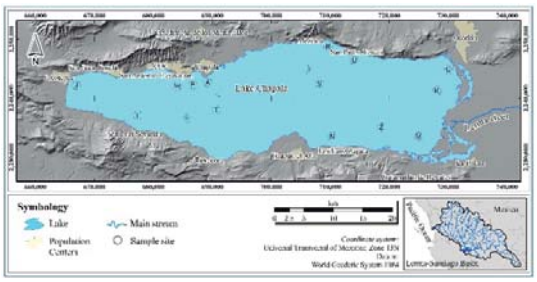

Fig. 1. Sites of carp capture, sediment and water collection in Lake Chapala, Jalisco, Mex.

Quality Control of Analysis

Perkin Elmer standard solutions (N9300174) was used to prepare the calibration curves, which presented $R^2 > 0.998$. Spiked samples from fish were used to determine the percentage of recovery, which ranged between 90 to 110%. Precision evaluation was performed using Perkin Elmer N9300211 solution. All samples were analyzed in

duplicate. The coefficients of variation did not exceed 9%.

Reference material DORM-4 (fish protein) for National Research Council Canada (CNRC, Canada) were digested and analyzed in triplicate and recoveries of heavy metals were within those indicated by certificate values for reference material according to used method. A blank was run for each digestion procedures to correct the measurements. For sets of every ten samples, a procedure blank and spike sample, involving all reagents, was run to check for interference and cross contamination.

RESULTS

The overall mean HgT in edible muscle of carp were 0.39 mg/kg, below the Mexican and International mercury limits for fish consumption (0.5-1.0 mg/kg). Figure 2 shows graphic representation of the fish HgT distribution in Lake Chapala.

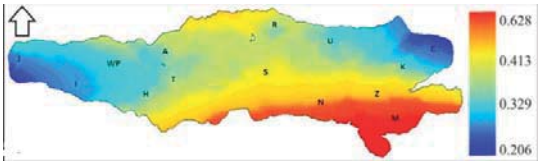

Fig. 2. Spatial distribution of HgT concentration in fish flesh captured in Lake Chapala, Jal. Mex. Blue color represent low concentration and red color high concentration.

Table 1 shows the mean HgT concentration in each site of sediments and fish muscle. HgT sediments concentrations (24.11 – 104.59 mg/kg) were similar than previous reports from Lake Chapala, but it were one or two magnitude order higher than reported for sediments from lakes in US and Canada (0.1 – 1.1 mg/kg) [3] .The total of 14 water samples were below the HgT limit of detection (0.19 µg/L) and it never exceed Mexican Standards [4] of water quality (Tab 2). It was observed that although heavy metals concentrations in sediments were high, water concentrations were low.

The correlation coefficient test (r) between sediment and fish HgT concentration was low: 0.394. Carp fish flesh HgT concentration did not have significant correlation with weight (r = 0.118), length (0.219) or girth (0.0419), although this is explainable because only carps with similar weight (about 1 kg) were captured.

Two Lake Chapala areas were detected with significant high HgT in sediments: ponit I Soyatlan in the sout-west area and M La Palma point at sout-est close to Lerma River mouth, but only last one was related with high fish HgT concentration. On the other way in the places with high fish HgT concentration like N, S and Z the concentration of HgT in sediments were relatively low. In general no correlation was observed between this variables.

Table 1. Mean mercury concentrations (HgT) in fish and sediments from Lake Chapala, Mex.

SITE	HgT Sediment	HgT Fish Flesh
	mg/kg	
A Chapala	80.77	0.3215
C Jamay	42.07	0.3751
H Tuxcueca	49.8	0.2897
I Soyatlan	104.59	0.3841
J Jocotepec	83.33	0.3048
K Rio Lerma1	84.71	0.2379
M La Palma	102.69	0.4065
N Rio Lerma2	29.32	0.5044
R Mezcala	26.38	0.4118
S Isla Mezcala	24.41	0.5067
T Chap-Tux	24.11	0.2651
U SP Itzican	24.42	0.3764
Z Petatan	28.53	0.6281
WP LaCristina	57.14	0.4014

One area in the southeast of the lake (points N, Z and M) was found with significant high HgT in fish muscle (p=0.000) than the rest of the areas. This points had mean HgT in fish of 0.514 mg/kg (red color in Fig. 2) while the rest of the points had a mean of 0.354 mg/kg. The southeast points had in common that were close to Lerma River mouth and the results agree with Ford *et al.* (2000) who reported higher HgT in fish of *Chirostoma sp*. living close to the Lerma river than those living farther from it in Lake Chapala. The sediment of site M had very high HgT concentration (102.69 mg/kg), but N and Z points had relatively low ones (29.32 mg/kg and 28.53 mg/kg respectively).

The red area in Fig. 2, found in southeast of Lake Chapala matches with a water vortex generated by the currents coming from Lerma River and with the higher sedimentation rates from the lake [6, 7]. That would explains why the high HgT concentrations from sediments and fish were found only in the south but not in the north of the Lerma river in the lake.

Bioavailability and toxicity of metals are largely controlled by a variety of chemical water parameters such as pH, alkalinity, hardness, dissolved organic carbon and particulate matter which in combination impact metal fluxes between water, sediment and biota. Metals may occur adsorbed onto particles or in dissolved form, but dissolved is generally the most bioavailable for fish [8]

In the case of Lake Chapala, previous reports showed a strong pH dependence of metals adsorption to sediment particles. Below pH 6, only 40% of metals are adsorbed to sediments and remaining metals could be found in solutions. But at pH 8 or higher, almost 100% of species are adsorbed to sediments, then no free metals are present in the water [9]. According with our results, at pH 8.1 or higher found in Lake Chapala (Tab 2), very low concentration of metals are available, as is demonstrated in the water results. The observation match with the studies of metal bioavailability and toxicity to fish in low-alkalinity lakes [10], explaining what we found in present work.

Has been demonstrated that food is the dominant pathway of mercury uptake by fish [11]. The feedings habits of the carp are dominated by the consumption of zooplankton like *Cladocera* and *Copepoda*, benthic aggregates with sediment particles and larvae forms of insects, earthworm and seed shrimp [12]. Taking in count that carp move only short distances and remain in the same area for long periods of time, then it could reflect well the conditions of the places where it was captured [13].

Despite the high concentrations and the big differences between HgT in sediments from different points, no correlation was observed with the HgT concentration in the carp HgT, making evidence that other factors not only HgT sediment concentration, are playing a roll in the metal bioaccumulation by fish.

Table 2. Summary of water quality parameters in sites of fish and sediment collection.

Parameter	Lake Chapala	Mexican standard
pH	8.1-9.5	6.5-8.5
Temperature (°C)	17.2-27.7	NA
Conductivity (µS/cm)	82.8-90.4	NA
Hardness (mg $CaCO_3$)	223.22-231.56	500
Cu (µg /L)	< 10-29	2.0
Zn (µg /L)	< 1-3	5.0
Cd (µg/L)	0.010-0.019	5.0
Pb (µg/L)	0.330-0.369	10.0
As (µg/L)	9.22 – 14.0	25.0
Hg (µg/L)	<0.19	1.0
CN^- (mg/L)	<0.02	0.07
Free residual chlorine	<0.1	0.2-1.5
Cl^- (mg/L)	59.8-75.8	250.0
Phenols (mg/L)	0.07 - 0.12	0.3
Fluoruros (mg/L)	0.84 - 1.32	1.50
NO_3^- (mg/L)	0.49 - 0.79	10.0
NO_2^- (mg/L)	<0.02	1.0
NH_4^+ (mg/L)	<0.5	0.5
Total dissolved solids	409 – 425	1000
SO_4^{2-} (mg/L)	114.5 – 177.11	400.0

CONCLUSIONS

The lack of correlation between HgT in sediments and fish flesh from Lake Chapala could be explained by the alkalinity in Lake Chapala water that prevents metal solubilization and reduce the metal bioavailability and subsequent fish metal accumulation.

Only sites on the southeast area of the lake showed higher concentration of HgT in sediment and fish flesh and this matches with a vortex in the water current and with higher sedimentation rate in Lake Chapala, making evident the importance of sediments in the lake.

Carp is an herbivorous fish and this represent some protection, more studies must be done in carnivorous specie like catfish, once has been reported these are more likely to introduce mercury in their diet. In addition, other heavy metals like Pb, As and Cd must be analyzed and other tissues like liver and gills, in order to get a broad overview of the phenomenon.

ACKNOWLEDGEMENTS

We are thankful to National Science and Technology Ministry of Mexico (CONACYT) for financial support through project number 216110.

REFERENCES

[1] Trasande L, “Methylmercury exposure in a subsistence fishing community in Lake Chapala, Mexico”, Env Health. 2010: 1-10.

[2] Hollis L, “Effects of long term sublethal Cd exposure in rainbow trout during soft water exposure”, Aquat Tox 2000.51:91-105.

[3] Hansen AM, “Metales pesados en el Sistema Lerma-Chapala: distribución y migración”, Ingeniería Hidráulica en México 1992. May-Dec:92-98.

[4] NOM-127-SSA1-1994, “Water permissible limits of quality for human use and consumption”, 2000. DOF Mexico.

[5] Ford T, Ika R, Shine J, et al. “Trace metal concentrations in Chirostoma sp. from Lake Chapala Mexico: elevated concentrations of mercury and public health implications”, 2000. J Environ Sci Health A. 35:313-325.

[6] Berezowsky V, Escalante E, leon V, “Calculo hidrodinámico del lago de Chapala”, 2007. IMTA report. Mexico.

[7] Fernex F, Zarate P, Ramírez H, et al. “Sedimentation rates in Lake Chapala (western Mexico): posible active tectonic control”, 2001, Chem Geol 177:3-4.

[8] Köck G and Hofer R, “Origin of cadmium and lead in clear softwater lakes of high-altitude and high-latitude, and their bioavailability and toxicity to fish”, in Braunbeck T (editor) Fish Ecotoxicoligy, 1998, Birkhauser verlag Basel. Switzerland.

[9] Hansen AM, "Adsorption-desorption behaviors of Pb and Cd in Lake Chapala, Mexico", Environment International 1997. 4:553-564.
[10] Spry DJ, "Metal bioavailability and toxicity to fish in low-alkalinity lakes: a critical review", Environmental Pollution 1991. 71:243-304.
[11] Hall BD, "Food as the dominant pathway of methylmercury uptake by fish", Water, air & soil poll 1997. 100:13-24.
[12] Sparatu P, Hepher B, Halevy A, "The effect of the method of supplementary feed application on the feeding habits of carp with regard to natural food in ponds", Hydrobiologia 1980. 72:171-178.
[13] Reynolds LF, "Migration patterns of five fish species in the Murray-Darling River system", Marine and Freshwater Research 1983. 34:857-871.

MINERALOGY AND GEOCHEMISTRY OF STREAM SEDIMENTS, FROM LA PURÍSIMA BASIN DAM, GUANAJUATO-MEXICO

Rueda Luisa[1], Miranda-Avilés Raúl[2], Puy-Alquiza María Jesús[2],. Zanor Gabriela A.[3]
[1]Engineering Faculty, Universidad de Guanajuato, Mexico
[2]Mines, Metallurgy and Geology Faculty, Universidad de Guanajuato, Mexico
[3]Life Sciences Faculty, Universidad de Guanajuato, Mexico

ABSTRACT

Nowadays the contamination of surface water and groundwater with heavy metals is a recurring problem, an example of this is the Guanajuato river basin, in México, where its sediments contains minerals from natural erosion of rocks and mining tailings [1], [2]. In the La Purísima Dam, different authors [3], [4], [5] have reported anomalous metal levels, such Lead (Pb), Mercury (Hg), Selenium (Se), Chromium (Cr), Nickel (Ni), Zinc (Zn), Copper (Cu), and Arsenic (As). This dam is part of the recharge area of the Silao-Romita aquifer; it is the main source of water for population of Guanajuato.

The draining basin of La Purísima Dam covers an approximate area of 482 Km^2 and is located south of Mesa del Centro and north of the Eje Neovolcánico, within the basin of the Lerma-Santiago River and sub-basin Guanajuato River. In the present research work, 35 samples of sediments were collected for its mineralogical and geochemical analysis in order to determine its origin (natural or anthropogenic) and pollution degree in the zone.

Keywords: Geochemistry, Stream Sediments, Provenance, La Purísima Dam.

INTRODUCTION

Different investigations in the study area have reported levels of metals and metalloids in water and sediments of the La Purísima Dam [2], [3], [5], in surrounding areas [1], [4] and in the groundwater of the Silao-Romita aquifer, whose main source of recharge is the dam [6], [7], [8].

Within the study zone is the mining district of Guanajuato, characterized by mineral deposits from the Cretaceous, Paleocene and Oligocene [9]. The oldest deposits are massive sulfides hosted in Mesozoic rocks and are located north of the district [9], the Paleocene deposits are located in the western sector and formed in the halo of alteration due to the intrusion of a granitic batholith [10]; while the youngest deposits are due to the volcanic activity of the Tertiary caused by subduction processes, forming epithermal deposits of low sulphuration [11], [12].

Reference [13] suggests that the minerals has had mining since pre-Hispanic times until now; during this period, the mining progress has been made with respect to exploitation sites, mineral extraction methods and waste processing. In 1548, smelting was used as a beneficiation process [13], in the year 1556 the mineral extraction system was established by amalgamation with mercury [14], the residual material from this process was poured into the natural streams [15]. In the following years the extraction of metals continued, new mineralized zones were discovered and waste continued emptying in to the riverbeds, this produced excess of sediment and deposited of it, caused flooding during the years 1760, 1770 and 1804 [14], by this situation in 1830 was proclaimed a decree where the emptying of residues to the rivers was banned [13]. In 1905 began the use of extraction techniques more productive, such as cyanidation, but the residual sludge continued to be emptied into the river bed, causing excess of sediment in the Guanajuato River in 1934 [13], during this year the first tailings dam was build, with the final purpose to reduce the risk of floods. In 1946 the Bulk flotation method was implemented, which is used currently [16].

The materials reported in the La Purisima dam are transported by rivers and streams that discharge their waters into it, and the sediment transport depends on factors such as the slope of the land, the intensity of rainfall, the composition of the rock, among others. Geochemical, mineralogical and morphometric studies of the basin and sediments will help to determine the mineralogical and elementary origin of the sediments, including the possible origin of the metals in the dam and its extension along rivers. In the country, several studies have applied sediment geochemistry to monitor, know the concentration, migration and possible source of pollutants in bodies of water and lands related to them [1], [17], [18], [19], [20], [21], [22], [23], [24], [25], [26].

STUDY AREA

The study area is located between the south sector of the Mesa del Centro and the north of the Eje Neovolcánico, in the state of Guanajuato, within the basin of the Lerma-Santiago river, sub-basin of

the Guanajuato river; it covers an approximate area of 482.67 Km^2 (Fig. 1). The region is characterized for presenting steep mountains with slopes that oscillate between 8 and 20 ° [23]; in the south predominates the basaltic plateaus, which are part of the El Bajío graben, with minor slopes of 5% (less than 3°). The area presents topographic variations from 1,700 to 2,900 meters above sea level.

The shape of drainage is detrital-subparallel and the main rivers are Guanajuato, El Chapín and El Cubo. According to the climatic zoning of the National Institute of Statistics and Geography of Mexico, the area has sub-humid climate, with temperatures ranging from 10°C to 22°C; the precipitation varies in the zone, the area of the Bajío presents rainfall of 700 mm, while the Sierra de Guanajuato records annual rainfall of 800 mm [23].

Geology of the study area

The study area is located in the southern region of the Sierra de Guanajuato and the north-eastern sector of Bajío Guanajuatense (Fig. 1); metamorphic, igneous, intrusive, extrusive and sedimentary events of the Mesozoic and Cenozoic ages constitute the current geology and geomorphology.

Stratigraphy

The oldest rocks in the area are mesozoic age and are represented by Diorita Tuna Mansa described as an intrusive igneous body of ultrabasic composition, with ages of 157.1 ± 8.8 M.a [25]. This intrusive body is metamorphosed and in tectonic contact below the volcanosedimentary sequence La Esperanza (Fig. 1), deposited in an geodynamic environment of intraoceanic island arc [28], [29]; at the end of the Lower Cretaceous is presented an intrusive phase of varied composition, related to the Nevadan orogeny [30], also occurred some events pre-Albian of intense compression [29], which caused metamorphism in the volcanosedimentary sequence. The sequence in the upper part are basaltic intercalations that correspond to the unit basaltic La Luz, described as basalt spills with massive and pillow structure. During the Maastrichtian occurs a compressive event related to the Laramide Orogeny [23], which causes the withdrawal of the seas and promotes a continental environment. At end of the Paleocene and beginning of the Eocene occurs an intense magmatism and emplaced of post-orogenic batholiths in the rocks of the Sierra de Guanajuato, with ages K-Ar and U-Pb 51 ± 1.3 and 51.7 ± 1.0 Ma, respectively (Granito de Comanja; [31] age K-Ar in feldspar; [32] age U-Pb in zircon). These events cause a typical deformation and faulting, favoring the accumulation in the depressions of conglomeratic red layers, known as the Conglomerado de Guanajuato, which are overlying the basal complex of the Upper Jurassic-Early Cretaceous [33], due to the angular and erosional unconformity that extends from the Upper Cretaceous to the Eocene [34]. Overlying the red layers are the Oligocene volcanic rocks, with ages K-Ar 33 and 39 Ma [35], tied to the subduction of the Farallón plate below the North American Plate [36]. Volcanic activity of siliceous character returns beginning of the Oligocene and extends until the Middle Miocene [37], during this extensional period, tectonic pits are produced and favor sediment deposition during the Neogene and Quaternary. The interaction between the North American and Cocos plates, during the Pliocene and beginning of the Quaternary period, caused spills of mafic and intermediate volcanic material related to the Eje Neovolcánico Transmexicano. In the Holocene occurs the most recent record and corresponds to the last volcanic events of the Eje Neovolcánico Transmexicano, and the soils derived from them in the Bajío.

Tectonics

The Sierra de Guanajuato is part of a failed anticline with NW-SE direction, is limited by the normal Bajío fault [34], with orientation N45°W and southwest inclination. The predominant orientation of the faults in the zone is northwest-southeast, the fractures appear in great density, well developed and with orientation similar to the faults (NW-SE).

During the Jurassic the region was affected by a ductile deformation phase, while in the Cretaceous the ductile-fragile deformation is evident in the folded and foliated rocks.

METHODOLOGY

The study area (Fig. 1) was delimited using tools from software ArcGis 10.1 (Spatial Analyst Tools - Hydrology – Watershed) and a mosaic of the digital elevation models of high resolution LiDAR (5m), scale 1:10,000 of the Mexican land (DEM, from the INEGI). The 35 sampling points were located in accordance with the hydrological, geological and geomorphological characteristics of the area.

The field campaign has been in the dry season, between the months of January and June of the years 2017-2018, following the parameters established by the United States Geological Survey and the British Geological Survey.

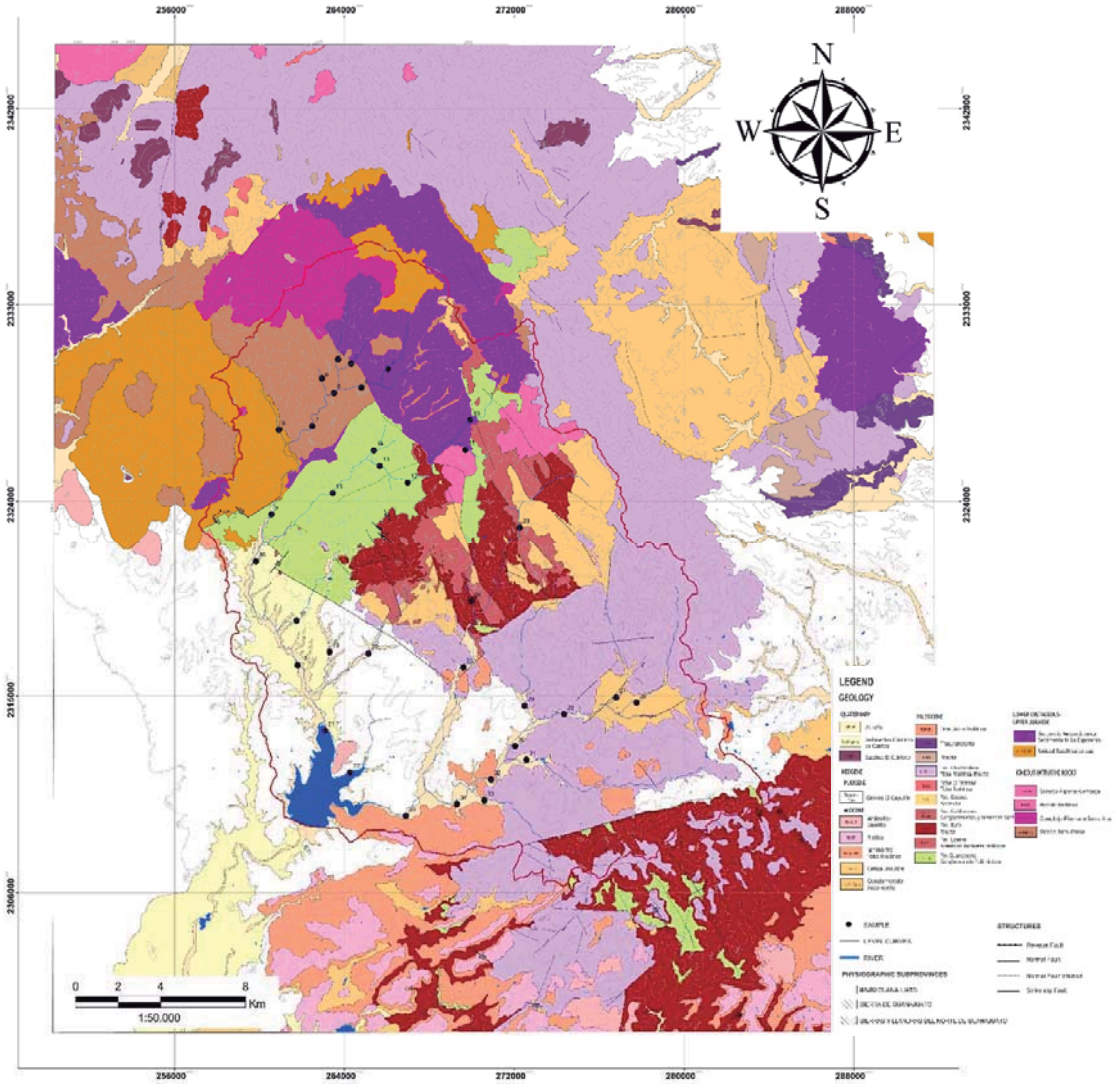

Fig. 1 Location and geological map of the study area. The area is outlined in red

In each station were collected 500 g of sediments sieved with nylon mesh # 18 (1.0 x 1.0 mm aperture), fraction heavy metals are concentrate in this [18], [38], [39], [40], [41]; the sediments were taken in the first 5-15 cm of depth, in the central bars of the streams and previously eliminating the mantle of organic matter, because it causes the attraction of other elements causing anomalies [42]. The samples were dried at room temperature for 48 hours and stored in polyethylene bags.

The morphometric characteristics of the study basin (Table 1) were quantified using ArcGis 10.1.

The mineralogy of the sediments was determined with the technique of X-ray diffraction (XRD), by means of the analysis of adjustment patterns of mineral with the database ICDD-PDF2.

The equipment used was a diffractometer Rigaku Ultima IV, with sweep angle 2θ of 5° to 70°, sweep speed was 2°/min and conditions 30 kV and 30 mA.

The chemical composition of major elements and traces of the sediments was calculated using the X-Ray Fluorescence (XRF) technique, with a spectrometer Rigaku Next CG, Helium atmosphere and conditions of 50 kV and 1.0 mA. Analyzes were done in the Laboratorio de Investigación y Caracterización de Minerales (LICAMM) of the Universidad de Guanajuato; the sediment sample were previously crushed in a porcelain mortar and pulverized in Agatha mortar.

The basal values of the study basin were calculated to identify the existence of anomalous concentrations in the sediments of the area.

The 2σ iterative statistical technique was used to estimate the background values (Fig. 2), which has been used and described by different authors [43], [44]. The grade of contamination of the sediments was calculated (Eq. (1)) by the geoaccumulation

index [45], which categorizes the level of contamination on scale of 1 to 6 (Table 3).

Table 1 Morphometric characteristic

SHAPE CHARACTERISTICS		
Length	Calculate with SIG	
Perimeter		
Area		
Gravelius index	$Cc = 0.282\left(\frac{P}{A^{0.5}}\right)$	Gravelius (1914)
Elongation	$Re = 1.1284\left(\frac{A^{0.05}}{Lc}\right)$	Schumm (1956)
Shape	$F = \frac{A}{Lc^2}$	Horton (1932)
TOPOGRAPHY CHARACTERISTICS		
Hypsometric curve	Generated with toold: Spatial analyst-Hydrology and Reclass	
Hypsometric index	$I = \frac{H_p - H_m}{H_M - H_m}$	Woody & Snell (1960)
Minimum, maximum and mean altitude	Analysis hypsometric curve	
Slope	Generate with tool Spatial Analyst-Surface-Slope	
DRAINAGE CHARACTERISTICS		
Stream type		
Drainage pattern		Zernitz (1932)
Stream order		Strahler (1952)
Length main river	Generate with tool Spatial Analyst-Hydrology	
Length drainage		
Average slope drainage		
Drainage density	$D_d = \frac{L}{A}$	Horton (1932)

$$I_{geo} = log_2\left(\frac{C_s}{1.5 \times B_n}\right) \quad (1)$$

Cs refers to the concentration of the element in the sediments, Bn is the geochemical concentration of this element (reference values) and 1.5 is the correction factor by lithogenic effects, applied to reduce the variations in background values caused by the environment [46].

RESULTS

The hypsometric curve of the study basin (Fig. 3) reflects a basin in a state of equilibrium (maturity phase), which occurs in mountainous systems with cumulative and degrading processes in equilibrium.

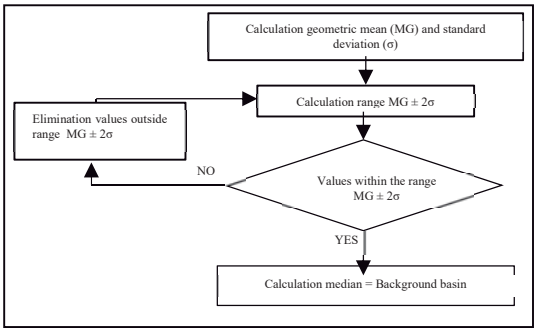

Fig. 2 Determination of background levels

Another important parameter is the slope of the basin (Table 2), it influences directly in erosive capacity; the study basin presents steep mountains in the northern area and towards the south predominance of plateaus, the slope varies between these two regions, but average slope of 19° (Table 3) corresponds to a very steep relief. The variations in the relief of the basin are related to the geology present in the area (Fig. 1), In the southern sector, low slopes are developed for volcanosedimentary rocks, sedimentary rocks and unconsolidated sediments (El Capulín gravels, Canitas clastic sediments, rhyolitic tuffs, among others); while in the northern section the slope increases as the hard rock units (Tuna Mansa granite, La Luz unit basaltic and La Esperanza metavolcanosedimentary sequence). According to [47] the study basin presents nine stream orders (Table 2), reflecting a high grade of branching drainage. The stream order and the high drainage density suggest a drainage well-developed (mature stage), allowing equilibrium between the processes of erosion and sedimentation.

Table 2 Morphometric properties of the Basin

PARAMETERS	UNIT	VALUE	DESCRIPTION
Length	km	27.600	
Perimeter	km	118.467	
Area	km2	489.108	
Size basin			Small
Gravelius index	dimensionless	1.511	Oval oblong to rectangular oblong
Elongation	dimensionless	0.904	Elongated-rounded
Shape		0.642	Moderately flattened
Minimum altitude	masl	1808	
Maximum altitude	masl	2822.000	
Mean altitude	masl	2155.150	Moderate
Hypsometric index	%	34.236	Madure and balanced basin
Slope	grades	19.000	Very inclined
Stream type			Permanent-temporary
Drainage pattern			Dendritic to subparallel
Length main river	km	41.061	
Length drainage	km	8070.572	
Average slope drainage	%	1.014	
Stream order	UND	9.000	High
Drainage density	km/km2	16.501	High

With respect to chemistry, the major elements and traces in the sediments have an average concentration similar to the earth's crust [48], but in some samples the concentrations are higher (Fig 4-5) than those reported [48]; this feature, together with the Ag-Au-Cu-Pb-Zn mineral deposits in the study area (according to [12] the epithermal of low and intermediate sulfuration), leads to the conclusion that the area of study presents natural anomalies, relate values obtained directly with values reported for the crust, would give us inaccurate results.

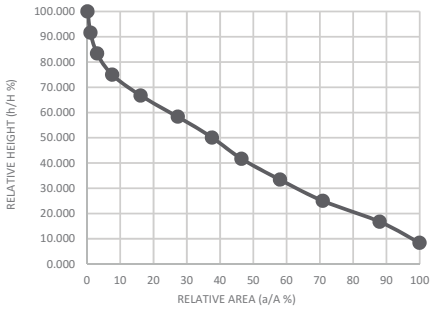

Fig. 3 Hypsometric curve of the study basin

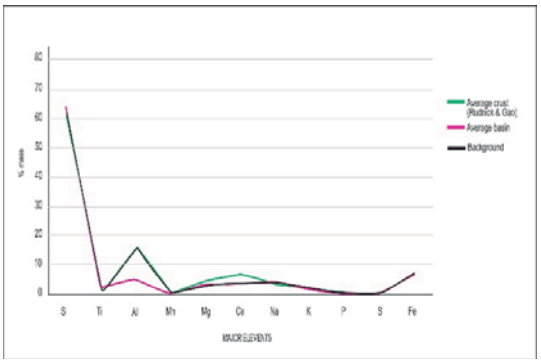

Fig. 4 Comparison values of baseline, average and reported by Rudnick & Gao for major elements

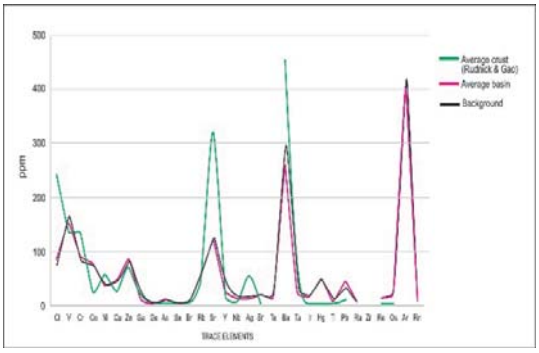

Fig. 5 Comparison values of baseline, average and reported by Rudnick & Gao for trace elements

Table 3 Geoaccumulation index basin

VALUE I_{geo}	CLASS I_{geo}	GRADE OF CONTAMINATION	ELEMENTS
0	$I_{geo} < 0$	No contaminated	
1	$0 < I_{geo} < 1$	No contaminated to moderately contaminated	Co-Cu-Br-Ge-Nb-Ti
2	$1 < I_{geo} < 2$	Moderately contaminated	As-Pb
3	$2 < I_{geo} < 3$	Moderate to heavily contaminted	Sn-Tl
4	$3 < I_{geo} < 4$	Heavily contaminted	Se
5	$4 < I_{geo} < 5$	Heavily contaminted to extremely contaminated	Ta
6	$5 < I_{geo} < 6$	Extremely contaminated	Ir-Hg-Re-Os

CONCLUSIONS

The geographic information systems facilitates the generation of morphological model of the basin from the DEM, help to management of this.

The basin of interest is a particular case of study, due geochemical anomaly with the average crust values, it must be analyzed and studied individually.

Some elements have higher concentrations than the levels of the crust, but comparing these with the background values (calculated basin), their concentrations are not high (except for certain elements such as Hg, which continues to be high).

REFERENCES

[1] Miranda-Avilés, R., Puy-Alquiza, M. J., & Pérez Arvizu, O. (2012). Anthropogenic metal content and natural background of overbank sediments from the mining district of Guanajuato, Mexico. Soil and Sediment Contamination: An International Journal, Vol. 21 (No 5), pp. 604-624.

[2] Ramos Arroyo, Y. R., Serafín Muñoz, A. H., Yánez Barrientos, E., Rodríguez Huerta, I., Wrobel, K., & Wrobel, K. (2013). Natural Decrease of Dissolved Arsenic in a Small Stream Receiving Drainages of Abandoned Silver Mines in Guanajuato, Mexico.Hossain MZ, "For a chapter in a book", Soil Mechics, 4th ed. Vol. 2, Sakai, Ed. Sankeisha: Publisher's Name, Year, pp. 11–60.

[3] Bravo Covarrubias, A., Serafín Muñoz, A. H., Cano Rodríguez, I., Gutiérrez Valtierra, M., Vera, R., Jeanneau, E., & Ramos Arroyo, Y.R. (2015). Spatial and temporal variability of the chemistry of a dam that receives mine drainage. Solución a la problemática del agua en México, Propuesta de jóvenes investigadores, Universidad de Guanajuato, Guanajuato, México.

[4] Cano Rodríguez, I., Gómez Vallejo, F., Ramírez Méndez, V., Martinez Barbosa, P., Rodríguez Rodríguez, E., & Aguilera Alvarado, A. (2000). Determinación de contaminantes en la presa la Purísima y su efecto en el sistema de pozos puentecillas de Guanajuato. International Water Management Institute, Serie Latinoamericana de México #20, pp. 123-133.

[5] García-Flores, M. E. & Zanor, G.A. (2016). Evaluación de la contaminación por elementos traza en sedimentos de la presa La Purísima, Guanajuato. Jóvenes en la Ciencia, Vol. 2 (No 1), pp. 475-479.

[6] Piña, V. (2016). Estudio de la calidad y sustentabilidad del agua subterránea del acuífero Silao-Romita mediante modelo geoestadístico (tesis de pregrado). Universidad de Guanajuato, Guanajuato, México.

[7] Arzola-Torres, D. M. y Li, Y. (2016). Estado de contaminación de arsénico y flúor en el acuífero de Silao-Romita. Jóvenes en la ciencia, Vol. 2 (No 1), p. 1101-1105.

[8] Esparza-Claudio, J. J. (2011). Simulación de flujo y trazado de partículas generadas por un depósito de jales mineros, para el análisis de riesgo en la zona de alta vulnerabilidad del acuífero Silao-Romita, en el municipio de Guanajuato. Tesis de Maestría. Universidad Autónoma Agraria Antonio Narro, Saltillo, Coahuila.

[9] Randall-Roberts, J.A., Saldaña, E., Clark, K.F., 1994, Exploration in a volcano-plutonic center at Guanajuato, México: Economic Geology, 89, 1722–1751.

[10] Martínez-Reyes, J., Vassallo, L.F., Franco, F.J., 1995, Geología y potencial minero de la porción central-poniente del Estado de Guanajuato: Guanajuato, México, Universidad Nacional Autonóma de México, Instituto de Geología, Estación Regional del Centro, Gobierno del Estado de Guanajuato, Secretaría de Desarrollo Económico, Dirección de Promoción Minera, 70 p.

[11] Clark, K.F., Foster, C.T., Damon, P.E., 1982, Cenozoic mineral deposits and subduction-related magmatic arcs in Mexico: Geological Society of America Bulletin, 93, 533–544.

[12] Heald, P., Foley, N.K., Hayba, D.O., 1987, Comparative anatomy of volcanic-hosted epithermal deposits: acid–sulfate and adularia–sericite types: Economic Geology, 82, 1–26.

[13] Antúnez, E.F., 1964, Monografía Histórica y Minera del Distrito Minero de Guanajuato: México, Consejo Nacional de Recursos Naturales no Renovables, Publicación 17-E, 589 p.

[14] Ramos Arroyo, Y. R., Prol Ledesma, R. M., & Siebe Grabach, C. D. (2004). Características geológicas y mineralógicas e historia de extracción del Distrito de Guanajuato, México. Posibles escenarios geoquímicos para los residuos mineros. Revista Mexicana de Ciencias Geológicas, Vol. 21 (No 2), pp. 268-284.

[15] Fernández, V., 1879, Práctica del beneficio de minerales de plata auríferos usado en el Distrito de Guanajuato llamado de patio: La Naturaleza, 4, 1877–1879.

[16] Archivo General de la Nación (1947), expediente 606.1/33. Informe del Gerente General Relativo a las operaciones de la Sociedad Cooperativa Minero-Metalúrgica "Santa Fé de Guanajuato" No 1, S.C.L., Noviembre de 1947. Se realizan pruebas de metalúrgicas para probar la factibilidad del método de flotación en minerals del Distrito Minero de Guanajuato: Dirección del Archivo Histórico Central, 42p.

[17] Posada-Ayala, I. H., Murillo-Jiménez, J. M., Shumilin, E., Marmolejo-Rodríguez, A. J., & Nava-Sánchez, E. H. (2016). Arsenic from gold mining in marine and stream sediments in Baja California Sur, Mexico. Environmental Earth Sciences, Vol. 75 (No 11), p. 1-16.

[18] Rangel-Peraza, J., De Anda, J., González-Farías, F. A., Rode, M., Sanhouse-García, A., y Bustos-Terrones, Y. A. (2015). Assessment of heavy metals in sediment of Aguamilpa Dam, Mexico. Environmental Monitoring and Assessment, Vol. 187 (No 3), p.134.

[19] Marmolejo-Rodríguez, A. J., Sánchez-Martínez, M. A., Romero-Guadarrama, J. A., Sánchez-González, A., & Magallanes-Ordóñez, V. R. (2011). Migration of As, Hg, Pb, and Zn in arroyo sediments from a semiarid coastal system influenced by the abandoned gold mining district at El Triunfo, Baja California Sur, Mexico. Journal of Environmental Monitoring, Vol.13 (No 8), p. 2182-2189.

[20] Aguilar-Ucán, C. A., Montalvo-Romero, C., Ramírez-Elias, M. A., & Barrera, C. G. (2009). Metales pesados en sedimentos del arroyo "La Caleta" de Ciudad del Carmen, Campeche, México: Estudio preliminar. Revista Latinoamericana de Recursos Naturales, Vol. 5 (No 3), p. 232-237.

[21] Miranda-Avilés, R., Puy-Alquiza, M. J. y Caudillo-González, M. (2009). Evidencias estratigráficas y geoquímicas de la variación temporal de sedimentos naturales y antropogénicos en la planicie aluvial del río Guanajuato. Rev. Mex. Cienc. Geol. 26(3), 564-574.

[22] Rodríguez-Meza, G. D., Shumilin, E., Sapozhnikov, D., Méndez-Rodríguez, L., & Acosta-Vargas, B. (2009). Evaluación geoquímica de elementos mayoritarios y oligoelementos en los sedimentos de Bahía Concepción (BCS, México). Boletín de la Sociedad Geológica Mexicana, Vol. 61 (No 1), p. 57-72.

[23] Hernández-Silva, G., Solorio-Munguía, J.G., Maples-Vermeersch, M., Vasallo-Morales, L., Flores-Delgadillo, L., Hernández-Santiago, D., Solís-Valdez, S., Hernández-Anguiano, M.E., Alcalá-Martínez, J.R. (2005). Monitoreo de contaminantes en las cuencas de los ríos Guanajuato, San Juan de Otates y Turbio y su Impacto en el río Lerma, Estado de Guanajuato, México. Boletín del Instituto de Geología de la Universidad Nacional Autónoma de México, Vol.112, 111p.

[24] Villaescusa Celaya, J. A., Flores Muñoz, G., & Gutiérrez Galindo, E. A. (1997). Materiales pesados en fracciones geoquímicas de sedimentos de la región fronteriza de Baja California, México, y California, EUA. Ciencias Marinas, Vol. 23 (No 1).

[25] Hansen, A. M., León, A., & Bravo, L. (1995). Fuentes de contaminación y enriquecimiento de metales en sedimentos de la cuenca Lerma-Chapala. Ingeniería Hidráulica en México, Vol. 10 (No 3), p. 55-69.

[26] Ponce-Velez, G., & Botello, A. V. (1992). Aspectos geoquímicos y de contaminación por metales pesados en la Laguna de Términos, Campeche. Hidrobiológica, Vol. 1 (No 2).

[27] Ortiz Hernández L. E., Chiodi M., Lapierre H., Monod O., Calvet Philippe, 1992, EL arco intraoceánico alóctono (Cretácico Inferior) de Guanajuato – características petrográficas, geoquímicas, estructurales e isotópicas del complejo filoniano y de las lavas basálticas asociadas; implicaciones geodinámicas: Universidad Nacional Autónoma de México, Instituto de Geología, Revista, vol. 9, núm 2, 1992, p. 125- 145.

[28] Martini, M.; Mori, L.; Solari, L. & Centeno-García, E. (2011). Sandstone provenance of the Arperos Basin (Sierra de Guanajuato, central Mexico): Late Jurassic-Early Cretaceous back-arc spreading as the foundation of the Guerrero terrane. The Journal of Geology, Vol. 119 (No 6), p. 597–617.

[29] Martini, M.; Solari, L. & Camprubí, A. (2013). Kinematics of the Guerrero terrane accretion in the Sierra de Gua¬najuato, central Mexico: new insights for the structural evolution of arc–continent collisional zones. International Geology Review, Vol. 55 (No 5), p. 574–589.

[30] Hernández-Laloth, N. (1991). Modelo conceptual de funcionamiento hidrodinámico del sistema acuífero del valle de León, Guanajuato: México, DF, Universidad Nacional Autónoma de México, Facultad de Ingeniería. 1991. Tesis Doctoral, 129 p.

[31] Stein, G.; Lapierre, H.; Monod, O.; Zimmermann, J.L. & Vidal, R. (1993). Petrology of some Mexican Meso¬zoic plutons-sources and tectonic environments. Journal of South American Earth Sciences, Vol. 7 (No 1), p. 1–7.

[32] Botero-Santa, P.A.; Alaniz-Álvarez, S.A.; Nieto-Samaniego, A.F.; López-Martínez, M.; Levresse, G.; Xu, S. & Ortega-Obregón, C. (2015). Origen y desarrollo de la cuenca El Bajío en el sector central de la Faja Volcánica Transmexicana. Revista Mexicana de Ciencias Geológicas, Vol. 32 (No 1), p. 84–98.

[33] Aranda-Gómez, J.J. & McDowell, F.W. (1998). Paleogene extension in the southern Basin and Range Province of Mexico; syndepositional tilting of Eocene Red Beds and Oligocene volcanic rocks in the Guanajuato Mining District. International Geology Review, Vol. 40 (No 2), p. 116–134.

[34] Nieto-Samaniego, A.F.; Alaniz Álvarez, S.A. & Camprubi Cano, A. (2005). La Mesa Central de México: estratigrafía, estructura y evolución tectónica cenozoica. Boletín de la Sociedad Geológica Mexicana, Vol. 57 (No 3), p. 285–318.

[35] Nieto-Samaniego, A.F.; Macías-Romo, C. & Alaniz-Álvarez, S.A. (1996). Nuevas edades isotópicas de la cubierta volcánica cenozoica de la parte meridional de la Mesa Central, México. Revista Mexicana de Ciencias Geológicas, Vol. 13 (No 1), p. 117–122.

[36] McDowell, F., & Clabaugh, S. E. (1981). The igneous history of the Sierra Madre Occidental and its relation to the tectonic evolution of western Mexico. Revista mexicana de ciencias geológicas, Vol. 5 (No 2), p. 195-206.

[37] Demant, Alain. (1978). Características del Eje Neovolcánico Transmexicano y sus problemas de interpretación. Revista mexicana de ciencias geológicas, vol. 2 (No 2), p. 172-187.

[38] Carriquiry, J. D.; Sánchez, A. (1999). Sedimentation in the Colorado River delta and Upper Gulf of California after nearly a century of discharge loss. Marine Geology, Vol. 158 (No 1), p. 125-145.

[39] Morton, A. C. (1985). Heavy minerals in provenance studies. Provenance of arenites. Springer Netherlands. p. 249-277.

[40] Rittenhouse, G. (1943). Transportation and deposition of heavy minerals. Geological Society of America Bulletin, Vol. 54, p. 1725–1780.

[41] Krumbein, W. C. & Rasmussen, W. C. (1941). The probable error of sampling beach sand for heavy mineral analysis. Journal of Sedimentary Research, Vol. 11 (No 1), p. 10-20.

[42] Martínez de la Cruz, M. (2000). Manual para realizar un levantamiento geoquímico de arroyo. (Tesis de pregrado). Universidad de San Luis Potosí, México.

[43] Matschullat, J., Ottenstein, R. and Reimann, C. (2000). Geochemical background—can we calculate it? Environmental Geology, Vol. 39 (No 9), p. 990–1000.

[44] Galuszka, A. (2007). Different approaches in using and understanding the term “geochemical background”—Practical implications for environmental studies. Polish Journal of Environmental Studies, Vol. 16, p. 389–395.

[45] Müller, G. (1969). Index of geoaccumulation in sediments of the Rhine River. Geo Journal. Vol. 2 (No 3), p. 108–118.

[46] Trujillo-González, J. M., y Torres-Mora, M. A. (2015). Niveles de contaminación en tres sectores de Villavicencio, a través del índice de geo-acumulación (I-geo). Orinoquia, Vol. 19 (No 1), p. 109-117.

[47] Strahler, A. N. (1957). Quantitative analysis of watershed geomorphology. Eos, Transactions American Geophysical Union, Vol. 38 (No 6), p. 913-920.

[48] Rudnick, R. L., & Gao, S. (2003). Composition of the continental crust. Treatise on geochemistry, 3, 659 p.

WATER QUALITY IN MEXICAN CARIBBEAN: ANALYSIS OF BENTHIC BIOINDICATORS AND PHYSICOCHEMICAL PARAMETERS OF WATER

Camacho-Cruz Karla[1,2], Ortiz-Hernández Ma. Concepción[1], Sánchez-González Alberto[2], Carrillo-Bibriezca Laura[1] and -Navarrete Alberto de Jesús [1]
[1]Departamento Ciencias de la Sustentabilidad, El Colegio de la Frontera Sur, Chetumal, México**;**
[2]Departamento de Oceanología, Instituto Politécnico Nacional, Centro Interdisciplinario de Ciencias Marinas, La Paz B.C.S., México

ABSTRACT

Pollution of Mexican Caribbean is mainly associated with increase of tourism infrastructure and poor wastewater treatment. Geomorphology and groundwater discharges (GWD) facilitate drag of organic matter, altering the environment. In order to evaluate a water quality and detect possible contributions of contamina-tion by GWD, physicochemical parameters and bioindicators were evaluated in coastal points and cenotes, along Riviera and Costa Maya during October, February and June (2015-2016). According with the results, cenotes had higher concentrations of silicates and nitrates than coastal points. We identify influence of GWD in Caleta Tankah and Chavez and Shambala. Isotopic values showed that enrichment of N in Akumal Bay and Tulum (T2), come from wastewater. The presence of faecal enterococci had overshoot the maximum allowable limit for recreational waters for Costa Maya and Cenote Manatí. The dominance of 2A group of nematodes in Riviera and Costa Maya is related to eutrophic environments. According to the results, Cenote Encantado, Manatí, Akumal, Chávez, and the points of Costa Maya did not comply chemistry or bacteriologically with the standards required by ecological criteria and Mexican norms in this period of study.

Keywords: Water Quality, Stable Isotopes, Nematodes, Nutrients, Mexican Caribbean

INTRODUCTION

In the Mexican Caribbean water quality is threatened by increasing tourism/population development, and impact of natural phenomena [8], [23, 24] and the lack of regulation environmental. This is reflected in a limited sewerage system and the use of septic tanks in poor condition, which leads to filtration of anthropic waste (eg, faecal matter) into the aquifer [2], which flows into coasts through groundwater discharge (GWD). The increase in nutrient concentration along mexican Caribbean coasts [3], [22] has caused environmental deterioration, such as damage to the Mesoamerican Barrier Reef which could affect the state economy.

In the last five years (2010-2015) hotel occupancy in Riviera Maya and Costa Maya grew exponentially; in 2010 highest hotel occupancy (February) was 82.5% (573,478 tourists), while in 2015 it was 90.1%, (730,719 tourists) [24].

Periodic evaluation of water quality by means of bioindicators ($\delta^{15}N$ in *Thalassia testudinum* [14], meiofauna as nematodes and faecal enterococci), variations in physicochemical properties (temperature, salinity, dissolved oxygen, pH, ammonium, nitrates, nitrites, total nitrogen, total phosphorus, orthophosphate and silicates) and also by the location of the GWD through the relationship between silicates and salinity [26], help to understand the state of water quality, generating evidence to support the implement of measures to improve water quality.

The objective of this work was to evaluate the water quality of cenotes and coastal environments through physicochemical data of water column and bioindicators, comparing sites with medium anthropic development: Maya Riviera (Akumal-Tulum) and low: Costa Maya (Mahahual - Xahuaxhol), as well as the location of possible GWD towards the coast. Physicochemical parameters and the faecal enterococci were compared with the permissible standards by Mexican normativity.

METODS

Study Sites

All samplings were made in the months of October 2015, February and June 2016 in 13 sites: ten coastal and three continental (cenotes) (Fig. 1). Nine of the selected sites are cataloged with a medium anthropic impact located in Riviera Maya and four sites with low anthropic impact in Costa Maya [23].

Sample Collection and Processing the Water Chemistry

Physicochemical parameters of water column were measured *in situ* with a Horiba® U-10 multiparameter probe. Water samples were collected manually in triplicate after wave breaking zone, at 1 m depth. Bottles of 500 ml were previously washed with 15% HCl, and rinsed with distilled water. Samples were preserved at 4ºC.
Nutrients were determined according to [27], [7] and [11]. Colorimetric readings were performed in a UV-visible spectrophotometer, SHIMADZU, UV-1700.

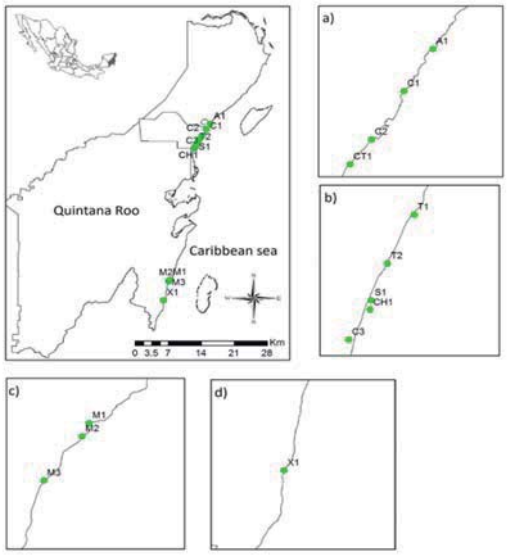

Fig. 1 Location of the study area and sampling sites. a,b) Riviera Maya (Akumal-Tulum); c,d) Costa Maya (Mahahual-Xahuaxhol). A1: Akumal, C1: cenote Manatí, C2: cenote Xcacel, CT1: Caleta Tankah, T1: public beach Tulum, T2: Tulum el Pez, Sh1: Shambala, Ch1 Chávez, C3: cenote Encantado, M1: Mahahual 1, M2: Mahahual 2, M3: Mahahual 3 y Xh1: Xhahuaxol

δ^{15}N in *Thalassia testudinum*

Leaves of *T. testudinum* were collected and placed in ice for preservation. In the lab, the leaves were rinsed with deionized H_20 and scraped to remove epiphytes, then acidified with 10% HCl. All tissues were dried at 60 °C and pulverized. The analyses were measured at the Laboratorio Espectrometria de Masas (LEsMA), CICIMAR IPN using standard elementsl-analyzer isotope-ratio mass spectrometer (EA-IRMS) procedures. The EA was coupled on a Thermo Delta-V plus isotope-ratio mass spectrometer in a continuous-flow mode.

To considering abundance of heavy isotopes with respect to light isotopes, values are defined by the following Eq (1).

Analytical precision of isotopic measurements was <0.2 ‰

$$\boldsymbol{\delta 15N(vs.air) = ((15N/14Nsample/15N/14Nreference) - 1)x1000} \quad (1)$$

Fecal Enterococci

In sterile bottles, water samples were collected (triplicate) after wave break zone, at 1 m depth and preserved at 4ºC. The method recommended by [19] chromogenic substrate [9] was used.

Nematodes

Sediment was collected with PVC core (0.10 m diameter), sediment columns were cut in two depth fractions at 0.05 and 0.10 m. Samples were fixed with formaldehyde (10%). Nematodes were separated manually from the rest of the meiofauna, mounted in anhydrous glycerin, and identified feeding type using a Nikon-brand optical microscope (Eclipse E 100 model) under an increase of 100 x. Nematodes were classified by their oral structure: selective and non-selective deposit feeders (1A, 1B), surface feeders (2A) and omnivores / predators (2B) [29].

Mexican Regulations

Results of fecal enterococci and nutrients were compared with maximum permissible limits established in [4], ecological criterion for the protection of marine / freshwater life and as use of drinking water, [20], Mexican standard for the use of water as a drinking source and [21], norm that regulates maximum number of fecal enterococci in water for recreational use.

Statistical Analysis

To identify the differences or similarities between nutrients concentrations for environment was used a multivariate analysis of variance permutation (PERMANOVA), on the PRIMER 6.I.II & PERMANOVA + 1.0.1 platform. Behavior of nutrients was observed in a multidimensional scaling, data was normalize and using euclidian distances.

RESULTS

Groundwater Discharges and Water Chemistry

The nutrient concentrations (nitrates, ammonium and phosphorus) between continental and coastal bodies differed significantly ($p = 0.0001$, $\alpha < 0.05$),

while, among sites classified with medium and low anthropic impact, no differed significantly ($p = 0.78$, $\alpha < 0.05$). In multidimensional scaling, evident grouping were observed by continental and coastal sites, with the exception of the Caleta Tankah, Shambalá and Tulum Pez, which were grouped with the continental bodies (Fig. 2).

Silicates concentrations were significantly higher in cenotes with an average of 76.03 µM, however the highest was in the Caleta Tankah (100.6 ± 0.09 µM). Sites on the coast, like Shambalá (37.1 ± 1.49 µM) and Chavez (18.8 ± 0.79 µM) had the highest silicates concentrations (Fig. 3).

Fig. 2 Multidimensional scaling, using euclidian distances. Stress 0.1

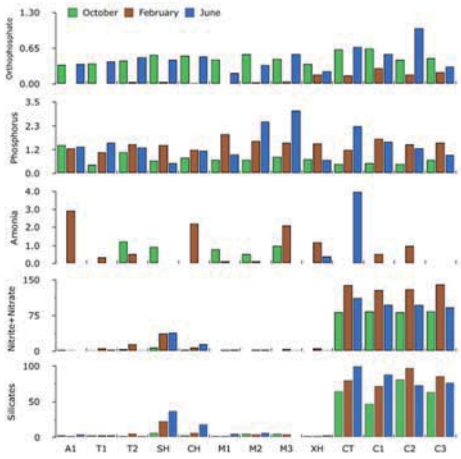

Fig. 3 Concentration of nutrients µM along Riviera and Costa Maya between 2015 and 2016

The highest concentration of NO_3^- + NO_2^- was in cenotes, cenote Encantado registered 140.6 µM, followed by cenote X-cacel (130 µM). Of coastal sites, Caleta Tankah (138.7 µM), Shambala (28.5 µM) and Chavez (14.2 µM) were the highest (Fig. 3). The highest concentrations of ammonium were recorded for the Caleta Tankah (3.98 ± 0.01µM), Mahahual 3 (2.1 ± 0.75µM), Akumal (2.92µM) and Chavez (2.2 ± 1.05µM) (Fig. 3).

Highest concentrations of total phosphorus were in Mahahual 1 (1.93 ± 0.09 µM), Mahahual 2 (2.54 ± 0.44 µM) and Mahahual 3 (3.08 ± 0.16 µM). Cenotes did not present greater than 1.56 µM. Orthophosphates in coastal sites presented an average of 0.31 ± 0.221µM, while in cenotes the mean value was 0.46 ± 0.26 µM (Fig. 3).

$\delta^{15}N$ in *Thalassia Testudinum*

Isotope values of *T. testudinum* are summarized in Table 1. In sites with medium tourist development (Akumal, Tulum public beach, Tulum Pez, Shambala) $\delta^{15}N$ of *T. testudinum* was > 4 ‰. Sites of low development had values of $\delta^{15}N$ < 3 ‰ with the exception of Mahahual 2.

Table 1 *Thalassia testudinum* leaf tissue stable isotope values ($\delta^{15}N$ vs. air), along Riviera and Costa Maya between 2015 and 2016

Localities	October (2015)	February (2016)	July (2016)
A1	5.45	-	2.42
T1	-	4.62	-
T2	4.76	6.11	6.48
Sh1	-	-	4.15
M1	-	0.37	-
M2	1.45	0.72	4.4
M3	0.64	1.1	-
Xh1	0.36	0.95	2.27

Faecal Enterococci

Bacteriological analysis in Riviera Maya showed concentrations <1 NMP / 100 ml, only cenote Manatí showed concentrations of 170 NMP / 100 ml, on October. In Costa Maya, Mahahual 3 showed 410.6 and 320.6 NMP / 100 ml on October and February respectively; Mahahual 1 and Xhahuaxhol recorded levels of up to 160 and 181 MPN / 100 ml, during October and June respectively.

Nematodes

During the sampling periods 6,568 nematodes were obtained. All feeding types were present in both areas of Mexican Caribbean.

Surface feeders (2A) dominated in all the sampling. Along the sities in Riviera Maya surface feeders represented with 38 % and Costa Maya with

42 %, deposit feeders and predator represented with less percentage.

Applied Regulations

Based on Mexican ecological standards and criteria, during this study coastal sites such as Chávez, Akumal, the Costa Maya (Mahahual-Xahuaxhol) and the cenote Encantado, Xcacel and Manatí were exceeded maximum permissible limits established by [4], [20] and [21].

DISCUSSION

Contrary to our expectations, nutrient concentrations between zones of low and medium anthropic impact did not show significant differences, probably because of the anthropic effect begins to be similar, or the load of leachates coming from different areas was a factor that impacted the similar way during the present study.

Groundwater Discharge and Nutrients

The concentrations of silicates and NO_3^- + NO_2^- detected in cenotes indicate that groundwater is enriched with siliceous and organic matter. Possibly the latter has anthropic origin which influences flow and increase of nitrogen from continental zone to coast. In Mexican Caribbean the GWD has been characterized by low concentrations of salinity, temperature and high concentrations of nitrates and silicates [18], [12], [22].

In particular, the coastal site of Caleta Tankah showed high concentrations of silicates and NO_3^- + NO_2^- low temperature and salinity, similar to the effect caused by the GWD. In places like Shambala and Chavez a small decrease in temperature and salinity was detected with high concentrations of silicates and NO_3^- + NO_2^-, in these two sites a more exhaustive sampling is recommended since the field observations showed the presence of GWD, however, sampling was hampered by coastal dynamics.

On the other hand, in cenotes the high concentrations of inorganic nitrogen dominated by NO_3^- also is influenced by several processes such as: the fixation of terrestrial nitrogen, precipitation, change of land use, and the refills of untreated wastewater, in addition of the effect of aerobic processes [17,18] In aquatic systems, the excess of N with respect to their assimilation capacity causes a rapid deterioration in the water quality mostly for an exponential growth of primary producers, such as microalgae.

In cenotes of Mexican Caribbean nitrate levels have increased considerably, values > 5 μM represent an excess [5]. In this study, the cenotes showed concentrations > 100 μM; for example in February, the cenote X-cacel showed high levels of nitrates (130.6 μM), and ammonium (0.998 μM), similar case to cenote Manatí, which also showed 50 NMP /100 of fecal enterococci. Suggesting that tourist use or filtration of contaminated groundwater are modifying water quality.

In costal sites like Akumal registered ammonium concentrations similar to those detected by [12], evidencing a continuous flow of nutrients to environment. In Costa Maya, the presence of ammonium related to high concentrations of fecal enterococci (160-410 NMP/100), indicate an enrichment through untreated wastewater.

Moreover concentration of phosphorus in karst systems it tends to be relatively low because $CaCO_3$ adsorbs phosphate molecules, limiting their availability in environment [14].

During February phosphorus on coastal sites of Riviera Maya showed an increase with respect to previously recorded by [6]. These concentrations are enough to generate algal blooms [16] and indicate that a phosphorus concentration> 0.1 μM can lead to a deterioration in water quality due to environmental eutrophication.

$\delta^{15}N$ in *Thalassia Testudinum*

The concentrations of $\delta^{15}N$ was different between sites with medium tourism activity compared to the sites of low tourism. Analysis allows us to deduce source of this element considering that primary producers leave an isotopic ratio of $\delta^{15}N$ (-1-0 ‰), treated wastewater (10-22 ‰) and untreated (4-9 ‰) [1], [18].

Bahia Akumal, Tulum, Shambala and Mahahual 2, showed that the isotopic composition of $\delta^{15}N$ in leaves was higher 4 ‰, suggesting a nitrogen enrichment via untreated wastewater, similar to that recorded in previous works [17, 18], [23]. In Akumal bay it is likely that the N load will be significantly affected not only by the climatic season, but also by the effect of tourist seasons and leachate. During this work in October, concentrations were detected that indicated an enrichment by untreated wastewater, that differ from the sampling season with the studies by [23]. The use of the bay as a recreational area has been increasing due the bay went from receiving 30 thousand people to more than 150 thousand a year [25], reaching the limit of the load capacity in this coastal system (per. com. Dr. Héctor Lizárraga Cubedo, Director of the Ecological Center of Akumal).

Nematodes

Free-living nematodes are one of the best represented groups (60-90%) in benthos, composition of community is influenced mainly by the type of sediment and food availability [28], which means that

the distribution of this group will be affected by environmental disturbances, like nutrient charge.

Based on classification proposed by [29], which related buccal morphology of organisms and type of environment, group 2A (surface feeders) dominated in both regions, Rivera and Costa Maya, in this case the abundance of this group allows to infer that environment is enriched with organic matter.

Dominance of surface feeder nematodes (2A) has been related to eutrophic environments [5], reflected in the high concentrations of nitrogen and phosphorus detected in coastal waters (Fig. 2). Dominance of group 2A can also be influenced by coastal swell generating the removal sediment in addition to the entry of water rich in phosphate compounds, which favor algal blooms [10], leaving food available for these organisms.

CONCLUSIONS

In conclusion, behavior of physicochemical parameters and stable isotopes of nitrogen showed an increase in sites such as Cenote Manatí, Akumal and Tulum. This trend was registered in a period of 10 years, inferring deterioration in the water quality. Coastal sites such as Chávez, Akumal, the Costa Maya (Mahahual-Xahuaxhol) and cenote Encantado, Xcacel and Manatí require attention, since they exceeded the maximum limits allowed by water quality standards.

The high concentrations of nutrients and the presence of four types of feeder nematodes occurred in both areas of Mexican Caribbean, reflect the lack of sanitary regulation, since hotels and restaurants along the coast could be contributing significant amounts of organic matter to the aquifer through their discharges of untreatreated wastewater.

In contrast to what was expected, the classified sites with medium and low anthropic impacts showed no differences in water quality. This must be highlighted because it can infer that deterioration of water quality is influenced not only by the specific effect of tourism or the local population, but also the leachates resulting from the rest of the region.

On the other hand, the GWD detected in Caleta Tankah, Chavez and Shambala, were the coast sites with the highest concentrations of inorganic N, evidencing the close relationship with groundwater loaded with organic matter and its importance as a source of nutrients.

It is important to mention that in Mexican Caribbean flow of tourism can generate a significant effect in the increase of certain nutrients to the environment. That is why it is recommended not only to conduct studies based on climatic variations, but also to consider effect of tourist seasons.

Also the use of integrative variables resulted useful to determinate the conditions of water quality.

ACKNOWLEDGEMENTS

This work was supported by Consejo Nacional de Ciencia y Tecnología (CONACYT) through a master's scholarship. Support was received from the SIP-IPN 20160046 project of Instituto Politécnico Nacional (CICIMAR-IPN). We also thank Adriana Zavala, Alejandro Arana and Ángel Ruvalcaba for their support in the field and laboratory work.

REFERENCES

[1] Aravena R, Evans ML y Cherry JA. Stable isotopes of oxygen and nitrogen in source identification of nitrate from septic systems, Groundwater, Vol. 31, Mar. 1993, pp. 180–186. DOI: 10.1111/j.1745-6584.1993.tb01809.x

[2] Beddows PA, Smart PL, Whitaker FF, Smith SL. Density stratified groundwater circulation on the Caribbean coast of Yucatan peninsula, Mexico J. Hydrol. Vol. 346, Jan. 2002, pp. 18–32 10.1016/j.jhydrol. 2007.08.013.

[3] Carruthers TJ, Van Tussenbroek BI y Dennison WC. Influence of submarine springs and wastewater on nutrient dynamics of Caribbean seagrass meadows. Estuar. Coast. Shelf.,Vol. 64, Apr. 2005, pp. 191–199. 10.1016/j.ecss.2005.01.015.

[4] Criterios Ecológicos de Calidad de Agua. CE-CCA-001-89. Acuerdo en el que se establecen los criterios Ecológicos de Calidad de Agua. Comisión para la Cooperación Ambiental. DOF. 13 de diciembre de 1989.

[5] De Jesús-Navarrete A y Herrera-Gómez J. Vertical distribution and feeding types of nematodes from Chetumal Bay, Quintana, Roo, Mexico. Estuaries, Vol. 6, Dec. 2002, pp. 1131-1137.

[6] De la Laza-Espino G, Hernández-Pulido S, Penié-Rodríguez I y Gómez-Rojas JC. Calidad del agua de las playas del municipio de Solidaridad. Medio Ambiente Turismo y Sustentabilidad, Vol. 2, Jun. 2006, pp. 25–43.

[7] Durán AH. Manual de microtécnicas para nutrientes. El Colegio de la Frontera Sur, Chetumal, México 2008.

[8] Enfield DB y Mestas-Nunez AM, "Global modes of ENSO and non-ENSO SST variability and their associations with climate", El Niño and the Southern Oscillation: multiscale variability and global and regional impacts. Cambridge, UK, Cambridge University Press, Ed. Diaz HF y Markgraf V., 2000, pp. 89–112.

[10] Enterolert. Defined Substrate Technology, DST and Quanti-Tray are trademarks or registered trademarks of IDEXX Laboratories, Inc. or its affiliates in the United States and/other countries, 2013.

[11] Escobar E, Mass M, Alcocer Durand J, Azpra Romero E, Falcón Álvarez LI, Gallegos García A, García FJ, García`Oliva F, Jaramillo V, Lecuanda Camacho R, Magaña V, Martínez`Yrízar A, Muhlia VA, Rodríguez Sobreyra R y Zavala-Hidalgo J "Diversidad de procesos funcionales en los ecosistemas", Capital natural de México, CONABIO, México, Ed. H Cotler, O Masera y P Moreno-Casasola, 2008, pp. 161-189.

[12] Hansen HP y Koroleff F. "Determination of nutrients", Methods of seawater analysis Wiley, Online Library, Ed. Grasshoff K, Kremling K y Ehrhardt M, 1983 pp. 159–228. 10.1002/9783527613984.
Hernández-Terrones LM, Rebolledo-Vieyra M, Merino-Ibarra M, Soto M, Le-Cossec A y Monroy-Ríos E. Groundwater pollution in a karstic region (NE Yucatan): baseline nutrient content and flux to coastal ecosystems. Water Air. Soil. Poll, Vol. 218, Jun. 2011, pp. 517–528. https://doi.org/10.1007/s11270-010-0664-x

[13] Hernández-Terrones LM, Ortega-Camacho DY, Nava-Ruíz VM, Sánchez-Navarro RP y Iván-Penié S. Reporte Final-Etapa II. Red de monitoreo de calidad de aguas naturales en la microcuenca de Tulum. Segunda etapa. Instrumentación y validación de la red de monitoreo de calidad de agua en los cuerpos naturales de agua continental y marino costero en la microcuenca Tulum. Centro de Investigación Científica de Yucatán, A.C. Unidad de Ciencias del Agua. Feb. 2013. 37 pp.

[14] König C. Addition to M. Cavolini's treatise on *Zostera oceanica* L. Ann. Bot., Vol. 2, 1805, pp. 91–97.

[15] Lapointe BE, O'Connell JD y Garrett GS.. Nutrient couplings between on-site sewage disposal systems, groundwaters, and nearshore surface waters of the Florida Keys. Biogeochemistry, Vol. 10, 1990, pp. 289–307

[16] Lapointe BE. Nutrient thresholds for bottom-up control of macroalgal blooms on coral reefs in Jamaica and southeast Florida. Limnol. Oceanogr., Vol. 42, 1997, pp. 1119-1131. 10.4319/lo.1997.42.5_part_2.1119

[17] Mutchler T, Dunton K, Townsend-Small A, Fredriksen S. y Rasser M. Isotopic and elemental indicators of nutrient sources and status of coastal habitats in the Caribbean Sea, Yucatan Peninsula, Mexico. Estuar. Coast. S, Vol. 74, Jun. 2007, pp. 449–457. 10.1016/j.ecss.2007.04.005

[18] Mutchler T, Mooney RF, Wallace S, Podsim L, Fredriksen S y Dunton KH, "Origins and fate of inorganic Nitrogen from land to coastal ocean on the Yucatan península, Mexico", Coastal Lagoons. Critical habitats of environmental change. Ed. Kennish MJ y Paerl HW, Taylor & Francis Group, Boca Raton, Florida, EUA. 2010, pp. 283–305.

[19] Norma Oficial Mexicana Secretaria de Salud NOM-210-SSA-2002. Productos y servicios. Agua y hielo para consumo humano, envasados y a granel. Especificaciones sanitarias. Diario Oficial de la Federación. 12 de sept del 2002.

[20] Norma Oficial Mexicana Secretaria de Salud NOM-127-SSA-1994. Salud ambiental, agua para uso y consumo humano-Límites permisibles de calidad y tratamientos a que debe someterse el agua para su potabilización. Secretaria de Salud. Diario Oficial de la Federación. 30 de nov de 1995.

[21] Norma Mexicana Secretaria de Economía NMX-AA-120-SCFI-2016. Que establece los Requisitos y Especificaciones de sustentablidad de Calidad de Playas, 2016.

[22] Null KA, Knee KL, Crook ED, de Sieyes NR, Rebolledo-Vieyra M, Hernández-Terrones L y Paytan A. Composition and fluxes of submarine groundwater along the Caribbean coast of the Yucatan Peninsula. Cont. Shelf. Res, Vol. 77, Jun. 2014, pp. 38–50. 10.1016/j.csr.2014.01.011.

[23] Sánchez A, Ortiz-Hernández MC, Talavera-Sáenz A y Aguíñiga-García S. Stable nitrogen isotopes in the turtle grass *Thalassia testudinum* from the Mexican Caribbean: Implications of anthropogenic development. Estuar. Coast. S., Vol. 135, Feb. 2013, pp. 86–93. http://dx.doi.org/10.1016/j.ecss.2013.01.021.

[24] SEDETUR. Indicadores Turísticos. [en línea] web:http://192.185.48.194/~argimx/estadisticas/indicadores/2014/Indicadores%0Turisticos%20Septiembre%202014.pdf. 10/02/15.

[25] SEMARNAT. Estudio técnico justificativo área de refugio para proteger especies marinas denominada bahía de Akumal, Quintana Roo. 2015, pp. 1–41.

[26] Smith SV, Camacho-Ibar V, Herrera-Silveira JA, Valdés D, Merino DM, Buddemeier RW. "Quantifying groundwater flow using water budgets and multiple conservative tracers",. Mexican and Central American coastal lagoon systems: Carbon, Nitrogen, and Phosphorus fluxes (Regional Workshop II), Ed. Smith SV, Marshall JI, Crossland y Crossland CJ. LOICZ Reports & Studies, Texel, The Netherlands, 1999, pp. 96–105.

[27] Strickland JDH y Parsons TR. A practical handbook of seawater analysis. Fish. Res Board Can. Bull, Vol. 167, 1968, pp. 127–139.

[28] Varela`Benavides I. Las comunidades de nemátodos como indicadores ambientales. Tecnología en Marcha, Vol. 31, 2013, pp. 30-37.

[29] Wieser T. Die Beziehung zwischen Mundhohlengestalt, Emahrungsweisw und Vorkommen bei freilebenden marine Nematoden. Ark. Zool, Vol. 4, 1953, pp. 439-448

IDENTIFICATION OF ENVIRONMENTAL COVARIABLES THAT INFLUENCE GULLY FORMATION IN THE MIXTECA REGION

Toledo-Medrano María Lorenza [1], Fernández-Reynoso Demetrio S. [1], Martínez-Menez Mario R.[1], Rubio-Granados Erasmo[1], and García-Rodríguez José Luis[2]
[1]Hidrociencias, Colegio de Postgraduados, México, [2]Universidad Politécnica de Madrid, España.

ABSTRACT

This work identifies, through multivariate analysis, environmental covariables related to gully formation in the Mixteca region of Oaxaca State. There were identify covariables reported in the literature associated to gully formation and by statistical analysis were discriminate those covariables with high correlations among them. From this process were selected: distance to geological faults, distance to volcanic peaks, slope, vertical curvature, horizontal curvature, topographic position index, slope length, topographic index of humidity, population density and NDVI. On these covariables, the Principal Component Analysis was applied and Supervised Classification was made on six components (condensing 96.7% of data). In order to validate the areas classified as susceptible for gully formation, with a probability greater than 50%, in Google Earth were verified incidence of gully erosion. The reliability of the resulting map, based on absence and presence of gullies, for a buffer radio of 15 m, 50 m, 100 m, and 150 m it was 96.2% 83.4%, 81.7% and 77.9%, respectively. From this work, it was concluded that the covariables with greater influence in gully formation in the study area, in order of importance, were: distance to geological faults, distances to volcanic peaks, topographic index of humidity, NDVI, land slope and population density.

Keywords: Maximum Likelihood, Multivariate Analysis, Monitoring Points, Elevation Models.

INTRODUCTION

Gullies are advanced forms of erosion where the detached soil particles produce low water quality and alteration of the hydraulic properties of downstream infrastructure, such as sedimentation of channels and siltation on reservoirs [20]. Gullies result from anthropogenic activities, such as overgrazing of grasslands, agriculture without runoff control, expansion of the agricultural frontier on slopes and deforestation [20].

The variables intervening in gully formation are anthropic and physical. Among the anthropic ones, overgrazing result from high animal charge in the ecosystems; agriculture expansion frontier on steep slopes; poor management of cultivated land; and deforestation [17]. According to [19] and [16], among the physical variables influencing gully erosion are: geology, climate, soil properties, topography, hydrology, land use, vegetation and crop management. For geological variables, the parental material stands out [16], among climatic factors are those related to distribution, intensity and magnitude of extreme rain events [20]; [17]; edaphic, related to the spatial distribution of physical and mechanical soil properties [3]; topographic, related to speed and concentration of runoff, such as slope orientation, terrain curvature, topographic humidity index, topographic position index, length and grade of slope [13] and [23]; hydrological, in relation to the size and shape of the basin [2].

The multi-criteria analysis allows to analyze the covariables influencing gully erosion [24] and the supervised classification, through main components analysis, categorizes statistically layers of information according the classes observed in the field. This method starts by defining categories, outlining the distribution of the sampling sites and visiting such locations [5].

According to [6], the ecosystems of the Mixteca Alta experienced a series of transformations from the late Pleistocene to the Holeocene. After the Spanish conquest, the area has experienced deforestation, overgrazing with goats [15] and expansion of the agricultural frontier; alteration that have caused extensive problems of gully erosion in the region. Given the advanced stage of gully erosion that suffer the soils of the Mixteca, the present work aims to identify the main environmental covariates that influence their formation and identify susceptible areas for their formation through environmental covariates. For this purpose, the results of the multivariate analysis (Principal Components Analysis) and the supervised classification were validated using field observations.

METHODOLOGY

The study area is located northwest of the state of Oaxaca and covers 39.3% of the Mixteca Oaxaqueña. The work area covers 6,167.5 km^2 and it

is located between the geographic coordinates 16° 55' 32.46" and 18° 7' 2.74" north latitude and 97° 58' 13.35" and 97° 01' 7.42" west longitude (Fig. 1).

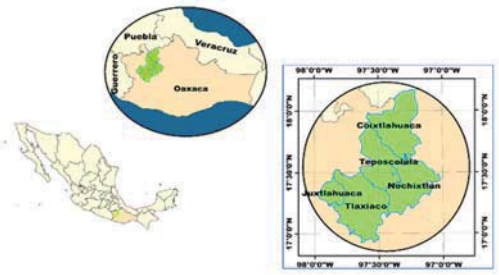

Fig. 1 Geographic location of the study area

The study area is located in the physiographic province known as *Sierra Madre del Sur* [7] originated by the collision between the Cocos and North America tectonic plates, generating the uplift of the sierra and great geological complexity in the region.

According to [22] the study area, in chronological order, the oldest rocks are from the Precambrian and cover 4.3% of the surface. During the Paleozoic were conformed lithologies of polygenic conglomerates such as shale-sandstones, sandstones-shales and limestone-shales; which cover 0.6% of the study area.

The 31.2% of the area has a Mesozoic origin and is composed by limestone, limestone with dolomite, limestone-shale, marge-limonite, shale-limestone, sandstone-shale, sandstone and andesitic tuff. During the recent period (Cenozoic era), 63.8% of the lithology was formed by volcanic eruptions and alluvial removal from andesitic tuff, andesitic-sandstone tuff and polygenic-sandstone conglomerates. All these volcanic materials have been accumulated in the lower parts of the region due to the erosion produced in the upper lands.

According to SGM [22] in the study area are at least 15 stratigraphic formations, however, the Tamazulapam formation (39.72% of the region) is controlled mainly by the fault of the same name and a long this line is where the largest concentration of gullies are observed. According to [9] the study area has following climates: temperate with rain in summer (74.1%), dry (17.06%) and semi-hot (8.83%). The soils present in the work area [8] are leptosols (38.18%), luvisols (25.13%), phaeozem (15.60%), regosols (11.31%), vertisols (5.44%), cambisols (3.66%), gleysols (0.42%) and fluvisols (0.11%). Among the main land use and vegetation covers [26] are grassland (20.99%) with important gully erosion problems, oak forest (19.11%), pine-oak and pine oak forest (16.60%), agriculture (12.92%), and bushes (12.12%).

The methodology began with a bibliographic review of the environmental covariables that influence the formation of gullies, thus, the covariables selected for analysis were ten: slope of the terrain (PEN), according to [4]; vertical or profile curvature (CV) and flat or horizontal curvature (CH), according to Moore [16]; slope length (LP), according to Moore [16]; topographic position index (IPT), as indicated [25], topographic humidity index (ITH); distance to peaks (DP) corresponds to the Euclidean distance measured from ridges generated by IPT; distance from Tamazulapam fault (DF); normalized difference vegetation index (NDVI); and population density (D) based on the 2010 population census [11].

In order to obtain these environmental covariates, for the study area was integrated a geographic information system with the following basic information: digital elevation model [10], soil distribution [8], geology units [22], climate data [11], physiography [7], vegetation and land use polygons [26], population locations [11], satellite images, and field surveys. The ERMEX system receiving station provided three images of the Spot 7 satellite (two for January 29, 2015 and one for November 4, 2015) and three from Spot 6 (for February 16, 2015), which were corrected by radiance and reflectance with the Top of the Atmosphere method. In the field, were visited 503 training points and were generated its training polygons in Google Earth Pro 6.0.

Each covariate was scaled (between 0 - 250) and its impact on gully formation was weighted through Principal Component Analysis (PCA). The PCA simplified the information from the original ten layers, into six main components. These components were used to identify, based on the training areas and the maximum likelihood method, the probability of presence of gullies on each pixel. According to Rossiter recommendation [21] the results validation had a density of 1.1 inspection points per km^2, in total were analyzed 289 random points. In order to observe the percentage of gully coverage for several distances, from the predicted point, were analyzed three concentric areas with radios of 50, 100 and 150 m (Fig. 2).

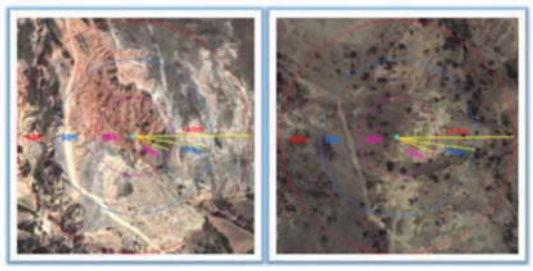

Fig. 2 Concentric areas for gully verification

RESULTS AND DISCUSSION

Based on 503 training areas, according to the magnitude of each covariate, following is described where gully erosion occurs.

Slope (PEN): in the study area gullies are observed on slopes between 1 and 77%, but more frequently in the range 2.5 to 6.5% (29.16%) and in the interval 7.5 to 22.5% (51.57%). The lower slopes are associated to entrenchments in the vicinity of intermontane valleys and the higher gullies are located in hillsides composed of residual materials. For this covariate, it is reported [18] for central Mexico that gullies are usually developed on slopes between 2 and 8%.

Horizontal Curvature (CH): in the area gullies are located between -4.75 and 5.65 (adim.), more frequently in the ranges from -1.75 to -0.45 (32.7%) and between 0.05 and 1.75 (64.5%). In general, the negative range corresponds to convergent flows associated with areas nearby valleys where currents are generated with greater accumulation of flow and bigger erosive potential, on the other hand, positive curvatures are linked to divergent flows like conical topographies (volcanic) of steeper slopes.

Vertical or profile curvature (CV): gullies are observed in vertical curvatures between -3.4 and 3.45; mainly in the range -0.75 to -0.05 (27.15%) and from 0.05 to 1.05 (68.49%). The negative range indicates that flow velocity increases as it descends, which generates flows with greater potential to cause erosion on gullies beds. On the other hand, the positive values are related to gullies located in areas where sedimentation is the dominant process, that is, they are located in the vicinity of alluvial valleys.

Slope length (LP): in the study area gullies occur on slopes lengths from 0 to 1,300 m, but mainly between 10 and 30 m (22.18%) and ranges varying from 35 to 110 m (33.52) %. In general, it is observed that the lower range corresponds to areas conformed by alluvial deposits and the greater lengths are associated to hillside terrains.

Topographic Position Index (IPT): it was found that gullies are mainly located for TPI> 1 and TPI <1, that is, in ridges (49.69%) and in intermontane valleys (42.22%), respectively. Thus, gullies occur mainly in the crests conformed by residual materials of volcanic tuff and nearby intermontane valleys where the runoffs produce, in previously deposited alluvial materials, entrenchments.

Topographical moisture index (ITH): it was found that gullies occur between 0 and 14 $m^2\ m^{-1}$ °; but mainly between 0.0 and 2.0 $m^2\ m^{-1}$ ° (42.43%); which are related to average accumulations of water, moderate slopes and residual materials of volcanic tuff. Also are observed between 2.0 and 7.0 $m^2\ m^{-1}$ ° (56.64%), specifically in areas with greater accumulations of water, lower slopes and alluvial materials; as happens in the periphery of the intermontane valleys.

Distance to peaks (DP): gullies in the study area are found at distances, to the nearest topographic peaks, from 0 to 1,300 m, however are concentrated at distances between 100 and 400 m (46.91%) and between 500 and 900 m (29.66%). Thus, gullies closer to topographic peaks are associated with residual materials surround ancient volcanic structures, and the farthest ones to alluvial deposits around intermontane valleys.

Distance to faults (DF): in the area of study gullies are located between 0 and 12,000 m from Tamazulapam fault. The highest frequency occurs between 0 and 4,000 m (49.87%), followed by the range from 4,000 to 10,000 m (45.87%). Therefore, gullies closest to the fault are associated with greater volcanic activity and the most distant to the formation of alluvial valleys. In has been observed [12] that failures closeness contributes on soil masses instability.

Normalized Difference Vegetation Index (NDVI): gullies show NDVI values between -0.54 and 0.29, occurring mainly in a range between -0.16 and 0.2 (99.02%), that is, on bare soil [14] where it is difficult to establish vegetation [1].

Population Density (D): it was found that gullies are located in places with densities between 0 to 170 inhabitants per km^2, distributed mainly in the ranges 5 - 30 inhabitants per km^2 (60.91%) and 30 - 70 inhabitants per km^2 (31.40%). Low population densities are for gullies located in sites of harder access and thin soils, on the other hand, gullies located in places with higher densities correspond to deeper soils, as occurs around alluvial valleys.

Environmental covariates on gully erosion

The covariance matrix, resulting from Principal Component Analysis (PCA), shows through its diagonal (Table 1), in order of importance, that distances to the Tamazulapam fault has mayor variability (55.8%), followed by the distance to peaks (12.3), topographic humidity index (11.1%), NDVI (9.0%), slope (5.0%), topographic position index (2.8%), population density (1.5%), slope length (1.3%)), vertical curvature (0.6%) and horizontal curvature (0.5%). This implies that DF, DP, ITH, NDVI explain 88.2% of information's variability, in other words, they contribute the most on results.

The correlation matrix (Table 2) shows that the vertical and horizontal curvature have high correlation (0.73), this means that one of them can be withdraw without altering significantly the results. Between slope length and topographic humidity index, there is an intermediate correlation (0.52), because the moisture index considers the shape and length of the slope to model water concentration.

Table 1 Covariance Matrix from PCA

Covariable	CH	CV	D	DF	DP	ITH	LP	NDVI	PEN	ITP
CH (Adim.)	15.14	11.87	-0.01	0.00	-2.79	-23.19	-6.12	3.02	-5.24	12.52
CV (Adim.)	11.87	17.68	0.01	-0.38	-0.99	-26.81	-8.00	2.28	-1.48	8.96
D (hab km^{-2})	-0.01	0.01	42.86	15.45	-1.11	5.62	-1.34	2.51	-5.07	-0.37
DF (m)	0.00	-0.38	-15.45	1590.44	-10.34	-17.74	1.70	44.64	27.83	0.60
DP (m)	-2.79	-0.99	-1.11	-10.34	349.72	32.37	14.53	-22.28	-13.56	-40.53
ITH (m^2 m^{-1} °)	-23.19	-26.81	-5.62	-17.74	32.37	317.26	56.79	-9.97	-20.56	-45.25
LP (m)	-6.12	-8.00	-1.34	1.70	14.53	56.79	37.04	-1.64	1.22	-14.97
NDVI	3.02	2.28	2.51	44.64	-22.28	-9.97	-1.64	256.60	-0.10	9.51
PEN (%)	-5.24	-1.48	-5.07	27.83	-13.56	-20.56	1.22	-0.10	143.48	-13.82
IPT (Adim.)	12.52	8.96	-0.37	0.60	-40.53	-45.25	-14.97	9.51	-13.82	79.31

Table 2 Correlation matrix from PCA

Covariable	CH	CV	D	DF	DP	ITH	LP	NDVI	PEN	IPT
CH (Adim.)	1.0	0.73	0.00	0.00	-0.04	-0.33	-0.26	0.05	-0.11	0.36
CV (Adim.)	0.73	1.0	0.00	0.00	-0.01	-0.36	-0.31	0.03	-0.03	0.24
D (hab km^{-2})	0.00	0.00	1.0	0.06	-0.01	0.05	-0.03	0.02	-0.06	-0.01
DF (m)	0.00	0.00	0.06	1.0	-0.01	-0.02	0.01	0.07	0.06	0.00
DP (m)	-0.04	-0.01	-0.01	-0.01	1.0	0.10	0.13	-0.07	-0.06	-0.24
ITH (m^2 m^{-1} °)	-0.33	-0.36	0.05	-0.02	0.10	1.0	0.52	-0.03	-0.10	-0.29
LP (m)	-0.26	-0.31	-0.03	0.01	0.13	0.52	1.0	-0.02	0.02	-0.28
NDVI	0.05	0.03	0.02	0.07	-0.07	-0.03	-0.02	1.0	0.00	0.07
PEN (%)	-0.11	-0.03	-0.06	0.06	-0.06	-0.10	0.02	0.00	1.0	-0.13
IPT (Adim.)	0.36	0.24	-0.01	0.00	-0.24	-0.29	-0.28	0.07	-0.13	1.00

The eigenvalues of each component provide the percentage of variation that explains the amount of original data, this information was useful to select the number of principal components for clustering. The eigenvectors, generated by PCA (Table 3), show the covariates with higher weight over each component, thus, for component one (PC1) the dominant covariate is distance to Tamazulapam fault; for PC2 and PC3 are distances to peaks and topographic index of humidity, for PC4 it corresponds to NDVI, for PC5 is the slope, for PC6 the topographic position index, for PC7 the population density, for PC8 the length of the slope, for PC9 the vertical and horizontal curvatures follow by length of the slope, and for PC10 the horizontal and vertical curvatures.

Table 3 Eigenvectors Matrix from PCA

Covariable	Principal Components (PC)									
	1	2	3	4	5	6	7	8	9	10
CH (Adim.)	0.00	0.05	0.06	0.01	0.07	0.14	0.02	0.23	0.59	-0.75
CV (Adim.)	0.00	0.05	0.07	0.01	0.04	0.09	0.03	0.35	0.66	0.65
D (hab km^{-2})	0.01	-0.01	-0.02	0.01	0.05	-0.03	0.99	-0.13	0.03	0.00
DF (m)	1.00	-0.02	0.00	-0.03	0.02	0.00	-0.01	0.00	0.00	0.00
DP (m)	-0.01	-0.74	0.62	0.20	-0.01	0.12	0.01	0.00	-0.03	0.00
ITH (m^2 m^{-1} °)	-0.01	-0.59	-0.75	0.02	-0.02	0.20	0.01	0.19	0.00	0.00
LP (m)	0.00	-0.13	-0.13	0.01	-0.06	-0.06	-0.13	-0.86	0.45	0.05
NDVI	0.03	0.17	-0.11	0.98	-0.04	-0.02	-0.01	0.00	-0.01	0.00
PEN (%)	0.02	0.07	0.04	-0.04	-0.96	0.24	0.06	0.03	0.01	-0.02
IPT (Adim.)	0.00	0.19	0.05	0.00	0.24	0.92	0.00	-0.18	-0.12	0.05

The Figure 3 shows that the first six principal components concentrate 96.7% of the original data to explain gully erosion. We can resume that PC1 is associated to geological covariates, PC2 to geohydrological process, PC3 to hydro-geological data, PC4 is associated to vegetal cover, PC5 to topographic aspects and the PC6 to topo-hydrological covariables.

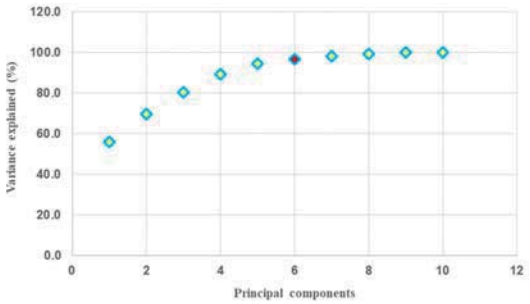

Fig. 3 Accumulative covariance for Principal Components

Susceptible areas for gully erosion

Based on the six principal components selected, the -

Table 4 Probability for gully presence

Probability Presence (%)	Area (km²)	Area (%)	Probability presence (%)	Area (km²)	Area (%)
0	5,560.92	90.17	75	75.7	1.23
0.5	5.68	0.09	90	27.56	0.45
1	5.07	0.08	95	6.4	0.10
2.5	18.75	0.30	97.5	2.6	0.04
5	39.16	0.64	99	1.23	0.02
10	90.01	1.46	99.5	0.35	0.01
25	186.76	3.03	100	0.32	0.01
50	146.95	2.38			
Total				**6,167.46**	**100.00**

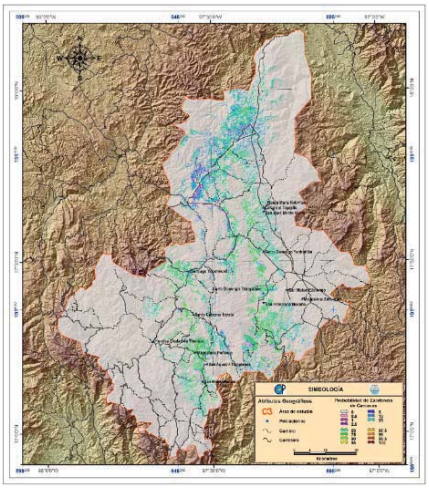

Fig. 4 Distribution of risk for gully formation

-Figure 4 shows the risk of gully formation. It was found that in 90.17% of the study area there is no risk for gully formation, while 9.83% of the surface (606.54 km^2) has a probability of presence of gullies greater than 0.5%. Likewise, 4.23% of the surface (261.11km^2) has a probability higher than 50% for this kind of soil erosion (Table 4).

Results Validation

Based on 289 verification points it was account the gullies presence with a probability of existence greater than 50%, resulting in 278 points affected by this kind of soil erosion and producing an overall reliability of 96.2% for the map generated (Fig. 4). If a 20% of risk is considered, then are observed 251 affected sites, which reduces certainty to 86.9%, which is consistent since there is a lower risk for gully formation.

Figure 5 shows the percentage of gully coverage for each radius of analysis, the trend is clear, the higher the radius the predicted sites with gully erosion decreases; taking in account a percentage of affectation for a range 30-40%, the radius for 50 m predicts a reliability of 83.4%, for 100 m reaches 81.7% and for 150 is 77.9%.

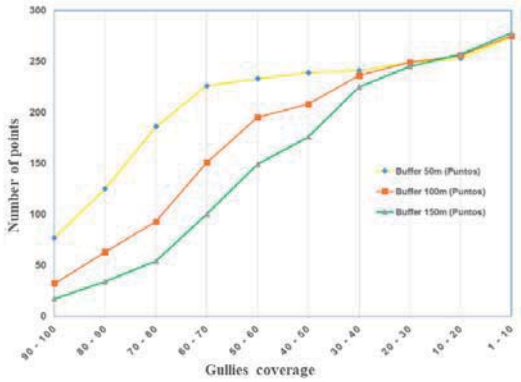

Fig. 5 Gully erosion on verification point for three analysis radiuses (50, 100 and 150 m)

CONCLUSIONS

In the study area the gullies occur in residual tuff soils on the foothills of old volcanic apparatus and on alluvial deposits that surround intermontane valleys.

At the regional level, the distance to the Tamazulapam fault and the presence of volcanic devices is conditioning gully formation, followed by geomorphological factors that control erosion and sedimentation processes as inferred through the topographic index of humidity, slope of the terrain, and the topographic position index.

The supervised classification method, using PCA, allows to identify areas with presence of gullies with an acceptable precision and was useful to determine a site potential to develop this kind of erosion.

ACKNOWLEDGEMENTS

This research was partially founded by WWF-Mexico, agreement OP19.

REFERENCES

[1] Alatorre, L. C., Beguería, S, " Identificación de zonas de erosión activa y áreas de riesgo mediante teledetección: un ejemplo en un paisaje de cárcavas sobre margas en el Pirineo Central Español", Cuadernos de investigación geográfica, Vol 35, No. 2, 2009, pp. 171-194.

[2] Bocco, G, "Gully erosion: processes and models", Progress in physical geography, Vol 15, 1991, pp. 392-406.

[3] Bull, L, J, Kirkby M, J, "Gully processes and modelling", Progress in Physical Geography, Vol. 21, 1997, pp. 354-374.

[4] Burrough, P, A, McDonell, R, A, "Principles of Geographical Information Systems", Oxford University Press, 1998, New York.

[5] Chuvieco, E, "Fundamentos de teledetección espacial", Rialp, 1990, Madrid, España.

[6] Guerrero-Arenas, R, Jiménez-Hidalgo, E, Santiago-Romero, H, "La transformación de los ecosistemas de la Mixteca Alta oaxaqueña desde el Pleistoceno Tardío hasta el Holoceno", Ciencia y Mar, Vol. 14, No.40, 2010, pp. 61-68.

[7] INEGI (Instituto Nacional de Estadística Geografía e Informática), "Conjunto de datos vectoriales Fisiográficos, escala 1:1 000 000", Instituto Nacional de Estadística, Geografía e informática, 2001, Aguascalientes, México.

[8] INEGI (Instituto Nacional de Estadística Geografía e Informática), "Conjunto de datos vectorial Edafológico, escala 1: 250 000, Serie II, Edafología", Instituto Nacional de Estadística, Geografía e Informática, 2006, Aguascalientes, Ags, México.

[9] INEGI (Instituto Nacional de Estadística Geografía e Informática), "Conjunto de datos vectoriales escala 1:1 000 000, Unidades climáticas", Instituto Nacional de Estadística, Geografía e Informática, 2008, Aguascalientes, Ags, México.

[10] INEGI (Instituto Nacional de Estadística Geografía e Informática), "Continental - Continúo de elevaciones mexicano, CEM, Modelo digital de elevaciones escala 1:50 000, Versión 3.0", Instituto Nacional de Estadística, Geografía e informática, 2012, Aguascalientes, México,

[11] INEGI (Instituto Nacional de Estadística Geografía e Informática), "Cartas topográficas

(E14B85, E14B86, E14D15, E14D16, E14D25, E14D26, E14D34, E14D35 y E14D44, E14D24, E14D36, E14D45, E14D46, E14D54 Y E14D55)", Instituto Nacional de Estadística, Geografía e informática, 2015, Aguascalientes, México,

[12] Irigaray, C, y Chacón, J, "Métodos de análisis de la susceptibilidad a los movimientos de ladera mediante SIG", Mapas de susceptibilidad a los movimientos de ladera con la técnica SIG, Fundamentos y aplicaciones en España, 2002, pp, 21-36.

[13] Kreznor, W, R, K, R, Olson, W, L, Banwart, D, L Johnson, "Soil, landscape, and erosion relationships in a Northwest Illinois watershed", Soil Science Society America Journal, Vol. 53, 1989, pp. 1763-1771.

[14] López-Pérez, A, Martínez-Menes, M, R, Fernández-Reynoso, D, S, "Priorización de áreas de intervención mediante análisis morfométrico e índice de vegetación", Tecnología y ciencias del agua Vol. 6, No.1, 2015, pp.121-137,

[15] Mendoza-García, E, "El ganado comunal en la Mixteca Alta: de la época colonial al siglo XX, El caso de Tepelmeme", Historia Mexicana, Vol. 51 No.4, 2002, pp. 749-785.

[16] Moore, I, D, Grayson R, B, Ladson A, R, "Digital terrain modelling: a review of hydrological, geomorphological, and biological applications", Hydrological Processes, Vol. 5, 1991, pp. 3-30.

[17] Nyssen, J, Poesen, J, Moeyersons, J, Luyten, E, Veyret-Picot, M, Deckers, J, Haile M, Govers, G, "Impact of road building on gully erosion risk: A case study from the Northern Ethiopian Highlands", Earth Surface Processes and Landforms, Vol. 27, 2002, pp. 1267-1283

[18] Palacio Prieto, J, L, "Determinación de áreas de erosión potencial en cárcavas: Un ejemplo en el centro de México", Investigaciones geográficas, Instituto de geografía, Boletín, Vol. 21, 1990, pp. 45-55, UNAM, México.

[19] Poesen J, Nachtergaele, J, Verstraeten, G, Valentin, C, "Gully erosion and environmental change: importance and research needs", Catena, Vol. 50, 2003, pp.91–133.

[20] Poesen, J, Hooke, J, M, "Erosion, flooding and channel management in Mediterranean environments of southern Europe", Progress in Physical Geography, Vol. 21, 1997, pp.157-199.

[21] Rossiter, D, "Texto base para el levantamiento del recurso suelo", International Institute for Geoinformation Science and Earth observation, 2002, ITC.

[22] SGM (Servicio Geológico Minero), "Cartas Geológico-Mineras y Geoquímicas E14-12 - Zaachila, 9 - Oaxaca y 6 - Orizaba escala 1: 250 000", Servicio Geológico Minero, 2000, México.

[23] Stolt, M, H, Baker, J, C, Simpson, T, W, "Soil – landscape relationships in Virginia: I, Soil variability and parent material uniformity", Soil Science Society America Journal, Vol. 57, 1993, pp.414-421.

[24] [Tamene, L, Park, S, J, Dikau, R, Vlek, P, L, G, "Analysis of factors determining sediment yield variability in the highlands of northern Ethiopia", Geomorphology, Vol. 76, No. 1, 2006, pp.76-91.

[25] Weiss, A, "Topographic Position and Landforms Analysis", ESRI User Conference, 2001, San Diego, CA.

[26] WWF (World Wildlife Fund), "Tasa de transformación de la vegetación en el área de intervención del proyecto Mixteca", Oficina de la WW en Oaxaca, 2014. Sitio web: http://www.proyectomixteca.org.mx/servidor-cartografico/ (consulted on april 2016).

SEDIMENT CHARACTERISTICS OF 18 TROPICAL, KARST LAKES IN CHIAPAS, MEXICO

Alcocer Javier [1], Oseguera Luis A. [1], Ardiles Vilma S. [1], Mora Lucy [2] and Prado Blanca [2]
[1]Proyecto de Investigación en Limnología Tropical, FES Iztacala, UNAM, México; [2]Instituto de Geología, UNAM, México

ABSTRACT

The "Lagunas de Montebello" National Park is a Mexican protected natural area and Ramsar site number 1325. Of the >50 lakes that make the "Lagunas de Montebello" karst lake complex, 18 were selected for this study. Several changes have occurred in some of the lakes since 2003, such as a change in the color of the water from crystal clear (pristine) to yellowish-green (deteriorated) and the occurrence of a yellowish-white supernatant, fetid odors from sulfur compounds, and fish mortality. Since the sediment determines many of the limnological characteristics and represents basic information that is required for follow-up studies, the goal of this study was to identify the sediment textural parameters and elemental composition. Deep lakes showed coarser sediments than the shallow ones. Pristine lakes have coarser sediments (silt > sand > clay) than the impacted ones (silt > clay > sand). Regarding elemental composition, there is a trend where the deep lakes showed higher content of C, H, N and S than the shallow ones. A similar trend is true for pristine lakes with higher content of C, H and N -but lower S- than the impacted lakes.

Keywords: Sediment Texture, Sediment Elemental Composition, Tropical Lakes, Karst Lakes, Lagunas de Montebello

INTRODUCTION

The "Lagunas de Montebello" National Park is located in the municipalities of La Trinitaria and Independencia in the state of Chiapas and was declared a protected natural area by a presidential decree that was published by the Diario Oficial de la Federación on December 16, 1959. Subsequently, the area was acknowledged as Ramsar Convention site number 1325 on November 27, 2003. In spite of the name of the national park and Ramsar site ("Lagunas de Montebello"), the limnological characteristics of the lakes are essentially unknown. Because the sediment determines many of its limnological characteristics and represents basic information that is required for follow-up studies, the goal of this study was to identify sediment textural parameters and elemental composition that are associated with the main water bodies of the Lagunas de Montebello to provide basic information to understand the functioning of the lake complex.

Since this study is strictly exploratory, it does not posit a hypothesis; however, it provides a foundation of information that can be used as the basis of a complete limnological study of the lakes because several changes have occurred to the lakes since 2003, such as a change in the color of the water from crystal clear to yellowish-green and the occurrence of a yellowish-white supernatant, fetid odors from sulfur compounds, and fish mortality.

METHODS

Study area

The study area covers 64.25 km^2 and is located in the physiographic province of Altos de Chiapas, which is also known as the Macizo Central Chiapas. The study area extends from 16°04'40'' N to 16°10'20'' N and from 91°37'40'' W to 91°47'40'' W (Fig. 1). Hydrologically, the basin is endorheic, is part of the RH30Gl sub-basin of the Comitán River, and is superficially fed by the Grande River. This sub-basin is part of the Lacatún River Basin, which is within hydrological region 30, Grijalva-Usumacinta.

Data from the meteorological station in Tziscao (16.1°N, 91.63°W; 1475 m a.s.l.) indicate that the mean annual temperature is 17.3°C, the mean annual precipitation is 2,279 mm, and the mean annual evaporation is 948 mm. The climate of the region is Cb(m)(f)ig, which represents a long cool summer that is humid and has a typical summer precipitation regime [1]. More than 10.2% of the annual precipitation falls during the winter. The climate is isothermal (less than 5°C) of a Ganges type. Lithologically, the entire area of interest is covered by a Lower Cretaceous limestone that is associated with the formation of a lake complex of karst origin; it includes solution lakes with dolines, uvalas and poljes. More than 50 lakes are present in the area displaying a wide array of bathymetric and

morphometric variables [2]. The lakes are aligned in a NW-SE orientation that coincides with the orientation of the main tectonic units [3].

Of the more than 50 lakes that make the Lagunas de Montebello karst lake complex, 18 were selected for this study; they cover the entire length of the NW-SE-oriented lake complex. The following 18 lakes (in alphabetical order) were studied: Agua Tinta (Aguatinta), Balantetic (Balamtetik), Bosque Azul, Chajchaj, Cinco Lagos, Dos Lagos (Dos Lagunas), Ensueño, Esmeralda, Kichail, La Encantada, Liquidambar, Montebello, Patianu (Patianú), Pojoj, San José, San Lorenzo, Tziscao and Yalalush (Fig. 1).

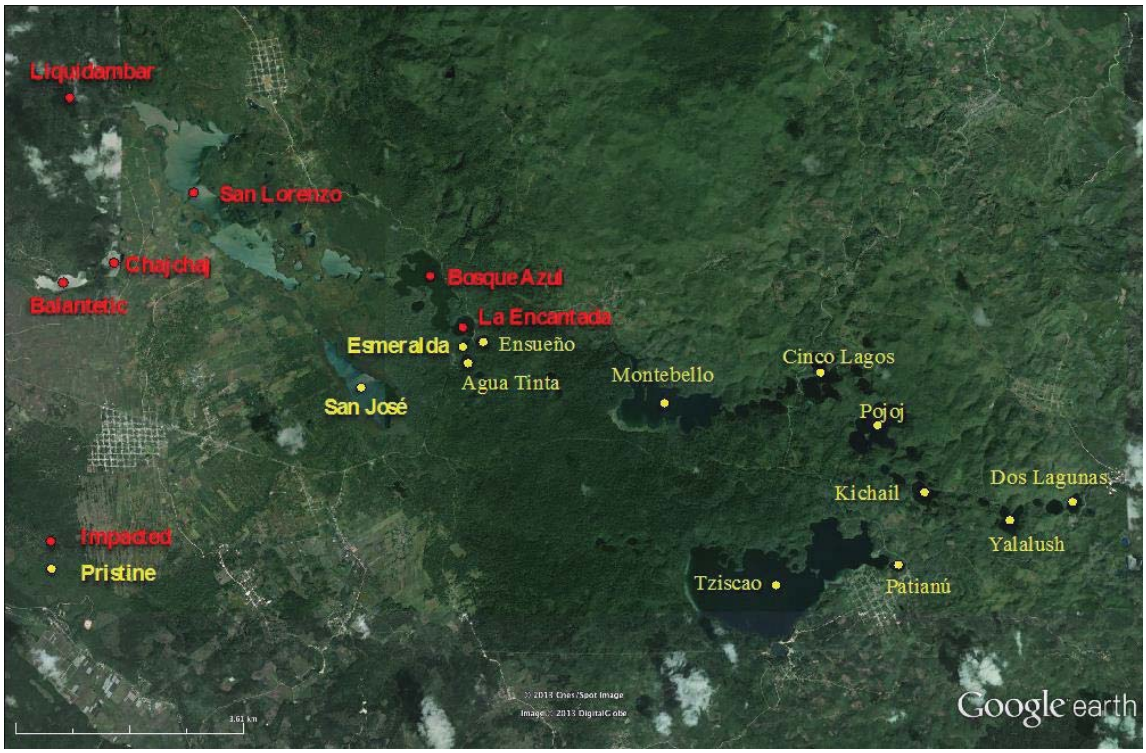

Fig. 1 The Lagunas de Montebello Lake District, Chiapas, Mexico. (The lakes considered in the study are indicated

Sampling

Surface sediments were collected from the central and deepest part of the lakes with an Ekman dredge (0.0225 m^2) from which two sediment aliquots (1 cm^3) were obtained with a manual corer (L=10 cm, Ø=1 cm), taking care not to disturb the surficial layer. The sediment subsamples were kept frozen in dark centrifuge tubes until analysis. Sediment texture was carried out in a Beckman Coulter LS230 laser diffraction analyzer. Samples for elemental analysis were treated by adding 10% HCl to eliminate inorganic C fraction. Sediment elemental composition was carried out in a Carlo Erba NC2100 elemental nitrogen/carbon analyzer at the Center for Marine Sciences, University of North California at Wilmington.

RESULTS AND DISCUSSION

Sediment particle size of the Montebello lakes along with their impact status (impacted or pristine) and maximum depth are provided in Table 1.

Concerning the particle size of the Montebello lakes' sediments (Fig. 2), there is a graphical trend (although not statistically different) where the shallow lakes sediments were finer (24 ± 27 µm) than the sediments of the deep lakes (58 ± 49 µm). A similar graphic tendency (Fig. 2) is true for impacted lakes with finer sediments (23 ± 24 µm), while the pristine displayed coarser sediments (64 ± 50 µm).

The lakes with the coarser sediments (> 50 µm) were La Encantada, Esmeralda, Agua Tinta, Ensueño, Cinco Lagos, Dos Lagos, Pojoj and Kichail; all of them but La Encantada, pristine (Fig. 3).

Silt dominates (> 60%) in both deep and shallow lakes (Fig. 4). Nonetheless, deep lakes showed coarser sediments (sand = 22 ± 28%, clay = 16 ± 12%) than the shallow ones (sand = 5 ± 6%, clay = 34 ± 20%). The shallow lakes receive the fine particles from the erosion of the watershed.

Table 1 Sediment particle size (Mode), impact status, and depth of the Montebello lakes. (P = pristine, I = impacted, Z_{MAX} = maximum depth)

Lake	P / I	Z_{MAX} (m)	Mode (µm)
Agua tinta	P	24	106
Balantetic	I	3	5
Bosque Azul	I	58	35
Chajchaj	I	12	4
Cinco Lagos	P	162	169
Dos Lagos	P	42	96
Ensueño	P	35	61
Esmeralda	P	7	61
Kichail	P	22	106
La Encantada	I	89	66
Liquidambar	I	24	15
Montebello	P	45	20
Patianú	P	26	12
Pojoj	P	198	88
San José	P	30	9
San Lorenzo	I	67	15
Tziscao	P	86	11
Yalalush	P	23	29

Moreover, according their impact status (Fig. 4), pristine lakes have coarser sediments (silt = 59 ± 20% > sand = 25 ± 29% > clay = 16 ±13%) than the impacted ones (silt = 67 ± 14% > clay = 28 ± 18% > sand = 5 ± 6%).

Clay dominated just in Chajchaj (53%), sands in Cinco Lagos (89%), Kichail (59%) and Pojoj (54%), while silt dominated in the rest of the lakes (Fig. 5).

Regarding elemental composition (Table 2, Fig. 6), there is a trend where the deep lakes showed higher content of C (11.9 ± 7.5%), H (2.5 ± 0.9%), N (1.0 ± 0.6%) and S (0.6 ± 0.6%) than the shallow ones (C = 4.3 ± 4.8%, H = 2.1 ± 0.6%, N = 0.7 ± 0.4%, S = 0.2 ± 0.2%).

A similar trend is true for pristine lakes (Fig. 6) with higher content of C (11.4 ± 8.2%), H (2.6 ± 1.0%) and N (1.0 ± 0.7%) than the impacted lakes (C = 5.5 ± 3.3%, H = 2.1 ± 0.4%, N = 0.8 ± 0.5%). S was higher in the impacted (8.8 ± 0.7%) than in the pristine (0.3 ± 0.3%).

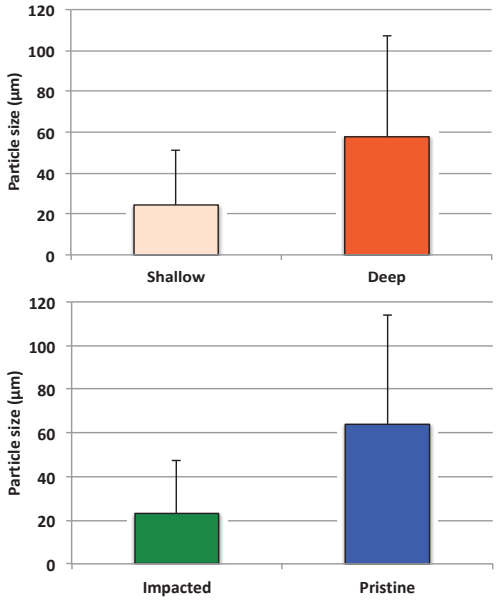

Fig. 2 Sediment mode size (µm) in shallow and deep (up) and impacted and pristine (bottom) lakes of Montebello. (No significant differences, P>0.05)

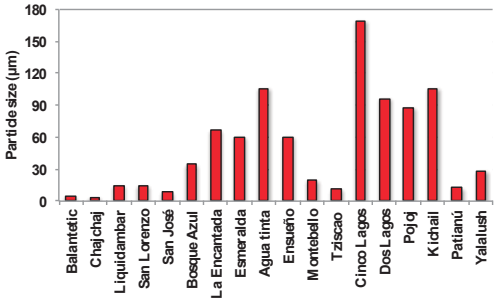

Fig. 3 Sediment particle size (µm) along a NW-SE gradient of the Lagos de Montebello

The lakes with the highest percentages of elemental composition (C > 9.4%, H > 2.4%, N > 0.9%, S > 0.5%) were the pristine Agua Tinta, Cinco Lagos and Kichail, and the impacted San Lorenzo. On the contrary, the lakes with the lowest percentages of elemental composition (C < 9.4%, H < 2.4%, N < 0.9%, S < 0.5%) were the impacted Balantetic and Chajchaj, and the pristine Esmeralda, Tziscao and Patianú (Fig. 7).

The C/N ratio was statistically larger in shallow (6 ± 12) than in deep (3 ± 5) lakes (Fig. 6). Opposite, the C/N ratio in impacted (11 ± 5) lakes was similar to pristine (13 ± 4) lakes (Fig. 6). The lake with the lowest C/N ratio was Chajchaj with 2.3 (N-enriched)

and the highest C/N ratio was Pojoj with 22.3 (C-enriched) (Fig. 8). The smaller the particle size the larger the N mineralization [5], therefore, the smaller the particle size, the lower the N content, and this increases the C/N ratio in lakes with fine sediments and low C content. The C/N ratio of small particle size is narrower than in large particles; also, smaller particles display larger contact surfaces than the larger ones [5].

The prevalence of finer sediments in the lakes of the NW section results from recent erosion. Regarding the deep lakes, the predominance of coarser particles could be a consequence of their filled up with sediments originated from the polymictic conglomerate (material with sands and conglomerates) located on the SW portion of the basin.

There has been placed a hypothesis [4] regarding the occurrence of a tectonic uplift that took place in the past. This raise conducted to the filled up of the lowest portion of the basin that resemble a paleolake.

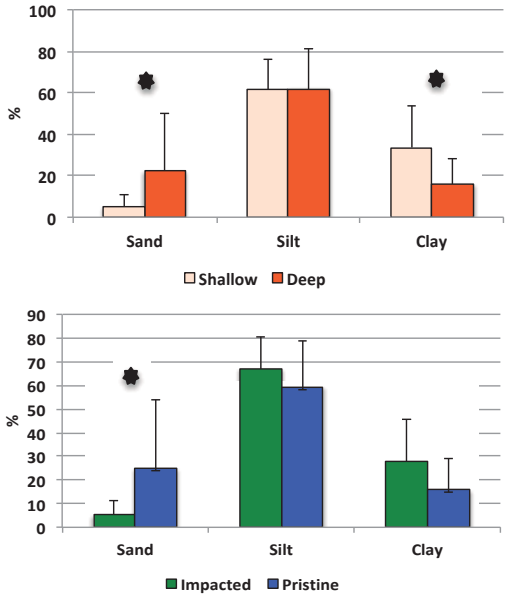

Fig. 4 Sediment texture in shallow and deep (up) and impacted and pristine (bottom) lakes of Montebello. (* Significant difference, P>0.05)

The coarser material that originally filled up the lakes was transported to the lowest portion, explaining the predominance of coarse material in the southernmost lakes. The chemical composition of the lakes provides further support to this hypothesis, since the polymictic block -at the SW- is enriched in sulfur.

The high content of organic C in the sediments of the deep lakes could result from the geomorphology of the area, with steep slopes favoring the erosion of the surrounding soils [4].

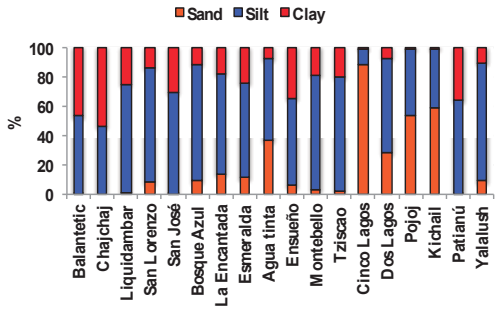

Fig. 5 Sediment textural composition (%) along a NW-SE gradient of the Lagos de Montebello

Table 2 Sediment elemental composition (%) of the Montebello lakes. (C = carbon, H = hydrogen, N = nitrogen, S = sulfur)

Lake	C	H	N	S	C/N
Agua tinta	20.1	3.4	1.4	0.6	14.2
Balantetic	2.0	1.8	0.4	0.0	5.6
Bosque Azul	8.0	2.5	1.2	1.5	6.9
Chajchaj	1.9	1.7	0.8	0.1	2.3
Cinco Lagos	25.0	4.2	2.3	0.7	11.1
Dos Lagos	11.3	1.8	0.7	0.5	17.1
Ensueño	3.4	2.1	0.4	0.0	9.5
Esmeralda	1.7	2.0	0.3	0.0	6.4
Kichail	25.2	4.3	2.3	1.1	11.1
La Encantada	7.8	2.0	0.5	0.5	17.0
Liquidambar	3.8	2.0	0.5	1.1	7.2
Montebello	6.3	2.5	0.7	0.3	8.7
Patianú	5.7	2.0	0.6	0.0	9.5
Pojoj	13.7	1.0	0.6	0.1	22.3
San José	4.1	2.1	0.5	0.1	9.1
San Lorenzo	9.4	2.5	1.5	1.8	6.2
Tziscao	8.6	2.3	0.8	0.1	10.7
Yalalush	11.6	3.0	1.2	0.4	9.7

The water bodies at the NW portion belong to a group of lakes where the dissolution processes are active, which means that they can receive a sediment supply via underground, which is supported by the increase of nutrients in the deepest lakes [6].

Furthermore, the adjacent vegetation of the deep lakes comprised forests, which are related with high C content soils. C/N ratio is often used to identify the origin of the C present in the sediments, and even, to distinguish between algal and land-plant origins of sedimentary organic matter [7].

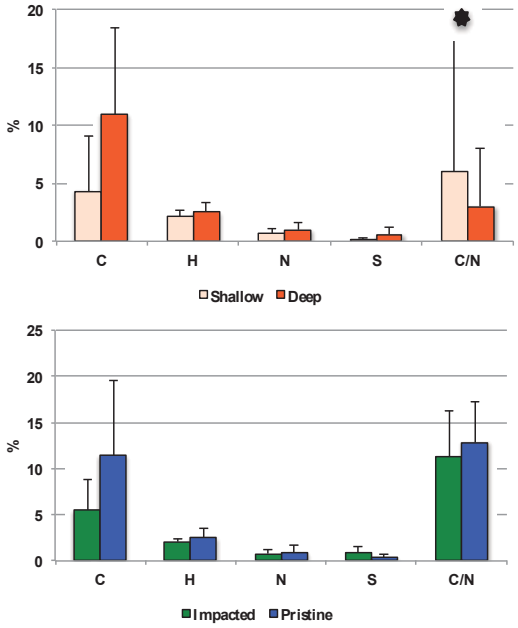

Fig. 6 Sediment elemental composition in shallow and deep (up) and impacted and pristine (bottom) lakes of Montebello. (* Significant difference, P>0.05)

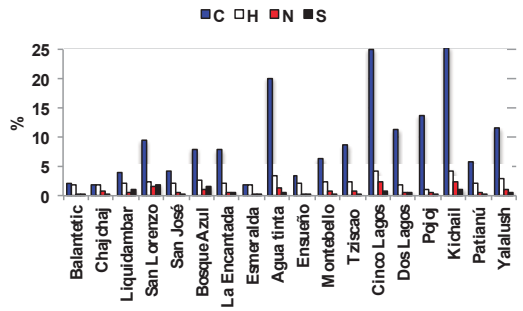

Fig. 7 Sediment elemental composition along a NW-SE gradient of the Lagos de Montebello

A C/N ratio > 20 derived from vascular plants, whereas the organic matter in the soil (organic matter associated with mineral surfaces) has a narrower C/N ratio [8] and decomposes more slowly than the mineral-free debris. The C/N ratio of the deep lakes of Montebello ranged from 9 to 22, that support the hypothesis that the lakes are being eroded receiving soil and vascular plants detritus that can be transported into the lakes from the catchment.

The impacted lakes Liquidambar, San Lorenzo, Bosque Azul and La Encantada exhibited the highest S concentration. S is a common element on the sediments of the region. The large concentration of organic matter in these lakes triggers anoxic conditions, which in the presence of S, derived in the formation of H_2S, CH_3SH [9].

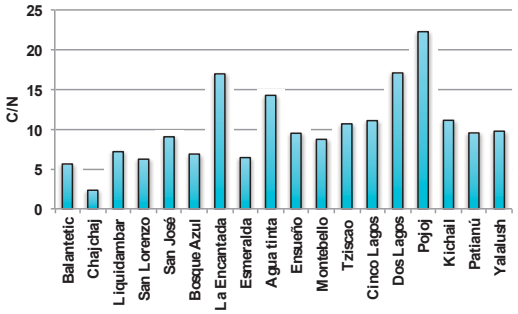

Fig. 8 Sediment C/N ratio (%) along a NW-SE gradient of the Lagos de Montebello

CONCLUSIONS

Even though the Montebello lakes belong to a lake district, there are differences in their bathymetric and morphometric parameters, as well as in their conservation status (pristine and impacted).

Regarding the particle size, we found a trend with coarser particles in the deeper lakes and finer in the shallower; nonetheless there were no significant differences. Silt was the dominant sediment class in all lakes, and significant differences were found in the sand contribution between shallow and pristine and pristine and impacted. The same is true in clay between shallow and deep lakes.

Elemental composition of the sediments displayed a trend with higher C, H, N and S content in deeper lakes, and lower in the shallower; however there were not significantly different. The same was true for C, H and N with higher content in pristine lakes and lower in impacted. The opposite was found for S with higher content in impacted lakes. Once again there were not significantly different. Only the C/N ratio was significantly higher in the shallow lakes than in the deeper.

The geomorphology of the basin, its geological evolution, and more recently, the anthropogenic impacts seem to explain the sedimentary differences between the lakes between those in the NW (plateau lakes and mostly impacted), and those in the SE (mountain lakes and mostly pristine).

ACKNOWLEDGEMENTS

This research was funded by the Fondo Sectorial de Investigación y Desarrollo Sobre el Agua (Sectorial Fund for Water Research and Development) (CONAGUA-CONACYT) through the project Estudio hidrológico y de Calidad del Agua del sistema Lagunar de Montebello, en el estado de Chiapas and by Dirección General de Asuntos del Personal Académico (PAPIIT-IN219215) through the project Factores que determinan el estado trófico de los lagos de Montebello, Chiapas. We thank René Morales Hernández for support during the fieldwork. We also thank the Parque Nacional Lagunas de Montebello, Comisión Nacional de Áreas Naturales Protegidas (CONANP) (Jesús A. León and Roberto Castellanos), the local community, and the Comisariados Ejidales from Antelá, Cárdenas, Miguel Hidalgo, Ojo de Agua and Tziscao for facilitating access to the lakes. We also thank the Comité de Administración de Tziscao (Sergio Marcos and Miguel A. Tomas), Presidente del Comité de Turismo de Tziscao (Armando Hernández), Comisario Ejidal de Tziscao (Enrique M. Hernández) and personnel of the Villas Tziscao Hotel (Rosemberg F. Jorge, Juan G. Espinoza and Gemuel P. Hernández) for offering their support and facilities for this study.

REFERENCES

[1] García E, Modificaciones al sistema de clasificación climática de Köppen. México: E. García, 1988.

[2] Alcocer J, LA Oseguera, G Sánchez, CG González, JR Martínez, R González, Bathymetric and morphometric surveys of the Montebello lakes, Chiapas, Journal of Limnology, Vol. 75, 2016, pp. 56-65.

[3] Durán Calderón JI, Análisis geomorfológico del Parque Nacional Lagunas de Montebello, Chiapas. México: UNAM, 2013.

[4] Mora L, R Bonifaz, R. López-Martínez, Unidades geomorfológicas de la cuenca del Río Grande de Comitán, Lagos de Montebello, Chiapas-México, Boletín de la Sociedad Geológica Mexicana, Vol. 68, Nr. 3, 2016, pp. 377-394.

[5] Cameron RS, AM Posner, Mineralizable organic nitrogen in soil fractionated according to particle size, Journal of Soil Science Vol. 30, 1979, pp. X5-577.

[6] Durán CL, Escolero OF, Muñoz EFM, Castillo MCS, Rodríguez GSR, Cartografía geomorfológica a escala 1:50000 del Parque Nacional Lagunas de Montebello, Chiapas (México), Boletín de la Sociedad Geológica Mexicana Vol. 66, Nr. 2, 2014, pp. 263–277.

[7] Jasper JP, Gagosian RB, The sources and deposition of organic matter in the Late Quaternary Pygmy Basin, Gulf of Mexico, Geochimica et Cosmochimica Acta, Vol. 54, Nr. 4, 1990, pp. 1117-1132.

[8] Spycher G, Sollins P, Rose SL, Carbon and nitrogen in the light fraction of a forest soil: vertical distribution and seasonal patterns, Soil Science, Vol. 135, 1983, pp. 79-87.

[9] Schubert CJ, Ferdelman TG, Strotmann B, Organic matter composition and sulfate reduction rates in sediments off Chile, Organic Geochemistry, Vol. 31, Nr. 5, 2000, pp. 351-361.

EFFECT OF THICKNESS AND SEDIMENT TYPE ON SEISMIC AMPLIFICATION IN THE URBAN AREA OF CHIAPA DE CORZO, CHIAPAS

Moreno Ceballo Roberto [1], González Herrera Raúl [1], Paz Tenorio Jorge Antonio [1], Aguilar Carboney Jorge Alfredo[2] and del Carpio Penagos Carlos Uriel[1]
[1]Universidad de Ciencias y Artes de Chiapas, Maestría en Ciencias en Desarrollo Sustentable y Gestión de Riesgos, México
[2]Universidad Autónoma de Chiapas, Facultad de Ingeniería Civil, México.

ABSTRACT

Local variations of the soil type and topography to a lesser extent, determine the seismic amplification and have established a pattern in the damages observed during large earthquakes, such as the one occurred on October 6th of 1975 and September 7 of 2017; the latter of Mw 8.2, being the most important in the seismic history of the last century in the region. With these bases an analysis is made to indentify the participation of the thickness and the type of sediment in the seismic amplification in the urban zone of Chiapa de Corzo, Chiapas. To obtain the thickness in the study area, the fundamental periods of soil vibration obtained by Salgado *et al.* (2004) were used, which vary between 0.14 s and 0.39 s. In addition, through the model used by Newmark and Rosenbleuth (1976), the variation of the sediment thicknesses that lead the site effect in the area was determined, for which an average cutting wave velocity of 150 m/s is considered. Finally, through the use of GIS-type software, a map was drawn up representing the sediment thicknesses in the city of Chiapa de Corzo, which oscillate between 7.12 m and 14.62 m and a spatial correlation was made with the historical earthquake damage recorded in the place.

Keywords*: Seismic Amplification, Sediment Thickness, Soil, GIS*

INTRODUCTION

There are various natural phenomena that are capable of representing a serious threat to humans and their properties. Among them, the ones that cause a greater number of victims and of material losses per unit of time are, probably, the earthquakes (Perepérez, 2014). With the occurrence of the earthquakes that have affected the state of Chiapas, it has become clear that local soil conditions have a fundamental role in the structural response.

The developments plans of the populations must contemplate the seismic response of the subsoil, in order to define the specific parameters of structural design seismo resistant, according to the seismic history of the region (IPCMIRD, 2010).

Generally, the dynamic response of the soils against earthquakes is very variable. In addition to the soils, in studies of this type, which basically consist in the elaboration of a micro-zoning, include the effects induced by failures, liquefaction and others, and its danger valued. The resulting maps, or microzoning maps, are presented in a useful cartographic base for building and urban planning purposes (Tupak, 2009).

Chiapa de Corzo, in the center of the state of Chiapas, has suffered constantly different earthquakes at different times over the time, in the earthquake of 1975 was one of the most affected cities, causing radical changes in its original structure as were their traditional adobe houses that were inhabited since its foundation, as these systems failed and most of the city was affected. The earthquakes in this region are irremediable as a result of the subduction of the tectonic plate of Cocos under that of North America (García and Suárez, 1996) (Figure 1).

A fundamental aspect to determine the amplification zones and in turn to do seismic hazard studies in a specific zone is the analysis of the historical damage by earthquake, table 1 shows some of the most significant earthquakes that have affected the city of Chiapa de Corzo.

For this work two seismic events were considered in particular, which were selected by the fact of having sufficient information of both that allowed to carry out a thorough analysis of its characteristics and its consequences for the city:

Monday, October 6th, five minutes to 01:00 in the morning, an earthquake of a magnitude of 4.8 shook the city of Chiapa de Corzo, causing major damage. The epicenter was located in Ribera de Cupía, Amatal and América Libre; rural localities located approximately 4 km at the southeast of Chiapa de Corzo, earthquake produced by the cortical failure, induced by the filling of the reservoir of the dam "La Angostura" (Nandayapa, 2011).

On september 7 of 2017, an earthquake with magnitude 8.2 was located in the Gulf os Teahuantepec, 133 km southwest of Pijijiapan, Chiapas, causing heavy damage in the metropolitan area of the state of Chiapas (SSN, 2017).

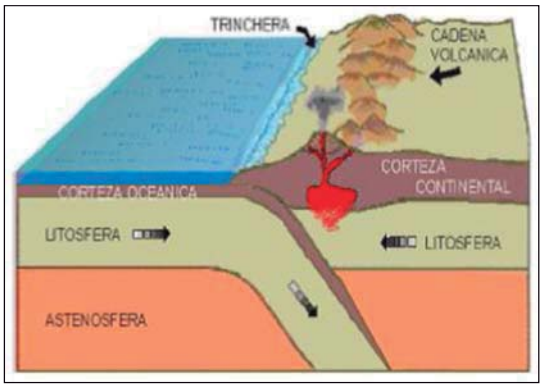

Figure 1. Subduction process between Cocos and North American plates (IPCMIRD, 2010).

The existence of buildings with high patrimonial value, the high degree of deterioration of the housing fund and the presence of areas with a high degree of marginalization are factors that make inminent the need to carry out zoning studies in the city of Chiapa de Corzo.

Table 1. Historical and recent local seismicity of Chiapa de Corzo (Salgado *et al.,* 2004; SSN, 2017)

Date	Latitude	Longitude	Magnitude
05/06/1897	16.30	-95.40	7.4
19/04/1902	14.90	-91.50	7.5
23/09/1902	16.60	-92.60	7.7
14/01/1903	15.00	-93.00	7.6
09/12/1912	15.50	-93.00	7.0
30/03/1914	17.00	-92.00	7.2
10/12/1925	15.50	-92.50	7.0
28/06/1944	15.00	-92.50	7.1
26/09/1955	15.50	-92.50	6.9
09/11/1956	17.45	-94.08	6.3
29/04/1970	14.52	-92.60	7.3
05/10/1975	16.74	-92.92	4.8
10/09/1993	14.20	-92.80	7.2
14/03/1994	15.98	-92.43	6.8
21/10/1995	16.81	-93.47	7.1
18/11/2001	15.45	-93.60	6.3
16/01/2002	15.58	-93.60	6.3
07/09/2017	15.76	-93.70	8.2

Geological characteristics of the study area

In general, the surface of the metropolitan region of the state of Chiapas presents seven types of rock and is composed of quaternary soils, it means, recent deposits where three types predominate, limestone

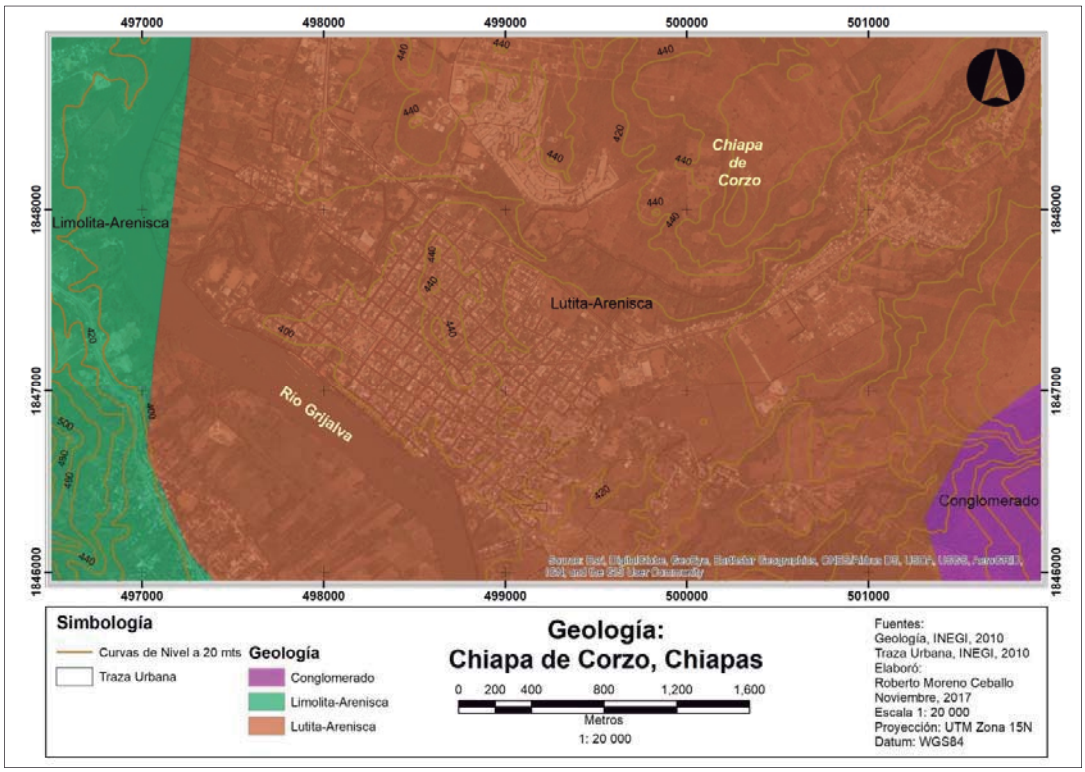

Figure 2. Detail of the geological map of the urban area of Chiapa de Corzo

(34.46%), limolita-sandstone (29.01%), and shale-sandstone (16.55%).

Also cretaceous deposits: limolita (8.99%) and alluvial (7.22%) (Figure 2). Other varied soil compositions make up the remaining 5.40% of the region´s surface area (PDM, 2017).

Chiapa de Corzo lies at the margins of the Grijalva river, therefore, all the urban spot is part of the flood plain, which, geomorphologically, is a form of land composed primarily of unbound deposited material, derived from sediments transported by the river in question (Schmudde, 1968).

The shales are fine-grained rocks that are departed in laminated slabs more or less parallel to the stratification. The particles of these rocks are so small that it is very difficult to determine the precise mineral composition. It is important to note that they contain clay minerals, as well as silt, quartz, feldspar, calcite and dolomite particles (Don Leet & Judson, 1980).

The sandstone is formed by the consolidation of individual grains of the size of the sand (1/16 mm to 2 mm diameter). Sandstone occupies, then, an intermediate position between the conglomerate, which is coarse-grained, and the lodolite, which is fine-grained. Since the size of the grains varies from one sandstone to another. Sanstones and shales constitute about 99% of all sedimentary rocks, the shales being the most abundant (Don Leet & Judson, 1980).

METHODS

The methodology proposed in this work consists of three fundamental stages, as illustrated in the diagram below (Figure 3).

In the first instance the mathematical model was defined to calculate the thickness, then the fundamental periods of vibration of the soil were obtained, this time the results were used of the investigation of Salgado (2004) and finally was made a comparison with the historical damage to correlate the soil thickness with the seismic amplification in the city of Chiapa de Corzo.

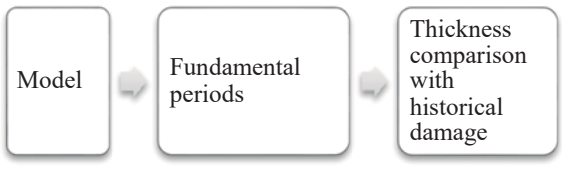

Figure 3. Methodological steps to determine the incidence if sediment thickness in the seismic amplification in the urban spot of Chiapa de Corzo.

Model

In 1976, Newmark and Rosenbleuth coined an expression that relates the thickness of the sediments with their fundamental period of vibration and the propagation rate of cutting waves:

$$\boldsymbol{T = 4 \sum_i^n \frac{h_i}{\beta_i}} \quad (1)$$

Where T represents the natural period of the terrain, H is the thickness of the i-th stratum and β is the propagation rate of cutting waves. The number of sedimentary strata is represented by n. From this model, we simply clear to obtain the definitive equation with which it will feed the ArcMap software with the purpose of obtaining the values that were subsequently interpolated:

$$\boldsymbol{h_i = \frac{(T x \beta_i)}{4}} \quad (2)$$

To estimate the thickness of sediments under the urban spot of Chiapa de Corzo, the model described above was used, complementary to the calculation of the natural periods of vibration of the city´s soils. For this we used a velocity β average of 150 m/s, the periods used correspond to those found by Salgado and collaborators (2004).

Fundamental periods of soil vibration

Table 2 shows the fundamental periods of soil vibration, obtained by Salgado (2004). You can see that the periods range from 0.14 s to 0.39 s, where periods close to 0.3 s predominate.

Table 2. Fundamental periods of soil vibration, measured in the urban spot of Chiapa de Corzo, Chiapas by Salgado and collaborators (2004)

Stat.	Location	Period
01	Emiliano Zapata, junto al río Grijalva	0.19
02	Benito Juárez, junto al río Grijalva	0.23
03	Mexicanidad Chiapaneca, esquina con Av. Independencia	0.27
04	Cap. Luis Vidal, esquina con Av. Independencia	0.32
05	C. 21 de Octubre, esquina con Av. Independencia	0.39
06	Francisco I. Madero, esq. Benito Juárez	0.38
07	Cap. Luis Vidal, esquina con Av. Julián Grajales	0.32
08	C. 21 de Octubre, esq. Av. Julián Grajales	0.36
09	C. 21 de Octubre, casi esq. Con Av. 21 de Octubre	0.27

Table 2. Continue

Stat.	Location	Period
10	Mexicanidad Chiapaneca, esq. Francisco I. Madero	0.38
11	Mexicanidad Chiapaneca, esq. Av. 21 de Octubre	0.26
12	Cap. Luis Vidal, esq. Av. 21 de Octubre	0.24
13	Benito Juárez, esq. Av. Zaragoza	0.37
14	5 de Febrero, esq. Av. Ángel Albino Corzo	0.14
15	Mexicanidad Chiapaneca, esq. Av. Ángel Albino Corzo	0.21
16	Mexicanidad Chiapaneca, esq. Av. Hidalgo	0.22
17	Santos Degollado, casi esq. Av. Cuauhtémoc	0.17
18	Tomás Cuesta, esq. Av. Cuauhtémoc	0.24
19	5 de Febrero, esq. Av. Hidalgo	0.27
20	5 de Febrero, esq. Av. Hidalgo	-

Historical Damage

The last step was to develop a database in Excel (Figure 4), with a compilation of the damage presented with the occurrence of two earthquakes mainly: the earthquakes of October 6th of 1975, and which of them persist to the present day, defining the use that was given to the property at the time and the one that it receives today and the earthquake of September 7 of 2017 of 8.2 Mw considered the one of greater magnitude in the last century in the region.

Points were taken that correspond to the buildings that presented damage by the aforementioned phenomena, which were geographically referenced and with them generated the vector information catalogued as historical damages.

The factors that generally influence the distribution of the damage that have been presented in the constructions are associated to the constructive systems employed, the properties of the soil and the materials used, in addition to the topographical characteristics of the site, that can be a source of site effects as they have a considerable influence on the frequency and amplitude characteristics of earthquake land movements and thus on the extent of local structural damage by earthquake (Meslem *et al*., 2012).

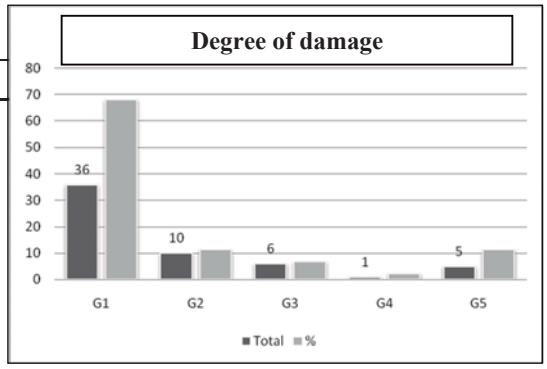

Figure 4. Degree of damage presented in the buildings of the municipal head of Chiapa de Corzo with the earthquakes of October 6th of 1975 and September 7 of 2017.

RESULTS

To have a first approximation of the dynamic behavior of the soil to the occurrence of an earthquake, making a micro zoning is a solid alternative to support the territorial management and planning programs, as well as having elements for the construction regulations.

In figure 5 a map is presented in which a variation of the natural periods of vibration is observed, it was created by means of a linear interpolation using the spline function of the ArcMap software.

The sediment thicknesses calculated with the model proposed above range from 7.12 m to 14.62 m (Figure 6). These thicknesses were compared with the historical damage by earthquake in the municipal head of Chiapa de Corzo (Figure 7), where it was observed that the areas with greater thickness, coincide with the damages of greater degree, that is, those that correspond to serious structural damage and even partial or total collapses.

The seismic threat does not govern or conditions the use of the soil, only conditions the structures subjected to this threat (Cardona, 2008), nor does it condition the use of urbanizations or constructions, nor does it in the case of land use urban planning. This threat only conditions the characteristics of the structures where such uses lie (Padrón *et al*., 2011), for this reason it is important to study the typical structures of the area, it means that the vulnerability that the structures have when they are subjected to structural resonance in the presence of the earthquake.

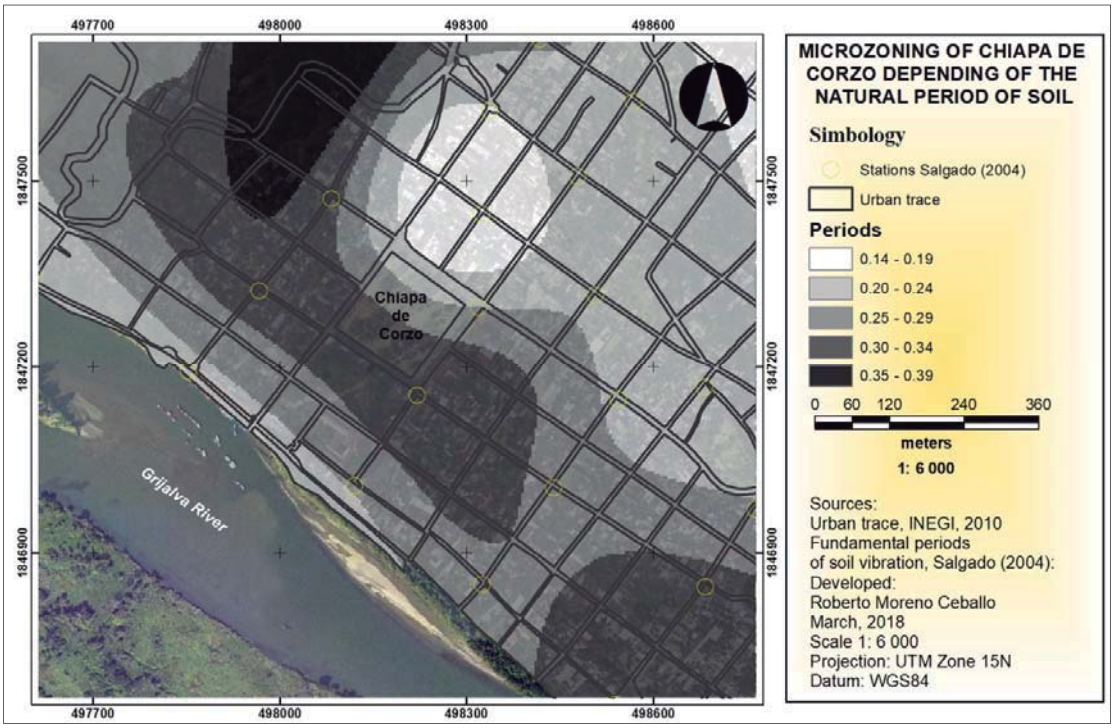

Figure 5. Micro zoning of the city of Chiapa de Corzo depending on the natural period of the soil, the circles represent the location of the measuring stations.

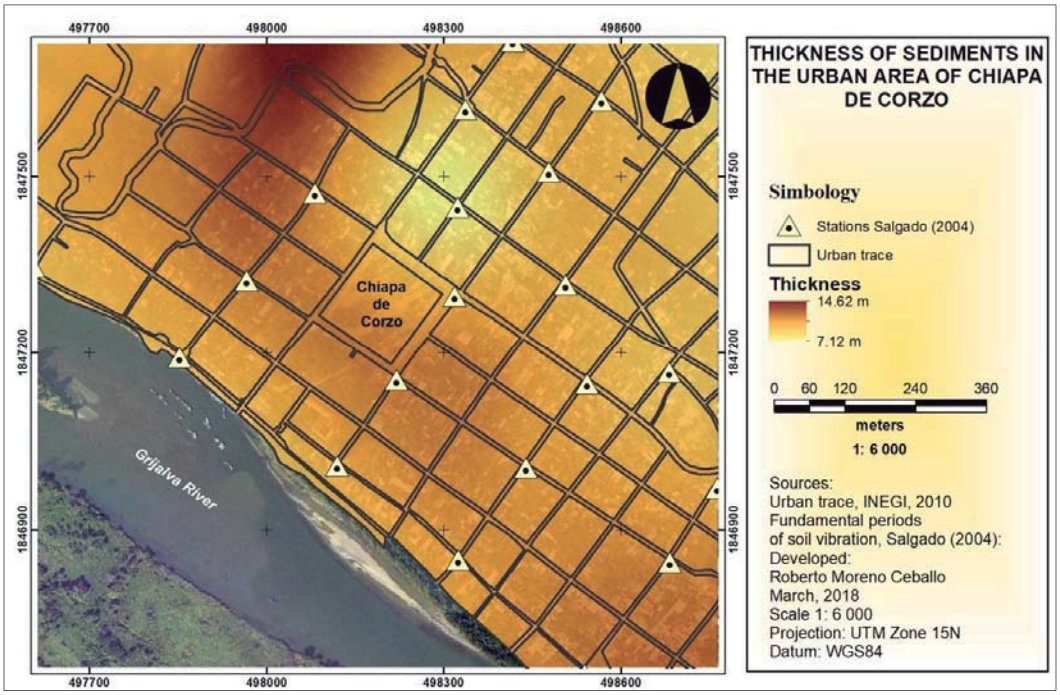

Figure 6. Representation of the thickness of sediments in the urban area of Chiapa de Corzo.

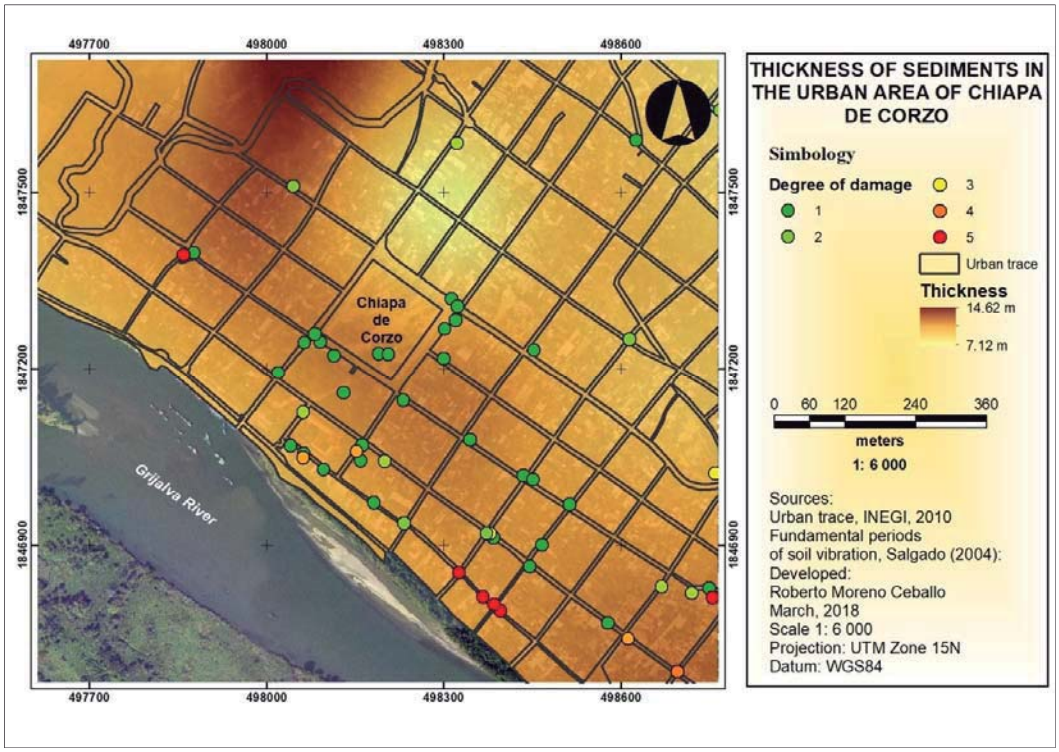

Figure 7. Comparison of sediment thicknesses with respect to historical damage by earthquake in the urban area of the municipal head of Chiapa de Corzo

CONCLUSIONS

The difference in values corresponding to the thicknesses enunciated above is due to the little variation between the natural periods of vibration. The results of this work are a fundamental input for the calculations of dynamic response of soils and the definition of micro zones in the city of Chiapa de Corzo.

This study revealed the importance of carefully considering site conditions; if the seismic behavior is not related to the system or the materials used, it is evident a considerable effect of site due to the behavior that have had the same constructive systems located indifferent zones of the city.

The topography is also an element to be considered, in order to obtain more security in the structural design of the buildings in the study area, since sometimes it receives a minor attention in the engineering works.

Evaluate the distribution of damage in a city such as Chiapa de Corzo, which presents homogeneous constructive pathologies, led to an analysis that considered not only the structural characteristics of the buildings, but also the conditions of subsoil.

The results obtained in this work should be supplemented by more detailed studies that include current measurements located throughout the urban spot of the municipal head, since in recent years population growth has been considerable.

REFERENCES

[1] Arbeláez, A. C., Posada, L., & Vélez, M. V.: "Usos de suelo en la zona inundable del río San Carlos, Colombia". *XV Seminario Nacional de Hidráulica e Hidrología*., 2002.

[2] Blanquer, J. M., Ibáñez, S., & Moreno, H. : "Vertisoles". *Universidad Politécnica de Valencia*., 2011.

[3] Cardona, O. (Transcripción de entrevista personal). En Padrón, C. (Comp), Lineamientos para la consideración de riesgo sísmico en la planificación urbana del municipio Chacao, estado Miranda (pp. 254-271). Informe de pasantía (véase Padrón, 2009), Universidad Simón Bolívar, Caracas., 2008.

[4] Don Leet, L., & Judson, S.: "Fundamentos de Geología Física". México, D.F.: Limusa.

[5] INEGI.: "*Prontuario de información geográfica municipal de los Estados Unidos Mexicanos"*., 2008.

[6] IPCMIRD.: "Sistema Estatal de Protección Civil del Estado de Chiapas. Plan Operativo de

Protección Civil por Riesgo Sísmico", Tuxtla Gutiérrez, Chiapas, 2010.

[7] Meslem, A., Yamazaki, F., Maruyama, Y., Benouar, D., Kibboua, A., & Mehani, Y. "The Effects of Building Characteristics and Site Conditions on the Damage Distribution in Boumerde`s after the 2003 Algeria Earthquake". *Earthquake Spectra , 28* (1), 185-216., 2012.

[8] Nandayapa, A. Temblores de 1975 en la ciudad de Chiapa de Corzo. Tuxtla Gutiérrez., 2011.

[9] Narcía López, C., Cruz Díaz, R., Aguilar Carboney, J., Ramírez Centeno, M., & González Herrera, R. "El período natural de vibración del suelo en la ciudad de Tuxtla Gutiérrez, Chiapas". *Quehacer Científico en Chiapas , 1* (1), 22-36., 2006.

[10] Newmark, N. y Rosenbleuth, E.Fundamentos de Ingeniería Sísmica, 1ª ed., Diana, México, D.F, 1976.

[11] Salgado, A., Escamirosa, F., & Calvo, A.: "Zonificación sísmica de tres centros históricos del sureste mexicano". *Sociedad Mexicana de Ingeniería Estructural*, 11-15. 2004.

[12] Schmudde, T.H.: "Floodplain"in R.W. Fairbridge, The Encyclopedia of Geomorphology. New York: Reinhold, pp. 359-362., 1968.

[13] SSN. "Reporte especial: SismodeTehuantepec2017-09-0723:49M8.2)"., 2017.

[14] Padrón, C., Mendes, K. C., Schmitz, M., & Hernández, J.J. "LA MICROZONIFICACIÓN SÍSMICA EN EL PROCESO DE PLANIFICACIÓN URBANA. CASO DE ESTUDIO: MUNICIPIO CHACAO". *Revista de la Facultad de Ingeniería U.C.V , 26* (2), 89-101., 2011.

[15] Pérez Pérez, B. (2014). La peligrosidad sísmica y el factor de riesgo. *Informes de la Construcción,* 66(534): e018, doi: http://dx.doi.org/10.3989/ic.

ASSESSMENT OF METHODS FOR EXTRACTION OF METAGENOMIC DNA FROM SEDIMENTS OF LAKES OF THE NATIONAL PARK "LAGUNAS DE MONTEBELLO", CHIAPAS, MEXICO

García-Rodríguez Jorge Arturo[1], Castañón-González José Humberto[1], Gutiérrez-Miceli Federico Antonio[1], Peña-Ocaña Betsy Anaid[1], Trejo-Valencia Radames[2] and Ruíz-Valdiviezo, Víctor Manuel[1]
[1]Tecnológico Nacional de México-Instituto Tecnológico de Tuxtla Gutiérrez, Chiapas, Mexico;
[2]Tecnológico Nacional de México-Instituto Tecnológico de Minatitlán, Veracruz, Mexico

ABSTRACT

A natural protected area of great importance is the National Park "Lagunas de Montebello", Chiapas, Mexico[1]. In this aquatic ecosystem, the lakes have different abiotic and biotic components[1], one of the biotic components are the microbial communities, which can play an important role in the different biogeochemical processes, and also used as bioindicators of the quality of the water[28]. However for our knowledge there are no scientific reports that reveal the diversity and abundance of prokaryotic communities (bacteria and archaea) associated with the sediments of the Montebello lakes. For this reason, the sediments were collected in three points from "Esmeralda" and "Encantada" lakes in two seasons of the year (2017). The samples were characterized physic-chemically and the protocols combine the application of mechanical (sterile sand and vortex), chemical and enzymatic (lysozyme) lysis methods for extraction of total DNA from sediments of lakes followed by its quantification and purity assessment using the nanospectrophotometer[1,9]. The extracted DNA was used to successfully amplify 16S rRNA region. The method of enzymatic lysis is simple, rapid and allowed to obtain an appropriate DNA quality for future metagenomic studies of diversity and exploration of functional genes in sediments of lakes of Montebello, Mexico.

Keywords: Metagenomic, 16S rRNA, Montebello, Bacteria and Archaea Communities.

INTRODUCTION

The composition and microbiological structure of ecosystems are very complex, as is the case of soils and sediments as an important point to have a better understanding of the physiology of the microbial communities present in these environments. The study of ecosystems allows the development of new approaches such as bioremediation, recycling and the discovery of new applications with a biotechnological approach [19]. Especially in aquatic biodiversity defined as the variety of life forms of a aquatic system, which involves multiple dimensions, different levels of organization of genes up to the biosphere, passing through species, populations, communities and ecosystems [13], so that the microbial communities present can be a very sensitive indicator of pollution in aquatic ecosystems [16], contamination could be by the presence of heavy metals, for example, can lead to a process of reducing bacterial diversity [20]. However, there are studies where an increase in microbial diversity was observed along with contamination by heavy metals [26]. Not only this effect, also microorganisms mainly bacteria have been recognized as main components within the benthic food webs, after their important participation in the decomposition of organic matter, on certain nutrient cycles these within biogeochemical cycles, and in food networks and the re-mobilization of heavy metals. By other hand, these microorganisms affect the benthic metabolism in general by regulating the pH and the redox conditions through the consumption of hypolimetic oxygen, nitrates and sulphates [11, 33]. The biological communities are the ones that inhabit the aquatic ecosystems [18], where the prokaryotic microorganisms come from the aquatic soil related as sediment, and that is reflected in it´s geochemical and physical composition that are specific to a site, such as: oxygen (O_2), methane (CH_4), organic and inorganic carbon, certain minerals, water (reflecting its quality) and depth of sediment [5, 15]. The sediments are composed of fractions of: Sand, Clay and Silt, as well as between other loose particles of the soil that are deposited in the bottom of a mass or body of water, in addition that they can come from the erosion of the soil or of the very decomposition of plants and animals. Wind and water are transport factors of these particles that get deposited up to rivers, lakes, lagoons and streams [2]. The characteristics presented by the sediments not only reflect the quality of the water, but also reflect the trophic state of an aquatic system [32].

Unfortunately knowledge of the structure of microbial communities (bacteria and / or archaea) in sediments is still limited, and even more so in sediments from lakes, lagoons and rivers, due to anthropogenic factors that intervene in the system producing effects adverse effects especially aquatic ecosystems [6, 32]. Therefore, in order to acquire a representative description of the microbial diversity, the molecular methods are found, and DNA extracts in a quantitative and qualitative reliable way are needed for their study. In other words, DNA extractions represent sub-surface communities, being challenging due to the low concentrations of nucleic acids that can be extracted, along with the adsorption of cells to sediment-rock particles, and a frequent co-determination extraction of enzymatic inhibitors (concentrations of heavy metals, colloids, fulvic and humic acids, among others). In other words, DNA extraction procedures allow the estimation of microbial diversity, although these require combination and optimization with other molecular methods [3]. On the other hand, the efficiency of the extraction methods are adequate, easy to handle, time-saving and accessible, which is desirably expected, although the methods have been universal in their application, allowing to reduce the number of extraction procedures, and make the calibrations different from more detailed molecular techniques [12]. In turn metagenomics as one of the most advanced methods to discover and describe environmental microorganisms inaccessible in all its complexity, and providing a global view of the potential that microbial communities may have.

The DNA extractions in sediments were evaluated under the management of three protocols mainly: Valenzuela-Encinas et al. (2008), Winston & Hoffman (1987) and Enzymatic Lysis (Saambrok et al., 2001). The objective of this study was to establish selected extraction methods applied to environmental samples such as aquatic sediments, regarding the quantity, quality and purity of the extracted DNA. The quantification of extracted DNA was carried out with a UV-Vis micro-volume spectrophotometer. The procedure, management, costs in terms of preparation and the difficulty to establish extraction protocols for aquatic sediments are very complex.

MATERIALS AND METHODS

Study site and collection of samples

The study was conducted in two aquatic systems called Laguna Esmeralda (Es) and Laguna Encantada (En) within the Lagunas de Montebello National Park (PNLM) aquatic system in the state of Chiapas, Mexico. The experimental site is located in the `Comiteca' region [1], characterized by having a humid temperate C type (fm) with rains throughout the year and in the extreme northwest with a warm climate (cm) with abundant rainfall in summer [23] Montebello a Karstic system with an approximate area of 454 km^2, constituted by diverse bodies of water, many of them connected hydraulically. It is an area dominated by sedimentary rocks from the Cretaceous and also because there are deposits of shallow platforms [14]. Besides being representative as one of the most beautiful natural settings nationwide, characterized by the different colorations of the waters within the more than 60 lacustrine bodies, of karstic origin those vary in extent and shape [23]. The collection of sediment samples in the littoral zone of three afore mentioned aquatic systems was carried out from the lakes hore 1.00 m away, and from that point 1.00 m depth (water-sediment). The collection of samples was carried out in two seasons of the year with dates between March 28, 2017 and August 18, 2017, corresponding to these seasons of low water and rain, in addition to three sampling points. For the sampling, 50 mL sterile polypropylene tubes were used, for each sampling point they were obtained in triplicate. For transport, portable coolers were operated with refrigeration conditions of 4 ° C for subsequent laboratory analyzes [8, 29, 31].

DNA extraction procedures

Three DNA extraction procedures were performed in triplicate. The preserved samples that were frozen were put to thaw gently at room temperature before beginning DNA extraction. The sediment samples were prepared by two processes prior to DNA extraction; From 2.5 g of sediment sample, they were added to 15 mL polypropylene tubes, adding 10 mL of sodium pyrophosphate buffer solution ($Na_4P_2O_7$.10 H_2O, remove organic material) 0.15 M, vortexing 1 minute, followed centrifugation at 4.000 g for 10 minutes at room temperature, the supernatant was decanted and the procedure was repeated until a clear supernatant was obtained. Subsequently, 10 mL of sodium phosphate buffer (NaH_2PO_4, excess sodium pyrophosphate) pH 8.0 was added to the same 15 mL tube, the procedure was repeated until a transparent supernatant was obtained again. The extracted DNA was through three modified procedures as described below.

Procedure one was performed according to Valenzuela-Encinas et al. (2008), the treatment corresponds to a mechanical and chemical method. Adding 500 µL of Lysis I solution (0.15M NaCl, 0.1 M EDTA at pH 8) and resuspending with the help of a vortex, and again adding 500 µL of Lysis II solution (0.1 M NaCl, 0.5 M Tris-HCl pH 8; 12% SDS at pH 8), together with the addition of a sterile sand volume of 0.5 g per sample washed. Shaking 15 mL tubes with a vortex at maximum speed for 20

minutes, and then incubated for 30 minutes at -70 ° C using liquid nitrogen. After the time, the samples were transferred still thermobath at a temperature of 70 ° C for 30 minutes. Finally, it was centrifuged at 4,000 g for 10 minutes at room temperature, so that the supernatant generated was transferred to a new and sterile 1.5 µL tube.

Procedure two was carried out according to Winston & Hoffman (1987), the treatment corresponds to a chemical and mechanical method adding 700 µL of Winston & Hoffman solution (Tris-Cl pH 8, Triton X-100 2%, SDS 1%, NaCl 100 mM and EDTA pH 8, 1 mM), together with this a volume of 0.5 g of sterile sand, vortexing until the sample is completely resuspended for 20 minutes, centrifuged at 4,000 g for 10 minutes at room temperature, the supernatant is transferred to a new and sterile 1.5 µL tube.

Procedure three was performed according to Saambrok et al., 2001, treatment corresponding to a chemical, mechanical and biological method. Adding 1 mL of lysozyme buffer solution (0.25 M EDTA to pH 8), and adding 80 µL of Lysozyme (10 mg / mL), was incubated for 1 hour at 37 ° C. After the time, 1 mL of 10% SDS solution and a volume of 0.5 g of sterile sand were added, and stirring at maximum speed with the aid of the vortex for 20 minutes. Finally centrifuge at 4,000 g for 10 minutes at room temperature, and again the supernatant is transferred to a new sterile 1.5 µL tube.

After each 1.5 µL tube with the supernatant of each procedure used, purification and elimination of proteins continues. Added 1/5 volume of 0.5 M EDTA solution pH 8, and 1/10 volume of 5 M potassium acetate solution pH 5. They were incubated for 40 minutes at 4 ° C, centrifuged at 13,000 g for 10 minutes at 4 ° C. The supernatant was transferred to a new and sterile 1.5 µL tube, where 500 µL of chloroform: isoamyl alcohol solution (24: 1) was added, and vigorously shaking at maximum speed, centrifuge at 13,000 g for 10 minutes at room temperature. In this process, an aqueous phase tends to form, which was transferred again to a new and sterile 1.5 µL tube, this step was repeated three times. That said, a volume of 13% Polyethylene glycol (PEG) in 1.6 M NaCl was added, and vortexing was incubated at -20 ° C overnight. Then centrifuge at 13,000 g for 10 minutes at 4 ° C, removing the supernatant by decanting, trying not to eliminate the DNA pellet stuck in the wall of the tube. The DNA pellet was washed with 500 µL of cold 70% ethanol and centrifuged at 13,000 g for 10 minutes at 4 ° C, again decanting trying not to eliminate the pellet, repeating twice.

Finally, the tube was given a spin with the micro-centrifuge trying to eliminate excess ethanol in the walls of the tube, drying the DNA pellet approximately 10 min, and adding 50 µL of ultrapure water at the end of each procedure.

DNA quantification

The quantification of double chain through the UV-Vis spectrophotometry test, being a next generation instrument in the Nanodrop series of micro-volumes. DNA quality was analyzed by measuring the A260 / A280 ratio (DNA / protein), and the A260 / 230 ratio (DNA / Humic Acid) to verify contamination by protein and humic acid substances, respectively [25]. The quantification of 1 µL of each sample was carried out through Nanodrop One (Thermo Fisher Scientific). The calibration of the equipment is through a target composed of ultra-pure water

RESULTS

Three different procedures were-evaluated and applied to sediment samples from two aquatic systems of the "Lagunas de Montebello National Park" in two seasons of the rainy and dry season.

DNA extraction

The extraction procedures were-obtained a considerable amount of DNA and a purity value according to absorbance values of the A260 / 280 ratio, so the enzymatic Lysis procedure is located as the method with an acceptable quality, on the other hand the procedure Winston & Hoffman (1987) shows in its absorbance an even greater quantity of quality. In comparison with the procedure Valenzuela-Encinas et al., (2008) denoting its value of quality still low.

Analyzing the values of DNA concentration of the three procedures, Valenzuela-encinas et al. (2008) modified the possibility of obtaining a higher concentration of DNA (598.18 ng / µL) unlike two other procedures, which manage to recover a considerable amount of DNA is Enzymatic Lysis (316.83 ng / µL), and finally Winston & Hoffman, (1987) with a certain concentration (7.24 ng / µL), and with a very low quality (Fig. 1).

This is because the procedures used can be different in three ways within their process as mechanical, chemical and enzymatic methods, and their combination allows them to become more efficient the procedures of DNA extraction reflected through quality and quantified quantity. Figure 2 shows the results in their A260 / 280 ratio obtained in the DNA extractions with the three different procedures described in the materials and methods section. For its part Fig. 3 shows the results in their relation A60 / 230 on the same procedures used.

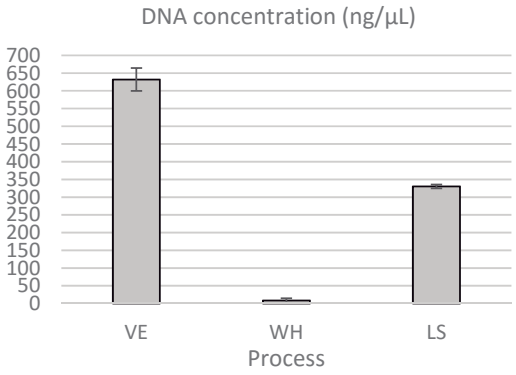

Fig. 1 Extraction methodology vs DNA concentration in units of ng/µL, Valenzuela-Encinas et al., 2008 (VE) recovering the largest amount of DNA, who precedes it is enzymatic lysis (LS) and finally Winston & Hoffman, 1987 (WH)

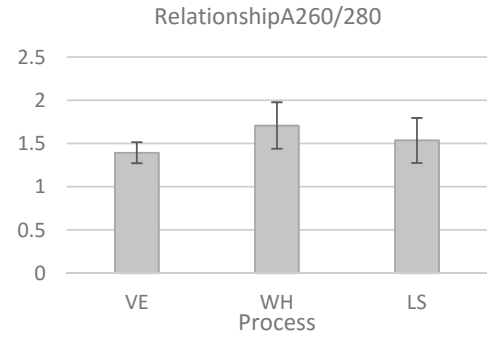

Fig. 2 Extraction methodology vs. Absorbance (A260 / 280), although there is no diversity in its values, Winston & Hoffman, 1987 (WH), procedure with better DNA quality, according to the readings found, in comparison with the two methods, which may be due to the presence of phenols, proteins that intervene in the reading

DNA quantification

Taking into account that the most important parameters within a DNA extraction are the quantity, quality and, respectively, its integrity. Therefore, the values reported as optimal in terms of DNA purity are between the ranges of 1.7-1.9, in terms of DNA purity are between the ranges of 1.7-1.9. The ones that indicate the quality are the spectrophotometric measurements, so analyzing the DNA values shows its high variability in these procedures, however, it is clear that procedure who recovers a greater amount of DNA up to 2519.3 µL, as was reported by Valenzuela-Encinas et al. (2008) with respect to the other two enzymatic Lysis and Winston & Hoffman, (1987) these values were very low. Tables 1, 2 and 3 showed the results obtained in DNA extractions under the three procedures for the rainy season, and for tables 4, 5 and 6 denote the results for the dry season.

Table 1 Values of DNA extraction by procedure No. 1, for the rainy season

System	Point	RAIN SEASON		
		Valenzuela-Encinas et al. (2008)		
		ng/µL	**A260/280**	**A260/230**
Lake "Esmeralda"	Es-A	36.90	1.587±0.431	0.737±0.206
	Es-B	481.60	1.30±0.036	0.653±0.023
	Es-C	941.53	1.313±0.030	0.660±0.01
Lake "Encantada"	En-A	2519.3	1.26±0.015	0.62±0.00
	En -B	3766.1	1.27±0.005	0.65±0.00
	En -C	1103.0	1.29±0.017	0.677±0.005

Table 2 Values of DNA extraction through procedure No. 2 for the rainy season

System	Point	RAIN SEASON		
		Winston & Hoffman, (1987)		
		ng/µL	**A260/280**	**A260/230**
Lake "Esmeralda"	Es-A	8.6	1.72±0.111	0.17±0.025
	Es-B	5.4	1.85±0.258	0.36±0.051
	Es-C	6.6	1.813±0.225	0.337±0.33
Lake "Encantada"	En-A	7.0	1.61±0.057	0.79±0.181
	En-B	0.9	2.08±0.561	0.38±0.013
	En-C	0.53	2.27±1.99	0.347±0.122

Table 3 Values obtained from DNA extractions by means of procedure No. 3 for the rainy season

System	Point	RAIN SEASON		
		Enzymatic lysis		
		ng/µL	**A260/280**	**A260/230**
Lake "Esmeralda"	Es-A	7.0	1.86±0.26	0.08±0.01
	Es-B	209.7	1.29±0.040	0.37±0.16
	Es-C	53.73	1.417±0.04	0.2±0.052
Lake "Encantada"	En-A	37.8	1.51±0.11	0.52±0.01
	En-B	25.4	1.66±0.15	0.38±0.03
	En-C	30.73	1.56±0.02	0.313±0.14

In Tables 1-6 it is possible to observe the behaviour of the procedures between seasons through the sampling points or concentration and their quality, while Fig. 1, 2 and 3 show which of the methods is more efficient in terms of its concentration value, and quality between both absorbance ratios. The enzymatic lysis procedure turns out to be the best procedure in terms of the extraction of metagenomic DNA applied to aquatic sediments, because there is

no variability of the data found, unlike the other two procedures.

Table 4 Values of DNA extraction by procedure N ° 1, for the low season

System	Point	DRY SEASON Valenzuela-Encinas et al. (2008)		
		ng/µL	**A260/280**	**A260/230**
Lake "Esmeralda"	Es-A	7.1	1.5±0.431	0.6±0.30
	Es-B	5.767	1.55±0.50	0.54±0.23
	Es-C	1.5	1.2±0.46	0.2±0.09
Lake "Encantada"	En-A	27.80	1.96±0.20	0.27±0.18
	En-B	3.6	1.90±0.23	0.20±0.21
	En-C	5.13	2.05±0.56	0.18±0.12

Table 5 DNA extraction values through procedure No. 2 for the low season

System	Point	Dry SEASON Winston & Hoffman (1987)		
		ng/µL	**A260/280**	**A260/230**
Lake "Esmeralda"	Es-A	52.6	1.44±0.06	0.637±0.06
	Es-B	28.93	1.51±0.12	0.58±0.17
	Es-C	66.33	1.42±0.02	0.59±0.17
Lake "Encantada"	En-A	196.23	1.58±0.12	0.97±0.24
	En-B	25.20	1.45±0.60	0.54±0.29
	En-C	13.5	1.59±0.27	0.56±0.12

Table 6 Values obtained from DNA extractions by means of the N° 3 procedure for the low season

System	Point	Dry SEASON Enzymatic lysis		
		ng/µL	**A260/280**	**A260/230**
Lake "Esmeralda"	Es-A	18.33	1.9±0.30	0.30±0.197
	Es-B	10.83	2.0±0.13	0.37±0.22
	Es-C	40.33	1.81±0.20	0.28±0.17
Lake "Encantada"	En-A	58.76	1.73±0.05	0.27±0.19
	En-B	51.23	1.71±0.24	0.14±0.07
	En-C	102.8	1.61±0.38	0.49±0.54

DISCUSSION

Three DNA extraction methods was applied to sediments from Montebello lakes and were compared with respect to the concentration, quality and efficiency of the methods used. These were modified in order to obtain acceptable DNA concentrations that allow us to continue with molecular studies such as next-generation sequencing (NGS).

In general, the extraction protocols follow a series of steps, which are based on the fact that the ions (mainly positive saline) are attracted to the negative charges of the DNA, allowing its dissolution, and later the extraction of the cell. These sequential steps consist mainly of: lysing the walls and cell membranes by the action of a detergent, followed by the degradation of the protein fraction and some cellular debris, and finally precipitation of the nucleic material [4, 17].

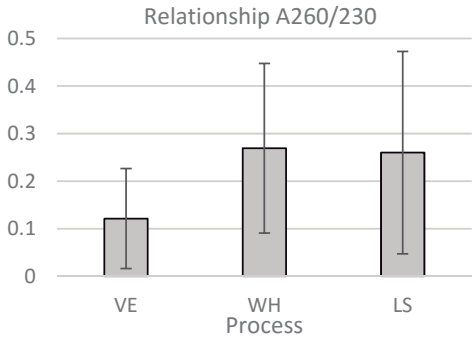

Fig. 3 Procedure used vs. Absorbance (A260 / 230), Valenzuela-Encinas et al., 2008 method with the lowest values and may be due to the presence of ac. Humic

DNA extractions from sediments or soils with low organic content are less problematic [23], in contrast to those that contain a high organic content that requires pre-processing to the samples through $Na_4P_2O_7$ .10 H_2O and followed by NaH_2PO_4. DNA extracts tend to be very impure in order to allow molecular analysis and need further purification. There is no effective purification method, but extraction methods that seem to be idiosyncratic and effective for a specific type of samples in which it was developed, on the other hand there are those that apply in a general manner, but it turns out to be variable in the results [27], and in our study the three evaluated procedures apply in a general manner but differ considerably in the results. That within the extraction process there are substances such as humic acids and try to eliminate them is critical, so again falls in the treatment with $Na_4P_2O_7$.10 H_2O and NaH_2PO4.

Lahiri & Nurberger (1981) reported that a gradient extraction method of salts ($MgCl_2$, KCl, NaCl, EDTA, Tris-HCl) allows to extract´s DNA of sufficient quality to be able to carry out an analysis molecular like PCR 'Polymerase Chain Reaction' [18]. If the samples are environmental, can be precipitated in addition to DNA, polar molecules and, in the case of marine samples, organic and inorganic ions, as well as polysaccharides and residues of chemicals used during the extraction [4, 10, 24]. However, it is known Proteinase K, lysozyme and sodium dodecyl sulphate (SDS) reduce contamination by this component [21]. In

comparison with the procedures used, interaction of the components and their variability of the process is observed (Tables 1-6 values of the three protocols, in terms of the efficiency of said procedures are Fig.1, 2 and 3).

The application of molecular techniques begins with the extraction of DNA, and the obtaining of reliable and reproducible data, dependent to a large extent on the extraction of a complete and pure DNA, within the same process include isolation and purification of DNA molecules that they are based on the physicochemical characteristics of the molecule [7].

Finally, the comparison of three methods of DNA extraction, with an acceptable quality for the last generation sequencing (NGS), the results of these molecular tools will allow to study the diversity of microoganisms present in aquatic sediments from Lagunas de Montebello, besides being able to compare the results in detail with the extent of the use of shotgun.

CONCLUSIONS

In this study was allowed to establish the extraction protocols of metagenomic DNA for sediments, achieving to generate real parameters of quantity, quality and purity of DNA. In addition to generating information on the possible microbial communities that inhabit these ecosystems for future metagenomic studies of diversity and exploration of functional genes.

The best extraction method as the case of enzymatic lysis, finding more stable values in DNA.

Finally, there are no studies at the molecular level in sediments of lakes of the national park “Lagunas de Montebello”, This work is the initial evidence on studies at the molecular level.

ACKNOWLEDGEMENTS

The project was funded by project “6287.17-P” from ‘Tecnológico Nacional de México’ (TNM, Mexico). This work was funded by the "Science Technology Council" (CONACyT) receiving a Master of Science scholarship at the Technological Institute of Tuxtla Gutierrez.

REFERENCES

[1] Alcocer J., Oseguera L. A., Sánchez G., González C. G., Martínez J. R. & González R. Bathymetric and morphometric surveys of the Montebello Lakes, Chiapas. México. Journal Limnology, 2016; 75(s1): 56-65.

[2] Arias-Madrid D., López-Paz O. & Jiménez-Builes J. Análisis de Sedimentos Utilizando un Enfoque de la Programación Estructurada. Rev. Tecno Lógicas No. 29. 2012; pp. 49-67.

[3] Alain K., Callac N., Ciobanu M. C., Reynaud Y., Duthoit F. & Jebbar M. DNA extractions from deep subseafloor sediments: Novel cryogenic-mill-based. Journal of Microbiological Methods 87 (2011); 355–362.

[4] Blanco-Jarvio A., Martinezz-Lopez A. & Bautista-García A. Optimización de un protocolo de extracción de dna total para la amplificación de marcadores moleculares funcionales específicos de organismos desnitrificantes. CICIMAR Oceánides, 29(2). 2014: 37-44.

[5] Calva-Benítez L. G. & Torres-Alvarado R. Organic carbon and textural characteristics of sediments in areas with turtlegrass Thalassia testudinum in coastal ecosystems of the southeastern gulf of Mexico. Researchgate. 27, 2, (2011):133-144.

[6] Castelo-Branco R., Barreiro A., Silva F.S., Carvalhl-Gomes S.B.V., Fontana L. F., Mendonça-Filho J. G. & Vasconcelosm F. Bacterial community characterization and biogeochemistry of sediments from a tropical upwelling system (Cabo Frio, Southeastern Brazil). Continental Shelf Research 130 (2016); 1–13.

[7] Chávez-Medina J. A., García-Negroe C. B., Soto-Lopez F. J.,Góngora-Gomez A. M., Flores-Zamora G. L., Gómez-Peraza R. L., MArtínez-Carrillo J. L. Estandarización de la técnica de extracción del dna de *spodoptera frugiperda* j. e. smith (*lepidoptera: noctuidae*) colectados en maíz en guasave, sinaloa. Entomología mexicana, 3 (2016): 781−785.

[8] Cheng H., Li M., Zhao C., Yang K., Li K., Peng M., Yang Z., Liu F., Liu Y., Bai R., Cui R., Huang Z., Li L., Liao Q., Luo J., Jia S., Pang X., Yang J. & Yin G. Concentrations of toxic metals and ecological risk assessment for sediments of major freshwater lakes in China. Journal of Geochemical Exploration 157, (2015); 15–26.

[9] Díaz-Vargas M, Elizalde-Arriaga EE, Quiroz-Castelan H, García Rodríguez J, Molina-Estudillo I. Caracterización de algunos parámetros físico, químicos del agua y sedimentos del algo Zempoala, morelos, México. Mayo. Año/vol 15, 2005, pp. 57-65.

[10] Espinosa-Asuar, L. Guía práctica sobre la técnica de PCR. In: Eguiarte, L., V. Souza & X. Aguirre (Eds.), Ecología molecular. SEMRNAAT-INE-UNAM-CONABIO, México. 2007; 608p.

[11] Haller L., Tonalla M., Zzopfi J., Peduzzi R., Wildi W. & Poté J. Composition of bacterial and archaeal communities in freshwater sediments with different contamination levels (Lake Geneva, Switzerland). Water research 4 5 (2 0 1 1); 1 2 1 3 -12 2 8.

[12] Kunh R., Böllmann J., Krahl K., Mbir-Bryant I. & Martienssen M. Comparison of ten different DNA extraction procedures with respect to their suitability

for environmental samples. Journal of Microbiological Methods 143 (2017); 78–86

[13] Mancera-Pineda J. E., Gavio B. & Lasso-Zapata J. Principales amenazas a la biodiversidad marina. Bogotá. Colombia. Actual Biol 35 (99). 2013; 111-133, 2013.

[14] Palomino L. M., García L. A., Ramos Y. R., Bonifaz R. & Escoleroa O. Description of chemical changes in a large karstic system: Montebello, Mexico. México, D.F. Procedia Earth and Planetary Science 17 (2017); 829 – 832.

[15] Póte J., García-Bravo A., Mavingui P., Ariztegui D. Wildi W. Evaluation of quantitative recovery of bacterial cells and DNA from different lake sediments by Nycodenz density gradient centrifugation. Ecological Indicators 10 (2010) 234–240.

[16] Pronk, M., Goldscheider, N., Zopfi, J. & Zwahlen, F. Percolation and particle transport in the unsaturated zone of a karst aquifer. Journal of Water and Health .Ground Water 47 (3). 2009; 361–369.

[17] Ríos-Sánchez, E., Calleros, E., González-Zamora, A., Rubio, J., Martínez, O. C., Martínez, A., Hernández, S., & Pérez-Morales, R. Análisis comparativo de diferentes métodos de extracción de DNA y su eficiencia de genotipificación en población mexicana. Acta Universitaria, 26(4). 2016; 56-65.

[18] Rodiles-Hernández R., González-Díaz A. A. & González-Acosta A. F. Ecosistemas acuáticos. La biodiversidad en Chiapas: Estudio de Estado. Comisión Nacional para el Conocimiento y Uso de la Biodiversidad (conabio) y Gobierno del Estado de Chiapas, México. 2014; pp. 45-57.

[19] Rojas-Hernández R., Narváez-Zpata J., Zamudio-Maya M. & Mena-Martínez M. E. A Simple Silica-based Method for Metagenomic DNA Extraction from Soil and Sediments. Mol Biotechnol (2008) 40:13–17.

[20] Sandaa R. A., Torsvik W., Enger Ǿ., Daae F.L., Castberg T. & Hahn D. Analysis of bacterial communities in heavy metalcontaminated soils at diferent levels of resolution. FEMS Microbiol. Ecol. 30 (1999); 237-251.

[21] Sagar K., Singh S. P., Goutam K. K. & Konwar B. K. Assessment of five soil DNA extraction methods and a rapid laboratory-developed method for quality soil DNA extraction for 16S rDNA-based amplification and library construction. Journal of Microbiological Methods 97 (2014) 68–73

[22] Sambrook J, Rusell D. W. Molecular cloning: a laboratory manual. (Cold Spring Harbor Laboratory Press, NY, eds). 3rd ed (2001); pp.

[23] Secretaría de Medio Ambiente y Recursos Naturales "SEMANH" (2007). Programa de Conservación y Manejo Parque Nacional Lagunas de Montebello, MÉXICO. 1era. Edición. ISBN 978-968-817-848-5 e 968-817-848-9.

[24] Serrato-Díaz, A., L. Flores-Rentería, J. Aportela-Cortez & E. Sierra-Palacios. In: Cornejo-Romero, A., A. Serrato-Díaz, B. Rendón-Aguilar & M. G. Rocha-Munive (Eds.), Herramientas moleculares aplicadas en ecología: Aspectos teóricos y prácticos. INECC, México. (2014); 274 p.

[25] Solomon S., Kachiprath B., Jayanath G., Sajeevan T. P., Bright Singh I. S. & Philip R. High-quality metagenomic DNA from marine sediment samples for genomic studies through a pre-processing Approach. Kerala, India. Springer- Biotech (2016) 6:160.

[26] Sorci, J.J., Paulauskis, J.D. and Ford, T.E. 16S rRNA-restriction fragment-length polymorphism analysis of bacterial diversity as a biomarker of ecological health in polluted sediments from New Bedford Harbor, Massachusetts, USA. Mar. Pollut. Bull. 38 (1999); 663-675.

[27] Schneegurt M. A., Dore S. Y. & Kulpa Jr. C. J. Direct Extraction of DNA from Soils for Studies in Microbial Ecology. Curr. Issues Mol. Biol. (2003) 5: 1-8.

[28] Tan B, Ng C, Nshimyimana JP, Loh LL, Gin KYH, Thompson Jr. Next-generation sequencing (NGS) for assessment of microbial water quality: current progress, challenges, and future opportunities. Frontiers in microbiology, Vol. 6, 2015; pp.1027.

[29] Tian K., Hu W., xing Z., Huang B., Jia M. & Wan M. Determination and evaluation of heavy metals in soils under two different greenhouse vegetable production systems in eastern China. Chemosphere 165 (2016); 555-563.

[30] Valenzuela-Encinas C., Neria-GonzálezI., Alcántara-Hernández R.J., Enríquez-Aragón J. A., Estrada-Alvarado I., Hernández-Rodríguez C., Dendooven L. & Marsch R. Phylogenetic analysis of the archaeal community in an alkaline-saline soil of the former lake Texcoco (Mexico). Springer- Extremophiles (2008), 12: 247–254.

[31] Vera-Franco Maya N., Hernández-Victoria P. P., Alcocer J., Ardiles-Gloria V. & Oseguera L. A. Concentración y distribución vertical de la clorofila-a fitoplanctónica en los lagos de Montebello, Chiapas. Tlalnepantla, Estado de México, México. Tendencias de Investigación en Limnología Tropical. 2015; 1-9.

[32] Wang Z., Su Y., Zhang Y., Guo H., Meng D. & Wamg F. Ecology-types determine physicochemical properties and microbial communities of sediments obtained along the Songhua River. Biochemical Systematics and Ecology 66 (2016); 312-318.

[33] Winters A. D., Marsch T. L., Brenden T. O. & Faisal M. Molecular characterization of bacterial communities associated with sediments in the Laurentian Great Lakes. Journal of Great Lakes Research 6, (2014); pp.

[34] Winston F. & Hoffman C. S. A ten-minute DNA preparation from yeast efficiently releases autonomous plasmids for transformation of Escherichia coli. Elsevier-Gene, 51 (1987); 267-212.

QUANTIFICATION OF PESTICIDES AND HEAVY METALS IN SEDIMENTS OF THE "ENCHANTED" LAKE OF THE NATIONAL PARK PONDS OF MONTEBELLO, CHIAPAS, MEXICO

Díaz-Cancino, Carolina Elizabeth[1], Castañón-González José Humberto[1], Villalobos-Maldonado Juan José[1], Ruíz-Valdiviezo Víctor Manuel[1], Báez-Sañudo Reginaldo[2], Adrián Gómez-De Jesús[3] and Trejo-Valencia, Radames[4]

[1]Tecnológico Nacional de México-Instituto Tecnológico de Tuxtla Gutiérrez, Chiapas, México; [2] Centro de Investigación en Alimentos y Desarrollo AC, Sonora, México. [3]Catedra CONACyT-Universidad Autónoma de Chiapas [4]Tecnológico Nacional de México Instituto Tecnológico de Minatitlán, Veracruz, México

ABSTRACT

The "La Encantada" lake was selected from the lagoon complex of the Lagunas de Montebello National Park, declared a RAMSAR Site in 2003 [1], due to its characteristics of color change over time few scientific studies reported [2]. The physicochemical parameters in the water were monitored *in situ* using electronic equipment and sensors in two seasons of the year (rains and low water) of 2017. The sediments were collected in three point and two seasons of the year. After, the quantification of heavy metals and pesticides in sediments was determined. The results showed the presence of lead (Pb), cadmium (Cd), iron (Fe) and mercury (Hg), found that the concentrations of these metals were higher values than the maximum permissible limits of the official Mexican standard NOM-127-SSA-1994. The reported chemical oxygen demand values indicate site contamination (24 to 87 mg / L OD). Likewise, pH, electrical conductivity, temperature and dissolved oxygen values were determined, finding significant differences in the sampling seasons [4]. Finally, the pesticides organochlorines (endosulfan, dieldrin, endrin, heptachlor) and organophosphorus (triadinefin, parathion, malathion) were not detected in sediment, even though these pesticides were employed by the populations near the study site, for the cultivation of corn, tomato and squash (4). Currently, techniques are established for the identification of microorganisms present in the sediments of the study sites within lakes of Montebello, México.

Keywords: Lagunas de Montebello National Park, Heavy Metals, Pesticides, Physico chemical parameter, RAMSAR

INTRODUCTION

The geographical position, the physiographic complexity and geology of Chiapas, causing a great diversity of ecosystems and species. In order to protect these ecosystems Protected Natural Areas (ANP) they were created.

In Chiapas, a protected great importance, it is the natural area Montebello Lakes National Park (PNLM), introducing a biodiversity in their soil, flora, fauna and hydrology [2].

This site is characterized by a diversity of lakes with different shades that make them attractive to tourism. In recent years, it has been affected by a change of color in the water of the lakes, as is Lake La Encantada.

Adjoining the National Park are various agricultural crops such as corn, beans and tomato; It is further believed that sewage from the city of Comitan infiltrate this lagoon system to not have a wastewater treatment.

The research focused on the pellets, as they serve as sinks and are potential secondary sources of heavy metal [5].

In aquatic systems, heavy metals and pesticides have high affinity for particulate matter and, therefore, accumulate in the sediment surface [6].

The objective of this project is to study heavy metals and organochlorine pesticides that may be present in the sediments of Lake La Encantada, to determine the degree of contamination in which this can be found.

MATERIALS AND METHODS

Study area

The Lagunas de Montebello National Park (PNLM) is located in South-East region of the State of Chiapas, on the border with Guatemala CA, covers an area of 6, 425 ha it comprises part of the Municipalities independence and Trinitaria. Its coordinates are 16º 04 ' 40 " and 16º 10 ' 20 " North Latitude and 91º 37 ' 40 " and 91º 47 ' 40 " West Longitude [2].

The PNLM has an altitude range of 1,200 to 1,800 meters, has humid climate with semi-warm rain throughout the year, with an annual

precipitation of 1,800 mm and average annual temperature of 17 ° C [7].

It consists of 60 lakes, within which the La Encantada lake, which belongs to Tepancoapan lagoon system is.

Lake La Encantada, has an altitude of 1434 meters, is characterized as a turbid lake with a connection to Lake Blue Forest, the dominant vegetation in the periphery is pine forest and on the banks of sawgrass by *Cladium jamaicense* [8] has a shape a semicircular area of 8.2 ha a maximum depth of 89 m and a depth of 29.4 m and a volume of 2,410,000 m^3 of water [3].

Time of sampling

The samplings were conducted during two seasons; drought, comprising the months of February to May with rainfall and no rainfall during the months of July to September with an average rainfall of 1.83 mm according to records obtained from the EMA located 15DA7496in Montebello facilities. The sampling for the dry season was held on March 13, 2017 and the rainy season on August 18, 2017.

Sample design

Mexican 112-1995-SCFI standard defines the sample as a representative entity of a place and it is an integral and fundamental part of any program evaluation of the quality of the aquatic environment.

In order to obtain a representative sample site, sampling three areas were selected, which they were geographically located equidistant and whose sampling points were named with letters A, B, and C (Fig. 1).

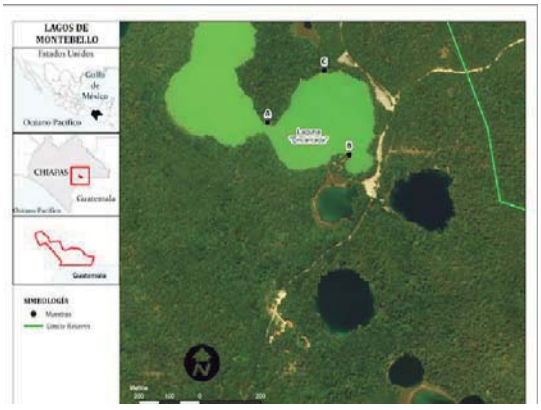

Fig. 1 Sampling points Encantada Lake

Sampling

Water samples were taken at a depth of 50 cm from the lake, in amber glass bottles previously sterile colored. Each sample was taken in triplicate at each sampled point, for transporting samples sulfuric acid was added until pH 2 in order to prevent growth of bacteria and they were representative of the place and time when it was carried out the sampling. Samples in coolers to 4 ° C were transferred, and then stored at -4 ° C until use.

Sediment samples were obtained by a simple 50 cm of the lake surface and 50 cm from the periphery there of, the sampling equipment used was a stainless steel dredger Ekman® type. Samples were taken in triplicate at each sampling point, once taken the samples were placed in sterile polyethylene bags black 30 x 45 x 16 cm to avoid exposure to sunlight and pollution. They were transported to the laboratory in ice chests at 4 ° C and stored at -20 ° C until use.

Treatment of samples (sediment)

To remove moisture of the samples they were placed in porcelain capsules and dried in an oven at a temperature of 30 ° C. Samples were crushed in a mortar to a fine homogeneous powder, then was sieved with a mesh (2x1 mm) and stored in sealed bags at room temperature until use.

Determination of physicochemical parameters

Physicochemical parameters were taken in situ it was performed by an automated multiparameter meter mark Global Water® ultrasensitive sensors. Measurements were taken at a distance of 2 m deep. The parameters measured were temperature (° C), pH and electrical conductivity (mS / cm).

Determination of Chemical Oxygen Demand (COD)

It was performed using the methodology of NMX-AA-030-SCFI- 2001 for COD determination by closed reflux, using commercial kit HACH® COD of the mark. 2 mL of sample was taken and placed into kit vials digestion, which were placed in the digester equipment (preheated) at 180 ° C for 2 hours, were removed from the digester and allowed to cool at room temperature for reading in the spectrophotometer at a wavelength of 620 nm. COD (mg O2 / L) of the samples was determined by the equation of the line obtained from the calibration curve potassium biphthalate ($C_8H_5KO_4$), previously obtained.

Determination of heavy metals

Heavy metal analysis was conducted in the laboratory of toxic waste from the Center for Food Research and Development (CIAD) of the city of Hermosillo, Sonora. The heavy metal analyzes were

performed by atomic absorption spectroscopy flame, graphite furnace and hydride generator according to NMX-AA-051-SCFI- 2001.

The extraction of heavy metals in sediment was performed with a strong acid digestion, 0.5 g of dried and sieved sediment was weighed into a flask of 120 mL Teflon brand savillex®; They were added 5 mL of concentrated nitric acid 70% (HN03), 5 mL of concentrated hydrochloric acid 37% (HCl) and 15 mL of deionized water using an extraction chamber. Acid digestion was carried out in an autoclave at 125 ° C and 15 lb pressure in a time of 50 minutes, after this time the samples were cooled and again placed in the autoclave for another 50 minutes this to achieve complete disintegration of the sample in the acid solution.

Once cooled digested and the samples were filtered with a Whatman # 40 (125 mm) membrane where the filtrate was recovered in volumetric flasks balls 50 mL and the volume with deionized water gauging completed.

Identify metals were Cd, Cr, Cu, Fe, Pb, Mn, Zn and Hg. They were selected for their high level of toxicity, its relation to mining and its continued presence in other studies [9].

Equipment gas chromatography was used for atomic absorption Pb, Cd and Cr metals in graphite furnace. For Cu, Mn, Fe and Zn equipment gas chromatography was used for atomic absorption flame and Hg, the gas chromatography equipment was used by flame atomic absorption with hydride generator.

Determination of organochlorine pesticides

Quantification of organochlorine pesticides was performed by gas chromatography Detector Electron Capture (ECD) under the methodology of the AOAC 990.06, where the scope of the method include determining Heptachlor, Triadimefon Hexaconazole, Dieldrin, Endrin, and Iprodione pesticides [14].

The results were verified by gas chromatography with mass detector according to the method determined by Anastassiades *et al*. (2003). Where certain pesticides were: Parathion, Parathion-Methyl, Malathion, Pirimiphos-Methyl, Triadimefon, Endrin, Dieldrin [13].

Extraction Method Organochlorine Pesticides

A sample of 10 g was taken in a centrifuge tube of 50 ml, in triplicate. A white method (where the matrix was 10 mL of water, unfortified) to determine interference of the reagents involved in the extraction process was prepared. 10 ml of acetonitrile was added and stirred vigorously for 10 minutes. Subsequently it was added 4 g of anhydrous magnesium sulfate and 1g sodium chloride, mixed by vortexing at maximum speed for 1 minute in order to avoid clusters. I was centrifuged for 5 minutes at 5000 rpm at 15°C, transferred 1 ml of supernatant to a 2 ml Eppendorf tube which contained 25 mg of PSA and 150 mg of anhydrous magnesium sulfate, was vortexed for 30 seconds and centrifuged 2 minutes at 6000 rpm at 15°C, the liquid phase was transferred into autosampler vial.

Injection of samples

Virgin sample extract was injected to identify potential organophosphate or organochlorine present and confirm that there is no presence of peaks at elution time of the internal standard.

A gas chromatograph was used with electron capture detector (^{63}Ni) for injection by gas chromatography with electron capture detector (ECD), with a capillary column chrompack Cp-Sil 5 CB 15 meters length and 0.25 mm internal diameter and nitrogen (UAP) as carrier gas.

The results of the concentration of organophosphate and organochlorine sediment by gas chromatography mass spectrometry were corroborated; a gas chromatograph was used with a system coupled to mass spectrometry with a capillary column of DB5ms 30 meters, 0.25 mm internal diameter and helium (UAP) as carrier gas.

RESULTS AND DISCUSSIONS

Physicochemical parameters in water

The physicochemical parameters of the water varied from season to season (Table 1). The temperature for the dry season found in levels ranging from 25.3 ° C to 27.2 ° C; in the rainy season they were found at a lower level (22.8 to 25.6 ° C).

Table 1 Physiochemical parameters La Encantada lake in the two sampling periods

Parameter	Season	
	Dry	Rainy
pH	9.05 ± 0.13	9.43 ± 0.07
EC (**µ**S / cm)	401.33 ± 5.51	339.48 ± 3.13
Temperature (° C)	26.37 ± 0.97	24.5 ± 1.49

Note: T = temperature, pH = hydrogen potential, CE = electrical conductivity.

La Encantada present a basic pH, which had different behavior in both seasons; the dry season showed levels ranging from 8.9 to 9.14, while the pH in the rainy season was higher compared to shallow water, where the values were within 9.35 to 9.47 pH levels found were above those reported by

Orozco in 2016, who reports to pH 8.01 ± 0.53 delighted.

The electrical conductivity varied in all points of both seasons. As the rainy season who had the lowest parameters (337-343µS / cm) and the highest season dry season (396-407 µS / cm). The values of both seasons are within the values reported in this lake Orozco, 2016, who reported an electrical conductivity of 372 ± 62.3 µS / cm.

Chemical Oxygen Demand

The chemical oxygen demand was higher concentrations in the rainy season, where the minimum value found was 77.72 mg O2 / L and a maximum of 8701 mg O2 / L; while in the dry season only point C present a high value (78.65 mg O2 / L) (Fig. 2).

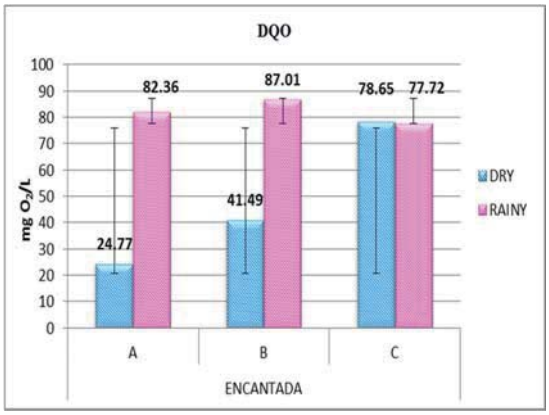

Fig. 2 Chemical oxygen demand at lake La Encantada

The Secretariat of Environment and Natural Resources (SEMARNAT) and the National Water Commission (CONAGUA) in 2012, conducted a study in Mexico for the determination of chemical oxygen demand (COD) and biochemical oxygen demand (BOD) in different water bodies of the country. Where water pollution categorized according COD levels, the levels range from < 10 mg / L for water with excellent quality; > 10 and < 20 (mg / L) good water; > 20 and < 40 (mg / L) acceptable water; > 40 and < 200 (mg / L) contaminated water and > 200 heavily contaminated water [10].

Referencing these values, lake La Encantada can be categorized for point B and C of the dry season as contaminated water and the point A, water acceptable. While in the rainy season the water is categorized as polluted water, since the values reported in the three sampling points are within the range > 40 and < 200 (mg / L).

This may be the various changes that have taken Montebello in recent years, where the change in land use, loss of vegetation cover, anthropogenic activities have led to changes in aggregate stability and soil structure making them more vulnerable to erosion processes lead to the mobilization of soil material and chemicals products to the base of the basin where the lagoon system is located [11].

Heavy metals

Metals had different behavior in the two different seasons; where levels in the rainy season of Pb, Cu, Zn and Hg were higher than the dry season.

While in the dry season found levels of Cr, Cd, Mn and Fe were higher than those of the rainy season (Table 2).

Table 2 Heavy metals La Encantada lake in the two sampling periods

	Seasons	
Metals	Dry	Rainy
Pb	6.51 ± 0.2	11.6 ± 0.2
Cr	1.11 ± 0.2	0.87 ± 0.04
CD	2.95 ± 0.2	2.75 ± 0.3
Cu	35.65 ± 0.4	40.61 ± 0.4
Mn	5.28 ± 0.02	4.68 ± 0.3
Faith	171.66 ± 6	122.21 ± 3
Zn	119.43 ± 4	138.38 ± 2
Hg	0.80 ± .04	0.84 ± .04

Note: Cd = Cadmium, Cr = Chromium, Cu = Copper, Fe = Iron, Hg = Mercury, Mn = Manganese, Pb = Lead, Zn= Zinc. The results are expressed in mg / kg.

Although there is no Mexican Standard that endorses concentrations permitted metals in sediments in Mexico, data with CEQG (Quality Guidelines Environment Canada (for its acronym in English, Canadian Environmental Quality Guidelines) for sediments of water bodies were compared continental). In the section ISQG: Interim Guidance Quality Sediment (for its acronym in English, Interim Sediment Quality Guideline) (12).

Cu levels in the dry season (35.65 ± 0.4 mg / kg) and in the rainy season (40.61 ± 0.4 mg / Kg) they are above the maximum permissible limits of the Canadian Standard, which handles a minimum concentration of 35.7 mg / Kg.

This same behavior is seen in determining the Zn in the rainy season, where the value found (138.38 ± 2 mg / kg) is more than is allowed in the Canadian Standard (123 mg / kg).

The results of the analysis suggest that heavy metals Hg concentrations detected in the study area exceed the maximum permissible limits of the Canadian standard, since el Hg in both seasons, found above the maximum permissible levels (0.17 mg / kg).

Organochlorine Pesticides

When injecting the samples into the gas Chromatograph with Electron Capture (EDC) no presence of peaks at elution time of the internal standard was found, indicating that there aren't organochlorine or organophosphate in the sample.

To ensure that the data were reliable was corroborated on a gas chromatograph coupled to a mass spectrometer (GC-mass), which also gave negative results.

CONCLUSIONS

The results of this study demonstrate the presence and increase of Pb and Hg in the intrinsic zone sediments La Encantada lakes Montebello Chiapas, according to the Mexican NOM-127-SSA-1994 which sets the permissible limits of quality and treatment of water.

Levels of Pb, Cu, Zn and Hg show variations according to the time of sampling, this variation of the metal indicates a higher bioavailability of the metal during the rainy season.

From according to Interim guidance Canadian Sediment Quality (ISQG), representing the concentration below which it is not expected occurring adverse biological effects; Cu in both seasons are above the maximum permissible limits, likewise the Zn in the rainy season, so the Hg in both seasons exceeds the maximum permissible limits in this standard.

Although two methodologies perform analysis organochlorine and organophosphate pesticides, these were not detected; it may be because these are not accumulated in the sediments of Montebello.

ACKNOWLEDGEMENTS

National Technology Mexico, for project financing 6287.17-P, "Environmental and molecular diagnosis of aquatic ecosystems protected from Chiapas". The laboratory of toxic waste (heavy metals and pesticides) Center for Food Research and Development (CIAD) of the City of Hermosillo, Sonora, Mexico. CONACYT for the scholarship granted to scholarship program Master of Science in Biochemical Engineering, Institute of Technology Tuxtla Gutierrez (TecNM) Carolina E. Diaz Cancino (605758).

REFERENCES

[1] RAMSAR (09 September 2003). Mexico wetlands. Retrieved on January 19, 2017. http://ramsar.conanp.gob.mx/docs/sitios/FIR_RAMSAR/Chiapas/PN%20Lagunas%20de%20Montebello/Parque%20Nacional%20Launas%20de%20Montebello.pdf.

[2] National Commission of Natural Protected Areas (CONANP). (2011). Conservation and management program of the Lagunas de Montebello National Park. Mexico DF: SEMARNAT.

[3] Alcocer, J., Oseguera, LA, Sanchez, G., Gonzalez, C., Martinez, JR, & Gonzalez, R. (2016). Morphometric and bathymetric surveys of the Montebello Lakes, Chiapas.

[4] Diaz, CC (2015). Characterization of agricultural production systems in the Tepancoapan Lagunar PNLM System. Comitan, Chiapas.

[5] Wang, Y., Yang, L., Kong, L., LIUC, E., Wang, L., & Zhu, J. (2015). Spatial distribution, ecological risk assessment and source identification for heavy metals in surface sediments from Lake Dongping, Shandong, East China. Soil Science, 200-205.

[6] Sundaray, SK, Nayak, BB, Lin, S., Bhatta, D., 2011. Geochemical speciation and risk assessment of heavy metals in the river estuarine sediments-A case study: Mahanadi basin, India. J. Hazard. Mater. 186, 1837-1846.

[7] Mora, PL, Garcia, LA Rene, RY, Bonifaz, R., & Escolero, O. (2017). Description of chemical changes in a large karstic system: Montebello Mexico. Appropriate, Earth and Planetary Science, 829-832

[8] Orozco, MC (2016). Effects of physicochemical variables in the structure of the community of aquatic macroinvertebrates in the lakes of Montebello. Mexico, DF: UNAM.

[9] Garcia-Garcia, N., Pedraza-Garciga, J. Montalvo, JF, Martinez, M., & Leyva, J. (2012). preliminary assessment of risks to human health from heavy metals in the bays of Buenavista and Remedios, Villa Clara, Cuba. Cuban Journal of Chemistry, 24 (2), 126-135.

[10] Ministry of Environment and Natural Resources (SEMARNAT) and the National Water Commission.Percentage distribution of monitoring sites for surface water chemical oxygen demand (COD), 2012. The environment in Mexico.http://apps1.semarnat.gob.mx/dgeia/informe_resumen14/06_agua/6_2_1.html.

[11] Martinez M. 2015. Characterization of soils in the Rio Grande as support for understanding the dynamics of pollutants reaching the lagoon system of Montebello, Chiapas. Thesis. School of Higher Studies Zaragoza. National Autonomous University of Mexico. DF, Mexico.

[12] Canadian Environmental Quality Guidelines (for its acronym in English, Canadian Environmental Quality Guidelines), establishing water quality parameters for the

protection of aquatic life concerning the presence of metals in inland waters; Interim Sediment Quality Guideline) and Probable Effect Level).

[13] Anastassiades, M. Lehotay, S.J, Stajnbaher, D y Schenck F,J. (2003). Fast and easy multiresidue method employing acetonitrile extraction / partitioning and dispersive solid phase extraction for the determination of pesticide residues in produce. J. AOAC International. Vol. 86, No. 2, Pag. 412-431.

[14] Association of Official Analytical Chemists (AOAC) International. Official Methods of Analysis, Edition 2000. , Cap. 10, Pag. 14-18. AOAC International, 2200 Wilson Boulevard, Arlington, VA 22201

PHYSICOCHEMICAL CHARACTERIZATION, ELEMENTAL SPECIATION AND HYDROGEOCHEMICAL MODELING OF SANTA LUCÍA PELOID USED FOR THERAPEUTIC USES

Suárez Muñoz Margaret [1], Martínez-Villegas Nadia [2], González-Hernández Patricia [3], Melián Rodríguez Clara [1], Barrios Cossio Josiel [1], Hernández Rebeca [4], Fagundo Juan R. [3], Díaz Rizo Oscar [1], Gelen Rudnicas Alina [1], Díaz López Cristina [3]and Pérez-Gramatges Aurora [5]

[1]Department of Radiochemistry, Higher Institute of Technology and Applied Sciences (InSTEC), Havana, Cuba,[2]Applied Geoscience Department, Institute for Scientific and Technological Research of San Luis Potosi (IPICYT), Mexico,[3]Faculty of Chemistry, Havana University, Cuba,[4]Technique Sciences Faculty, University of Pinar del Río "Hermanos Saíz", Pinar del Río, Cuba, [5]Department of Chemistry, Pontifical Catholic University of Rio de Janeiro (PUC-Rio), Brazil.

ABSTRACT

Santa Lucía peloid is a sediment, extracted from salt mines, used in pelotherapy in Cuban primary health care services. Therefore, in addition to classical quality control analyses of total metal concentrations in sediments, speciation and complementary analyses are required to understand potential geochemical element availability for their use in human health.

The present study was conducted to characterize the Santa Lucía peloid, based on the total metal content and geochemical speciation of major elements and transition metals (Cr, Cu, Fe, Ni, Mn, Pb and Zn), using a sequential extraction procedure and inductively couple plasma emission techniques. In order to predict the distribution of majoritarian and trace elements in different geochemical fractions, the physicochemical parameters, the particle size (electronic microscopy), mineralogy (X-ray diffraction), and the hydrogeochemical models (Pourbaix phase diagrams) were used. The results showed that the predominant cation was Na with high mobility and exchange capacity; meanwhile most of the trace elements studied (Cr, Pb, Ni) in this investigation appeared in the less mobile fractions, which suggested low availability in the sediment, under the studied conditions. The findings were useful to predict the behavior of the metals regarding solubility, potential motility and availability in the sediment, and it was concluded that most of the metals are strongly retained in the peloid and that sediment was considered as non-polluted, according to USEPA normative.

Keywords: Peloid, Trace elements, Pelotherapy, Sediment, Santa Lucía

INTRODUCTION

Peloids are multi-component systems which consist of mineral water and clay minerals, organic matter and organo mineral complexes that are applied in healing procedures [1]. Peloids can be formed by the interaction of geo materials with mineral waters over long periods of time in a natural environment or can be formulated in an artificial maturation process focused in a product with suitable properties for the treatment of specific pathologies [2].

During the last decades, several investigations have been done to get insights on the chemical composition and biological mechanism of action of peloids for the significance in their correct application and use in the treatment called Pelotherapy [2]. Tendencies of the chemical studies in peloids have been related with the determination of chemical species (organic and inorganic compounds with biological activities); changes in maturation process; determination of physicochemical and rheological properties of peloids, organic contaminants and toxic elements (As, Cd, Hg, Pb Se, Tl, etc.); and the establishment of standard criteria for the certification of the quality and suitability of the peloids devised for specific therapies [2]-[4].

In particular, mobile and/or exchangeable toxic elements (e.g. Fe, Mn, Cu, Zn, Pb, Cr, As, Cd, Hg), are of special concern, since they can be scavenged by the skin sweat [4]. These metals have therefore become important discussion issues in the "certification" of the quality of sediments for therapeutic uses [2]. However, there are only a few comprehensive studies related to the presence and availability of these metals in peloids, despite being a key knowledge to understand the possible beneficial and/or dangerous effects to human health [2], [4]. Particularly, there is a need for studies related to the geochemical composition of peloids used in balneotherapy due to the risk of heavy metals in peloids, the interaction between metals and other components of the peloid matrix, and with the

human biomembranes, with possible re-adsorption through the skin [2].

Besides the total content, metals can be partitioned into different chemical forms that are associated with a variety of organic and inorganic phases, depending on chemical and geological conditions [2], [5]. Thus, speciation analysis of metallic elements and mineralogical studies might provide useful information regarding the potential mobility and bioavailability of a particular element, which consequently can offer a more realistic estimation of its effects [5].

In Cuba, there is still a great reserve of natural peloids, used in pelotherapy. The profuse resources are related with coastal and salt mine (brine) sediments due to a wide distribution through the island coastal line. Santa Lucía peloid is a sediment extracted from "El Real" salt mine, located in Santa Lucía locality, in Camaguey Province, Cuba, at 20° 52′ 03″ of north latitude and 90° 22′ 20″ west longitude. This peloid has been used in pelotherapy for many years, mainly associated with Cuban primary health care centers and services, for the routinely treatment of inflammatory (osteoarthritis, rheumatoid arthritis, bursitis) and dermatological (eczemas, psoriasis, cutaneous seborrhea and mycosis) processes. As far as the actual knowledge, there are no reports of operational speciation and geoavailability of metals in this peloid; either or studies on its relation with the physicochemical and geological conditions, to predict the metallic elements mobility and establish the inorganic quality for its use in pelotherapy.

The present study was conducted to characterize the Santa Lucía peloid, based on the total metal content and geochemical speciation of major elements and transition metals (Cr, Cu, Fe, Ni, Mn, Pb and Zn), using a sequential extraction procedure and inductively couple plasma emission techniques. In order to predict the distribution of majoritarian and trace elements in different geochemical fractions, the physicochemical parameters, the particle size (electronic microscopy), mineralogy (X-ray diffraction), and the hydrogeochemical models (Pourbaix phase diagrams) were used.

MATERIALS AND METHODS

Field methodology

Surface samples of the peloid (20-40 cm) were collected directly in the "El Real" salt mine, 50 m away from the coastal line. A composite sample was prepared from 10different subsamples. "In situ" measurements of pH, oxidation–reduction potential (Eh),electric conductivity (EC), temperature and dissolved oxygen in the peloid samples were carried out using a HANNAHI-8424 pH/Eh meter, a WTW LF197 conductimeter with internal temperature probe and a HANNA HI 914 oxymeter, respectively.

Sediment samples were sealed in clean polyethylene containers, placed in a cooler at 4 °C, and transported to the laboratory immediately for further analysis.

Laboratory methodology and hydrogeochemical modeling

The sequential extraction method followed a modified Tessier diagram [6], to obtain five different fractions: (i) exchangeable(EXC), (ii) bound to carbonates (CARB), (iii) bound to easily reducible oxides (Fe/Mn oxide-bound fraction) (ERO), (iv) bound to organic matter and sulfide (MO), and (v) residual (R-RES). Total metal concentration (digestion using HNO_3 (65%) and $HClO_4$ (60%)(3:1.5)) and sequential extraction procedures used in this study were previously described by Suárez [2]. The final extracts were analyzed using an inductively coupled plasma optical emission spectrometer (ICP-OES, Varian: 730-ES Optical Emission Spectrometer) to determine metals commonly present in sediments (Cu, Cr, Fe, Mn, Ni, Pb and Zn). Total metal concentrations were compared with results obtained from the sequential extraction procedure of the sediment samples. Quality control was assured by the analysis of triplicate samples and standard reference materials with recoveries ranged from 86 to 116% and analytical precision better than 10%.

The Pourbaix phase diagrams were used as hydrogeochemical model to predict the dominant aqueous species of each metal and sulfur in the sediment, defined by the Eh and pH values [7].

Solid phase analysis (XRD, SEM-EDS, particle size)

Bulk mineralogy was determined by X-Ray Diffraction (XRD) using PANalytical X'Pert PRO X Ray Diffractometer with Cu Kα radiation. Analyses were performed in a 2θ range of 5 to 90° at a scan rate of 0.02° s^{-1}. Phase identification was carried out by comparison with the Joint Committee of Powder Diffraction Standard 2007 Data Base. Mineral semi-quantification was estimated by the Reference Intensity Ratio (RIR) method using the X'pert High Score Plus software.

For the Scattering Electronic Microscopy (SEM), the peloid samples were observed using a scanning electron microscope Phillips XL 30, EE.UU. The particle size was determined using at least 10 different areas of each sample microphotography; and the image processing was obtained by the ImageJ IJ 1.46r software. The obtained data was classified by the International System of Texture of Soils and Sediments [39], and the normalized

classification of soils attending to different normatives (DIN (4022), British, ASTM) [8].

Sediment quality assessment

In the present work, the peloid was considered and evaluated as a generic sediment, using standard quality guidelines (USEPA, 1977) [9] to establish chemical inorganic quality criteria, since it was not possible to find in the literature any specific requirements regarding metal content in peloids.

Elemental results are then compared with background concentrations to determine if the metal content in the analyzed peloid represents a natural concentration or a contamination value. These background values are used for the calculation of the contamination factor (Cf) and the contamination degree (Cd) calculated as described in [2], [10].

The mobility factor (MF), as the relation of the content in the more labile fractions against all the fractions determined [10], were calculated as Eq. (1).

$$MF = \frac{(EXC + CARB)}{(EXC + CARB + ERO + MO + R - RES)} * 100 \quad (1)$$

RESULTS AND DISCUSSION

Physicochemical, elemental characterization

The results obtained for physicochemical parameters show very low (negative) oxidation–reduction (Eh) potential (−0.413 ± 0.002V) and anoxic conditions with rather neutral pH values (6.79 ± 0.02). The main aspect is that electric conductivity (EC) is high with values of 120.86 ± 0.03 mS/cm due to the salinity contributed by sea water. Both EC and Eh values show extreme geochemical conditions of the peloid and they can have a decisive effect in the chemical and biological reactions which are responsible for the properties of the peloid, since they can affect metal mobility due to changes in metal-binding capacity of humic materials, metal sulfide formation (or sulfide oxidation), and changes in Fe/Mn-oxyhydroxides [4], [12].

Elemental content analysis of major and minor elements of Santa Lucía showed that Ca, Na, Mg, and K are the main cations that contribute to sediment composition, and are also responsible for the high values of electric conductivity (Fig. 1). The concentration of these four major elements was found in the range of 190-61680 mg·kg^{-1}. These cations are present in the sediment as result of the lithological contribution (terrigen-carbonated deposits and sands with composition rich in carbonates, gypsum and halite) and also the salts coming from the concentrated sea water. Other metals (Cr, Cu, Ni, Pb and Zn) appeared at lower concentrations (5.20-25.4 mgkg^{-1}) (Fig. 1) as a result of lithological origin from the geochemical cycle in the ecosystem [2].

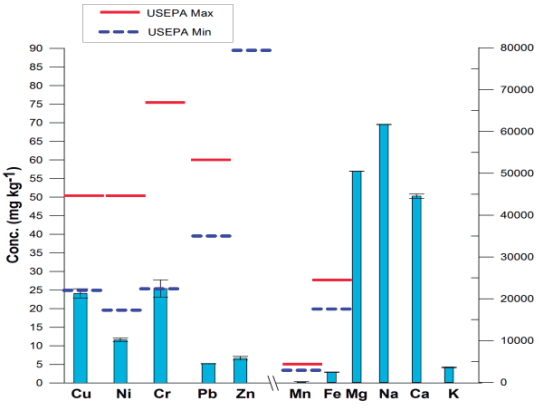

Fig. 1 Metal concentration in mg/Kg.

Solid phase analysis (XRD, SEM-EDS, particle size)

Table 1 shows the granulometric or particle size analysis obtained by SEM. The results demonstrate that the main sizes are related with fine sand distribution (near 60%) followed with a distribution as silty particle size (30%).

This distribution corresponds with the coastal environment, with high percent of sand and low percent of clay (Table 1). Therefore, these results indicates that the retention of transition metals in the sediment is poor (it is reported that clayed materials with lower sizes (2 μm and < 63 μm) favor the retention and cation exchange having higher specific superficial area) [13]. Therefore, the distribution of the particle size may play an important role in the geoability, mobility and finally bioability of the metals showing Santa Lucía peloid, in this case, less retention capacity of metals than other peloids reported in literature [4], [13].

Bulk XRD analysis shows a homogeneous composition dominated by gypsum and halite. Phyllosilicates contribution (clayed material), in concordance with particle size analysis, is not high or significant. Other precipitated minerals in low magnitude are calcite as well as quartz, common in terrestrial crust (Table 2).

The use of theoretical Pourbaix Eh–pH phase diagrams in hydrogeochemical modeling, contributes to understand the potential mobility of metals. As can be seen in Fig. 2, the reducing conditions determine that all the metals are situated in the lower zone of water stability, corresponding to sub-aqueous sediment accumulations and in the so-called “euxinic” environments of poorly ventilated marine water bodies or organic-rich brines pools [14].

Table 1 Granulometric analysis

Classification	%	Classification		%
Clay	12.08	Sand	Fine	60.59
Silt	27.13		Thick	0.2

Table 2 Mineralogical composition

Mineral	%	Mineral	%
Phyllosilicates	10	Calcite	8
Halite	29	Pyrite	5
Gypsum	44	Quartz	4

Hydrogeochemical modeling

In the case of the major elements, Na and K are predicted in their monovalent soluble species meanwhile Mg and Ca are described to be present in their divalent species and also $MgHCO_3^+$ and $CaHCO_3^+$ species with the same behavior than reported in [2]. For the trace elements (Fig. 2 a–h), the Pourbaix Eh–pH diagrams predicts that all elements, with exception of Cu (Cu $_{(s)}$), are in their soluble form (Cr, Fe and Pb forming metal(OH)$^{n+}$ species and Zn, Mn and Ni soluble divalent cations). These results predict a low retention of transition metals in the peloid in agreement with the findings of the particle size analysis and mineralogy.

The sulfur species were also modeled due to the relevance for metal mobility in highly reductive environments. In the case of sulfur species (S), it is predicted to appear in the form of H_2S.

In these environments, the salinity is such that the water is no longer solvent and the thermodynamic conditions preclude the use of the PHREEQC software with conditions described [2], and a special database must be designed for the environments of the samples.

Metal speciation in Santa Lucía peloid

Although total metal content can be used as a preliminary approach to evaluate quality and suitability of peloids for therapeutic uses, chemical speciation is of supreme importance to elucidate possible mechanisms of distribution and mobility in these complex systems. In peloids, no matter the total content, elements can only cause a positive or toxic response in biological systems, if they are mobile and available and can interact with sweat and biological barriers (skin or mucous membranes).

The analysis of the different fractions obtained after sequential extraction showed the distribution of the species according to their affinity with the different phases (Fig.3 a and b). In general, the major elements are distributed in the leachable fractions (EXC, CARB and ERO). This behavior is due to the high solubility of the elements of the alkaline and alkaline-earth metal groups.

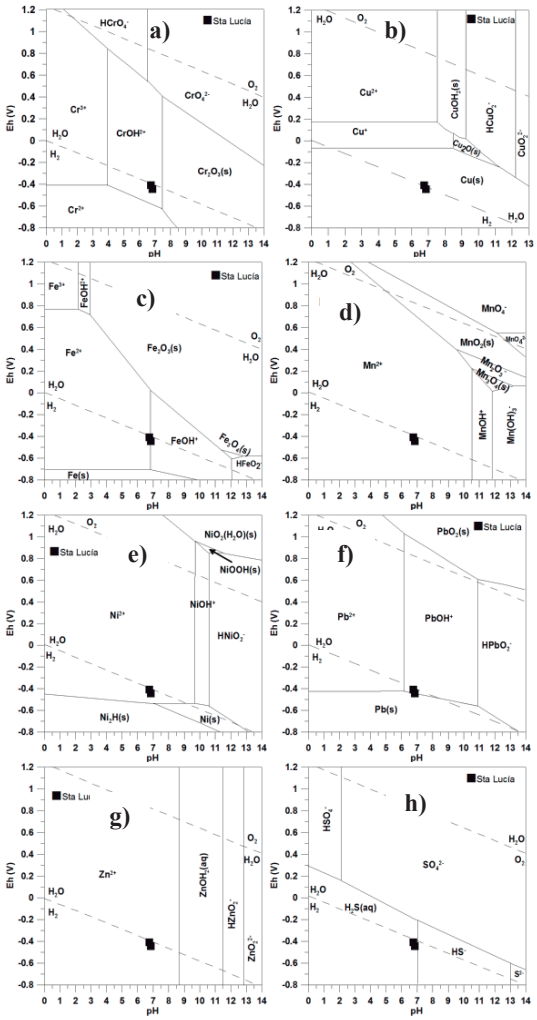

Fig. 2 Pourbaix Eh–pH diagrams of the transition metals (Cr (a), Cu (b), Fe (c), Mn (d), Ni (e), Pb (f), Zn (g)) and sulfur (h) speciation in RSD and PSD sediments.

For transition metals, shown in Fig. 3b, the main distribution is associated to ERO, MO and R-RES fractions, with the exception of Mn with 67% in the CARB fraction. The percentages of metals in the ERO fraction are of 22%, 15%, 77% and 10 % for Cr, Pb, Cu, Ni, respectively. Those values were higher than those obtained for another Cuban peloid (San Diego de los Baños), where the mentioned metals are linked in the less mobile fractions (MO and R-RES) and ERO fraction percentages were lower than 10% [2]. The results show that these transition metals in Santa Lucía peloid are less retained than in San Diego peloid, as predicted with the hydrogeochemical modeling and their particle size and mineralogical composition.

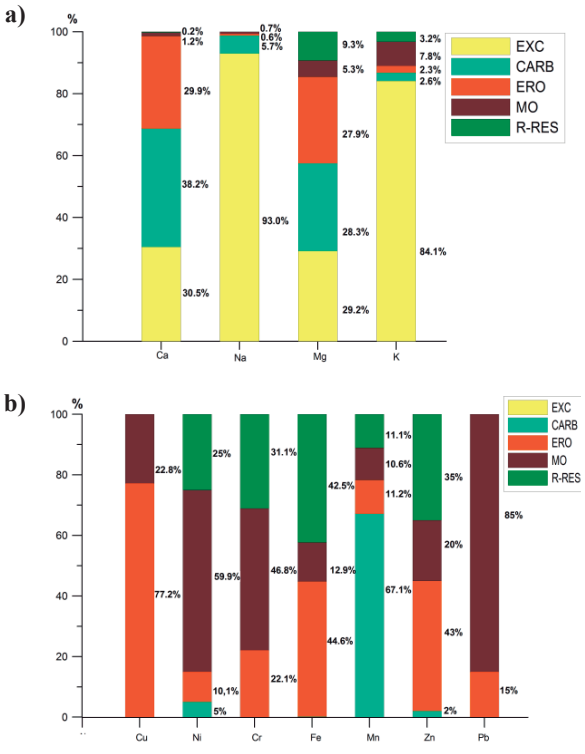

Fig. 3 Distribution of majoritarian (a) and trace (b) metals in the different extraction fractions.

Specialized literature reports that in low salinity environments, the main factor controlling metal distribution is pH, meanwhile in cases with high salinity the distribution of metals is influenced by pH, EC and salinity, the last two intimately related [15] [16]. The trace metals at high salinity can be easily exchanged by alkaline metal and the saturation of the cationic exchange capacity of the sediment can occur. This phenomenon can decrease the retention and storage of trace metals in sediment matrix, as reported for Pb (II), Cu (II), Cd (II) and Cr (III) [12], [15]. These mechanisms are also conditioned by the high particle size that provides small specific superficial area causing low retention of trace metals.

On the other hand, Mn is the more labile trace element with more of 67% in the CARB fraction. This behavior of Mn in sediments has been reported in the interaction with solutions with high NaCl concentration originating that Mn solubility arises due to the exchange reactions of this cation with Ca and Na, which preclude the sorption reaction of Mn over the ERO particles (Fe/Mn oxides), although other mechanisms as the formation of complexes with Cl^- y SO_4^{2-} have been proposed [16], [17].

Despite the difference in the behavior of trace elements in Santa Lucía peloid, in comparison with other reported peloids, under the studied conditions, still Cr, Ni and Pb are highly immobilized (MO and R-RES (78-85%)). The literature reports that Cr, Ni and Pb, showed a high affinity for the organic matter. Lead has been mostly distributed in MO fraction and is reported to form strongly bounded complexes with the organic matter, and that slighted alkaline pH inhibits the mobility of this element [2]. Ni and Cr, are mostly located between MO and R-RES phases and it is reported that for Ni is expected that brusque changes in sediment conditions would lead to a slight redistribution between the MO and ERO fractions as observed in the sequential extractions [2]. Also the same behavior is reported for Cr, with the variation of salinity (higher salinity makes Cr less bounded to MO) [2].

Quality assessment

Due to the therapeutic use of peloids, a further analysis of the concentration values of transition metals regarding possible contamination was made by comparing with the limits reported by the USEPA (Fig. 1). It can be seen that the concentration values for all the sediments were below the minimum limit reported by the USEPA, so the peloid can be considered as non-polluted. Also using the background of the marine sediments for terrestrial crust can be considered with low contamination factor (Cf) and low degree of contamination (Cd). Meanwhile the FM index shows that all the elements exhibit low mobility with the exception of Mn (Table 3).

Special care should be paid to the chemical equilibrium and distribution of trace metals, as well as to the conditions of application of the peloid, because, despite the results obtained for FM index, Santa Lucía trace metals exhibit lower retention than the obtained for San Diego de los Baños peloid, mostly related with oxido-reduction changes (ERO fraction). Particular is the case of Mn species that are highly soluble and mobile, and can increase its bioavailability; however the dermal absorption of this metal is considered minimal and not a risky exposition pathway in normal conditions [2].

Table 3 Contamination factor (Cf), contamination degree (Cd) and FM index for trace elements

Element	(Cf)	FM
Cr	0,28	0,00
Cu	0,09	0,00
Fe	0,04	0,20
Mn	0,03	67,15
Ni	0,05	5,00
Pb	0,06	0,00
Zn	0,04	2,00
(Cd)	0,56	

CONCLUSIONS

The results showed that the major cations were Na, Ca, Mg and K, and that Na was the predominant element with high mobility and exchange capacity. Some of the trace elements studied in this investigation (Cr, Pb, Ni) appeared in the less mobile fractions, but the effect of salinity and particle size are observed with the displacement of a percentage of all the elements distribution toward the ERO fraction. Even so, still the results based in the FM index suggest low availability in the sediment, under the studied conditions. Also the peloid is considered as non-polluted, according to USEPA normative and not contaminated in relation with the background levels of marine sediments. The findings were useful to predict the behavior of the metals regarding solubility, potential mobility and availability in the sediment, and it was concluded that most of the metals are strongly retained in the peloid.

REFERENCES

[1] Tserenpil Sh, Dolmaa G, Voronkov M.G. "Organic matters in healing muds from Mongolia". Applied Clay Science, Vol. 49, 2010, pp. 55–63.

[2] Suárez Muñoz M, Melián Rodríguez C, Gelen Rudnikas A, et al. "Physicochemical characterization, elemental speciation and hydrogeochemical modeling of river and peloid sediments used for therapeutic uses". Applied Clay Science, Vol. 104, 2015, pp 36–47.

[3] Centini M, Tredici MR, Biondi N, et al. "Thermal mud maturation: organic matter and biological activity". International Journal of Cosmetic Science, Vol. 37, 2015, pp 339–347.

[4] Carretero MI, Pozo M, Martín-Rubí JA, et al. "Mobility of elements in interaction between artificial sweat and peloids used in Spanish spas". Applied Clay Science Vol. 48, 2010, pp. 506–515.

[5] Yang Z, Wang Y, Shen Z, et al. "Distribution and speciation of heavy metals in sediments from the mainstream, tributaries, and lakes of the Yangtze River catchment of Wuhan, China". J. Hazard. Mater. Vol. 166, 2009, pp. 1186–1194.

[6] Oluwabukola A, Olayinka KO, Alo BI. "Comparison of three sequential extraction protocols for the fractionation of potentially toxic metals in coastal sediments". Environ. Monit. Assess. Col. 172, 2011, pp. 319–327.

[7] Research Center for Deep Geological Environments, Naoto TAKENO. "Atlas of Eh–pH diagrams. Intercomparison of Thermodynamic Databases". In: Geological Survey of Japan (Ed.), Open File Report No. 419, 2005, 287 pp.

[8] Barrios Cossio J. "Caracterización inorgánica del peloide de Playa Cajío". Thesis. INSTEC. 70 pp.

[9] United States Environmental Protection Agency (USEPA). "Guidelines for Pollution Classification of Great Lakes Harbor Sediments". USEPA Region V, Great Lakes Surveillance Branch, Chicago IL, 1977, 8 pp.

[10] Kwon YT, Lee CW. "Application of multiple ecological risk indices for the evaluation of heavy metal contamination in a coastal dredging area". Sci. Total Environ. Vol. 214, 1998, pp. 203–210.

[11] Turekian K, Wedepohl K. "Distribution of the elements in some major units of the Earth´s crust". Geological Society of America Bulletin, Vol.72, 1961, pp 175-192.

[12] Laing GD, Rinklebe J, Vandecasteele B, et al. "Trace metal behavior in estuarine and riverine flood plain soils and sediments: a review". Sci. Total Environ. Vol. 407, 2009, pp. 3972–3985.

[13] Pozo M, Carretero MI, Maraver F, et al. "Composition and physico-chemical properties of peloids used in Spanish spas: A comparative study". Applied Clay Science Vol. 83-84, 2013, pp 270-279.

[14] Leeder MR. "The origin of terriginous clastic grain". Sedimentology. Process and Products. First edition 1982 (Reprinted 1994), Published by CHapmand & Hall, London, UK, pp. 3-14.

[15] Keniston Ch. "Increasing salinity effects on heavy metal concentration". Thesis. Cary Institute of Ecosystem Studios. California State University. United States, 2015.

[16] Du Laing G, De Vos R, Vandecasteele B, et al. "Effect of salinity on heavy metal mobility and availability in intertidal sediments of the Scheldt estuary". Estuarine, Coastal and Shelf Science Vol. 77, 2008, pp. 589-602.

[17] Lores E, Pennock B. "The effect of salinity on binding of Cd, Cr, Cu and Zn to dissolved organic matter". Chemosphere Vol. 37 (5), 1998, pp. 861–874.

VALORIZATION OF WATERWAYS SEDIMENTS IN WALLONIA (BELGIUM): STUDY OF A LANDSCAPED MOUND

Florian Liénard [1] and Laurence Haouche [1]
[1]Institut Scientifique de Service Public (ISSeP), Belgium

ABSTRACT

Due to the shallow relief in Belgium and northern France, the dredging of their waterways generates significant quantities of sediments for which there are few valorization pathways. Waterways operators and administrations are still waiting for efficient valorization solutions. The VALSE project, funded by the Interreg V program FWVL, aims to validate valorization pathways through the implementation of large-scale works that promote a good integration in territories and a sustainable use. In this context, a sediment-based mound is ecologically and ecotoxicologically monitored to determine its influence magnitude on the environment over time. An earth slope near the studied site was chosen as a control. The monitoring consists of *in situ* flora and substrate-living invertebrates inventories on the one hand. On the other hand, ecotoxicological tests are carried out on sediments and soil respectively taken from the mound and the control: the reproduction of an earthworm (*Eisenia fetida*) and the activity of nitrifying bacteria potentially present in these substrates are studied. First results show that the sediments do not impact negatively plant colonization or the settlement of underground invertebrates. About laboratory testing, *E. fetida* reproduction seems significantly better in mound sediments than in control soil. Even lower than the nitrification process in the control, a nitrifying activity has taken place in the sediments. These promising initial results tend towards a good integration of the mound in the surrounding environment for the monitored parameters.

Keywords: Wallonia, Sediments, Valorization, Landscape development, Ecology, Ecotoxicology

INTRODUCTION

The shallow relief in Belgium and northern France favours a high sedimentation rate in the waterways, requiring many dredging works to maintain the navigability. This work generates significant quantities of sediments for which there are few valorization pathways. Waterways operators and administrations are still waiting for efficient valorization solutions [1].

The VALSE project, funded by the Interreg V FWVL program aims to validate these valorization pathways through the implementation of large-scale works that promote a good integration in territories and a sustainable use [2].

In this context, a sediment-based mound (Fig. 1), built to deal with wild dumping of household trash, was ecologically and ecotoxicologically monitored to determine its influence magnitude on the environment over time [3]. An earth slope near the studied site is chosen as a control.

The ecological monitoring includes *in situ* fauna and flora surveys. The fauna inventory focuses on substrate-living invertebrates to determine if the mound hosts a sediment-specific fauna compared to the slope soil [3]-[4]-[5]. Similarly, the flora inventory is carried out to determine if the sediments are home to particular plants [6]-[7].

Ecotoxicological testing consists in the study of the nitrifying activity [8] and an earthworm (*Eisenia fetida*) reproduction rate [3]. The first test aims to determine the potential nitrifying activity taking place within the sediments in comparison to the control soil. Indeed, microbial metabolism is directly responsible of soil nitrification which plays a role in its quality because it generates assimilable nitrogen by plants [9]. The second test aims to study the influence of a sediment-based substrate on *E. fetida* life cycle in comparison with the slope soil. This earthworm specie is actually known as a good toxicity bioindicator for soils and is widely used to detect possible harmful effect on soil invertebrates [3]-[10].

Fig. 1 The studied sediment-based landcaped mound (October 2017)

MATERIALS AND METHODS

Ecological monitoring

Fauna and flora surveys were carried out on the mound and the control slope in June and October 2017. This procedure was used to note any change in fauna composition through the seasons and identify as many plants as possible growing throughout the year on the mound and the control.

Fauna inventory

The sampling of the substrate-living invertebrates was carried out according to ISO 23611-5 (2011) [11] and took place on 4 locations equally distributed on the mound, and on the control. The methodology was as follows: an area of 30cm x 30cm bare soil was watered with 0.2% formalin water to chase the invertebrates out towards the surface. They were then collected and fixed in formalin according to their sampling location. The identification was done in the laboratory using reference books [12]-[13]. A comparison was then made between the mound and the control inventories.

Flora inventory

The flora inventory consisted in a simple identification of the plants growing on the mound and the control but also in an estimation of the trees, shrubs, herbs and moss cover percentage. The mound vegetal cover and inventory were then compared to the control ones.

Ecotoxicological monitoring

Ecotoxicological monitoring was carried out on samples collected in June and October 2017 on the sediment mound and the control slope. The samples were taken with a hand auger over the first 15cm from the surface. They were collected in June on the mound at 4 locations (Station 1, 2, 3, 4) to ensure its homogeneity. The June results actually reflected mound homogeneity, thus a single sample composed of substrate from twenty points scattered along the whole mound was collected in October. As the slope area is small, the sampling method for the control was not modified between June and October.

Determination of nitrification potential

This nitrification test was carried out according to the norm ISO 15685 (2012) [14] which describes a method to inhibit the second step of ammonium oxidation (nitrate formation from nitrite oxidation by nitrating bacteria) by KCl addition. The following nitrite accumulation is measured over an incubation period of 6 hours and is used to estimate the potential nitrifying activity of bacteria which convert ammonium into nitrite.

Efficiencies of the nitrification taking place in the mound sediments and in the control soil in June and October were then graphically compared.

Earthworm reproduction test

This test was carried out according to the norm ISO 11268-2 (2015) [15] which consists in the introduction of 10 *E. fetida* adults with a mass comprised between 300mg and 600mg into test containers. These containers are filled with 500g of dry substrate wetted with deionized water to reach 40% to 60% of the total water holding capacity. The earthworms are left for 4 weeks in the containers and weekly fed with 5 to 10g of wet horse dung. After this time, adult worms are removed from the test containers where they laid egg cocoons. *E. fetida* reproduction rate is measured after an additional period of 4 weeks by counting the number of offspring hatched from the cocoons.

ANOVA test was used for statistical analysis of the results related to the samples collected in June (Station 1 to 4 of the mound, and control soil) and t-test was used to interpret the results related to the samples collected in October (homogenous sediment sample from the mound and control soil). ANOVA was followed by Tukey's pairwise test. Open source software R was used for all the graphs and statistics. A 5% significance threshold was chosen by default for all the tests (95% confidence intervals).

RESULTS

Ecological monitoring

Fauna inventory

The substrate-living inventory (Table 1) shows that the most abundant organisms in the mound sediments are moudlouses (*Porcellio scaber*), centipedes (*Necrophloeophagus longicornis*) and earthworms (*Lumbricus terrestris*) while the most abundant organisms in the control soil are earthworms only (*Lumbricus terrestris*). A lot of worker ants were also observed on both sites (*Lasius niger* on the mound and *Lasius flavius* on the control). The other identified organisms were very few (1 or 2 specimens by specie). Overall, more species were recorded on the mound than on the control.

Flora inventory

Plants growing on the sediment mound and control slope in 2017 were identified while the coverage variation of different plant layers between June and October was determined. The mound is

characterized by a low shrub cover (< 5% of the surface), a particularly large herbaceous cover (> 90% of the surface) and a low proportion of bare soil (~5% of the surface). The tree layer is nonexistent on the mound and mosses do not seem to grow on the mound. No variation was observed between June and October concerning the mound vegetal layers. The control is covered by ~60% of herbaceous plants. The remaining 30% of cover were bare soil in June and colonized by moss in October. No trees or shrubs are growing on the slope.

Table 1 Substrate-living invertebrates identified in the sediments mound and the control soil

Identified invertebrate species	Number of specimens (mound)	Number of specimens (control)
A. gracilens	1	0
B. guttulatus	1	0
C. septempunctuta	1	0
D. lapidosus	1	0
D. ruber	1	0
F. auricularia	1	0
F. rufa	0	1
L. flavius	0	7
L. niger	8	0
L. rotundum	0	1
L. terrestris	8	8
N. longicornis	8	0
P. scaber	30	0
P. spumarius	1	0
S. caesarus	1	0
S. cingulata	1	0
T. albipes	2	1
T. hypnorum	1	0

The mound is populated by a total of 46 plant species distributed in 21 families, the control by 10 species distributed in 6 families (Fig. 2).

Both biotopes share some species which are *Medicago lupulina*, *Trifolium pratense*, *Trifolium repens*, *Plantago lanceolata*, *Rubus* sp. and *Taraxacum* sp. More than 50% of the entire mound herbaceous cover is represented by 4 Poaceae species (*Fetusca pratensis*, *Lolium perenne*, *Phleum pratense* and *Poa pratensis*) although the nettle (*Urtica dioica*) also forms large bouquets along its length. Meanwhile, the control dominant species are *Bellis perennis*, *Trifolium repens* and *Plantago lanceolata*.

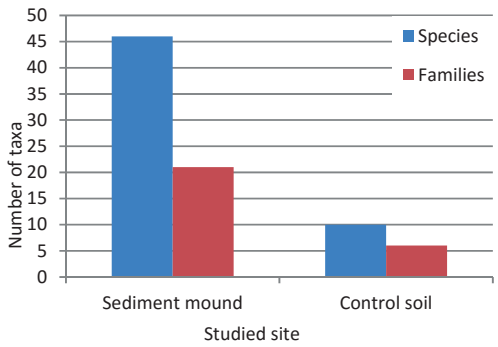

Fig. 2 Plant species and families distributions on the mound and the slope

Ecotoxicological monitoring

Determination of potential nitrification

Nitrification occurred linearly in all samples taken in June and October, either in the mound sediments or in the control soil. About the June samples, nitrification efficiency was equivalent from one station to another. Nitrification in the homogeneous sample collected in October did not differ from the different stations measurements. Nitrification efficiency in control soil was higher in the June sample than in the October sample. Despite this decrease, nitrification remained much more effective in the control soil than in the mound sediments (Fig. 3).

Earthworm reproduction test

About the June samples, ANOVA test showed a result below the 5% threshold which means *E. fetida* reproduction rate is significantly different between at least 2 tested substrates. *Post-hoc* pairwise testing indicated that the significant differences were between control soil and Station 1 sediments. Indeed, the graphical representation of the results (Fig. 4) shows that the higher reproduction rate took place in the station 1 sediments. However, there was no significant difference between the reproduction rate related to the three other stations and the control soil.

Concerning October samples, although data transformation was needed for the statistical testing, t-test showed a result below the 5% threshold, which means *E. fetida* reproduction rate is significantly different between mound sediments and control soil. The statistical results obtained are consistent with their graphical representation (Fig. 5) which indicates a drastically more efficient reproduction in mound sediments than in control slope soil.

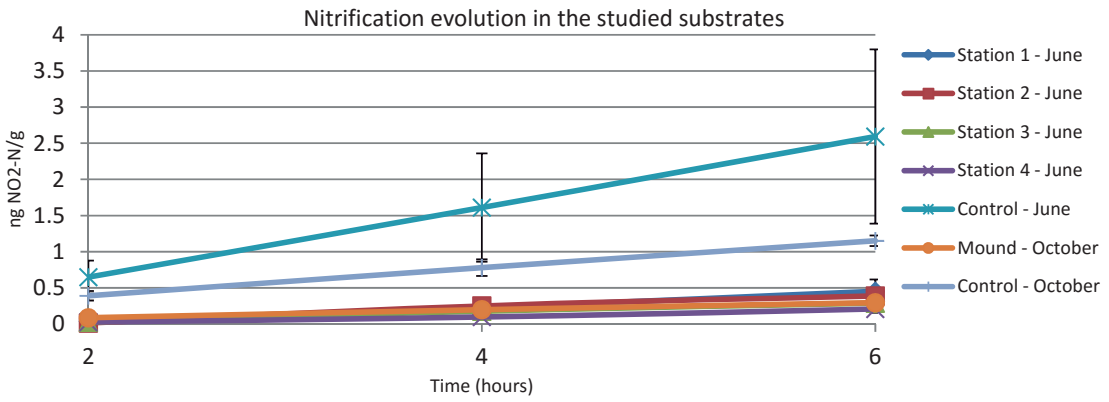

Fig. 3 Nitrification efficiency in the sediments mound and the control soil (June and October)

Control soil reproduction rate is equivalent between June and October. Also, October reproduction rate in sediments is similar to the June reproduction rate observed in the various stations.

DISCUSSION

Fauna inventory

The mound and control dominant species are represented by detritophages organisms (moudlouses, centipedes, earthworms). Concerning the worker ants observed, a single anthill near the studied sites is enough to explain the presence of several specimens.

The presence of these common animals is not surprising since the studied biotopes are located on a roadside which is not an environment that favors the settlement of demanding species [16]-[17].

The mound richness seems higher than the control one because more species were identified in the sediments but they were only represented by isolated specimens. It is possible that these organisms are not specific to the mound and just transit through the area. Plus, the surface of the mound is larger than the control one therefore there is a higher likelihood to find a transiting specie in the sediments. Hence the higher richness of the mound is not really significant and the sediments seem to be a habitat equivalent to the control soil.

Flora inventory

The uniform abundance of four species of Poaceae along the whole mound means that they were probably sown right after its creation. However, their presence does not seem to prevent other species as nettle, dandelion, plantain and clover from also settling along the whole mound. It is difficult to determine where these species come from because they may have been spread by the wind. Some undergrowth species (*Gallium aparine*, *Ranunculus repens*, *Rubus* sp.) seem to spread from a wooded area near the sites or even from the control itself (*Medicago lupulina*). It is also possible that seeds or root fragments initially present in the sediment are involved in the mound plant colonization. This hypothesis is corroborated by the fact that one common reed plant (*Phragmites australis*) was recorded during the October inventory. Thus, it is possible that some identified plants come from the sediment itself.

The control plant community appears to be stable over time because the same species were identified during June and October surveys. The only noted change concerns the moss cover which was nonexistent in June and reached 30% in October. The drought in June probably reduced the moss population meanwhile autumnal humidity allowed them to recolonize the bare soil areas. The stability of the flora may be due to the high number of Fabaceae (clover species) symbiotic with nitrifying bacteria which feed the soil with nitrogen nutrients [9] and thus allows the other control species to survive for long periods of time. Various environmental factors as a regular mowing of the slope may also prevent other species from settling permanently [18].

Determination of potential nitrification

As pointed out in the previous section, the slope is populated by a high density of Fabaceae which are symbiotic plants of nitrifying bacteria [9]. Therefore, it is logical that a high nitrification rate takes place in the control soil. The decrease in nitrification effectiveness between June and October is probably related to the fact that the metabolism of nitrifying bacteria was highly stimulated by summer temperatures and less stimulated by early autumn conditions.

Nitrification effectiveness in the mound is stable since it is equivalent in June and October. In addition, although nitrification in sediments is not as high as in the control soil, it is equivalent to nitrification of an agricultural soil which was used as a positive control in another research project (VALSOLINDUS) [19]. These results assume that the nitrifying bacteria activity in the slope is particularly high while the sediment one is similar to that of a reference soil. This nitrification rate can be explained by the colonization of the mound by several Fabaceae species as shown by the flora inventory. Nitrification effectiveness is also indicated by the development of nettle populations on sediments since they are nitrophilous plants [20].

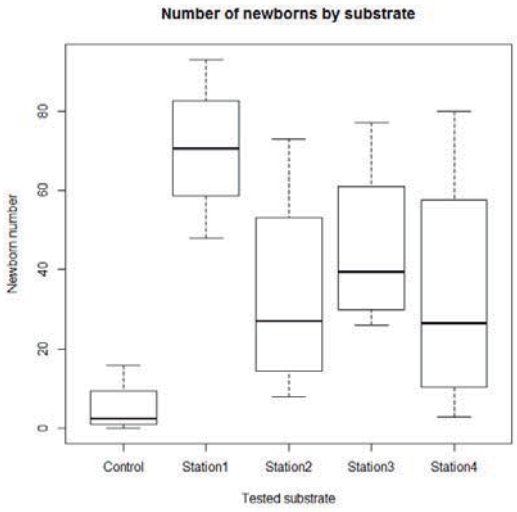

Fig. 4 *Eisenia fetida* reproduction rate in sediments samples from the mound (Station 1, 2, 3, 4) and from the slope (Control) - June 2017

Earthworm reproduction

E. fetida reproduction rate appears equivalent in sediments and soil in June samples because only one station supports a reproduction rate significantly higher than in the control. This result reflects that the sediments influence on reproduction compared to soil is nonexistent or slightly positive. Concerning October samples, *E. fetida* reproduction rate is significantly better in sediments than in control soil which means again that the sediments do not negatively impact reproduction.

These encouraging results indicate at worst that the mound does not influence *E. fetida* reproduction more than a soil collected in the same geographical area. However, these are only preliminary results and the potential mound ecotoxicity will continue to be investigated for the duration of VALSE project (until 2020).

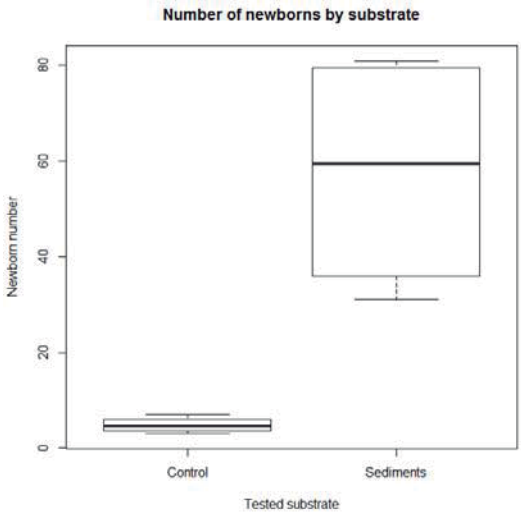

Fig. 5 *Eisenia fetida* reproduction rate in homogenous sample from the mound (Sediments) and sample from the control slope (Control) - October 2017

CONCLUSIONS

Although the studied aspects do not allow drawing any definite conclusion, the monitored parameters tend towards a good integration of the mound in the surrounding environment. Indeed, this first approach does not indicate that sediment-based landscape development constitutes an ecological nor ecotoxicological problem:

Substrate-living invertebrate fauna of the mound, including earthworms, is poor in species but seems equivalent to control soil one. Control flora seems very stable while ongoing plant colonization of the mound appears to arise from different origins (close environment, control slope, sediments). These observations lead to the conclusion that sediments do not represent an issue for flora and underground fauna settlement.

About laboratory testing, the nitrifying activity taking place in the sediments, although lower than the control one, is similar to the nitrification rate observed in a reference agricultural soil. Concerning *E. fetida* reproduction test, reproduction rate appears to be similar or slightly better in sediments than in soil.

However, these promising initial results may vary over time because the mound is, as most habitats, a complex system that depends on a large number of factors, often interconnected. Thus, ecological inventories and laboratory analyses will be repeated throughout the duration of the VALSE project to observe the evolution of sediments ecology relative to the one of the surrounding environment.

Subsequent analysis of the functional diversity of mound-dependent microbial communities will also be conducted. It will provide information about the metabolic profile of the mound sediments and then characterize their functionality in order to compare it to other types of soil.

ACKNOWLEDGMENTS

We gratefully acknowledge financial support from the Walloon region and from the Interreg V FWVL program. The authors would also like to thank the VALSE team for their support.

REFERENCES

[1] Lemiere B *et al.*, "The GeDSeT Project: constitution of a decision support tool (DST) for the management and material recovery of waterways sediments in Belgium and Nothern France", WASCON event, 30 May-1 June 2012, Gothenburg, Sweden.

[2] Lemiere B *et al.*, "InterReg Project VALSE", Newsletter SedNet, Sept. 2017.

[3] Blair J M *et al.* "Soil Invertebrates as Indicators of Soil Quality", Methods for Assessing Soil Quality, Jan. 1996, pp 273-291.

[4] Lavelle P *et al.*, "Soil invertebrates and ecosystem services", European Journal of Soil Biology, Vol. 42, Nov. 2006, pp 3-15.

[5] Santorufo L *et al.*, "Soil invertebrates as bioindicators of urban soil quality", Environmental Pollution, Vol. 16, Feb. 2012, pp 57-63.

[6] Godefroid S, "Temporal analysis of the Brussels flora as indicator for changing environmental quality", Landscape and Urban Planning Vol. 52, nº 4, Jan. 2001, pp 203-224.

[7] Henneresse T, "Inventaire floristique des Centres d'Enfouissement technique de Habay et de Tenneville (province de Luxembourg, Belgique)", Dumortiera, Vol. 8, 2016, p 8.

[8] Hooper A B *et al.*, "Enzymology of the Oxidation of Ammonia to Nitrite by Bacteria", Antonie van Leeuwenhoek, Vol. 71, nº 1-2, Feb 1997, pp 59-67.

[9] Van Der Heijden M G A *et al.*, "The Unseen Majority: Soil Microbes as Drivers of Plant Diversity and Productivity in Terrestrial Ecosystems", Ecology Letters Vol. 11, nº 3, March 2008, pp 296-310.

[10] Sanchez-Hernandez J C, "Earthworm Biomarkers in Ecological Risk Assessment", Reviews of Environmental Contamination and Toxicology, 2006, pp 85-126.

[11] NBN "Soil quality – Sampling of soil invertebrates – Part 5: Sampling and extraction of soil macro-invertebrates." EN ISO 23611-5:2013 F, 2011, 12 p.

[12] Bellmann H. "Insectes et principaux arachnids", Vigot, 2006.

[13] Chinery M. "Insectes de France et d'Europe occidentale", Flammarion, 2005.

[14] NBN "Soil quality – Determination of potential nitrification and inhibition of nitrification – Rapid test by ammonium oxidation", ISO 15685 F, 2012, 12 p.

[15] NBN "Soil quality – Effects of pollutants on earthworms – Part 2: Determination of effects on reproduction of *Eisenia fetida*/*Eisenia andrei*", ISO 11268-2, 2012, 21 p.

[16] Muskett C J and Jones M P, "The dispersal of lead, cadmium and nickel from motor vehicles and effects on roadside invertebrate macrofauna", Environmental Pollution Series A, Ecological and Biological, Vol. 23, nº 3 Nov. 1980, pp 231-242.

[17] Rotholz E and Mandelik Y, "Roadside Habitats: Effects on Diversity and Composition of Plant, Arthropod, and Small Mammal Communities"; Biodiversity and Conservation, Vol. 22, nº 4, April 2013, pp 1017-1031.

[18] Williams D W *et al.*, "Effects of Frequent Mowing on Survival and Persistence of Forbs Seeded into a Species-Poor Grassland", Restoration Ecology Vol. 15, nº 1, March 2007, pp 24-33.

[19] Bouhoulle E *et al.*, "Valsolindus, a demonstration project of sediment valorization", 5th International Symposium on Sediment Management, 11-13 July 2016, Montréal, Canada.

[20] Dulière J-F *et al.*, "Répertoire des groupes écologique du fichier écologique des essences", Ministère de la Région wallonne, 1995.

PHOSPHOLIPID ESTER FATTY ACIDS (PLFA) IN BOTTOM TRAWLING FISHING AREAS IN THE GULF OF CALIFORNIA

Aguíñiga-García Sergio[1,2], Sánchez-González Alberto[1,2], Torres-Rojas Yassir Edén[3], Carreón-Palau Laura[4], Marmolejo-Rodríguez Ana Judith[1,2], Dorantes-Hernández J. Manuel[1,5], Pérez-Falls Zenia[1,5], Olivares-Rodríguez Elsy Alejandra[1], LLadó-Cabrera Dayli[1,5]and Camacho-Cruz Karla Andrea[1,5]
[1]CICIMAR, Instituto Politécnico Nacional, México,[2]Becario-COFAA-IPN México,[3]EPOMEX, Universidad Autónoma de Campeche, México,[4]CIBNOR, México,[5]Becario-BEIFI-IPN

ABSTRACT

Wastes from bottom trawling fisheries that flow directly into the environment can have an important effect on the function of sedimentary ecosystems [1,2]. In this study, we analyze the composition of fatty acid of phospholipid esters (PLFA) and the environmental impact conclusions based on sedimentological ($CaCO_3$, grain size), and sedimentary organic matter geochemical data ($\delta^{13}C$, $\delta^{15}N$, C/N) in pristine areas and bottom trawling fisheries areas of Sonora and Sinaloa in the Gulf of California, Mexico [4]. While the PLFA ratios (Σ monounsaturated/ Σ branched and iso+anteisoC15/C16) [5,6] showed statistically significant differences indicating oxic/anoxic sedimentary environments. The multivariate analysis of sedimentological and geochemical data showed no significant differences between pristine and impacted areas. These results lead to the conclusion that the ecosystem under the effect of the waste produced by bottom trawling fisheries in the Gulf of California can absorb this impact [4]. Our results show that PLFAs are highly sensitive to the impact of bottom trawl fisheries because they indicate predominantly anoxic bacterial biomass in areas influenced by fisheries waste. The distinct microbial community composition in trawling affected stations compared to pristine can explain the PLFA of the functional groups of microorganisms.

Keywords: PLFA, Bottom Trawling Fisheries, Carbon Nitrogen Stable Isotopes

INTRODUCTION

Evaluating the effects of bottom trawling on benthic communities is complicated but crucial for impact assessment as anthropogenic activities in the marine coastal zone, which are increasing in Mexico. The damage caused in the benthic marine ecosystem varies with the type of sediments and biota, hydrodynamic parameters, bioturbation and trawling intensity, which lead to a very complex relationship that compromises diversity and abundance of species [1], [2]. Although some studies have been conducted on the impact of trawling on the seafloor, these investigations have focused on specifically evaluating changes and/or successions that occur in benthic communities before, during and after bottom trawling. Lately, trawl marks visible on the seabed have been studied using vessel monitoring system [2]. Some studies of sedimentary geochemical aspects of shrimp fishing areas have been focused in evaluating some properties of the sediment (grain size: sands *vs.* silts and clays) [3]. Elemental and isotopic carbon and nitrogen isotopes (C/N, $\delta^{13}C$, $\delta^{15}N$) have been contrasted for areas of intensive trawling (disturbed areas and unconsolidated sediments) and non-trawling (pristine zones characterized by rocks, gravel, pebbles or sunken ships) [4]. The multivariate analysis did not show a spatial distribution as indicative of a preferential grouping by any sedimentological and geochemical variable in the pristine and impacted areas, suggesting that there is no significant impact of bottom trawling in the Gulf of California [3, 4]. In order to increase knowledge about geochemical disturbances produced by trawling fisheries in the same stations previously reported [4], we present results of phospholipid ester fatty acids (PLFA) from surficial sediments of areas of disturbance *versus* virtually undisturbed sites in shrimp fishery areas in the Gulf of California, Mexico.

METHODS

The sampling period (May) corresponds to the end of the season of the shrimp fishery in Sonora and Sinaloa, Mexico. Surficial sediment (2 cm) were collected with a Smith-Grad dredger at depths of 8 to 47 m at Sonora and Sinaloa coast of Mexico. From the total of 38 stations reported [4], subsamples were taken for the PLFA analysis and 5 pristine stations (1, 3, 5, 14, 19) and 6 stations impacted by trawl fisheries were considered (20, 21, 30, 31, 33, 38) as described in Fig. 1. Analysis of PLFAs were performed using the methodology of [5] based on fractionation of the total lipid extract

(ELT) obtained with dichloromethane: methanol (1.8:1 v/v) and using silica gel columns (S/P 60A) activated. The polar fraction eluted with methanol was derivatized with methanol at 39 °C for two hours. It was purified and stored under an N_2 atmosphere at -20 °C until its chromatographic analysis (GC-MS) at CIBNOR. In this study, fatty acids (FA) were classified to establish functional groups of microorganisms: monounsaturated (MUFA), polyunsaturated (PUFA), branched (branched FA) which permitted to contrast the presence of these biomarkers in the study area. Database of 56 PLFA per sample of 5 pristine stations and six impacted stations were classified according to [5]: Σpair FA <19C, Σbranched FA, ΣMUFA <20C, ΣPUFA.

RESULTS

The PLFA were determined within a gradient considering to represent possible environmentally dissimilar zones due to the effect of the bottom trawl shrimp fishery. The relative dominance of microorganisms' characteristic of an environment was estimated based on the different proportions of fatty acid groups according to [5], which were evaluated in pristine and impacted stations. Statistically different sedimentary environments were found in the spatial scale identifying areas and degrees of disturbance associated to the effect of trawling fisheries.

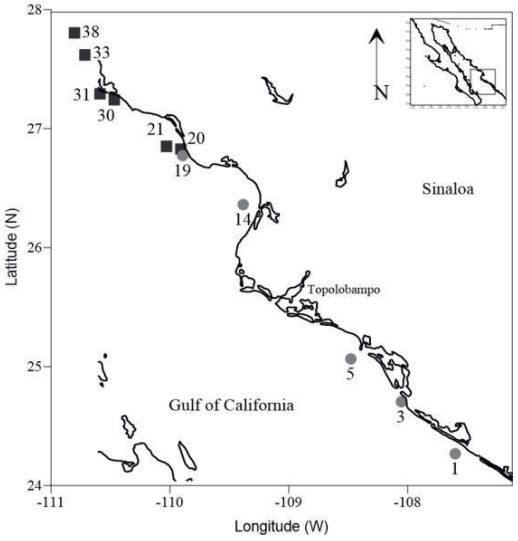

Fig. 1 Study area in the Gulf of California, Mexico. Black squares are trawl fishery stations. Stations 20, 21, 30, 31, 33 and 38 were considered for PLFA analysis. Gray dots are pristine stations. Stations 1, 3, 5, 14 and 19 were considered for PLFA analysis

In our study, the low percentages of the polyunsaturated PLFA reported as characteristic of phytoplankton, indicated that the eukaryotic microorganism's contribution is minor in the superficial sediments. The presence of high percentages of branched + monounsaturated PLFA (and the low percentages of polyunsaturated) indicate that bacteria are the main contributors of fatty acids to surface sediments and therefore, it is inferred that they are the predominant source of monoenoic fatty acids (*e.g.* C16:1w9 and C18:1w9) in these sediments. However, stations 1, 3, 5, 14 and 19 showed very low rates (0.03) of i+aC15:0/C16:0 indicative of high proportions of eukaryotic microorganisms in the pristine stations. These ratios contrast with 0.8 ratio in station 30 and similar values along stations 20, 21, 31, 33, 38 were a strong trawling fishing effort were associated with high i+aC15:0 percentages.

Ratios of monounsaturated/branched PLFA were calculated for pristine and impacted stations. These PLFA ratios allow evaluating the predominance of bacterial groups that circumscribe oxic and anoxic environments of the benthos. Very high ratios (3.5) detected in pristine stations indicate aerobic conditions with lower bacterial FA contribution and more phytoplankton organic matter nature in the surficial sediments. In contrast, ratios as low as 0.35 (with 41% of branched PLFA in station 30) indicate anaerobic conditions as an effect of trawling fisheries (Fig. 2).

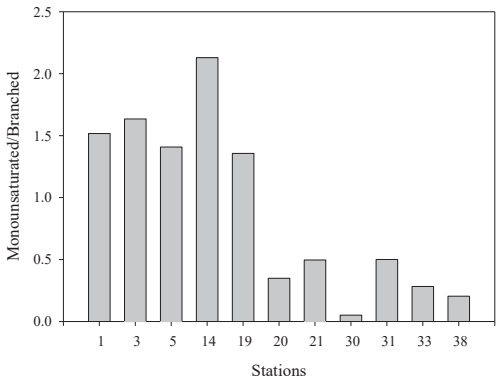

Fig. 2 Monounsaturated/branched PLFA ratios in pristine soft bottom stations and bottom trawl shrimp stations (20, 21, 30, 31, 33, 38) in Sonora and Sinaloa, Mexico.

The branched, monounsaturated, cyclopropyl and saturated AG pairs <20 carbons have been attributed to bacterial populations "*in situ*" of marine sediments [5]. Of the 56 fatty acids identified in every single sample, > 50% are of bacterial origin. In our study, Σbranched PLFA averaged 4.7% in pristine stations in contrast to 20.6% in trawling

affected stations. PLFA *trans/cis* ratios have been used as stress indicators. During starvation-induced phospholipid loss, the cis-monoenoic fatty acids would, therefore, be preferentially utilized increasing *trans/cis* ratios. [6]. In our study, the 18:1n9*cis* were abundant and consistent with very low ratios of monounsaturated/branched described previously in trawling affected stations in Sonora and Sinaloa area. In contrast, *trans*-monoenoic acids were very low practically inexistent indicating low turnover rates of cis-monoenoic fatty acids of membrane phospholipids and the availability of enzymes for the metabolism of these isomers. The very low *trans/cis* value ratios of our study are consistent with ratios of mangrove, and estuarine sediment ecosystems (from 0.01 to 0.09) previously reported [6], which are well correlated with the anoxic environment and low grain size (silt). These results suggest that, in trawling affected areas, there is no bacterial membrane stress, such as that caused by starvation. Results of factor analysis explain 85% of the variability (Fig. 3). The factor 1 (70%) is weighted by 18:1n9*trans* fatty acid (18: 1n9T) and monounsaturated/branched ratio PLFA (mono/bran). This factor includes pristine stations (1, 3, 5, 14, 19). Factor 2 explained 15% of the variability and is weighted by saturated fatty acids (pairs <20, odd <20 saturated >20), monounsaturated and polyunsaturated fatty acids (mono, PUFA), branched fatty acids (bran) and 18:1n9*cis*. The factor 2 includes trawling affected stations (20, 21, 30, 31, 33 and 38).

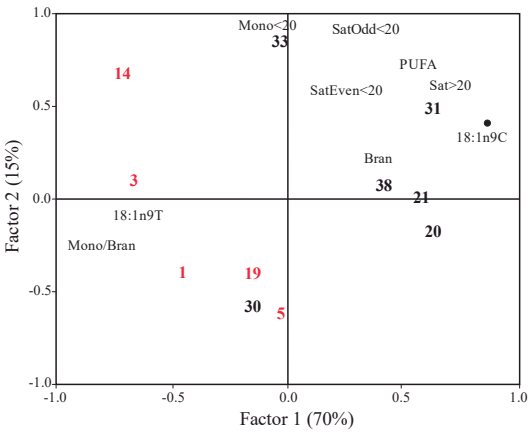

Fig. 3 Analysis multivariate factors of the study area. Red numbers indicate pristine stations and black numbers indicate trawling affected stations

Sánchez et al. [4], based on sedimentological and isotopic data multivariate analysis, concluded that not significant differences were found between pristine and impacted areas, which implicate that the ecosystem under the effect of the waste produced by bottom trawling fisheries in the Gulf of California can absorb this impact, must be reviewed. Statistically significant differences of our PLFA based study, indicated oxic/anoxic sedimentary environments, different organic matter nature, and type of bacteria existent in pristine and trawling affected stations. Factor analysis corroborates that the trawling affected stations are characterized by bacterial communities growing in predominant anoxic conditions. Whereas in the pristine stations, the PLFA data indicate bacterial communities are growing in predominant oxic conditions.

CONCLUSIONS

Wastes from bottom trawling fisheries that flow directly into the environment affect the amount of bioavailable sedimentary organic matter involved in remineralization process and consequently the structure and physiological state of bacterial community in our study site. The distinct microbial community composition in trawling affected stations compared to pristine can explain the PLFA of the functional groups of microorganisms. The phospholipid ester fatty acids (PLFA) of the surface sediment are highly sensitive to the environmental impact of bottom trawling fisheries since their profiles can indicate bacterial biomass that grows in predominantly anoxic conditions, specifically in the areas influenced by fishery waste. Our results indicate that specific organic compounds must be considered to assess the impact of bottom trawling fisheries. The insensitivity of the geochemical variables to the impact of wastes flow reported [4], may be due to the biogeochemical processes that determine the intervals of these variables and that do not make them statistically different.

ACKNOWLEDGEMENTS

We thank to Multidisciplinary Project 1906, SIP20180551, SIP20171669, and 20172233 all granted by IPN. We also thank to SEMARNAT-CONACYT 263401 Project: Análisis de $\delta^{13}C$ y $\delta^{18}O$ en otolitos de peces marinos presentes en el Área de Protección de Flora y Fauna Laguna de Términos, Campeche: indicadores del cambio climático.

REFERENCES

[1] Clark MR, Rowden AA. Effect of deepwater trawling on the macro-invertebrate assemblages of seamounts on the Chatham Rise, New Zealand. Deep Sea Research Part I: Oceanographic Research Papers, Vol. 56, 2009. pp. 1540-1554.

[2] Mérillet L, Kopp D, Robert M, Salaün M, Méhault S, Bourillet JF, Mouchet M. Are trawl marks a good indicator of trawling pressure in

muddy sand fishing grounds?, Ecological Indicators, Vol. 85, 2018. pp. 570–574.

[3] Carriquiry JD, Sanchez A., Camacho-Ibar VF. Sedimentation in the Northern Gulf of California after the elimination of Colorado River Discharge. Sedimentary Geology, Vol. 144, 2001. pp. 37-62.

[4] Sánchez A, Aguíñiga S, Lluch-Belda D, Camalich-Carpizo J, Del Monte-Luna P, Ponce-Díaz G, Arreguín-Sánchez F, Geoquímica sedimentaria en áreas de pesca de arrastre y no arrastre de fondo en la costa de Sinaloa-Sonora, Golfo de California. Boletín de la Sociedad Geológica Mexicana, Vol. 61, 2009. pp. 25-30.

[5] Findlay RH and FC Dobbs, Quantitative description of microbial communities using lipid analysis. In Section II, Cap. 32, Handbook of methods in aquatic microbiology. Kemp, Sherr, Sherr y Cole (eds.), 1993, pp. 271-284.

[6] Guckert JB, Hood MA, White DC, Phospholipid ester-linked fatty acid profile changes during nutrient deprivation of Vibrio cholerae: Increases in the trans/cis ratio and proportions of cyclopropyl fatty acids", Applied and Environmental Microbiology in Proc. Vol. 52, No. 4, 1986, pp. 794-801.

IDENTIFICATION OF ORGANIC COMPOUNDS IN CAJÍO PELOID (CUBA)

Suárez Muñoz Margaret[1], Martinez-Villegas Nadia[2], González-Hernández Patricia[3], Melián Rodríguez Clara[1], Barrios Cossio Josiel[1], Hernández Díaz Rebeca[4], Fagundo Castillo Juan R.[3], Díaz Rizo Oscar[1], Díaz López Cristina[3] and Pérez-Gramatges Aurora[5]
[1]Department of Radiochemistry, Higher Institute of Technology and Applied Sciences (InSTEC), Cuba, [2]Applied Geoscience Department, Institute for Scientific and Technological Research of San Luis Potosi (IPICYT), Mexico, [3]Faculty of Chemistry, Havana University, Cuba, [4]Technique Sciences Faculty, University of Pinar del Río "Hermanos Saíz", Cuba, [5]Department of Chemistry, Pontifical Catholic University of Rio de Janeiro (PUC-Rio), Brazil.

ABSTRACT

Thermal muds ("peloids") are a typical example of natural sediments used in the treatment of different pathologies. Nowadays, because of their use in therapeutics, relax and cosmetic issues, a proper management of peloids is of increasing importance. Peloid characterization and monitoring for quality control purposes are therefore the main aspects of peloid management. Organic chemical quality is directly related with the biological active compounds and the therapeutic properties of peloidsto be used in human health and with the determination suitable contamination.

This study was performed to characterize the organic fraction of Cajío peloid (Cuba) in order to identify the organic components with possible biological effects and establish its natural or anthropogenic origin. For this purpose, a procedure with chromatographic analysis and mass spectrometry detection has been performed.

More than 40 compounds were identified, in Cajío peloid, mainly of natural origin. Among them were found alkanes, steroids, fatty acids, alcohols and other heteroatoms compounds, some of them with reported biological activity in their isolated form as antioxidant, analgesic, anti-inflammatory, and others. The results provide evidence for medical interpretation of the therapeutic action of Cajío peloid in the treatment of inflammatory and dermatological diseases and contribute to the understanding of pelotherapy, giving some scientific basis for its future development.

Keywords: Peloids, Peotherapy, Organic Characterization, Sediment, Cajío

INTRODUCTION

Thermal muds ("peloids") are a typical example of natural sediments used in the treatment of different pathologies [1]. Nowadays, because of their use in therapeutics, relax and cosmetic, the correct management of peloids is increasing its importance [1]. This situation highlights the significance of scientific research on the chemical characterization of thermal muds, firstly, to find the organic and inorganic substrates of their therapeutic activity, which provides some support for their medical use, and secondly, to certify their quality to be used in medical treatments [1]. The characterization and monitoring of these sediments (quality control) are main aspects in the management of these mineral resources. Organic chemical quality is directly related with the biological active compounds and the therapeutic properties of peloids to be used in human health and with the determination suitable contamination.

Peloids are complex and variable matrixes, and their chemical composition depends on different factors such as: the mineralogical composition of clay (geomaterials), organic matter, type of water, and micro-organisms involved in the maturation process. Therefore, the total organic chemical characterization of peloids becomes a complex procedure in chemical analysis. That fact justifies that, although inorganic and quality controls are established, the requirements for organic composition are scarcely described [2]. Current literature reports only few and specific studies of different organic fractions of peloids (non-polar compounds such as long-chain hydrocarbons, carboxylic acids, lipids, vitamins and pigments, and of polar compounds such as amino acids and proteins) [1]-[5], but there is still lack of literature on general characterizations. The identification of organic compounds of biological relevance in peloids is this reports are done mainly using gas-liquid chromatography coupled with mass spectrometry.

Cajío Beach is a locality of the Güira de Melena municipality in the eastern part of Cuba, and contains one of the most important deposits of peloids of the region. This peloid have been used in an empiric way for the residents of the province to

improve inflammatory (osteoarthritis, rheumatoid arthritis, bursitis) and dermatological (psoriasis, acne, cutaneous seborrhea and mycosis) processes and as an analgesic for painful processes of osteomioarticular system. Although in Cuba there are different deposits of peloids in dissimilar stages of characterization and exploitation, no reports have been found of chemical characterization of Cajío peloid.

This study was performed to characterize the organic fraction of Cajío peloid (Cuba) in order to identify the organic components with possible biological effects and establish its natural or anthropogenic origin.

MATERIALS AND METHODS

Sampling and pretreatment procedures

Sample pretreatment of Cajío peloid sample was done following previously reported procedures used for a similar peloid [1].

Briefly, the thermal mud was collected from two sampling stations in Cajío Beach deposit, where different subsamples were obtained, and afterwards a composite sample was prepared *in situ*, sealed in clean polyethylene containers, placed in a cooler at 4ºC, and transported to the laboratory immediately for further analysis.

Total organic matter (TOM) was determined using the Walkey Black volumetric method [6], and the n-hexane removable substances were determined using the gravimetric method [6].

Clean-up procedures

Sulfur removal was done according to a previously reported procedure [1], based on solvent extraction of the peloid sample with solvents of different polarity. The clean-up procedures were followed by centrifugation and drying at room temperature to constant weight. The solids obtained were grounded and sifted to a particle size of 125 mm, constituting the solid phases for the separation procedures.

Separation procedures

After removal of sulfur interference, the solid phases were subjected to specific analytical procedures for separation and identification of non-polar and polar organic compounds. In the case of non-polar compounds, the solid obtained for non-polar compounds analysis was macerated with 100 mL of n-hexane for 14 h in a stirring machine at room temperature, at a frequency of 200 min^{-1}, followed by centrifugation for phase separation. The liquid phase (non-polar fraction) was then reduced by rotary evaporation down to 1.5 mL and injected in a reverse phase (RP18) column and eluted with 2 mL of eight solvents (n-hexane, cyclohexane, di-isopropyl ether, acetone, ethyl acetate, acetonitrile, ethanol, methanol). The resultant fractions were later analyzed by gas chromatography–mass spectrometry (GC-MS).

For the polar compounds, the solid obtained, after removal of sulfur, was macerated with methanol for 14 h at room temperature. The extract of this polar fraction was analyzed by GC-MS.

A blank study was also carried out, as reported by [2], to determine if some of the organic compounds could be present because of contamination during the analytical procedure.

Instrumental analysis

Separation by gas chromatography (GC) was achieved using a fused silica capillar column HP 5MS of intermediate polarity (5% phenyl) column (15.0 m x 250 μm x 0.1μm) with intermediate polarity in a Agilent GCMS-7890A-5975C equipment.

The GC operating conditions were the following: temperature is held at 100°C for 1 min, increased from 100 to 215°C at a rate of 20ºC min^{-1}, hold for 10 min, increasing again to 290°C at a rate of 20°C min^{-1}, with a final isothermal hold at 290°C for 20 min; the pressure was 72.3 kPa, and the flow of 1.0 mL min^{-1}, using helium as carrier gas. The samples were split injected (2μL) with the injector temperature at 250°C. The mass spectrometer was operated in electronic impact mode (EI) at 70 eV ionization energy at 200°C, and scanned from 40 to 900 Da. Identification of individual compounds was performed using the GC-MS Solution 1.10 software for the spectrum construction, and by comparison of mass spectra with library data or interpretation of mass spectrometric fragmentation patterns. Other chemical software and databases (MS Windows NIST Mass Spectral, AMDIS Search Program Version 1.7-2005, MS Windows NIST Mass Spectral Search Program, Version 1.5-1997, and the MSDB NIST Standard Reference Data Base Series 1a. Version 4.5-1994: NIST 21, NIST 98, Wiley 229) were also used in the analysis of the results. Match qualities of 90% or greater against NIST 107 and 21 (National Institute of Standards and Technology) libraries were assumed to give reliable identifications. Tentative identification refers to qualities between 70% and 89% against these libraries. Analytes yielding match qualities of 69% or less were assumed to be not identified (unknown).

RESULTS AND DISCUSSION

Total organic matter determination

The levels of organic matter in the sediment allows for the classification of peloids into two possible groups, one with low content of organic matter (1%–5%) and high mineral composition (e.g. mud or fangi, limus), and the other with high organic matter content (e.g. peat, bioglea, sapropel) [7]. On the basis of that Cajio peloid classify in the first group (TOM=1.42%). A further classification can be done according to the characteristics of the water used in the maturation process. In general, mineral peloids formed from hydrothermal waters are known as mud or fangi, while the limus type is associated with seawater. In the case of Cajío peloid, formed in the sea, it can be classified as limus.

On the other hand, the n-hexane removable substances value was 1.34%, representing 94% of the compounds present in the TOM, indicating the predominance of organic non-polar (e.g. alkanes, steroids) over the polar (e.g. carboxylic acids, alcohols, aldehydes) compounds (6%) in Cajío peloid.

Organic characterization

Table 1 shows that, in Cajío peloid, separated (S) and identified (I+TI) compounds are 52 and 46 compounds respectively, for 88% percentage of identification. All the fractions show high identification percentage, with the exception of acetonitrile. These results indicate that the chromatographic methodology employed was appropriate for the characterization of Cajío peloid. The majority of the compounds (65%) were separated in the n-hexane and cyclohexane fractions demonstrating the prevalence of non-polar compounds over the polar ones in the as indicated by the values of n-hexane removable substances. The blank study indicates that no organic compounds product of the contamination from sample manipulation during the analytic procedure was found.

Non-polar fraction

Figure 1a-h shows the chromatograms of the eight non-polar fractions separated in Cajío peloid, in general, with good resolution and low base line. The only affected fractions in resolution are n-hexane and cyclohexane, were the main non-polar compounds are extracted, however high percentages of identification (>90%) were still obtained. These chromatograms contain the alkane region that frequently is characterized by complex mixture of linear, branched and cyclic hydrocarbons of difficult resolution [1]. Also it is important to remark that no interference of sulfur can be observed in the base line of the obtained chromatograms, indicating that the clean-up procedure was effective.

In the n-hexane fraction (Table 2), the identified compounds were mainly paraffins (alkanes and other members of the homologous series such as alkenes, alcohols and aldehydes). In the cyclohexane and di-isopropyl ether fractions (Table 2), the organic compounds that were identified consisted mainly in linear or cyclic paraffins, members of the homologous series such as (alcohols and ketones, carboxylic acids) and the presence of isoprenoids and steroids as squalene and fucosterol. In the acetone fraction the compounds identified correspond to the homologous series of alkanes of short chain (alcohols, carboxylic acids). The most polar compounds in this non-polar fraction (Fig. 1e-h) show few separated compounds corresponding to long chain alcohols, the dodecanoic (lauric) acid and citrate (Table 2).

Some of the organic compounds found in Cajío peloid, such as alkanes, alkenes and monocyclic hydrocarbons, steroids, lactones, hydroxy acids, carboxylic acids, ketoacids, esters, aromatic compounds, fatty carboxylic acids and terpenoids, have been reported in sediments of different origin and few reports in peloids [1]-[5], [8]-[11].

Table 1 Resume of compounds separated in each fraction

Fraction	S	I	TI	U	% (I+TI)
Fraction of Non-Polar Compounds					
n-hexane	20	5	13	2	90
cyclohexane	14	3	10	1	93
di-isopropyl ether	4	2	1	1	100
acetone	4	1	3	0	100
ethyl-acetate	1	1	0	0	100
acetonitrile	2	1	0	1	50
ethanol	2	1	1	0	100
methanol	1	0	1	0	100
Fraction of Polar Compounds					
methanol	4	1	2	1	75
Total	**52**	**15**	**31**	**6**	

S-Separated compounds, I-Identified compounds, TI-Tentatively Identified compounds, U-Unknown compounds.

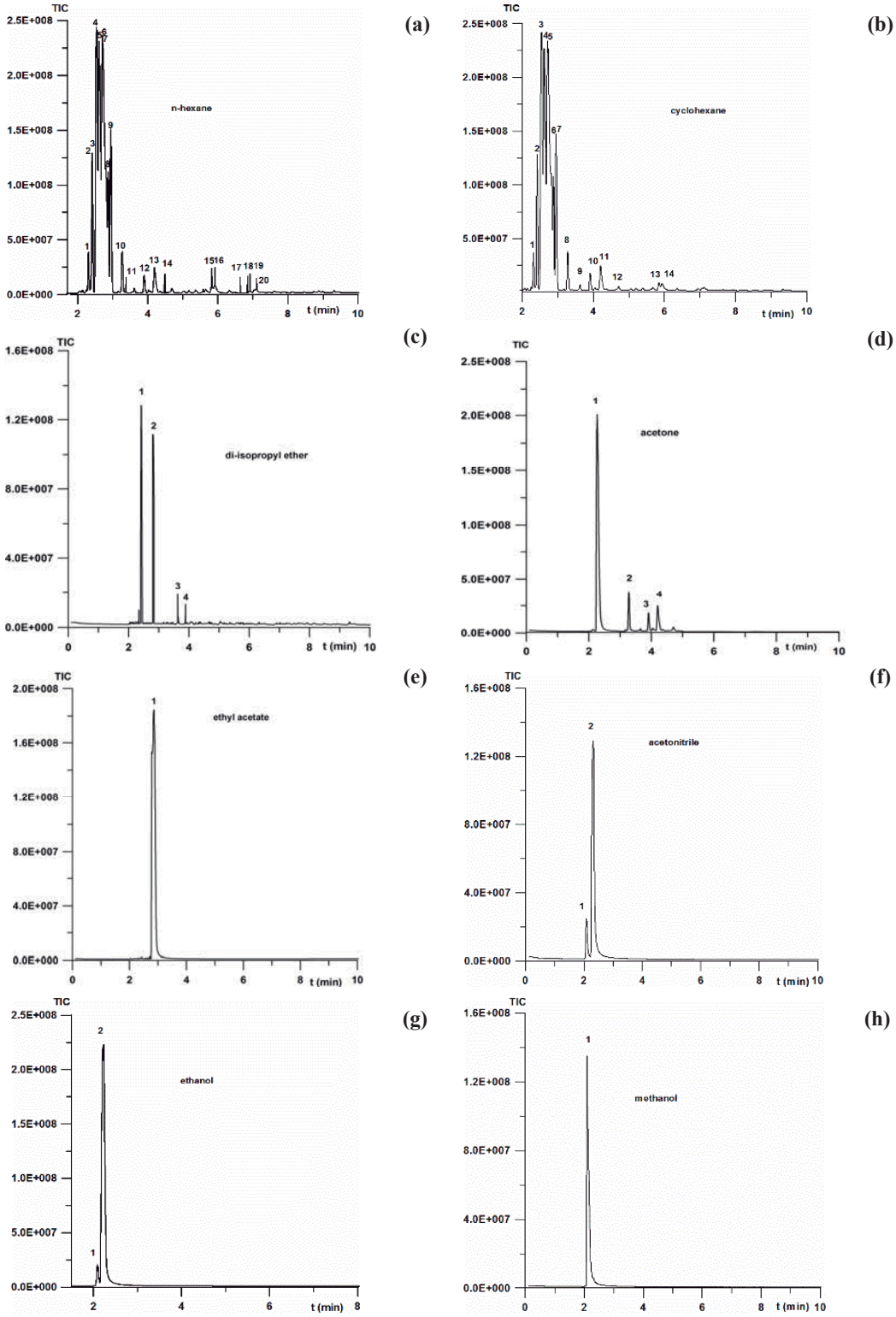

Fig. 1 Chromatographic profile of eluted non-polar fraction of Cajío peloid sample: a) n-hexane, b) cyclohexane, c) di-isopropyl ether, d) acetone, e) ethyl acetate, f) acetonitrile, g) ethanol and h) methanol

Polar fraction.

Good resolution and identification percentage (75%) was obtained for polar methanol fraction (Fig. 2). In this fraction only four compounds were separated, corresponding mainly to fatty carboxylic acid group. The poor compound separation is expected by the n-hexane removable substances analysis, but other factors can be influencing these results: probable decomposition of thermolabile and volatile polar organic compounds (presumably vitamins and proteins), during sample heating in the GC experimental procedure and/or the fact that higher molecular weight compounds (such as fulvic and humic acids), which contribute to the total organic matter, could not be determined by the procedure developed in the present work [11]. The polar fraction have been less investigated and only few reports have been found in sediments related to saccharides and some carotenoid derivatives [9].

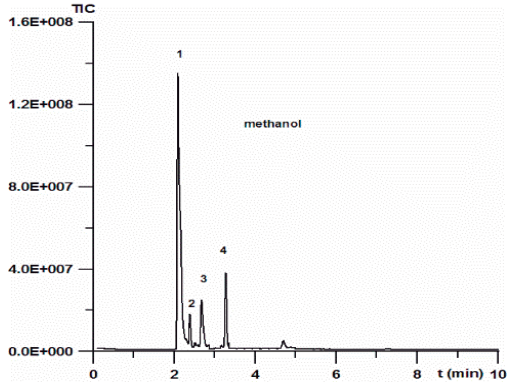

Fig. 2 Chromatographic profile of eluted methanol polar fraction of Cajío peloid sample

General organic composition of Cajio peloid

The main group of compounds identified (35%) in Cajío peloid is the hydrocarbons from C5 to C29 (straight, ramified or cyclic alkanes). These compounds are present in natural sediment as a result of plant biomolecule degradation and as microbiota byproducts [10].

As reported in previous works, paraffins (long, lineal or substituted alkanes) can strongly influence the physico-chemical properties of thermal therapeutic muds, related to heat retention, caloric capacity, humidity conservation, and toxins adsorption [1] and therefore the paraffin content in Cajío peloid could be related to its empirical reported thermotherapeutic and anti-inflammatory effects.

The next important fraction also represents approximately 35 % and it is dominated by the homologous compound series of n-alkanes (n-alkenes, n-alkanals, n-alkanols, n-alkanoic acids, n-alkanones and aliphatic carboxylic acids). These compounds reported to be mainly derived from the degradation of terrestrial plants, pheromones, essential oils and other biomolecules [10]. It has been not found reported the biological activity for these compounds.

Another 14.6 % of the total identified compounds is formed by various compounds of diverse nature, predominantly the nitrogenous compounds such as N-ethyl-N-methyl acetamide, the ubiquitous antioxidant BHT and compounds with oxygen. The origin of some of these compounds could not be assigned [10].

The fatty acids and terpenoids/steroids (phytosterols) represent approximately the remaining 12% of the total identified compounds. The fatty acids found in Cajio peloid were stearic acid (C18:0), palmitic (C16:0) and oleic (C18:1). Carboxylic acids are common in organisms and they are mainly originated from animal and plant internal lipid components such as essential oils of terrestrial plants, pheromones, and other biomolecules [10], [11]. These fatty carboxylic acids have also been reported to act as antioxidants, and membrane regulators in its isolated form and with significant anti-inflammatory activity [2]. Also these compounds were shown to play a protective roleagainst free radicals and UV radiations [2].

On the other hand, the terpenoids and steroids found in Cajío peloid are also important compounds identified. Squalene, particularly, has reportedly immune stimulant, antineoplastic and detoxicant action, and it is commonly used in pharmaceutical and cosmetic products because it acts protecting the unsaturated fatty acids of the lipid peroxidation, which is the cause of natural or premature aging [12]. In addition, the steroids (fucosterol) possess a well-studied and known biological activity in its isolated form, as hormones, analgesics and anti-inflammatory agents [13].

The absence of petroleum biomarkers (hopanes, pristane and others) suggests that the main sources of paraffins are typical plant wax alkanes [11] and no anthropogenic contamination.

These results provide strong evidence for medical interpretation of the therapeutic action of Cajío peloid in the treatment of inflammatory diseases and as analgesic.

Table 2 List of the identified compounds

Fraction	No.	Compound	Ident.	Fraction	No.	Compound	Ident.
Fraction of Non-Polar Compounds							
n-hexano	1	pentane	I	di-isopropyl ether	1	unknown	U
	2	unknown	U		2	octadecanoic acid (stearic acid)	I
	3	unknown	U		3	hexadecanoic acid (palmitic acid)	I
	4	1,2-dimethyl cyclopropene	TI		4	fucosterol	TI
	5	4-Pentenal	TI	acetone	1	2-butenoic acid	I
	6	cis 1-ethyl-2-methyl cyclopropane	TI		2	3-methyl-1-penten-3-ol	TI
	7	tetramethyloxirane	TI		3	3-methyl-1,3-pentadiene-5-ol	TI
	8	1-cyclopropyl-1-propanone	TI		4	3 hexen-2-ona	TI
	9	methyl benzene	TI	ethyl acetate	1	dodecanoic acid (lauric acid)	I
	10	butilatedhidroxytoluene (BHT)	TI	acetonitrile	1	2-octadeciloxy-ethanol	I
	11	hexadecane	I		2	unknown	U
	12	2,3-butanediol	TI	ethanol	1	2-hexadeciloxy-ethanol	I
	13	heptadecane	I		2	2-octadeciloxy-ethanol	TI
	14	3,4-dimethyl-2-pentene	TI	methanol	1	Citrate	TI
	15	eicosane	I	**Fraction of Polar Compounds**			
	16	heneicosane	TI		1	Citrate	TI
	17	tetracosane	TI	Methanol	2	hexadecanoic acid (palmitic acid)	I
	18	pentacosane	TI		3	9-ctadecenoic acid (oleic acid)	TI
	19	hexacosane	I		4	unknown	U
	20	2-methyl octacosane	TI				
Cyclo-hexane	1	unknown	U				
	2	pentiloxiran	TI				
	3	cis 1-ethyl-2-methyl-cyclopropane	TI				
	4	butilatedhidroxytoluene (BHT)	I				
	5	bencene	TI				
	6	3-ethyl-2,2-dimethyloxirano	TI				
	7	3-methyl-2-pentanona	TI				
	8	4-methyl 3-penten-2-ona	TI				
	9	3,4-dimethyl-2-pentene	TI				
	10	2,3-butanediol	I				
	11	methyl decanoate	TI				
	12	heptadecanoic acid	I				
	13	N-ethyl-N-methyl acetamide	TI				
	14	squalene	TI				

CONCLUSIONS

The analytical procedure developed in this work allowed the organic characterization of Cajío peloid permitting that 52 and 46 compounds were separated and identified respectively; most of them of natural origin. All the fractions show high identification percentage, and total percentage reached 88%. The majority of the compounds (65%) were separated in the n-hexane and cyclohexane fractions demonstrating the prevalence of non-polar compounds over the polar compounds as indicated by the values of n-hexane removable substances.

The main group of compounds identified in Cajío peloid is the hydrocarbons from C5 to C29 (straight, ramified or cyclic alkanes). Also were identified compounds of the series of n-alkanes (n-alkenes, n-alkanals, n-alkanols, n-alkanoic acids, n-alkanones and aliphatic carboxylic acids), fatty acids, terpenoids, steroids and various compounds of diverse nature. An important result derived from this research is the identification in this peloid of relevant organic compounds such as paraffins, squalene, fucosterol and fatty carboxylic acids, with reported biological activity in their isolated forms as antioxidants, hormones, analgesics and anti-inflammatory agents. These results provide strong evidence for medical interpretation of the therapeutic action of Cajío peloid in the treatment of inflammatory diseases and as an analgesic for painful processes of osteomioarticular system.

REFERENCES

[1] Suárez M, Domínguez R, González P, et al. "Identification of organic compounds in San Diego de los Baños peloid (Pinar del Río, Cuba)". Alternative and Complementary Medicine, Vol. 17, 2011, pp. 1-11.

[2] Centini M, Tredici MR, Biondi N, et al. "Thermal mud maturation: organic matter and biological activity". International Journal of Cosmetic Science, Vol. 37, 2015, pp. 339–347.

[3] Curri S, Gonzato, "Chromatographic analyses of peloide lipid and steroid fractions". Biochimica e Biologia Sperimentale. Journal of the AbanoTerme, Italy, 2004.

[4] Odabasi H, Gul E, Macit M, et. al."Lipophilic Components of Different Therapeutic Mud Species". Journal of Alternative and Complementary Medicine, Vol. 13, 2007, pp. 1115-1118

[5] Tserenpil Sh, Dolmaa G, Voronkov MG. "Organic matters in healing muds from Mongolia". Applied Clay Science, Vol. 49, 2010, pp. 55–63.

[6] Hiromi Sato J, Celio de Figueiredo C, Leandro Marchão R, et. al. "Methods of soil organic carbon determination in Brazilian savannah soils". Scientia Agricola, Vol, 71, 2014, pp. 7-10.

[7] Oficina Nacional de Normalización. "Norma Cubana de Peloides (NC 6: 98). Especificaciones". 1998. Habana, Cuba. 9 pp.

[8] Huang X, Zeng Z, Chen S, et. al. "Component characteristics of organic matter in hydrothermal barnacle shells from Southwest Indian Ridge". Acta Oceanologica Sinica, Vol. 32, 2013, pp. 60-67.

[9] Al-Mutlaq KF, Stanley LJ, Simoneit BRT. "Composition and sources of extractable organic matter from a sediment core in Lake Kivu, East African rift valley". Applied Geochemistry, Vol. 23, 2008, pp. 1023–1040.

[10] Oros DR, David N. "Identification and Evaluation of Unidentified Organic Contaminants in the San Francisco Estuary". RMP Technical Report. Regional Monitoring Program for Trace Substances: San Francisco Estuary Institute, 2002. SFEI Contribution 45. 119 pp.

[11] Rushdi AI, Kassim T, Simoneit BRT. "Organic tracers in sediments from the coastal zone of Ras Abu el-Darag, Gulf of Suez". Environ Geol, Vol. 58, 2009, pp. 1675–1687.

[12] Fox CB. "Squalene Emulsions for Parenteral Vaccine and Drug Delivery". Molecules, Vol. 14, 2009, pp. 3286-3312.

[13] Ardiles AE, González-Rodríguez A, Núñez MJ, et. al. "Studies of naturally occurring friedelane triterpenoids as insulin sensitizers in the treatment of type 2 diabetes mellitus". Phytochemistry, Vol. 84, 2012, pp. 116-128.

DETERMINATION OF ARSENIC IN SEDIMENT SAMPLES FROM A WELL IN THE COMARCA LAGUNERA, MEXICO

Mejía Miguel [1], González Luis [1], Briones Roberto [2], Ojeda María del Carmen [2], Cardona Antonio [2] Soto Pedro [3]
[1]Mexican Institute of Water Technology, Mexico [2]University of San Luis Potosí, Mexico [3]National Water Commission, Mexico

ABSTRACT

In order to elucidate the processes that incorporate arsenic to the groundwater of the Comarca Lagunera, México, Scanning Electron Microscopy (SEM) studies of the sediment of a well were carried out, as well as dissolved oxygen profiles, redox potential and arsenic in the water column inside the well. The results of the analyses indicate that the sediment contains Arsenopyrite (FeAsS), Sulfides of (Pb-Cu-As) and Oxides of (Pb-Fe-As). The results also demonstrated the reductive dissolution of iron oxides containing arsenic. The results obtained through the field and laboratory parameters of the groundwater, and the mineralogical characterization of the sediments at the different depths of the well, allowed to establish two possible mechanisms that would contribute to the incorporation of arsenic into groundwater that are: in anoxic conditions the reductive dissolution of iron oxide that would be arsenic carrier phases, and in oxic conditions the incorporation of arsenic from the primary phases of polymetallic sulphides containing arsenic (arsenopyrite).

Keywords: *Scanning Electron Microscopy, Sediment, Comarca Lagunera Aquifer, Arsenic, Arsenopyrite and Arsenical Sulphides.*

INTRODUCTION

Since the early 1960s, the health institutions of Mexico reported health problems in humans and animals, in the Laguna Region, in North central Mexico, due to consumption of groundwater with high arsenic concentrations ([1], [2]). Groundwater is the main source for drinking, agricultural and industrial use. Studies ([3], [4]) have outlined extensive areas of the La Laguna where arsenic levels are above 25 μg/L, the maximum level adopted in Mexico [5].

Hydrochemical and isotopic studies ([4], [6], [7], [8], [9]) have been performed to understand the geochemical behavior of arsenic and other components in the groundwater. However, the studies made to date are based on the analysis of arsenic concentrations in the groundwater themselves, and do not provide any information on the geochemistry of the aquifer sediments. This study examines both the geochemistry of the sediments and the groundwater in a newly constructed well, in order to establish the relationship between the aqueous and solid phase and understand the factors influencing mobilization of arsenic.

STUDY AREA

The study area is located in the North central part of Mexico and occupies southwestern portions of Coahuila and northeastern of Durango (Fig. 1). This area is located in a region named "La Comarca Lagunera" in Mexico. It is bounded on the west and south by the Sierra Madre Oriental and the east and north by isolated mountains.

Fig. 1 Geographic location of the Comarca Lagunera, Mexico

The Laguna Region is an endorheic basin fed by rivers Nazas and Aguanaval [10]: The Nazas, with 220 km of length, drains the western with a 60,000 km^2 basin covering the states of Coahuila and Durango, and Aguanaval River, 305 km of length, drains the southeastern with a 25,500 km^2 basin. The

rainy season covers four months, from June to September, with an annual average rainfall of 200-300 mm. The annual average temperature is 20.6 ºC. In the eastern part of the region is located a vast plain of alluvial lacustrine deposits.

Under natural conditions the direction of the groundwater flow was predominantly from southwest to northeast, showing a certain parallelism with the channels of the Nazas and Aguanaval rivers [11]. The overexploitation of the aquifer and the regularization of the Nazas and Aguanaval rivers, has produced the presence of depression cones and the disappearance of the lakes that gave the area the name of Comarca Lagunera (Fig. 2). The well object of this study is located at coordinates 25.72° and 103.56° (Fig. 2).

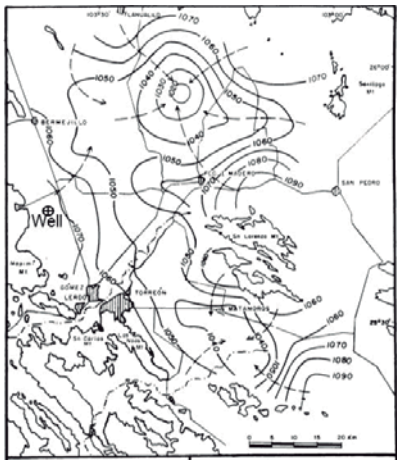

Fig. 2 Groundwater flow in the present time and well location [11]

The construction characteristics of the well under study are presented in Fig. 3.

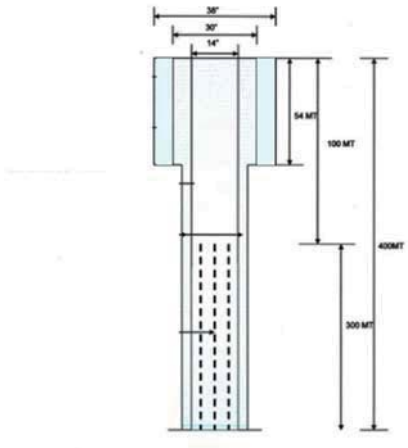

Fig. 3 Construction characteristics of the well under study

METHODOLOGY

Groundwater

The measurement of the field parameters and the collection of water samples in the vertical inside the well was carried out two months after the well was built. The well was not purged before measuring or taking samples. To measure the dissolved oxygen and the redox potential in the vertical inside the well, a multiparameter probe YSI 6600 V2 was used. Water samples were also taken vertically inside the well for laboratory analysis. The collected water samples were packed in high density polyethylene bottles and acidified to pH <2. The samples were filtered through cellulose membranes with 0.45-micron pore size using positive pressure.

After measuring the field parameters and taking the water samples, the well was pumped three times its volume and allowed to stand for 24 hours. Subsequently, the field parameters were again measured.

Analysis of sediments

Four samples of sediment from the cuttings of the well drilling were analyzed, from the following depths: 130m, 190m, 250m and 350m. The samples were homogenized and quartered using the cone technique to form representative batches for the corresponding studies.

A batch of sample was taken and separated into two fractions according to the mesh number corresponding to the F50, the products being denominated as coarse and fine. Mineralogical analyzes were performed for each fraction; For this purpose, the test specimens were prepared taking approximately 5 g of each and were encapsulated in epoxy resin. Once the specimens were hardened, they were roughened and polished to obtain smooth surfaces of the minerals. Subsequently the samples were coated with carbon wire to make the surface conductive and be analyzed in Scanning Electron Microscopy (SEM) equipment.

The mineralogical characterization of the sediment by Scanning Electron Microscopy SEM allowed to study the morphological details of the primary and secondary phases, the morphological variations, the inclusions on majority phases and chemical composition. The characterization was carried out using a PHILIPS XL 30 microscope equipped with a disperse energy X-ray spectrometer EDAX DX460 (EDS).

RESULTS

Groundwater

Before purging the well

The dissolved oxygen in the vertical inside the well before purging is shown in Fig. 4, the redox potential in Fig. 5, and the arsenic content in Fig. 6.

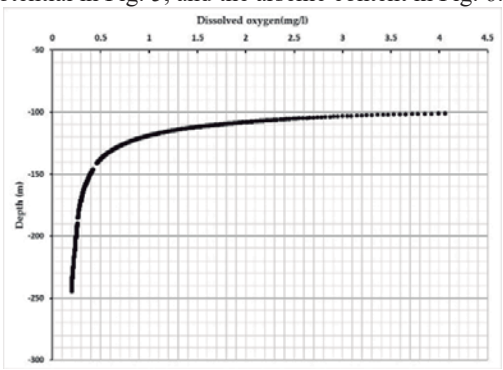

Fig. 4 Concentration of dissolved oxygen in water inside the well before purging

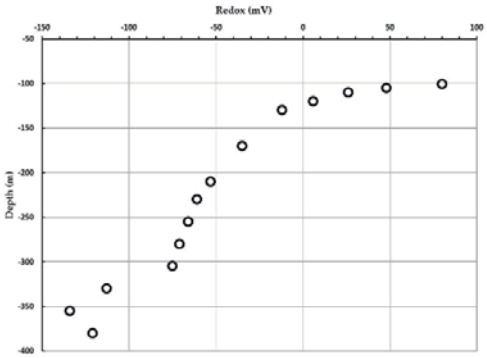

Fig. 5 Redox potential in the vertical inside the well before purging

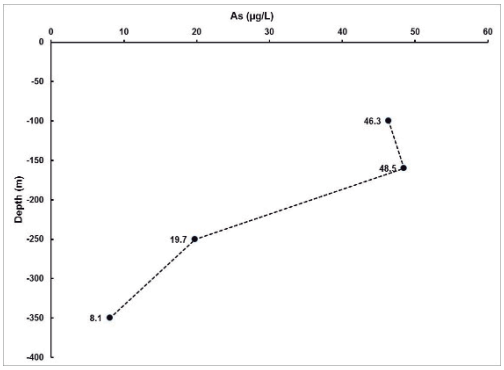

Fig. 6 Dissolved arsenic concentrations in the vertical inside the well before purging

After purging the well

The oxygen dissolved in the vertical inside the well after purging is shown in Fig. 7.

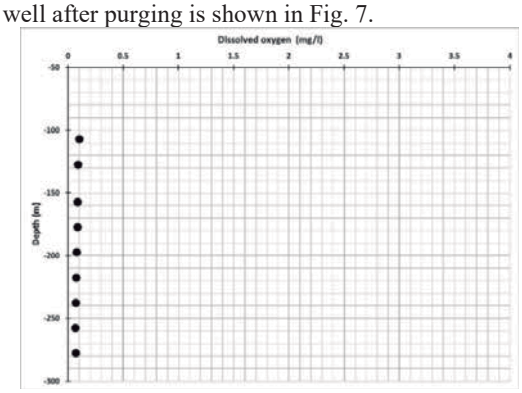

Fig. 7 Concentration of dissolved oxygen in the vertical inside the well after purging

Sediment

Sample of 130 m

Species identified in the sample, as well as the shapes and sizes of the particles, obtained in SEM, are shown in Fig. 8 and 9.

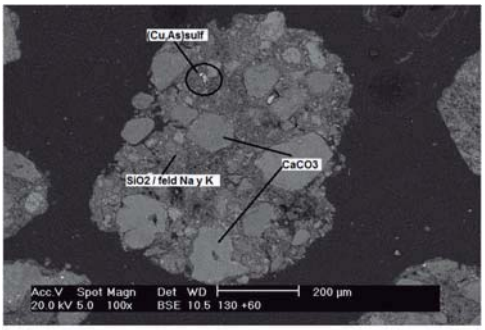

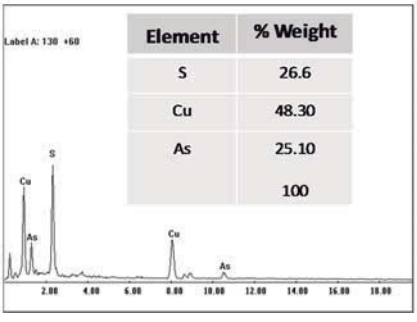

Fig. 8 Sulfides of (Cu, As) occluded in calcite-quartz-feldspar agglomerates

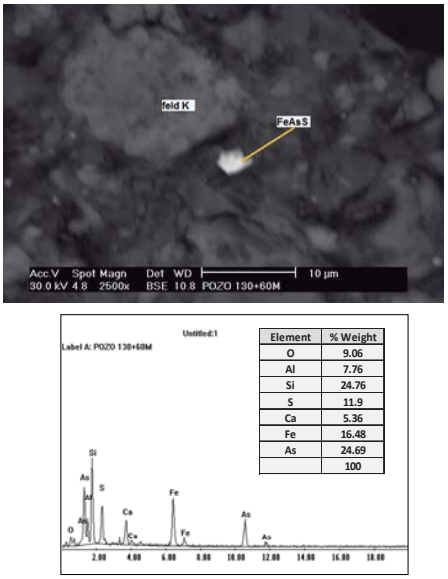

Fig. 9 Arsenopyrite in K feldspars

Sample of 190 m

Species identified in the sample, as well as the shapes and sizes of the particles, obtained in SEM, are shown in Fig. 10.

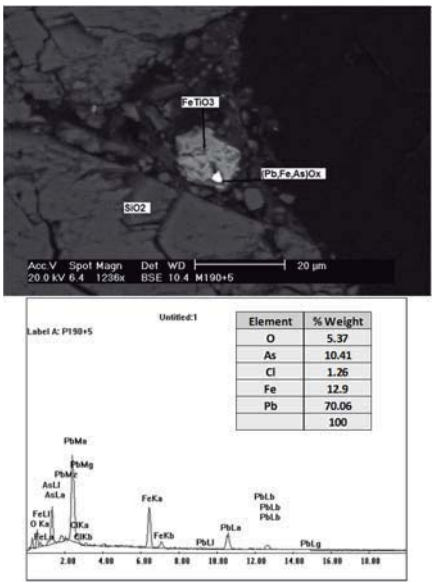

Fig. 10 Oxides of (Pb, Fe, As) occluded in ilmenite

Sample of 250 m

Species identified in the sample, as well as the shapes and sizes of the particles, obtained in SEM, are shown in Fig. 11.

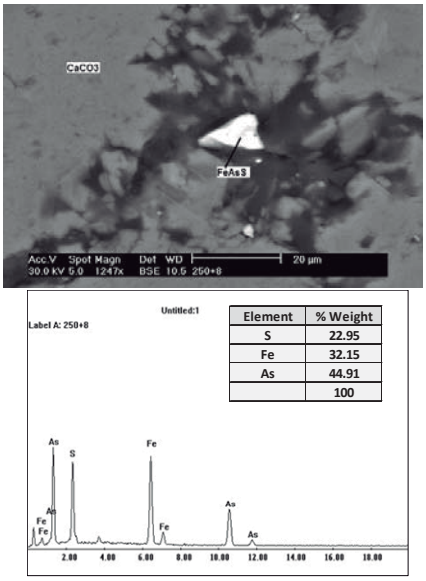

Fig. 11 Free arsenopyrite between calcite mineral

Sample of 350 m

Species identified in the sample, as well as the shapes and sizes of the particles, obtained in SEM, are shown in Fig. 12.

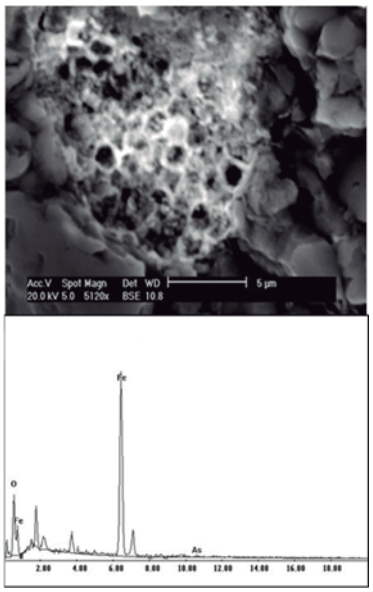

Fig. 12 Reductive dissolution of iron oxides carrying arsenic

DISCUSSION

In the Fox River Valley aquifer in Wisconsin, high concentrations of arsenic have been measured [12]. In wells with arsenic greater than 100 µg/L, it was identified that the oxidation of a layer of

sulfides containing arsenic is the process that mobilizes the arsenic of the solid phase to the groundwater. Various mechanisms causing the oxidation of sulfides were proposed, but it was concluded that the well acts as a direct conduit for the entrance of oxygen from the outside. [13] collected water samples from three monitoring wells before purging them. The dissolved oxygen concentrations varied from 3 mg/l to 10 mg/l. After purging the wells, they all had concentrations around 0.1 mg/l.

As can be seen in Fig. 4 and 7, before purging the well the shallow water presents aerobic conditions, however, after purging the well the dissolved oxygen is very low (~0.2 mg/l). This seems to indicate that: (1) the aquifer is anaerobic, and (2) the well acts as a direct conduit for the entry of oxygen from the outside.

CONCLUSIONS

First

The results of the SEM characterization showed that the sediment contains arsenopyrite (FeAsS), polymetallic sulphides of (Pb-Cu-As); (Cu, Zn, As); (Cu, As) and Oxides of (Pb-Fe-As).

Second

The characterization also showed particles of iron oxides carrying arsenic with a high degree of reductive dissolution.

Third

The distribution of oxygen in the vertical in the well, without purging, shows a thick stratum under anoxic conditions underlying a thin shallow layer under aerobic conditions. Apparently, the aquifer presents anaerobic conditions but the well acts as a direct conduit for the entrance of oxygen from the outside, causing aerobic conditions in the water of the upper strata of the well. Possibly the oxygen is oxidizing the arsenopyrite and the sulfides that are in the sediment, mobilizing the arsenic from the solid phase to the groundwater. The distribution of arsenic dissolved in the water in the vertical in the well, without purging, shows that the concentrations in the shallow strata of the well exceed the Mexican Maximum Permissible Limit (25 µg/l).

Fourth

The results obtained through the parameters of field and laboratory of groundwater, and the mineralogical characterization of the sediments at the different depths of the well, allow to establish two possible mechanisms that would contribute to the incorporation of arsenic to the groundwater that are: under anoxic conditions the reductive dissolution of iron oxide that would be arsenic carrier phases, and in oxic conditions the incorporation of arsenic from the primary phases of polymetallic sulphides with arsenic content.

ACKNOWLEDGMENTS

The study of the sediments was financed by the "RESEARCH AND DEVELOPMENT FUND ON THE WATER", sponsored by CONACYT-CONAGUA

REFERENCES

[1] Albores, A., Cebrián M., Tellez I., Valdez B., 1979. *Estudio comparativo del hidroarsenicismo crónico en dos comunidades rurales de la Región Lagunera de México.* Bol. Of. Sanit. Panam 86 (3).

[2] García Salcedo, J., Portales, A.; Blakely, E., Díaz R., 1984. *Transverse study of a group of patients with vasculopathy from chronic arsenic poisoning in communities of the Francisco I. Madero and San Pedro Districts, Coahuila, México*. Revista de la Facultad de Medicina de Torreón. 1, 12-16.

[3] CINVESTAV, 1986. *Estudio de calidad del agua para la identificación de compuestos arsenicales en la Comarca Lagunera*. Informe técnico, Dirección de Calidad del Agua, Comisión Nacional del Agua, México.

[4] IMTA, 1992. *Estudio Hidrogeoquímico e isotópico del acuífero granular de la Comarca Lagunera,* Informe técnico, Instituto Mexicano de Tecnología del Agua, México.

[5] Modificación a la Norma Oficial Mexicana NOM-127-SSA-1994. Official Journal of the Federation.

[6] SICYGSA, 2000, *Estudio de la contaminación difusa del acuífero de la Comarca Lagunera, Coahuila*, Subdirección general técnica, Gerencia de Aguas Subterráneas, CONAGUA.

[7] Ortega A., 2003, *Origin and geochemical evolution of groundwater in a closed-basin clayey aquitard, Northern México,* Journal of hydrology 284 (2003) 26-44.

[8] Molina, A., 2004. *Estudio hidrogeoquímico en la Comarca Lagunera, México.* Tesis de maestría en ciencias de la tierra. UNAM.

[9] Ortega A., 2017. *Evaporative concentration of arsenic in groundwater: health and environmental implications, La Laguna Region, Mexico*. Environ Geochem Health 39:987–1003.

[10] PIFSV-SARH, 1991, *Estadística de la producción agropecuaria y forestal y su valor de los ciclos otoño-invierno y primavera-verano.* SARH subdelegación de la política y concertación, unidad de información y estadística, Cd. Lerdo, Durango, México.

[11] CNA, 1992. *Revisión geológica e interpretación de la geometría del Acuífero Principal de la Comarca Lagunera, en los estados de Coahuila y Durango, México.* Reporte Interno Comisión Nacional del Agua.

[12] Schreiber, M.E., Gotkowitz, M.B., Simo, J.A., Freiberg, P.G., 2003. *Mechanisms of arsenic release to ground water from naturally occurring sources, eastern Wisconsin.* In: Welch, A.H., Stollenwerk, K.G. (Eds.), Arsenic in Groundwater: Geochemistry and Occurrence. Kluwer, Boston, pp. 259–294.

[13] Pelczar, J.S., 1996, *Groundwater chemistry of wells exhibiting natural arsenic contamination in east-central Wisconsin.* M.S. Thesis. University of Wisconsin-Green Bay, 206 p.

4. Sediment-driven reactions and transport of pollutants in rivers and groundwater

Session chairs: Graciela Herrera[1] and Blanca Prado[2]
[1]Departamento de Recursos Naturales, Instituto de Geofísica de la UNAM, México
[2]Departamento de Edafología, Instituto de Geología de la UNAM, México

Sediment-driven reactions and transport of pollutants is often referred to as "reactive transport modelling" (RTM), and it represents the culmination or coming together of theoretical and empirical chemical and physical data to generate predictive models of system behaviors, often in very complex multicomponent, multiphase systems. The requirement for RTM is growing, especially in the fields of carbon storage, unconventional hydrocarbon extraction and mineral exploration and mine development. This session looks to bring together the researchers whose work has direct implications to RTM and those who utilize RTM. The objective is to explore the capabilities, the growing requirements for data and data production, and to find the gaps and enhance the future of RTM based research.

COHESIVE SUSPENDED SEDIMENT TRANSPORT MODEL FOR THE GRIJALVA AND USUMACINTA RIVERS, MEXICO

García-Aragón J. A.[1], Izquierdo-Ayala K[1], Castillo-Uzcanga M.M.[2] Carrillo, L.[3]. and Salinas Tapia H.[1]
[1]CIRA-Fac. Eng., Univ. Aut. Estado de Mexico, Mexico. [2] El Colegio de la Frontera Sur, unidad Villahermosa, Tabasco, Mexico. [3]El Colegio de la Frontera Sur, unidad Chetumal, Quintana Roo.

ABSTRACT

Suspended sediment transport in large rivers is constituted mainly by cohesive sediments, which form aggregates or flocs with primary particles less than 65 μm [1], [2]. Due to its size, density and shape, the hydrodynamic behavior of flocs is very different from that of non-cohesive sediments as they depend on the interaction with the water column.

A classical model to calculate suspended sediment concentration profiles for steady flow conditions is the Rouse equation, which has been extensively validated for non-cohesive suspended sediment. Some authors have demonstrated that when applied in some large rivers in conjunction with non-cohesive settling velocity models it does not perform very well [1], [4]. The difficulty comes from the fact that most of the suspended sediment charge in large rivers is constituted by cohesive sediments.

Suspended sediments from Mexico's two largest rivers Usumacinta and Grijalva, with a mean flow rate near mouth of 2020 m^3/s and 1150 m^3/s respectively, were analyzed in a rotating circular flume. The shear velocity obtained in the field was reproduced in the circular flume and size and shape of flocs were obtained by means of PTV. Settling velocity was also obtained to calibrate a settling velocity model appropriate for cohesive sediments. The general model obtained was used to calculate the Z_R parameter in Rouse equation. This allowed us to reproduce suspended sediment concentration profiles of rivers Usumacinta and Grijalva. The estimated concentration profiles were able to reproduce the measured concentration profiles in the field.

Keywords: cohesive sediments, Concentration profiles, PTV, Rotating annular flume, Settling velocity

INTRODUCTION

Most of the suspended sediment charge in large rivers is constituted by cohesive sediments [1]. Cohesive sediments form flocs that behave in a very different way than non-cohesive sediments. Measuring in-situ flocs settling velocities in rivers is not possible with normally used sediment sampling instruments. Only recently in-situ optical instruments are being used for floc size measurement in the ocean [2-3]. In this chapter a method based on suspended concentration sampling and laboratory particle size analysis in a rotating annular flume is used to obtain flocs size and with an appropriate settling velocity model, deduce the settling velocity to be used in the Rouse equation. The method is validated with sediments from Usumacinta and Grijalva rivers the two major rivers in México.

The settling velocity of cohesive sediments is an important design parameter in aquatic environments such as water treatment installations, storm water ponds, sediment filling in lakes, sedimentation in estuaries and dredging in rivers.

Optical techniques like Particle Tracking Velocimetry (PTV) [4] were used in this study to measure particle velocities. Flocs performed as particles in the PTV technique, which also allowed us to measure particle size and shape.

METHODS

Suspended cohesive sediments were sampled in two locations, one in the Grijalva and one in the Usumacinta river in Centla, Tabasco, upstream from the confluence of both rivers. Suspended sediment concentration profiles were obtained at cross-sections at each sampling site. In order to analyze suspended cohesive sediments coming from the Usumacinta and Grijalva rivers in México a annular rotating flume was used.. The hydrodynamic conditions prevailing in the river were reproduced and the flocculation process was studied during long range experiments in the annular rotating flume,1.3 m diameter and flume cross section (15 cmx 15 cm) made of Plexiglas, (Fig. 1). The cohesive sediments were analyzed during 1.5 h long experiments and images were taken each 15 minutes. Floc sizes were obtained and settling velocities.

Fig. 1 Rotating annular flume

Theoretical settling velocity models

The main difficulty for the proposal of a settling velocity model for flocs is the adequate definition of their density. Many models have been formulated for floc density [5]. In this research we applied the model proposed by Kranenburg [6], Eq. (1)

$$\rho_f - \rho_w = (\rho_p - \rho_w)\left(\frac{D}{d}\right)^{F-3} \quad (1)$$

Where ρ_f, ρ_w, ρ_p are densities of floc, water and primary particles, D is the floc diameter and d is the primary particles diameter. F is the fractal dimension and the model assumes that the floc is constituted of spherical primary particles of equal diameter. The model can be used for non-spherical particles with equivalent diameters.

A balance of drag forces and gravitational forces gives Eq. (2)

$$W_s^2 = \frac{4(\rho_f - \rho_w)gD}{3C_{Df}\rho_w} \quad (2)$$

Where W_s is the floc settling velocity and C_{Df} is the permeable particle drag coefficient. Using Eq. (1) and (2) the following relationship for the settling velocity is obtained Eq. (3)

$$W_s = \sqrt{\frac{4(S-1)g(D)^{F-2}}{3C_{Df}(d)^{F-3}}} \quad (3)$$

Where S is the primary particles relative density

Using Particle Tracking Velocimetry methods (PTV), Garcia Aragon et al. [7] have shown that a useful relationship for the drag coefficient of a permeable floc has the form of Eq. 4.

$$C_{Df} = \frac{15}{R_{ep}^{\,n}} \quad (4)$$

Where the coefficient n depends on the kind of floc and varies, according to a comparison of results of different authors [8], between 1.1 and 1.25. R_{ep} is the particle Reynolds number defined as $R_{ep}=W_sD/\nu$ where ν is the kinematic viscosity of the fluid.

Replacing this relationship in Eq. (3) the following relationship (Eq. 5) for the settling velocity is obtained

$$W_S = \frac{\left[13.08(S-1)\right]^{\frac{1}{2-n}} D^{\frac{F+n-2}{2-n}}}{15^{\frac{1}{2-n}} \nu^{\frac{n}{2-n}} d^{\frac{F-3}{2-n}}} \quad (5)$$

Where W_s is in m/s and D and d in m.

The fractal dimension changes with floc diameter, we used in this paper a relationship similar to that proposed by [9] that has the following form

$$F = 3 - \alpha\left[\frac{D}{d}\right]^{\beta} \quad (6)$$

Where α and β are constants that depend on the kind of cohesive sediment.

Application to suspended load estimation in large rivers.

Authors working with the Mississippi river sediment transport Colby [10-11], realized that the predicted Rouse number was not equal to the measured Rouse number in a series of vertical profiles sampled in the Mississippi. Also researchers working in the three Gorges Reservoir in the Yangtze river showed that settling velocities calculated with diameters obtained from particle size analyzer do not reproduce observed settling velocities indicating flocculation existence [12]. The formation of flocs in large rivers is the reason why Rouse equation cannot be used with particle sizes from classical granulometric measurements in conjunction with non-cohesive settling velocity equations. Recently researchers working in the Amazon River and tributaries also found similar results [1]. Their conclusion was that granulometric measurements did not represent the real particle size because cohesive sediments agglomerate to form flocs [13] and after sampling, these flocs are destroyed and could not be measured appropriately in laboratory.

The Rouse equation is generally accepted to estimate the suspended sediment profile in stationary flows (Eq. (7)) [14],

$$\left(\frac{C(y)}{C(a)}\right)=\left(\frac{H-y}{y}.\frac{a}{H-a}\right)^{Z_R} \quad (7)$$

Where $Z_R=Ws/Ku^*$, $C(y)$ is the suspended sediment concentration at height y above bed, a is a reference depth above bed, H is the flow depth and K is Von-Karman constant that for low sediment concentration is equal to 0.4.

In this work the Eq. (5) was used to estimate the settling velocity Ws and in conjunction with the Rouse equation (Eq. (7)) estimate suspended sediment profiles in the Grijalva and Usumacinta rivers.

RESULTS

From the sampling of suspended cohesive sediments in the Grijalva and Usumacinta rivers, the following suspended sediment concentration profiles were obtained (Fig. 2 and 3).

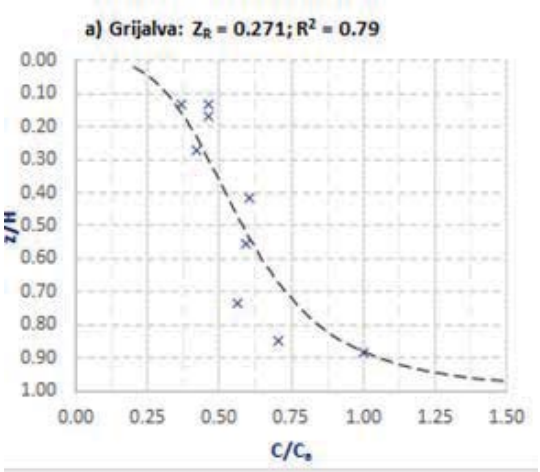

Fig. 2 Suspended sediment concentration profile for the Grijalva river

An average value of Rouse parameter Zr=0.271 was obtained in the Grijalva River. Which is representative of a small increase of suspended sediment charge near the bottom.

An average value of Zr=0.065 was obtained in the Usumacinta River. This value is representative of near constant suspended sediment charge in the water column.

Experiments in the rotating annular flume using samples for the Grijalva and Usumacinta rivers were performed at shear rates similar to those encountered in the field. Table 1 shows the values of shear velocity (u_*) obtained in the sampling stations of the Grijalva (width 220 m at the sampling of December 2016) and Usumacinta (width of 265 m) rivers, using the fluctuating velocities u',w'($\boldsymbol{u_*^2=\overline{u'w'}}$) measured in the field by an Acoustic Doppler Current profiler (ADCP).

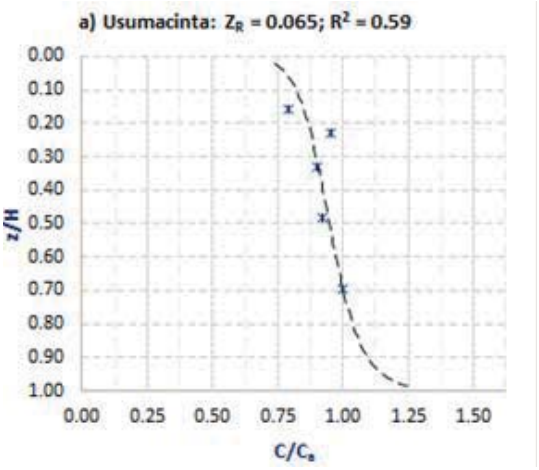

Fig. 3 Suspended sediment concentration profile for the Usumacinta river

Table 1 Shear velocity in Usumacinta and Grijalva rivers

River	Distance from left bank	u_* (m/s)
Grijalva	55 m	0.048
	90 m	0.045
	195 m	0.036
Usumacinta	25 m	0.064
	140 m	0.082
	210 m	0.065

Images of flocs after 1.5 hours experimental runs in the annular flume using PTV, gave us an average size of flocs in the rivers. Table 2 shows the statistical values of flocs obtained in large runs at a shear velocity u_*= 0.07 m/s the average value in the Usumacinta river (see Table 2). The mean value of floc size obatind for the Usumacinta river was 209 μm. Table 3 shows the values of D for u_*=0.04 m/s the average value at Grijalva river (Table 1). The mean value of floc size obtained for the Grijalva river was 307 μm.

The values of α and β in Eq. (6) were adopted from experiments performed in aquaculture recirculation tanks [7], 0.07 and 0.72 respectively.

Also microscopic images of some representative flocs were obtained with 40x magnification. An average value of primary particle, after a statistical analysis of 50 flocs images for each river, for the Grijalva river gave an estimated value of at 12 microns and 3.8 microns for the Usumacinta.

Table 2 Average floc size at the Usumacinta River from PTV experiments in the rotating annular flume

time (min)	D (μm)	# data
5	217	33200
20	188	17254
50	172	21500
120	164	12200
150	242	32560
180	247	25400
210	232	23450
mean	209	

Table 3 Average floc size at the Grijalva river from PTV experiments in the rotating annular flume

time (min)	D (μm)	# Data
0	306	33400
5	308	25550
20	313	22652
50	311	21320
85	297	23460
mean	307	

When Eq. (6) is used along with the already found average values of D and d, along with Eq. (7), with values of α=0.07 and β=0.72, the following values of settling velocity are obtained for different floc sizes (Table 4). Different values of n were used to show the sensitivity of the model to this compaction index.

Table 4 Estimated values of Ws and corresponding values of Zr

	W_s- mm/s Usumacinta	W_s- mm/s Grijalva	Zr Usumacinta	Zr Grijalva
n				
1.1	0.19	3.84	0.07	0.223
1.15	0.16	3.87	0.05	0.225
1.2	0.13	3.91	0.04	0.227
1.25	0.10	3.95	0.03	0.229

Table 4 shows that the best estimation of Zr for the Usumacinta river is obtained with n=1.1 because the average measured Zr (see Fig. 3) was Zr=0.065, also the best estimation of Zr for the Grijalva river is obtained with n=1.1 because the average measured Zr (see Fig. 2) was Zr=0.271.

These results indicate that flocs coming from both rivers are strong flocs, which is logical because shear rates at the Usumacinta and the Grijalva rivers are large. For comparison the average u* in the Amazon river at station Obidos is u*=0.08 m/s [1]. It is also observed that the value of Zr in the Usumacinta river is more sensitive to the change in the value of n. The lesson is that the larger the depth of flow it is more difficult to define n. The n value can change largely even in the same cross section of the river at different levels.

CONCLUSIONS

A method to calculate sediment concentration profiles for rivers with a large cohesive suspended sediment charge was presented. The necessary data to use this model are, average floc size which should be obtained by laboratory experiments in an annular rotating flume, the average shear rate of the flow in the field obtained by devices like ADCP and floc characteristics. These characteristics are fractal dimension and density of primary particles. The degree of floc compaction represented by the parameter n could be obtained by comparing estimated values of settling velocity with measured values.

In order to define the total annual transport of sediments it is necessary to make a monthly analysis, the data presented here are for large flow rates (December only).

REFERENCES

[1] Bouchez J., Metivier F., Lupker M., Maurice L., Perez M., Gaillardet J.and France-Lanord C. (2011) Prediction of depth-integrated fluxes of suspended sediment in the Amazon River: particle aggregation as a complicating factor. *Hydrological processes*, **25**, 778-794.2011.

[2] [Mikkelsen O.A., Milligan T., Hill P. , and Moffatt D. INSSECT—an instrumented platform for investigating floc properties close to the seabed. *Limnol. Oceanogr.: Methods* **2** : 226–236. 2004.

[3] Nimmo Smith W.A.M., Atsavapranee P. , Katz , and Osborn T.R. PIV measurements in the bottom boundary layer of the coastal ocean. *Experiments in Fluids* **33** : 962–971. 2002.

[4] Satake, S., Kunugi, T., Sato, K and Ito T., Digital Holographic Particle Tracking Velocimetry for 3-D Transient Flow around an Obstacle in a Narrow Channel. Opt. Rev., 11, 162–164. 2004.

[5] Li D.H. and Ganczarczyk J.J. Stroboscopic determination of settling velocity, size and

porosity of activated sludge flocs. *Wat. Res*. **21**(3); 157-262. 1987.

[6] Kranenburg C. The fractal structure of cohesive sediment aggregates. *Estuarine Coastal Shelf Science*. 39: 1665-1680, 1994.

[7] Garcia-Aragon J.A., Salinas-Tapia H., Moreno-Vega J., Diaz-Palomarez V and Tejeda-Vega S. A model for the settling velocity of flocs; Application to an aquaculture recirculation tank. *Int. J. of Comp. Methods and Exp. Measurements*. Vol 2, No. 3, pp:313-322, 2014. Doi:10.2495/CMEM-V2-N3-313-322.

[8]] Johnson C.P, Xiaoyan L.I, Logan B.E. Settling velocities of fractal aggregates. *Environ. Sci. Technol*. **30**: 1911-1918, 1996.

[9] Garcia-Aragon J.A., Droppo I., Krishnappan B., Trapp B and Jaskot C. Experimental assessment of Athabasca River cohesive sediment deposition dynamics. *Water Quality Research Journal of Canada*. Ed. IWA. 46 (1):87-96.2011b

[10] Jordan PR. Fluvial sediment of the Mississippi River at St. Louis,Missouri. *USGS Water-Supply Paper* **1802**. http://pubs.er.usgs.gov/djvu/WSP/wsp 1802.djvu.1965.

[11] Scott CH, Stephens HD. (1966) Special sediment investigations: Mississippi river at St. Louis, Missouri, 1961-63. *USGS Water-supply Paper* **1819-J**. http://pubs.er.usgs.gov/djvu/WSP/wsp 1819-J.djvu

[12] Li W, Wang J.,Yang S. and Zhang P. Determining the existence of the fine sediment flocculation in the Three Gorges Reservoir. *J. Hydraul. Eng.* 141(2), 05014008. 2015.

[13]] Droppo I.G. and Ongley E.D. Flocculation of suspended sediment in rivers of south-eastern Canada. *Water Research*, **28**, 1799–1809,. 1994.

[14]] Chien N and Wan Z. Mechanics of sediment transport. ASCE press. Pp:913. 1999.

NUMERICAL MODELING OF SEDIMENT TRANSPORT WITH LEVELES OF HYDROCARBONS IN A SHALLOW LAGOON

Herrera-Díaz Israel E.[1], Gutierrez-Vaca Cesar[1] and Saldaña-Robles Adriana[1]
[1]Depto. Ingeniería Agrícola, DICIVA, Universidad de Guanajuato, México

ABSTRACT

A particle tracking model was applied to estimate the sediment transport with presence of hydrocarbons inside a lagoon on the borders of the Grijalva River in Tabasco Mexico, for which purpose the calculation of the hydrodynamics of the study area was determined the three-dimensional velocity field [1], later, the calculation of particle transport was obtained, which was determined in any direction of the space caused by the velocity field and the turbulent dispersion (random movement of the Brownian type). The dispersion and re-suspension mechanisms of the particles used were represented by stochastic models, which describe the movement by means of a probability function [2]. The validation of the model was previously carried out by [3], obtaining average relative errors of less than 4.8%. The results obtained from simulating the particle transport, allow determining, under different hydrodynamic scenarios, the areas susceptible to accumulation of sediments within the lagoon, for its subsequent removal and treatment or final disposal.

Keywords: Sediment Transport, Shallow Lagoon, Hydrocarbons, Numerical Modeling

INTRODUCTION

The numerical computational model developed for the transport of the particles, is given under a Lagrangian approach; the particles are placed in bottom following an exponential law of concentrations or by an initial position in three-dimensional space. For the particle movement, the specific weight of each particle as well as the particle's fall velocity is considered [4], the analysis takes special interest on the particles in suspension. The Lagrangian model, it has the capacity to use the previous calculation of the hydrodynamics velocity filed, or in an integrated way to the hydrodynamic calculation, preferably it is developed and modeled separately, this for computational convenience. The results of the hydrodynamic calculation correspond to a stable field and converged in time, which indicates that the velocity fields and their turbulent parameters can be assumed as constants, but with an important spatial variation, in this way the simulation of the transport of particles is performed for times greater than those obtained in the hydrodynamic simulation. Therefore, for the transport of particles, the same hydrodynamic field can be used repeatedly, for all time intervals, (Dt) as many times as required, until the simulation period is completed. The velocities of the particles are obtained by linearly interpolating the velocities around the particle in the three-dimensional mesh. An advantage of separating the hydrodynamic simulation from the simulation of particle movement, allows us to develop large numbers of transport simulations [5], in this way we can simulate particle movements with: different locations and types of sources, several simulation durations, different transport parameters and different physical properties of the particles (specific weight and diameter), all this based on a hydrodynamic velocity simulation.

METODOLOGY

The governing equation hidrodynamical model

The Navier-Stokes equations in free surface flow, in cartesian coordinates; use the hypothesis of hydrostatic pressure and considering the postulates of Reynolds [6].

$$\frac{\partial u}{\partial t} + u\frac{\partial u}{\partial x} + v\frac{\partial u}{\partial y} + w\frac{\partial u}{\partial z} = -g\frac{\partial \eta}{\partial x} + div\left(\nu_e \overrightarrow{grad}(u)\right)$$

$$\frac{\partial v}{\partial t} + u\frac{\partial v}{\partial x} + v\frac{\partial v}{\partial y} + w\frac{\partial v}{\partial z} = -g\frac{\partial \eta}{\partial x} + div\left(\nu_e \overrightarrow{grad}(v)\right) \quad (1)$$

$$\frac{\partial \eta}{\partial t} = -\frac{\partial}{\partial x}\left(\int_{-zf}^{\eta} u\, dz\right) - \frac{\partial}{\partial y}\left(\int_{-zf}^{\eta} v\, dz\right)$$

where ν_e effective viscosity coefficient, obtained by adding the turbulent and molecular viscosity coefficient $\nu_e = \nu_t + \nu_m$, [7] proposes the following model to solve the turbulent viscosity:

$$\nu_t = \left\{ \ell_h{}^4 \left[2\left(\frac{\partial u}{\partial x}\right)^2 + 2\left(\frac{\partial v}{\partial y}\right)^2 + \left(\frac{\partial v}{\partial x} + \frac{\partial u}{\partial y}\right)^2 \right] + \right.$$

$$\left. \ell_v{}^4 \left[\left(\frac{\partial u}{\partial z}\right)^2 + \left(\frac{\partial v}{\partial z}\right)^2 \right] \right\}^{\frac{1}{2}} \quad (2)$$

where the vertical length scale $\boldsymbol{\ell_v = \kappa(z - z_b)}$ for $\frac{(z-z_b)}{\delta} < \frac{\lambda}{\kappa}$ and $\boldsymbol{\ell_v = \lambda\delta}$ for, $\frac{\lambda}{\kappa} < \frac{(z-z_b)}{\delta} < \mathbf{1}$ $\boldsymbol{\kappa}$ is the von Kármán constant typically 0.41, $(\boldsymbol{z - z_b})$ is the distance from the wall, $\boldsymbol{\delta}$ is the boundary-layer thickness and $\boldsymbol{\lambda}$ is a constant, typically 0.09. In the case of shallow-water flows, due to a steady current, the boundary-layer thickness may be assumed to be equal to the water depth h. The horizontal length scale is usually different than the vertical length scale, and the simplest assumption is to assume direct proportionality defined by $\boldsymbol{\ell_h = \beta\ell_v}$. The constant $\boldsymbol{\beta}$ has to be determined experimentally.

Free surface and bottom conditions

$$\tau_x^{fondo} = \nu_e \frac{\partial u}{\partial z}\Big|_{fondo} = \frac{g\sqrt{u^2+v^2}}{Cz^2}\,(u)$$
$$\tau_y^{fondo} = \nu_e \frac{\partial v}{\partial z}\Big|_{fondo} = \frac{g\sqrt{u^2+v^2}}{Cz^2}\,(v) \quad (3)$$

where $\boldsymbol{Cz}$ is the Chezy friction coefficient. The velocity components are taken from values of the layer adjacent to the sediment-water interface.

$$\boldsymbol{\tau_x^{sup} = \nu_e \frac{\partial u}{\partial z}\Big|_{superficie} = -\frac{\rho_{aire}}{\rho_{agua}} a_{viento}\omega_x|\omega_x|}$$
$$\boldsymbol{\tau_y^{sup} = \nu_e \frac{\partial v}{\partial z}\Big|_{superficie} = -\frac{\rho_{aire}}{\rho_{agua}} a_{viento}\omega_y|\omega_y|} \quad (4)$$

where $\boldsymbol{\rho_{aire}}$ = 1.29 kg/m3, $\boldsymbol{\omega_x}$ y $\boldsymbol{\omega_y}$ are the horizontal components at x and y respectively of the wind speed at 10 m altitude. The unidimensional coefficient $\boldsymbol{a_{viento}}$ can be obtained using the equation given by [8].

$$\boldsymbol{a_{viento} = 0.565 \times 10^{-3};\ si\ |\vec{\omega}| \le 5\ m/s}$$
$$a_{viento} = (-0.12 + 0.137|\vec{\omega}|)10^{-3}\ ;\ si\ 5 \le |\vec{\omega}| \le 19.22\ m/s \quad (5)$$
$$a_{viento} = 2.513 \times 10^{-3};\ si\ |\vec{\omega}| \ge 19.22\ m/s$$

The governing equation particle tracking model

The numerical model for particle transport is given under a Lagrangian approach; the particles are placed following an exponential law of concentrations or by an initial position in three-dimensional space [9]. For the movement of particles, a stochastic model is considered and discretized in three dimensions (Fig. 1), considering the specific weight of each particle as well as the fall velocity of the same [10] and it is verified if these are within the domain study for a single time step (Dt) from (n) to (n + 1) is given by:

$$\boldsymbol{x_i^{n+1} = x_i^n + u_{i,j,k}(\Delta t) \pm (2rand(iseed) - 0.5)\sqrt{(2\nu t_{i,j,k}\Delta t)}}$$
$$\boldsymbol{y_i^{n+1} = y_i^n + v_{i,j,k}(\Delta t) \pm (2rand(iseed) - 0.5)\sqrt{(2\nu t_{i,j,k}\Delta t)}}$$
$$\boldsymbol{z_i^{n+1} = z_i^n + w_{i,j,k}(\Delta t) \pm (2rand(iseed) - 0.5)\sqrt{(2\nu t_{i,j,k}\Delta t - w_s\Delta t)}} \quad (6)$$

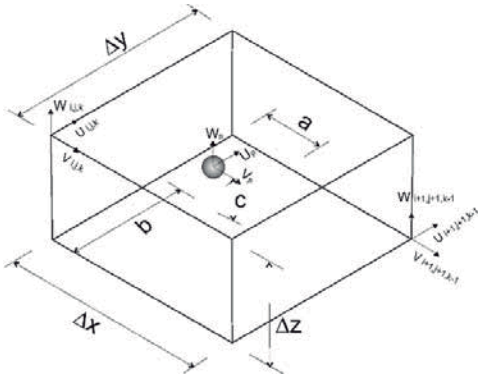

Fig. 1 Location in the three-dimensional space of the particle and its associated velocities

where $(\boldsymbol{x_i^n, y_i^n, z_i^n})$ is the position of the particle in time (*t*), (*u, v, w*) are the average velocities in (*i, j, k*), $(\boldsymbol{\nu_t})$ is the turbulent viscosity coefficient, (*Dt*) is the Lagrangean time step and $(\boldsymbol{w_s})$ is the velocity of sediment falling. The tracking of the particles is using the Eq. (6), therefore each particle is subject to a spatial displacement of magnitude $\pm(\boldsymbol{2rand(iseed) - 0.5})\sqrt{(\boldsymbol{2\nu t_{i,j,k}\Delta t})}$, in any direction of the domain, the sign is positive or negative depending on the sense of its location. In that moment of time the velocity field acts on each particle, in this way the movement has a sense in function of the main movement, given by the velocity fields. The term $(\boldsymbol{\nu_t})$ is found over the entire domain, represented by a field of positive scalars, which possesses information of turbulent intensities.

The shear forces in a turbulent flow, along its depth (z), can be written as:

$$\boldsymbol{\tau_i = \rho\nu\frac{dU}{dz} - \rho\overline{u_i w}} \quad (7)$$

where: $(\boldsymbol{\tau_i})$ bottom shear stress, $(\boldsymbol{\rho})$ fluid density, $(\boldsymbol{\nu})$ cinematic viscosity coefficient, (*U*) mean fluid velocity and $(\boldsymbol{\overline{u_i w}})$ bottom double correlation.

The critical shear stress that perform on the particles, is written:

$$\tau_{critico} = 0.03(\rho_s - \rho)gd_{50} \quad (8)$$

where: (ρ_s) solid density, (ρ) water density, (g) gravitational constant and (d_{50}) particle diameter 50%.

The probability function for the deposition of the particles is determined with the following equation:

$$P_{depósito} = \begin{cases} 0 \\ \left(1 - \frac{\tau_{x,y}}{\tau_{crítico}}\right) \end{cases}, \begin{matrix} \tau_{x,y} \geq crítico \\ \tau_{x,y} < crítico \end{matrix} \quad (9)$$

And the probability function for the resuspension of the particles is established in the following way:

$$P_{depósito} = \begin{cases} 0 \\ \left(1 - \frac{\tau_{crítico}}{\tau_{x,y}}\right) \end{cases}, \begin{matrix} \tau_{x,y} \leq crítico \\ \tau_{x,y} > crítico \end{matrix} \quad (10)$$

Velocity fall of sediment

To determine the velocity fall of sediment particles, these are considered to have non-spherical shape, so the effect of the shapes have a considerable influence on their velocity, mainly on relatively large particles (*>300μm*), the expressions that determine the magnitude of velocity fall [11] are expressed below.

$$w_s = \frac{(S-1)gd^2}{0.8v}; \quad 1 < d \leq 100\mu m$$
$$w_s = \frac{10v}{d}\left[\left(1 + 0.01\frac{(S-1)gd^3}{v^2}\right)^{0.5} - 1\right]; 100 < d \leq 1000\mu m$$
$$w_s = 1.1\left((S-1)gd^2\right)^{0.5}; \quad d > 1000\mu m \quad (11)$$

where (d) diameter of particle, (S) specific gravity, (υ) kinematic viscosity coefficient y (g) gravitational constant.

RESULTS AND APPLICATION

The lagoon called "El Viento" is located on the right bank of the Grijalva River, Tabasco, Mexico (Fig. 2). The lagoon has a maximum depth of 4.0 meters and is considered shallow by the surface area / depth relationship, the contributions of 3 rivers to this lagoon are contemplated, which make contributions of hydrocarbons from upstream areas.

The study area was worked with a mesh in finite differences (Fig. 3) with constant spacings in both directions (Dx = Dy = 50 m) with 135 cells in the "x" direction and 90 cells in the direction " Y"; 30 days of the month of November 2017 were simulated with increments of Dt = 1.0s.

The hydrodynamic model is used to generate the velocity field corresponding to the month of November, taking as force the magnitude and direction of the wind every hour, as well as the average monthly flow rate by the 3 rivers contribute to the lagoon (Table 1).

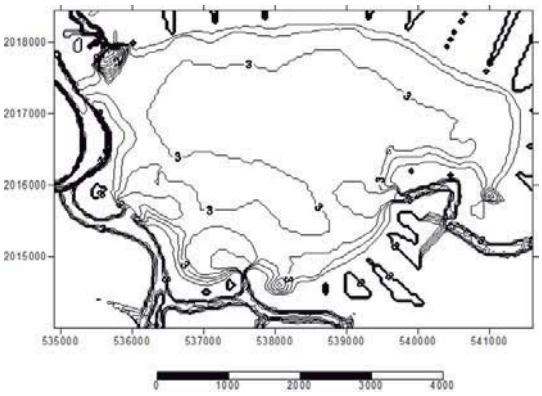

Fig. 2 Location “El Viento” lagoon

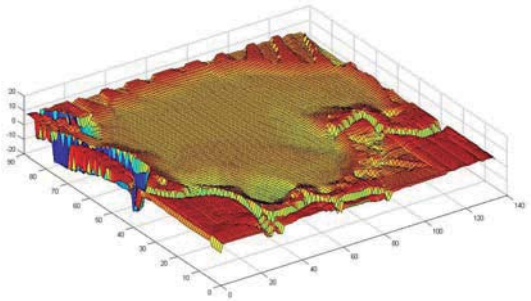

Fig. 3 Numerical mesh “El Viento” lagoon

Table 1 Flow rate Grijalva River in November

River-Reach	Flow Rate (m^3/s)
1	**8.07**
2	**4.67**
3	**2.96**

It is observed that the predominant circulation is due to the effect of the wind in its main cause, the contributions of the 3 rivers to the lagoon allow it to have superficial speeds of up to 0.015 m / s. There are 2 vortices in the lower part, product of the bathymetry of the lagoon and the contributions of the rivers.

The flow rates of the rivers that are poured into the lagoon, modify slightly the behavior of the hydrodynamics velocity field, exist a large vortex forms in the lower part of the lagoon; the contribution of the lagoon to the Grijalva river does not differ much, so it does not represent a significant alteration to the study area.

In the Fig. 4 the results of the behavior of the lagoon for the month of November to every 6 days

of simulation are presented, it is observed that the flood level of the lagoon covers 13% more compared to the rainy season of this year.

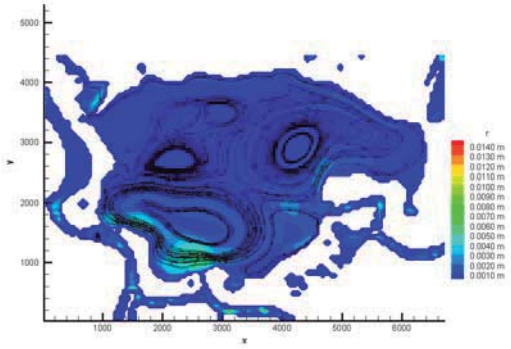

6 days simulation

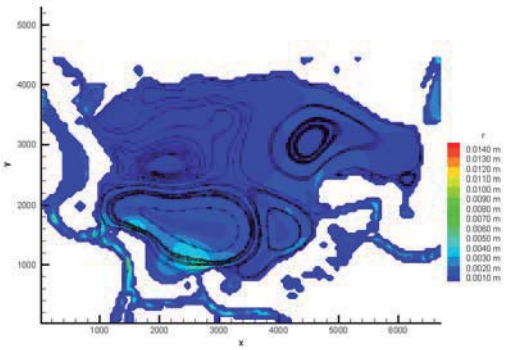

12 days simulation

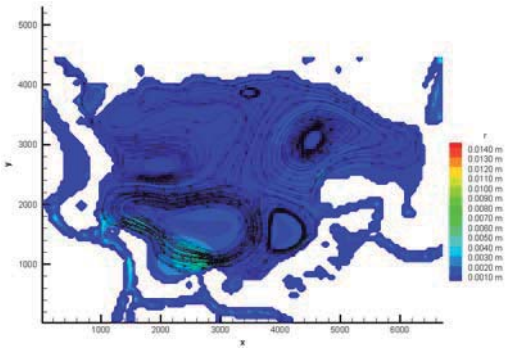

18 days simulation

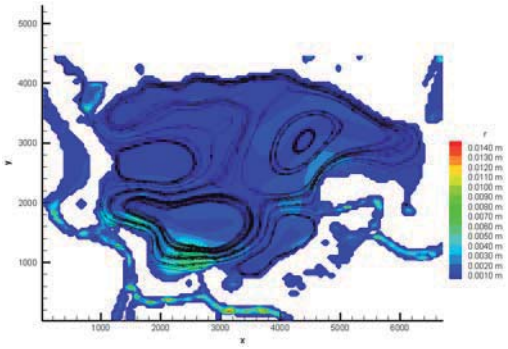

24 days simulation

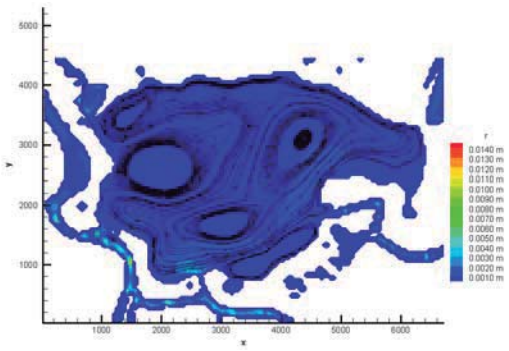

30 days simulation

Fig. 4 Hydrodynamic velocity field

Once the velocity field has been obtained, the seeding of sediment particles is placed at the bottom, the characteristic diameters of the sediment in the study area, which feed the sediment model are mentioned in the Table 2, the material is constituted in 87% sand and the remaining 13% is distributed in coarse and bulky material.

Table 2 Characterization of bottom sediments

Grid	Particle diameter (mm)
D05	**0.15**
D15	**0.19**
D25	**0.22**
D20	**0.24**
D35	**0.25**
D45	**0.27**
D50	**0.28**
D55	**0.3**
D65	**0.33**
D75	**0.38**
D85	**0.39**
D90	**0.42**
D95	**0.15**

The seeding of sediment particles in the bottom of the lagoon was established with an approximation by the PIC method (Particle in Cell), generalizing an initial concentration of sediments in a moment of time zero with 550,000 particles in this case. The concentration in an individual cell is obtained dividing the total mass in the cell by its volume.

The Fig. 5 presents the results of sediment transport for 30 days of study, in these images observed at different times (6, 12, 18, 24 and 30 days) the evolution of the transport in the bottom and consequently, the areas of sediment accumulation that translates into sediment and where the greatest amount of impregnated hydrocarbon is concentrated.

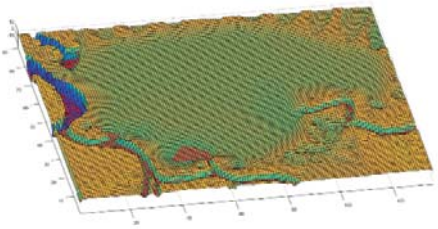

Simulation of tracer cloud size at 6 days

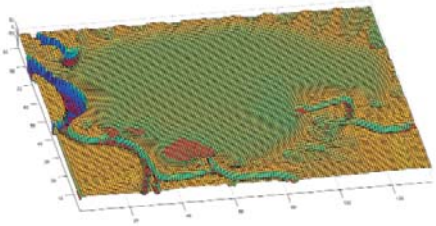

Simulation of tracer cloud size at 12 days

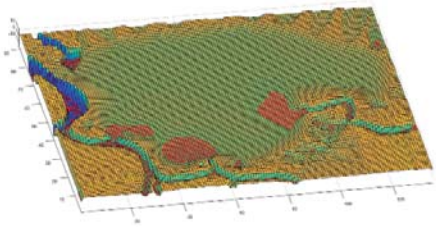

Simulation of tracer cloud size at 18 days

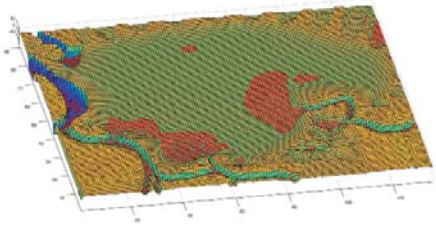

Simulation of tracer cloud size at 24 days

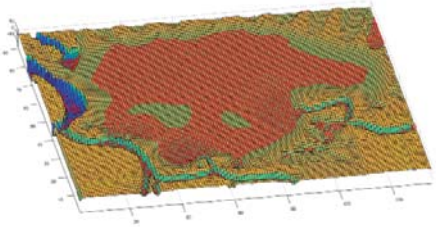

Simulation of tracer cloud size at 30 days

Fig. 5 Simulation of tracer cloud evolution

CONCLUSIONS

A general model for the sediment transport and dispersion of pollutants has been developed, based on a Lagrangian formulation. The model allows to describe the evolution of tracer cloud both in the near and far-field.

The model has the capacity to simulate 550,000 particles, limited only by the memory of the computer that is used. In this case, the evolution of tracer cloud is a function of the velocity field of the lagoon and sediment process.

The model requires a thorough calibration process, but the first results illustrate the possibility of considering the model a useful engineering tool to verify existing outfall designs and to predict future or hypothetical situations.

REFERENCES

[1] Rodríguez C., Couder C., Flores E., Herrera I.E., Cisneros R., “Modelling shallow water wakes using a hybrid turbulence model”, Journal of Applied Mathematics, Vol. 2014, pp.1-10.

[2] Herrera I.E., Rodríguez C., Couder C., Gasca J.R., “Modelación numérica hidrodinámico-hidrológica en zonas de inundación con presencia de infraestructura”, Tecnología y Ciencias del Agua, Vol. VI, Num. 1 Ene-Feb. 2015, pp. 139-152.

[3] Herrera I.E., Torres F.M., Moreno J.Y., Rodriguez C., Couder C., “Light particle tracking model for simulating bed sediment transport load in river areas”, Mathematical Problems in Engineering, Hindawi Publishing, Vol. 2017, pp.1-15.

[4] Trento A.E. and Vinzon S.B. “Modelo de partículas para el transporte de sedimentos finos”, Mecánica Computacional, XXIII: 2004, 1357–1374pp.

[5] Gu H.B., Causon D.M., Mingham C.G. and Qian L., “A Fast-Marching Semi-Lagrangian level set method for free surface flows”, Proc. of the Nineteenth International Offshore and Polar Enginnering Conference (ISOPE) 2009.

[6] Broomans, P. “Numerical accuracy in solutions of the shallow-water equations”, Master thesis, 2003, TU Delf & WL, Delf Hydraulics.

[7] Stansby, P. “A mixing-length model for shallow turbulent wakes”, Journal of Fluid Mechanics, Vol. 495, 2003, pp. 369-384.

[8] Flather R.A., “Results from surge prediction model of the North-West European continental shelf for April, November and December”, Institute of Oceanographic (UK), Report number 24, 1976.

[9] Robinson M., Monaghan J., and Mansour J. “SPH simulation of 2d wall-bounded turbulence”, SPHERIC, Smoothed Particle Hydrodynamics European Research Interest Community, Second International Workshop 2007, 107–110pp.

[10] Hernandez I., "Modelos euleriano-lagrangeanos en flujos a superficie libre: Aplicación al transporte de partículas suspendidas y al crecimiento de microorganismos", Tesis Maestría, 2003, DEPFI, UNAM.

[11] Van-Rijn L.C., Walstra D.J. and Van-Ormondt M. "Unified view of sediment transport by currents and waves IV: Application of Morphodynamic model", Journal of Hydraulic Engineering 2007, 133-7:776– 793pp.

EVALUATION OF SURFACE AND GROUNDWATER QUALITY RELATED WITH THE DISCHARGES COMPOSITION AND WATER-SEDIMENT INTERACTIONS, WITH AGRIWATER SOFTWARE

Bautista Francisco [1] and Pacheco Aristeo [2]
[1]Centro de Investigaciones en Geografía Ambiental, Universidad Nacional Autónoma de México, México,
[2]Skiu, Michoacán México.

ABSTRACT

The quality of the water for irrigation is the result of the composition of the discharges and it interaction with the sediments. It must be evaluated in each body of water used to irrigation of agricultural land, to avoid salinization and sodification of the sediments and soils, as well as toxicity in the crops; and also when it is used in industrial processes. Agriwater is a multiplatform software with which it can work in any operating system. With Agriwater it is possible to: a) organize, store and process water quality data from hundreds of wells in seconds; b) Conversion of units to improve data management and calculation of water quality indices; c) evaluate the salinity and sodicity of the water so as not to contaminate the soil; d) evaluate the toxicity of soluble ions in crops; e) identify water families; and f) evaluate changes in the quality of irrigation water over time and thus avoid the degradation of agricultural soils. In addition, the physicochemical parameters that Agriwater uses are those that are commonly measured to characterize water. With Agriwater the evaluation of irrigation water quality is simple, fast and reliable. Agriwater can be used in agroindustrial companies in extensive and intensive agriculture, as well as by all types of industry responsible for the environment that wants to regulate its effluents.

Keywords: Salinity; Sodicity; Salt toxicity; Water families; Agriculture

INTRODUCTION

The quality of irrigation water is a crucial factor in agriculture as well as in the study of sediments quality [1].

Studying, analyzing and evaluating large datasets on water quality to build indexes and graphs demand considerable time, and technician knowledge (chemical, agronomic and sedimentology). Furthermore, the management of data may be exposed to human errors. The process of analyzing irrigation water quality data can be automated through the use of software.

The aim of this work was to describe both structure and function of agriwater software.

STRUCTURE

The Agriwater software was designed with: a) Java programming language; b) Eclipse as integrated development environment; c) Apache Derby as database management system because it met the criteria of being: multi-platform, lightweight, embeddable, SQL-based and relational.

The software routines developed were optimized to require a minimum amount of computing resources: 1.0 GHz or higher Intel or AMD processor, 256 MB of dedicated RAM for optimal performance, VGA screen with a recommended resolution of 1200 x 800 and 32 MB of graphics memory to display the different graphical interfaces, a hard drive with at least 100 MB free for installation, Java Virtual Machine 1.8 (JVM), Windows Vista or higher, any version of Linux that supports JVM 1.8, any Mac OS version supporting JVM 1.8.

In the "File" menu contains "Exit" options and "Change Language", when some is selected, another window opens requesting confirmation of exit or changing languages. (English or Spanish) (Fig. 1).

In the "Edit" menu are the options "Copy", "Cut" and "Paste". This action is executed to data selected.

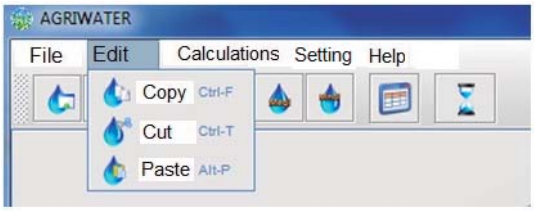

Fig. 1 Principal menu

FUNCTIONS

In the "Calculations" menu we find much of the software functions; with it is possible to modify or enter new data, view the already registered in any of the three units (mg L-1, meq L-1 y mmol L-1), to make graphs, descriptive statistics and tests for trend (Fig. 2).

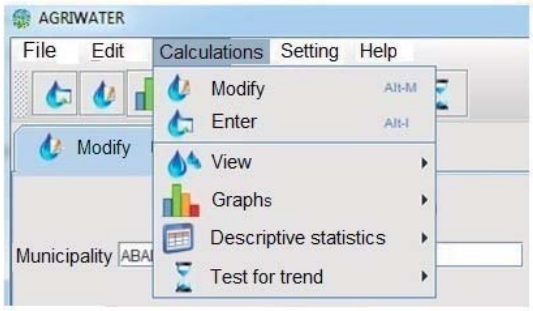

Fig. 2 Calculations menu

The equations necessary for converting units, calculating water quality indexes, the salinity and sodicity of irrigation water, chloride toxicity and classifying types of water, were turned into algorithms capable of processing the data stored in the DBMS and display the results in tabular and/or graphical format via different software interfaces.

The software has a set of routines for calculating parameters and indices:

a)) Storing and managing georeferenced physicochemical data of water quality;
b) Making quick queries and conversions of chemical units;
c) Sum of anions and cations[2, 3];
d) Simple correlation between all parameters.
e) Sodium Adsorption Ratio (RAS);
f) Potential Salinity (PS) (Fig. 3);
g) Effective Salinity (ES);
h) The name of the families of water (Fig. 4) [4];
i) The risk classification of the use of water from the relationship between RAS and CE (Fig. 5) [5];
j) The risk classification of the use of water from the concentration of chlorides;
k) The risk classification of water use from the sulphate concentration; and
l) The risk classification of water use from the sodium concentration.

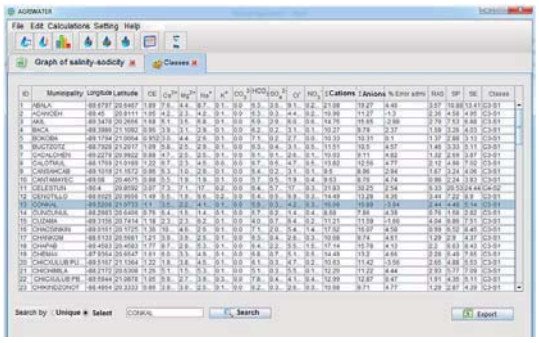

Fig. 3 Ions and salinity index

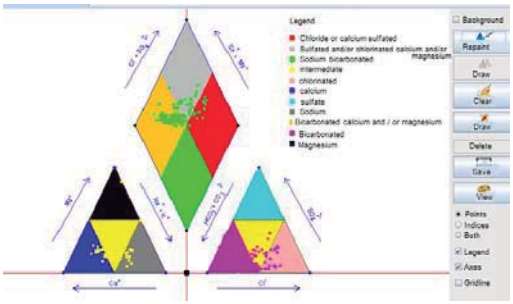

Fig. 4 Pipper diagram

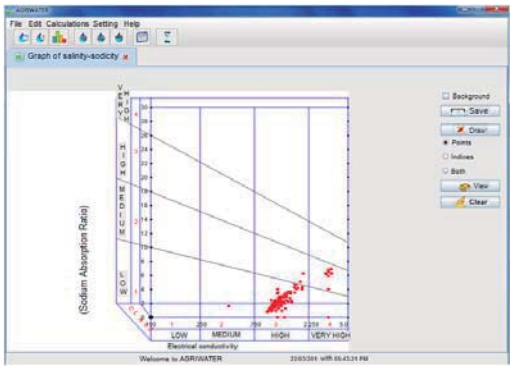

Fig. 5 Diagram o salinity and sodicity

CONCLUSIONS

The Agriwater software is a professional tool that allows users to organize, store and process large amounts of data of the chemical composition of water in a simple, fast and accurate way.

With agriwater, the quality of the water will be known and evaluated, and with it, better management and care will be taken of the sediments and soils surrounding the water sources.

REFERENCES

[1] Ayers, R.S. y Wescott, D.W. (1985). Water quality for agriculture. FAO Irrigation and Drainage Paper 29 Rev.1, Roma, 174, pp.

[2] Delgado, C., Pacheco, J., Cabrera, A., Batllori, E., Orellana, R., & Bautista, F. Quality of groundwater for irrigation in tropical karst environment: The case of Yucatan, Mexico. Agricultural Water Management, 97, 2010. pp. 1423–1433.

[3] Hounslow, A.W. Water Quality Data. Lewis Publishers., U.S.A. 1995.

[4] Piper, A. M. A graphical procedure in the geochemical interpretation of water analysis. Transactions American Geophysical Union 25.1944. pp. 914-928

[5] Richards, L.A. Diagnosis and improvement of saline and alkali soils. USDA Agricultural Handbook 1954. 60, 160 pp.

ROLE OF SEDIMENT AND SUSPENDED MATTER IN THE FATE OF FLAGRANCES FROM WWTP-EFFLUENT

Alary Claire[1], Belles Angel[1,2] and Franke Christine[2]
[1]IMT Lille Douai, LGCgE - Civil & Environmental Engineering Department, France; [2]MINES Centre for Geosciences and Geoengineering, France

ABSTRACT

Persistent pollutant in aquatic media (such as polycyclic musks) raised a specific concern in regard to the risk assessment of aquatic ecosystem. This study attempt to evaluate near to a WWTP-effluent the transport of 2 persistent polycyclic musks (i.e. galaxolide and tonalide) and the part of suspended matter and sediment in the fate of the musks. Fort de Scarpe-WWTP and Scarpe river were selected to evaluate in-stream fate of polycyclic musks because they take up the effluent of a large population of Douaisis agglomeration (France) and release effluent under a relatively small channelized river with a low water discharge. During the study period, dissolved contamination and contaminants sorbed to the SPM were monitored at different time scale and different location of the study area. Additionally, a set of laboratory experiments were conducted for evaluating the diffusive flux of compounds between the sediment bed and the water column. Finally, the transport of contaminants between the water column and the bedded sediment mediated by the settling of SPM was estimated as well as the amount of pollutants transported from the bedded sediment to the water column by the sediment re-suspension. Results show that attenuation due to sedimentation of SPM lead to reduce by half the contamination of the dissolved phase after ~30 km. Diffusive exchanges with bedded sediment are likely canceled out over long term period and instream fluxes in dissolved phase dominate on fluxes of compounds sorbed onto SPM. One concern remain as what will happen to sediment-sorbed contaminants if surface water contamination come to be durably reduced notably due to the growing water quality regulation. In this condition, significant diffusive contaminant transport from sediment is expected leading to minimize the positive effect of our efforts to reduce the surface water contamination.

Keywords: Sediment, WWTP-effluent, Pollutants, Musks

INTRODUCTION

Waste water treatment plant (WWTP) effluents are complex mixture of various anthropogenic pollutants among which pharmaceuticals, musks and surfactants are commonly reported in the litterature. Many of them are not fully eliminated by the conventional WWTP that lead to the significant release of these substances in surface water [1] [2]. The potential impacts of these contaminants on aquatic ecosystem are widely reported notably in regard of compounds with genetic damage and endocrine disruptor activities [3] [4] [5]. However, with the increasing of water demand and growing population and effluent load, there is a need for a better understanding of the persistence and fate of such pollutants. Several processes drive the transport and the persistence of WWTP-related pollutants in the aquatic environment. Dilution by mixing with upstream water is one of the main processes providing the contamination level attenuation needed to preserve the qualities of hydro-systems. However, multiple other processes occur simultaneously making difficult to identify the fate of substances. Currently, sorption [6], biodegradation [7] volatilization [8], photolysis [9] and hydrolysis are the main investigated processes (most of the time separately).

This study attempt to evaluate near to a WWTP-effluent the transport and the apportionment between the dissolved phase, the bedded sediment and the suspended particulate matter (SPM) of 2 persistent polycyclic musks (*i.e.* galaxolide and tonalide).

EXPERIMENTAL METHODS

Site description and sampling strategy

Fort de Scarpe-WWTP and Scarpe river were selected to evaluate in-stream fate of polycyclic musks because they take up the effluent of a large population of Douaisis agglomeration (156 000 unit per capita loading) and release effluent under a relatively small channelized river with a low water discharge Q (regulated at 1 m^3/s). The study site is situated in the lower basin (after the city of Douai) and flow through 2 km without connection with other canal. The configuration of the site allow easily the characterization of the “background” and “waste water impacted” stream over several km. The

WWTP has an average annual discharge of 0.31 m^3/s (31 % of the river flow).

Study site has 14 transect separated by a distance included between 60 and 80 m (total length: 1000 m). The effluent of the treatment plant is located between transect n°12 and transect n°13. An initial campaigns consisting of water sample collection on 5 points along each transect were conducted in December 2016 (sampling size of 70 samples). Cross sectional composite samples of sediment were also collected at each transect. In addition, for evaluating time dependence of dissolved contamination (C_{diss}), water sample were also collected at St1 station -located upstream to the effluent- and at St2 station -located downstream to the effluent- during a period of 1 month with at least 2 samples collected per week and per location. Large volume water sample were collected at these stations 5 times over the study period for determining the average load of SPM (φ_{SPM}) its contamination (C_{SPM}) and the C_{SPM} to C_{diss} ratio (noted K_{SPM}) for each compound. 3 SPM traps aiming to determine the settling rate of SPM Settling rate (R_{sett}) were also disposed at 50 cm above the sediment floor for 67 d period.

Conceptualization of the model

A model of transport of contaminants and apportionment between the dissolved water phase, the SPM and the bedded sediment was used in order to evaluate the behavior of pollutants in the local area of the WWTP-outflow. The developed model takes into account the contaminants fluxes mediated by the following processes:

- The settling of contaminated SPM (F_{sett}), where

$$F_{sett} = R_{sett}.C_{SPM} = R_{sett}.K_{SPM}.C_{diss} \quad (1)$$

- The contaminants transport mediated by the resuspension of the settled SPM (F_{ress}). Assuming that SPM trap provide a measurement of the settling rate alone -negligible resuspension is expected in the trap- the resuspension rate was estimated from the difference between the settling rate and the annual sediment accumulation (Eq. (2)) calculated over the 2 last decades using ^{137}Cs and ^{210}Pb radionuclide. Estimation of long term sedimentation rate was provided in the companion paper by [10].

$$F_{ress} = (R_{sedimentation} - R_{sett}).C_{SPM} = (R_{sedimentation} - R_{sett}).K_{SPM}.C_{diss} \quad (2)$$

- The bidirectional diffusive flux of contaminants between the bedded sediment and the overlaying water (F_{diff}). In this work, the pore water contamination level is regarded as the dissolved concentration of contaminants when equilibrium is reach with the surficial sediment ($C_{diss,eq}$). It was determined by incubating 300 g of wet sediment collected at each transect with 1 L of water collected at St1 station poisoned with sodium azide. After 14 d of equilibration, the dissolved phase was analyzed for the targeted compounds. The final dissolved concentration is assumed to be the concentration of dissolved contaminant when equilibrated with surficial sediment. Therefore, direction of flux of compounds was assessed by comparison of the effective concentration of the overlaying water (C_{diss}) with $C_{diss,eq}$. According the modified equation of the 2nd Fick law, the magnitude of sediment to water diffusive flux is assumed linearly proportional to the difference between the chemical concentrations in the water phase and the pore water phase in equilibrium with sediment ([11]; Eq. (3)).

$$F_{diff} = K_m(C_{diss} - C_{diss,eq}) \quad (3)$$

In order to evaluate the magnitude of F_{diff}, the mass-transfer coefficient (K_m) should be determined. For this purpose F_{diff} were measured through a set of laboratory experiments simulating various values of (C_{diss}-$C_{diss,eq}$). K_m were then determined by a linear regression analysis of F_{diff} when plotted as a function of (C_{diss}-$C_{diss,eq}$). For simulating different (C_{diss}-$C_{diss,eq}$) conditions, 10 L of sediments collected at St2 station were disposed in a 27-L experimental unit supplemented with 15 L of uncontaminated tap water maintained under controlled stirring. Water was renewed at different rates (3, 8, 13, 21, 33 and 58 L/d) which have dictated various dissolved contamination of the overlying water (C_{diss}). During the experiments, C_{diss} were measured every day and F_{diff} were calculated as the product of the renewing rate of water and the contamination level divided by the exchange area between water and the sediment (346 cm^2).

-The in-stream transport of contaminants sorbed to the SPM (F_{SPM}), where

$$F_{SPM} = Q.\varphi_{SPM}.C_{SPM} \quad (4)$$

Because C_{SPM} to C_{diss} ratio (K_{SPM}) is expected almost constant, F_{SPM} could also be calculated as:

$$F_{SPM} = Q.\varphi_{SPM}.K_{SPM}.C_{diss} \quad (5)$$

- And the in-stream transport of contaminants dissolved in the water column (F_{diss}), where

$$F_{diss} = Q.C_{diss} \quad (6)$$

RESULTS AND DISCUSSION

The Dissolved contaminants

The initial campaign conducted on 70 locations of the study site show for galaxolide and tonalide higher contamination downstream of the WWTP outflow and an over contamination at the nearest sampling point of the effluent (Fig. 1). In the same way, the SPM contaminations were higher at St2 station than St1 station for the WWTP-related contaminant. All over transect 1 to 11, the dissolved concentration of galaxolide and tonalide are similar indicating that upstream water and the effluent are rapidly homogenized. Galaxolide and tonalide contamination appear highly variable at St2 sampling location. Effectively, over 48 h period galaxolide and tonalide concentrations vary by a factor of 2 likely due to the variable outflow of fragrance from WWTP-effluent.

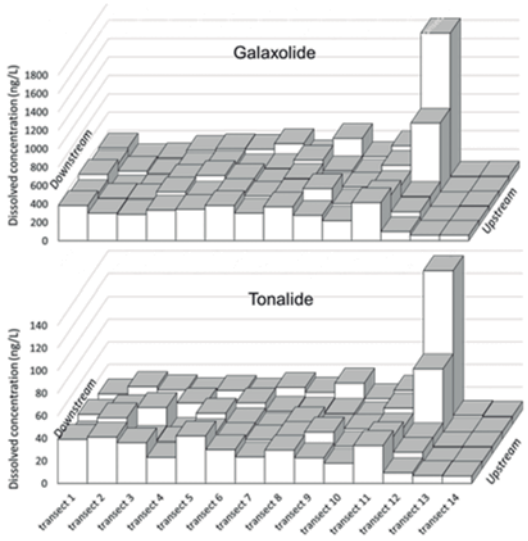

Fig. 1 Dissolved concentration of galaxolide and tonalide during the initial sampling campaign. Transect 12 is located near to the WWTP-outlet

Sediment activity

Below the WWTP-effluent, the average dissolved concentration of contaminants at steady state with the collected sediments ($C_{diss,eq}$), were respectively of 555 ± 111 ng/L and 54 ± 10 ng/L for galaxolide and tonalide. Upstream, the values for galaxolide and tonalide are approximately 2 fold lesser (Fig. 2).

The concentration difference with the dissolved contamination of the overlaying water (C_{diss}) indicates the direction of diffusive flux of contaminants between the bedded sediment and the water column. During the initial campaign, the dissolved concentrations of the WWTP-related contaminants were below the equilibrium concentration with sediment at all location of the study area. Therefore, at the moment of sampling, sediment bed was acted as source of pollutants.

During the 1-month monitoring, galaxolide and tonalide at St1 and St2 stations appear to alternate between contamination levels above and below the equilibrium concentration. This indicates that the direction of compounds flux was inverted several times during the study period following C_{diss} values.

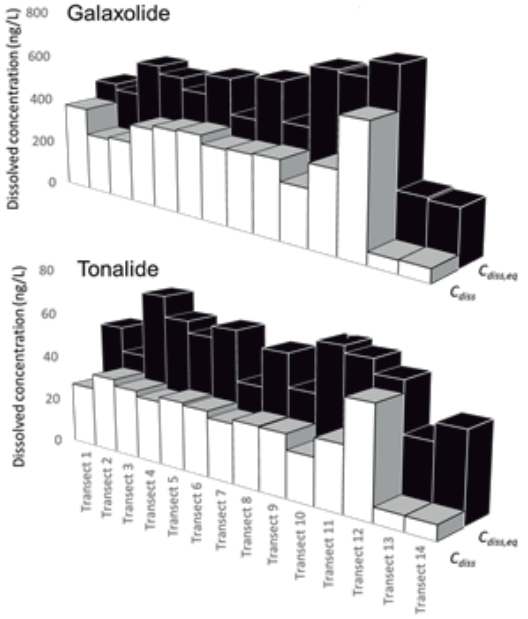

Fig. 2 Dissolved concentration of galaxolide and tonalide in equilibrium with sediment ($C_{diss,eq}$) and dissolved concentration measured in the water column (C_{diss})

Fluxes at St1 and St2 stations

During the monitoring period, F_{diss} and F_{SPM} were respectively 5 times and 3 times higher at St2 than at St1 station for galaxolide and 3 times and 2 times higher for tonalide (see Table 1 for galaxolide).

According to the compounds and the location, the SPM contribution into the overall in-stream transport of contaminants range between 0.7 and 4.9 %. For instance, SPM load required for F_{SPM} of tonalide (log K_{SPM}=4.1) dominate F_{diss} is about 80 mg/L. F_{SPM} should also dominate F_{diss} with similar SPM load condition (4.1 mg/L) for compounds with log $K_{SPM} \geq$ 5.4.

At St2 station, the resulting in-stream flux range between 16 and 68 g/d for galaxolide, and between 2 and 6 g/d for tonalide following the period while at St1 station contaminants fluxes were on average 4 times lower for WWTP-related contaminants.

Table 1 Average fluxes measured at St1 and St2 station during the 1-month monitoring for Galaxolide. Negative values depict fluxes from sediment to water column

	St1	St2
F_{diss} (g/d)	6.8 ± 2.8	35.8 ± 14.3
F_{SPM} (g/d)	0.2 ± 0.1	0.6 ± 0.3
F_{sett} (ng/cm²/d)	1.8 ± 0.4	22.4 ± 7.9
F_{ress} (ng/cm²/d)	-1.4 ± 0.3	-21.1 ± 7.5
F_{diff} (ng/cm²/d)	-5.2 ± 0.7	-1.9 ± 5.8

Exchanges of contaminants bounded to SPM with the bedded sediment (expressed by unit of sediment bed area), show that independently to the station, transport mediated by settling (F_{sett}) dominate on resuspension process. It exceeds the transport due to the resuspension (F_{ress}) that result in positive net fluxes (from the water column to the sediment bed). Over the monitored downstream area (≈800 m), this net flux of contaminants transported to the sediment mediated by sedimentation (i.e F_{set}-F_{res}) was of 0.24 g/d for galaxolide, and 0.04 g/d for tonalide that represent 0.6 and 1.3 % of the net in-stream flux.

Modelling of attenuation due to sedimentation of SPM has been performed. Results show that SPM deposit lead to reduce by half the contamination of the dissolved phase at 28 km downstream for tonalide (log K_{SPM}=4.1). For galaxolide the distance exceed >30 km due to lower K_{SPM} (log K_{SPM}=3.8).

During the 1-month monitoring period, upstream diffusive fluxes of galaxolide and tonalide were of -5.2 ± 0.7 ng/cm²/d and –1.2 ± 0.3 ng/cm²/d respectively. Downstream, fluxes are of same order of magnitude (-1.9 ± 5.8 ng/cm²/d and –0.6 ± 0.8 ng/cm²/d). The location heavily contaminated does not necessarily translate in higher diffusive flux of contaminants. Additionally, F_{diff} appear to alternate between negative and positive values, and is likely canceled out over an extended period. By comparison, the transport mediated by sedimentation is consistently positive and therefore dominate on F_{diff}.

CONCLUSIONS

The distribution and fate of WWTP-related contaminants was investigated by taking as example 2 persistent contaminants. For such substances, in-stream flux of dissolved substances appears to dominate flux mediated by SPM. However, transport mediated by SPM is expected dominate for highly turbid river (>80 mg/L) and much more hydrophobic compounds (log K_{SPM}>5.4).

Transport of contaminant bounded to SPM toward the sediment bed result in net flux in direction of sediment bed. This process is responsible of the contamination attenuation along the river course. Under the hydrologic condition of the studied site and on the basis of attenuation by sedimentation only, the contamination is reduced by half after 28 km for tonalide (which present the highest logK_{SPM}). However, the settled particles lead to an increasing pool of contaminants in sediment bed that could be transported again to the water column notably by passive diffusion processes. It was demonstrated that long term transport of contaminants by passive diffusion through the sediment to water interface is canceled because alternate between positive and negative fluxes.

However if the contamination of overlaying water tend to durably decrease, the contaminants stock will be slowly released into the overlaying water and sediment will became a significant source of pollutants.

ACKNOWLEDGEMENTS

This study was financially supported by the project “Traversière” of the French Institute Carnot M.I.N.E.S.

REFERENCES

[1] Tixier C., Singer H.P., Oellers S., Müller S.R. Environ. Sci. Technol., 2003, 37 (6), pp 1061–1068.
[2] Kimura K., Hara H., Watanabe Y. Environ. Sci. Technol., 2007, 41 (10), pp.3708–3714.
[3] Jonkers N., Kohler H-P.E., Dammshäuser A., Giger W. Environmental Pollution, 2009,157 (3), pp 714-723.
[4] Phillips P.J., Chalmers A.T., Gray J.L., Kolpin D.W., Foreman W.T., Wall G. R. Environ. Sci. Technol., 2012, 46 (10), pp 5336–5343
[5] Parolini M., Magni S., Traversi I., Villa S., Finizio A., Binelli A. Journal of Hazardous Materials, 2015, 285, pp 1-10.
[6] Belles A., Alary C., Mamindy-panjany Y., Abriak N-E. Environmental Pollution 2016, S0269-7491, 30465-1.
[7] Belles A., Alary C., Criquet J., Billon G. Chemosphere, 2016, 164, pp 347-354.
[8] Peck A.M., Hornbuckle K.C. Environ. Sci. Technol., 2004, 38 (2), pp 367–372.
[9] Godayol A., Gonzalez-Olmos R., Sanchez J.M., Anticó E. Chemosphere, 2015, 125, pp 25-32.
[10] Zebracki M., Alary C., Lefèvre I., Nan-Hammade V., Evrard O., Bonté P. J Soils Sediments, 2016, 16(1), pp 294-308.
[11] Liu H-H., Bao L-J., Zeng E.Y. TrAC Trends in Analytical Chemistry 2014, 54, pp 56-64.

5. Water-sediment interactions in rivers and hydraulic works

Session chairs: Joselina Espinoza[1] and Moisés Berezowsky[2]
[1]Coordinación de Hidráulica, Instituto Mexicano de Tecnología del Agua, México
[2]Subdirección de Hidráulica y Ambiental, Instituto de Ingeniería de la UNAM, México

Hydraulic structures include a broad spectrum of applications in engineering practices such as: dams, river flood controls, piers, protection works on rivers, like borders or dikes. The flow around hydraulic structures is complex, three dimensional and highly turbulent with sediment transport. Pier scour is influenced by flow structures, and sediment factors, as the vortices and turbulence structures around the piers, and sediments in water bodies. The dams in the rivers interact giving rise to upstream degradation and downstream erosion. Study of the interaction between hydraulic works, water and sediment is focused to understand of the effects of hydraulic structures on natural systems, through laboratory experiments, field campaigns, physical and numerical modeling, analysis of occurred events, and to obtain criteria, methods, to improvement in the design, construction, operation and maintenance of hydraulic structures. Works in this thematic are most welcome.

EXPERIMENTAL ESTIMATION OF STRUCTURES IMPACT PRESSURE OF A GRANULAR DEBRIS FLOW

Mendoza-López Francisco Alonso [1], García-Aragón Juan Antonio [2], Salinas-Tapia Humberto[3] and Díaz-Delgado Carlos [4]

[1,2,3,4] Interamerican Water Resources Center, Autonomous University of State of Mexico, Mexico

ABSTRACT

Debris flows are a particular phenomenon of sediment transport in mountain rivers, its occurrence represents a risk to people and infrastructure. Due to their effects, it is important to increase the knowledge about their occurrence and behavior in order to have basic data for protection works design. In this work an experimental study to estimate the rheology and impact pressure was developed employing the particle tracking velocimetry (PTV) [1] in order to obtain particle velocity fields.

A 6 m length rectangular flume was used with 150 mm x 300 mm of cross section. Granular materials taken from Xinantécatl volcano (Mexico) were employed (sediment densities from 1,420 kg/m^3 to 2,420 kg/m^3 and diameters from 2.36 mm to 6.32 mm). Channel slope, solid concentrations and solid - liquid flow rates were controlled to have frictional-collision debris flow conditions [2]. Debris flow image sequences were obtained with a system that is capable to turn on a LED array and synchronizing it with a high-speed digital camera. Particles displacements and velocities were obtained applying a modified PTV algorithm [3]. Then an image processing was made in order to determine velocity and impact pressure profiles.

Different pressure models were analyzed, from classical hydrostatic models, Hydrodynamic models [4] and a hydrodynamic modified model that was shown to produce the best results. These models can be used to obtain debris flow effects over structures [5].

Keywords: Granular debris flow, Rheology, Velocity profiles, Impact pressure.

INTRODUCTION

In mountain regions, at occurrence of low frequency rains, a kind of debris flow with a large concentration of granular material is triggered. This flow characterized by the absence of fine particles belongs to a particular flow regime, between a purely collisional flow and a quasi static rate-independent plastic regime. This latter flow is characterized by large frictional stresses developed between the grains that at high concentrations present multiple contacts between them. Also debris flow head, even with a tail with high fine contents, presents this hydrodynamic behavior.

To model the collisional flow regime Kinetic theories have been developed to treat rapid flows of granular materials for moderate and low concentrations [6], [7]. The frictional regime has been less intensively studied because the network of contact points changes randomly [8], [9].

The single-phase granular flow kinetic theories have been extended to include the effects of interstitial fluids by adding extra terms to account for particle drag forces and energy dissipation arising from the differences between the fluid and particle velocities [10], [11]. The main effect of the fluid is to dampen the energy of collisions which is reflected in a diminution of the granular temperature T.

The term granular temperature has been associated with the mean-square particle velocity fluctuations. We can define (for the three-dimensional case) a translational granular temperature $T = [c^2]/3$. Where the particle velocity fluctuation $c = (v - u)$, and v is the instantaneous particle velocity, $u = [v]$ is the mean transport velocity and the brackets designate an ensemble average. This parameter is very difficult to measure experimentally. Some authors [12] has attempted to do so by means of optical methods using polystyrene disks in chute flows.

In this research granular materials consisting of mixtures of lithic gravel and volcanic low density gravel (pumitic gravel) were used in chute flows. The interstitial fluid was clear water in order to represent geophysical flows. This is intended to represent debris flow head dynamics, because of grainsize segregation during debris-flow motion. This segregation led to development of a debris-flow head consisting of gravel, and the high permeability of this gravel promotes rapid dissipation of pore pressure therein. Thus, in the 100 m long flume experiments performed by Iverson [13] the flow head basal pore-fluid pressure was close to zero, much smaller than the pressure necessary for liquefaction.

The channel was able to tilt between 10° and 15° angles. Particle Tracking Velocimetry methods were

used in order to measure velocities, hence granular temperature and concentrations. A frictional-collisional flow regime, between purely collisional and quasistatic flow, was deliberately obtained. To do so a Bagnold number larger than 200 and a Savage number less than 0.1 [13] were obtained in each of the experiments. The aim of the work is to obtain experimentally the order of magnitude of the shear stress distribution in a granular-fluid chute flow.

METHODS

The experiments were performed in a rectangular channel with variable slope from 10 ° to 15 °. The channel is 6 m long, 150 mm x 300 mm cross section with transparent walls and Manning bed roughness of 0.015 (see Fig. 1). Granular materials from the Nevado de Toluca volcano were used, with densities between 1,420 kg/m^3 and 2,420 kg/m^3 and diameters between 2.36 mm and 6.32 mm. Solid concentrations, solid and liquid flow rates were controlled to generate the conditions of a frictional-collisional chute flow. The collisional and frictional stresses predominance were ensured with Savage numbers (N_{Sav}) less than 0.1 and Bagnold numbers (N_{Bag}) greater than 200.

Liquid flow rates were controlled by a valve previously calibrated. An estimation of solids concentrations was obtained in preliminary essays. During these essays the volume of solids were previously measured. When the sliding gate was open a mean concentration near 50% by volume was already guaranteed.

Fig. 1 Tilting flume (a) and lifting mechanism (b)

During the experiments the required conditions for a frictional-collisional flow, like tilting angle, solids volume, and liquid flow rate were adjusted in order to obtain the required Bagnold number (N_{Bag}) and savage number (N_{Sav}).

The ratio between collisional stresses τ_c and viscous stresses τ_v is given by the Bagnold number N_{Bag} (Bagnold 1966)

$$N_{Bag} = \frac{\lambda \rho_s d^2 (du/dz)}{\mu} \quad (1)$$

Where d is the average particle diameter, u is the average transport velocity, ρ_s is the density of particles , μ is the viscosity of the interstitial fluid and λ is the linear concentration defined as

$$\lambda = \frac{1}{\left(\frac{C_{max}}{C}\right)^{1/3} - 1} \quad (2)$$

where C is the volumetric concentration of solids and C_{max} is the closest pack concentration.

In inertial flows with large collisional stresses N_{Bag} is larger than 200.
The ratio between collisional stresses and frictional stresses τ_f is given by the Savage number N_{Sav} [2].

$$N_{Sav} = \frac{\rho_s d (du/dz)^2}{N(\rho_s - \rho) g \tan \emptyset} \quad (3)$$

where *N* is the number of particles above an height *z*, ρ is the density of the interstitial fluid, $\emptyset$ is the particles friction angle and g is the acceleration of gravity.

Reference [13] states that friction stresses are dominant over collisional ones if Savage number is lower than 0.1. This is possible if volumetric concentration is high, larger than 51% after Bagnold [14]. Also Takahashi [15] states that friction stresses are dominant for volumetric concentrations larger than 50%.

Materials used

Two kind of materials were used in the experiments coming from nearby Toluca volcano (see Table 1 and Fig. 2). Lithic gravel with high density and pumitic gravel from volcano origin with low density.

Table 1 Properties of materials used in the experiments

Parameter	Unit	Material	
		Lithic gravel	Pumitic gravel
Solids density, ρ_s	kg/m^3	2,420.0	1,424.9
Solids specific weihgt, γ_s	N/m^3	23,740.2	13,978.3
Submerged specific weight	N/m^3	13,930.2	4,168.3
Porosity	%	42.0	58.5
Sizes range	mm	2.36 - 6.35	2.36 - 6.35
Representative diameter, *d*	mm	4.35	4.35
Settling velocity, D_{50}	m/s	0.24	0.07
Internal friction angle	°	36.0	31.9

After some initial experiments it was decided to use experiments with only lithic gravel and experiments with a mixture 50%-50% by volume lithic gravel and pumitic gravel.

Optical technique

Images were taken laterally through the transparent wall of the channel and analyzed using PTV. Fluctuating velocities of the particles were obtained in order to estimate granular temperatures. Also concentration values were obtained. A LED arrangement was used and controlled by a software in order to obtain light pulses.

The software *SofCamDan* was developed for image capture. Camera triggering and illumination are controlled with the software. Input parameters are; exposure time of camera sensor, type of capture (one pulse or multipulse), lag time, time between pulses and number of images required.

The images were treated with the software Matlab (2017) in order to define the free flow surface, the perimeter of near wall particles and their centroids. This was done for each two images sequence obtained. The technique used follows the next steps:

I. Some filters are applied to the original image in order to avoid noises, adjust intensities and identify edges (Median Filter and Sobel module).
II. Some low intensities (representing the far away particles from the wall) are eliminated.
III. Apply a threshold intensity value in MATLAB (2017) (the greyscale image is converted to a binary image) in order to obtain only the closest particles from the channel wall.
IV. Image segmentation of the binary image in order to individual particle show up.
V. Particle geometric characteristics determination (area, centroid and equivalent diameter) with RegionProps module of MATLAB (2017),
VI. Process is repeated for other images,

Once the particles are identified in each pair of images. They were analyzed with the software PTVpairs developed at CIRA. Vectors of movement were obtained with the particles centroids and particles velocity vectors were obtained taking into account time between light pulses. Because of the large particle concentrations classical PTV algorithms fail during pair identification. To avoid errors three different criteria were adopted; a criteria of minimum and maximum displacement, a criteria of minimum and maximum angle and a criteria of similar equivalent diameter.

The length criteria considered a minimum distance of 50% of the mean diameter and a maximum distance of 200% of the mean diameter. The angle criteria considered a 10° arch for valid particles. The equivalent diameter of a particle should not exceed ± 5% of the diameter of a particle that fits the angle and velocity criteria. All these criteria are shown in Fig. 2.

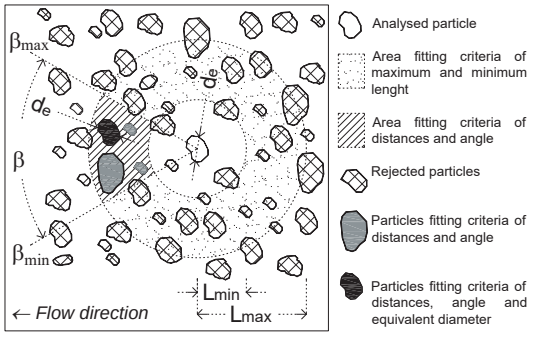

Fig. 2 Criteria for pair detection in PTV algorithm

Impact pressure calculations.

Three kind of models are presented in the scientific literature for impact pressure (P) calculations; the hydrostatic [16], hydrodynamic [17] and a modified hydrodynamic [18], see Table 2.

Table 2 Impact pressure models

Hydrostatic model	$P= C_s*\rho*g*h$
Hydrodynamic model	$P= C_d*\rho*U^2$
Modified Hydrodynamic	$P= 5*\rho*(g*h)^{0.6}*U^{0.8}$

In Table 2, P is the impact pressure of debris flow in N/m^2, Cs y Cd are adjusting coefficients, U is the average velocity in m/s and *h* is flow depth in m.

RESULTS

The experiments were performed changing the tilting angle of the channel from 10° to 15° and the solids volume supplied to the channel from 7.5 L to 15 L. An initial set of experiments were done in order to define flows into the frictional-collisional regime according to Bagnold and Savage numbers. Liquid flow rate and solid flow rate were changed and the experiments shown in Table 1 were selected for image acquisition. The experiments consisted of lifting suddenly a gate with incoming constant liquid flow rate and with a solid volume behind the gate previously defined. The images of the flow were taken laterally at 3.5 m from the entrance (1 m from the gate) with CCD JAI camera model CV-

M2CL(1024x1040 pixels spatial resolution and 250 fps temporal resolution) in a region illuminated with an array of 40 LEDS of 3 W (wavelength 490-590 nm). The LEDS were organized in two groups in order to emit different pulses.

Two types of material were used lithic gravel (called G) and a mixture 50% lithic gravel and 50% pumitic gravel (called M). Table 3 summarizes some of the parameters used in the experiments selected to show in this paper. For identification a key was designed in the form; tilting angle (°)-G or M-solids volume (L)-letter.

Based on already defined centroids, images overlap shows the displacement of the particles. The displacements were transformed into velocity vectors and velocity fields for all pair of images. Figure 3 shows velocity vectors and the velocity field for the chute flow 10-G-10-g.

Table 3 Parameters of experiments selected for image acquisition

Tilting angle	Material	Liquid flow rate (l/s)	Solid Volume (liters)	Estimated Savage number	Estimated Bagnold number	Key for Identification
10°	G	1.37	10	0.05	792	10-G-10-g
		1.37	15	0.06	1,012	10-G-15-h
	M	1.84	15	0.11	1,421	10-M-15-e
		2.28	15	0.08	1,230	10-M-15-f
12°	G	1.37	10	0.05	1,056	12-G-10-a
		2.28	15	0.03	834	12-G-15-b
	M	1.84	10	0.06	1,063	12-M-10-e
		2.28	10	0.11	1,758	12-M-10-f
15°	G	1.71	7.5	0.09	616	15-G-7.5-l
		2.28	10	0.10	1,217	15-G-10-o
	M	1.96	7.5	0.10	1,302	15-M-7.5-b
		2.62	10	0.10	1,248	15-M-10-f

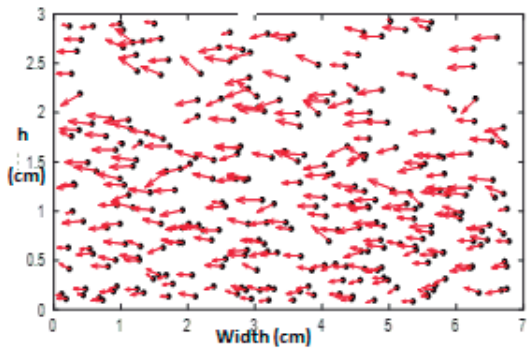

Fig. 3 Velocity vectors of particle velocities for the chute flow 15-G-10-o (flow direction is from right to left)

The velocity vectors were used to calculate the mean total velocity, the mean normal velocity and the mean longitudinal velocity over a 1.125 mm horizontal layer. This allowed us to obtain velocity profiles for each of the experiments. Figure 4 shows the experimental data for the tilting angle of 10°, also is shown the best fit curve, that will be used in order to calculate the shear rate (du/dy). Additionally, the model proposed by Takahashi [15] is shown, to estimate the mean fluid velocity for granular-fluid chute flows. It is observed that for large tilting angles the Takahashi model largely underestimates flow velocities.

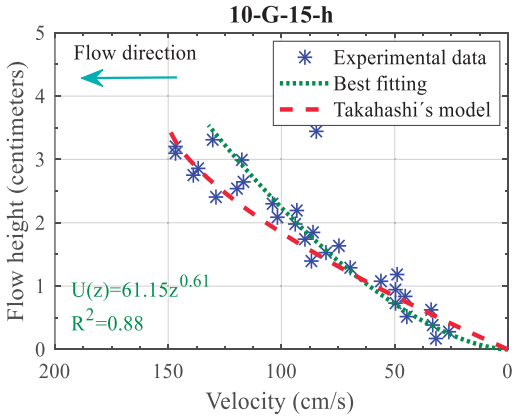

Fig. 4 Experimental data of particle velocities and best curve fit for 10°

With particle velocities already obtained a mean velocity of the debris flow can be calculated. This allowed us to obtain the impact pressure of a debris flow (see Table 2) over structures, using Cs=5 and Cd=1.5 recommended values [16]. An example is presented in Fig. 5 for gravel in a 10° tilting angle with 15 liters of gravel a 1.37 L/s of liquid flow rate.

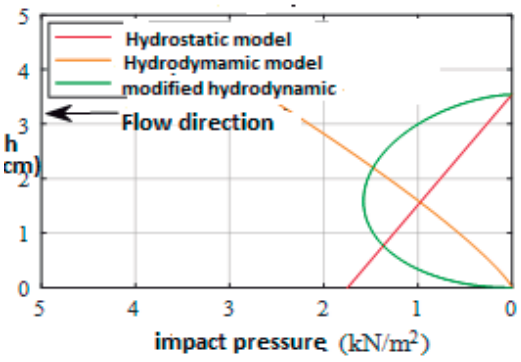

Fig. 5 Example of flow pressure calculation, 10-G-15-h

It is observed that the hydrostatic model overestimate flow pressure for high flow depths and

underestimate it for low depths. The opposite is observed for the hydrodynamic model. The best estimation is obtained with the modified hydrodynamic model and it is recommended for protection structures design purposes.

CONCLUSIONS

An experimental research of geophysical debris flows was developed in a rectangular channel provided with optical access. Particle Tracking Velocimetry (PTV) was used in order to obtain main flow characteristics. Deliberately debris flows in the collisional-frictional regime were analyzed. This kind of debris flows causes the greatest impact over protection structures. It was found that a modified hydrodynamic model gives the most realistic results.

REFERENCES

[1] Ido, T., Murai, Y., y Yamamoto, F. (2002). Post-Processing Algorithm for Particle-Tracking Velocimetry Based on Ellipsoidal Equations. Exp. Fluids. Vol. 32. Pp. 326-336.

[2] Iverson, R. M. (1997). The physics of debris flows. Reviews of geophysics, Vol. 35, No. 3. Pp 245-296.

[3] Salinas-Tapia, H., Robles-Rovelo, C. O., Chávez-Carlos, D. y Bautista-Capetillo, C.F. (2014a). Caracterización geométrica y dinámica de un chorro pulverizado empleando la técnica óptica PTV. Tecnología y Ciencias del Agua. Vol. 5, No. 3. Pp. 125-140.

[4] Hu, K., Wei, F., y Li, Y. (2011). Real- time measurement and preliminary analysis of debris- flow impact force at Jiangjia Ravine, China. Earth Surface Processes and Landforms. Vol. 36 No. 9. Pp 1268-1278.

[5] Teufelsbauer H., Yongqi Wang, Shiva P. Pudasaini and Wei Wu DEM simulation of impact force exerted by granular flow on rigid structures. Acta Geotechnica · September 2011. DOI: 10.1007/s11440-011-0140-9 on GEOMAT, 2011, pp. 8-13.

[6] Lun, C. K. K., Savage, S. B., Jeffrey, D. J. & Chepurniy, N. 1984 Kinetic theories for granular flow: inelastic particles in Couette flow and slightly inelastic particles in a general flow field. *J. Fluid Mech*. 140, 223-256.

[7] Sela, N. & Goldhirsch, I. 1998 Hydrodynamical equations for rapid flows of smooth inelastic spheres Burnett order. *J. Fluid Mech*. 361, 41-74

[8] Behringer, R. P. & Baxter, G. W. 1994 Pattern formation and complexity in granular flows. In Granular Matter (ed. A. Mehta), pp. 85-119. Springer.

[9] Gutfraind, R. & Pouliquen, O. 1996 Study of the origin of shear zones in quasi-static vertical chute flows using discrete element simulations. *Mech. Mater*. 24, 273-285

[10] Zhang Y. and Reese J.M. 2000 The influence of the drag force due to the interstitial gas on granular flows down a chute. *International Journal of Multiphase Flow* 26, 2049-2072.

[11] García Aragón, J.A. 1995 Granular-fluid chute flow: Experimental and numerical observations. *Journal of Hydraulic Engineering. ASCE*. 121(4), 355-364.

[12] Larcher, L., Fraccarollo, L., Armanini, A. y Capart, H. 2007 Set of measurement data from flume experiments on steady uniform debris flows. *Journal of hydraulic research.* 45, 59-71.

[13] Iverson, R. M. 2003 The debris-flow rheology myth. In Debris-Flow Hazards Mitigation: Mechanics, Prediction, and Assessment, Rickenmann & Chen (eds). Millpress, Rotterdam, ISBN 90 77017 78 X

[14] Bagnold RA.1966 An approach to the sediment transport problem from general physics.US Gov. printing office. PP: 137.

[15] Takahashi, T. 2014 Debris Flow, Mechanics, Prediction and Countermeasures. 2nd Edition. CRC Press. U. S.A. Pp: 118.

[16] *Scotton P y Deganutti AM. (1997).* Phreatic line and dynamic impact in laboratory debris flow experiments. In Debris Flow Hazards Mitigation: Mechanics, Prediction, and Assessment. ASCE: New York. Pp 777–786.

[17] *Hungr O, Morgan GC, Kellerhals R. (1984).* Quantitative analysis of debris torrent hazard for design of remedial measures. Canadian Geotechnical Journal 21. Pp. 663–677.

[18] *Hübl, J., Suda, J., Proske, D., Kaitna, R., & Scheidl, C. (2009*). Debris flow impact estimation. In Proceedings of the 11th international symposium on water management and hydraulic engineering, Ohrid, Macedonia. Pp 1-5.

EROSION DISTRIBUTION IN THE DJORF-TORBA DAM AREA (SOUTHWEST OF ALGERIA: BECHAR)

Belaout Fateh[1], Mekerta Belkacem[1], Kalloum Slimane[1] and Semcha Abdelaziz[1]
[1] Laboratory of energy, environment and information system Faculty of technology, Ahmed Draia University, Algeria [2] IMT Lille Douai, France

ABSTRACT

The soil erosion is caused by several factors, such as the climate conditions and the land morphology**.** In arid or semi-arid lands, this phenomenon is widely spread, because of the appreciate conditions that reinforce the erosion development such as (the lack of vegetation, sand, wind and seasonal floods...). Dam Djorf-Torba is located in an arid area; it spreads over a large area of sub-Saharan basin a surface of 22000 km^2 with an initial storage capacity of 350 million m^3. Soil erosion in the dam area causes siltation, which affects negatively on performance (reduction of the storage capacity, blocking the bottom drain and risk of instability of the dam) According to statistics of the National Dam and Transfer Agency (N.D.T.A, 2004), the rate agency silting up of the dam is about 25%, corresponding to an annual loss of 0.75 to 1% capacity clearance from the impoundment in 1969.

Our research works are intended to draw up an erosion distribution map which generates considerable volumes of different nature sediments.

Key words: Dam Djorf-Torba, Weather Conditions, Erosion, Siltation, Sediment mapping

INTRODUCTION

The sedimentation of dam reservoirs in Algeria is mainly influenced by accelerated and very marked annual erosion.

The phenomenon of erosion is more critical in watersheds located in an arid or semi-arid region.

The majority of dam reservoirs in Algeria are faced with the loss of silt storage volumes [1], [2].

According to ANBT statistics in 2016, there is approximately a large volume of sediment, estimated at 403 million m^3 in the west, 230 million m^3 in the east, 428 million m^3 in the center and 87 million m^3 south of Algeria.

The Djorf-Torba dam is a real example of the silting problem rapidly from year to year.

Our study area is characterized by an aggressive climate with alternating periods of floods and rains, with a windy and dry period, knowing that the vegetation cover in the watershed is reduced and sometimes don't exist.

The sediments that fill the reservoir can be perceived as a producer of raw materials and their valuations in the event of dredging the reservoir dam will be one of the prospects to be developed.

The objective of our research is to study the erosion behavior at the dam zone and its influence on sedimentation of the dam. We will consider the variation of different parameters, the soil size or the geological nature of the site and also the climatic conditions of the region.

PRESENTATION OF THE STUDY AREA

The Djorf-Torba dam is located about fifty kilometers (50 km) west of the Bechar's town. It is a gravity dam which is located on Oued Guir, it encloses a very large bowl in a particularly flat environment.

The dam is the fourth important in Algeria, with an estimated capacity of 350 hm³, intended for the water supply of the agricultural perimeters of Abadla, and a drinking water supply in the region of Bechar and Kenadsa (15 hm^3 /year). Figure 1 shows an overview of the dam [3].

Fig. 1 Dam of Djorf-Torba

BASIN OF THE OUED GUIR

Oued Guir controls a vast sub-Saharan watershed with an area of about 22,000 km^2 at the head of the Saoura Valley (Fig. 2), [4]. Geographically, the Oued Guir basin is limited to the North by the plain of Tamlal and the High Atlas, to the East by the Oued Bechar watershed, to the West by Hamada de Guir, to the South by Chebket Mennouna [5].

The Guir-Saoura hydrological system is the biggest river in the Algerian Sahara, with a length of more than 900 km. This river descends from the Moroccan Atlas and flows substantially from north to south. Saoura is considered as an allogeneic river according to the crossed areas.

Oued Guir has its source on the southern slope of the Moroccan Atlas, under peaks around 2700 m altitude [5].

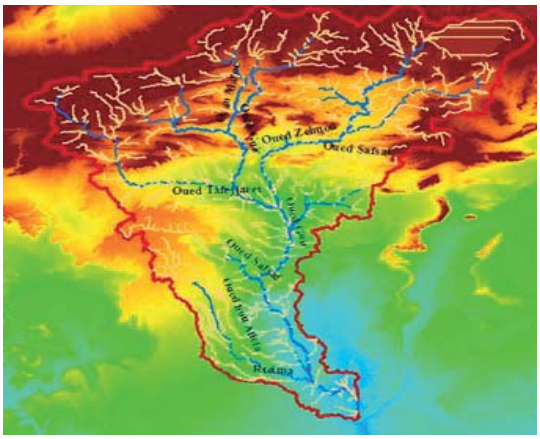

Fig. 2 Watershed of Oued Guir [5]

RAINFALL TRENDS ANALYSIS

Rainfall is characterized by a regime with two rainy periods, one in winter (from September to December), the other in spring (March, April and early May) separated by two dry periods in summer (June and August) with the month of July without precipitation and in January and February. Rainfall increases with altitude and heads west [4].

According to the engineering consulting firm (Coynie and Bellier) [6], that provided the technical study of the dam, the exceptional flood is characterized by a liquid supply estimated as one billion m^3. Since 1952 and over 22 years, there have been recorded 1 or 2 floods over 300 hm^3, almost 4 times more than 200 hm^3, 11 times more than 110 hm^3. The recurring problem of very high floods reaching the milliard de m^3 of sediments, with points at 15.000 to 20.000 m^3/s.

ESTIMATION OF EROSION IN THE BASIN OF OUED GUIR

The physical features of a basin that affect erosion and solid transport are primarily concerned with relief, geological features, soil, vegetation, land use, and drain system morphology.

Estimate of the solid matters of wadi Guir

Hydrological features include climatic factors, such as precipitation and temperature. The volume and intensity of precipitation play an important role in the erosion process, as a result of their effects in the dynamics of particle detachment by flow.

The estimate of the solid input makes it possible to evaluate the silted volume of the dam. In our study, the Djorf-Torba dam has a height of 37 meters and creates one of the biggest reservoirs in Algeria. He receives the violent and few floods of Wadi Guir.

The Oued Guir watershed takes an area of 23887.2 km^2 (surface treated by Arc-Gis software), it is located upstream of the dam and has an elongated shape.

The floods of the region by its extreme violence are characterized by a large volume of inputs also resulting in solid particles. The intake is very variable depending on the year, it is around 180 million m^3 of water per year on average [5].

The estimation of solid transport is based on the formula of TIXERONT according to Eq. (1), [4].

$$As = 200\ (Lr)\ 0.15 \quad (1)$$

Knowing that: As: Average specific solid input (Tons / Km^2 / year). Lr: The water slide in (mm).

In order to estimate erosion in the watershed of Guir wadi, we proceed first by calculating the water slide, with the empirical formulas, we calculate the specific solid input average of the watershed.

The water slide is evaluated by the following Eq. (2).

$$Lr = A_L / SB \quad (2)$$

With: A_L: Average annual water supply in m^3;
SB: Area of the catchment area in m^2

The Water Blade (Le) or the water slide (Lr) is the volume flowing at the outlet of a dam area (A_L) divided by basin area (SB). If we count the area in km^2 and the height in mm, we have the following Eq. (3).

$$Lr\ (mm) = (Q\ (m^3 / s)\ 365.\ 86400) / SB\ (km^2) \quad (3)$$

For the Djorf-Torba'dam, the last bathymetric survey was carried out in 2004 by the ANBT [5]. This has made it possible to update dam's storage capacities, the rate of siltation is estimated at 25%. The amount of sediment up to the year 2004 was determined by the bathymetric survey.

In order to estimate the solid inputs that will arrive at the level of the reservoir, the statistics of the A.N.B.T are considered for the period from 2005 to 2016) [6].

Other methods are used for estimate the solid input, one can quote the method of FRIGUI or the model of FRIGUI which is defined by the Eq. (4). Table 1 summarizes the variation of solid inputs according to TIXERONT and FRIGUI.

$$As = 498 * (Lr)^{0.89}. (SB)^{-0,26} \quad (4)$$

Table 1 Variation of solid particuls

Période	TIXERONT	FRIGUI
(AL) ; m³/an	3461	3461
(SB) ; km²	22000	22000
(Lr) ; mm	4961.18	4961.18
(As) ; T/km²/an	71675	71989.41

The soils of our study area are fragile, with very low vegetal cover, this state of affairs is accentuated by soil degradation following the plowing of land located in or near the banks of the beds of the wadi, thus accentuating the process erosion of these soils.

In order to be able to estimate the rate of abrasion or specific degradation of the Guir wadi basin, experimental formulas applied to Algerian conditions are used.

The TIXERONT formula is based on the correlations established from the measurements made in the major wadis. The estimate of the specific solid inputs of the Djorf-torba dam is 71675 Tonnes / km² / year: with the TIXERONT method, and according to the FRIGUI method the specific solid contribution is 71989.41 Tonnes / km² / year.

Estimation of the specific erosion of the watershed

To estimate the annual specific erosion, FOURNIER (in OLIVRY, 1991) [2] proposed a formula using rainfall and morphology of the watershed. The nature of the precipitation and the morphological characteristics of the watershed studied allow the application of this formula according to Eq. 5 [2].

$$Es = (1/36). (Ps^2 / Pa)^{2.65}. (H^2 / SB)^{0.46} \quad (5)$$

With :
Es = specific annual solid input (T / km² / year),
Ps = average monthly rain of the wettest month (mm),
Pa = annual rainfall (mm),
H = average slope,
SB = area of the BV of wadi Guir (S = 22000 km²).

The Oued Guir watershed area occupies an area of 22000 km², with a highly variable terrain [5]. Annual precipitation data were provided by the National Water Resources Agency (ANRH-Bechar) for a period of 21 years (1985 to 2006). These data show that the average monthly rain of the wettest month appears in November, it is Ps = 12 mm, the minimum is in July with 0.39 mm.

The annual rainfall is given by the climatic stations involved in these studies, which are (Fig. 3): Djorf Torba (A, 55 mm / year), Boukais (B, 76 mm / year), Bouanane (C, 103 mm / year), Boudnib (D: 101 mm / year), Ain flesh (E: 105 mm / year), Ait Aissa (F: 102 mm / year), Bouarfa (G: 112 mm / year), Blessed Tajjet (H 100 mm / year), Figuig (I, 136 mm / year). The sum of the annual rainfall of the different stations is 890 mm / year [4].

Fig. 3 Different climatic stations (A.N.R.H-Béchar) [4]

Tables 2 and 3 show the different values of the specific erosion of each watershed in two different zones 1 and 2.

Table 2 Specific erosion in zone 1

Station	A	B	C	D	E
Pa (mm)	55	76	103	101	105
H (%)	4.84	10.11	9.98	12.28	14.22
SB (km²)	4032	1537	1352	3582	1737
Es (T/km² /an)	4.83	6.32	2.41	2.42	3.42

Table 3 Specific erosion in zone 2

Station	F	G	H	I
Pa (mm)	102	112	100	136
H (%)	10.10	14.05	9.35	4.30
SB (km^2)	2153	2875	1843	2889
Es (T/km^2 /an)	2.45	2.30	2.60	0.66

The annual average specific solid input in T / km^2 / year, is the sum of the specific erosion for the two (2) zones: Es = 27,865 T / km^2 / year.

METHODS OF SAMPLING

In order to focus on the nature of the samples at different points accessible to the dam, a sampling campaign was conducted in November 2017. Five samples were taken at different points upstream and downstream of the dam. Figure 4 shows sample collection points (P1, P2, P3, P4 and P5) at different locations in the dam containment and attached the different photos.

The samples studied were taken from three different sites using a hand shovel. The first samples from site 01 were taken at two points (P1 and P2) distributed upstream of the dam at varying distances.

The second sample of site 02 was taken at a point (P3) at the dam gallery, located at a depth of 30 m (inside the gallery).

The third sample of site 03 was taken at two points (P4 and P5) distributed downstream of the dam. The different sediment samples were packaged in closed and preserved plastic bags.

Due to the characteristics of the difficult region, whether in terms of terrain morphology or geographical location of the dam, access to the reservoir is very difficult. All these disadvantages did not allow us to take enough samples to reach the greatest number of points.

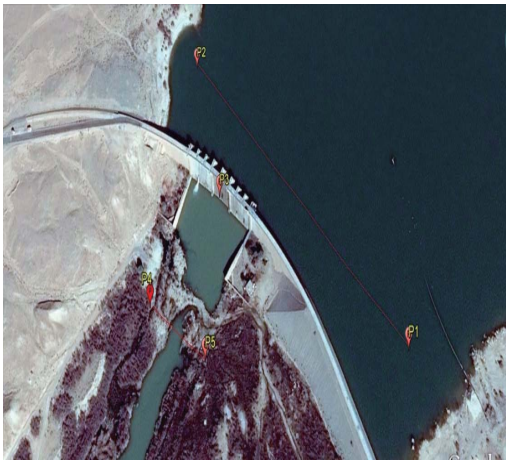

Fig. 4 Location of the different samples at the reservoir dam Djorf-Torba

Synthesis on the nature of the samples

The five samples taken at different points from upstream to downstream of the dam and even at the level of the gallery, show without any doubt that the nature of soils is very variable from one point to another. Samples (1) and (2) are almost sands. The third sample is a low sandy loam, the sample (4) is a red clay, and finally the sample (5) consists of alluvium.

GENERAL CONCLUSIONS

We have estimated that over than 20 million hectares of watersheds in Algeria have 50% risks of erosion. The life of a dam is calculated basing on its rate of siltation.

Most dams in Algeria have a lifespan of about thirty years because of the phenomenon of siltation, they are in a critical situation and their farms remain below their real capacities. Dredging of the dams is becoming an indispensable solution to extend the life of the structure.

The importance of the annual solid contribution of the different watersheds, as well as the distribution of erosion at the Djorf-Torba dam and the knowledge of the nature of the sediments collected, will surely make it possible to target the areas to be dredged in particular the zone at the foot of the dam (sample P3).

The analysis of the various factors involved in the erosion phenomenon makes it possible to know the behavior, the direction and the points which represent the zone producing the sediments at the level of the different wadis (Fig. 3). Our study contribute to the knowledge of the erosion phenomenon's efforts on storage capacity dams and also establish a protection system to protect our structure [7], [8], [9], [10], [11] and [12].

REFERENCES

[1] Mekerta B, Semcha A, Sadok A, Guessas H et Rahmani M.C. Moyens de lutte pour la prédiction de l'envasement des retenues de bartages d'Ouizert, Bouhanifia et Fergoug. Conf. I2SM Montréal, 2016.

[2] Mekerta B, Semcha A, Rahmani F et Troalen JP. Erosion spécifique et caractérisation de la résistance au cisaillement des sédiments du barrage de Fergoug. Xèmes Journées Nationales Génie Civil – Génie Côtier, Tome 1, Sophia Antipolis France, 14-15 et 16 octobre 2008, pp. 135-144.

[3] Agence Nationale des Barrages et Transfert. Levées bathymétriques des barrages en exploitation, Avril 2004, 40 pages.

[4] Brahimi Tidjani. Etude de la problématique de l'envasement du barrage Djorf-Torba. Mémoire

de Master, Université Ahmed Draïa, Adrar (Algérie), Juin 2016, 55 pages.

[5] Kabour A, Mekkaoui A et Chebbah L. Le barrage de Djorf Torba (Béchar, sud-ouest Algérien), sous contraintes du climat, de l'environnement et de gestion. Conf. ISSN 2310-6743 Mila-Algérie, 2016.

[6] Barrage Djorf Torba sur l'Oued Guir, Monographie, A.N.B.T, 1985, 156 pages.

[7] Baali Hafsa.. Exploitation, maintenance et stabilité du barrage Djorf-Torba pour une meilleure préservation des ressources en eau de la wilaya de Bechar. Mémoire de Master, Université Ahmed Draïa, Adrar (Algérie), Juin 2016, 80 pages.

[8] Diab Djeffal Imane. L'envasement dans les barrages de l'Algérie. Séminaire International sur l'Hydrogéologie et l'Environnement SIHE, Ouargla (Algérie), 2013, pp. 415-418.

[9] MEKERTA Belkacem. Étude des propriétés géomécaniques des sédiments d'envasement de la retenue du barrage de Génissiat. Thèse de Doctorat, Institut National Polytechnique de la Lorraine (France), Juillet 1995, 195 pages.

[10] SOUADI Youssef. L'érosion hydrique au Maghreb étude d'un cas : le bassin versant de l'oued Barbara (Tunisie Septentrionale). Mémoire de magister, Université du Québec (Canada), mars 2011, 143 pages.

[11] AMMARI Abdelhadi. Vulnérabilité à l'envasement des barrages (Cas du bassin Hydrographique des Côtiers Algérois). Thèse de Doctorat, Faculté des Sciences et de la technologie, Université Mohamed Khider– Biskra (Algérie), septembre 2012, 195 pages.

[12] Ouallali A, Moukhchane H, Aassoumi H, Berrad F et Dakir I. Evaluation et cartographie des taux d'érosion hydrique dans le bassin versant de l'oued Arbaa ayacha (rif occidental, nord Maroc). Conf. ISSN : 2458-7184 Rabat-Maroc, 2016.

Photo 2 : Sample P1 upstream of the dam

Photo 3 : Sample P2 Upstream of the dam

Photo 4 : Sample P3 in the galery

Photo 5 : Sample P4 downtream of the dam

Photo 6 : Sample P5 downstream of the dam

Appendix: Sampling photos of the different samples (P1, P2, P3, P4 and P5).

SCOUR ESTIMATION OF A BRIDGE PIER, A CASE OF STUDY

González V. José Alfredo [1], Espinoza A. Joselina [1] and Bonola A. Isaac [2]
[1]Mexican Institute of Water Technology, Mexico, [2]DIV Ingeniería S.A, de C.V., Mexico

ABSTRACT

The results of a case of study of scour damage in a river in the southwestern of Mexico are presented. The scour was determined using empirical methods and data available from literature to evaluate it. This was done considering the design discharge and the bottom material of the channel at the study site.The scour in rivers is a complex phenomenon, where the effects of water flow, the bottom material, channel geometry and modifications involved in time combine to act together at bridge foundations. The use of the methods presented provide good estimate of scour, combined with field measurements and observations. It is recommended analyze the results using an interdisciplinary team to determinate their reliability and adequacy for the bridge.

Keywords: Bridge, Scour, Piers, Sediment characterization

INTRODUCTION

The total scour in the channels is composed of long-term degradation, general scour and local scour. The components add up. Additionally, lateral displacement of a current can cause or increase scour at the base of the bridge.

Local scour is caused by the interference of the piers and abutments with the flow and is characterized by the formation of scour holes immediately at the bridge pier or abutment.

Factors that may affect the depth of scour at bridge foundation are: Geomorphic, hydrologic, flood-flow transport, bed sediment and bridge geometric.

Geomorphic factors influencing bridge scour can be divided into catchment characteristics and river characteristics. These influences are more important for general scour than for localized scour.

River characteristics of importance are valley setting, the channel cross-sectional shape, its planform shape, its planform shape and the channel boundary.

Planform shape is also important. Meandering rivers are characterized by continual development of the meander bends, so that there is a high potential for problems associated with bank erosion and channel migration. In wide braided rivers, the deep water channels can shift significantly and unpredictably during floods.

The geometry of the bridge piers can be described by the type, shape length, width and alignment with the flow.

The total scour depth at a foundation is calculated on the basis of superposition of general and localized scour at the foundation.

The calculation of scour with different methodologies shows great variability in the results. That indicates that the phenomenon has not been fully explained and is still lacking to be able to interpret more closely the variables that intervene in the scour and the interrelation between them.

The methodologies use dimensionless relations between the main parameters that intervene in the phenomenon, and the Froude number, generally using laboratory results and few real data.

There exist many equations for the estimation of local scour depth at bridge foundation and fewer methods for estimation of other types of scour. However, there is a need for documentation of cases of application of the available methods.

In this paper the study site is a reach of the Carrizal River. It is an alluvial sand bed typical river in terms of sediment characteristics and hydrological regime.

RESULTS

For the quantitative scour analyses at the site of the bridge, the design discharge to a return period of 20 years at this site is 902 m^3/s

The sediment was sampling in six sections of the channel. The characterization of the sediment in laboratory was carried out, the granulometric curves and the characteristic diameters were obtained. The sediment is composed of cohesion less alluvial sands with silt.

Data for the quantitative scour analyses at the bridge are summarized in Table 1.

The scour at the site is caused the effects of numerous floods magnitudes, and river migration. In this case total scour is obtained quantitatively as composed by: general scour, bend scour together with local scour.

Table 1 Basic Data for the Present Quantitative Scour Analyses

Parameter	
Channel Width W (m)	149.2
Radius of curvature for bend r_c (m)	400.11
Average upstream unscoured flow depth y_u(m)	5.685
Bed material	
Median size d_{50} (mm)	0.31
Discharge Q(m^3/s)	902.
Discharge intensity q (m^2/s)	6.045

General Scour

General scour occurs irrespective of the existence of bridge and as either long-term or short-term scour. Short term general scour develops during a single or several closely spaced floods. This type of scour includes scour at channel confluences, scour arising from a shift in the channel thalweg or a scour at bends, and bed form migration. Long term general scour has a considerably longer time scale, normally of the order of several years.

Field and subsurface observations, together with engineering judgement, provides the best approach to initial evaluation of mean scoured flow depth y_{ms}.

Regime formula of Lacey, applicable to alluvial rivers and tidal channels of sand beds [2].

$$y_{ms} = 0.47 \left(\frac{Q}{f}\right)^{1/3} \quad (1)$$

$$f = 1.76\, d_m^{0.5}$$

f is the Lacey silt factor a function of grain size.

This approach is indicated to be too conservative for large sediment. The relation for *f* applies for d_m<1.3 mm.

d_m= 0.31 mm

f= 1.76 $(0.31)^{0.5}$

f= 0.9799

y_{ms}= 0.47 $(902/0.9799)^{1/3}$ = 4.56 m

y_{ms}= 4.56 m

The mean scoured flow depth, y_{ms} (m) below the free surface can be determined based on the mean discharge per unit channel width as in reference [1]:

$$y_{ms} = 1.20 \left[\frac{q^{2/3}}{d^{1/6}}\right]^{1.20} \quad (2)$$

q= Q/W= 902/149.2= 6.045 m^3/m/s

$$y_{ms} = 1.20 \left[\frac{q^{\frac{2}{3}}}{d^{\frac{1}{6}}}\right]^{1.20} = 1.20 \text{ x } 4.03 = 4.8379 \text{ m}$$

y_{ms}= 4.84m

The general scour is presented in Table 2

Table 2 Evaluation of the Degraded Channel

Scour analyses	
Lacey (1930)	4.56
Blench (1969)	4.8379
y_{ms} (m)	4.6989

Bend Scour

The scour in curves leads to deep sections at the foot of the outer margin of the curve. Secondary currents and larger strains in the outer margin cause high velocities in this range. The secondary currents transport the bottom sediment towards the inner margin of the curve.

Empirical methods use observed data to develop rules, constants, or regression equations for the estimation of the scour.

Maynord. The maximum scoured flow depth in a bend y_{bs} can be evaluated using [4]:

$$y_{bs} = F_s(y_{ms})_c \left\{1.8 - 0.051\left(\frac{r}{W}\right) + 0.008\,[W/(y_{ms})_c]\right\} \quad (3)$$

Where a conservative safety factor of F_s=1.19 is adopted herein. This method is valid for $W/(y_{ms})$ c < 1.25 and r_c /W =1.5 being adopted for r_c/W< 1.5, and $W/(y_{ms})$c=20

The expression by Thome [9] found that bend scour for 70 bends in a reach of the Red River between Arkansas and Louisiana in the United States of America could be reasonably described by:

$$y_{bs} = (y_{ms})_c \left\{2.07 - 0.19\, ln\, \left[\left(\frac{r}{W}\right) - 2\right]\right\} \quad (4)$$

Where this method is valid for r_c/W>2. Eq. (3) and (4) are recommended to be limited to flows of overbank depths upstream the bend of less than 20% of the main channel depth. The bend scour is presented in Table 3.

Table 3 Evaluation of Scoured Channel Section

Flow depth y_{ms} (m)	5.68 m
Average Veloc V(m/s)	1.064
Critical velocity for sediment entrainment V_c(m/s)	
Flow rate Q(m^3/s)	902.97
Channel Width W(m)	149.2
r_c (m)	400.2
Average scoured flow depth $y(ms)_c$ (m)	
Maximum scoured flow depth in bend y_{bs}(m)	
Maynord	10.7
Thorne	12.1859
Selected value of y_{bs}	
S_c Maynord	5.02
S_c Thorne	6.505
S_c	5.7625

Local scour depth d_s by HEC-18

The basic mechanism causing local scour at piers is the formation of vortices at their bases known as the horseshoe vortex at pier. The horseshoe vortex results from the pile up of water on the upstream surface of the obstruction and subsequent acceleration of the flow around the nose of the pier. The action of the vortex removes bed material from around the base of the obstruction [8].

An equation developed by fitting laboratory data based on the Colorado State University (CSU) [6] and [7-8] was recommended by the Federal Highway Administration for both live-bed and clear-water pier scour. The study of 22 scour equations using field data presented by [3] indicate that the HEC 18 equations was good for design because rarely under predicted the observed scour. The data contained 384 measurements of scour at 56 bridges.

This equation has been progressively modified over the years and is currently one of those recommended by the U.S. Department of Transportation for estimating local scour depths at bridge piers. This equation is expressed as:

$$\frac{y_s}{y_1} = 2.0\, K_1 K_2 K_3 K_4 K_w \left(\frac{a}{y_1}\right)^{0.65} F_1^{0.43} \qquad (5)$$

In terms of y_s/a, Eq. (5) is

$$\frac{y_s}{a} = 2.0\, K_1 K_2 K_3 K_4 K_w \left(\frac{a}{y_1}\right)^{0.35} F_1^{0.43} \qquad (6)$$

$y_s \le 2.4\, a$ $F_1<0.8$

$y_s \le 3a$ $F_1>0.8$

Where:

y_s= scour depth, m, ft

y_1= flow depth directly upstream of the pier, m, ft

K_1= correction factor for pier nose shape

K_2 = correction factor for angle of attack of flow

K_w = correction factor for very wide pier, piers

a= pier width, m, ft,

L= length of pier, m, ft

F_1= Froude number= $V_1/(gy_1)^{1/2}$

$V_{1=}$ mean velocity of flow directly upstream of the pier, m/s, ft/s

Considering the following conditions:

A design discharge Q= 902 m^3/s, T_r= 20 years, V=1.24 m/s, y_1= 10.65 m

The geometry of the bridge can be described by the type, shape, length, width and alignment with the flow, and considered by means of different factors in the equation:

$F_1= V_1/ (9.81 \times 10.65)^{0.5} = 0.120$

F_1=0.120

K_1 is the correction factor by shape of the pier nose, for a rounded pile K_1=1,

K_2 per angle of attack, K_2= 1.0.

K_3 by the underlying condition, in the case of clear water scour and small dunes K_3 = 1.1

K_4 correction factor for the kind of the bed material K_4 =1 if D_{50} < 2 mm

In this case D_{50} < 2mm and K_4=1

K_w is a factor for the width of the pier

$K_w= 2.58\ (y/a)^{0.34}\ F^{0.65}$ para $V/V_c < 1$

$K_w = 2.58\ (10.65/10.8)^{0.34}\ (0.120)^{0.65}$

K_w= 0.65

Substituting in the previous equation

$y_s/y_1=2.0x1x1x1.1x0.65(10.8/10.65)^{0.65}x(0.120)^{0.43}$

y_s/y_1 = 0.579

y_s= 0.579x 10.65 =6.17 m

y_s= 6.7m

Total Scour

The Total scour at a highway crossing is composed of long-term degradation, general scour and local scour. The components are assumed to be additive. In addition, lateral shifting of a stream can cause or increase the scour. Each of the three types of scour and stream instability are introduced separately [6]. The total scour is presented in Table 4.

As can be seen, the evaluation of the scour is done as a sum of processes that act separately to give the total scour. As a result of applying empirical equations those estimate separately the different types of scour. However, scour occurs as the

interaction of different processes that are presented in a river according to the conditions of bathymetry, flow and transport of sediment in it and its evolution over time.

Table 4 Total Scour

Total Scour	
General Scour (m)	4.699
Bend scour (m)	5.76
Local Scour (m)	6.7
Total Scour (m)	17.159

The lack of measurements of scour in the field and its follow-up, is the reason why there is some uncertainty when applying them. However, further improvement will be necessary to understand the mechanism of river scouring.

Planform shape of the river is also important, meandering rivers are characterized by continual development of the meander bends, so that there is a high potential for problems associated with bank erosion and channel migration. In wide braided rivers, the deep water channels can shift significantly and unpredictably during floods.

Measurements of cross sections and bed elevation histories in a particular place can be used to provide indications of maximum general scour depths to be expected.

CONCLUSIONS

The scour at the site is caused for the effects of numerous floods, general scour, bend scour and local scour, together with channel migration. In this case the total scour was 17.16m.

Empirical equations are based on laboratory data derived from idealized models of bridge. The equations have limitations due to this idealized approach. Field data measurements of scour at bridges, which are necessary to better understand the problem of scour and to evaluate analytical methods for scour prediction, are extremely limited.

In the literature, expressions for determination of the various scour components are generally presented as: general scour, scour in curves, local scour. Total scour is obtained as the linear superposition or sum of the effects of these individual processes as if were separate scour processes.

However scour is a complex phenomenon, where the effects of water flow, the bottom material, channel geometry and modifications involved in time combine to act together at bridge foundations.

Physical model studies are still recommended for complex piers.

The use of the methods presented provide good estimate of scour, combined with field measurements and observations. It is recommended analyze the results using an interdisciplinary team to determinate their reliability and adequacy for the bridge, flow and site conditions, safety and costs.

REFERENCES

[1] Blench,T. Mobile bed fluviology, University of Alberta Press, Edmonton, Canada.1969

[2] Lacey, G (1930). Stable channels in alluvium. Paper 4736, Minutes of the Proc. Of the Instn. Of Civ. Engrs., Vol. 229, William Clowes and Sons, London, 259-292.

[3] Landers, M.N., Muller, D.S., and Marten, G.R., Bridge scour data management system user's guide manual. U.S. Geological Survey Open FileReport 95-754, Reston, Va, 1996.

[4] Maynord, S.T. (1996) "Toe scour estimation in stabilized bend ways", J. Hydr. –Engr. ASCE, 122(8), pp.460-464

[5] Melville, B.W. and Coleman, S.E, Bridge Scour. Water Resources Publications, Littleton Colorado. 2000.

[6] Richardson, E.V., Simons, D.B. and Julien, P.Y., Highways in the river environment. Federal Highway Administration, U.S. Department of Transportation, Washington, D.C, 1990.

[7] Richardson, E.V., Simons, D.B., and Lagasse, P.F., River engineering for highway encroachments-Highways in the river environment. Hydraulic Design Series 6 (HDS6) Publ, No FHWA NH1 01-004, Federal Highway Administration, U.S. Department of Transportation, Washington, D.C.,2001.

[8] Richardson, J.R. and Richardson E.V., "Bridge Scour Evaluation", Sedimentation Engineering Process, Measurements, Modeling, and Practice, ASCE Man. Edited by Marcelo H. García, ASCE, 2007, ch.10.

[9] Thorne, C.R. Bank processes on the Red River between Index, Arkansas and Shreveport, Louisiana" Final Rep to the US: Army Eur. Res. Ofc. Dept. of Geography, Queen Mary Collegue, London, 1988

VOLUMETRIC MEASURING OF SEDIMENTS IN A TRANSPORTABLE PRISMATIC CHANNEL

Mundo-Molina Martin[1]
[1]Engineering Faculty, Chiapas State University, Mexico

ABSTRACT

Teaching the transporting mechanics of sediments in the civil engineer undergraduate program is not an easy task. It is difficult to achieve the following objectives: transmit theoretical concepts and empiric equations to students in order to motivate them to have interest in these matters and make use of knowledge. Thus, the combination of theory, practice and measurements in the laboratory are necessary. The vast majority of public universities of Mexico lack laboratories for this objective, so in the Research Centre of Engineering Faculty of Chiapas State University (UNACH by its acronym in Spanish) was designed a transportable prismatic channel (CPPV by its acronym in Spanish) which is used to teach and achieve the aforementioned objectives. In this paper, the constructive process for the channel is presented as well as the methodology used to teach the volumetric sediment measurement in the CPPV.

Keywords: Volumetric Measurement of Sediment, Sediment Transport, Transportable Prismatic Channel, Measurement of Sediment in Laboratory.

INTRODUCTION

One of the serious problems of provincial universities in Mexico is the lack of economic resources to acquire the necessary equipment for their laboratories. Thousands of students of the open channel hydraulics class in the civil engineering degree program receive theoretical classes in a traditional way (blackboard hours). The academic program of the Faculty of Engineering (FI by its acronym in Spanish) of the UNACH contains the class “open channel hydraulics" , whose thematic content is: theoretical concepts and principles, specific energy and critical regime, rapidly varied flow, uniform flow, hydraulic transitions and the principles of sediments transport. The last topic is not usually studied for three reasons: lack of training of teachers in this subject, lack of time (especially in the so-called short semesters) and because there is no infrastructure for the student to experiment and analyze: the initiation of sediments transport, the mechanics of their transport, bed forms and the scour phenomena. Thus, the properties of the sediments particles and their main characteristics can be explained on the blackboard without major effort, however the issues of sediment transport, forces and velocities that occur in the movement of particles, tractive force, resistance to flow, bed forms, flow regimes, transport, movement mechanics, and the criteria for sediment quantification require a greater effort because students fail to internalize the concepts without experimentation. For these reasons the academic objectives are not achieved, meaning that the student does not appropriate knowledge through the internalization of concepts and their materialization through visualization and experimentation. This is why the aim of this investigation is not only to demonstrate the methodology of the construction of a CPPV, but also describes the methodology for volumetrically estimating the amount of sediments that transport a stream in order to later develop semi-empirical or empirical equations that allows for the quantification of the volume of sediments transported by water.

BACKGROUND

The emergence of physical modeling as a scientific topic forms part of the solution which responds to theoretical limitations [1]. The development of physical models and the construction of artificial channels in laboratories allows for the solving of many problems that theory is not capable of solving, either due to their mathematical complexity or lack of computational tools and computing power. However, by 1950 the appearance of computers and the application of numerical methods marked the beginning of the weakening of hydraulic experimentation in research centers. Thus, in the early 80’s, the mass production of personal computers, costing less and less money, furthered the possibilities of these calculation methodologies. Experimentation in public and private universities declined. At present, hundreds of schools or faculties (especially those in the province) that teach civil engineering and / or water sciences in Mexico do not have a hydraulics laboratory. Concerned by this problem, the Research Center

(RC) of the FI of the UNACH, Mexico, designed and built an economic prismatic channel, with a rectangular cross section and variable slope with the objective of carrying out hydraulic experiments which include the transport of sediments in order to improve teaching and promote investigation. The materials and methods used to construct the CPPV and a technique for the volumetric measurement of the sediments in the laboratory are presented below.

MATERIALS AND METHOD

Materials

The materials that were used to build the CPPV were the following [2]: tubular metal with a rectangular profile (PTR by its acronym in Spanish), 10 cm wide and 5 m long, to build the base (Fig. 1); hydraulic jack to change the slopes of the CPPV (Fig. 2); acrylic sheets to build the walls and the bottom of the channel (Fig. 2); two tripods constructed with three piece of steels of 3 inches diameter in order to support the weight of the channel (Fig. 2); volumetric tank that serves not only as "reference model" for validate Q but also as a deposit "water intake" for the circulation of the flow rate (Q) into the CPPV (Fig. 3); 4 HP gasoline pump (Fig. 4) with 2 inches diameter of output to drive water from the deposit "water intake" to the CPPV and to circulate the flow in a closed system. Once the CPPV was designed, it was built as shown in Fig. 1 and 2.

Fig. 1 Metallic PTR for the base of the channel

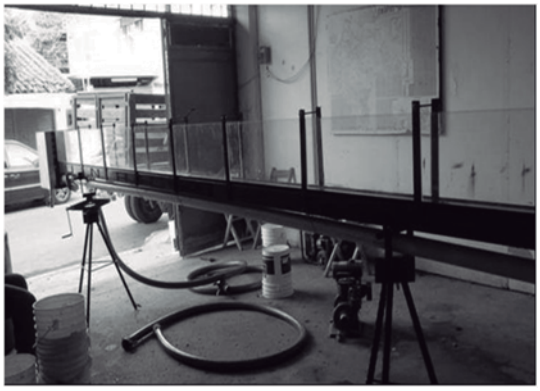

Fig. 2 Hydraulic jack, tripods and energy dissipation tank

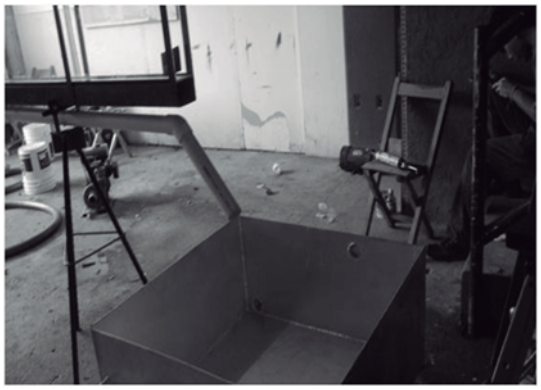

Fig. 3 Calibrated volumetric tank

Fig. 4 4 HP gasoline pump

Method

Thus, once the CPPV was built the volumetric tank shown in Fig. 3 was calibrated. The calibration curve is shown in Fig. 5. With this curve, the flow rate of the CPPV can be estimated using Eq. (1).

$$\boldsymbol{Q = \frac{V}{t}} \quad (1)$$

Where Q is the flow rate (l/s), V is the volume (l) and t is the time (s).

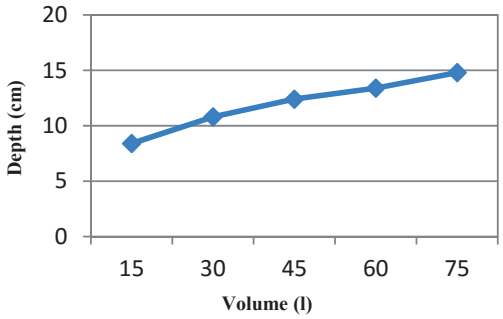

Fig. 5 Calibration curve

Subsequently, 1.2m^{3}of silt from the Grijalva River was collected (located 12 km from the RC of the FI of the UNACH).The sediment that was collected is inorganic silt with an approximate diameter of 0.004 mm that was transported to the soil mechanics laboratory of the UNACH where its submerged specific weight was estimated to be 1200 kg/m^3. Before placing the silt in the channel, the CPPV was weighed with a mechanical scale. Its weight was 110 kg. Subsequently, a uniform layer of silt 10 cm thick was spread over the base of the CPPV's entire 5 m length and 9 cm width (Fig. 2). The weight of the soil mass (W) of the extended layer, according to Eq. (2), was 54 kg.

$$\boldsymbol{W = \gamma V} \quad (2)$$

Where W is the weight of the soil mass in kg,$\boldsymbol{\gamma}$ is the specific weight of the soil in kg/m^3 and V is the volume in m^3. Thus the total weight of the CPPV and the extended silt is 164 kg. Once the CPPV and the extended layer of silt were weighed, a flow rate of 3.5 l/s was circulated through the CPPV to empirically estimate Manning's "n" using the following equation:

$$n = \frac{A_h R_h^{0.666} \sqrt{S_o}}{Q} \quad (3)$$

Where Q is the flow rate m^3/s, A_h, is the hydraulic area in m^2, R_h is the hydraulic radius in m, and S_o is the slope of the CPPV. The "n" obtained was 0.034. This value is consistent with the equation of [3]-[4]:

$$n = \frac{D_m^{\frac{1}{8}}}{16.27} \quad (4)$$

Where D_m is the mean diameter of the sediment. The lost sediment was replaced and then a flow rate of 3.5 l/s for 8 continuous hours was circulated in the CPPV. The average velocity of the flow was 0.66 m/s. The velocity curve is presented in Fig. 6.

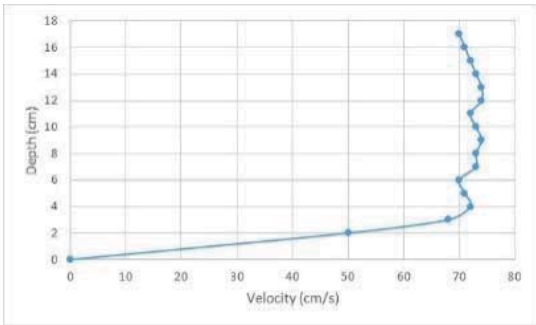

Fig. 6 Velocity profile

During this period of time, an intense sediment transport (biphasic flow) was generated that allowed to observe: beds form, transport mechanics, slight scouring in the head of the CPPV, as well as the transport and accumulation of sediments (by suspension, saltation and depositing) in the volumetric tank shown in photo 3. The hydraulic and geometric data of the experiment were as follows: Q = 3.5 l/s, n = 0.034, b = 0.09 m, S_o = 0.05. The total amount of sediment (suspension plus bottom deposits) transported by the CPPV during 8 continuous hours was: V=0.008325 m^3. This volume was collected in the volumetric tank of the CPPV shown in photo 3. Thus, according to equation 2, this volume corresponds to a weight W = 9.991 kg, which means that an average layer of 1.85 cm thick was lost in the whole extension of the CPPV that corresponds to 18.5% of the original thickness of 10 cm. For this reason the final weight of the CPPV with the silt, after the realization of the experiment, was 154.10 kg, which is consistent with the described estimates.

CONCLUSIONS

The following objectives were obtained: the traditional teaching of the mechanical transport of sediments in the civil engineering undergraduate program of the FI of the UNACH was overcome. Not only were the theoretical concepts of sediment transport transmitted, but they also implemented and observed the phenomenon in practice. This was achieved by building a transportable variable slope

prismatic channel. Thus, in this paper was presented the constructive process of the CPPV (patent pending) and the methodology used to teach the mechanics of sediment transport and it volumetric measurement. In order to achieve the final objective, a layer of 10 cm thick inorganic silt from the Grijalva River was placed in the CPPV, then was generate a flow rate in the CPPV of 3.5 l/s with a slope S_o = 0.05 and an average velocity of 0.66 m/s associated with a n = 0.034, whereby an estimated volume of 0.008325 m^3 of sediment was collected and measured in the CPPV volumetric tank. The total sediment transported during the 8 hours of the experiment represents a thickness of 1.85 cm (loaded in its two phases: monophasic and biphasic).

It is suggested that at a later date the results of these experiments are used to develop empiric and semi-empiric equations to quantify the volume of transported sediments, both in suspension and settled. Finally, it is suggested that a thematic area called "Teaching and training in sediment management" is included in the "7th International Symposium on Sediment Management", in order to promote teacher training in the subject of "transport and sediment management".

REFERENCES

[1] Lopardo, R. (1995). La formación del ingeniero hidráulico para el siglo XXI. Revista Ingeniería del Agua, vol. 2, no.4, pp.67-76.

[2] Mundo, M.M. (2014). "Diseño y construcción de una canal económico en el laboratorio de hidráulica de la Facultad de Ingeniería de la UNACH. Congreso Latinoamericano de Hidráulica, Santiago de Chile.

[3] Maza A. J. A., García Flores M. (1986). Distribuciones de los tamaños de los sedimentos del fondo en cauces naturales. Memorias del XII Congreso Latinoamericano de Hidráulica, volume 3, pages 104 to 109, Sao Paolo, Brasil.

[4] Maza, A. J., García, F.M. (1996). Manual de Ingeniería de Ríos. Series del Instituto de Ingeniería de la UNAM.

IMPORTANCE OF THE AN ANALYSIS OF THE ALTERATIONS IN THE FLOODPLAIN OF THE PROPOSED LAS CRUCES DAM

Gracia Jesús and Ramos Judith[1]
[1]Instituto de Ingeniería, Universidad Nacional Autónoma de Mexico, Mexico

ABSTRACT

It has been postulated that the analysis of a river should include its floodplain, otherwise the connectivity between the two will go unnoticed resulting in an incomplete assessment. In order to identify the changes that have occurred in the river and its floodplain traditional aspects as well as changes in the structure of the fluvial and riparian microhabitat among others need to be attended, moreover when building a dam in the river basin. This article seeks to answer the question whether Las Cruces dam will result in a direct detriment of the vegetative populations and their environment? Thus, a morphodynamics study of the San Pedro River and its floodplain was carried out. The geoforms including the soil and vegetation were studied through remote sensing techniques. The results show that the vegetative communities downstream have a relationship with the presence of sand sediments between 0.1 and 1 mm in diameter and fine sediments < 0.1 mm. Additionally, this type of material can sediment in the delta of the dam after an extraordinary flood event. Therefore, there are significant alterations in the geoforms as well as in the sediment load generated and transported. As a consequence some measures are proposed to avoid the loss of sediments downstream of the dam.

Keywords: Wetlands, Dam Las Cruces, Sedimentation, Floodplain, Remote Sensing

INTRODUCTION

For several decades now, rivers have stopped to be considered as conveyors of water, to become as a part of the ecosystem with several biological, fluvial and ecological processes. Rivers maintain habitats and, transform and transport matter received from the catchment and produced in the streams themselves [1]. When rivers overflow they create terrestrial and aquatic transitional zones (floodplains) that also are an important part of the ecosystem since different processes have placed in it [2]. Floodplains become a natural storage for water (from the rivers or precipitation, or groundwater), habitat for biodiversity, and provide many vital functions to the river such as nutrient supplied, improving water quality, among others. As a transitional zone floodplains are very dynamic and heterogeneous ecosystems, showing complex patterns of variation over a wide range of temporal and spatial scales [3]. Reference [4] observed that some processes could be inferred by observing patterns that can be organised or random. The most important aspect in the generation of patterns is the capability to represent reality and, in consequence, to produce confident hydrological predictions. In this case, these predictions are related to changes on the river main channel, river corridor and floodplain.

Based on this, in the last decade it has been postulated that the analysis of a river should include its floodplain in order to achieve an ecologically driven catchment management. As river and floodplain are connected in order to maintain an equilibrium, water, energy, sediment, and debris are in balance. Under this condition there is not gain or loss of sediments in the channel and bed, respectively. For this, the connectivity between the river and its floodplain needs to be attended in order to avoid incomplete assessments. Reference [5] mentioned that hydrological connectivity, as a dynamic process, interrelates the spatial continuity and the spatio-temporal heterogeneity of the biodiversity that characterises river-floodplain.

In general, the floodplain ecosystems are flat and fertile lands as a consequence of continuous floods which provide deposit of sediments and soil to ecosystems that are adapter to, and reliant upon, the regular inundation of waters [6]. The different types of habitats shelter a variety of species that require lotic conditions at some point during their life history stages [7]. For that the transition from flooding laterally to terrestrial provides inundated areas, which act like a reservoir that temporarily stores water that after some time return to the river. However, these areas gradually sank and erode forming very productive estuaries separated from the river by barriers but affected by the constant ebb and flow. The estuaries are characterised by a great dynamism with important habitats and natural resources. These areas are suitable for speciation being the main characteristic of the new species its high adaptation capability that enable them to survive during an adverse period of drought or flood and even benefit from it [8] in [2]; [3].

When rivers have been altered by regulation or hydraulic structures, its fluvial dynamics is altered

affecting the connectivity of the river and its floodplain and the biodiversity. As result some alterations could be observed in the runoff pattern, the quality of river discharges, the size distribution and the load of the transported sediments, as well as changes in the structure of the fluvial and riparian microhabitat. Also, additional to the climate and land cover change, it is important to consider the development of aquatic resources, irrigation zones, and expansion of the industrial sector.

When building a dam, special attention needs to be performed in order to evaluate the benefits and also the negative impacts in the channel and floodplain. In dammed rivers, the sediment regime changes are the most impacting aspect because a dam interrupts the natural flow of a river and impedes a continuous sediments transport. Other resulting changes are water quality degradation, downstream flow regime, bed morphology and ecosystem [9]. As a dam acts as blocking of the transported sediments, thus a lack of sediments downstream could become critical to maintain the floodplain ecosystem. Reference [9] indicates that it is possible to achieve a sediment management in order to maintain the sediments downstream. Some techniques used for this purpose are flushing, sluicing and bypassing [10], [11]. The last one avoids accumulation at the reservoir head or inside using tunnels known as sediment bypass tunnels (SBT see Fig. 1) that routing sediments after the dam embody them into the channel [12]. On one hand, a direct positive result is the restabilising of sediment connectivity, thus the downstream flow will have the same conditions than pre-dam. However, on the other hand, a negative result just after the dam is the morphological changes in the river bed and the effect in the river habitats than are going to impact morphologically and ecologically the floodplain close to the deposition. Thus it is required to maintain the integrity of the floodplain ecosystem.

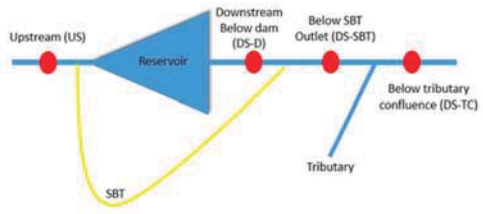

Fig. 1 Sediment Bypass Tunnel scheme. Source: [9]

This article addresses a morphodynamics study of the San Pedro River and its floodplain. The soil and vegetation conditions are analysed, as well as the dynamics of the geomorphology of the river and its floodplain in order to answer the question *will the Las Cruces dam result in a direct detriment of the vegetative populations and their environment?*

STUDY SITE

The San Pedro River is located in the lower basin of the San Pedro-Mezquital system, in the Hydrological Region RH-11. The river is born to the northwest of La Sauceda River in the city of Durango changing abruptly from south to west at the town of San Pedro Ixcatán and Tuxpan, until its mouth in the Mexcaltitán Lagoon at the Marismas Nacionales, to finally end in the Pacific Ocean as shown in Fig. 2 [13].

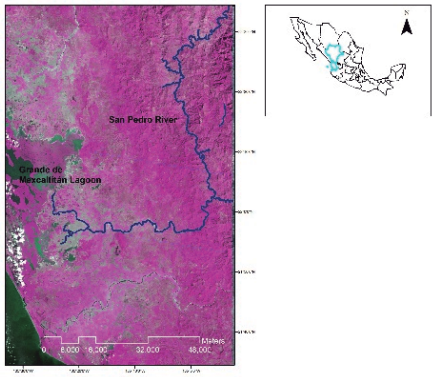

Fig. 2 San Pedro River at the Hydrological Region RH-11 in the Durango and Nayarit States.

The northern part of the sub-basin of the San Pedro River is a mountain area, included within the sub-province of the Neovolcanic Axis with soft hills and residual soils associated with plains. The coastal zone is located in the physiographic province of the Coastal Plain of the Pacific, in the subprovince of the Delta of the Santiago River, on the lands of the deltaic landscape system, marshes with coastal lagoons and parallel bars of old coastlines. The presence of dynamic processes is manifested in the erosion (in the channel) and deposition along the floodplain (terraces and dams) [14],[15]. Basically the main type of soils are fluvisols, cambrisols and feozem with some gleysols. The foezem are well-drained, fertile and productive soils.

In the lower part of the San Pedro-Mezquital basin, the climate is subhumid warm with summer rainfall A (w) and semi-warm subhumid Aw1 (h '). The average annual temperature varies from 26 to 28 ° C, and the average annual precipitation is 634.1 mm, with the highest values of the order of 1,000 to 1,500 mm reaching 2,000 mm in the rainiest months (September and October). Winds correspond to humid monsoon coming from the sea during June, July and August. Rainfall in this zone is also associated with the presence of the Mexican

Monsoon, which causes rains above the average, although not always in the same intensity. Additionally, this zone is subject to the occurrence of hurricanes and tropical storms, which may appear between the months of June to October of each year.

The rain presented gives rise to the processes of washing in the soil, modifying the age of the plain and generating sediments from medium to light texture (loam, silty loam, sandy loam to sandy). Mangrove is the dominant vegetation with species reaching up to 20 or 30 m in height. Mangroves are fundamental for the ecosystem as well as for the local economy. However, agriculture is the main water consumption since in the upper part of the basin is allocated the Irrigation District (DR) 052, various Irrigation Units and, in the lower part, is the Irrigation District (DR) 043.

METODOLOGY

In order to establish the magnitude of the morphological changes in any system, the geoforms were studied through remote sensing techniques, particularly with respect to accretion, erosion, destruction, reductions in their heights, and the equilibrium downstream of the sedimentary load.

Changes along the San Pedro River

The morphodynamics study of the San Pedro River and its floodplain embraces from the Pajaritos Hydrometric Station to its arrival in the wetland area. It is important to mention that the feeder to the core-wall of the dam is almost 50km and from the core-wall to the deltaic zone the river longitude is approximately 80km.

Basically, one is looking for that the areas that have altered the dynamic equilibrium on the river. This means those areas subject to erosion and accretion, in order to stablish how the river has been adapting through years to morphodynamic transformations as results of large floods. This adaptation implies that the driving and resisting forces at the river should remain constants. For the driving force it is necessary to measure changes in discharge and slope, whereas for the resisting force in the sediment load and bank stability. Thus, to describe the morphodynamic changes, data acquisition consider water depth, mean flow velocity, wetter width and substrate, and other aspect to be analysed is the confluence of tributaries since they could contribute with the hydrodynamics and morphodynamics control of a river. Also, in order to define the critical shear stress, the sediment characteristics are basic. In particular, the size of the grain is highly relevant as one is interested to understand the impact in the mangroves areas.

Spatial and Temporal Analysis of the San Pedro River

The history of the river provides important information that can be addressed by remote sensing techniques since morphological changes can be determined using different techniques [16],[17]. Reference [6] mentions that different spatial and temporal scales need to be considered to stablish the land characteristics. It can be observed that at mesoscale, features such as the bed-form change from temporal scales of 1 to 10 years. The results at this scale modify observations at microscale, but probably microhabitats such as substrate composition, that change within days or weeks, could not be analysed only inferred.

In this paper, the approach is to define the observed patterns on the base that the controlling processes are known and follow the preferential flow through soil. This flow favoured the wetness creating very productive soils where vegetation is healthy. Also, the presence or absence of geoforms are crucial to establish patterns for the channel and floodplain width. Reference [20] establish that the width of a river indicates the amount of water flowing by the channel, the sediment load, the composition of the bed and banks, and the influence of local topography, soil properties and vegetation communities. These are the patterns to be perceived in the river and its floodplain.

DATA

Several sources of information were used.

Sedimentation load

Sedimentation load data were used from a previous work carried out by [21], where some variables were measured in order to estimate the sediment load such as: the reservoir bathimetry obtained from LiDAR information and hydrometric information as average discharges for monthly, annual and for extreme events in July to November. Data were processed in a sediment mathematical software.

Landsat data

Raster information available at this stage of the project, includes Landsat images with MSS, TM and OLI sensors. Landsat images correspond to the day of the year (DOY) 349 for 1973, DOY312/1993, DOY290/2002 and DOY280/2013 that corresponds to the rainy season and the presence of tropical cyclones. But also DOY142/83 from drought season. The pre-processing of the images consisted in the radiometric correction, this is the calculation of the reflectance values from the digital levels of the

scenes. Geometric and atmospheric corrections were not necessary. Once the reflectance values are taken, a spatio-temporal analysis was carried out, which allows the identification firstly of the land cover changes that have taken place over time and then of the spatial patterns.

Geospatial ancillary datasets

The vector data obtained from the [22] include topics such as natural resources: geology, soil science, hydrology, land and vegetation use, climatology, physiography, potential land use, potential wetlands and island territory. In addition, the data of urban cartography, cadastre, geodesy, national geostatistical framework and topography were acquired.

Other available data, also obtained from [22] are relief data, whose cells have elevation values in meters above sea level (msnm). These elevation models are called Continuo de Elevaciones Mexicano Edition 3 (CEM 3.0) and are available in several resolutions: 120m, 90m, 60m, 30m and 15m. The meteorological information (basically, temperature and precipitation) was obtained from climatological stations [23] located within the sub-basin area.

RESULTS

Identify potential land cover changes

The approach was designed to capture the main land change disturbances and to update the land cover for those changed areas. The spatio-temporal analysis of the sub-basin of the San Pedro River made it possible to visualize the dynamics of deforestation, and to quantify these changes over a period of 40 years (1973-2013). The land classification was based on vegetation indices and the most relevant observation is that from 1973 to 1983 the San Pedro-Mezquital Basin presented a severe deforestation (see Fig. 3) at the upper and middle part. This practice was continue through 1993 losing more than 60% of the forested area, which were converted into grass or agricultural lands. Although an apparent increment in the forest area was observed for 2003 and improved in 2013, compared to the year 1973 it represents a lower percentage, and also there is the doubt if it is a new specie or really the forest was recovered.

At the lower part of the basin, in the coastal plains, vegetation showed a loss of mangroves, although there are other type of vegetation that could be considered as emergent wetland as [24] pointed out from 1990 to 2000 period. The authors associated the losses to the presence of hydrometeorological events such as hurricanes like Rosa in 1993. At this time, it is important to mention that two hurricanes category 2 and 4 hit the coast of Nayarit in 1983: one in May 27th (Adolph) with an important wind shear and the other in October 16th (Tico), respectively. Thus, important changes were observed after these dates, maximised the deforestation in this decade.

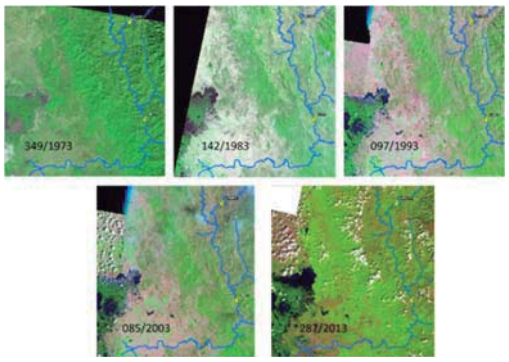

Fig. 3 Loss of the forest cover through a 40 year period

Geoforms and spatial patterns

The San Pedro River is very dynamic particularly in the coastal plains. [14] divided geomorphologically this landscape into: intermediate fluvial plain (second level of fluvial terrace at 5 to 10 m heights, from which the rivers overflow during extraordinary avenues), low plain with fluvio-marine influence and fluvial floodplain subjected to the action of the systematic flooding of the Santiago, San Pedro and Acaponeta Rivers, where a rejuvenation process is activated and manifested by the presence of fluvic material in the first 50 cm thick soil.

The river width was obtained after applying some filters in order to differentiate as best as possible water, sediments, bare soils and vegetation. Then using the *zonal change* and *Imagen differences* and *Highlight change* commands from ERDAS (2011), it was assessed the percentage of change for the time periods of 1973-1983, 1983-1993, 1993-2002, 2002-2013 and 1973-2013. In the upper part of the subbasin sediments did not modify the channel width at all, thus the floodplain is recovered after some extraordinary event. However, after the confluence of the El Naranjo stream there are important areas with erosion and deposition of sediments (see Fig. 4). Also the El Naranjo stream contributes significantly to the morphodynamics observed downstream at the San Pedro River.

Sedimentation load

Results showed that the total sediments contribution for the Las Cruces dam could be of approx. 5.3 Millions of m^3 per year ($Mm^3 \cdot year^{-1}$).

From this quantity, it is expected that the coarse material sediment overpass easily the core-wall since the fine material is < 0.1mm. The latter is because the short retention times reduce the sedimentation capacity. Coarse sediments (0.1 and 1.0 mm) will be deposited in the reservoir, representing only the 10% of the total sediment load load, thus the real contribution is around 0.53 $Mm^3 \cdot year^{-1}$. Also, it was demonstrated that the coarse sediment retained should be useful downstream of the dam maintaining the wetlands zone. Due to this material is effectively sedimented, it can be mechanically translated from the upstream deposit in the reservoir, to the downstream zone of the dam just after the core-wall.

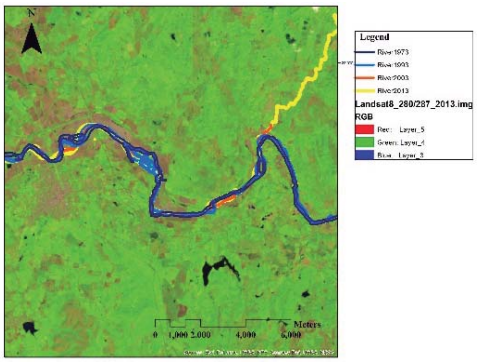

Fig. 4 Part of the San Pedro River at the coastal plains

The size of the grain is highly variable since there are an irregular distribution of the content in organic matter and/or materials of different texture, due to the systematic flooding of the river, which buries the horizon A of the preceding soil. However, fine sediments are going to be transported as suspended material (>0.1mm) thus it could overpass the core-wall of the dam.

Soils in the delta go from an alluvial to a clay formation or sedimentation process, of medium depth, with a franc-loamy/clay texture forming unusual features in the high and intermediate terraces. Thus, it is highly recommended that a grain size between 0.1-0.2 can be maintained after the dam construction.

Considering this size of grain, and the sediment load and discharge upstream of the dam, it was estimated a total sediment volume of 100,000 m^3 per year to be transported out the dam. However, this volume needs to be deposited after the core-wall in order to allow the river conveyed the sediments downstream. Of course, in the place and immediately some short distance downstream, there is going to be a change in the morphology not only in the channel, but also in the floodplain, which needs to be studied. Therefore, no consequences affecting the ecosystem are expected downstream in the floodplain zone, because there it is not lack of sediment.

CONCLUSIONS

The monitoring and mapping of the land cover changes are important ways to support the evaluation of the status and transition of ecosystems. Also, they facilitate the identification of morphological changes at different scales in the San Pedro River, particularly in its lower part, that corresponds to the deltaic area. Basically, these changes observed correspond to a severe deforestation making highly vulnerable the upper part of the subbasin. These changes were initiated from the 70's and followed for almost 30 years until 2000's where some recovering was observed. As a consequence of the deforestation, the sediment load increased in volume and it was composed by a mixture of sediment size and origin (organic matter, rock, etc.). Also, this implies the deposition or erosion of the channel bed and banks but modifications also for sediments in the flood plain by the lateral overflow of the river and the transfer of material from the floodplain into the channel.

The spatial patterns obtained show the width variation through 40 years of the river being more important in the deltaic zones and, in consequence, the impact is major in the habitats. This action have abated the mangrove area passing from homogeneous covered areas to patches and in the surrounding new adapted species.

As there is significant evidence of the positive and negative effects of building a dam in the river basin, some downstream measures need to be proposed to avoid sediment shortage and habitats decay. One of the strategies to be considered is the sediment bypass from upstream for a specific grain size into the channel after the core-wall of the dam. However, a more detailed analysis of the morphodynamic, sediment transport and dominant discharges need to be investigated further.

ACKNOWLEDGEMENTS

This work was supported by the "Programa de Apoyo a Proyectos de Investigación e Innovación Tecnológica (PAPIIT)", UNAM [Project grants Num. IN106818.]

REFERENCES

[1] Madsen J D, Chambers PA, James WF, Koch EW, Westlake DF, "The interaction between water movement, sediment dynamics and submersed macrophytes", Hydrobiologia, Vol. 444, issue 1-3, 2001, pp.71–84.

[2] Bramlett K, "Flood Plain Form, Function, and Connectivity in River Restoration", River

Restoration, 2012. Web Page consulted on January 20th, 2018

[3] Tockner K, Lorang MS, Stanford JA, "River Flood Plains are Model Ecosystems to Test General Hyrogeomorphic and Ecological Concepts" River Research and Applications Vol. 26, 1, 2010, pp. 76-86. doi: 10.1002/rra.1328

[4] Grayson R, Blöschl G, "Spatial Processes, organisation and Patterns", in R. Grayson and G Blöschl (eds), Spatial Patterns in Cathment Hydrology: Observations and Modelling, 2000, Cambridge Uni8versity Press, United Kingdom

[5] Holubová K, Čomaj M, Mravcová K, "Recoonnection of the Danube floodplain channels as a vital step to restore river morphology and fluvial dynamics", River Sedimentation, Wieprechy et al., Editors, 2016, pp. 825-832.

[6] Berger V, Niemann A, Feld CK,"River restoration in sand-dominated lowland streams – a comparison of morphodynamic impacts and response", in Proc. 13th International Symposium on River Sedimentation, Wieprechy et al., Editors, 2016, pp. 833-840.

[7] Barko VA, Herzog DP, O'Connell MT, "Response of Fishes To Floodplain Connectivity During and Following a 500-Year Flood Event in the Unimpounded Upper Mississippi River", Wetlands, Vol. 26, No. 1, 2006, pp. 244-257. doi: https://doi.org/10.1672/0277-5212(2006)26[244:ROFTFC]2.0.CO;2

[8] Junk W J, Bayley PB, Sparks RE, "The Flood Pulse Concept in River-Floodplain Systems", in Proc. of the International Large River Symposium, 1989, 110-127

[9] Auel C, Kobayashi S, Sumi T, Takemon Y, "Effects of sediment bypass tunnels on sediment grain size distribution and benthic habitats", in Proc. 13th International Symposium on River Sedimentation, Wieprechy et al., Editors, 2016, pp. 825-832.

[10] Kondolf GM, Rubin ZK, Minear JT, "Dams on the Mekong: Cumulative sediment starvation", Water Resour. Res., Vol. 50, 2014, pp. 5158–5169. doi: 10.1002/2013WR01465

[11] Morris GL, Fan J, "Reservoir Sedimentation Handbook", 1998, Chapter 13, pp13.1-13.25, McGraw-Hill Book Co., New York.

[12] Sumi T, Okano M, Takata Y, "reservoir sedimentation management with bypass tunnels in Japan", in Proc. 9th International Symposium of River Sedimentation, Yichang, China, 2004, pp. 1036-1046

[13] DOF, Diario Oficial de la Federación 09/07/2014 Web Page consulted on November, 2015 [https://app.vlex.com/#vid/518891230]

[14] Bojórquez I, Nájera O, Hernández A, Flores F, González A, García D, Madueño A, "Particularidades de formación y principales suelos de la llanura costera norte del estado de Nayarit, México", Cultivos Tropicales, Vol. 27, No. 4, 2006, pp. 19-26

[15] Bojórquez I, Hernández A, García D, Nájera O, Flores F, Madueño A, Bugarín R, "Características de los suelos de las barras paralelas, playas y dunas de la llanura costera norte del estado de Nayarit, México", Cultivos Tropicales, Vol. 29, No. 1, 2008, pp. 37-42

[16] Alam JB, Uddin M, Uddin Ahmed J, Cacovean H, Habibur Rahman M, Banik BK, Yesmin N, "Study of Morphological Change of River Old Brahmaputra and Its Social Impacts by Remote Sensing", Geographia Technica, No.2, 2007, pp. 1-11

[17] Mohammadi A, Alaghmand S, Mosaedi A, "Study and Determination of Morphological Changes of Dough River in North of Iran Using GIS", in Proc. The International Archives of the Photogrammetry, Remote Sensing and Spatial Information Sciences. Vol. XXXVII. Part B8. Beijing 2008

[18] Miller JA, Rogan J, "Using GIS and remote sensing for ecological mapping and monitoring", in Vistor Mesev Ed. Integration of GIS and Remote Sensing , Chapter 10, 2008, pp. 233-268

[19] Finnegan NJ, Roe G, Montgomery DR, Hallet B, "Controls on the channel width of rivers: Implications for modelling fluvial incision of bedrock", Geology, Vol. 33; No. 3; 2005, pp. 229-232. doi: 10.1130/G21171.1

[20] Blöschl G, Grayson R, "Spatial Observations and Interpretations", in R. Grayson and G Blöschl (Eds), Spatial Patterns in Cathment Hydrology: Observations and Modelling, 2000, Cambridge University Press, United Kingdom pp. 17-50

[21] Gracia J, Luna Bahena JC, Osnaya Romero J, Ortíz MArtínez V, Carrizosa Elizondo E, Franco V, "Estudios Complementarios en Materia de Políticas de Operación, Diagnóstico de Zonas Costeras, Transporte de Sedimentos y Manejo de Cuenca, del Proyecto Hidroeléctrico Las Cruces, Nayarit (2da Etapa). (Informe Final Modelos Físicos)", Project 5336 founded by the Federal Commission of Electricity, Mexico, 2016

[22] INEGI, Web Page consulted on November, 2017 [http://www.beta.inegi.org.mx/app/mapas/]

[23] SMN, Servicio meteorologico Nacional, Web Page consulted on November, 2017 [http://smn.cna.gob.mx/es/climatologia/informacion-climatologica]

[24] Hernandez-Guzmán R, Ruiz Luna A, Berlanga Robles CA, "Cambios de cobertura y usos del terreno de la sub-cuenca Río San Pedro (Nayarit, México) y su efecto sobre los humedales costeros", Thematic área: Conservación de los ecosistemas y la biodiversidad. 2008.

APPLICATION OF EMPIRICAL METHODS TO DETERMINE THE CHANGE IN THE CURVE ELEVATIONS AREAS-CAPACITIES TO THREE RESERVOIRS LOCATED IN THE MEXICAN REPUBLIC

Morales-Saldivar Jorge Antonio[1], González Verdugo José Alfredo[2] and Espinoza Ayala Joselina[3]
[1]Comisión Nacional del Agua, México; [2,3] Instituto Mexicano de Tecnología del Agua, México

ABSTRACT

The sedimentation in reservoirs is a problem of great importance, from the technical, economic, environmental and social points of view, since the reservoirs behave like sediment traps that retain most of the materials transported by the river. In the great majority of countries, of which México is not the exception, the best sites for hydraulic exploitation have already been selected and the best works have already been built from the technical, economic, social, environmental and legal points of view; the possible projects to be developed in the future have, in addition to technical and economic difficulties, great social, environmental and resource availability pressures. Nowadays in Mexico there are no exclusive programs for the measurement of sediments, the measurements are limited to climatological, hydrometric, hydroclimatological and water quality measurement stations and, in hydrometric stations, routine measurements of solids concentration are made, near the surface, with this last measurement, as a reference base, a methodology of the forties. Given the scarcity of data on sediments, to make the necessary estimates, the bathymetries turn out to be an economical and reliable practice to obtain a numerical approximation to the sedimentation that occurred in each reservoir. Empirical methods have been developed to determine the distribution of the deposit of sediment within the vessel as a function of depth, which allows to calculate the future displacement of the curve elevation-areas – capacities. This document presents the application to three reservoirs located in different states of the Mexican Republic of the Area-Reduction methods proposed by [2], as well as the empirical methods developed by [14] and [11], with what is intended to provide a criterion that allows to set the design thresholds of the different structures of the dam.

Keywords: sedimentation, reservoirs, empirical methods, México.

INTRODUCTION

The sedimentation in reservoirs is a problem of great importance, from the technical, economic, environmental and social points of view, since the reservoirs behave like sediment traps that retain most of the materials transported by the river. The sediments that can be transported are those that provide the bottom and banks of the channel, in addition to the very fine particles from the basin lands. Likewise, the phenomenon can adversely impact these reservoirs, as they are subject to a continuous silting process that reduces their storage capacity.

In the vast majority of countries, of which Mexico is not the exception, the best sites for hydraulic exploitation have already been selected and the best works have already been built from the technical, economic, social, environmental and legal points of view; the possible projects to develop in the future have, in addition to technical and economic difficulties, great social, environmental and resource availability pressures.

One of the traditional concepts in the design of reservoirs is linked to the useful life: the reservoir must operate efficiently for the purposes it was designed for a number of years. The concept of useful life has a radical change; on the one hand, in an environmentally sustainable vision, it is unacceptable that at the end of the useful life the work should be left as it was; therefore, today it is required to dismantle it; of course, the dismantling process must be ecologically monitored. In the USA and Europe, they seek to leave the river in ecological and morphological conditions as close as possible to those that were before the construction of the dam.

The retention of sediments is one of the limitations of the useful life of reservoirs; if it is considered that a design standard was that the infrastructure had a useful life of 50 to 100 years, many works in the world and particularly in Mexico are close to that limit, both in its operation and silting aspects. Given that there are neither the resources nor the sites to carry out new projects of significant magnitude, the available infrastructure should be used as much as possible.

It is important to highlight here the importance of making measurements of sediment inputs; In addition to the fines that are measured in the gauging stations, you have to measure the solid expenditure in the background.

Nowadays in Mexico there are no exclusive programs for the measurement of sediments, the measurements are limited to stations measuring weather, hydrometric, hydroclimatological and water quality measurement stations and eventually in the hydrometric stations are made routine measurements of concentration of solids near the surface, with this last measurement, as a reference base, a methodology of the forties. From these measured values, solid expenses are calculated, often from unreliable assumptions without formal verification; In general, there are no routine measurements of bottom trawl transport in Mexico, so trying to infer it from suspended load implies serious errors, especially during the flood season where the bottom load is greater [17].

Given the scarcity of data on sediments, to make the necessary estimates, the bathymetries turn out to be an economical and reliable practice to obtain a numerical approximation to the sedimentation that occurred in each reservoir. The existence of bathymetries allows to estimate the total volume of sediments deposited in the reservoir vessel and even its evolution.

In Mexico, the most accurate estimation of sediment contributions is made through the topobatimetric surveys of reservoirs with a certain frequency, the National Water Commission carries them out in the Investment Program K139 called Investment for the Integral Management of the Hydrological Cycle, in charge of the Technical General Subdirectorate.

The sediments are deposited in the reservoirs at all elevations, making the area-capacity curve (ASC curve) change. Empirical methods have been developed to determine the distribution of sediment deposition within the vessel as a function of depth, which allows to calculate the future displacement of the ASC curve. These methods are much faster and easier to use than mathematical models and also require less data. When sediment input data from an existing deposit is available, the observed deposit pattern can be used to select the appropriate empirical relationship to calculate the change in the ASC curve.

The theoretical approaches to reservoir sedimentation forecasting are mathematical methods that can be divided into analytical and numerical. Regardless of the type of theoretical model used, it is necessary to calibrate or verify the results of the calculations. Such verification is carried out in comparison with the results of field tests, which often form the basis of empirical methods. The results allow knowing the evaluation of the approximate course of the phenomenon or process analyzed.

Churchill [7], Brune [5], Borland and Miller [2], among others, studied sediment deposition processes, for the US Department of the Interior Bureau of Reclamation (1989), as well as, examined the methods, both empirical as numerical, of estimation of the long term deposit in the reservoirs. They approached the management of the Dams, emphasizing the possibility of preserving their capacity for their future use and carried out real case studies showing the problems related to the sedimentation of reservoirs. Among the first empirical models to determine the distribution of sediments within the vessel of the Dams, we can distinguish several, for example models described by Cristofano [6], Borland and Miller [2], Lara [13], Hobbs [10], Borland [3], in addition to Pemberton [16], Qian [18], Annandale [1], Mohammadzadeh and Heidarpour [14], Rahmanian and Banihashemi [19], Bogusław [4] and Hosseinjanzadeh-Kaveh-Mousavi [11].

Empirical methods for the prediction of sediment distribution have been developed through the investigation of large reservoirs. One of the most used is the one proposed in 1958 by Borland and Miller [15], the so-called Empirical Area-Reduction Method (EARM), which was established on the basis of the results of sedimentation measurements of 30 reservoirs with a capacity of 1.36 million m^3 to 38 billion m^3. This method, verified by [13] and [15], is based on the conclusion that the change in the thickness of the deposits along the length of the reservoir is characteristic for the groups of reservoirs with similar uptake properties, vessel shape, method of operation and characteristics of deposited sediments.

Reference [14] used a new empirical method for the prediction of sediment distribution in reservoirs with storage capacities from 484 thousand m^3 to 39 billion m^3 based on the data of the corresponding original and secondary elevation ASC curves the latter to subsequent sedimentation survey data of 40 reservoirs in the United States of America. In its proposed method, the distribution of sediments in a deposit is related to the volume of sediments and the original characteristics of storage.

Reference [11] propose a new empirical method for the prediction of the distribution of sediments in reservoirs with storage capacities from 392 to 1,491,924 acre-ft based on the data of the original and secondary ASC curves corresponding to 25 topobatimetric surveys of 16 reservoirs in the United States of America. The proposed method is similar to that used by [14], also considering that the distribution of sediments in the vessel is related to the volume of sediments and the original storage characteristics. It is worth mentioning that [12], carried out the application of adjustment of the ASC curves to the Mosul Dam, in Iraq; for two existing ASC curves, using the methodology of [14] and [11], as well as 11 reservoirs operated by the USBR modifying the adjustment theories of [14] and [11]. They determined that there is a linear variation of

the storage coefficient (N) defined by these authors over time, they conclude according to the dams analyzed, that there is a better fit with the Kaveh equations, for the medium term, so that the method of area reduction presented the highest percentage of error when applying it to infer the behavior of the Mosul Dam, Iraq, for 50, 75, 100 and 125 years.

In this study three different empirical methods were evaluated. These methods are: the area reduction method proposed by [2] that has been adopted by the U.S. Bureau of Reclamation and the methods reported by [14] and [11]. The methods were applied to determine the ASC curves and maximum water depth or depth of sediment in the site of the dams Jesus María (JMD), La Chirimoya (CHD), boths in the State of Guanajuato and Manuel Felguérez, Lobatos (LD), State of Zacatecas. The results provided by these methods were compared with the original and secondary bathymetric survey data for these three reservoirs located in the Mexican Republic.

Thus, the main objective of this study was: evaluating these methods with reference to the bathymetric survey for determining ASC curves and maximum sediment depth at dam site.

The evaluation of these methods can help decision makers, planners and designers, to use these methods to determine the ASC curves for reservoirs that were used to estimate their useful life.

THE DAMS AND AVAILABLE DATA

For the present study, three reservoirs located in the Mexican Republic were selected: Jesús María Dam (JMDR), Municipality of San Felipe, State of Guanajuato; The Chirimoya Dam (CHDR), Municipality of San Felipe, State of Guanajuato, and The Lobatos Dam (LDR), Municipality of Valparaíso, State of Zacatecas, which meet the following conditions: 1) At least two different surveys are available; 2) The storage is not used as a side vase, 3) There are no upstream of your vat retaining dams, diversion dams or storage dams and 4) His wall has not been raised.

Some of its main characteristics are described below:

The Jesús María Dam, Municipality of San Felipe, State of Guanajuato

Was built by S.A.R.H. during the period from 1986 to 1991, entering into operation this last year (1991). It is located on the De La Laja River, tributaries of the Lerma River and the purpose of its construction was to make more efficient use of the runoff from the river and the contributing streams of the basin. This dam benefits an area of 2,100 hectares and controls the avenues to protect the communities of San Antonio de Jesus Maria, San Pedro de la Palma and Tepozán, all in the municipality of San Felipe in the State of Guanajuato. The bathymetric survey of the Jesús María Dam, Guanajuato, was carried out during the month from January 2012.

The Chirimoya Dam, Municipality of San Felipe, State of Guanajuato

The Chirimoya Dam, Municipality of San Felipe, State of Guanajuato, was built in 1975-1981, by the construction company ICA, S. A., the construction supervised by the residence of the Undersecretary of Hydro-Agricultural Infrastructure of the Ministry of Agriculture and Hydraulic Resources, is located in the Northwest portion of the State of Guanajuato, with the purpose of taking advantage of and controlling the avenues of the San Bartolo River, tributaries of the Santa María River that discharges 10 km from the community of Jaral de Barrios, forming part of the River basin Pánuco, this dam was destined to irrigate 751 ha, although the original project was 905 ha and its useful design capacity was 4.87 hm^3. Its operation is in charge of the user association. The bathymetric survey of the Chirimoya Dam, Guanajuato, was carried out during the month from January 2012.

The Manuel Felguérez Dam (Lobatos), Municipality of Valparaíso, State of Zacatecas

Is built on the Pajaritos River, which in turn is a tributary of the Valparaíso River, which discharges into the Bolaños River, upstream of the vessel, is located the Arroyo Pomas that downloads in this. The dam has a total capacity of 9.80 million m^3 and is used to control the Pajaritos River, to take advantage of its irrigation waters of 667 ha of land immediately adjacent to the towns of Lobatos, Mala Noche, El Vergel and Ejido Valparaíso. The bathymetric survey of the Chirimoya Dam, Guanajuato, was carried out during the month from April 2012.

The survey

Was conducted according to U.S. Army Corps of Engineers standards [20] for the distances between transverse sections, boat type and calibration methods. The error values of water depth measurements were 0.03 to 0.07 m depending on the water depth within the reservoir.

The survey results were also used to construct ASC capacity curves (Figs. 1, 2, and 3), the original characteristics of the studied reservoirs are presented in the same figures.

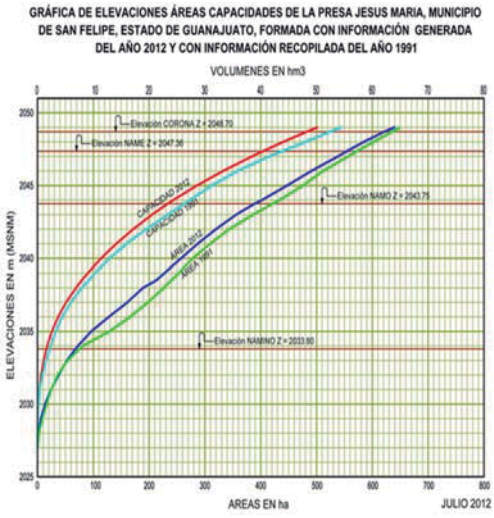

Fig. 1 Area-storage capacity curves for the JMDR

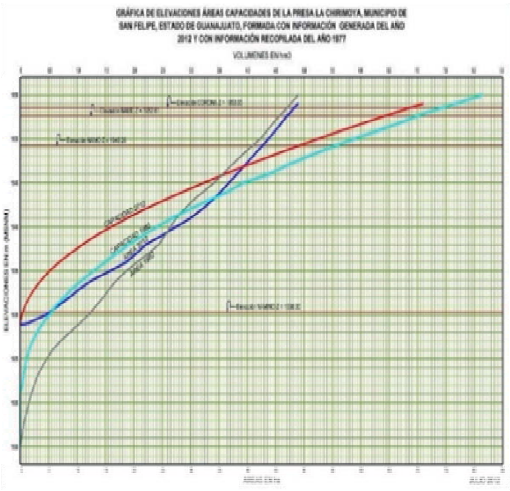

Fig. 2 Area-storage capacity curves for the CHDR

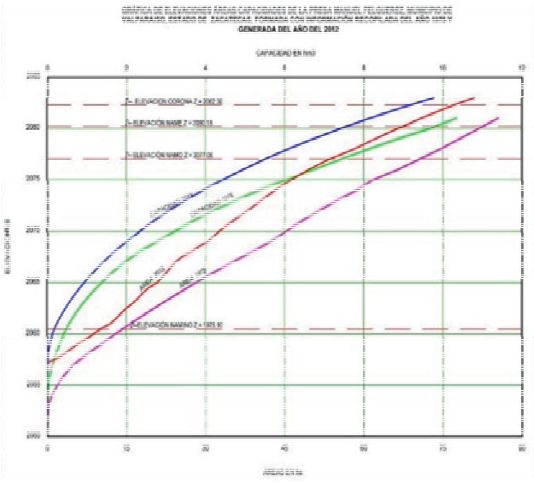

Fig. 3 Area-storage capacity curves for the LDR

TECHNIQUES AND METHODS USED

Empirical techniques are used to determine the amount of sediment deposited in a reservoir as a function of water depth or to determine ASC curves. These methods are widely used for engineering purposes. Consequently, large numbers of empirical methods have been reported but the most commonly used is the area reduction method that was developed and adopted by the U.S. Bureau of Reclamation [15].

The first empirical method was developed by [2] referred to as area increment method. This method assumed that the reduction on water surface area at any depth above the new zero depth is constant, meaning that an equal amount of sediment will be deposited in each depth increment of the reservoir [2],[20].

The following methods were used in this study:

The Area-Reduction Method (EARM)

The EARM is the most commonly used method for predicting the impact of sediment deposition in a reservoir or the change in the ASC curves with reservoir sedimentation. The method was proposed by [2] based on an analysis of sedimentation data for 30 reservoirs in the USA. This technique is based on the adjustment of the water surface area above zero depth to a new area due to sedimentation that reflects the relationship between reduction in water surface area and sedimentation rate and reservoir characteristics. Reservoirs are classified in to four categories based on the shape factor of the reservoir "M" (Table 1). The shape factor "M" represents the reciprocal slope of the straight line that can be calculated from plotting the relationship of water depth at the dam site as the Y-axis against the storage capacity as the X-axis on a logarithmic scale plot [2], [11], [14] and [12]. The area reduction method involves four different sedimentation pattern curves that were developed from the resurvey data assembled for 30 reservoirs (Fig. 4). These curves are dimensionless and are used to determine the change in the ASC curves due to sedimentation. This technique is usually used when the sedimentation rate and characteristics of the reservoir are available.

Table 1 Reservoirs classification according shape factor "M", source: Borland & Miller (1958)

Type of reservoir	Classification	Shape factor M
I	Lake	3.5-4.5
II	Flood plain-foot hill	2.5-3.5
III	Hill	1.5-2.5
IV	Gorge or normally empty	1.0-1.5

The Mohammadzadeh-Habili semi-empirical method

Reference [14] proposed a dimensionless equation for the relationship between water depth and storage capacity using the similarity between the natural logarithmic function curve and the stage-storage capacity curve. This equation depends on only one unknown dimensionless parameter called the reservoir coefficient "N" as follows:

$$V_y = V_m \left[e^{\ln 2 * \left(\frac{y}{y_m}\right)} - 1 \right]^{\frac{1}{N}} \quad (1)$$

where Vy is reservoir capacity at depth y, Vm is reservoir capacity at maximum pool level, y is the water depth above the stream bed at the dam site and ym is the maximum water depth at the dam site. The water surface area and reservoir coefficient equations were derived from Eq. (1) as follows:

$$A_y = \frac{V_m * (\ln 2)}{N * y_m} * e^{\ln 2 * \left(\frac{y}{y_m}\right)} * \left[e^{\ln 2 * \left(\frac{y}{y_m}\right)} - 1 \right]^{\frac{(1-N)}{N}} \quad (2)$$

$$N = 2(\ln 2) \frac{V_m}{A_m * y_m} \quad (3)$$

where Ay is reservoir water surface area at depth y, and Am is the water surface area of reservoir at maximum pool level.

The equations obtained were compared with the resurvey data for 16 reservoirs. The comparison of the results demonstrated good agreement, especially with reservoirs that had smoothed stage-storage capacity curves. Furthermore, the results were used to develop an empirical relationship between the reservoir shape factor "M" and its coefficient (Eq. (4), [12]).

$$\mathbf{N = 1.075M^{-0.9063}} \quad (4)$$

Reference [14] modified the reservoir coefficient equation (Eq. (3)) based on the original and secondary ASC curves of 40 resurveyed reservoirs in the United States as:

$$N = 2(\ln 2) \frac{N_{SSE}(Minimization\ of\ SSE)}{N} \frac{V_m}{A_m * y_m} \quad (5)$$

where N_m is the modified reservoir coefficient and N_{SSE} is the reservoir coefficient obtained using minimization of the sum of squares of the errors (SSE) of the original normalized water depth–capacity curve and the curve from Eq. (3).

The Kaveh et al. method

A parabolic equation is used to represent the general form of the relationship between storage capacity and depth which can be expressed as follows:

$$\mathbf{V_y = a + b * y + c * y^2} \quad (6)$$

where a; b; c are the coefficients that are usually computed using the ACAP computer program adopted by the U. S. Bureau of Reclamation [8] and [11] differentiated the simple dimensionless capacity equation using a parabolic equation for reservoir capacity. Kaveh's equation depends on one reservoir coefficient parameter as:

$$\mathbf{V_y = V_m * \left(\frac{y}{y_m}\right)^{\frac{2}{N_*}}} \quad (7)$$

where $\mathbf{N_*}$ is the reservoir coefficient proposed by Kaveh et al. (2013).

The water surface area equation for a reservoir at different elevations and the reservoir coefficient equation were obtained as a derivative of the above Eq. (7) as follows:

$$\mathbf{A_y = \frac{2 * V_m}{N * y} \left(\frac{y}{y_m}\right)^{\frac{2}{N_*}}} \quad (8)$$

$$N_* = \frac{2 * V_m}{y_m * A_m} \quad (9)$$

In addition Kaveh et al. (2013) [11] derived a relationship between the reservoir coefficient and the shape factor based on the above equations, which is:

$$\mathbf{N_* = \frac{2}{M}} \quad (10)$$

It should be noted here, the three approaches suggested by [14] and [11] that are described above, mainly depend on the dimensionless parameters (N or N_*) in their calculation which are called reservoir coefficients. These coefficients depend on the dimensionless relationship between the ratio of volume $\frac{V}{V_m}$ and ratio of water depth at dam site $\frac{y}{y_m}$ as stated in Eqs. (1) and (7) for N and N_* respectively. These coefficients depend on the sedimentation condition. Therefore, the reservoir coefficient value changes with time depending on these conditions too. It should be mentioned however, that last three mentioned methods did not take in to consideration future variation in this relationship or reservoir coefficient in response to sedimentation.

Methodology

The three methods described above were firstly applied for the JMDR, CHDR and LDR to generate ASC curves for the reservoir after 21, 35 & 32 years

of dams operation, respectively. To apply the EARM, the first step necessitated selecting the type of reservoir or type of sediment deposition pattern. This process depends on the shape factor, the mode of operating the reservoir and the predominant grain size of the sediment deposited [15]. This information was used to select the appropriate empirical curve that was used to predict the sediment distribution within the reservoir.

According to data the classification for the JMDR, CHDR and LDR based on the slope of the original depth–capacity curve plotted on log–log paper is clasified as Type IV, Type III & Type III, wich represents Gorge or normally empty and Hill reservoir type, respectively (Table 1). The empirical curve type was used to develop a stage-capacity curve for 21, 35 & 32 years for JMDR, CHDR and LDR, respectively. (Figs. 4, 5 and 6).

In addition to the above, the methods proposed by Mohammadzadeh-Habili and Heidarpour and Kaveh et al., were used to determine ASC curves and maximum water depth at the dam site using the sedimentation survey data for JMD, CHD and LD as follow: The dimensionless relationship of depth–capacity curve of JMD, CHD and LD for 1991-2012, 1977-2012 and 1980-2012 surveys, respectively, were used to calculate its reservoir coefficients (N, N_m and N_*) that were employed by Mohammadzadeh-Habili and Heidarpour and Kaveh et al. respectively.

The storage capacity for different elevations for JMD, CHD and LD were computed using Eqs. (1) and (7) based on its reservoir coefficients that were computed from the dimensionless relationship of its original depth–storage capacity curve.

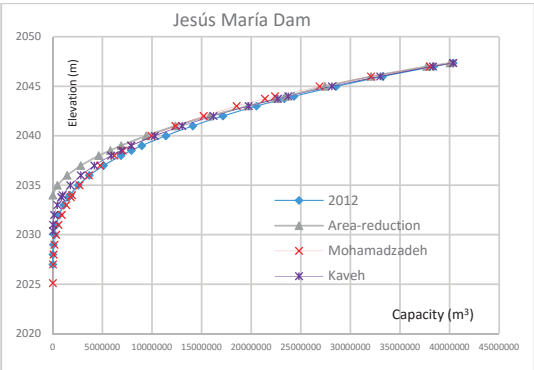

Fig. 4 Stage storage-capacity curves for the JMDR for 21 year of dam operation

Eqs. (2) and (8) were used to compute the water surface area for the same elevations using the same reservoir coefficients.

These results obtained from the above steps were used to construct the stage-storage capacity curves (Fig. 5, 6 and 7).

Eqs. (3), (5) and (9) were used to determine water depth at the dam site for the methods of [14] and [11] respectively (Table 2).

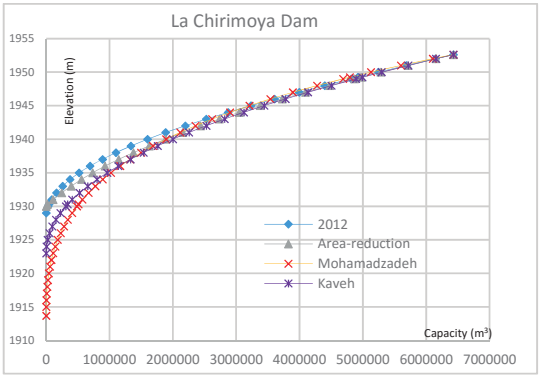

Fig. 5 Stage storage-capacity curves for the CHDR for 32 year of dam operation

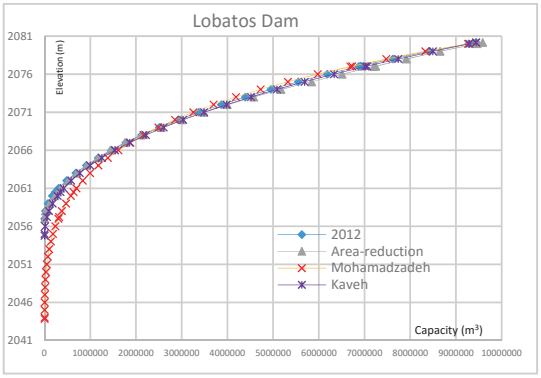

Fig. 6 Stage storage-capacity curves for the LDR for 35 year of dam operation

Table 2 Variation of maximum water depth at dam site with sedimentation.

Source of water depth:	water depth and % Error	JMD	CHD	LD
Secondary Survey	y_m (m)	20.36	23.61	20.36
Mohamad-zadeh et. al.	y_m (m)	22.24	38.95	22.18
	% Error	-9.23	-64.97	-8.94
Kaveh et. al.	y_m (m)	16.98	29.62	36.37
	% Error	16.60	-25.46	-78.64
Area-reduction	y_m (m)	13.36	22.61	25.42
	% Error	34.38	4.19	-24.85

EVALUATION AND COMPARISON OF THE TECHNIQUES USED

The three methods described in the previous sections were evaluated by testing them against the bathymetric survey data for the JMD, CHD and LD obtained by a bathymetric survey conducted in 2012. The percentage errors for the maximum water depth at the dams site for all methods based on the bathymetric survey results are tabulated in Table 2. For estimating maximum water depth at the dam site all three methods yielded approximate results with errors that ranged between 4.19 and 78.64% but the method of [14] gave results close to those obtained by the bathymetric survey. The other methods, however, predicted a water depth greater than that provided by the bathymetric survey. This implies that the deposition depth predicted by these methods is less than that represented by the actual sedimentation rate at the site of the dam. This could be because the presented algorithms suppose the non-variation of the maximum area and therefore a similar secondary volume measured in the secondary survey (Table 3), achieving a better fit for the higher values of the ASC, reducing the residuals and the sum of squared errors (SSE), a criterion that was used to evaluate the precision of the results (Table 4).

Table 3 Variation of secondary reservoir volume at maximum water level at dam with sedimentation

Reservoir volume secondary	V_s and % error	JMD	CHD	LD
Secondary Survey	V_s ($10^6 m^3$)	40.36	6.43	9.44
Mohamad-zadeh et. al.	V_s ($10^6 m^3$)	40.36	6.43	9.44
	% Error	0	0	0
Kaveh et. al.	V_s ($10^6 m^3$)	40.36	6.43	9.44
	% Error	0	0	0
Area-reduction	V_s ($10^6 m^3$)	40.03	6.43	9.58
	% Error	0.817	0	-1.5

Table 4 Sum of squared errors (SSE)

Secondary reservoir volume	JMD	CHD	LD
Mohamad-zadeh et. al.	$2.8x10^{13}$	$3.2 x10^{12}$	$1.8 x10^{12}$
Kaveh et. al.	$1.2 x10^{13}$	$2.5 x10^{12}$	$2.9 x10^{11}$
Area-reduction	$5.0x10^{13}$	$7.3 x10^{11}$	$7.3 x10^{11}$

The stage-storage capacity curves show that the the method of [11] provided results that were in close agreement with the actual survey data, when compared to other methods. The results showed that all methods converge and produce good agreement with the survey data (Figs. 7-15).

The results of these three methods showed that the method of [11] gave convergent results with low percentage of errors (Table 4).

According to the above results the method proposed by [11] is considered a good approach for computing and predicting the ASC curves due to its accurate results and its ease of use.

Empirical methods have been developed to determine the distribution of sediment deposition within the vessel as a function of depth, what allows to calculate the future displacement of the ASC curve. Three empirical methods for deriving these curves were applied to the JMD, CHD and LD.

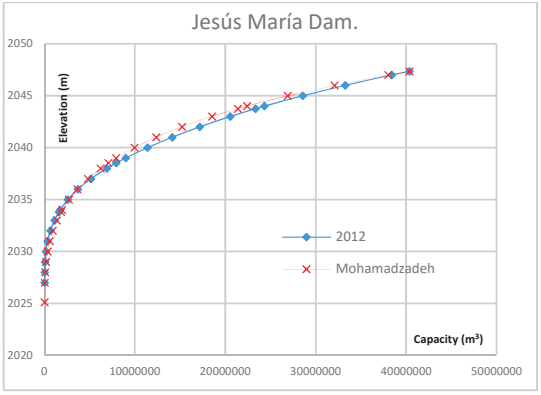

Fig. 7 Original and secondary elevation-capacity data of JMD, Mohammadzadeh-Habili and Heidapour method (2010)

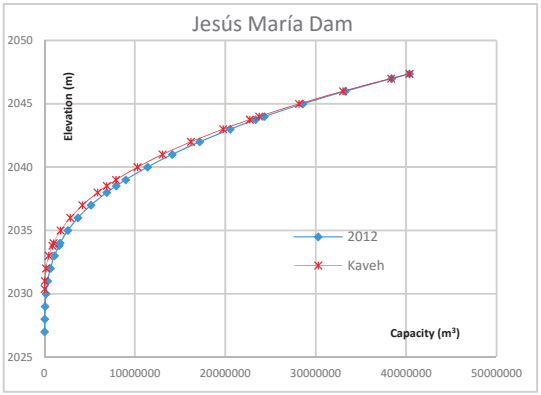

Fig. 8 Original and secondary elevation-capacity data of JMD, Kaveh et al. method (2013)

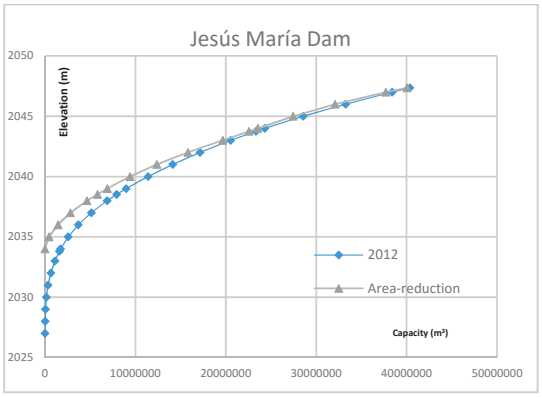

Fig. 9 Original and secondary elevation-capacity data of JMD, Area-Reduction method (2013).

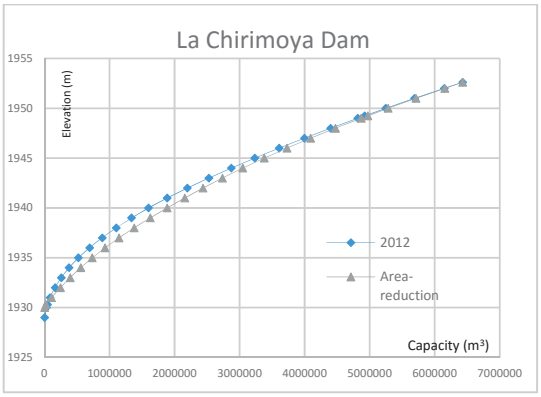

Fig. 12 Original and secondary elevation-capacity data of CHD, Area-Reduction method (2013)

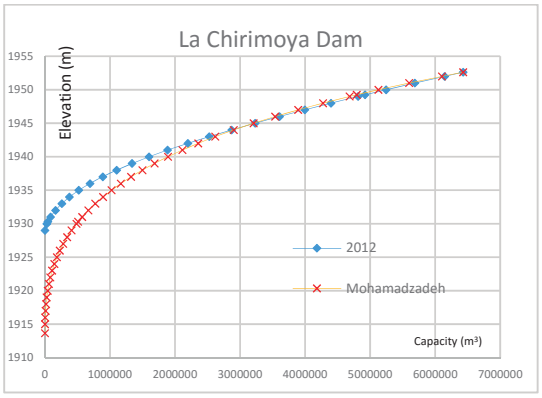

Fig. 10 Original and secondary elevation-capacity data of CHD, Mohammadzadeh-Habili and Heidapour method (2010)

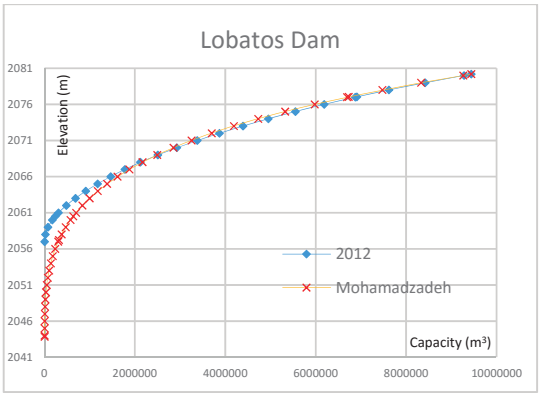

Fig. 13 Original and secondary elevation-capacity data of LD, Mohammadzadeh-Habili and Heidapour method (2010)

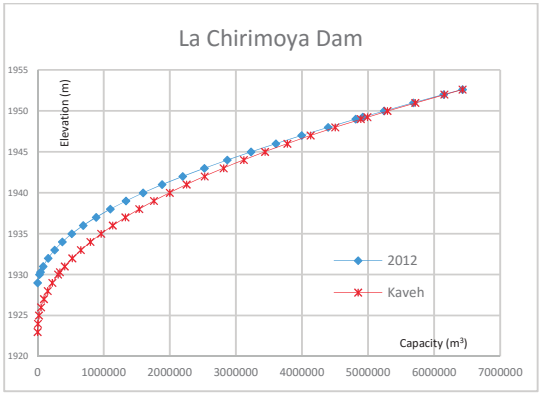

Fig. 11 Original and secondary elevation-capacity data of CHD, Kaveh et al. method (2013)

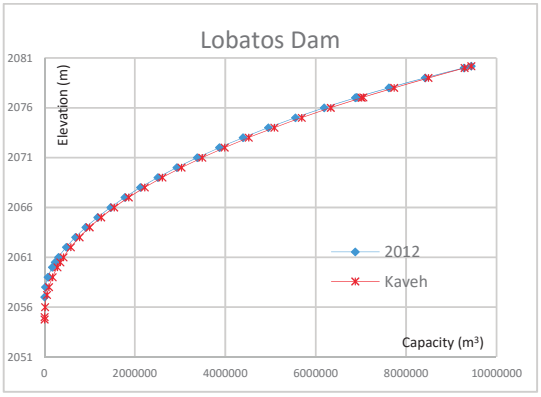

Fig. 14 Original and secondary elevation-capacity data of LD, Kaveh et al. method (2013)

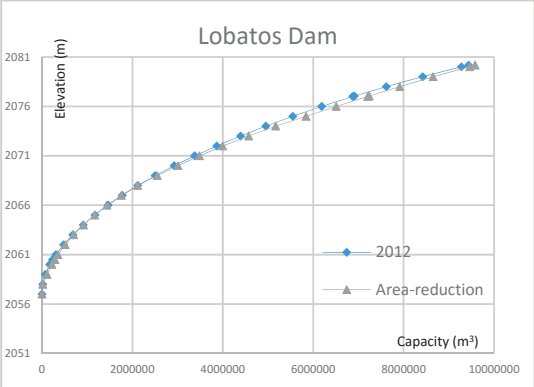

Fig. 15 Original and secondary elevation-capacity data of CHD, Area-Reduction method (2013)

CONCLUSIONS

The sediments are deposited in the reservoirs at all elevations, making the ASC curve change.

These methods include the area reduction method Borland & Miller and those proposed by, Mohammadzadeh-Habili and Heidarpour and Kaveh et al. The results were compared with those obtained using the bathymetric survey conducted in 2012 after 21, 35 & 32 years of operating, respectively. The comparison of the results for establishing the ASC curves showed that the method proposed by Kaveh et. al. gave good agreement with bathymetric results. For maximum water depth at the dam site or sedimentation depth the Mohammadzadeh-Habili and Heidarpour and Kaveh et. al. methods were more accurate for determining sedimentation depth at the dam site with a percentage errors that ranged between 4.19 and 78.64%.

REFERENCES

[1] Annandale, G.W. Predicting the distribution of deposited sediment in southern African reservoirs. Challenges in African Hydrology and Water Resources (Proceedings of the Harare Symposium, July 1984); International Association of Hydrological Sciences Publication: Harare, Zimbabwe; Volume 144, pp. 549–558.

[2] Borland, W. M., & Miller, C. R. (1958). Distribution of sediment in large reservoirs. Journal of the Hydraulics Division, 84(2), 1587.1–1587.10.

[3] Borland, W.M. Reservoir Sedimentation, River Mechanics; Shen, H.W., Ed.; Water Resources Publisher: Fort Collins, CO, USA; 1970, Chapter 29, pp. 1–38.Annnn B, “Unpublished work but accepted”, accepted, Year.

[4] Bogusław M. The Use of Modified Annandale’s Method in the Estimation of the Sediment Distribution in Small Reservoirs-A Case Study. Water 2014, 6, 2993-3011; doi:10.3390/w6102993.Islam MR, “Conference proceedings”, in Proc. 2nd Int. Conf. on GEOMAT, 2011, pp. 8-13.

[5] Brune, G.M. Trap efficiency of reservoirs. Transactions, American Geophysical Union, Volume 34, Number 3:1953, pp. 408-415.

[6] Cristofano, E.A. Area-Increment Method for Distributing Sediment in a Reservoir; US Bureau of Reclamation: Albuquerque, NM, USA, 1953.

[7] Churchill, M. A. Discussion of “Analysis and Use of Reservoir Sedimentation Data,” by L. C. Gottschalk, 1948, pp. 139-140, Proceedings of the Federal Inter-Agency Sedimentation Conference, Denver, Colorado.

[8] Ferrari, R. L., & Collins, K. (2006). Reservoir survey and data analysis In: Bureau of reclamation, erosion and sedimentation manual. Chapter 9. Denver, Colorado, USA: Sedimentation and River Hydraulics Group, http://www. usbr.gov/pmts/sediment.

[9] Churchill, M. A. Discussion of “Analysis and Use of Reservoir Sedimentation Data,” by L. C. Gottschalk, 1948, pp. 139-140, Proceedings of the Federal Inter-Agency Sedimentation Conference, Denver, Colorado.

[10] Hobbs, B.L. Forecasting Distribution of Sediment Deposits in Large Reservoirs; Appendix I,.ETL 1110-2-64; Department of the Army, Office of the Chief of Engineers: Washington, DC, USA, 1969.

[11] Hosseinjanzadeh, H.; Kaveh, K.; Mousavi Sayed-Farhad. New proposed method of reservoir sedimentation distribution. International Journal of sediment Research. Publicado por International Research and Training Center on Erosion y Sedimentation/the World Association for Sedimentation and Erosion Research. Elsevier B. V., 2015.

[12] Issa. I. et al. Evaluation and modification of some empirical and semi-empirical approaches for prediction of area-storage capacity curves in reservoirs of dams International Journal of sediment Research, 2016, http://dx.doi.org/10.1016/j.ijsrc.201.12.001

[13] Lara, J.M. Revision of the Procedure to Compute Sediment Distribution in Large Reservoirs; US Bureau of Reclamation: Denver, CO, USA, 1962.

[14] Mohammadzadeh-Habili, J., & Heidarpour, M. (2010). New empirical method for prediction of sediment distribution in reservoirs. Journal of Hydrologic Engineering, 15 (10), 813–821. http://dx.doi.org/10.1061/(ASCE)HE.1943-5584.0000259.

[15] Morris, G.L., & Fan, J. Reservoir sedimentation handbook, design and management of dams, reservoirs, and watersheds for sustainable use. NewYork, USA: McGraw-Hill Book Co., 1998, pág. 10.31.

[16] Pemberton, E.L. Reservoir Sedimentation. Proceedings of the US-Japan Seminar on Sedimentation and Erosion, Honolulu, HI, USA, 20–24 March 1978.

[17] Peters, J. J. Diseño de sistemas (Métodos y Procedimientos) Aplicables en México para la Medición de Sedimentos en Suspensión y Arrastre de Fondo, Prepared by the World Meteorological Organization and the National Water Commission under the Agreement CNA-OMM, Ginebra, december 1998. pp. 5.

[18] Qian, N. Reservoir sedimentation and slope stability, technical and environmental effects. General Report, G.R.54. Proceedings of the 14th International Commission on Large Dams Congress, Rio de Janeiro, Brazil, May 1982, pp.14–17.

[19] Rahmanian, M.R.; Banhashemi, M.A. A new empirical reservoir shape function to define sediment distribution pattern in dam reservoirs. IJST Trans. Civ. Eng. 2012, 36, 79–92.

[20] Strand, R. I., & Pemberton, E. L. (1982). Reservoir sedimentation In: Technical guideline for bureau of reclamation, technical services engineering and research center (p.55) Denver, Colorado: Bureau of Reclamation's Sedimentation and River Hydraulics Group.

[21] U.S. Army Corps of Engineers (2004). Engineering and design hydrographic surveying. Department of Army, Washington, DC 20314-1000. Em1110-2- 1003/ toc.htm.

SUSPENDED SEDIMENTS CONTENT ALONG THE USUMACINTA RIVER, THE MEXICAN TROPICS

Oseguera Luis A. [1], Alcocer Javier [1], Cuevas Daniel [2] and Cortés Guzmán Daniela [2]
[1]Proyecto de Investigación en Limnología Tropical, FES Iztacala, UNAM, México; [2]Programa de Posgrado en Ciencias del Mar y Limnología, UNAM, México

ABSTRACT

The Usumacinta is the most important river in Mexico (2,678 $m^3 s^{-1}$). 58% of its watershed is in Guatemala and the remaining 42% in Mexico representing 4.7% (91,345 km^2) of the total Mexican territory. As other tropical fluvial systems, its role in transporting materials is assumed to be important, yet not measured at the time. Herein we present the first report of the suspended sediment (SS) along the Usumacinta River and its tributaries. Samples were taken during the dry (DS, May 2017) and the wet (WS, November 2017) seasons. The SS in WS (6.8–131 mg L^{-1}) was higher than in DS (6.1–90.3 mg L^{-1}). The largest amount of SS in DS was found in San Pablo (59.9 ± 17.7 mg L^{-1}), and the lowest in Boca del Cerro (7.1 ± 1.1 mg L^{-1}). Differently, the SS largest amount in the WS was found in Lacantún (118.9 ± 14.0 mg L^{-1}), while the lowest was in San Pedro (8.0 ± 1.2 mg L^{-1}). There were differences among sampling stations during both seasons, although no correlation between concentration and discharge was found. SS fluxes were also higher in WS, with a maximum value of 38,359.7 ± 6,784.1 in the Usumacinta- Grijalva confluence and the minimum was in Tzendales, while maximum value during DS was 1,339.5 ± 783.4 at Grijalva station and minimum in Tzendales. F_{SS} showed a downstream increase along the basin during WS while remained similar in DS.

Keywords: Suspended Sediments, Tropical Rivers, Mexico, Sediment Transport, Hydrology

INTRODUCTION

The Usumacinta River is the largest fluvial system at regional scale; it is a priority region based on its hydrological resources and high biodiversity [1]; it is located within the remaining largest area of tropical forest in Mexico. Estimates on global carbon transport have shown that tropical rivers on wet climates have the greatest contributions of carbon discharges toward the ocean [2]. Nevertheless, size and composition of transported sediments in tropical fluvial systems has not been characterized, even though their contribution is disproportionately higher compared to high latitude rivers.

Rivers with massive sediment load and water flow play an important role in transporting particulate materials from terrestrial environments to the oceans, and through their path from headwaters to river mouth, temporal variations on its discharges, sediment loads, and concentration of transported materials takes place [3]. In this sense, water and materials that flows through the river may come from regions with different climate [4], whereby longitudinal and seasonal measurements of the transported material in several points of the basin are of great importance.

The fluxes of materials in fluvial systems are driven by different sets of environmental factors and conditions, like basin area, slope, temperature, runoff, lithology and human activities [5]. Many researches in riverine particulate material fluxes and inputs to the ocean consider few sampling points across the basin. A better understanding of temporal and spatial variations in river concentrations of this material will improve the identification of material and its fate in riverine environments [6].

"Suspended sediments" (SS) is a collective concept for all particulate material present in water, including biotic and abiotic components [7]. Synonyms of this are "seston" and "total suspended matter". To avoid confusion, from now on we will use SS throughout the paper. These suspended particles contribute significantly to river sediment budget, their importance is related to the nutrients and contaminants that are transported with them, their dependence on hydrological events and its implications on river water quality and sediment management plans [8].

Anthropogenic activities drive changes in transporting materials through the river. Those related to changes in land use, as mining, agriculture and urban growth, have significant consequences on the fluxes and material processing [2]. On the other hand, hydraulic engineering, water extraction, wastewater treatment, dredging and damming increase or diminish the sediment load [9].

The research and global estimates of riverine material fluxes has been susceptive to the lack of studies and data concerning to tropical latitudes. Frequently, the Amazon River has been used as model for tropical rivers, and there has been a rise in

the data availability from other tropical systems in Latin America and other regions in the planet over the last decade [10].

Here we present results from two campaigns carried out in wet (WS) and dry (DS) seasons over the Mexican portion of the Usumacinta River, that covers the mid and the low portions of the watershed. Our purpose is to assess the variations on the amount and fluxes of suspended sediments along the river, its main tributaries and the river mouth in Gulf of Mexico, in two contrasting seasons.

MATERIALS AND METHODS

Study Area

The Usumacinta River belongs to the No. 30 Grijalva-Usumacinta hydrological region, at the Mexican SE. The headwaters of the river is in the Cuchumatanes mountain range, Guatemala. In the Mexican territory, the river crosses the states of Chiapas and Tabasco; the Grijalva River joins –artificially- the Usumacinta 15 km before the river mouth, at the Gulf of Mexico coastline [11]. Both rivers make up the largest fluvial system of Mexico, and the 10th in North America [11], with a length of ~1,100 km, an area of ~112,000 km^2 and an annual discharge of ~2,678 m^3 s^{-1}[12].

The basin of these rivers is characterized by an important discharge associated to the wet climate with a mean annual precipitation over 2,000 mm, although spatial distribution of rains is variable [1], [11]. The wet season (WS) takes place between May and October, and the dry season (DS) between November and April [13]. Intense rainfalls produce sudden increases of the Usumacinta discharges, causing frequent flooding lowland [11].

Sampling Methods

Two sampling campaigns were carried out in May (DS) and November (WS) 2017. Logistics prevented the access to some portions of the river during DS that allow us to samples at just 7 stations, whereas in 18 stations during WS. The extent of the whole Usumacinta watershed comprises Guatemalan and Mexican territories. Nonetheless, this study considered only the Mexican side; for description purposes, we named high (A1–B3), middle (C–E3) and low basin (F–H) (Fig. 1).

At each station, the cross section bathymetric profile was measured with an Echo Sounder Garmin GPSMap 526S. Three points located at the center and 1/3 towards both sides across the river section were selected to measure physicochemical parameters with a Hydrolab DS5 multiparametric probe, and water velocity with a Swoffer 3000 current meter. Bathymetric profiles along with stream velocities were used to calculate water discharge (m^3 s^{-1}).

At the same three points, at 1/3 of maximum depth, water samples were taken with a horizontal Van Dorn-like bottle. A known volume of these samples was filtered in the laboratory through previously combusted (550°C / 4 h) and weighed Whatmann GF/F filters. After filtration, the filters were weighed again to obtain by subtraction the SS concentrations.

Fig. 1 Sampling stations along the Usumacinta River, Mexico

The concentrations along with the water discharge data were used to calculated SS fluxes (F_{SS}), following Eq. (1) [4]:

$$F_{SS} = M_Q * M_{SS} \quad (1)$$

Where, M_Q is the arithmetic mean of the discharge, and M_{SS} is the arithmetic mean of the suspended sediment concentration during the sampling days. The values were transform and reported in units of ton per day (t d^{-1}).

Differences between data were tested through Anova on Ranks and Student t test.

RESULTS AND DISCUSSION

Physicochemical Parameters

Temperature was higher during the DS with a maximum of 30.8°C in Frontera Corosal (C) and minimum of 27.3°C in Lacantún (A3). Whereas in the WS, the maximum of 30.2°C was observed in

Grijalva (G2) and the minimum of 20.8°C in Ixcán (A1) (Table 1). Dissolved oxygen was very similar in both seasons, only in Grijalva (G2) and San Pablo (H) were lower during the WS (Table 1).

Electric conductivity (K_{25}) was usually higher during the DS. Moreover, K_{25} in the stations near the river's mouth (Usumacinta, Grijalva and San Pablo) were 100-fold higher than through the WS (Table 1). The above is due the fact that during the DS there is a marine wedge. Contrary to K_{25}, turbidity was larger during the WS with exception of San Pablo (H), where the higher turbidity occurred through the DS (Table 1).

Table 1 Physicochemical parameters measured in the sampled stations during the dry (DS) and wet (WS) seasons, the Usumacinta River, Mexico. (Zmax = maximum depth, Temp = temperature, DO = dissolved oxygen, K_{25} = electric conductivity, Turb = turbidity, - = no data). (The stations are ordered upstream to downstream)

	Station	Zmax (m)		Temp (°C)		DO (mg l^{-1})		K_{25} (µS cm^{-1})		Turb (NTU)	
		DS	WS	DS	WS	DS	WS	DS	WS	DS	WS
High	A1	-	1.4	-	20.8	-	8.6	-	319	-	102
	A2	-	4.0	-	21.3	-	8.4	-	241	-	99
	A3	3.5	6.0	27.3	22.2	6.3	8.5	395	374	77	101
	A4	1.4	3.0	27.8	23.4	7.2	8.0	931	539	10	8
	A5	-	7.0	-	22.4	-	8.4	-	384	-	99
	B1	-	10.4	-	24.2	-	6.4	-	288	-	80
	B2	-	10.3	-	25.9	-	1.6	-	319	-	5
	B3	-	11.9	-	25.1	-	4.0	-	304	-	60
	Mean	2.45	6.8	27.4	24.0	6.5	5.6	512	330	57	57
	S.D.	1.5	3.8	0.6	1.5	0.4	2.7	223	53	35	38
Middle	C	4.9	15.1	30.8	24.3	6.5	5.8	706	317	11	57
	D	25.0	35.0	30.6	24.9	6.4	6.6	839	359	7	52
	E1	-	11.5	-	27.0	-	4.6	-	737	-	5
	E2	-	13.8	-	25.2	-	6.5	-	355	-	49
	E3	-	20.3	-	25.5	-	6.3	-	400	-	40
	Mean	14.95	19.1	30.7	25.1	6.5	6.2	789	386	9	45
	S.D.	14.21	9.4	0.1	0.7	0.1	0.5	65	100	3	13
Low	F	-	3.9	-	26.6	-	4.7	-	362	-	46
	G1	13.6	16.9	29.9	26.7	3.2	4.6	32440	361	10	48
	G2	11.0	12.3	30.2	27.9	3.9	1.4	28631	337	8	82
	G3	-	15.1	-	27.4	-	2.8	-	357	-	61
	H	4.8	5.0	29.8	27.5	5.1	1.9	54825	395	188	55
	Mean	9.8	10.6	30.0	27.3	3.8	3.0	34192	358	36	50
	S.D.	4.5	5.9	0.8	0.5	2.1	1.5	17944	19	92	17
Total	Mean	9.2	11.3	29.6	25.2	5.8	5.2	10625	357	26.3	51
	S.D.	8.2	7.9	1.4	1.7	1.5	2.3	19322	73	43.4	27
	Min	1.4	1.4	27.3	20.8	1.2	1.3	393	317	5	2
	Max	25.0	35.0	31.1	28.0	7.2	8.6	58072	438	339	110

Suspended Sediments Concentrations

SS during the DS varied between 6.1 and 90.3 mg L^{-1}, its maximum mean value, 59.9 ± 17.7 mg L^{-1}, was found in San Pablo (H), and its minimum, 7.1 ± 1.1 mg L^{-1}, in Boca del Cerro (D). We found significant differences among stations ($H = 22.7$, $p < 0.001$) but without a trend along the basin. Instead, the data showed a decrease from high to middle basin, and then an increased from mid to low basin (Fig. 2). Furthermore, we found a negative correlation between concentration data and discharge ($r = -0.4$, $p < 0.05$). This relationship, although weak, is significant, which points out a reduction of concentration with the increment of water discharge, opposite to the expected.

SS concentrations during WS showed an increase compared with DS. The values ranged from 6.8 to 131.0 mg L^{-1}. Highest value was recorded in Lacantún (A3), with mean of 118.9 ± 14.0 mg L^{-1}, and lowest mean value, 8.0 ± 1.2 mg L^{-1}, in San Pedro (E1). The range between 0.1 and 483 mg L^{-1} in African rivers [14]–[16] resulted similar to our data, while lower comparing to the estimated global average of 500 mg L^{-1} [17]. Statistical differences were found among stations ($H = 63.4$, $p < 0.001$)

and a general trend of decrease on concentrations along the basin (Fig. 3). There is a strong SS concentrations seasonality in the Tana River (Kenya), with values varying over several orders of magnitude (24- 9,386 mg L^{-1}) [18].

We did not find a significant correlation between SS concentrations and water discharge ($r = 0.04$, $p > 0.05$). The fluvial sediment transport is a power function relative to the seasonality of the river discharge [6], [19]. Higher discharges usually imply an increase in turbulence, associated with a higher transport capacity of bed material in suspension [8]. This discharge increase frequently is a result of soil erosion and fine sediments input due to precipitation events and runoff in the river basin.

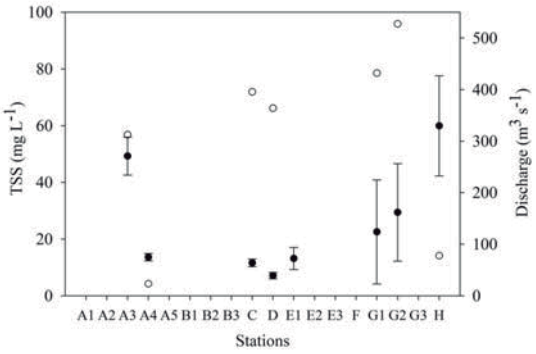

Fig. 2 SS concentration (± S.D.) (filled circles) and discharge values (open circles) at each sampled station during DS

Our results indicated a raise on the SS concentrations values during the WS compared to the DS, however there was no correlation between discharge and SS. The Tana River display a clear trend to decrease suspended matter from upstream to downstream, being most pronounced during high discharge conditions [18].

As mentioned, SS concentrations and water discharges are not always synchronized. The initial rains of the WS produce movement of surface soil layers and sediments; as the discharge continue to raise, the relative SS concentrations diminish, as observed by displacement of maximum concentration and discharge peaks [8], [18].

Suspended Sediments Fluxes

During the DS, the highest SS flux was found in Grijalva River (G2), with a mean of 1,339.5 ± 783.4 t d^{-1}, and the lowest in Tzendales (A4) with a mean of 27.2 ± 2.6 t d^{-1}. The values during the DS ranged from 25.4 to 2,388.3 t d^{-1}. The regression line shows relatively constant values along stations (Fig. 4).

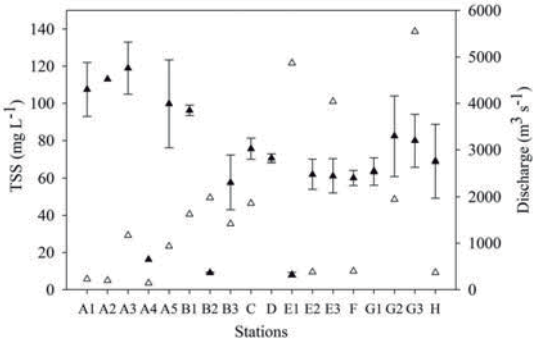

Fig. 3 SS concentration (± S.D.) (filled triangles) and discharge values (open triangles) at each sampled station during WS

During WS, the highest SS flux was found in the Usumacinta–Grijalva confluence (G3), with a mean of 38,359.7 ± 6,784.1 t d^{-1}, and the lowest in Tzendales (A4) with a single value of 13.6 t d^{-1}.The values varied from 13.6 to 48,269.2 t d^{-1}. The trend observed by regression line is an increase in fluxes along the basin (Fig. 4).

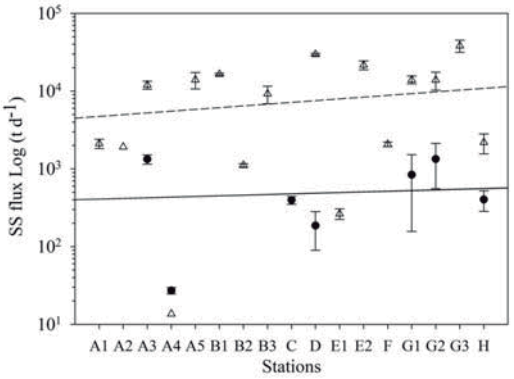

Fig. 4 SS mean fluxes (± S.D.) of sampled stations during DS (black circles) and WS (open triangles) seasons, and its regression lines (DS = continuous line, WS = dotted line)

We found seasonal differences in Lacantún (A3, $t = 18.3$, $p < 0.001$), Boca del Cerro (D, $T = 57$, $p < 0.05$), Usumacinta (G1, $t = 18.8$, $p < 0.001$), Grijalva (G2, $t = 8.3$, $p < 0.001$) and San Pablo (H, $t = 6.8$, $p < 0.001$), with highest values during WS, as expected, and increases of one order of magnitude or larger.

Large differences in the relative contributions of fluxes between dry and wet seasons are common. DS showed a lower contribution in the annual flux although an important water flow was maintained, indicating a larger reduction in the sediment content but not in the water discharge [10].

These findings suggest water discharge and sediment load have different dynamics. Thereby, SS concentrations in the Usumacinta River decrease during wet season, but SS flux increases, suggesting that fluxes rely strongly on water amount.

SS concentrations and fluxes were also calculated by zone, to help visualize the trends, which cannot be clearly seen in Fig. 4. In the DS there was a decrease from high to middle basin, then an increase from middle to low basin; the maximum values were found at the high zone for both SS concentrations and fluxes. The SS concentration in the WS decreased from high to middle, and an increment from middle to low basin. The SS fluxes increased from high to middle basin, and then decreased from mid to low zones (Table 2).

Overall, values from the WS were higher in all zones comparing with the DS, and differences in SS between zones were more pronounced during the DS, but large changes in SS fluxes were seen in both seasons. Mean values reported from Tana River ranged approximately from 2,500 to 51,250 t d^{-1}. In the wet season, their highest values were found in the middle portion of the river, with a mean of 51,250 t d^{-1} and the lowest mean of 10,000 t d^{-1} in the low section. In the dry season, again the highest value was in the middle section, with a mean of 5,000 t d^{-1}, and the lowest was in the high section, with a value of 2,500 t d^{-1} [18]. These values of fluxes are higher than ours, even when this river has lower values of water discharge (25- 922 m^3 s^{-1}) than Usumacinta (23- 5,550 m^3 s^{-1}).

Table 2 Mean (± S.D.) of SS concentrations and fluxes (F_{SS}) by zones of the basin. (DS = dry season, WS = wet season)

Zone	SS (mg L^{-1})		F_{SS} (t d^{-1})	
	DS	WS	DS	WS
High	40.3 ± 17.5	78.5 ± 41.6	1,003.8 ± 621.9	9,291.6 ± 6,135.3
Middle	10.1 ± 3.0	59.4 ± 21.4	291.0 ± 131.4	20,499.8 ± 11,680.6
Low	37.3 ± 23.6	72.3 ± 17.0	860.8 ± 690.8	15,878.2 ± 13,726.6

The difference between incoming flux at upstream points and outgoing flux at downstream, determines whether the river act as a retention or source section for the sediment, which fate can be either storage in the stream or the floodplains or processing within the river [10].

A comparison between upstream and downstream sediment fluxes in a tropical river indicates a significant mobilization of materials upstream, while retention occurs downstream [19]. Our results point out a negative difference (-6,586.4 t d^{-1}) between incoming and outgoing values during the WS, suggesting mobilization of suspended sediments. During DS this difference was positive (143.0 t d^{-1}), showing retention.

In fluvial environments the role of the vegetation as particulate matter traps improves the retention of sediments during floods [20]. The role of floodplains has been reported as regulating downstream transport of riverine suspended matter, particularly in large rivers with extensive inundation areas and deltas [8], [17]. Nevertheless, the flux estimates showed a decrease only over the river from mid to low sections in WS, probably related with the extended floodplains including the Centla swamps at the river mouth [12]. Accordingly, it has been found that the retention of suspended sediments on the floodplains is particularly high during high flow regimes [18].

Certainly, floodplains have been shown to act as sink of riverine material, like WS results, but in some cases, they have been considered sources of suspended material too [18], which may be the case for the mid and lower Usumacinta River during the DS.

River systems often deliver their fluvial sediment load to estuaries instead of directly to the ocean [19]. Lacking an estuary, the sediment load of the Usumacinta River seems to discharge directly into the Gulf of Mexico coastal ocean. Finally, the actual quantity of SS that flows to the Gulf of Mexico must be close to the one measured at the river mouth. The Usumacinta River has two mouths, one after the confluence with the Grijalva River (G3), and another, 24 km NE, at San Pablo station (H). During the WS the recorded values were 38,359.7 ± 6,784.1 t d^{-1} (G3) and 2,193.1 ± 628.7 t d^{-1} (H), which resulted in 40,552.8 t d^{-1}. During the DS, the values were 840.1 ± 683.6 t d^{-1} (G1) and 402.6 ± 118.7 t d^{-1} (H), which resulted in 1,242.7 t d^{-1}. The input during WS is two orders of magnitude larger than during the DS, showing the importance of seasonality on the SS input to the ocean.

CONCLUSIONS

Statistical differences in SS amount were found among stations during both seasons, with higher values during the WS. The Usumacinta River SS amount range (6.1–131.0 mg L^{-1}) is similar to those reported from other tropical rivers, but lower compared to the global mean of 500 mg L^{-1}. There was no correlation between SS concentrations and water discharge; the lack of synchrony has been reported elsewhere. Finally, SS concentrations and fluxes showed different dynamics, suggesting that the river could change the rate of mobilization or retention of materials seasonally.

ACKNOWLEDGEMENTS

We acknowledge the funding received through the project FORDECYT- CONACYT 273646 "Fortalecimiento de las capacidades científicas y tecnológicas para la gestión territorial sustentable de la Cuenca del Río Usumacinta y su Zona Marina de Influencia (CRUZMI), así como su adaptación ante el cambio climático". Jorge Ramírez, Julio Diaz and Regina Ramírez helped with fieldwork and data collecting and processing. Natura y Ecosistemas Mexicanos AC foundation supported us with logistic services at Chajúl Biological Station. Local fishermen at several stations helped with transportation along the river.

REFERENCES

[1] Arriaga L et al., Aguas continentales y diversidad biológica en México. Ciudad de México: Comisión Nacional para el Conocimiento y uso de la biodiversidad, 2000.

[2] Li M et al., "The carbon flux of global rivers: a re-evaluation of amount and spatial patterns", Ecological Indicators, Vol. 80, May 2017, pp. 40-51.

[3] Ward ND et al., "Where carbon goes when water flows: carbon cycling across the aquatic continuum", Frontiers in Marine Science, Vol. 4 Jan. 2017, pp. 1-27.

[4] Kempe S et al., "Biogeochemistry of European rivers", Biogeochemistry of major world rivers, 1st ed. Vol. 42, Degens et al., Ed. J Wiley- and Sons, 1991, pp. 169-211.

[5] Syvitsky JPM and JD Milliman, "Geology, geography and humans battle for dominance over the delivery of fluvial sediment to the coastal ocean", The Journal of Geology, Vol. 115, Jan. 2007, pp. 1-19.

[6] McKee BA et al., "Transport and transformation of dissolved and particulate material on continental margins influenced by major rivers: benthic boundary layer and seabed process", Continental Shelf Research, Vol. 24, 2004, pp. 899-926.

[7] Wetzel RG, Limnology: lake and river ecosystems. San Diego: Academic Press, 2001

[8] Hillebrand G et al., "Dynamics of total suspended matter and phytoplankton loads in the river Elbe", Journal of Soils and Sediments, Feb. 2018.

[9] Wang S et al., "Reduced sediment transport in the Yellow River due to anthropogenic change", Nature GeoScience, Vol. 9, Jan. 2016, pp. 38-41.

[10] Geeraert N et al., "Seasonal and inter-annual variation in carbon fluxes in a tropical river system (Tana River, Kenya)", accepted 2017.

[11] Muñoz- Salinas E et al., "Using three different approaches of OSL for the study of young fluvial sediments at the coastal plain of the Usumacinta- Grijalva river basin, southern Mexico", Earth Surfaces Processes and Landforms, Vol. 41, Jan. 2016, pp. 823-834.

[12] Benke AC, "Streams and rivers of North America: western, northern and Mexican basins", Encyclopedia of Inland Waters, 1st ed., Likens, Ed. Elsevier Boston, 2009, pp. 425-437.

[13] Grodsky SA and JA Carton, "The intertropical convergence zone in the South Atlantic and the equatorial cold tongue", Journal of Climate, Vol. 16, Feb. 2003, pp. 2052-2065.

[14] Coynel A et al., "Spatial and seasonal dynamics of total suspended sediment and organic carbon species in the Congo River", Global Biogeochemical Cycles, Vol. 19, Dec. 2005.

[15] Buillon S et al., "Distribution, origin and cycling of carbon in the Tana River (Kenya): a dry season basin scale survey from headwaters to the delta", Biogeoscience, Vol. 6, Jun. 2009, pp. 2475-2493.

[16] Buillon S et al., "Organic matter fluxes and greenhouse gas exchange in the Oubangui River (Congo River basin)", Biogeoscience, Vol. 9, Jun. 2012, pp- 2045-2062.

[17] Milliman JD and KL Farnsworth, River Discharge to the Coastal Ocean, A global synthesis. New York: Cambridge University Press, 2011.

[18] Tamooh F et al., "Sediments and carbon fluxes along a longitudinal gradient in the lower Tana River (Kenya)", Biogeoscience, Vol. 119, Jul. 2014, pp. 1340-1353.

[19] Meade RH, "River sediment inputs to major deltas", Sea level rise and coastal subsidence, 1st ed. Vol. 2, Milliman and Haq Ed. Springer, 1996, pp. 63-85.

[20] Rouled M et al., "Methylmercury in water, seston, and epiphyton of an Amazonian river and its floodplain, Tapajós River, Brazil", The Science of the Total Environment, Vol. 261, Apr. 2000, pp. 43-59.

SEDIMENT MODELING TO DEVELOP A DEPOSITION PREDICTION MODEL AT LA GAVIA RIVER, MEXICO

Tejeda Samuel [1], Bernal-Banda Rodolfo[2], Flores-Gutiérrez Leonarda María[2], Salinas Tapia Humberto[3], López-Rebollar Boris Miguel[2], Zarazúa-Ortega Graciela[2]
[1]Instituto Nacional de Investigaciones Nucleares.
[2]Universidad Autónoma del Estado de México, Estado de México, México.
[3] Centro Interamericano de Recursos del Agua, Estado de México, México.

ABSTRACT

The present study focuses on the sediment transport and consequent deposition issues in La Gavia river and the Ramirez reservoir. The river section under study is located between Benito Juarez town at upstream, and discharge to reservoir at downstream. One-dimensional (1D) HEC-RAS numerical model in conjunction with Arc-GIS was employed for the study of erosion and sedimentation in the river. Direct runoff hydrograph and bed gradation were used as input parameters. Different return periods were used as critical scenarios considering annual hydrographic survey data from climatologic gauges available in the public archives of Comisión Nacional del Agua. Calibration and validation of the hydrodynamic was performed using measured water surface elevation and velocity at measured sections. The capability of (1D) HEC-RAS quasi-unsteady model was assessed in prediction of sediment accumulation downstream of the river. A temporal deposition prediction model was developed to determine the dredging schedule. This model could potentially be used as a decision support tool to analyze the long term impact of sedimentation in the river and reservoir.

Keywords: Modeling, Sediments, HEC-RAS.

INTRODUCTION

Rivers are affected by natural and human factors; rivers usually undergo severe erosion on bed or banks, sedimentation and sectional movements. These factors cause dramatic changes to rivers at long run leading to what is known as geomorphological changes. One of the key topics in river engineering is to investigate river morphology that describes: the river geometry, bed shape and longitudinal profile, cross-sections and changes of river shape [1].

Sediment accumulation is a problem in many rivers and reservoirs in Mexico and around the world. Available storage capacity is decreasing while demand for water is increasing. La Gavia river and Ramirez reservoir are very important water sources due to the increase in the demand of drinking water for the city of Toluca and its metropolitan region. Removal of accumulated sediment from reservoirs tends to be prohibitively expensive. This underscores the need to reduce: soil degradation, the scour of the rivers and the need to optimally operate reservoirs to reduce sediment deposition.

The storage capacity of the Ramirez reservoir is 20.5 Mm^3 and its use is mainly for agricultural purposes. Its climate is temperate with rains during the summer between the months of June to October; The average annual environmental temperature is 16ºC. One of the main problems of the basin is the high deforestation and inefficient agricultural practices, which contributes to the increase of erosion and sediment transport to La Gavia river and Ramirez reservoir. Ramirez is a small reservoir in the Lerma river basin that serves for flood control, recreation, and environmental benefits. Ramírez reservoir discharges to the Lerma River that in turn benefits other water consumers in the states of Mexico, Michoacan, Guanajuato and Jalisco.

The purpose of this study is to determine the sediment transport along a stretch of 4.7 km of the lower course of La Gavia river, using field measurements (indirect method) and applying Meyer–Peter y Müller model in order to do the first approximation of sediment transport.

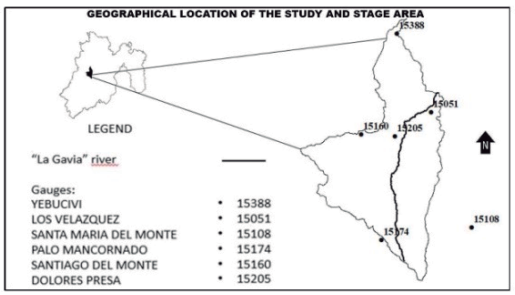

Figure 1. Geographical location of the study and stage area.

Study area: La Gavia river, with a length of 24.1 km is the shortest river of the state of Mexico state. The river with a basin of 224.84 km^2 is situated in center of the country (Figure 1). Turcio y Rosario branches in the north of Almoloya de Juarez forming La Gavia river. There are two hydrometric gauges including Los Velazquez and Atotonilco stations in the study region (Figure 2). In present research, Puente Los Velazquez station was used as for calibration upstream boundary. La Gavia river flows through numerous tows with a great number of private farms. As there is great residing population along this river there is a need the extensive study of potential arising of sedimentation including formation of sand bars at the entry to the Ramirez reservoir.

MODEL HEC-RAS

The HEC-RAS model was developed by the Hydrologic Engineering Center, which is a part of the Institute for Water Resources, U S Army Corps of Engineers, Davis, California. The software was released in 1995, and initially it was a one-dimensional numerical model for the computation of water surface profiles in steady and unsteady flow in a non-prismatic channel together with gradually varied profile, rapidly varied profile and mixed profile. After that, HEC-RAS, was enhanced for the analysis of water quality and the computation of sediment transport together with the movable boundary condition. The advantage of HEC-RAS is that it is developed on object-oriented programming and the object are shared by subroutines without data duplication [3]. In this paper, HEC-RAS 5.0.3 version was used.

HEC-RAS includes a one dimensional sediment transport model that updates channel bathymetry based on sediment mechanics. The model solves the sediment continuity equation over control volumes centered on each cross section. HEC-RAS compares the transport capacity computed for each grain class to the sediment supply entering the control volume. The program computes a localized sediment deficit or surplus from the difference between the capacity and the supply, which translate into erosion and deposition respectively each cross section [4].

INPUT DATA

This section describes the geometric data, hydraulic boundary condition, sediment data and sediment boundary condition which are inputs required for modeling with HEC-RAS.

GEOMETRIC DATA

To specify the geometric data, the model section of the La Gavia River was divided into 316 river stations obtained physically by topographic survey (Figure 2). The upstream river station 4740 is located at the community Benito Juarez, after this site the average distance between two river stations is about 15 m, and the downstream river station 15 is located at the Ramirez reservoir. The Manning´s roughness coefficient n was 0.02 for main channel and 0.03 for left and right over bank. The coefficients of contraction and extraction were 0.1 and 0.3, respectively.

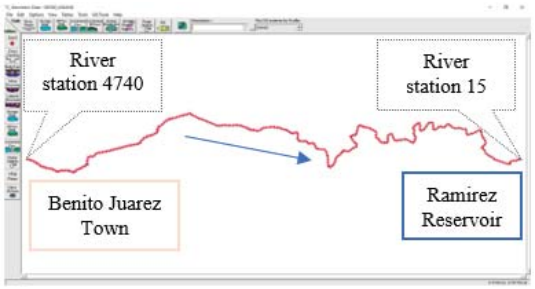

Figure 2. River stations 4740 upstream and 15 downstream close to Ramirez reservoir.

HYDRAULIC BOUNDARY CONDITIONS

In this study, the simulations of sediment transport were carried out by the quasi-unsteady hydraulic data.

The direct runoff hydrograph was used as the upstream condition in river station 4740 and Normal Depth was used as the downstream condition in river station 15.

The hydrograph for the return period of 2 and 5 years were obtained, with the help of HEC-HMS software, with the SCS method, as input data were used 6 meteorological stations that are within the basin, with identification number: 15388, 15051, 15108, 15160, 15174 y 15205, whose data was obtained directly from Comisión Nacional del Agua (Mexico). Using a curve number of 75.17, which was obtained based on current land use. The hydrographs are shown in figure 3.

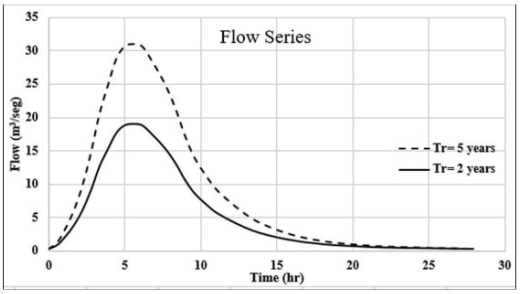

Figure 3. Hydrographs for return period of 2 and 5 years.

SEDIMENT DATA

The sediment data include sediment transport functions, particle fall velocity, bed gradation, sorting of bed sediment and boundary conditions.

Several sediment transport functions are available in HEC-RAS for the computation of the sediment transport capacity.

The available sediment transport capacity functions are: Ackers-White; Englund-Hanen; Laursen; Meyer-Peter Muller; Toffaleti; MPM-Toffaleti; Yang and Wilcock-Crowe.

The Meyer-Peter-Muller bed load transport function was used, is based primarily on experimental data and has been extensively tested and used for rivers with relatively coarse sediment. (Reference Manual HECRAS).

The general transport equation for the Meyer-Peter-Muller function is represented by: Ecuation 1.

$$\left(\frac{k_r}{k_r'}\right)^{3/2} \gamma RS = 0.047(\gamma_s - \gamma)d_m + 0.25\left(\frac{\gamma}{g}\right)^{1/3}\left(\frac{\gamma_s - \gamma}{\gamma_s}\right)^{2/3} g_s^{2/3}$$

Where: g_s = Unit sediment transport rate in weight/time/unit width; k_r = A roughness coefficient; k_r' = A roughness coefficient based on grains; γ = Unit weight of water; γ_s = Unit weight of sediment; g = Acceleration of gravity; d_m = Median particle diameter; R = Hydraulic radius; S = Energy gradient

The suspension of a sediment particle is initiated once the bed-level shear velocity approaches the same magnitude as the fall velocity of that particle. For the fall velocity, the formula of Rubey was applied. This equation has been shown to be adequate for silt, sand, and gravel grains. Ecuation 2.

$$\omega = F_1\sqrt{(s-1)g d_s}$$

in which, Ecuation 3.

$$F_1 = \sqrt{\frac{2}{3} + \frac{36v^2}{gd^3(s-1)}} - \sqrt{\frac{36v^2}{gd^3(s-1)}}$$

Bed gradation data at each sample site were entered bases on the sieve analyses at the sediment taken from 4 sites, and the data were interpolated for cross sections between the sample sites. The average d50, d90 and d84 value for the entire reach was 0.215, 0.619, 0.190 mm respectively. Bed surface material consist of coarse sand and gravels, with specific weight 2.68 T/m^3

In this study, maximum erodible depth values were set at 2 m for each cross section based on observed data, and the entire extent of each cross section was allowed to erode.

SEDIMENT BOUNDARY CONDITIONS

Sediment boundary condition controls the amount of sediment passing through a cross section. The boundary condition is required for the first and last cross sections.

An equilibrium load was selected as the upstream sediment boundary condition at river station 4740.

RESULTS AND DISCUSSION

CALIBARTION AND VALIDATION OF HYDRODINAMICS

Hydrodynamic calibration was carried out with the velocity and depth data in the control sections. The velocity was measured with the use of a water velocity meter (sensitivity of 0.01 cm/s), two field measurements in October 2017 and in February 2018 were made. For the calibration in HEC RAS, the parameter adjusted was the Manning coefficient value resulting from 0.025 for the main channel. Table 1 shows the comparison between the result of the simulation and the experimental, the mean square error for the velocity (V) and the depth (h) in the control section. The RMSE is acceptable, and the established Manning n was considered adequate.

Table 1. Mean Quadratic Error for the velocity and the depth in the control section.

		October (2017)	February (2018)
Measurements	Q (m^3/s)	0.907	0.280
	V (m/s)	0.44	0.32
	T (m)	0.38	0.18
HEC-RAS	V (m/s)	0.57	0.34
	T (m)	0.36	0.20
RMSE	V	**13%**	**2%**
	T	**2.0 %**	**1.73%**

Figure 4 shows the figure a comparison of the flow profile for the two return periods, it is observed that the behavior of the flow is similar, however the flow is highly turbulent upstream of the reservoir due to the high slope that causes erosion in the ground.
In addition, the sections located near the reservoir have an irregular shape.

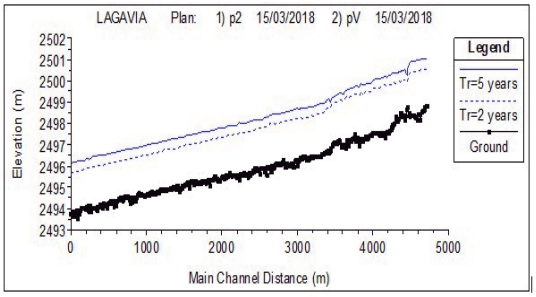

Figure 4. A comparison of changes in elevation for return period of 2 and 5 years.

SEDIMENT TRANSPORT

The mass balance to obtain the sediment load of the La Gavia river towards the dam was made, considering the maximum flow for two return periods of 2 and 5 years. The results of the simulation indicate that the transport of sediments in the bottom layer were 0.7813 Kg / s and 0.8846 Kg / s for the corresponding periods, which means that 9298 m^3/year, and 10527 m^3/year respectively. As it was observed, the sediment load is high in relation to the size of the basin; this is attributed to the soli degradation in the hills and the inefficient agricultural practices that cause a considerable contribution of sediments to the Ramirez reservoir.

The results of the simulation allowed to identify that the river presents erosion of 20 to 30 cm in the bottom layer upstream and deposition of sediments downstream (Figure 5) for the maximum flow and a return period of 2 years. In the area near the reservoir, the deposition of sediments from 10 to 20 cm was observed.

Figure 6 shows the sections of the river that reach the greatest erosion of 50 cm and the deposit of sediments for the return period of 5 years, as it is observed, as the flow increases, the drag of the bottom layer increases, which indicates that there is more transport of material to low areas.

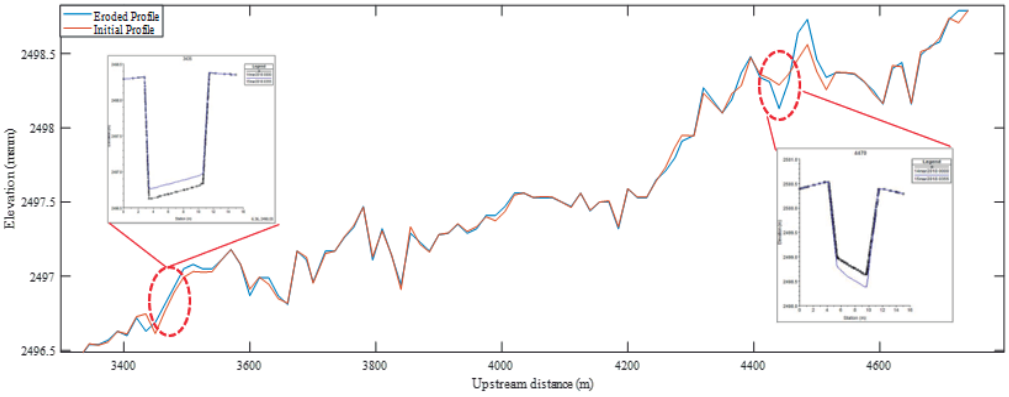

Figure 5. Model results of initial and eroded profile in two stations.

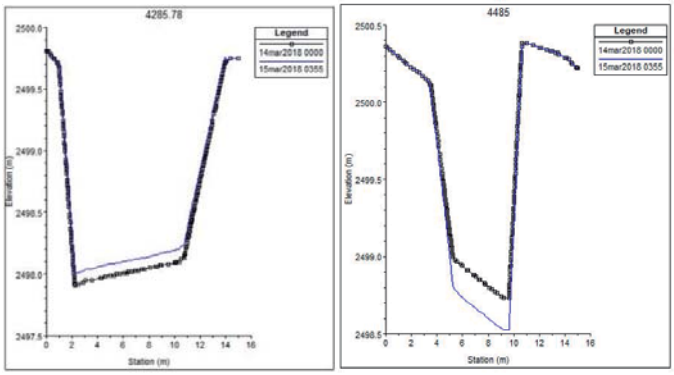

Figure 6. Model results for two cross sections of the river for a return period of 5 years.

It is important to highlight that HEC-RAS allowed reproducing the hydrodynamic behavior of the river, and identifying potentially degradable river areas, as well as zones with high deposition of sediments, this will allow to have tools to establish a dredging plan that allows conserving the La Gavia river, the Ramirez reservoir and maintaining its water storage capacity.

CONCLUSIONS

This paper described the initial development of a one-dimensional HEC-RAS .0 mobile-bed model for modeling and predicting sediment accumulation in La Gavia river. This model utilizes new features in HEC-RAS 5.0.3 including Unsteady Sediment.

This model demonstrates the utility of HEC-RAS for sedimentation analysis of small rivers. Future work will quantify the reduction in sediment accumulation possible at Ramirez reservoir through construction of gabion check dams.

ACKNOWLEDGEMENTS

Authors acknowledge the Instituto Nacional de Investigaciones Nucleares for financial support to carry out the said work under the Institutional Project on “Strengthening the surveillance systems and monitoring programs by hydraulic facilities in the region, using the nuclear techniques to assess the sedimentation impacts as environmental and social risk”. Authors are also grateful to Universidad Autónoma del Estado de México, National Water Commission (Govt. of Mexico), and Almoloya de Juarez Municipality for providing data to carry out the present investigation.

REFERENCES

[1] Hamzeh Haghiabi A., Zaredehdasht E. (2012). Evaluation of HEC-RAS Ability in Erosion and Sediment Transport Forecasting. World Applied Sciences Journal 17 (11): 1490-1497.

[2] Shelley J., Gibson S., Williams A. Unsteady flow and sediment modeling in a large reservoir using HEC-RAS 5.0. U.S. Army Corps of Engineers, Kansas City District. https://acwi.gov/sos/pubs/3rdJFIC/Contents/9C-Shelley.pdf

[3]Brunner, G.W. (2002). HEC-RAS, River Analysis System Hydraulic Reference Manual. U.S. Army Corps of Engineers, Hydraulic Engineering Center (HEC), Davis, 350 pp.

[4] Gibson, S.A., Pak, J.H., Fleming, M.J. (2010). Modeling Watershed and Riverine Sediment Processes with HEC-HMS and HEC-RAS. Watershed Management 2010. 1340-1349. https://www.researchgate.net/profile/Jang_Pak/publication/269138827_Modeling_watershed_and_riverine_sediment_processes_with_HEC-HMS_and_HEC-RAS/links/549340bd0cf25de74db4f100.pdf

6. Sediments and environmental regulation

Session chairs: Ma. Antonieta Gómez[1] and Pilar Saldaña[2]
[1,2] Coordinación de Tratamiento y Calidad del Agua, Instituto Mexicano de Tecnología del Agua, México

Dealing with sediments is becoming an increasingly urgent task due to the importance of natural processes and the impact of anthropogenic activities. At the basin level, it is important to preserve connectivity among ecosystems as well between riverbed and flooding areas. Sediment transport and deposition is a limiting factor for the conservation of wetlands of international concern due to its importance as substrate, nutrients source, and water residence areas during floods. Dams have interrupted sediments fluxes and dredging is an increasing activity worldwide, with effects barely known and regulated. Besides, while solving hydrological cycles by mimicking temporal and historical variations through environmental flows, registration of sediments are rare at hydrometric gauges, and it is therefore not possible to identify patterns, alterations and trends. Sediments as means of transportation, transformation and final fate of pollutants are issues of great concern and advances in modelling and regulation are of benefit in this context. Examples on guidelines, approaches and regulations are highly welcome to help in advancing in this topic, still unsolved in many parts of the World.

QUALITY OF SEDIMENTS IN TWO RIVERS IMPACTED BY INDUSTRIAL ACTIVITIES

Saldaña Fabela Pilar y Gómez Balandra María Antonieta
Instituto Mexicano de Tecnología del Agua, México.

ABSTRACT

Sediment as the last environmental compartment of the aquatic ecosystem is where pollutants are deposited and stored; they can be reincorporated into the water column, affecting their quality. In two industrial zones with petroleum activities, sediment samples were taken for the analysis of heavy metals. In the first system, the sediments were analyzed before being dredged in a section of the river to know the concentration of heavy metals that can be incorporated into the Coatzacoalcos River. In the second system, the section of the Lerma River that directly receives the discharge of wastewater from a refinery, the heavy metal analysis was carried out before and after the discharge. The results were compared with standards or criteria from the United States and Canada, because in Mexico there are currently no criteria or quality standards for sediments. In the Coatzacoalcos River, metals such as barium, mercury and nickel were detected. The Lerma River, lead, copper and chromium, while cadmium, vanadium and manganese twice exceeded the guide value established by Canada.

Keywords: Sediments, Dredging, Criteria, Standards

INTRODUCTION

The aquatic environment has suffered the pressures of industrialization by industrial discharges without treatment or with deficient treatment, which causes the contribution of pollutants that are distributed in the various compartments such as: water, biota and sediments. One of these compartments where the pollutants that enter the environment are deposited are the sediments, which represent the final destination of the toxic substances that are introduced by punctual and diffuse sources affecting the health and quality of the aquatic ecosystem. In industrial development zones, the presence of organic and inorganic compounds in the water column, which are discharged into the system, follow several environmental routes as a result of transport, transformation and degradation. [1].

The industrial and municipal discharges that contain mixtures of toxic compounds and that are adsorbed and assimilated by the suspended material in the water column have as final destination the sediments of the riverbed, lakes and estuaries and historically act as concentrators of toxic substances, which by resuspension processes can be incorporated into the water column.

In Mexico, the development of the petrochemical and refining industry in the two study areas is located in the lower part of the Coatzacoalcos river basin, Veracruz and in the Lerma river basin in Guanajuato. The installation and operation of the industrial zone has a significant effect on the environmental quality and has caused the loss of habitat, due to the change in quality, sediment dynamics, characteristics of the fluvial bed and an increase in the entry of hydrocarbons and metals heavy due to the discharge of wastewater [2].

STUDY AREA AND METHOD

The Coatzacoalcos River belongs to the hydrological region No. 26 located in the southeast of Mexico at 17 ° 46 'and 18 ° 10' north latitude and 92° 25 'and 94° 31' west longitude (Fig. 1), the The study section is 5.4 km, and 3.3 km downstream from the refinery, six sediment collection sites were located.

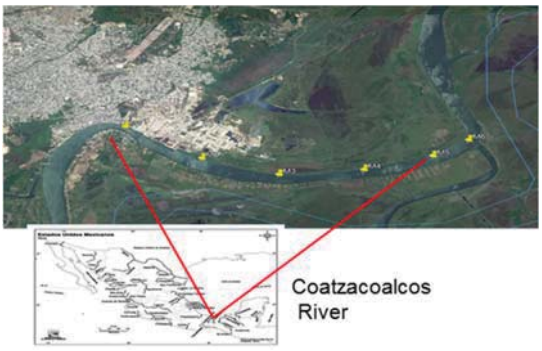

Fig. 1 Monitoring sites on the Coatzacoalcos River

The Lerma River belongs to hydrological region No. 12, the 4 km study section is located between 101° 11'39 " west longitude and 20° 34'22 " north latitude (Fig. 2). Three sediment monitoring sites were located in the section, one upstream of the

discharge, in the discharge and another downstream of the refinery discharge.

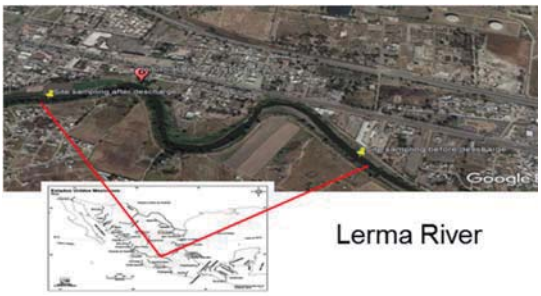

Fig. 2 Monitoring sites on the Lerma River

The samples were collected with Van Been dredger and transported in glass jars or sterile bags at a temperature of 4° C for the subsequent analysis of five total heavy metals analyzed by means of the atomic absorption spectrophotometer equipment for analysis by flame, hydride generator and graphite furnace.

The keys used for each river were: Site L1 for the Lerma river, Site C1 for the Coatzacoalcos river and only the discharge of the Lerma river refinery was analyzed. The concentration is in milligrams per kilogram of dry weight.

In the Coatzacoalcos River, metal analyzes were carried out in the selected section, due to programmed dredging actions, so for the disposal of the dredged material, it is necessary to know the concentrations of the metals.

The results obtained were analyzed and compared with the antecedent geochemical concentration [3], as well as with the concentrations of the metals that cause adverse effects to biological test organisms of a set of data used to calculate them obtaining the ERM and ERL that are defined as:

ERM (Effects Range Median)—Determined values for each chemical as the 50th percentile (median) in a database of ascending concentrations associated with adverse biological effects.

ERL (Effects Range Low)—Determined values for each chemical as the 10th percentile in a database of ascending concentrations associated with adverse biological effects [4].

The analysis of the results is carried out with the comparisons of the data presented in Table 1 (Bn, ERM and ERL), given that in Mexico there are no sediment quality standards or guides.

RESULTS

Five heavy metals were analyzed: cadmium, chromium, copper, lead and vanadium in the monitoring sites and in the discharge of the Lerma river refinery. The five metals are indicators of industrial activities and related to oil extraction among other activities.

The results of the five metals are presented in Table 1 and Fig 3.

Table 1 Results of metals in sediments in the Lerma river (L), refinery discharge and Coatzacoalcos river (C) ($mgkg^{-1}$). Bn is the geochemical background value. ERM Effects Range Median. ERL Effects Range Low

Site	Cd	Cr	Cu	Pb	Va
L1	1.3	15.3	19.2	16.5	70.9
Discharge	2.3	314.8	306.4	416.4	513.8
L2	1.2	36.4	16.5	17.9	62.5
C1	0.64	16.50	12.9	12.1	20.4
C2	0.58	16.38	11.9	11.1	18.9
C3	0.49	15.31	22.8	14.6	17.9
C4	0.69	16.75	15.9	13.1	24.5
C5	0.71	16.40	20.1	11.4	26.4
C6	0.40	14.42	9.2	8.3	14.7
Bn	0.17	72	33	19	105
ERM	9.6	370	270	218	ND
ERL	1.2	81	34	46.7	ND

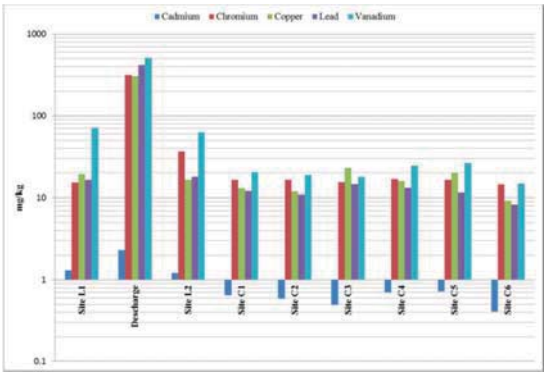

Fig. 3 Results of metals in sediments from the Lerma and Coatzacoalcos rivers

The discharge of the refinery located in the Lerma River, presents the highest concentrations for the five metals, as well as the values that represent adverse biological effects to the organisms that could be present near the discharge site.

Vanadium is the metal with the highest concentration of 513.8 $mgkg^{-1}$ and cadmium with the lowest concentration (2.3 $mgkg^{-1}$) in the refinery discharge in the Lerma river.

Vanadium due to the minimum capacity to pass into the environment under natural conditions is a good indicator of contamination by oil exploitation [5].

The concentrations of chromium, copper and lead in the sediments of the Lerma and Coatzacoalcos rivers were compared with the ERM and ERL values that represent adverse effects for the test organisms in 50% and 10% respectively.

Only cadmium in sediments from the Lerma River slightly exceeds the sediment quality standard for sites L1 and L2 that are upstream and downstream of the refinery discharge for the ERL value that may cause adverse effects to organisms that live in the sediment.

The comparison of the geochemical background values, indicated that the cadmium in all the sampling sites, exceeded the value which can indicate a possible enrichment and / or storage of the metal, if we consider that the cadmium is also present in the formulation of several pesticides and that both rivers pass through agricultural areas, this activity could be the main cause of the metal in the sediments.

The concentrations obtained in the Coatzacolacos River are lower than those obtained in the Lerma River, mainly due to the fact that the Coatzacoalcos River is more abundant than the Lerma River.

CONCLUSIONS

Heavy metals were detected in the sediments of both rivers and the detected concentrations were compared with standard quality values in sediments of the Environmental protection agency of the United States.

In Mexico there are water quality guidelines for metals and other pollutants, however for sediments there are no criteria or standards to define the degree of contamination of industrial activities

REFERENCES

[1] Rand G. M. and Petrocelli S. R. Fundamentals of Aquatic Toxicology. Methods and Applications. Ed. Hemisphere Publishing Corporation, 1985, pp. 666.

[2] L. Rosales-Hoz, A. B. Cundy, J. L. Bahena-Manjarrez, 2003, Heavy metals in sediment cores from a tropical estuary affected by anthropogenic discharges: Coatzacoalcos estuary, Mexico, Estuarine Coastal and Shelf Science, 56 (2003) 1-10.

[3] Salomon W. and Forstner U. 1984. Metals in the Hydrocycle. Springer-Verlang New York. Pp. 479. Ch. 3. ISBN 3-540-12755-0.

[4] EPA, 2012. National Coastal Condition Report IV. EPA-842-R-10-003. pp 334. April

[5] Villacreces Luis. Evaluación de vanadio como indicador de contaminación de origen petrolero. Informe Petroecuador

SEDIMENTS AS PART OF THE ENVIRONMENTAL FLOW REGULATIONS

Gómez-Balandra María Antonieta[1], Saldaña-Fabela María del Pilar[1] and Llerandi-Juárez Rosa Dina[2]
[1]Instituto Mexicano de Tecnología del Agua, México; [2]Comisión Federal de Electricidad, México.

ABSTRACT

Environmental flows are known as a master variable and many approaches to deal with its management or regulation have been developed worldwide to imitate flow regimes, with its seasonal and inter-annual variations. However, both water and sediment are fundamental drivers of aquatic ecosystems. Therefore, e-flow approaches must be completed with the analysis of sediment processes, even though they are strongly modified by humans. Due to the importance of connectivity between fluvial, estuary and wetland ecosystems, the Article 60 Ter of the Wildlife Act in Mexico prohibits remove, fill or any activity that affects the hydrological flow integrity in mangroves, its productivity and load capacity for tourism projects as well its habitats and interactions with marine and corals zones. Hydrological integrity is related to preserve attributes in magnitude, frequency, timing, duration and rate of change. This paper analyzes the scope of sediment regulations currently applied in Mexico, which is minimal. Available data are scarce and methodological approaches correspond to sediment transport to design hydraulic infrastructure, analytical methods to quantify associated pollutants in mining areas and petrochemical or industrial complexes that discharge into rivers or connected water bodies. Thus, it is imperative to promote normative instruments that activate this field of knowledge and conservation.

Keywords: Flows, Sediments, Regime, Regulation

INTRODUCTION

Knowledge of sediment dynamics currently represents the barrier facing for many disciplines since their generation, transport, deposit and movement in general are related to several macro processes at the basin level such as land use change and erosion: In addition to others once they reach the channels, for example: the volumes of sedimentation, their transport, deposit, as well as at the micro level by the adsorption of pollutants, among others.

Most of these aspects have been studied in isolation and poorly understood, so sediment measurement has been focused in a timely manner to respond to issues with reduced vision of being able generate data useful by other disciplines and focused mainly on designing storage with dead loads, estimate a balance, check the stability of channels, geomorphological studies and in a lesser proportion environmental assessments. Sediment measurement has also been reduced to few hydrometric gauges and over time, due to limited economic budget to support or increase the stations in this network by the two most interested institutions in the country National Commission of water (Conagua) and Federal Commission of Electricity (CFE).

Due to the lack of maintenance of the stations and instruments, as well as the infrequent verification of river sections, the quality control of the data is poor and its applications. Limited work has been done on the interrelation of issues associated with sediments, especially from the point of view of watershed management, aquatic ecosystem dynamics, ecosystem services and fluvial - coastal connectivity.

Although the concept of ecological or environmental flow is fundamentally related to the amount of water that must be left (instream flow) or assigned to a water body under competition schemes (ecological flow) or for conservation and rehabilitation of ecosystems, coexisting with other uses by the populations that depend on the associated resources (environmental flow), it has been recognized that in order to develop effective environmental flow proposals, the habitat availability for species of interest and the trophic structure that makes them possible must be included. Therefore, it leads to the analysis of channel geomorphology, its evolution and sediment transport that determine habitats diversity and connectivity for species and between the ecosystems e.g. rivers and wetlands

It has also been recognized the importance of deposit and drag processes during floods, either for cleaning the channel, distribute nutrients and determine plant profile and successions in the margins or riparian vegetation. These processes alongside fluvial dynamics determine channel configuration and stability. Besides flooding regimes determines humidity that must be maintained in the mangroves and other wetlands connected with the river.

Fluvial ecosystems models, generally share ideas on the geomorphology and the habitat as zones of functional processes [1].

They recognize a dynamics of patches in the lotic systems, longitudinal and lateral connectivity, as well as spatial heterogeneity and temporal variability in the rivers that affect populations, communities and ecosystems [2], [3].

Currently, environmental flow methodologies are mainly applied to rivers, considering the hydrological variable as a starting point for a general, regional or mostly water quantity, while the conservation needs of aquatic communities and the ecosystem services, require the application of other methods, such as hydro-biological, of habitat preference by species and holistic, which include the substrate characterization from micro or meso-habitat to landscape units, incorporating the importance of flooding and sediment dynamics, riparian vegetation and water uses.

This has been translated into a reference standard in Mexico NMX-AA-159-SCOFI-2012 [4] to deal with the procedure to determine environmental flow in hydrological basins. The standard points out methods should be used in an indicative, but not limitative manner from hydrological to holistic analysis. In applying these methods a set of protocols for each topic that have been developed, with some advances for channel geomorphology, substrates, floods and its relationship with habitat availability.

SCOPE OF REGULATIONS

Many Latin American countries such as Peru, Venezuela, Brazil, Mexico, etc., have developed their water acts since more than 25 years ago. These laws have been reformed, as well as complementing their regulations, standards and other associated instruments to incorporate the topics of watersheds integrated management and ecological flows, among others. Nevertheless, with scarce attention to sediments, despite its importance for the design of infrastructure and the issues already mentioned.

The National Waters Act in Mexico [5] makes a single mention to sediments mainly considering the effects caused in the irrigation infrastructure (Article 77). However, this Law and its regulations indicate specifications on the concession permits and the management conditions of the stone material banks (sand, gravel, stone and any other used in the construction (Article 113 Bis, 176).

Watersheds limits

Delimitation of hydrological basins is considered a fundamental aspect for the study and management of sediments. Thus, in Mexico, 757 watersheds are officially recognized in 37 hydrological regions, from which their sub-basins or corresponding sections have been defined for the purpose of administration and water availability estimation availability at control points or hydrometric gauges, where it has been indicated sediment loads are poorly measured [6]. (Fig. 1)

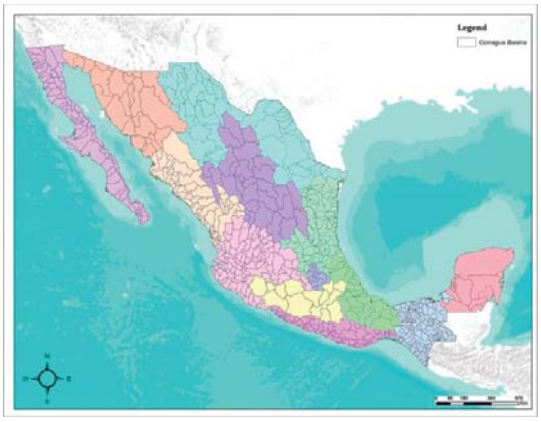

Fig. 1 CONAGUA basins and watersheds

Based on topographic and hydrographic criteria (surface drainage network), there is also a delimitation of river watershed scale 1:250,000 (Fig. 2) [7], as surface morphological units, delimited by partways, which can be subdivided into sub-basins or a lower order and differentiated into functional zones according to its position: a) head-catchment and b) transport-emission, or alternatively by their altitudinal level (upper, medium and low basin). The 1:50000 hydrographic network is currently in Beta version INEGI: http://www.inegi.org.mx/

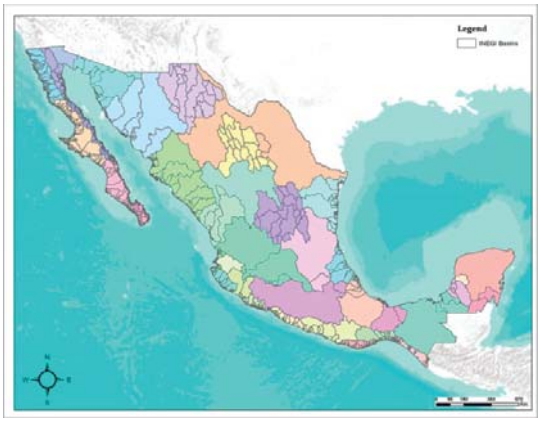

Fig. 2 INEGI basins and watersheds

Water availability in the basins

Based on the application of Mexican Standard NOM-011-Conagua in 2000 and its update in 2015, the average annual availability of surface water in the 757 watersheds in the country [8], is calculated as a balance between (Fig. 3):

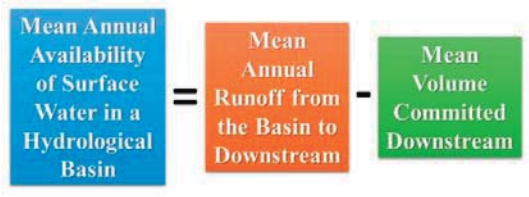

Fig. 3 Balance of the average annual availability of surface water

The mean annual runoff from the basin to downstream MARds is determined by applying the following expression Eq. (1):

$$MARds = MARus + MANR + AVR + AVim - AVex - AVxt - MAVevem - MAVvasr \quad (1)$$

Where:
MARds = mean annual runoff from the basin to downstream
MARus = mean annual runoff from the watershed upstream
MANR = mean annual natural runoff of the basin
AVR = Annual Volume of Returns (percentages estimated by use, for example: agricultural 10-30%, urban public 70-80% and hydroelectric generation 95 -100%.
AVim = annual volume of imports
AVex = annual volume of exports
AVxt = annual volume of surface water extraction
MAVevem = mean annual volume of evaporation in reservoirs
MAVvasr = mean annual volume of storage variation in reservoirs.

Volumes generated in the basin and those that travel from upstream to downstream, constitute criteria that are reviewed to estimate ecological flows.

Ecological flow

The NMX-AA-159-SCFI-2012, states ecological flow as the quantity, quality and variation of the flow or levels of water reserved to preserve environmental services, components, functions, processes and the resilience of aquatic and terrestrials ecosystems that depend on hydrological, geomorphological, ecological and social processes.

The regime of ecological flows is an instrument of water management, based on the ecological principle of natural regime and the gradient of biological condition, which seeks to establish a regime and not a minimum flow.

The NMX-AA-159-SCFI-2012 of ecological flow introduces the concept of environmental objective (OA) to each basin or section of the basin (757 watersheds of the country), which is determined by its ecological importance, related to the presence of endemic species or with any conservation status according to NOM-059-SEMARNAT-2010[9]; presence of Ramsar sites, natural protected areas and by water pressure (percentage of water allocated) by basin (Fig. 4).

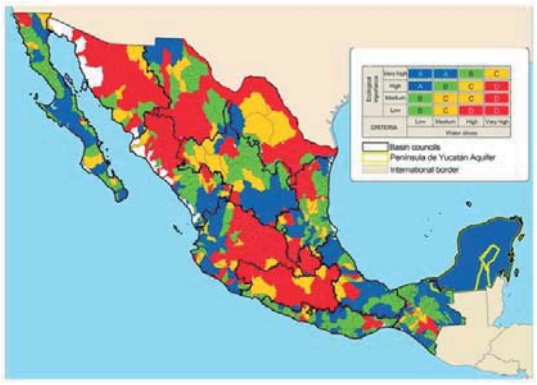

Fig. 4 Classification of watersheds by environmental objectives [10]

In the formulation of the ecological flow standard NMX-159-SCFI-2012, it was recognized there is a national problem related to water decreases, derived from the competition between uses and increase of water demand in the high and middle parts of the hydrological basins, which hinder the conservation of a runoff in the channels and towards the lower parts. In addition of depletion of groundwater recharge, which in the long term decreases the discharge of the aquifer towards surface water bodies, as base flow.

The procedures ecological flows must recognize the natural conditions of hydrological regime, its state of alteration, possibilities of conservation or recovery of components of hydrological regime to maintain and achieve an environmental objective that improves river conditions.

The reference values apply for the allocation of volumes, being greater for the environmental objective "A", either the monthly flow or annual reserve volume. The alteration degree of hydrological regime is also used as a reference. It is calculated by comparing two periods of hydrometric data time series to establish whether the most recent period of 20 years (generally) deviates by more than 50% from the 90th and 10th percentiles per month and years of the previous period for which better flow conditions are assumed, comparing historical hydrographs.

Hydrological methods

The standard of Ecological Flow in its "A" appendix indicates for the 731 basins of the country

the corresponding environmental objective. In Appendix B, the procedure for determining monthly and annual hydrological alterations is indicated. Appendix C shows annual and monthly reference percentages for each environmental objective and describes the Tennant method modified by E. García [4] to determine the ecological flow on a monthly or seasonal basis. (Fig. 5)

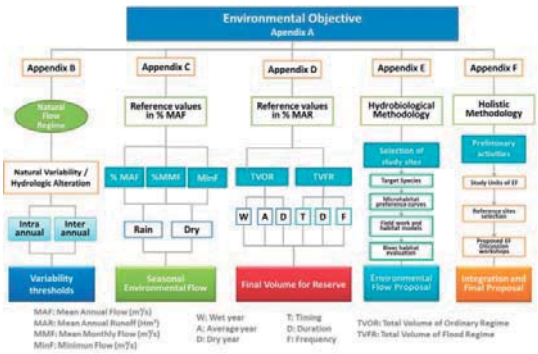

Fig. 5 NMX-AA-159-SCOFI-2012 Structure

Appendix D. indicates reference percentages of the annual volume to be reserved as EF according to environmental objective (Table 1), as well as the procedure for estimating annual volume, composed by an ordinary flow regime, plus a volume associated to floods.

Table 1 Reference values for EF

Environmental Objective	Conservation condition	(% MAR) Creek or river	
		Perennial	intermittent
A	Very Good	>=40 %	>=20 %
B	Good	25-39 %	15-19 %
C	Moderated	15-24 %	10-14 %
D	Deficient	5-14 %	5-9 %

An annual reserve is calculated and can be decreed for each river or catchment area of the 757 indicated for Mexico. In a synthetic way, it consists of:

Regime of seasonal flows

According to the environmental objective defined for the river, the frequencies of occurrence in 10 years of each type of year (wet, medium, dry and very dry) is used to integrate the monthly volume as is shown in Table 2.

Total seasonal volume is calculated by multiplying the volume of each month by the frequencies indicated according each type of year, Eq. (2).

Table 2 Frequency of hydrological conditions for environmental objectives

Environmental Objective	Conservation condition	Frequency			
		Humid	Medium	Dry	Very dry
A	Very good	0.1	0.4	0.3	0.2
B	Good	0.0	0.2	0.4	0.4
C	Medium	0.0	0.0	0.4	0.6
D	Deficient	0.0	0.0	0.0	1.0

$$TSV = (fH * vH) + (fM * vM) + (fD * vD) + (fVD * vVD) \quad (2)$$

Where:

TSV = Total seasonal volume;

f = frequency of occurrence in a hydrological condition "i";

H, M, D and VD = hydrological conditions

Flood Regime estimation

This analysis tries to identify those floods that activate key processes (ecological, hydrological and geomorphological) which are needed to maintain ecosystems in the long term.

Of these, floods that are repeated annually and are estimated to flood the riverbed are Category I; those that have a return period of 1.5 years, they overflow to the riparian vegetation, maintaining its structure (Category II) and those with a frequency of 5 years (Category III) that maintain the area of flood and infiltration to maintain the base flow.

During a period of 10 years the frequency of each described floods are presented according to the environmental objective. Its estimation is according to their attributes of: magnitude, duration, and exchange rate (Table 3). For an environmental objective A, all floods must be reproduced.

Table 3 Criteria to integrate floods and frequency of occurrence

	Floods Regime		
Environmental Objective	Category I	Category II	Category III
A	10	6	2
B	5	3	2
C	3	2	1
D	2	1	1

Floods regime volume (FRV) is calculated using Eq. (3):

$$FRV = (fI * dI * VI) + (fII * dII * VII) + (fIII * dIII * VIII) \quad (3)$$

Where:

FRV=Floods regime volume
f=frequency of each flood
d=duration of each flood
V=Volume of each flood

This volume is divided by 10 to obtain the volume associated with the annual floods regime, which is added to the seasonality to obtain the Final Annual Reserve Volume (FARV) in Hm^3/year, Eq. (4).

$$FARV = TSV + FRV \quad (4)$$

Finally, the standard indicates in appendices E and F hydro-biological and holistic methods that apply to detailed studies for the conservation of species, communities, ecosystems and their environmental services, as well as to build scenarios with operation of new infrastructure with impacts on flow regime and regional distribution of water. Thus, it requires the application of criteria and methods to characterize habitat, including geomorphological aspects.

These methods have been adapted and have developed own protocols for monitoring and analyzing sediments such as: Rosgen classification, applied to stretches; variables such as depth, substrate, current speed for the PHabSim and Meso HabSim models, as well as register of position and actions doing by fish. Spreadsheets have also been designed that relate different types of floods with depths and structure in channel [11]

National Water Reserves

Through article 78 of the NWA (National Water Act, Federal government may decree national water reserves, among others to the purposes of:

a) Guarantee the minimum flows required by the stability of the channels, lakes and lagoons, and the maintenance of aquatic species, and
b) The protection, conservation or restoration of an aquatic ecosystem, including wetlands, lakes, lagoons and estuaries, as well as aquatic ecosystems that have historical, tourist or recreational value.

Therefore, the sites with the greatest potential were identified [12] (Fig. 6).

Technical support studies were carried out from more than 10 basins and two have been decreed from 189 that were proposed for the country in the last National Hydric Program 2014 - 2018 [13].

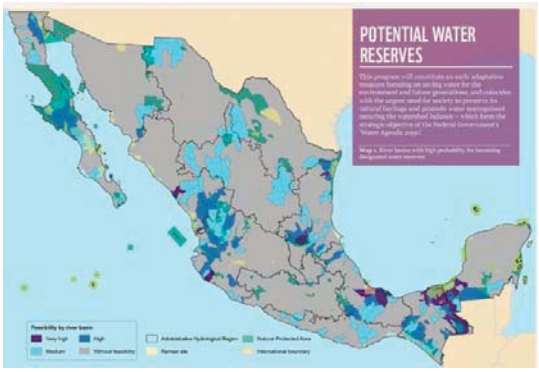

Fig. 6 Potential Water Reserves [12]

Sediment management for EF

The approaches are currently based on the design of new dams that include bottom discharges or actions to connect sediment transport according to hydrological regime in order to maintain healthy and productive ecosystems, as well as to conserve most species.

Even though watershed transformation it is important to maintain sedimentation levels between interval of equilibrium to protect soils and hydrological processes (infiltration, evapotranspiration, and runoff) and cycles. Moreover, to recognize climate changes.

It is about recovering partially the natural dynamics between erosion and sedimentation, as well ecosystems complexity and attenuate the accelerated geomorphological changes in rivers and watersheds, conserving and improving their environmental services [14]; [15].

In doing so, it is important to recognize reference sites in terms of the least alteration to the hydrological, geomorphological and biological cycles, as well as to strengthen and promote the integration of databases and time series in these topics [16] .

Operation of dams reduces diversity of materials transported in the river downstream, creating uniform habitats with components of sand and silt that are discharged, whether they come from hydro peaks centrals or from storage dams for agriculture or public supply purposes. [17]

In dismantling works of small and old dams in various countries, sections of rivers and ecosystems are re - connected again, as well as with re-operation of hydroelectric power plants or cascade systems, t flow regime and the sediment contributions of under a management system are simulated by an. adaptive approach [15], [18].

CONCLUSIONS

Measurement and management of sediments represents an important area of work and research for the country due to its relationship with the design, operation and conservation of dams for energy, irrigation and water supply. Nevertheless, data, technical reports and scientific publications remain scarce.

Some available information is related to navigation activities, dredging, floods protection but few to environmental protection.

Through ecological flows new dimensions for its characterization and management is arisen.

It is important to review methods, protocols and produce data time series necessary to make better decisions since, gaps of information are recognized in general and for this specific topic.

The watershed approach, although fundamental, is important to disintegrate and reintegrate to explain phenomena related to channel dynamics, river banks, floodplains and habitat availability for the species to be conserved, as well as control in case of aquatic invasive plants.

Specific measurements are needed for these issues, in addition to considering the already established guidelines. At present, they have been pointed out for each level of micro to meso-habitat and landscape studies. Therefore, it is relevant integrate data from different institutions that are responsible for forestry, water, watersheds, for the continuity and scope of the measurements, and management analysis practices at the micro to Cuenca level, and strengthening the current regulatory framework.

Design of new dams, as well as the re-operation of others have allowed recovering hydrological features of a regime, including some floods and sediment transport. Both regimes are considered important to conserve rivers, their biodiversity and ecosystem services, with examples of benefits mainly in developed countries.

REFERENCES

[1] L. BENDA, N. L. POFF, D. MILLER, T. DUNNE, G. REEVES, G. PESS, and M. POLLOCK, "The Network Dynamics Hypothesis: How Channel Networks Structure Riverine Habitats," *BioScience*, vol. 54, no. 5, p. 413, 2004.

[2] R. L. Vannote, G. W. Minshall, K. W. Cummins, J. R. Sedell, and C. E. Cushing, "The River Continuum Concept," *Canadian Journal of Fisheries and Aquatic Sciences*, vol. 37, no. 1, pp. 130–137, Jan. 1980.

[3] K. O. Winemiller, A. S. Flecker, and D. J. Hoeinghaus, "Patch dynamics and environmental heterogeneity in lotic ecosystems," *Journal of the North American Benthological Society*, vol. 29, no. 1, pp. 84–99, 2010.

[4] NMX-AA-159-SCFI-2012, *Norma Mexicana. Que establece el procedimiento para la determinación del caudal ecológico en cuencas hidrológicas". DOF 20 de septiembre de 2012.* México, 2012, p. 123.

[5] Comisión Nacional del Agua (CONAGUA), *Ley De Aguas Nacionales y su Reglamento*. México, 2017, p. 234.

[6] DOF 07/07/2016, *ACUERDO por el que se actualiza la disponibilidad media anual de las aguas nacionales superficiales de las 757 cuencas hidrológicas que comprenden las 37 regiones hidrológicas en que se encuentra dividido los Estados Unidos Mexicanos.* Mexico, 2016, p. 76.

[7] INEGI, INE, and CONAGUA, "Documento técnico del mapa de Cuencas hidrográficas de México (escala 1: 250 000).," Mexico, 2007.

[8] NOM-011-CONAGUA-2000, *"Norma Oficial Mexicana. Conservación del recurso agua. Que establece las especificaciones y el método para disponibilidad media anual de las aguas nacionales". DOF 17-Abril-2002*. México, p. 20.

[9] NOM-059-SEMARNAT-2010, *NORMA Oficial Mexicana, Protección ambiental-Especies nativas de México de flora y fauna silvestres-Categorías de riesgo y especificaciones para su inclusión, exclusión o cambio-Lista de especies en riesgo. DOF: Jueves 30 de diciembre de 2010*. México, 2010, p. 77.

[10] WWF, Fundación Río Arronte, and CONAGUA, "Norma mexicana de caudal ecológico - Una política pública para la gestión del agua a través de la conservación del régimen hidrológico," Mexico, D.F., 2012.

[11] Conagua, Fundación Gonzalo Río Arronte, and WWF, "Cuaderno de trabajo de la Norma Mexicana NMX-AA-159-SCFI-2012," Mexico, 2012.

[12] CONAGUA, *Identificación de reservas potenciales de agua para el medio ambiente en México*, Primera Ed. Mexico: Comisión Nacional del Agua, Alianza WWF-Fundación Gonzalo Río Arronte I.A.P, 2011.

[13] CONAGUA, "Decretos de reservas de agua para el medio ambiente," *20 de febrero de 2017*, 2018. [Online]. Available: https://www.gob.mx/conagua/acciones-y-programas/decretos-de-reservas-de-agua-para-el-medio-ambiente-publicados. [Accessed: 16-Mar-2018].

[14] B. D. Richter, A. T. Warner, J. L. Meyer, and K. I. M. Lutz, "A collaborative and adaptive process for developing environmental flow recommendations," *River Research and Applications*, vol. 22, no. 3, pp. 297–318, Mar. 2006.

[15] B. D. Richter and G. A. Thomas, "Restoring Environmental Flows by Modifying Dam Operations," *Ecology And Society*, vol. 12, no. 1, p. 12, 2007.

[16] N. Lloyd, G. Quinn, M. Thoms, P. A. Arthington, P. Humphries, and K. Walker, "Does flow modification cause geomorphological and ecological response in rivers? A literature review from an Australian perspective," Canberra, 2004.

[17] P. Wood and P. Armitage, "Biological Effects of Fine Sediment in the Lotic Environment," *Environmental Management*, vol. 21, no. 2, pp. 203–17, 1997.

[18] N. L. Poff and J. K. H. Zimmerman, "Ecological responses to altered flow regimes: a literature review to inform the science and management of environmental flows," *Freshwater Biology*, vol. 55, no. 1, pp. 194–205, Jan. 2010.

GROWING MEDIA MANUFACTURING FROM FLUVIAL SEDIMENTS AND GREEN WASTES FOLLOWING E.U ECOLABEL FRAMEWORK

Mamindy-Pajany Yannick[1], Scribot Cyril[2] and Abriak Nor-Edine[3]
[1,2]Univ. Lille, Laboratoire de Génie Civil et Géo-Environnement, Département Génie Civil & Environnemental, France [3]IMT Lille Douai, France

ABSTRACT

To maintain their economic activities, inland ports, rivers and canals have to be dredged. In French legislation, dredged sediments have to be managed onshore when their environmental characteristics, i.e. trace element and organics concentrations, are suggesting it. In this case, dredged sediment are considered as waste and their reuse as secondary aggregates for agronomic products is allowed under some conditions. These conditions include checking the sediment is not hazardous and the new product will not cause environmental and sanitary risks. In this context, the European Union Ecolabel framework establishes environmental, technical, and economics criteria for waste reusing as growing media for plants in landscaping. In this research, dredged sediments from French waterways are reused as aggregates in the preparation of growing media according to the rules of E.U ECOLABEL. Given their organic matter and nutrient contents, dredged sediments are relevant for manufacturing growing media. Addition of composted green waste residues and construction demolition wastes aggregates followed by sufficient tillage time allowed obtaining growing media for non-food purposes in compliance with ecolabel and legislation requirements. Also, besides the agronomic parameters, environmental characteristics of agronomic products were studied through leaching tests in order to check their conformity.

Keywords: Dredged sediments, Composted green waste residues, Growing media, E.U Ecolabel

INTRODUCTION

Sediments, which result from natural processes, are an essential, integral and dynamic part of river basins, including estuaries and coastal zones. Generally, sediments come from the weathering and erosion of minerals, organic material and soils in upstream areas and from the erosion of riverbanks. They are susceptible to being transported downstream by surface water. Deforestation and urbanization tend to facilitate the washing of superficial soils by rain which increases the amount of particles down the bottom of rivers, channels and harbors. Nowadays sediments have become an economic and environmental issue due to their accumulation in navigational infrastructures and the occurrence of chemical substances. In France, dredged sediments are considered as wastes and their reuse as secondary aggregates is allowed if there is no risk for environment. In this context, the framework SEDIMATERIAUX on the circular economy of sediments was launched in 2009 to establish environmental, technical, and economics criteria for sediment reuse [1]. In this framework, numerous collaborative projects have studied scenario for substituting a percentage of marine sand by seaport sediments in the preparation of embankment, mortar, concrete [2]. In the VAL'AGRO project, the aim is to study the possibility of preparing growing media from sediment waterways and green wastes following EU ECOLABEL requirements. Whether alone or in mixtures, peat is the substrate most commonly used in horticulture to grow seedlings and soilless plants. But quality peat is a scarce resource in southern Europe, where there is a significant soilless crop production sector. Peat must therefore be imported from northern and central Europe and recently has become more expensive [3], but resort to low cost products involves problems of quality and heterogeneity. In addition, peat is a very slowly renewable natural resource and its exploitation entails C emissions which could greatly influence climate change [4], so environmental pressure against its extraction has risen. In response to these concerns and the need for efficient recycling of wastes, the EU Commission [5] has established the ecological criteria for the award of the Community's eco-label to growing media. The EU Ecolabel is a voluntary scheme promoting environmental excellence which can be trusted. It may be awarded to products and services that have a reduced environmental impact throughout their life cycle, from the extraction of raw material through to production, use and disposal. To apply for the European Eco-label the products have to meet requirements for raw materials, hazardous substances, contaminants, nutrient loadings, product performance and product safety. A growing media shall only be considered for the award of the eco-

label if it does not contain peat and its organic matter content is derived from the processing and/or re-use of waste. In the organic constituents content of heavy metals (Zn, Cu, Ni, Cd, Pb, Hg and Cr) is limited, and also other hazardous substances (Mo, Se, As) for products containing materials from industrial processes. Products have to show low level of primary pathogens (absence of salmonella and Escherichia coli) and of viable weed seed/propagules. Besides, growing media must not adversely affect plant emergence or subsequent growth and its electrical conductivity.

Some project focused on the potential of various types of sediments as growing media and nutrient sources For example, AGRIPORT project demonstrated the environmental and economic benefits of innovative phyto-treatment processes to recycle slightly polluted dredged sediments from ports into reusable soil. The project has a high replication potential in the EU and the Mediterranean area as it offers an eco-sustainable alternative to the current expensive methods for treatment and disposal of dredged sediment. The end product is land that can be employed for gardening, environmental restoration of degraded areas and landscaping. Another example is the LIFE HORTISED project which demonstrated the suitability of dredged remediated sediments as an alternative to peat in the preparation of growing media in horticulture. It will demonstrate the potential of an innovative sediment-based growing media in the cultivation of pomegranate and strawberries, as representative plants at farm scale in Italy and Spain. Results were compared with the typical cultivation of the same fruits grown with the use of the traditional peat-based growing media. Finally, the project drew up guidelines for the safe and sustainable use of sediments as components of horticultural growing media. Dredged sediment is a material available in good quantities around the world. The aim of this research was to obtain a sediment based substrate for non-food purposes and fulfilling the requirements for award of the European Union eco-label.

EXPERIMENTAL SECTION

Sediment sampling and treatment

Sediment sample was collected in Scarpe channel in France (Saint Laurent Blangy, Pas de Calais) by using mechanical dredging techniques (Fig. 1). In a first step, the dredged sediment was characterized for chemicals (Table 1), and then it was prepared at large scale by natural attenuation and addition of composted green waste residues and construction and demolition wastes aggregates to produce suitable growing media for non-food purposes (Fig. 2).

Fig. 1 Sediment sample collection in Scarpe channel (Saint Laurent Blangy, Pas-de-Calais, France)

Table 1 Chemical parameters detected in the collected sediment sample

Chemical parameters (mg/kg)	Sediment sample	E.U Ecolabel guidelines
As	5,8	30
Cd	0,8	2
Cr	38,7	150
Cu	33,2	100
Hg	0,2	1
Ni	18,1	50
Pb	44,5	100
Zn	266	300
Total hydrocarbons (C10-C40)	1600	-

Fig. 2 Sediment samples after treatment by natural attenuation and formulation with mineral or organic amendments

Three formulations, denoted DV0, DV25, and DV50, integrating different dosages of amendments

were prepared. The mixtures were prepared on large scale by BAUDELET Company in the framework VAL'AGRO on 2 cubic meter of sediments for each formulation according to the composition reported in Table 2.

Table 2 Composition of growing media prepared by natural attenuation and amendments integration

% (v/v) Constituents	DV0	DV25	DV50
Sediment	75	75	50
Green wastes	0	25	50
C&D wastes	25	0	0

Note: Green wastes are composted by green wastes residues obtained after composting.

The use of amendments aims at to aerate the sediment sample and improve their treatment by natural attenuation and properties as growing media. The treatment by natural attenuation consist in daily mechanical returning of each formulation during 7 weeks.

RESULTS SECTION

Hydrocarbons remediation by natural attenuation

The high concentration of total hydrocarbons in the sediment sample must be decreased in order to prepare growing media owing chemical composition similar to inert wastes. In this sense, the natural attenuation of the sediment in presence of amendments was followed during 7 weeks. Results are reported in Table 3 for total hydrocarbon concentrations in each formulation.

Table 3 Total hydrocarbon concentrations (C10-C40) expressed as mg/kg in each formulation (DV0, DV25, DV50)

Time in weeks	DV0	DV25	DV50
0	1600	1600	1600
7	949	891	891

After 7 weeks the total hydrocarbon concentrations decreased by 60-55% in each formulations suggesting that the treatment by natural attenuation is efficient to improve the chemical quality of sediments. The treatment is slightly more efficient in sediment mixed with construction and demolition wastes (DV0) suggesting that the presence of aggregates improve biological degradation process by physical aeration.

At this stage, the treatment is ongoing to reduce hydrocarbon carbon concentrations near to guidelines for inert wastes (500 mg/kg). This level will ensure a low availability of this substance in leaching waters and a high protection regarding the transfer towards groundwater.

E.U Ecolabel parameters

Applicability of the different criteria to each type of product covered by E.U Ecolabel is reported in the EU commission decision 2015/2099 of 18 November 2015 establishing the ecological criteria for the award of the EU Ecolabel for growing media, soil improvers and mulch. The following criteria should be checked for growing media: Constituents (Criterion 1), Organic constituents (Criterion 2), Mineral growing media and mineral constituents (Criterion 3), Recycled/recovered and organic materials in growing media (Criterion 4), Limitation of hazardous substances (Criterion 5), Stability (Criterion 6), physical contaminants (Criterion 7), Viable weed seeds and plant propagules (Criterion 9), Plant response (Criterion 10), Growing media features (Criterion 11), Provision of information (Criterion 12) and Information appearing on the E.U Ecolabel (Criterion 13). According to results obtaining on three tested formulations DV0, DV25, and DV50, all growing media are in compliance with E.U Ecolabel criterion. On criterion 5, metals and PAHs (List of 16 PAHs from US EPA) concentrations measured in the sediment and the formulations are in compliance with E.U ECOLABEL levels (Table 4). Although, no guidelines is proposed for total hydrocarbons (C10-C40), this parameter should be checked for all substrates formulated from waterways sediments.

Table 4 Chemical parameters measured on each growing media (DV0, DV25, and DV50) after 7 weeks

Chemical parameters (mg/kg DW)	DV0	DV25	DV50	Ecolabel product content
Cd	0.4	0.4	0.4	3
Cr	29.2	29.9	32	150
Cu	37.0	37.6	40.8	100
Hg	-	-	-	1
Ni	15.2	16.2	16.7	90
Pb	53.4	77.5	59.6	150
Zn	282.9	289.4	291.4	300
Total PAHs	2.89	3.01	3.9	6

Note: Total PAHs = sum of napthtalene, acenaphtylene, acenaphtene, fluorine, phenantrene, anthracene, fluoranthene, pyrene, benzo(a)anthracene, chrysene, benzo(b)fluoranthene, benzo(k)fluoranthene, benzo(a)pyrene, indeno(1,2,3-cd)pyrene,dibenzo(a,h)anthracene and benzo(ghi)perylene.

CONCLUSIONS

The study is ongoing for improving the final quality of the product formulated from waterways sediments, construction and demolition wastes, and composted green waste residues. After 7 weeks, the products (DV0, DV25 and DV50) are in compliance with EU ECOLABEL criteria, however, the total hydrocarbons concentrations in the sediment should reduce at acceptable level similar to inert waste to ensure its environmental guarantee.

In the next step of the project, the treatment will be continued during few months (around 5 months) in order to decrease chemical content in hydrocarbons (C10-C40) and then lysimetric experiments will be performed at various scale (in lab and field) to check the environmental impact and agronomic properties of the three formulated growing media.

ACKNOWLEDGEMENTS

The project was financed by “Conseil Régional Hauts-de-France” within the framework SEDIMATERIAUX. Authors thanks other partners from the project VAL’AGRO for treatment application at large scale (BAUDELET ENVIRONNEMENT and NEO-ECO companies) and CU ARRAS for providing the sediment.

REFERENCES

[1] Abriak N-E., « Conference talk » In : LGCgE, *Salon Environord*. Lille grand Palais, juin 2015.
[2] Mamindy-Pajany Y., « Conference talk » In : cd2e, Congrès Eco-technologies pour le futur, Journées Nationales Sédiments, Lille grand Palais, juin 2014.
[3] H.M. Ribeiro, A.M. Romero, H. Pereira, P. Borges, F. Cabral, E. Vasconcelos Bioresour. Technol., 98 (2007), pp. 3294-3297
[4] A.Boldrin, K.R. Hartling, M. Laugen, T.H. Christensen Resour. Conserv. Recycl. 54 (2010), pp. 1250-1260.
[5] EU commission decision 2015/2099 of 18 November 2015 establishing the ecological criteria for the award of the EU Ecolabel for growing media, soil improvers and mulch.

7. Reuse and management of sludge from water treatment

Session chairs: Gabriela Mantilla[1] and Guillermo Quijano-Govantes[2]
[1]Coordinación de Tratamiento y Calidad del Agua, Instituto Mexicano de Tecnología del Agua, México
[2]Laboratorio de Investigación en Procesos Avanzados de Tratamiento de Aguas, Instituto de Ingeniería de la UNAM, México

One of the main challenges during water and wastewater treatment is the management of the produced sludge. The sustainability and economic feasibility of water and wastewater treatment plants are strongly impacted by the technologies used for sludge management. In the 21th century conception, the sludge could be considered as a raw material to produce added-value products, including fertilizers, soil conditioners, and renewable energy, among others. The main characteristics of the resulting sludge depend on the composition of water and/or wastewater and the treatment technology used, which in turn will determine the possible benefit obtained from the sludge. Contributions to this subject are most welcome, especially those related with (i) biogas production, (ii) pathogens characterization in digestates and challenges towards the reuse in agricultural activities, (iii) added-value products, and (iv) recovery of chemical products

ESTIMATING H_2S CONCENTRATION IN BIOGAS PRODUCED BY ANAEROBIC SLUDGE FROM SULFUR-RICH WASTEWATERS

Quijano Guillermo, Figueroa-González Ivonne, Moreno Gloria and Moreno-Andrade Iván[1]
[1]Laboratory for Research on Advanced Processes for Water Treatment, Unidad Académica Juriquilla, Instituto de Ingeniería, Universidad Nacional Autónoma de México, México

ABSTRACT

Sulfur-rich wastewaters such as wine vinasses (WV) or cheese whey (CW) have the potential to produce biogas highly loaded with hydrogen sulfide (H_2S), which is a pollutant that must be removed prior the use of biogas for thermal/electrical energy generation. The presence of H_2S in biogas leads to the formation of H_2SO_4 after contact with water producing damage to engines, turbines and internal parts of devices running on biogas to generate energy. The H_2S concentration in biogas must be maintained below 500 ppm_v to avoid corrosion issues. Therefore, the estimation of the H_2S concentration in biogas produced from sulfur-rich effluents is of paramount relevance to anticipate and design adequate desulfurization technologies. In this work, a correlation based on the biochemical biogas potential and other characteristics of the target effluent was developed to estimate the H_2S concentration in the resulting biogas. The model predictions were compared with H_2S concentrations experimentally quantified in biogas produced from WV, CW and organic fraction of municipal solid waste (OFMSW) by an anaerobic sludge. The model accurately predicted the H_2S concentration in biogas from WV and CW, while slightly underestimated the H_2S concentration from OFMSW, which was attributed to the complex composition of this waste.

Keywords: Anaerobic Sludge, Biogas, H_2S, Sulfur-rich wastewaters

INTRODUCTION

Sulfur-rich effluents are ubiquitous in industrial processes. This is the case of wine vinasses (WV) or cheese whey (CW). These effluents might contain sulfate concentrations from 0.5 up to 50 g L^{-1} [1],[2]. Likewise, these effluents contain high concentrations of organic matter that can be converted into biogas by means of anaerobic digestion processes performed by anaerobic sludge [1]. The biogas produced from sulfur-rich effluents might contain H_2S concentrations up to 20,000 ppm_v (2% v/v) [3]. The presence of H_2S limits the use of biogas to produce heat and power as it causes corrosion to internal combustion engines and industrial pipes. The maximum allowable concentration of H_2S in biogas to be used in combined heat and power processes is in the range of 80-400 ppm_v [4]. Therefore, important efforts must be made to purify highly H_2S-laden biogas for energy production.

In this context, the estimation of the H_2S concentration in biogas is quite useful towards anticipating the suitable biogas purification system given the type of sulfur-rich effluent. The present work presents a relatively simple equation to estimate the maximum H_2S concentration in biogas (Eq. 1):

$$H_2S_{\%} = \frac{\left(\frac{TS}{MW}\right)22.4}{BBP} \times 100 \quad (1)$$

where, TS, MW and BBP represent the total mass of sulfur per gram of COD fed (gS $gCOD^{-1}$), the sulfur molar weight (32 g $mole^{-1}$) and the biochemical biogas potential (normalized L of biogas produced per g of COD fed), respectively. The factor 22.4 stands for the molar volume at normal pressure and temperature conditions (normalized L of H_2S per mole). Equation (1) assumes that all the sulfur fed is fully converted into H_2S during the anaerobic digestion process, estimating therefore the maximum H_2S concentration that can be reached. H_2S concentration in ppm_v units can be obtained as:

$$H_2S_{ppmv} = H_2S_{\%} \times 10{,}000 \quad (2)$$

Equation (1) was used to estimate the H_2S concentration in the biogas obtained from WV, CW and diluted OFMSW. Model estimations were then compared with experimental measurements of H_2S concentration. Nowadays, these effluents are used worldwide to produce renewable energy in the form of biogas. Hence, it is important to develop tools for anticipating the H_2S concentration in the resulting biogas given the characteristics of the target effluents and the operating conditions (e.g. level of effluent dilution).

MATERIALS AND METHODS

Biochemical Biogas Potential

The BBP tests were performed in an Automatic Methane Potential Test System (AMPTS II, Bioprocess Control, Sweden). This experimental system allowed the testing the three effluents in the same experimental run with automatic methane gas quantification (triplicate experiments for each effluent). The raw biogas composition (CH_4, CO_2 and H_2S) was also characterized by gas chromatography to obtain the BBP. The tests were performed in 500 mL glass bottles (370 mL of liquid working volume) at 37°C. Agitation at 144 rpm was provided for 1 min every 3 minutes by means of a rotating shaft. The bottles were inoculated with 50 g of anaerobic granular sludge (brewery wastewater treatment plant, Guadalajara, Mexico). A ratio of 0.5 gCOD of substrate per gTVS of inoculum was used. Controls without effluent (to evaluate the endogenous production of the inoculum) and controls with glucose (to evaluate the activity of the inoculum) were also performed in triplicate. Besides providing 4.4 mL of mineral salt medium and $NaHCO_3$ to each bottle, as recommended by Angelidaki et al. [5], distilled water was added to reach a working volume of 0.37 L in all the bottles.

Inoculum and effluents characterization

In order to set a 0.5 ratio of gCOD to gTVS in the BBP tests, the effluents were prepared as follows: 150 g of restaurant OFMSW were diluted in 1.5 L of distilled water, while raw WV and CW were diluted by factors of 8.4 and 2.3 in distilled water, respectively. Total volatile solids (TVS), density of the inoculum and COD of effluents were determined according to standard methods. Total sulfur content in the inoculum and effluents was determined by plasma-mass spectrometry (ICAPq, Thermo, USA). A summary of the main characteristics of the sludge and effluents is given in Table 1.

Table 1 Characteristics of the inoculum and substrates used in the BBP tests

Effluent / Inoculum	COD effluent[1] ($g\ L^{-1}$)	Sulfur content[1] ($gS\ L^{-1}$)	Volume in the BBP (L)
WV	25.0	1.7×10^{-3}	0.104
CW	25.0	2.0×10^{-3}	0.101
OFMSW	15.5	4.4×10^{-3}	0.161
Sludge[2]	-	3.0×10^{-2}	0.050

[1]Data corresponding to diluted effluents.
[2]TVS and density of the sludge were 0.1 g g^{-1} and 1.0 g mL^{-1}, respectively.

RESULTS AND DISCUSSION

The biogas production from the three effluents tested was similar, ranging from 0.35 to 0.39 L_{Biogas} per gram of COD fed. The WV showed the highest biogas production, while the OFMSW exhibited the lowest biogas production (Fig. 1). These results are in agreement with the literature as BBP values from 0.33 to 0.50 L_{Biogas} $gCOD^{-1}$ have been so far reported for these effluents [6]-[8].

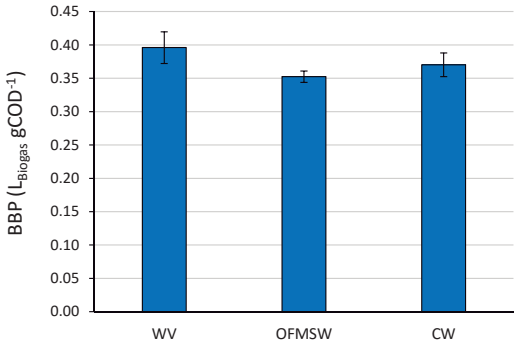

Fig. 1 Biochemical biogas production of the effluents investigated

The biogas composition in terms of CO_2 and CH_4 percentages is shown in Fig. 2. It was observed that in all effluents, the CH_4 percentage was at least 60%, this percentage being up to 67% in the case of WV. These results showed that even when effluents and the inoculum contained a relatively high sulfur content, the resulting biogas had enough quality to be used in energy production devices considering its CH_4 and CO_2 content.

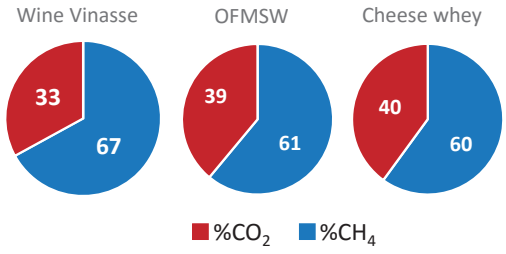

Fig. 2 Composition of the biogas obtained from the three effluents investigated in terms of CH_4 and CO_2 percentage

In a first approach, Eq. (1) was used to estimate the H_2S concentration in biogas considering only the sulfur contained in the effluents. This approach was tested since the total sulfur concentration of the inoculum is not a common operating parameter reported for setting up BBP tests. Under this approach, the estimated H_2S concentration in biogas

is assumed to be produced only from the sulfur contained in the substrates. As shown in Fig. 3, when comparing the experimental H_2S concentrations with model estimations an important underestimation was observed when the sulfur content of the inoculum was neglected. Based on these estimations, it could be erroneously concluded that the biogas do not require a further desulfurization process as the H_2S concentration was below the limit of 500 ppm_v to be used in industrial energy production devices.

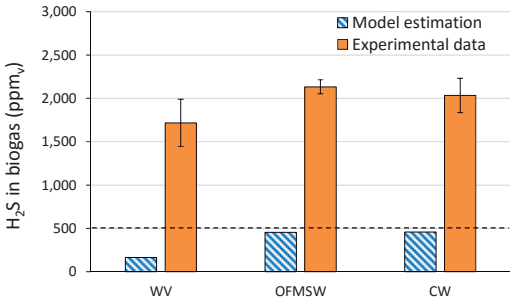

Fig. 3 Model estimations and experimental H_2S concentrations in the biogas. Model estimations only considered the sulfur contained in the substrates

In a second approach, the sulfur contained in the inoculum was also considered to calculate the total mass of sulfur per gram of COD fed in the BBP tests. Interestingly, the sulfur content of the inoculum was up to 18 times higher than that contained in the diluted effluents, which clearly showed that the sulfur content in the inoculum must be considered to retrieve realistic estimations of H_2S concentration from Eq. (1). Figure 4 shows that the model estimations for the three effluents were very similar to the experimental data when the sulfur content of the inoculum was considered.

It is important to stress that while model estimations were in full agreement with the experimental H_2S concentrations of WV and CW, for OFMSW the estimation was ~20% higher than that observed experimentally. This overestimation was attributed to the complex nature of the OFMSW. An important fraction of the sulfur content in the OFMSW is contained in particles of suspended solids, and it is available for reduction to H_2S once complex hydrolytic processes have occurred. In fact, the amount of total solids in the OFMSW (32.1 g L^{-1}) herein studied was 2 and 10 times higher than that in WV and CW, respectively.

A fundamental assumption of Eq. (1) is that all the sulfur content is converted into H_2S during the anaerobic digestion process. This assumption was very reasonable for liquid effluents such as WV and CW. This ~20% overestimation factor must be considered when using Eq. (1) for estimating the H_2S concentration in biogas obtained from effluents rich in complex macromolecules such as OFMSW. The magnitude of this overestimation factor is expected to be a function of both the OFMSW dilution used and the size of the particles, which depends on the grinding process used.

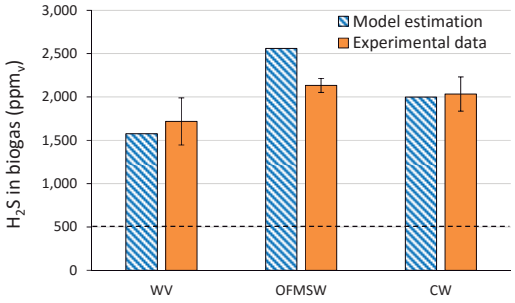

Fig. 4 Model estimations and experimental H_2S concentrations in the biogas. Model estimations considered the sulfur contained in substrates and inoculum

When the sulfur contained in substrates and inoculum is considered, the model estimations clearly showed that a desulfurization process is required before the biogas produced can be used in energy production devices. In fact, the H_2S concentration in the biogas obtained from all the effluents must be reduced (at least) 3-5 times to enable its use for energy production.

CONCLUSIONS

As far as the authors know, this is the first report on the successful application of a simple model for the estimation of H_2S concentration in biogas produced from liquid effluents. From a process implementation point of view, the model here presented constitutes a very useful tool for anticipating the potential desulfurization process that will be required based on relatively simple parameters such as sulfur content, COD fed and BBP data. The model yielded highly accurate estimations of H_2S concentration for liquid effluents. In the case of effluents with a high content of particles of suspended solids (e.g. OFMSW), the model overestimates the H_2S concentration in biogas by a factor of approximately 20%. This magnitude of this overestimation is expected to be a function of the dilution of the waste and the size of the particles in the case of OFMSW. This factor must be considered when using Eq. (1) to estimate the H_2S concentration in complex effluents rich in suspended solids.

ACKNOWLEDGEMENTS

The financial support granted by "Fondo de Sustentabilidad Energética SENER– CONACYT (Mexico)", through the project 247006 Gaseous Biofuels Cluster, is gratefully acknowledged.

REFERENCES

[1] Lens PNL, Visser A, Janssen AJH, Pol LWH, Lettinga G, "Biotechnological Treatment of Sulfate-Rich Wastewaters", Crit. Rev. Environ. Sci. Technol., Vol. 28, Jun. 1998, pp. 41-88.

[2] Rubio-Rincon F, Lopez-Vazquez C, Welles L, van den Brand T, Abbas B, van Loosdrecht M, Brdjanovic D, "Effects of electron acceptors on sulphate reduction activity in activated sludge processes", Appl. Microbiol. Biotechnol., Vol. 101, Aug. 2017, pp. 6229-6240.

[3] Fortuny M, Baeza JA, Gamisans X, Casas C, Lafuente J, Deshusses MA, Gabriel D, "Biological sweetening of energy gases mimics in biotrickling filters", Chemosphere, Vol. 71, March. 2008, pp. 10-17.

[4] Aita BC, Mayer FD, Muratt DT, Brondani M, Pujol LB, Denardi LB, Hoffmann R, da Silveira DD, "Biofiltration of H_2S-rich biogas using Acidithiobacillus thiooxidans", Clean Technol. Environ. Policy, Vol. 18, March. 2016, pp. 689-703.

[5] Angelidaki I, Alves M, Bolzonella D, BorzacconiL, Campos JL, Guwy AJ, Kalyuzhnyi S, Jenicek P, van Lier JB, "Defining the biomethane potential (BMP) of solid organic wastes and energy crops: a proposed protocol for batch assays", Water Sci. Technol., Vol. 59, March. 2009, pp. 927-934.

[6] Lalov IG, Krysteva MA, Phelouzat JL, "Improvement of biogas production from vinasse via covalently immobilized methanogens", Bioresour. Technol., Vol. 79, Aug. 2001, pp. 83-85.

[7] Demirer GN, Duran M, Erguder TH, Guven E, Ugurlu O, Tezel U, "Anaerobic treatability and biogas production potential studies of different agro-industrial wastewaters in Turkey", Biodegradation, Vol. 11, Nov. 2000, pp. 401-405.

[8] Rodríguez-Pimentel RI, Rodríguez-Pérez S, Monroy-Hermosillo O, Ramírez-Vives F, "Effect of organic loading rate on the performance of two-stage anaerobic digestion of the organic fraction of municipal solid waste (OFMSW)", Water Sci. Technol., Vol. 72, Aug. 2015, pp. 384-390.

CHARACTERIZING THE EVOLUTION OF SEDIMENT-LIKE WASTES EXPOSED TO AMBIENT CONDITIONS IN OPEN RESERVOIRS

Hernández D.[1,2,3], Astudillo C.A.[2], Fernández-Palacios, E.[3], Cataldo, F.[1,2], Tenreiro, C.[2], Gabriel D.[3]
[1]Instituto de Química de Recursos Naturales, Universidad de Talca, Chile
[2]Facultad de Ingeniería, Universidad de Talca, Chile
[3]Grupo de investigación GENOCOV. Departamento de Ingeniería Química, Biológica y Ambiental, Universidad Autónoma de Barcelona, Bellaterra, España.

ABSTRACT

The main impact of olive mill wastes stored in open reservoirs is the emanation of unpleasant odorous substances. This manuscript focuses on the study of Alperujo and Orujo, two wastes that behave as sediments when stored in open pools. The aim was to monitor the changes in their physical-chemical parameters (ash, humidity, phenols, pH, proteins, fibers, oils and fats) and microbial biodiversity (through Ilumina platform for bacteria and fungi) as well as to characterize the evolution of volatile organic compounds as a consequence of waste decomposition. Gaseous emissions were analyzed during six months using thermal desorption gas chromatography mass spectrometry. A statistical analysis was performed in order to measure the impact of ambient conditions in the most relevant physical-chemical parameters. During the first three months, a decrease in the concentrations of compounds responsible for the scent was recorded, while compounds responsible of unpleasant odors appeared after three months. The dynamics of these odor compounds was related to the degradation of organic matter, the increase of microorganism's diversity and the influence of the environmental variables that directly impacted physical-chemical parameters as well as the concentrations of fats.

Keywords: Agroindustrial waste, Odor, Alperujo, Orujo, Fatty acids.

INTRODUCTION

In the process of olive oil extraction, 20% olive oil is obtained and about 80% corresponds to waste [1]. Two of these residues, alperujo and orujo, obtained from the two-phase and three-phase systems, are mixtures of water, oils, cellulose, lignin, proteins, carbohydrates, nitrogen, organic acids, pectins, tannins, polyalcohols and a small fraction of active phenolic compounds and other derivatives [2]. Currently, due to the properties of its content, these systems can be used for the generation of electrical energy, composting, biodiesel, etc. as long as they have a low percentage of humidity [1].

Currently in Chile, the alperujo and orujo have no specific final destination, transforming them into a waste without use that accumulates in the same agricultural land where it is produced (oil mills) or stored in specially constructed reservoirs for these purposes, so that the high temperatures (from winter to spring) reduce their moisture and volume. This situation generates two important environmental problems: a) undesirable odors for the surrounding population; and b) damage to land, surface effluents and groundwater.

On the other hand, when oil mills come into operation they have a direct effect on the environment since the liquid and solid residues accumulated (alperujo, orujo, alpechin and washing water) generate emissions of Volatile Organic Compounds (VOCs) that are generally odorous [3]. A study conducted by Brenes [4] shows that one of the compounds responsible for unpleasant odors in the olive paste stored for 8 months under uncontrolled conditions is the 4-ethylphenol with concentrations of 476 mg kg^{-1} in the liquid phase. Subsequently, it was shown that the 4-ethylphenol formation in alperujo, was a result of the growth of lactic acid bacteria, particularly *Lactobacillus pentosus* [5].

The growth of other microorganisms such as *Saccharomyces sp., Candida boidinii and Geotrichum candidum* has also been reported in alperujo as substrate [6]. The authors of [7] describe that the growth of certain species in olive brine, alpechin, and other olive products, are unique because of their particular chemical composition.

There is no information about the mechanisms of orujo and alperujo decomposition in relation to emissions. In addition, the microbial diversity and its evolution in alperujo and orujo wastes have not been described. Therefore, the present research aims at studing the evolution of physical-chemical and microbiological characteristics as well as the generation of VOCs from alperujo and orujo when they naturally degrade in storage reservoirs under uncontrolled ambient conditions. The influence and physical-chemical parameters of the ambient

conditions on the evolution of the characteristics of the residues and their microbial diversity in a period of 6 months from winter to spring were evaluated in order to find existing relationships between environmental and physical-chemical parameters.

MATERIALS AND METHODS

Samples

Three samples of each residue were used, one from the two-phase system and another from the three-phase system, from two different oil mills: a) Orujo, hereinafter O, Almazara del Pacifico, Alto Pangue, Talca, Chile; b) Alperujo, hereinafter A, Agrícola y Forestal don Rafael, Molina, Chile. Each oil mill in its processes had treated the varieties of fruit called Arbequina, Leccino and Picual. The samples were extracted directly from the oil mills, which were emptied from the only waste outlet duct towards 200 L plastic containers. The samples were moved and stored at the Universidad de Talca, Curicó, Chile (Latitude -35.0059 and Longitude –71.22.52) and kept open and outdoors between the months of June-November (Winter to spring).

Samples from each container were taken using a 250 cm^3 dredger sediment sampler (Van Veen, 12.110 model, Sidmar). Initially, one sample from each contained was extracted, analyzed and considered as reference. Subsequently, all the ends of the month, four kilograms from each container were extracted. Two kilograms from the upper part, hereinafter AT (alperujo) and OT (orujo), respectively and two kilograms from the intermediate part (half of the height and diameter of each container), hereinafter AM and OM for A and O, respectively. One kilogram of the upper part and one kilogram of the intermediate part were kept frozen at -18ºC for later analyzes and controls, while the other remaining kilogram from the intermediate part were used to make different physicochemical analysis in triplicate.

Analytical methods.

A and O samples were monthly analyzed, conducting standardized physical-chemical analyzes. For all these procedures, excluding pH and total phenolic, the samples were dried at 103±2ºC using a Memmert brand oven model W02WVU.

Every two months, a Fatty Acids Methyl Esters (FAMEs) analysis was carried out by taking one g from each wet A and O sample and using the method described by [8]. Later, the organic phase was extracted and brought to dryness using a rotavapor (Steroglass strike, model 300), to be finally reconstituted in 1.0 mL of hexane and analyzed in a gas chromatograph with mass detector (GC/MS), Thermo Fisher Scientific, model Trace 1300/ISQELTL, in Splitless mode at 50-280 ºC, injector temperature 250ºC; Split Flow 50 ml/min; Split Ratio 33.i; Constant flow 1,5 ml/min. Detector: MS transfer line temp: 200ºC, Ion source temp 230ºC and using a capillary column Rtx-5MSD.

The composition of VOCs was also measured and quantified by Thermal Desorption Gas Chromatography Mass Spectrometry (TD-GC/MS). Every two months, two grams of each sample (A and O) were extracted from the solid phase of the containers and deposited in 20 mL vials (Restek), and then conditioned for 60 minutes in a thermoregulated bath (Memmert, 14 Lt WNB) at a temperature of 30°C. Subsequently, with a suction pump (Markes Easy VOC, LP-1200), 10 ml of the gas phase was extracted through adsorption tubes (Markez C2-BAXX-5315 odor/sulfur. C6/7-C30, thiols and mercaptans). The desorption of the tubes was carried out using a thermal desorption cold trap injector (TD, Markes, Unity-xr). The gases were extracted in split mode, driven with helium, to the hot trap programmed at 300°C for 1 minute, then cooled to 20°C in the cold trap, to finally be heated at 300°C for 5 minutes. The volatiles were transferred by means of a transfer line heated at 200°C to a column (Rtx-5MS) installed in a GC/MS (Split oven mode Tº 40-220 ºC). Flow de 1,2 ml/min; Split Ratio de 10 ºC/min. Detector MS transfer line 200 ºC, y Ion source a 250 ºC). The qualitative identification of VOCs was carried out using the Chromeleon software package with the NIST library using standard retention times. Quantification was performed using Merck, Sigma-Aldrich and Lancaster standards. The Limit of Detection (LOD) of each compound was greater than or equal to 3 times the signal-to-noise ratio.

Ambient conditions.

For six months and every day, the conditions of temperature, moisture, wind speed and amount of rainfall were measured. The results are shown in Table 1, as a monthly average of each.

Table 1 Average monthly meteorological conditions

	Units	Jun	Jul	Aug	Sep	Oct	Nov
PPT	mm	10.6	25.6	4.5	3.2	15.1	2.5
Tmin	ºC	4.5	5.2	6.0	5.6	8.3	9.8
Tmax	ºC	13.0	14.2	19.0	21.5	22.5	25.2
Wind	Km h^{-1}	4.0	10.4	7.5	8.5	9.2	10.5
RH	%	86.0	86.0	81.0	77.0	71.0	58.0

Precipitation (PPT); Temperature min. (Tmin); Temperature max. (Tmax); Wind speed (wind); Relative humidity (RH)

Statistical methods.

In order to find relationships between the chemical and environmental variables, we conducted a series of correlation analysis. The corresponding plots were obtained using the R package "PerformanceAnalytics" and the estimators provided there [9].

Illumina sequencing analysis.

Identification of the microbial population in samples of A and O was performed using next-generation sequencing at day 30 (June) and after 6 months (November), the samples were extracted as a mixture of each container. DNA was extracted from samples by applying the protocol of MoBio PowerSoil™ DNA extraction kit (MoBio Laboratories, USA). The quantity and quality of the extracted DNA were evaluated by using a NanoDrop 1000 Spectrophotometer (Thermo Fisher Scientific, USA). Paired-end of the extracted DNA was performed on an Illumina MiSeq platform by an external service (Scsie UV, Valencia). Bacterial 16S rRNA variable region V3-V4 was targeted using the primer pair 341F-806R. A fungus-biased primer set consisting of ITS1/ ITS4 was employed to amplify the fungal internal transcribed spacer ITS1 region.

RESULTS AND DISCUSSION

Evolution of physicochemical parameters of wastes.

Table 2 shows the results of the initial physicochemical parameters of the samples of A and O. In general, the values found were similar to those referenced by different authors [1], [10]. Therefore, the samples used were considered to be representative of the typology of residues studied.

Table 2 Physicochemical parameters of the initial samples of A and O

Analysis		Units	A	O
mc *	AOAC 945.15	%	58.3	67.2
cp *	AOAC 979.09	%	8.7	7.7
mhv*	DIN 51.900	MJ kg^{-1}	21.9	20.1
ashes*	AOAC 940.26	%	1.8	2.5
cf*	AOAC 920.169	%	86.7	79.1
fats*	AOAC 963.15	%	8.7	7.6
pH**			5.7	5.8
tp**	folin-ciocalteu´s	g kg^{-1}	13.2	17.2

moisture content (mc)*; crude protein *(cp); measuring heating value* (mhv); crude fiber* (cf); total phenolic (tp)**. *dry base; **wet base

Table 3 shows the data of the evolution of the parameters analyzed throughout the study period for both waste (A and O) in the upper and intermediate areas of containers. Table 3 also shows the percentage of relative variation between the maximum and minimum data for each parameter over the period. Those data with a difference greater than 8% between the maximum and the minimum were considered as statistically variable, mainly moisture, proteins, fats, phenols and ashes; while fibers, heating value and pH were considered constant and did not present major changes in time, behaving similar to the values indicated in Table 2 for initial A and O, therefore, they are not indicated in Table 3.

Table 3 Evolution of the physicochemical parameters of the samples of A and O

Analysis	Jun	Jul	Aug	Sep	Oct	Nov	% change
AT							
mc	56.9	62.7	57.7	43.0	37.9	32.9	47.5
cp	8.5	8.6	8.2	7.5	6.4	6.0	30.1
ashes	1.9	1.8	1.7	1.9	2.1	2.3	27.0
fats	12.0	11.0	10.4	9.5	8.8	8.2	31.4
tp	13.1	8.8	8.6	8.4	12.4	12.3	35.9
AM							
mc	60.4	68.9	60.8	56.0	47.8	43.0	37.7
cp	8.3	8.2	8.1	7.0	6.9	6.5	21.6
ashes	1.9	1.3	1.3	1.9	2.1	2.2	42.1
fats	8.5	8.6	8.6	8.3	8.0	7.8	9.5
tp	13.3	8.6	8.9	8.5	12.3	12.4	36.1
OT							
mc	69.9	70.7	72.7	69.0	56.9	41.5	42.8
cp	8.4	8.0	7.6	7.1	6.3	5.8	31.5
ashes	2.9	3.2	3.5	3.7	3.9	4.3	31.0
fats	11.4	11.3	10.8	10.5	10.0	9.6	16.1
tp	13.6	13.4	13.6	16.4	18.4	22.3	40.1
OM							
mc	68.4	72.8	73.8	68.0	57.4	47.3	35.8
cp	8.3	8.1	7.9	7.0	6.5	6.1	26.9
ashes	3.5	3.6	3.7	4.0	4.5	5.0	30.4
fats	8.3	7.1	7.3	6.6	6.0	5.6	33.0
tp	14.6	12.5	13.8	15.2	19.2	21.2	41.2

At a general level, it is important to highlight the results described here (Table 3), because they show important differences between both residues (A and O). Moisture, ash content and total phenols were revealed as the parameters that showed to be significantly variable over time, presenting higher average values in orujo than in alperujo. The

moisture of O was between 13% and 33% higher on average than that of A, ash content between 129% and 84% higher in O than in A, while phenols registered 53% and 51% higher in O than in A.

Statistical relationship between environmental factors and the physicochemical parameters of wastes.

The values reported in Table 1 for Tmax, Tmin and RH correlated significantly with most of the physical-chemical parameters in Table 3. The moisture of the containers with Tmax and Tmin values, reported negative Pearson values, since the moisture in the containers decreased due to the increase in temperatures during warmer months (Jun-Nov), there being a linear trend. On the other hand, the moisture of the containers correlated positively with RH, which means that, if RH decreases, then the moisture of the containers decreases because a lower degree of RH in the environment favors the evaporation of water. It can also be observed that the moisture of the containers decreased more in the upper part (AT and OT), than in the intermediate part (AM and OM), where this consequence is a product of the high correlation that exists with the temperatures, wind and solar radiation that favored more the evaporation in the upper area of the containers, since these were open. In addition, it is evident that between the samples of O (OT and OM) and A (AT and AM), there are no significant differences in moisture loss.

On the other hand, the container proteins correlated negatively with the Tmax and Tmin values, which means that when the temperatures increased, the proteins decreased in a proportionally linear manner. These data coincide with those reported by [11], which indicate that, at higher temperature and aging time of stored fruits, soluble proteins decrease their concentration, due to the different metabolic pathways that involve the synthesis of proteins. A positive correlation between proteins and RH is also observed, where the relative humidity of the air decreases coincidently with a reduction of the proteins.

An inverse dependence between fats and temperatures was also observed. When the temperatures increased, the fats of the containers decreased both for O (OT and OM) and A (AT and AM), as reported by [12], because at a higher temperature the autooxidation is favored and, therefore, a reduction in the amount of fats in the containers is produced.

Temporal evolution and interrelation between FAMEs and VOCs.

FAMEs that come from the fatty acid alkyl ester (FAAEs) can be a two-way product by esterification of free fatty acids or the transesterification of the alkyl ester with methanol [13].

Table 4 describes the most important FAMEs found in samples of O and A, which are similar in compounds to those reported by [14] for vegetable oils. It is evident to observe that the concentrations of FAMEs were affected in time, showing a significant change in the samples of O and A.

Table 4 also shows that the composition and general concentrations of FAMEs for O and A are relatively similar. Particular case is the C18:1 n9 that increased the concentration, while the rest of fatty acids decreased. In a different study, the authors of [15], evaluated changes in the fatty acids of Spanish olive oils stored at room temperature for 21 months, observing that the linoleic acid was reduced between 2.1% and 3.8% and the linolenic acid between 5.8% and 10.0%, whereas the oleic acid showed no significant changes. However, in our study, if we analyze in detail the changes over time presented by C18:1 n9, it is observed that its concentration was approx. 40% higher in O than in A. This tendency may be due to its high initial concentration compared to the rest of fatty acids or it may be due to its greater degree of establishment, since polyunsaturated fatty acids with more than one double bond oxidize more quickly than those monounsaturated.

Table 4 Main fatty acids identified over time in samples of A and O, measured in mg kg^{-1}. Where the notation Cx:y,nz indicates x= number of carbon atoms; y= number of double bonds; z= C atom where the double bond is located

FAMEs	Alperujo			Orujo		
	Jul	Sep	Nov	Jul	Sep	Nov
C16:1n9	0.4	0.3	0.2	0.2	0.1	0.1
C16:0	1.8	1.7	1.7	1.9	1.3	1.0
C17:1 n10	0.4	0.3	0.3	0.5	0.3	0.3
C18:0	0.1	-	-	0.3	0.2	0.2
C18:1 n9	5.1	6.0	6.7	5.0	6.3	7.6
C:18:0	1.2	1.0	0.9	1.1	1.0	0.5
C20:1 n11	0.5	0.1	-	0.5	-	-
C19:0	0.5	0.5	0.2	0.2	0.1	0.1
C20:0	2.3	2.2	2.1	0.3	-	-
C30:6n2,5,9,13,17,20	1.8	1.7	1.7	2.4	2.2	2.1

Table 5 shows the results of VOCs found and their evolution in A and O, observing that some of these molecules decreased their concentration, while others increased at the end of six months. VOCs are molecules with low molecular weight, high vapor

pressure and that under ambient conditions of pressure and temperature go into the gaseous state [16]. More than 100 volatile odorant compounds have been identified in vegetable oils, such as hydrocarbons, alcohols, aldehydes, ketones, esters, acids, terpene compounds and furan derivatives [16].

Table 5 Main volatile organic compounds identified in samples of O and A (mg kg^{-1})

	Alperujo			Orujo		
VOCs	Jul	Sep	Nov	Jul	Sep	Nov
n-pentane	6.6	0.11	-	7.8	5.8	3.6
n-hexane	1.9	-	-	0.1	-	-
n-heptane	3.8	2.8	0.5	0.8	0.5	0.1
2-heptanone	-	-	1.0	-	-	0.5
n-octane	4.8	1.8	1.1	3.8	2.6	1.2
ethyl butanoate	0.9	0.4	-	0.9	0.6	-
phenol	4.7	3.3	2.8	1.3	1.1	0.6
butanal. 3-methyl	-	-	3.0	-	-	4.2
butanal. 2-methyl	-	-	2.8	-	-	4.4
butanoic acid	-	-	4.9	-	-	5.9
hexanoic acid	-	-	1.2	-	-	1.8
heptanal	-	-	1.1	-	-	2.1
octanal	-	-	2.2	-	-	4.9
nonanal	-	-	2.6	-	-	2.7
decanal	-	-	0,8	-	-	0,4

The upper part of Table 5 shows the molecules that decreased their concentration over time for A and O. These families of compounds, n-pentane, n-hexane, n-heptane, n-octane and phenol, as well as others (alcohols, aldehydes, ketones, etc.), are responsible for the aroma of oils, which last while kept in closed containers and away from high temperatures and light, preventing fatty acids from suffering oxidation, [17]. On the contrary, as in our case (open containers and high temperatures), lipid hydroperoxides should have been generated, which decompose easily in alkoxy radicals to form different secondary compounds. The ethyl butanoate also decreases its concentration, possibly because it is oxidized to carboxylic acid (butanoic acid), appearing only in the month of November. Its presence must be a product in addition to the existence of *clostridium* colonies that grew in the last months, which also coincides with what was reported by [18]. Another compound that appears at the end of the process is 2-heptanone, where its presence must be the product of the growth of different species of the genus *Aspergillu*s, together with *ascomicetos,* and *Penicillium notatum*, that have the ability to oxidize free fatty acids [19].

The 3-methylbutanal and 2-methylbutanal, which are odorant molecules and appear in high concentrations in recent months for both samples, may be a product of the metabolism of amino acids (total proteins), which decrease their concentration for O and A, as the months progressed (see Table 3) as it also reports [20]. The heptanal, octanal, nonanal and decanal appear only in the last month for both samples, as a product of different mechanisms of degradation, such as the autoxidation of fatty acids and the enzymatic activity of lipases [19].

Microbial community.

Illumina MiSeq was used to examine the evolution of the microbial community in the samples of orujo (O) and alperujo (A) during a period of 6 months. With that purpose, samples on month 0 (O1, A1) and on month 6 (O2, A2) were analyzed. The initial mixture of olive wastes (O1, A1) was dominated by members of the *phylum Proteobacteria* with a relative abundance of 99% and 85% respectively, followed by phylum *Actinobacteria, Bacteroidetes* and *Firmicutes*. These results are similar to those obtained by [21] where *Actinobacteria, Bacteroidetes, Firmicutes and Proteobacteria* were the main phyla detected as well. These may indicate that conditions similar as those reached during a composting process of oil mill waste were achieved during our process.

Interestingly, the abundance of *Cellulomonas, Dysgonomonas* and other representatives of the *Bacteroidetes* and *Actinobacteria* phylum increased at the completion of the process. *Actinomycetes* are known as active cellulose decomposers, and typical residents of compost and *Bacteroidetes* are able to degrade macromolecules such as chitin and cellulose. Possibly species of these taxa were more competitive in the final mixtures due to their metabolic properties.

CONCLUSIONS

The paper analyzed the impact of olive mill waste stored in open reservoirs. The study focused on two residuals, namely the Alperujo and Orujo, and their impact in the emanation of unpleasant odors. A physical-chemical and biological analysis evidenced the influence of the environmental parameters, specially the external temperature and the relative humidity. The analysis FAME, COV and Ilumina revealed a progressive decomposition of the residuals as a result of the chemical and biological mechanisms. The biological analysis showed an increase in bacteria and fungi as time proceeds. Based on the calorific power measured in the samples, our results show that the residuals are appropriate for the elaboration of pellets of biomass.

Acknowledgements

This work was funded by the project PIEI Quim BIO, Universidad de Talca. Thanks to Agricola y Forestal don Rafael and Almazaras del Pacifico, for providing us with the final residues of their processes..

REFERENCES

[1] Hernández D, Astudillo L, Gutiérrez M, et al., "Biodiesel production from an industrial residue: alperujo", Industrial Crops and Products, Vol. 52, 2014, pp. 495-498.

[2] Alburquerque JA, González J, García D, et al., "Agrochemical characterization of "alperujo", a solid by-product of the two-phase centrifugation method for olive oil extraction", Bioresource Technology, Vol. 91, 2004, pp.195-200.

[3] Font X, Artola A, Sánchez A, "Detection, composition and treatment of volatile organic compounds from waste treatment plants", Sensors, Vol. 11, 2011, pp. 4043–4059.

[4] Brenes M, Romero C, García A, et al., "Phenolic compounds in olive oils intended for refining: Formation of 4-Ethylphenol during olive paste storage", J. Agricultural Food Chemestry, Vol. 52, 2004, pp. 8177−8181

[5] Castro A, Asencio E, Ruiz-Méndez MV, et al., "Production of 4-ethylphenol in alperujo by Lactobacillus pentosus" J. Sci. Food Agric., Vol. 11, 2015, pp. 30-95.

[6] Giannoutsou EP, Meintanis C, Karagouni AD, "Identification of yeast strains isolated from a two-phase decanter system olive oil waste and investigation of their ability for its fermentation" Bioresource Technology, Vol. 93, 2004, pp. 301-306.

[7] Middelhoven WJ, "Identification of yeasts present in sour fermented foods and fodders" Mol. Biotechnology, Vol. 21, 2002, pp. 279-292

[8] Cert A, Moreda W, Perez-Camino MC, "Methods of preparation of fatty acid methyl esters (FAME). Statistical assessment of the precision characteristics from a collaborative trial", Grasas y Aceites, Vol. 51(6), 2000, pp. 447-456.

[9] Peterson B, Car P, Boudt K, et al., "Package 'PerformanceAnalytics'", 2014, http://r-forge.r-project.org/projects/returnanalytics/.

[10] Rincón B, Bujalance L, Fermoso FG, et al., "Effect of ultrasonic pretreatment on biomethane potential of two-phase olive mill solid waste: Kinetic approach and process performance" Scientific World Journal, 2014, pp. 648-624.

[11] Camargo C, Dunoyer A, García-Zapateiro L, "The effect of storage temperature and time on total phenolics and enzymatic activity of sapodilla (Achras sapota L.)", Rev. Fac. Nac. Agron., Vol. 69 (2), 2016, pp. 7955-7963.

[12] Kiritsakis A, "El aceite de oliva" Ed. A. Madrid Vicente, Madrid, pp. 127.

[13] Biedermann M, Bongartz A, Mariani C, Grob K, "Fatty acid methyl and ethyl esters as well as wax esters for evaluating the quality of olive oils", European Food Research and Technology, Vol. 228, 2008ª, pp. 65-74.

[14] Zielinska A, Nowak I, "Fatty acids in vegetable oils and their importance in cosmetic industry" CHEMIK, Vol. 68, 2014, pp. 103-110.

[15] Gómez-Alonso S, Mancebo-Campos V, Salvador MD, Fregapane G, "Evolution of major and minor components and oxidation indices of virgin olive oil during 21 months storage at room temperature" Food Chemistry", Vol. 100, 2007, pp. 36–42.

[16] Angerosa F, Servili M, Selvaggini R, Taticchi A, Esposto S, Montedoro GF, "Volatile compounds in virgin olive oil: occurrence and their relationship with the quality" Journal of Chromatography A, Vol. 1054, 2004, pp. 17–31.

[17] Chimi H, Rahmani M, Collard J, Collard P, "Rôle des Composés phénoliques", Rev. Fr. Corps Gras, Vol. 37, 1990, pp. 363–367.

[18] Angerosa F, Lanza B, Marsilio V, "Biogenesis of "fusty" defect in virgin olive oils", Grasas y Aceites, Vol. 47, 1996, pp. 142-150.

[19] Romero del Rio I, "Evaluación de indicadores de la calidad del aceite de oliva virgen: fortalezas, debilidades y oportunidades" Tesis Doctoral, Universidad de Sevilla, España, 2015.

[20] Luna G, "Caracterización de aceites de olive vírgenes europeos: implicaciones del análisis sensorial y la actitud de los consumidores. Tesis Doctoral. Universidad de Sevilla, España, 2003.

[21] Tortosa G, Castellano-Hinojosa, A, Correa-Galeote D, et al., "Evolution of bacterial diversity during two-phase olive mill waste (''alperujo") composting by 16S rRNA gene pyrosequencing", Bioresource Technology, Vol. 224, 2017, pp. 101–111.

TRACE METALS STIMULATION OF BIOCHEMICAL METHANE POTENTIAL FROM PRETREATED WASTE ACTIVATED SLUDGE

Peralta E. D., Noyola A., Barrios J. A., Durán U.
Instituto de Ingeniería, UNAM, México.

ABSTRACT

The treatment of waste activated sludge (WAS) through anaerobic digestion (AD) allows its stabilization by the organic matter (OM) reduction and conversion, which generates methane-rich biogas that can be used as heat energy or electricity. A disadvantage of this technology is the low solubilization of OM in WAS, several pretreatments have been studied, but chemical methods as electrooxidation (EOP) and peracetic acid addition (PAP) increase the hydrolysis rates significantly and hence the OM bioavailability. There are reports about the addition of trace metals (TM) as micronutrients in order to improve the methane production during AD. However, only a few research has been done on combined some TM such as iron (Fe), nickel (Ni), cobalt (Co) and molybdenum (Mo) on AD of WAS pretreated. Therefore, in this research biochemical methane potential (BMP) assays were carried out testing EOP and PAP in combination with the addition of two different solutions of four TM (Fe, Ni, Co, and Mo) as AD biostimulants. First of all, WAS were pretreated with the following conditions: EOP at current density of 28.6mA/cm^2, 3% of total solids (TS) and a food/microorganism ratio (S/X_0) of 0.15 kg VS_f/kg VS_i, and PAP with 500 ppm of peracetic acid, 2% of TS and a S/X_0 ratio of 0.45 kg VS_f/kg VS_i. Afterward, the BMP assays were performed for 21 days at 310 K, pH= 7 and stirring at 150 rpm. The following TM solutions were used (mg/L): (a) 5.0 of Fe, 0.79 of Ni, 0.52 of Co and 0.02 of Mo, and (b) 126.0 of Fe, 20.0 of Ni, 13.0 of Co and 0.4 of Mo. WAS pretreated with PAP, obtained respectively for assays (a) and (b): removal efficiencies of volatile solids (VS) of 21.8 and 51.9%, and for chemical oxygen demand (COD) of 40.9 and 64.7%, as well as BMP of 109.5 N-L CH_4/kg VS_i and 72.8 N-L CH_4/kg VS_i. When WAS were pretreated with EOP had respectively for assays (a) and (b): removal efficiencies of VS of 62.3 and 62.4%, and for COD of 56.2 and 57.4%, as well as BMP of 72.4 N-L CH_4/kg VS_i and 67.3 N-L CH_4/kg VS_i. Overall, the addition of TM in AD of WAS increased the methane production in both pretreatments, but its greatest biostimulated in PAP assays and specifically with the lower TM solution (a).

Keywords: Waste Activated Sludge, Anaerobic Digestion, Trace Metals, Electrooxidation Pretreatment, Peracetic Acid Pretreatment

INTRODUCTION

The generation of waste activated sludge (WAS) in Mexico is estimated at around 3,201 ton/day [1], which represents an important issue when the sludge has to be treated before its final disposal, this is due to the fact that its management can represent up to 60% of the total cost of operation and maintenance for a wastewater treatment plant (WWTP) [2].

Nowadays anaerobic digestion is one of the most commonly used sludge treatment processes, 70% of the sludge is stabilized by this method [3]. This process has a major advantage biogas production, which can be used as an energy source.

Given that WAS is the excess biomass from biological wastewater treatment systems, most of the organic content of WAS consists microbial cells that are hard to degrade. In order to increase the efficiency of anaerobic digestion of WAS, the rate of hydrolysis needs to be accelerated since it is the limiting stage of the process [4], [5].

To increase WAS degradability pretreatments prior to anaerobic digestion change the structure of cellular content and improve the solubility of organic matter so that dissolved the components and make them easier to use by microorganisms in subsequent biological processes [6].

Chemical pretreatments including oxidative processes like the addition of acids or bases have been studied. Peracetic acid has a high oxidizing power that generates $^{\cdot}OH$ radicals during its reaction with organic matter, which can break the cell wall and release the intracellular content [7]–[9].

Electrooxidation is another oxidation process that can efficiently decompose the organic substances of macromolecules into the smaller ones by generating free radicals ($^{\cdot}OH$). Electrooxidation was used before for conditioning of sludge [10], or as a pretreatment for aerobic and anaerobic digestion [11]. Another important factor in the anaerobic digestion seen as a biogas generating process is the methanogenic microorganisms which are responsible for the production of methane by the decomposition of the organic matter present. Due to metals are involved in aspects of microbial growth, metabolism, and differentiation [12], these have

been the subject of research since beneficial effects can be obtained by adding concentrations in trace levels. Metals such as iron (Fe), nickel (Ni), cobalt (Co), molybdenum (Mo) and selenium (Se), are stimulants for methanogenic microorganisms, amplifying their cellular reproduction and resulting in increased production of methane in the composition of biogas [13]. These metals function as micronutrients and cofactors of the enzymes involved in the different stages of the anaerobic process [14]. They give the cell membrane stability, favor the transfer of nutrients and help to save energy in methane-producing bacteria [15].

Despite the literature on the stimulating effect of trace metals (TM) or pretreatments in the anaerobic digestion of different substrates, research has not yet been carried out to know the combined influence of a mixture of trace metals as micronutrients in anaerobic digestion of WAS that has been subjected to a pretreatment by different chemical methods. Therefore, the objective of this work is to evaluate the effect of two mixtures of Fe, Ni, Co and Mo in WAS pretreated by electrooxidation and by the addition of peracetic acid.

MATERIALS AND METHODS

Sludge Samples

WAS was collected from a secondary clarification of a WWTP in Mexico City (Cerro de la Estrella, Iztapalapa), which have a biological treatment process of activated sludge and treats 2 m^3/s. Plastic containers were used to transport the samples to the laboratory and then they were cooled to 4 °C.

Peracetic Acid Pretreatment

To carry out the pretreatment by the addition of peracetic acid (PAP), a pitcher test equipment (Phipps & Bird 7790-400) was used to treat samples of 1 L of raw WAS with an initial concentration of 2% total solids (TS). This concentration was reached by sedimentation of the raw sludge samples (24 h) and supernatant decantation, followed by centrifugation at 1,400 g for 20 minutes. TS was adjusted to the fixed values with the supernatant collected. Then, 500 ppm of peracetic acid was added and stirred at 300 rpm for 30 minutes as the contact time at room temperature (25 °C).

Electrooxidation Pretreatment

The electrooxidation pretreatment (EOP) was carried out in a single compartment electrochemical cell (DiaClean®, WaterDiam Sarl, Switzerland). Diamond-based material (p-Si–boron-doped diamond) was used as anode and cathode. Both electrodes were circular (100 mm diameter) with a surface area of 70 cm^2. Raw WAS (1 L) was mixed in a glass reactor with an overhead stirrer and the speed was low (100 rpm) to keep the sludge homogenous and avoid phase separation. The temperature of the system was kept constant (25 °C) with a water bath/heat exchanger. The system worked in recirculation mode, with a peristaltic pump (JP Selecta Percom N-M328) that continuously feeding the DiaClean® reactor (2.8 L/min). Power was supplied by a Delta Elektronika ES030-10, during 30 minutes applying a current density of 28.6 mA/cm^2 to WAS with a concentration of 3.0 % of TS.

Biochemical Methane Potential (BMP) assays

Anaerobic digestion batch assays for WAS pre-treated with the two different methods were performed in an OxiTop® Control OC 110 (WTW, Germany). A working volume of 80 mL was used, and a volume of 170 mL in the bottles was left as headspace for the generated biogas. Anaerobic sludge from mesophilic laboratory reactors adapted each one to different substrates was used as inoculum: 1) raw WAS (UT: untreated), 2) WAS with PAP and 3) WAS with EOP. Assays in duplicate were carried out using as substrate also WAS with the conditions above 1), 2), and 3) in separates bottles. The amount of inoculum and substrate were dosed according to the S/X_0 ratio (VS_f/kg VS_i) and the solids concentration for each pretreatment as it is shown in Table 1. During the preparation of the tests two solutions with different doses of TM were used with the following concentrations (mg/ L): (a) 5.0 of Fe, 0.79 of Ni, 0.52 of Co and 0.02 of Mo, and (b) 126.0 of Fe, 20.0 of Ni, 13.0 of Co and 0.4 of Mo [16], [17]. There also were used controls without TM (c) for each assay. The operating conditions of the batch assays were mesophilic temperature (37±2 °C), pH adjusted to 7, and shaking at 150 rpm for 21 days [18], [19].

All assays were analyzed at the beginning and at the end with the determinations according to the *Standard Methods* [20]: TS, volatile solids (VS), fixed solids (FS), total chemical oxygen demand (COD). The biogas composition was analyzed by gas chromatography (FISHER chromatograph with thermal conductivity detector, TCD, and column Porapak Q).

Table 1 Experimental design used in BMP assays

Pretreatment	% TS	S/X_0	TM
UT1	2	0.45	a, b, c
PAP	2	0.45	a, b, c
UT2	3	0.15	a, b, c
EOP	3	0.15	a, b, c

UT: untreated, EO: electrooxidation, PA: peracetic acid, TM: trace metal doses.

RESULTS AND DISCUSSION

According to the results shown in Fig. 1, about the total biogas production express as methane normalized liters by kilogram of initial volatile solids, it can be observed that for the two pretreatments evaluated and their controls without pretreatment (UT1, UT2) BMP was slightly higher for PAP assays in general. Although when comparing the assays with an addition of TM, it can be observed that the highest value corresponding to PAP with the lowest concentration of TM in the solution (a), which obtained a significant increase respect to its control without addition of TM (c) with a methane production of more than double. Even PAP-(a) methane production is 40.7% superior to PAP assay with the solution (b) of TM.

This effect on the increase of BMP by the addition of TM has a similar tendency to the aforementioned for both solutions used (a, b) in all the other WAS assays with EOP, UT1, and UT2. However, the difference is not significant between the effects of the two solutions used but it becomes important in comparison with the assays without the addition of TM. This tendency is according to [21], [22] about the addition of TM in WAS caused the enhancement of methane production no matter which pretreatment method was used. They report that one reason for pretreated sludge showing a great methane yield could be due to a high MT release depending on the medium conditions generates by each pretreatment.

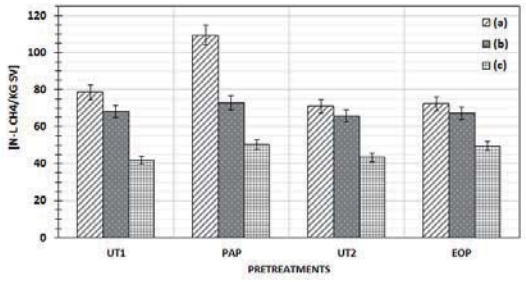

Fig. 1 Normalized PBM from WAS in assays

Table 2 summarizes the response variables for all the assays. The organic material removals for each assay based on the initial and final measurements of VS and total COD are indicated. In the VS removal efficiency, values were obtained in the order of 12.3-14.6% for UT1 and 20.2-28.2% for UT2, low values when compared to those of the assays with PAP (13.9-51.9%) and with EOP (57.5 -62.4%).

On the other hand, for the removal efficiency of COD, more evident differences were obtained with values between 4.1-9.3% for UT1 and between 6.0-21.3% for UT2, compared with 40.9-64.7% of PAP and with 53.2-57.4% of EOP. These results are clearly in agreement with the fact that pretreatments increased the soluble material in WAS due to cell rupture and release of intracellular compounds and make them availability as is mentioned in [23], [24], and it also responds to [25], [26], about the addition of TM tested are necessary to increase the growth of methanogenic bacteria but it is also important understood that the characteristics of medium propitiated by pretreatments may turn into no bioavailable these TM and then decrease their effect [27] [22].

Table 2 Resume of results obtained in BMP assays

ASSAYS	N-L CH_4/kg VS	VS removal efficiency (%)	COD removal efficiency (%)
UT1-(a)	78.6	14.6	4.1
UT1-(b)	68.3	12.3	9.3
UT1-(c)	42.0	14.1	7.4
PAP-(a)	109.5	21.8	40.9
PAP-(b)	72.8	51.9	64.7
PAP-(c)	50.3	13.9	59.2
UT2-(a)	70.9	28.2	6.9
UT2-(b)	65.7	25.3	21.3
UT2-(c)	43.4	20.2	6.0
EOP-(a)	72.4	62.3	56.2
EOP-(b)	67.3	62.4	57.4
EOP-(c)	49.4	57.5	53.2

UT: untreated, EO: electrooxidation, PA: peracetic acid

CONCLUSIONS

The highest BPM (109.5 N-L CH_4/kg VS_i) was reached by the PAP assay with the (a) TM solution. This solution [mg/L: 5.0 of Fe, 0.79 of Ni, 0.52 of Co and 0.02 of Mo] proved to be better by stimulating anaerobic digestion in all WAS assays proved. Hence the addition of TM in WAS shown to be needed for a more competitive energy production by optimizing methane generation regardless of the type of pretreatment.

By pretreating WAS, it is possible to reduce the maximum methane production times, which was reported in [18], [19] as 30 days of minimum duration for this kind of assays, nevertheless, in this work optimal conditions were carried out. Although in some cases substrates were not completely consumed for biogas production due to the WAS hydrolysis producing more organic matter available than the inoculum can consume, this may be likely by a reduction of TM effect in methanogens microorganism growth caused by alterations in the medium induced by pretreatments effects.

ACKNOWLEDGMENTS

This work was made with CONACYT economic support number CVU: 779935. The authors gratefully acknowledged the financial support from the gaseous biofuels cluster project 247006 of the Energy Sustainability Fund 2014-05 (CONACYT-SENER) of the Mexican Centre for Innovation in Bioenergy (Cemie-Bio).

REFERENCES

[1] Secretaría de Medio Ambiente y Recursos Naturales (SEMARNAT), "Programa Nacional para la Prevención y Gestión Integral de los Residuos 2009-2012," 2009.

[2] P. Camacho, S. Deleris, V. Geaugey, P. Ginestet, and E. Paul, "A comparative study between mechanical, thermal and oxidative disintegration techniques of waste activated sludge," *Water Sci. Technol.*, vol. 46, no. 10, pp. 79–87, 2002.

[3] V. K. Tyagi and S. L. Lo, "Application of physico-chemical pretreatment methods to enhance the sludge disintegration and subsequent anaerobic digestion: An up to date review," *Rev. Environ. Sci. Biotechnol.*, vol. 10, no. 3, pp. 215–242, 2011.

[4] L. Appels, J. Baeyens, J. Degrève, and R. Dewil, "Principles and potential of the anaerobic digestion of waste-activated sludge," *Prog. Energy Combust. Sci.*, vol. 34, no. 6, pp. 755–781, 2008.

[5] L. Appels, A. Van Assche, K. Willems, J. Degrève, J. Van Impe, and R. Dewil, "Peracetic acid oxidation as an alternative pre-treatment for the anaerobic digestion of waste activated sludge," *Bioresour. Technol.*, vol. 102, no. 5, pp. 4124–4130, 2011.

[6] J. A. Müller, "Prospects and problems of sludge pre-treatment processes," *Water Sci. Technol.*, vol. 44, no. 10, pp. 121–128, 2001.

[7] E. V Rokhina, K. Makarova, E. A. Golovina, H. Van As, and J. Virkutyte, "Free radical reaction pathway, thermochemistry of peracetic acid homolysis, and its application for phenol degradation: Spectroscopic study and quantum chemistry calculations," *Environ. Sci. Technol.*, vol. 44, no. 17, pp. 6815–6821, 2010.

[8] C. Barrios, J.A, Jimenez, B, Maya, "Treatment of sludge with peracetic acid to reduce the microbial content," *J. Residuals Sci. {&} Technol.*, vol. 1, no. 1, 69–74, pp. 69–74, 2004.

[9] R. Colgan, S. y Gehr, "Disinfection: Peracetic acid gains favor as an effective, environmentally benign disinfection alternative for municipal wastewater treatment applications.," *Wat. Env. {&} Tech*, pp. 29–33, 2001.

[10] H. Yuan, N. Zhu, and L. Song, "Conditioning of sewage sludge with electrolysis: Effectiveness and optimizing study to improve dewaterability," *Bioresour. Technol.*, vol. 101, no. 12, pp. 4285–4290, 2010.

[11] L. J. Song, N. W. Zhu, H. P. Yuan, Y. Hong, and J. Ding, "Enhancement of waste activated sludge aerobic digestion by electrochemical pre-treatment," *Water Res.*, vol. 44, no. 15, pp. 4371–4378, 2010.

[12] S. Mancillas-Salas, J. A. Rodríguez-de la Garza, and L. Ríos-González, "Bioestimulación de la digestión anaerobia," *Revista Científica de la Universidad Autónoma de Coahuila*, vol. 4, no. 8, pp. 56–59, 2012.

[13] Y. Lorenzo Acosta and M. Obaya Abreu, "La digestión anaerobia. Aspectos teóricos. Parte I," *ICIDCA. Sobre los Deriv. la Caña Azúcar*, vol. 39, no. 1, pp. 35–48, 2005.

[14] G. Jurado-Mariscal, "Efecto de iones metálicos sobre la metanogénesis en la digestión anaerobia de residuos sólidos orgánicos urbanos," Universidad Nacional Autónoma de México, 2014.

[15] S. K. Patidar and V. Tare, "Soluble microbial products formation and their effect on trace metal availability during anaerobic degradation of sulfate laden organics," *Water Sci. Technol.*, 2008.

[16] A. Noyola and A. Tinajero, "Effect of biological additives and micronutrients on the anaerobic digestion of physicochemical sludge," *Water Sci. Technol.*, vol. 52, no. 1–2, pp. 275–281, 2005.

[17] A. Espinosa, L. Rosas, K. Ilangovan, and A. Noyola, "Effect of the trace metals on the anaerobic degradation of volatile fatty acids in molasses stillage," *Water Sci. Technol.*, vol. 32, no. 12, pp. 121–129, 1995.

[18] I. Angelidaki, M. Alves, D. Bolzonella, L. Borzacconi, J. L. Campos, A. J. Guwy, S. Kalyuzhnyi, P. Jenicek, and J. B. Van Lier, "Defining the biomethane potential (BMP) of solid organic wastes and energy crops: A proposed protocol for batch assays," *Water Sci. Technol.*, vol. 59, no. 5, pp. 927–934, 2009.

[19] G. Esposito, L. Frunzo, F. Liotta, A. Panico, and F. Pirozzi, "Bio-Methane Potential Tests To Measure The Biogas Production From The Digestion and Co-Digestion of Complex Organic Substrates," *Open Environ. Eng. J.*, vol. 5, no. 1, pp. 1–8, 2012.

[20] - APHA, - AWWA, and WEF, *Standard methods for the examination of water and wastewater*. Washington D.C.: American Public Health Association, American Water Works Association, Water Environment Federation, 2015.

[21] D. Zhang, Y. Chen, Y. Zhao, and X. Zhu, "New Sludge Pretreatment Method to Improve Methane Production in Waste Activated Sludge Digestion," *Environ. Sci. Technol.*, vol. 44, no. 12, pp. 4802–4808, Jun. 2010.

[22] M. H. Zandvoort, E. D. van Hullebusch, F. G. Fermoso, and P. N. L. Lens, "Trace metals in anaerobic granular sludge reactors: Bioavailability and dosing strategies," *Eng. Life Sci.*, vol. 6, no. 3, pp. 293–301, 2006.

[23] J. Xu, H. Yuan, J. Lin, and W. Yuan, "Evaluation of thermal, thermal-alkaline, alkaline and electrochemical pretreatments on sludge to enhance anaerobic biogas production," *J. Taiwan Inst. Chem. Eng.*, vol. 45, no. 5, pp. 2531–2536, 2014.

[24] J. A. Barrios, U. Duran, A. Cano, M. Cisneros-Ortiz, and S. Hernández, "Sludge electrooxidation as pre-treatment for anaerobic digestion," *Water Sci. Technol.*, vol. 75, no. 4, pp. 775–781, 2017.

[25] B. Demirel and P. Scherer, "Trace element requirements of agricultural biogas digesters during biological conversion of renewable biomass to methane," *Biomass and Bioenergy*, vol. 35, no. 3, pp. 992–998, 2011.

[26] A. J. Ward, P. J. Hobbs, P. J. Holliman, and D. L. Jones, "Optimisation of the anaerobic digestion of agricultural resources," *Bioresour. Technol.*, vol. 99, no. 17, pp. 7928–7940, 2008.

[27] H. Pobeheim, B. Munk, J. Johansson, and G. M. Guebitz, "Influence of trace elements on methane formation from a synthetic model substrate for maize silage," *Bioresour. Technol.*, vol. 101, no. 2, pp. 836–839, 2010.

SLUDGE WASTEWATER TREATMENT PLANTS A RAW MATER TO PRODUCE A GREEN-CEMENT

Djafari Driss[1], Zentar Rachid[2], Mekerta Belkacem[1] and Semcha Abdelaziz[1]
[1]Faculty of Sciences and Technology, University of Ahmed DRAIA, ADRAR; ALGERIE,
[2]Ecole des Mines de Douai, Laboratoire de Genie Civil et géo-Environnement (LGCgE), Lille du Nord de France.

ABSTRACT

The present study is a contribution to consider sludge from wastewater treatment plants (WWTPs) a raw material to produce a green-cement.

Physic-chemical and mineralogical characterizations were carried out on the sludge of WWTPs as well as the ash obtained after calcinations under a temperature equal 500°C.

The green-cement is realized by substitution of ash (5%, 10% and 15%) obtained into the clinker. Mortar and concrete using the green-cement were tested in the fresh and hardened state. The results obtained showed an increase in the apparent viscosity of mortar in the fresh state thus a remarkable improvement in the strength of concrete in the cured state.

Physic-chemical and mineralogical characterizations were carried out on the sludge of WWTPs as well as the ash obtained after calcinations under a temperature equal 500°C.

The valorization of sludge from wastewater treatment plants to produce a green-cement remains a beneficial sector in both approaches; environmental and economic-technological.

Keywords: Sludge, Characterization, Green-cement, Viscosity.

INTRODUCTION

Economic growth, urban development and demographic growth induce an important consumption in drinking water and, in return, a greater generation of wastewater in the receiving environment is recorded. Then, in front of the constraint related to the insufficiency of the water resource and the need for rationalizing its use, the wastewaters generated are treated and recycled. Unfortunately, the wastewater treatment plants (WWTPs) installed for this purpose, still encounter enormous problems, in terms of solid waste management. Indeed, whatever the treatment system adopted, the treatment of wastewaters is accompanied ineluctably by a production of a considerable quantities of sludge. The sludge produced thereby, require a space for storing; constitute an additional environmental problem to solve by the managers of the WWTPs. Several ways exist for the elimination of this sludge, but the choice remains often related to the cost of the installation, the origin of sludge, the added-value of the product which results from this and the impact of solution retained on the environment. The dumping (also called storage) is legally prohibited in many countries and will more and more restrained in other countries (Directives 1999/31 / EC).

The present study describes a new way of sludge management from WWTPs by valorizing the latter in the manufacturing an ecological and economical cement (eco-cement). Economical and ecological by using the calorific power of the sludge to improve preheating for example of raw materials prior to clinkerisation, by reducing the amount of clinker in the developed cement, by improving the management of solid wastes from wastewater treatment plants and finally by reducing the CO_2 emission in the cement industry. In this work after a detailed characterization of raw and calcinated sludge of WWTPs, various eco-cements with increasing amount of substitution in the raw cement were made. The use of such materials which are mostly considered as industrial wastes or by products, leads to a significant reduction in CO_2 emissions [1]-[2]-[3]-[4]. To evaluate the performance of these new binders, mortar and concrete using the green-cement were tested in the fresh and hardened state.

MATERIAL AND METHOD

Use the samples of the studied sludge were taken from the WWTPs known "Rochet" in the district of Sidi Bel Abbes (west of Algeria, 400 km from Algiers (Algeria)). The taken samples were preserved at a temperature of - 4 °C in order to eliminate any risk of fermentation.

Physical parameters of sludge are measured in accordance with AFNOR standards as shown in Table 1. For the preparation of the eco-cement; mixtures of clinker, of ashes resulting from the

incineration of sludge from WWTPs and Gypsum are carried out. Before carrying out a chemical and mineralogical analysis of the various components and the mixtures of the finished products realized, a crushing was made in a micro-crusher.

Table 1 Standards used to characterize the physical properties of the WWTPs sludge

Character	Indices	Standard
Dry matters	DM	NF EN 12879
Mineral matter	MM	NF U 44-160
Dry volatile matter	DVM	NF U 44-160
Humidity		NF U 44-171
Dry apparent density		NF EN 1097-6
Dryness	MBV	NF T 90-105-2
Methylene blue value		NF P 94-068

The compositions of formulated eco-cements are given in Table 2.

Table 2 Composition in mass of the developed eco-cements

Cements	Gypsum (%)	Clinker (%)	Ash (%)
EC_0	5	95	0
EC_5	5	90	5
EC_{10}	5	85	10
EC_{15}	5	80	15

Blaine surface measurements, chemical and mineralogical analysis are carried out. To evaluate the performance of the green-cement developed in there two state (fresh and hardened state). The mini-cone test has used for studding the rheological of the cement grouts developed (CGT, CG5, CG10 and CG15), prismatic samples (40x40x160 mm^3) of a mortar made of the green-cements and standard cement were tested (EC0, EC5, EC10 and EC15). The mortar used is composed in mass, of one part of cement (or green-cement), three parts of standard sand and a half part of water (in masse water/ cement is equal to 0.5).

Each batch for three test specimens comprises 450 g ± 2 g of cement, 1350 g ± 5 g of standard sand and 225 g ± 1 g of water. In total forty-five prismatic specimens were prepared.

RESULTS AND DISCUSSION

Physical characteristics of the studied sludge

The physical characteristics of the studied sludge are shown in Table 3. From these results, it is to note the high water content, the high OM (≈ DVM) levels and a relatively low value of methylene bleu value. Compared with the characteristics of other WWTPs sludge, these values are relatively comparable [5].

Table 3 Physical characteristics of sludge of WWTPs

Property	Value
Dry matter (%)	85.11
Dry volatile matter (% DVM)	39.87
Mineral matter (% DVM)	60.13
Humidity (%)	14.88
Particle density	0.69
Methylene blue of a soil by means of the strain test	0.85

Chemical characteristics of the studied sludge

The results presented in Table 4 show that the sludge contains a low metal trace elements compared to the thresholds in the standard NF U 44-051 and the values proposed in other studies [5]-[6]. In terms of the characterization of the green-cements designed, Blaine specific area is presented in Table 5. It should be noted a sensitive increase of the Blaine specific area (over 20%) of cement containing ashes of calcified sludge. However, it is not possible to relate solely the increase in specific surface area to the ashes content incorporated in different cements.

Table 5 Blaine specific area of developed green-cements

Designation	EC0	EC5	EC10	EC15
Specific area cm^2/g	3636	4497	4401	4379

Mini-cone test of cement grouts

To study the effects of adding ash of sludge studied on the rheological properties; tests on the cement grouts were carried out by the mini-cone test measurement according to standard NF EN 196-1. Fig. 1.

The results of this test were carried out and shown in Table 6.

From the results shown in the table above; a remarkable increase in the shear stress is observed between the CGT (control) and the other CGx (5%, 10% and 15%).

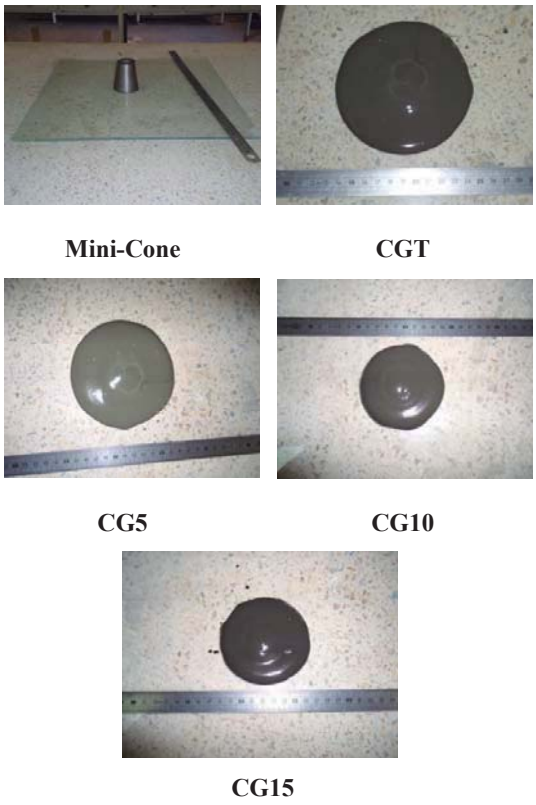

Figure 1 Mini-cone test of cement developed

Table 6

Designation	CG0	CG5	CG10	CG15
Flow test (mm)	104	90	89	85

Mechanical characteristics

The mechanical results presented in Fig. 2 show that the green-cements used make it possible to develop strengths at the early age (7days) and higher than the strength measured on samples including the standard cement (MT). This increase in strength can be attributed, in regard of the measured parameters, to the specific surface developed by the green-cements. The high specific surface area developed by the green-cements (see Table 5) probably allowed a more important reactivity, hence, high speed of formation of hydrates silicate calcium (H-S-C) gel. The high specific area of the green-cements could predict also finer grain size distribution of the green cement. This later fact could induce an increase of the strength by increasing the compactness of developed mortars.

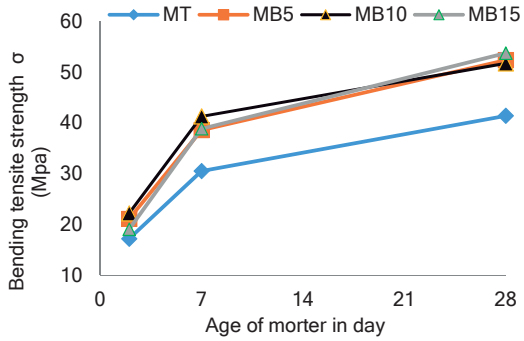

Fig. 2 Evolution of compressive strength

CONCLUSION

In this study, a valuation approach of WWTPs sludge, taken in the district of Sidi Bel Abbes (west of Algeria), in the cement industry has been proposed. A detailed characterization of the sludge and the ashes issued from the heat treatment of the sludge, are performed. This first step has allowed comparing the physical as the chemical characteristics of the studied sludge to the results published in other countries. From this comparative study, it appears that the sludge studied is comparable in terms of physical as chemical characteristics. Moreover, the chemical and mineralogical analyzes of the induced ashes, have allowed detecting elements comparable to those present in a clinker. Hence, in this work a substitution of the clinker by the ashes up to 20% is tested. In terms of mechanical performances of samples made of standard as green cements developed, it appears from this study that the compressive strengths obtained at different curing times, for mortars including the green-cements are higher than the measured values on specimens containing standard cement. It is to note that after 28 days of curing, the resistances of samples made with green-cements exceed 50 MPa. The same trend is observed with specimens tested in bending tensile strength.

REFERENCES

[1] Yang, K-H., Jung. Y-B., Cho, M-S., Tae, S-H., J. Clean. Prod, Vol. 103, 2015. Pp. 774-783.
[2] Zhao, H., Sun, W., Wu, X., Gao, B., J. Clean. Prod, Vol. 95, 2015, pp. 66-74.
[3] Bostanci, S.C., Limbachiva, M., Kew, H., J. Clean. Prod, Vol. 112, Part 1, 2016, pp. 542-552.
[4] Vargas, J., Halog, A., J. Clean. Prod, Vol. 103, 2015, pp 948-959.
[5] Pevere, A., Guibaud, G., Goin, E., Van Hullebusch, E., Lens, P., Biochem. Eng. J, Vol. 43, 2009, pp. 231-238.
[6] Karvelas, A., Katsoyiannis, A., Samara, C., Chemosphere, Vol. 53 (10), 2003, pp. 1201-1210.

8. Perspectives of the industry

Session chairs: Margarita Eugenia Gutiérrez[1] and Yann René Ramos[2]
[1]Laboratorio de Biogeoquímica Ambiental, Facultad de Química de la UNAM, México
[2]Departamento de Ingeniería Geomática e Hidráulica, División de Ingenierías, México

The role of the industry in the management of sediments is an important issue worldwide. Every year, rivers and other water bodies are impacted by industrial pollutants, representing a potential risks for aquatic life and for soil quality when affected by the river floods and deposits of dredged sediments. The perspective of the metallurgic and mining industries on the proper management of affected sediments varies widely from one country to another. Two visions prevail: 1) the fulfillment of regulations without more information; or 2) carrying out assessment evaluations or case studies, which apply recent engineering developments to protect populations and resources. The environmental risk is related not only with hazardous substances behavior, but also with the environment vulnerability (including human population). The environmental fate of the pollutants and the routes of exposure are mainly dominated by the physico-chemical process in water and sediments, and the prevailing geochemical conditions. Therefore, multidisciplinary scientific studies play a significant role in sediment management studies. The point of view of relevant stakeholders, like the industry, regarding the different options to properly manage sediments, can help development of environmental regulations and policies, as well as related private programs.

LEVELS OF MN, ZN, PB AND HG IN SEDIMENTS OF THE ZAMORA RIVER, ECUADOR

Mora Abrahan [1], Jumbo-Flores Diana [2] and Mahlknecht Jürgen [1]
[1]Escuela de Ingeniería y Ciencia, Tecnológico de Monterrey, México; [2]Universidad Nacional de Loja, Ecuador

ABSTRACT

Artisanal and small-scale gold mining activities (ASGM) are currently performed in the Zamora River basin (Ecuadorian Amazon), mainly in the Nambija and La Herradura-Chinapintza mining district. However, the effects of ASGM on these fluvial systems have not been yet assessed. Thus, the concentrations of Mn, Zn, Pb and Hg were measured in bottom sediments of rivers of the Zamora River basin and suspended sediments of the mining effluents. The results show that bottom sediments of several tributaries of the Zamora River (Congüime River and the lower Nangaritza River) are severely contaminated with Mn, Zn, Pb and Hg. This contamination is the result of the discharge of mining effluents coming from La Herradura-Chinapintza mining district, which are rich in sediments composed by polymetallic mineral. Bottom sediments of the Nambija and the upper Zamora River show a severe contamination with Hg, suggesting the existence of ASGM in the upper Zamora River basin. The contaminated bottom sediments of these rivers are re-suspended during high water discharge periods and are transported toward the Amazon River mainstream. According to international guidelines, the high levels of Mn, Zn, Pb and Hg in river sediments of the Zamora basin can have adverse effects on aquatic biota.

Keywords: Zamora, Heavy Metals, Contamination, Bottom Sediments, Mining

INTRODUCTION

The greatest mining potential of the Zamora Chinchipe Province (Southeastern Ecuadorian Amazon) can be found in the geological formations of the Nanguipa, Tzunantza and the Cóndor mountain ranges. These geological formations, located at the border area of northern Peru and southern Ecuador, are part of a metallogenic belt that extends in a northerly direction and contains gold skarn deposits, porphyry Cu-(Mo-Au) deposits and low-sulfidation epithermal Au-Ag deposits of poorly defined age [1]. The geology of this part of the eastern Ecuadorian Andes is dominated by Jurassic calc-alkaline I-type, granodioritic to tonalitic intrusions of the Zamora batholith [1]–[2]. Owing to the large gold deposits, there are several mining settlements in this zone, both in the Chinapintza sector and in the Nambija sector, which is one of the mining districts with the largest gold production in Ecuador since the decade of 80s [1]. However, the Nambija mining district is under concession to mining companies, and only a small number of artisanal miners are working in that zone. The artisanal and small-scale gold mining (ASGM) activities that have been performed and are currently still being performed in the Zamora River basin, especially in the Nambija mining district, have produced a strong contamination of the streams and rivers adjacent to mining zones with Hg and other heavy metals [3]–[5]. Indeed, this contamination is produced due to the inadequate management of mining effluents and metal rich tailings.

During the gold extraction process, the ore coming from the stone is crushed to a fine powder and then mixed with metallic Hg to form the "amalgam", which is a mixture composed of equal parts of Hg and Au. Thus, during the finely ground ore washing process, both the excess of Hg added during the amalgamation step and other heavy metals present in the ore are released into mining effluents in the dissolved and particulate phase. Indeed, these mining effluents can reach rivers and streams, which results in the contamination of water bodies.

It is estimated that in Ecuador, approximately 40% of gold production derives from the amalgamation process and 60% from the cyanidation process. Likewise, of the total miners who still use the amalgamation process, 50% use the retort (which is a device for recovering Hg from the metal amalgam), while 50% burn amalgam in an open pan or shovel, often in their own homes. Although the use of devices such as retorts and fume hoods can help decreasing Hg emissions, these could be inefficient and could release Hg to the environment, either in the vapor or in the liquid phase [6]. Moreover, if Hg is released into the environment in the vapor form, it eventually settles in soils and sediments of streams, rivers and lakes [7].

Although several studies have measured the concentrations of heavy metals in bottom sediments of rivers and streams of the Nambija River basin [3]–[5], only few reports refer to the pollution by ASGM in the Zamora River, Nangaritza River and

other rivers and streams of the southern Ecuadorian Amazon [8]. Therefore, the objectives of this study were to determine the concentrations of Mn, Zn, Pb and Hg in bottom sediments of streams and rivers of the Zamora River basin.

STUDY AREA

This Zamora River is located in the Ecuadorian Amazon region and it originates in the Podocarpus National Park at more than 3200 m.a.s.l., between the border area of the Zamora Chichipe and Loja provinces. In its headwaters, the Zamora River flows toward the northeastern direction. However, due to the influence of a major regional fault, the river abruptly changes its direction toward the southeast before it enters in the Zamora Chinchipe Province. During its course, the upper Zamora River receives the contributions of other tributaries such as Nambija, Timbara, Cumbaratza, Suapaca, Nanguipa, Yantzaza, Nangaritza and Muchime rivers. Owing to the high mean annual precipitation values in the basin (between 2800 and 3000 mm), the mean annual water discharge of the Zamora River reaches 667 m^3 s^{-1}, whereas the basin covers an area of 733.969 ha.

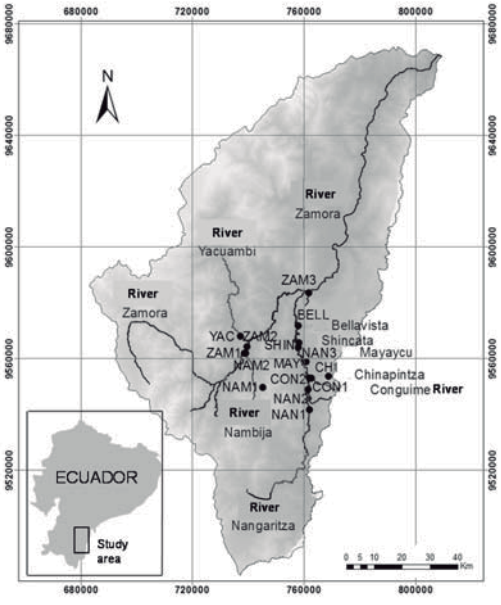

Fig. 1 Sampling sites along the Zamora River basin

The mining districts of Nambija and Chinapintza-La Herradura are the two main mining districts that release effluents rich in mine tailings to streams and rivers of the Zamora River basin. In the Nambija mining district, the mining effluents are discharged into the Nambija River, which is a tributary of the Zamora River. In Chinapintza-La Herradura district, mining effluents are discharged mainly to streams, which join to the Congüime River and then with the Nangaritza and Zamora rivers (Fig. 1).

MATERIALS AND METHODS

Collection of samples

The collection of bottom sediment samples was carried out between November 2014 and January 2015 due to the low water discharge of rivers and streams during these months, which favors the collection of bottom sediments. Three sediment samples were collected at each sampling site in order to obtain triplicate values. Bottom sediment samples from the Yacuambi River and the Bellavista, Shincata and Mayaycu natural streams were collected in order to assess background conditions for these regional rivers. Bottom sediments were also collected in the Nambija River (one site), in the Congüime River (two sites) and in the Nangaritza River in three sites (two before the confluence with the Congüime River and one after the confluence with the Congüime River). Also, bottom sediment samples were also collected in the Zamora River main channel at three sites (before and after the Zamora-Nambija rivers confluence and after the confluence with the Nangaritza River). The sediment samples were collected using a plastic shovel and put in pre-cleaned plastic bags. Additionally, two water samples (1 liter) were taken from the mining effluents of Nambija and Chinapintza-La Herradura mining districts. The total suspended sediment (TSS) concentrations in both mining effluents were analyzed by filtering the water samples over a pre-weighted 0.45 µm pore size filters. Figure 1 indicates the sampling sites along the Zamora River basin and Table 1 shows the codification and the metric coordinates of the sampling sites.

Table 1 Coordinates and codification of the sampling sites

River/Stream/Effluent	Code	Lat.	Long.
Yacuambi River	YAC	737350	9567930
Mayaicu stream	MAY	760991	9558706
Shinquata stream	SHIN	758225	9565594
Bellavista stream	BELL	758012	9571720
Zamora River	ZAM1	738863	9561859
Zamora River	ZAM2	739591	9564068
Zamora River	ZAM3	761939	9583562
Nangaritza River	NAN1	761963	9541506
Nangaritza River	NAN2	761680	9548859
Nangaritza River	NAN3	758188	9564036
Congüime River	CON1	762882	9552914
Congüime River	CON2	762110	9552912
Nambija River	NAM2	739180	9561778
Nambija Effluent	NAM1	745388	9549642
Chinapintza Effluent	CHI	768932	9553541

Analysis of Mn, Pb, Zn and Hg

Sediment samples were dried in a lab-oven at 40 °C. Then, these samples were disaggregated and homogenized in a mortar. Sediment and TSS samples of mining effluents were subjected to acid digestion using the USEPA method 3050B. After the acid digestion, the extracts were put in polyethylene kits and stored at 4 °C for subsequent determination of Mn, Zn and Pb by flame atomic absorption spectrometry (Shimadzu AA-6800). Samples for Hg analysis were digested with a mixture of HCl, HNO_3 and $KMnO_4$ in a water bath at 95 °C. The acid extracts were analyzed by atomic absorption using the cold vapor-generation technique (Shimadzu HVG-1 hydride generator).

The detection limits of the respective analytical techniques were 3 mg kg^{-1} for Mn, 9 mg kg^{-1} for Pb, 1 mg kg^{-1} for Zn and 0.02 mg kg^{-1} for Hg. The precision of the analyses (based on three samples collected at each sampling location) for all studied elements was considerable less than 20 %.

RESULTS AND DISCUSION

Concentrations of Mn, Zn, Pb and Hg in sediment and TSS of mining effluents

Figure 2 shows the mean concentrations (bars) and the standard deviations (error bars) of Mn, Zn, Pb and Hg in bottom sediments of the studied rivers and streams and in TSS of the mining effluents (NAM1 and CHI). In the Zamora River basin, there are two principal mining districts (Chinapintza-La Herradura and Nambija) where ASGM activities are performed. The mining effluent of the Chinapintza-La Herradura district (CHI) showed a TSS concentration of 4600 mg/l, which was much lower than the TSS concentration showed by the Nambija (NAM1) mining effluent (30800 mg/l). However, the TSS in the Chinapintza-La Herradura mining effluent had higher concentrations of Mn, Zn and Pb than the suspended material of the Nambija effluent (Fig. 2). Indeed, this fact can suggest that the suspended material of the Chinapintza-La Herradura mining effluent is constituted by recently crushed polymetallic ore, which has been discharged from mining areas after the gold extraction process and is enriched in Mn, Zn and Pb. On the other hand, the relative low concentrations of Mn, Zn and Pb in the suspended material of the Nambija effluent seems to indicate that this suspended material is mainly constituted by silt and clay minerals (aluminiosilicates), which are originated from the removal and erosion of soils in this zone. With respect to Hg concentrations, the TSS of both effluents showed elevated Hg levels, although higher Hg concentrations were found in the suspended material of the Chinapintza-La Herradura mining effluent.

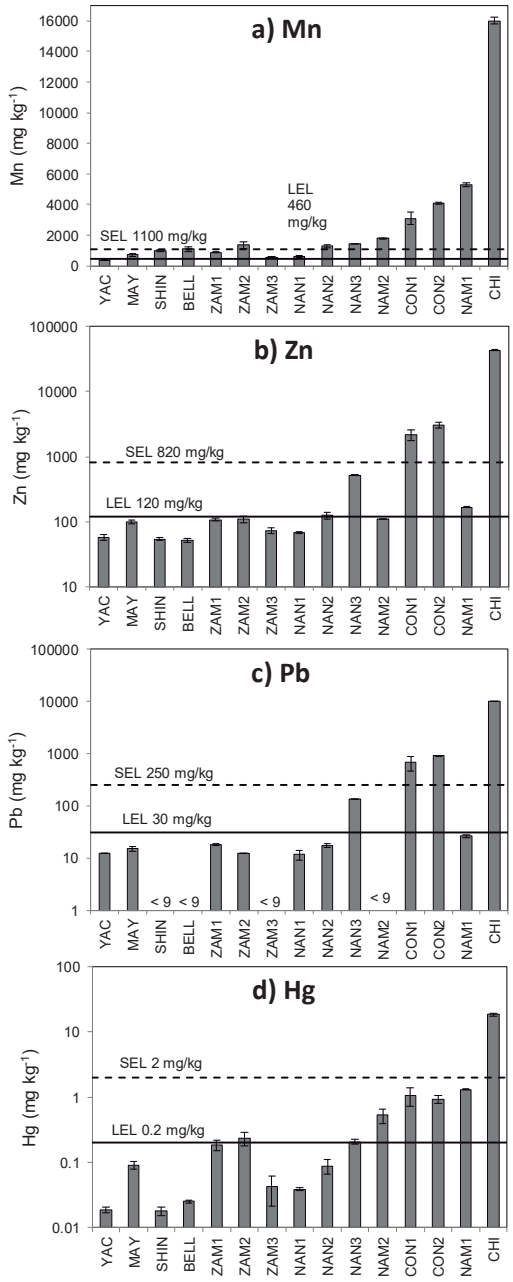

Fig. 2 Mean concentrations of Mn, Zn, Pb and Hg in bottom sediments from rivers and streams and suspended sediments from mining effluents (plots of Zn, Pb, and Hg are in logarithmic scale)

Figure 2 shows that bottom sediments from the unaffected streams Shincata, Bellavista and Mayaycu and from the rivers Yacuambi and Nangaritza (sites NAN1 and NAN2) showed similar

concentrations of all studied elements. Also, these sediments showed the lowest concentrations of Mn, Pb, Zn and Hg, suggesting that the presence of these heavy metals in these sediments is due to geological origin and these levels could be considered as regional values.

Conversely, sediments collected in the Congüime River and Nangaritza River in the site NAN3 (after the confluence with the Congüime River) showed the highest concentrations of Mn, Zn, Pb and Hg, because of the ASGM activities performed in the Chinapintza-La Herradura mining district. Moreover, the concentrations of these elements in sediments of the Congüime River were similar or higher than those reported for bottom sediments of the Puyango River, an Ecuadorian river that has been strongly impacted by the discharge of mine tailings from gold ore processing plants since the second half of the twentieth century [9]–[10]. Indeed, the high concentrations of the studied elements in bottom sediments of the Congüime River is due to the mining effluents coming from the Chinapintza-La Herradura mining district (effluent CHI), which flow into the Congüime River and bring a high content of TSS constituted by recently crushed polymetallic mineral. Similarly, the increase of Mn, Zn, Pb and Hg concentrations in sediments from the Nangaritza River after the confluence with the Congüime River (site NAN3) is due to the influence of the contaminated sediments coming from the Congüime River, which tend to be resuspended and deposited in the lower section of the Nangaritza River.

Toward the western Zamora River basin, the Mn, Zn, Pb and Hg concentrations in the Nambija River sediments were of the same order of magnitude as the values reported recently by other studies in sediments of this river [4]–[5]. Thus, this suggests that mining activities in this district have not increased in the last years. When comparing the concentrations of the measured elements in sediments of the Nambija River with those measured in sediments from the Congüime River, it is observed that the Nambija River sediments show lower concentrations of Mn, Zn and Pb. This fact could be due to the TSS from mining effluents of the Nambija sector (NAM1) are constituted by silts and clays (as the results of the remove and erosion of soils) and thus they have low levels of heavy metals.

Regarding to Hg concentrations, the Hg values in sediments of the Congüime, Nambija and Nangaritza rivers were similar that the Hg values found in sediments of rivers impacted by ASGM in Africa and South America [11]–[12]. However, the concentrations of Hg in sediments of the Zamora, Nambija, Congüime and Nangaritza rivers were higher than those found in rivers and streams of the Madre de Dios River basin (where the maximum value reported was 0.095 mg/kg), a region of the Amazon basin in Peru impacted by ASGM [13]. It is also important to mention that although bottom sediments of the Zamora River main channel showed Mn, Zn and Pb concentrations very similar to background values, the high concentrations of Hg found in the sediments from the sites ZAM1 and ZAM2 could indicate the existence of ASGM activities towards the upper and middle Zamora River basin.

Comparison with international guidelines

Figure 2 also compares the concentrations of the measured elements in bottom sediments of rivers and natural streams of the Zamora River basin with the Guidelines for the Protection and Management of Aquatic Sediment Quality in Ontario [14]. Based on the long-term effects which the heavy metals may have on the aquatic organisms, these guidelines have established three levels of effects: i) the no effect level (NEL) suggests that the metals in the sediment do not affect fishes or sediment-dwelling organisms; ii) the lowest effect level (LEL) specifies that at this level, the contamination has no effect on the majority of the benthic organisms; however, contamination that exceeds this level may require further testing. Finally, iii) the severe effect level (SEL) indicates heavily polluted sediments, which can affect seriously the health of sediment-dwelling organisms. Even though the mean concentrations of Mn in sediments from the Zamora and Nangaritza rivers exceeded the LEL level proposed, the concentrations of this metal was similar or slightly higher than those showed by sediments collected in non-impacted streams (MAY, SHIN and BELL). Therefore, these concentrations are close to background levels and no further assessments are needed. Mean concentrations of Mn, Zn and Pb in sediments from the Congüime River and mean levels of Mn in bottom sediments from the Nambija River and Nangaritza River in the site NAN3 are much higher than the SEL value proposed for these metals (about three or four-fold). Therefore, this fact indicates that the bottom sediments of the Congüime, Nambija and Nangaritza (site NAN3) rivers are considered highly contaminated and likely have an adverse effect on benthic organisms living in these fluvial sediments. Similarly, Fig. 2 also shows that although the Hg concentrations in sediments from the Congüime, Nambija, Nangaritza (NAN3) and Zamora (ZAM2) rivers exceeds the LEL value proposed for Hg in the Ontario guidelines, none of these riverine sediments had Hg concentrations higher than 2 mg kg^{-1}, a value above which the Hg could severely affect the macroinvertebrate communities living in aquatic sediments [14].

CONCLUSIONS

This study analyzed and evaluated the levels of heavy metals due to ASGM activities in sediments of rivers and streams of the Zamora River basin. Bottom sediments of the Congüime River are contaminated with Mn, Zn, Pb and Hg due to the high levels of these metals in the suspended material of mining effluents coming from the Chinapintza-La Herradura mining sector. This suspended material also contaminated the bottom sediments of the Nangaritza River, which showed an increase of Mn, Zn, Pb, and Hg in the lower section of the basin. Although fluvial sediments of the Zamora and Nambija rivers did not show contamination with Zn and Pb, these sediments are contaminated with Hg, probably due to the ASGM carried out in the Nambija mining district and in the upper Zamora River basin. The high concentrations of Mn, Zn and Pb in sediments of the Congüime River and Mn in sediments of the Nambija River and sediments of the lower Nangaritza River can have a harmful effect on sediment-dwelling organisms, according to the Ontario Guidelines for the Protection and Management of Aquatic Sediment Quality.

ACKNOWLEDGEMENTS

This investigation was supported by Secretaría de Educación Superior, Ciencia, Tecnología e Innovación de la República del Ecuador (SENESCYT) and Universidad Nacional de Loja. In addition, Tecnológico de Monterrey has supported the presentation of this work in the 6th International Symposium on Sediment Management.

REFERENCES

[1] Chiaradia M, Vallance J, Fontboté L, Stein H, Schaltegger U, Coder J, Richards J, Villeneuve M, Gendall I, "U-Pb, Re-Os and $^{40}Ar/^{39}Ar$ geochronology of the Nambija Au-skarn and Pangui porphyry Cu deposits, Ecuador: implications for the Jurassic metallogenic belt of the Northern Andes", Miner. Deposita, Vol. 44, May 2009, pp. 371-387.

[2] Vallance J, Fontboté L, Chiaradia M, Markowski A, Schmidt S, Vennemann T, "Magmatic-dominated fluid evolution in the Jurassic Nambija gold skarn deposits (southeastern Ecuador)", Miner. Deposita, Vol. 44, May 2009, pp. 389-413.

[3] Appleton JD, Williams TM, Orbea H, Carrasco M, "Fluvial contamination associated with artisanal gold mining in the Ponce Enríquez, Portovelo-Zaruma and Nambija areas, Ecuador", Water Air Soil Poll., Vol. 131, Oct. 2001, pp. 19-39.

[4] Ramírez ME, Ramos JF, Angélica RS, Brabo ES, "Assessment of Hg-contamination in soils and stream sediments in the mineral district of Nambija, Ecuadorian Amazon (example of an impacted area affected by artisanal gold mining)", Appl. Geochem., Vol. 18, Mar. 2003, pp. 371-381.

[5] Carling GT, Diaz X, Ponce M, Perez L, Nasimba L, Pazmino E, Rudd A, Merugu S, Fernandez DP, Gale BK, Johnson WP, "Particulate and dissolved trace element concentrations in three southern Ecuador rivers impacted by artisanal gold mining", Water Air Soil Pollut., Vol. 224, Feb. 2013, 1415.

[6] Counter SA, Buchanan LH, Ortega F, "Mercury levels in urine and hair of children in an Andean gold-mining settlement", Int. J. Occup. Environ. Health, Vol. 11, Apr. 2005, pp. 132-137.

[7] Tomiyasu T, Kono Y, Kodamatani H, Hidayati N, Rahajoe JS, "The distribution of mercury around the small-scale gold mining area along the Cikaniki River, Bogor, Indonesia", Environ. Res., Vol. 125, Aug. 2013, pp. 12-19.

[8] Ministerio de Energía y Minas Ecuador, "Monitoreo ambiental de las áreas mineras en el sur de Ecuador", Quito, Ecuador, UCP Prodeminca, 1999, pp. 212.

[9] Tarras-Wahlberg NH, Flachier A, Lane SN, Sangfors O, "Environmental impacts and metal exposure of aquatic ecosystems in rivers contaminated by small scale gold mining: the Puyango River basin, southern Ecuador", Sci. Total Environ., Vol. 278, Oct. 2001, pp. 239-261.

[10] García ME, Betancourt O, Cueva E, Guimaraes JR, "Mining and seasonal variation of the metals concentration in the Puyango River basin-Ecuador", J. Environ. Protect., Vol. 3, Nov. 2012, pp. 1542-1550.

[11] Niane B, Moritz R, Guédron S, Ngom P, Pfeifer H, Mall I, Poté J, "Effect of recent artisanal small-scale gold mining on the contamination of surface river sediment: Case of Gambia River, Kedougou region, southeastern Senegal", J. Geochem. Explor., Vol. 144, Sep. 2014, pp. 517-527.

[12] Pinedo-Hernández J, Marrugo-Negrete J, Díez S, "Speciation and bioavailability of mercury in sediments impacted by gold mining in Colombia", Chemosphere, Vol. 119, Jan. 2015, pp. 1289-1295.

[13] Diringer SE, Feingold BJ, Ortiz EJ, Gallis JA, Araújo-Flores JM, Berky A, Pan WK, Hsu-Kim H, "River transport of mercury from artisanal and small-scale gold mining and risks for dietary mercury exposure in Madre de Dios, Peru", Environ. Sci. Proc. Imp., Vol. 17, Feb. 2015, pp. 478-487.

[14] Persaud D, Jaagumagi R, Hayton A, "Guidelines for the protection and management of aquatic sediment quality in Ontario", Ontario, Ministry of Environment and Energy, Nov. 1993, pp. 27.

CHEMICAL AND MINERALOGICAL CHARACTERIZATION OF SEDIMENTS FORMED BY MINE WASTES LEACHATES

Valdez-Bernal Fátima [1], Ramos-Arroyo Yann [1], Escot-Espinoza Victor [2] and Briones-Gallardo Roberto [2]
[1]Engineering Department, University of Guanajuato, Mexico; [2] Institute of Metallurgy, Autonomous University of San Luis Potosi, Mexico

ABSTRACT

Exploitation of mineral ores of skarn type at La Aurora Mine in Xichu Guanajuato generated huge quantities of residues deposited without control in the banks of the river. This residue was oxidized during more than 60 years and has high contents of potentially toxic elements (PTE: arsenic, lead and selenium). Over the channel, great quantities of secondary minerals were formed, main mineralogy are iron oxides and hydroxi-sulphates as jarosite. These mineral phases can be dissolved with the rains and the runoff.

In this work, arsenic distribution in different mineralogical phases, and mobility conditions from tailings deposits were evaluated. For that, samples were collected from residues considering a topographic transect from the upper part of deposit to the base in the bank of the river.

Results of X ray fluorescence applied to some samples show that secondary minerals has elevated concentrations with maximum values of 36,559 mg/kg for As, 24,619 mg/kg of Pb, 90 mg/kg of Se. Granulometry is a very important factor for liberation of arsenic species, fine material of residues is composed by soluble secondary minerals, more abundant are.

Keywords: Xichú Guanajuato, Tailings of Skarn Ores Type, Soluble Minerals, Arsenic.

INTRODUCTION

Environmental regulations are increasingly stricter, which implies the development of new analysis and monitoring methodologies to generate information on the availability of potentially toxic elements in soil and sediments.

The mining Xichú district is located in the North-East of the state of Guanajuato, Mexico, in the physiographic region of Sierra Gorda. The mining activity in the district began at the end of the XIX century and ended in the middle of the twentieth century. There is a great amount of mineral deposits scattered in the area, formed by veins epithermal deposits and skarn found in calcareous rocks of the Upper Cretaceous. The La Aurora mine generated large volumes of tailing mines that were arranged on the banks of the Xichú River. These residues have been weathering during more than 60 years and contain large amounts of potential toxic elements (PTE: As, Pb, Se). The main ore minerals were: galena (PbS), chalcopyrite (CuFeS), sphalerite (ZnS), pyrite (FeS) and arsenopyrite (FeAsS) with trace of gold (Au) and silver (Ag). So the mined elements of commercial interest were Zn, Cu, Pb, Ag and Au

Geochemistry of arsenic

The main source of the As in the soil is the parental material; however, mining has contributed, together with other anthropogenic activities to the dispersion of this contaminant in the environment [1].

Arsenic behavior is typical of many calcophile elements which are released by sulphides oxidation through diverse biogeochemical processes, and attenuated by adsorption and co-precipitation with Fe-minerals, clay and organic matter [2].

Concentrations and relative proportions between As (V) and As (III) in solution depend of changes of physicochemical conditions (e.g. pH, redox potential), and divers kinds of biological activities. As (III) can be maintained in the waters anoxic by biological reduction of As (V) [3]. As (V) is the inorganic specie of As predominant in soil with oxidizing conditions and it is uptaked by reactions of adsorption in several mineral phases [4, 5, 6, 7]. The most important minerals that control the adsorption of As (V) in soil include Al and Fe oxides [8, 9, 10].

Unawareness of waste attenuation processes, their impacts over environment and public health risk require a diagnosis about geochemical characterization to identify secondary phases created in situ by waste weathering such as sulfates, jarosites and iron oxides (amorphous or crystalins) and their chemical stability.

METODOLOGY

Sample Collection

Solid samples of mine wastes and sediments formed from leachates of them were collected

according to Siebe's protocol and they are described in Table 1.

Two types of solid samples were identifying according to structure of tailing dump:

I. Residue from the top of tailing dump relate to a washing process on the surface (washing zone).

II. Terrigenous sediments produced by mixing of leachates and solid precipitation of them.

All samples were dried, quartering and homogenized. Total concentrations of PTE were determined using an X-ray fluorescence equipment (Axon, Olympus).

Table 1 Description of samples

Description	Key
Horizon 1 of waste solid located in the top of tailing dump (from 0 to -7 cm of depth)	WSPH1
Horizon 4 of waste solid located in the top of tailing dump (from -15 to -20 cm of depth).	WSPH4
Horizon 6 of waste solid located in the top of tailing dump (from -26 to -32 cm of depth).	WSPH6
Horizon 1 of terrigenous sediments located in the fluvial plain down of tailing dump (from 0 to -1 cm of depth)	TSPH1
Horizon 6 of terrigenous sediments located in the fluvial plain down of tailing dump (from -13 to -16 cm of depth).	TSPH6
Horizon 7 of terrigenous sediments located in the fluvial plain down of tailing dump (from -30 to -33 cm of depth).	TSPH7

XDR Analysis

All X-ray diffractometric analysis were carried out using a diffractometer Bruker (D8 Advanced Instrument). Solid samples were milled to mesh -400 to achieve a better spectral resolution for identification of mineral phases and semi-quantitative analysis of them.

Soluble and exchangeable fractions of PTE in solid samples

Solid samples were put in contact with 200 mL of deionized water for 20 min in an orbital agitator. In the filtered supernatant (Whatman filter #5) were determined pH and electrical conductivity (E.C.). The procedure was repeated until the value of E.C. of deionized water did not present modifications by contact with the solid sample. Subsequently, the solid-liquid separation was made by centrifugation at 3000 rpm for 15 min. The solid recovered were dried to 70°C until constant weight. The sample solid residual was milled and homogenized to -400 for later analysis by XRD and FRX.

The solid residual recovered in the previous extraction was placed twice in contact of 50 mL of 1M NaH_2PO_4 for 24 h each contact. The sample was then dried up to constant weight and XRD identification and total concentration quantification of PTE by FRX were performed again.

RESULT AND DISCUSSION

Table 2 shown total concentrations of arsenic, lead, selenium and antimony which exceeded the maximum permissible limits (MPL) stablished by the NOM 157. Arsenic in the waste solids located in the top of tailing dump is 15 to 70 times above the MPL stablished in the Mexican normative [12]. In the cases of terrigenous sediment arsenic concentration were 1.4 to 38 times the MPL value, and the highest value of arsenic was determined in the most deep horizon to profile. On the other hand, it is observed that the behavior of lead is completely different because in waste solid profile the Pb exceeds 12 to 43 times the MPL, presenting a significant increase in function to its depth for the profile located in the top of tailing dump. The highest lead concentration in the terrigenous sediments profile is located in an intermediate horizon (TSPH6). Antimony exceeds 1-19 times the MPL on the waste solid in the top of tailing dump profile and up to 6 times in the terrigenous sediment profile recollected in the fluvial plain.

Table 2 Total concentrations of arsenic, lead, selenium and antimony in the waste solid and terrigenous sediments

Sample	As	Pb	Se	Sb
WSPH1	1597	1268	**9**	100
WSPH3	6977	3374	24	190
WSPH4	5318	4366	27	148
TSPH1	141	83	3	--
TSPH6	9507	286	10	49
TSPH7	13868	149	7	60
MPL*	**100**	**100**	**20**	**10.6**

*MPL: maximum permissible limits stablished in NOM-157-SEMANRNAT-1996.

Figure 1 show the arsenic total concentrations in the three granulometric fractions analyzed (pd> 600 μm; 250<pd<600 and pd<250 μm; where pd correspond to particle diameter associated to mesh used).With regard to the arsenic, this element is concentrates in the deep part of the profile of the terrace of the deposit and preferably in the fine fraction. This behavior is opposite to its distribution

in the terrigenous sediments, where the As availability is distributed homogeneously in the different sizes of particle, but it is concentrated in the part superficial profile.

Figure 2a and 2b present the distribution of the soluble and exchangeable anionic fractions of the As, Pb, Se, Sb, Fe, Ca and S in the waste solid and terrigenous sediments, respectively, with respect to their depth and considering the finest granulometric fraction.

Figure 2a shows that the highest soluble and exchangeable concentrations of arsenic, selenium and antimony are present in the H3 horizon with respect to the H1 horizon. It can be assumed that the surface in the top of tailing dump is continuously washed by meteoric water, thus decreasing the total, soluble and exchangeable concentrations of these elements. With respect to arsenic, equimolar proportions of this element are observed between the two more available fractions evaluated (soluble / exchangeable).

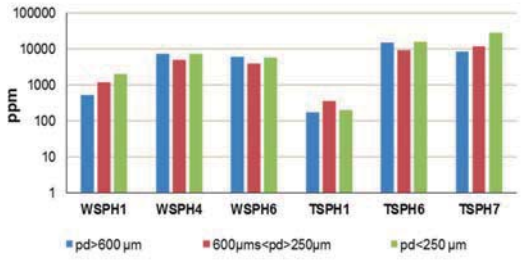

Fig. 1 Arsenic total concentration in different granulometric fractions of the residues analyzed (where WSP are waste solid profile and TSP terrigenous sediment profile)

Otherwise, the highest proportion available of selenium is in the soluble+exchangeable fraction in horizons H1 and H2 but opposite in H3. The percentages of the soluble+exchangeable anionic fractions of arsenic (from 32 to 50%) are related to those of iron (33 to 45%), probably associated with the dissolution of soluble mineralogical phases that contain them. In this regard, it is important to mention that between 73 and 90% of the calcium is in soluble form in the three horizons of the tailing dump profile and is related to ~ 35% of the sulfur solubilized in the surface horizon (H1) and with a 70 % with the deepest horizon (H3).

In the case of lead, the available fraction of this element corresponds to the exchangeable anionic fraction (between 10 and 20%) associated with the dissolution of secondary phases that contain it, such as gypsum, jarosites or amorphous iron oxides.

In Fig. 2b, which corresponds to terrigenous sediments profile, it is observed that the arsenic soluble fraction is highest in the top of profile (H1) and diminished with the depth, which may be due to the washing process in the surface migration fine particulate material, and exchangeable fraction is more important in the deepest horizon, passing from 9% in H1 to 30% in H3.

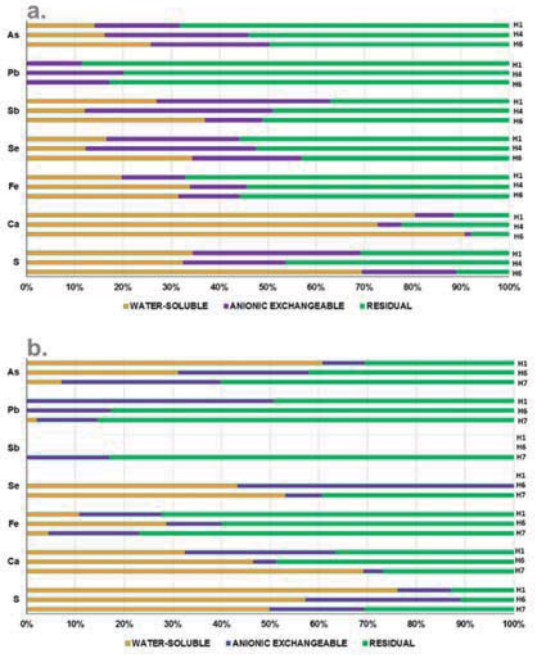

Fig. 2 Mineralogical composition of the samples of the deposits of the mining waste. (a) waste solid, (b) terrigenous sediments

Available fractions of lead were principally associated with the exchangeable fraction; this fraction also decreased from the superficial to the deep horizon, going from 50% in H1 to 15% in H7. A similar behavior to that observed with arsenic profile it was presented for the sulfur and calcium fractionations, where the most available fractions (soluble + exchangeable) were presented in the upper part. In Fig. 2b, for terrigenous sediments profile, there are not trace to selenium in the most surficial horizon, and the most available fraction of selenium (soluble and exchangele fractions) occurs at 100% in the horizon H6 (from -13 to -16 cm of deep) dropped to 60% at -30 cm of deep. A similar behavior to selenium is observed for antimony, but in this case, there is no trace of this element until -30 cm of deep. The behavior of Se and Sb permit stablish that these elements were the most available after that they were released. In the same way as it was observed with arsenic, because it was not possible to identify selenium, or antimony, mineral phases, it is very likely that those elements are associated, by adsorption or coprecipitation, to other

major phases such as gypsum, jarosites and amorphous iron oxides, that when they are chemically destabilized they release the associated arsenic, selenium or antimony.

Mineralogical characterization obtained by XRD allowed to identify the crystalline phases associated during stage of sequential extraction to the release of As, Pb, Se, Sb, Ca, S and F, lepidocrocite, wuistite and hannebanchite were identify as crystaline phases carriers of PTE. On the other hand the phase of feldspars compries tridymite, quartz, muscovite, rossular, gehlenite, anhortite (Fig. 3).

In particular, the phases associated with the release of the soluble fractions of As and Fe were related to gypsum and probably ferrous sulphates Since these phases disappear after solubilization with water. In the case of the exchangeable fraction, the phosphate anion used in this extraction promotes the chemical destabilization of secondary jarosite-like phases that were no longer observed as part of the mineralogical phases remaining in the XRD (Fig. 3).

The depth of the sample is a factor that influences the availability of As species and their association with other minerals such as gypsum and jarosites that have been completely removed after each extraction stage.

Pb availability was affected by the anionic interaction of the phosphates in the exchangeable anionic phase and seems to be related to lead retained in jarosites. Depending on the depth of the samples, the sulfur as sulfate is soluble and more available in the terrigenous sediments than in the washed waste solid in the top of tailing dump.

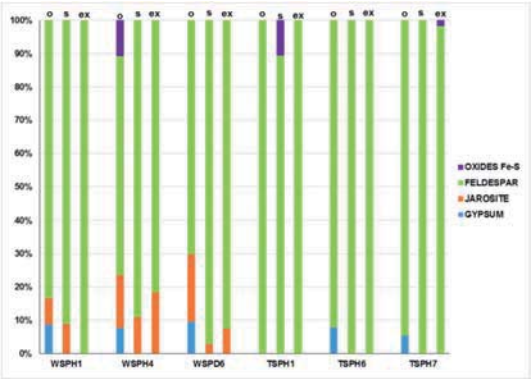

Fig. 3 Mineralogical characterization of waste solid and terrigenous sediments. From left to right: (o) original sample; (s) residual solid aftersoluble extraction; (ex) residual solid after anionic exchangeable extraction

CONCLUSIONS

The particle diameter is an important factor for release of PTE, since the fine fraction of the sediments or soils is easily draggable, transporting and releasing species such as As, Se and Sb.

The availability of As, Pb, Se and Sb is highly influenced by the depth of the samples and the solubility in the aqueous phase.

The chemical stability and the reactivity generated by the passage of meteoric water, also it is clear that the interaction with phosphates generates a significantly release of As, Se, Pb and SB from crystalline phases carrier of them.

ACKNOWLEDGEMENTS

The authors thanks to Ms. Tovar Tovar by X-ray Diffraction Laboratory in Institute of Metallurgy of Autonomous University of San Luis Potosi, Mexico.

REFERENCES

[1] Ongley L. K.; Sherman L.; Armienta A.; Concilio A.; Ferguson-Salinas C. (2007) "Arsenic in the soils of Zimapa´n, Mexico;"; Environmental Pollution 145, 793e799.

[2] Drahota P.; Filippi M. (2009) Secondary arsenic minerals in the environment: A review. Environ Int 35:1243-1255Author H, A Book. New York: Publisher, Yr, ch. 3.

[3] Lloyd J.R.; Oremland R.S. (2006) Microbial transformations of arsenic in the lake environment: From soda lakes to aquifers. Elements 2:85-90.Kimura S, "Journal paper title", J. of Computer Science, Vol. 1, Aug. 1987, pp. 23-49.

[4] Santini J.M.; Ward S.A. (eds) (2012) The metabolism of arsenite. In: Arsenic in the Environment 5. CRC Press, Boca Raton, Florida, pp. 189.

[5] Sadiq M.; Zaidi T. H.; Al-Mohana H. (1991) Bulletin of Environmental Contamination and Toxicology, Volume 47, Number 3, Page 335.

[6] Roy, W.R.; Hassett J.J.; Griffin R.A. (1986) Competitive coefficients for the adsorption of arsenate, molybdate, and phosphate mixtures by soils. Soil Sci. Soc. Am. J. 50:1176-1182.

[7] Goldberg S.; Gaubig R.A. (1988) Anion Sorption on a Calcareous, Montmorillonitic Soil Arsenic Soil. Sci. Soc. Am. J. 52:1297-1300.

[8] Jacobs, L. W., Syere, J. K., and Keeney. D. R. (1970). Arsenic sorption by soils. Soil Sci. SOC. Am. Proc.34, 750-754.

[9] Livesey, N.T.; Huang, P.M. (1981) Adsorption of arsenate by soils and its relation to selected chemical properties and anions. Soil Sci. 131, 88–94.

[10] Fuller, C.C.; Davis, J.A.; Waychunas, G.A. (1993) Geochim. Cosmochim. Acta, 57, 227-2282.

[11] Siebe C.; Jahn R.; Sthar K. (1996) "Manual para la descripción y evaluación ecológica de suelos en campo"; Universidad Autónoma de México.

[12] Diario oficial de la federación (2011) NOM-157-SEMARNAT-2009, Que establece los elementos y procedimientos para instrumentar planes de manejo de residuos mineros.

EVALUATION OF MANGANESE INSOLUBILITY ON BODIES OF WATER ON A MINING REGION IN MEXICO

Scheel-Hinojosa Patrick
Compañía Minera Autlán, S.A.B. de C.V., México

ABSTRACT

The Manganese (Mn) District of the State of Hidalgo, Mexico, contains the second largest deposit of manganese in Latin America. The nature of the region plus the extractive operations of Mn triggers an inherent movement of matter that transfers into the bodies of water of the area. The existence of Mn in the region is evident, although, the origins of its dispersion are uncertain. In past studies carried out to compare the sediments of bodies of water within the sphere of influence of mining-metallurgical activities versus a baseline, Mn was detected on 8/27 samples of water, and on 12/20 samples of sediments. It is possible that Mn detected on water is due to solid colloids (fine particles smaller than 0.45 microns) that are not retained on the filters used for water quality analysis. Manganese accumulates on sediments, and is considered negligible on water. It is concluded that Mn, available as Mn oxide, is not soluble from sediments, thus there is no effect on water quality. Certain factors can solubilize Mn on sediments, but represent an extremely unlikely scenario under the climatic conditions of the region. Therefore, transport of soluble Mn by water is improbable.

Keywords: Insolubility of Manganese, Sediment Contamination, Manganese Water Impacts, Colloidal Systems

INTRODUCTION

Manganese is the fifth most abundant metal in the Earth's crust, and its main mining areas spread all across the globe. The Mn District of the State of Hidalgo, Mexico is the second largest deposit in Latin America, and one of the top 10 worldwide. The most common Mn mineral found is the pyrolusite, containing manganese (IV) dioxide (MnO_2), it is also the most used on the Mn industry.

Manganese is a naturally occurring element found in rock, soil, water, and food, that plays an essential role as a micronutrient for all life forms. It is found mostly in bones, the liver, kidneys, and pancreas, used for many metabolic functions, including the development of the osseous system, the activation of enzymes, and the secretion of the reproductive hormone. It is also a component of the antioxidant enzyme superoxide dismutase, protecting cells against free radicals, and being necessary for normal brain and nerve function [1].

The excess of Mn stored on brain tissue, reaching toxic levels, has been related to causing Manganism, similar to Parkinson's Disease. Nevertheless, it is believed that Mn toxicity can only be reached by inhaling significant doses of Mn particles, while Mn ingestion is controlled by the physiological control system for absorption, distribution, and elimination of the element. The concentration of Mn on the body is regulated homeostatically by the liver, through the bile, and any excess is excreted accordingly.

In order to define the real impact of the mining-metallurgical activities over the bodies of water, samples of water and sediments have been collected, and a thorough analysis has been done to determine the amount of Mn and its impact on the environment.

Manganese oxides have been detected on water and sediments within the sphere of influence within the Mexican Mn District. Considering the properties of the mineral, being Mn(II) and Mn(IV) principally the main constitutents, and taken into account the climatic conditions of the region, Mn is not solubilized and is accumulated on sediments. In this paper, it is hypothesized that from 30% of water samples with Mn, with a median of 0.525 mg/L, the Mn identified consists of solid colloids which are not soluble but are still present on the results due to the fine Mn particles that are not retained by the 0.45 micron filters for the water analysis. In addition to this, Mn is very unlikely to solubilize and does not represent a risk for the flora and fauna of the riverbed, thus there is no effect on water quality.

METHODOLOGY

During 2015, 27 water samples and 20 sediment samples were collected on three different field visits. The locations were selected based on the most representative rivers and streams that flow besides the discharges of the mining-metallurgical activities.

The geographical location of the water sampling is shown on Fig. 1, while the sediment sampling location on Fig. 2. The procedure used for the sampling of sediments was based on the Mexican standard NMX-AA-132-SCFI-2006 and NMX-AA-014-1980 for water. Sediment and water samples were taken from the same spot, where possible,

excluding discharge sites. The analysis of samples was performed according to EPA 6010c and 9045D.

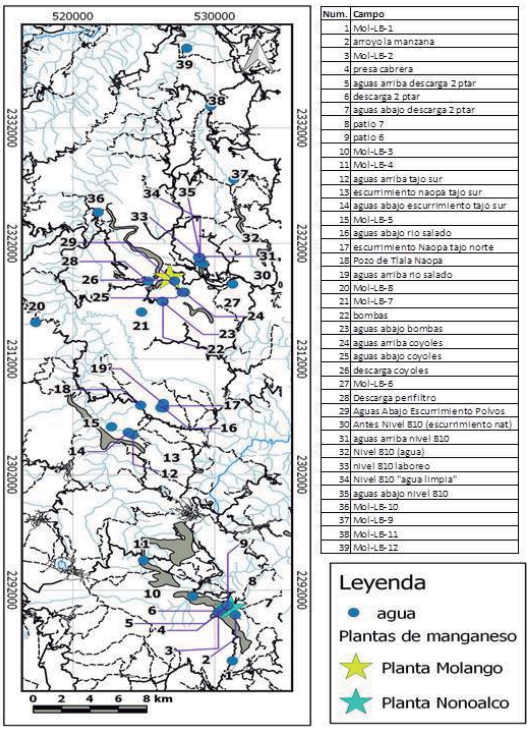

Num.	Campo
1	Mol-LB-1
2	arroyo la manzana
3	Mol-LB-2
4	presa cabrera
5	aguas arriba descarga 2 ptar
6	descarga 2 ptar
7	aguas abajo descarga 2 ptar
8	patio 7
9	patio 6
10	Mol-LB-3
11	Mol-LB-4
12	aguas arriba tajo sur
13	escurrimiento naopa tajo sur
14	aguas abajo escurrimiento tajo sur
15	Mol-LB-5
16	aguas abajo rio salado
17	escurrimiento Naopa tajo norte
18	Pozo de Tlala Naopa
19	aguas arriba rio salado
20	Mol-LB-8
21	Mol-LB-7
22	bombas
23	aguas abajo bombas
24	aguas arriba coyoles
25	aguas abajo coyoles
26	descarga coyoles
27	Mol-LB-6
28	Descarga perifiltro
29	Aguas Abajo Escurrimiento Polvos
30	Antes Nivel 810 (escurrimiento nat)
31	aguas arriba nivel 810
32	Nivel 810 (agua)
33	nivel 810 laboreo
34	Nivel 810 "agua limpia"
35	aguas abajo nivel 810
36	Mol-LB-10
37	Mol-LB-9
38	Mol-LB-11
39	Mol-LB-12

Fig. 1 Geographical Location of Water Sampling

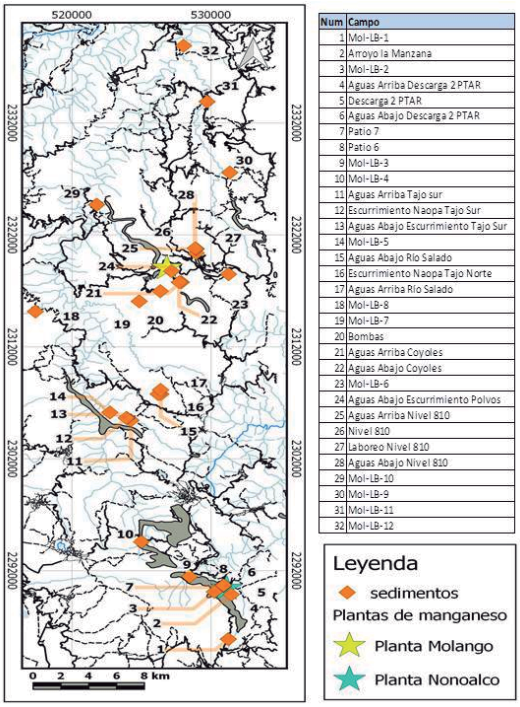

Num	Campo
1	Mol-LB-1
2	Arroyo la Manzana
3	Mol-LB-2
4	Aguas Arriba Descarga 2 PTAR
5	Descarga 2 PTAR
6	Aguas Abajo Descarga 2 PTAR
7	Patio 7
8	Patio 6
9	Mol-LB-3
10	Mol-LB-4
11	Aguas Arriba Tajo sur
12	Escurrimiento Naopa Tajo Sur
13	Aguas Abajo Escurrimiento Tajo Sur
14	Mol-LB-5
15	Aguas Abajo Rio Salado
16	Escurrimiento Naopa Tajo Norte
17	Aguas Arriba Rio Salado
18	Mol-LB-8
19	Mol-LB-7
20	Bombas
21	Aguas Arriba Coyoles
22	Aguas Abajo Coyoles
23	Mol-LB-6
24	Aguas Abajo Escurrimiento Polvos
25	Aguas Arriba Nivel 810
26	Nivel 810
27	Laboreo Nivel 810
28	Aguas Abajo Nivel 810
29	Mol-LB-10
30	Mol-LB-9
31	Mol-LB-11
32	Mol-LB-12

Fig. 2 Geographical Location of Sediment Sampling

Sampling was mainly focused on the area suspected to have higher impact or "Mining-Metallurgical Impact Area" (MMIA) based on the proximity of the mining-metallurgical activities, where 27 water samples were taken, and 20 from sediments. The MMIA was divided by each of the three mining units on the Mexican Mn District: Molango, Naopa, and Nonoalco. Sites potentially not affected by industrial activities were considered as well for sampling, divided in three areas: North, Center, and South. On these areas, 8 samples were taken from each, being 24 samples in total, 12 for water and 12 for sediments, the locations for both consisting on exactly the same spots.

The samplings were conducted by certified personnel, identifying the locations via GPS with the coordinates established on the initial planification. For the reliability of the sampling and quality control, 5% of duplicate samples were taken. Each sample was registered properly on a logbook, attaching photographs and specific details of each location.

Approximately 1 kg of sediment samples were collected on high density plastic bags, then sealed and introduced on a second bag for protection. In the laboratory, the samples were homogenized and spread on 2.5 cm layers over plastic trays, then dried at a controlled temperature of 33°C ± 3°C. The pieces larger than 2 cm were discarded, and the rest was then separated in a 10 mesh to obtain samples smaller than 2mm, which were again homogenized and evaluated for the physicochemical analysis. As for the Mn concentration, the samples were grinded to a size smaller than 100 mesh, then measured via ICP Spectrometer.

Approximately 1 liter of water was collected, stored in sealed containers and transported in a cooler to the laboratory, where the samples were validated based on the internal quality standards. The samples were agitated for the determination of pH, then they were let standing for 5 minutes for the determination of electrical conductivity (E.C.). For the Mn concentration, the samples were filtered on 0.45 micron filters and then acidified for its analysis on the ICP Spectrometer. This is a standard procedure followed by acidification with HNO_3 for analysis, where approximately 20 mL of water are filtered, depending on the level of solids present.

RESULTS

Water Sampling

Focusing on the MMIA, and excluding the baseline sampling, for the water analysis, out of the 27 samples, 8 were identified with Mn. The mean and the median being 0.5437 and 0.5250 mg/L, respectively, with a maximum of 0.88 and minimum of 0.21 mg/L. The 12 samples taken from

the baseline obtained Mn concentration levels below detection. Results are shown on Table 1. Samples with Mn concentration below detection levels were omitted from Table 1, but considered for statistical purposes.

Mexican legislation does not regulate concentration of Mn for natural bodies of water with industrial discharges, due to the nature and complexity of the element. Although, Mn concentration in drinking water is regulated, with a maximum permissible limit established by 0.15 mg/L. Nevertheless, local population does not drink water from rivers. In fact, Mn concentration in drinking water samples from each community were below the maximum permissible limit [2].

The pH values were practically neutral, with a small tendency towards basic, with a median of 7.9. There is no observable impact of the mining-metallurgical activities within this parameter. The pH values in water, and also in sediments, are always in the same range above 7 (with an anomalous exception of a minimum peak of 5.6), regarding upstream and downstream rivers, and discharges, within the MMIA. The pH from the baseline had a median of 8.15, also basic and similar to the result on the pH of the MMIA.

The E.C. had a median of 668 µs/cm and a maximum peak of 3,370 µs/cm within the MMIA. The baseline had a median of 301 µs/cm, indicating there exists an influence of the mining-metallurgical activities on water, regarding E.C.

Sediment Sampling

The sediment sampling included 20 samples within the MMIA, and 12 samples taken from the baseline, located at the exact same spots as the samples taken for water. The median obtained from the baseline was 820 mg/kg, with a maximum of 17,592 mg/kg. This maximum was used to establish the reference for the identification of Mn originated by the mining-metallurgical activities or related to the agriculture or cattle raising activities. Out of the 20 sediment samples, 12 were above the 17,592 mg/kg reference, resulting in a median of 30,731 mg/kg and a maximum of 194,160 mg/kg. As the remaining 8 samples were included inside the reference, it is considered that those levels of Mn concentration are due to the natural conditions of the region. Results are shown on Table 2.

Similar to the water sampling, the pH resulted slightly basic for the sediments within the MMIA, with a median of 8.3. While the pH of the baseline resulted more acidic in 7.8.

As for the E.C., the median of the MMIA, was similar to that of the baseline, being 268 and 158 µs/cm, respectively. The maximum value inside the MMIA was of 1,181 µs/cm, substantially lower than the results on the water samples. Only a small influence of the E.C. from the mining-metallurgical activities over the sediments could be identified.

Insolubility of Mn

Manganese oxidation states range from -3 to +7, the most common being +2 (Mn(II), manganese oxide [MnO]), +4 (Mn(IV), manganese dioxide [MnO_2]), and +7 (Mn(VII), potassium permanganate [$KMnO_4$]). Manganese exists in the aquatic environment in two main forms: Mn(II) and Mn(IV) [3].

Regarding the mining-metallurgical activities, Mn(II) and Mn(IV) are present, the rhodochrosite and kutnohorite containing Mn(II), and the pyrolusite and hausmannite containing Mn(IV).

Mn(II) is the simplest ionic oxide of Mn, with highly basic characteristics. Although, in a solution it is not corrosive and does not react on skin exposure. It is rarely found naturally in manganosite form, it is more often prepared by reduction or heating processes in an atmosphere low on oxygen, as it is the case with the mining-metallurgical activities, where the most common Mn compound found is Mn(II), due to the nodulization process of calcination and reduction of Mn carbonate.

Mn(IV) is the compound that occurs naturally on the pyrolusite. It is a black insoluble solid, which is essentially ionic [4]. Besides its insolubility in water, Mn(IV) is also known for its solubility in hydrochloric acid [3].

The logarithmic solubility product constants (pKs) are low for the Mn substances in question. For Mn(II), it has been reported as 10.93 and 12.5 for rhodochrosite and as 19.84 for kutnohorite, meaning that the quantity of Mn that can solubilize and react is practically negligible [5]. On the other hand, Mn(IV) presents a pKs of 17.84 for pyrolusite and 54.15 for hausmannite. Also, representing very low probability of solubilization.

The environmental chemistry of Mn is directly influenced by pH and redox conditions. An extremely acidic environment can increase the probability of dissolved Mn. There is a trend from ionic Mn(II) dominance at low pH to an increasing proportion of colloidal manganese oxyhydroxides above pH 5.5 in non-dystrophic waters [6].

Reference [7] analyzed waters receiving acid mine drainage, where dissolved Mn concentrations were below 0.04 mg/L when the pH was above 5.5; however, when the acidification increased below pH 3, the dissolved Mn concentrations peaked up to 4.4 mg/L. On the same consideration, reference [8] analyzed sediments, where Mn concentrations decreased from 400 mg/kg at pH 5.9 to 8 mg/kg at pH below 3, due to Mn dissolution influenced by acid mine drainage.

Other factors, such as acid precipitation, land use, and municipal wastewater discharges, can increase dissolved manganese levels [3].

The Mn(II) ion is more soluble than Mn(IV) [9]; therefore, with decreasing pH and under reducing conditions, Mn will tend to become more bioavailable. The presence of high concentrations of chlorides, nitrates, or sulfates may also facilitate Mn solubility and thus increase aqueous mobility and uptake by plants [10], but recent research has found the role of sulfate ions as prominent [11].

Considering the results from the analysis of the MMIA, the median pH of water and sediments being 7.9 and 8.3, respectively, the characterization of the MMIA is considered basic, where an extremely unlikely scenario would have to decrease the pH below 3 to dissolve Mn. On the case of the sediment sampling, the pH resulted more acidic on the baseline, meaning that the conditions within the MMIA are more appropriate as the pH is more basic.

Reference [12] analyzed the concentration of bioavailable elements in soil through an ICP Spectrometer to acknowledge that the soluble Mn was below the minimum levels of detection, indicating the low probability of solubilization that Mn has in the mineral forms presented in the MMIA, and its real impact on soils, concluding there exists a change in composition of the mineral fraction, but not an effect in the composition of the solution of the soil, nor in the sorption complex.

Reference [13] analyzed the concentration of Mn on a Mexican dam, where dissolved Mn was found to be present in its mayor proportion as solid colloids, being inert and slowly labile, identified as Mn particles that cannot be retained by filtration through a membrane of 0.45 microns, but that can be retained by a Chelex 100 resin after 24 hours of contact, thus not soluble.

Table 1 Water Samples Results (pH, electrical conductivity, and Mn concentration

Location	pH	E.C. (µs/cm)	Mn (mg/L)
810 Level DC - MU	8.2	2680	0.47
Coyoles DC - MU	7.8	3370	0.39
Bombas R - MU	8	668	0.21
Zacuala R - NaU	7.8	2450	0.37
Courtyard 6 - NoU	7.6	2340	0.83
La Manzana - NoU	7.6	1182	0.58
WWTP US - NoU	7.9	888	0.88
WWTP DS - NoU	7.8	882	0.62

Table 2 Sediment Samples Results (pH, electrical conductivity, and Mn concentration)

Location	pH	E.C. (µs/cm)	Mn (mg/kg)
810 Level - MU	8.8	539	34,939
810 Level DC - MU	8	1181	31,653
810 Level US - MU	8.3	257.5	16,567
810 Level DS - MU	8.4	462.5	44,334
Coyoles US - MU	8.8	61.5	13,299
Coyoles DS - MU	8.7	131.2	21,931
Bombas R - MU	8.5	486	179,311
Polvos R - MU	8.3	804.5	194,160
Salado R - NaU	7.8	310.5	9,436
Salado US - NaU	8.8	105.3	4,910
Salado DS - NaU	8.5	51.2	877
Zacuala R - NaU	8.3	375	1,552
Zacuala US - NaU	8.5	129.6	5,888
Zacuala DS - NaU	8.8	147.2	1,154
Courtyard 6 - NoU	7.5	817	134,250
Courtyard 7 - NoU	8.1	244	73,734
La Manzana - NoU	8.1	312.5	29,808
WWTP DC - NoU	7.8	278.5	97,125
WWTP US - NoU	8	158.3	87,884
WWTP DS - NoU	7.8	185.1	57,774
BL 1 - S	7.34	868	294
BL 2 - S	7.56	223	326
BL 3 - S	8.2	131.7	327
BL 4 - S	7.73	256	205
BL 5 - C	8.1	120.6	4,164
BL 6 - C	7.9	129	4,260
BL 7 - C	6.8	35.2	325
BL 8 - C	8.3	56.7	953
BL 9 - N	7.6	160.9	687
BL 10 - N	7.9	269	1,692
BL 11 - N	7.5	342	17,592
BL 12 - N	8	155.3	11,635

MU = Molango Unit
NaU = Naopa Unit
NoU = Nonoalco Unit
DC = Discharge
DS = Downstream
US = Upstream
R = Runoff
WWTP = Waste Water Treatment Plant
BL = Baseline
S = South
C = Center
N = North

DISCUSSION

Manganese can be found in nature in many different mineral forms. Colloidal Mn can be dissolved in dilute mineral acids [14], Mn chloride and Mn sulfate are soluble in water and alcohol. Potassium permanganate is soluble in water, acetone, and sulfuric acid. Leaving Mn dioxide and Mn tetroxide insoluble in water, but soluble in hydrochloric acid [15].

Considering the conditions of the MMIA, and its pH parameters being basic, soluble Mn is highly unlikely. Municipal and communities' wastewater is drained to the analyzed rivers. Nonetheless, the population of the region of influence is less than 20 thousand persons and are widely distributed across the mountain range in more than 30 communities. The wastewater discharged is not significant for the pH acidification of rivers, and it does not represent a risk for Mn solubility.

The solubility of Mn is controlled by the limestone that covers the facies of Mn, as it precipitates as Mn(II). Only in the scenario where large quantities of protons produced by the oxidation of pyrite present on the mineral, or where substantial amounts of wastewater are discharged to rivers with low flux, the reduction of Mn and its mobilization may be possible [5].

International levels of Mn concentration on river sediments range from 410 to 6700 mg/kg dry weight, considering no industrial impact, while sediments from lakes receiving discharges from industrial and residential areas contain Mn at concentrations ranging up to 13,400 mg/kg dry weight [3].

The Mexican Mn District has an actual deposit of nearly 30 million tons of mineral, while the probable reserves rise up to 250 million tons [16]. The nature of the region triggers an inherent movement of Mn that transfers into the bodies of water of the area. The baseline shows a maximum of 17,592 mg/kg, and based on the methodology of the sampling, this sample is outside of the known MMIA, where further analysis may be required to define the origins of Mn dispersion inside the baseline. Nevertheless, Mn found in sediments with a median of 30,731 mg/kg inside the MMIA represent a clear influence of the mining-metallurgical activities in the region within a controlled radius.

Mn oxides are omnipresent on soils and sediments, and due to their high chemical activity, they facilitate the degradation of potentially toxic metals and exert a great influence over the chemical compositions and behaviors of associated aqueous systems [17].

During the water analysis, the samples were filtered and a considerable difference was identified for the Mn concentration. While the maximum value of the filtered samples was 0.88 mg/L, a maximum from the unfiltered samples was detected by 2,101 mg/L. This significant gap demonstrates that Mn is found forming colloids.

Most toxicity tests that have been carried out on the rivers of the MMIA have been using ionic Mn, and not colloidal Mn, which happens to be more common. The investigation on the aquatic toxicity of this element, in colloidal, particulate, or complex form is very limited. However, it is assumed that toxicities of metals bound into these colloidal forms are less harmful than those of the aquo-ionic forms of soluble Mn [3].

CONCLUSIONS

Different minerals containing Mn are found on water and sediments inside the Mexican Mn District. The most common being Mn(II) and Mn(IV), respectively by priority. Both of which are considered insoluble due to characterization of basic pH of the rivers within the MMIA.

Mn found in the water samples may be due to solid colloids smaller than 0.45 microns, which are not soluble but neither retained by the size of the filters used for determining Mn concentration. The significant gap between the Mn concentration of filtered vs unfiltered samples demonstrates the existence of colloids.

A baseline was defined for Mn concentration on sediments, where 12/20 samples exceeded the reference levels within the MMIA. Determining there is a clear influence of the mineral-metallurgical activities on the district, but also that the region outside the MMIA, due to natural deposits of Mn, represent a significant source of Mn dispersion.

Mn is a naturally occurring element that plays an essential role as a micronutrient for all life forms. The presence of Mn on water and sediments do not represent a risk for the flora and fauna of the riverbed. Any excess ingested by animals is regulated homeostatically and excreted accordingly.

Further analysis may be required for the investigation of the origins of Mn dispersion.

ACKNOWLEDGEMENTS

The author is grateful to Dr. Margarita Eugenia Gutiérrez Ruiz and Dr. Roberto Gregorio García Fragoso, from the Laboratory of Environmental Biogeochemistry, Department of Chemistry, National Autonomous University of Mexico, for their valuable support and expertise on the topic. Also, special thanks to Autlan Mining Company, for funding the project for the analysis of Mn in wastes, sediments, water, plants, and soils, in order to identify the real impacts of the mining-metallurgical activities in the Mexican Mn District.

REFERENCES

[1] Ehrlich Steven, "Manganese", University of Maryland Medical Center, 2013, umm.edu/health/medical/altmed/supplement/manganese.

[2] Rodríguez-Agudelo, Y., Riojas-Rodríguez, H., Ríos, C., Rosas, I., Pedraza, E. S., Miranda, J., Santos-Burgoa, C., "Motor alterations associated with exposure to manganese in the environment in Mexico", Science of the Total Environment, Vol. 368, 2006, pp. 542-556.

[3] Howe P.D., Malcolm H.M., Dobson S., "Manganese and its compounds: environmental aspects", Centre of Ecology & Hydrology, Monks Wood, United Kingdom, 2004.

[4] Emsley, J., "Manganese", Royal Society of Chemistry, 2011, rsc.org/periodictable/element/25/manganese.

[5] Siebe C., Herre A., Cram S., Ramos-Arroyo Y.R., Riojas-Rodríguez H. "Manganese mobilization from quarries and tailings in four watersheds of the Molango Mining District, Mexico", Water-Rock Interaction, 2010, pp. 751-754.

[6] LaZerte BD, Burling K, "Manganese speciation in dilute waters of the Precambrian Shield", Canada Water Research, Vol. 24, 1990, pp. 1097–1101.

[7] Filipek LH, Nordstrom DK, Ficklin WH "Interaction of acid mine drainage with waters and sediments of West Squaw Creek in the West Shasta Mining District", California. Environmental Science & Technology, Vol. 21, 1987, pp. 388–396.

[8] Cherry DS, Currie RJ, Soucek DJ, Latimer HA, Trent GC, "An integrative assessment of a watershed impacted by abandoned mined land discharges", Environmental Pollution, Vol. 111, 2001, pp. 377–388.

[9] Heal KV, "Manganese and land-use in upland catchments in Scotland", Science of the Total Environment, Vol. 265, 2001, pp 169–179.

[10] Clement Associates, "Chemical, Physical and Biological Properties of Compounds Present at Hazardous Waste Sites", Prepared for U.S. EPA, Washington, D.C, 1985, pp. 312.

[11] Švec, P., Kováčik, J., Hedbavný, J., Babula, P., Rotková, G., & Klejdus, B., "Impact of Anions, Cations, and pH on Manganese Accumulation and Toxicity in the Green Alga Scenedesmus quadricauda", Water, Air, & Soil Pollution, Vol. 227, 2016, pp. 161.

[12] Gutiérrez-Ruiz Margarita, "Estudio Ambiental del Distrito Manganesífero de Molango, Hidalgo, México", Laboratorio de Biogeoquímica Ambiental, Facultad de Química, Universidad Nacional Autónoma de México, 2016.

[13] Barceló I, Solís H, González C, Bussy A, Ávila P, García J, "Determinación experimental de las especies de Fe, Mn y Cu en el agua de la presa J. A. Alzate, Edo. de México", Revista de la Sociedad Química de México, Vol. 43, 1999, pp. 43-49.

[14] Lide DR, ed., "CRC handbook of chemistry and physics", Boca Raton, FL, CRC Press, 1993.

[15] HSDB, "Hazardous substances data bank. Bethesda", National Institute of Health, National Library of Medicine, 1998.

[16] Arenas-Islas, D., "Análisis Tafonómico de rocas siliciclásticas del sinemuriano superior (Jurásico Inferior), en la Formación Huayacocotla, centro oriente de México: Hidalgo, México", Universidad Autónoma del estado de Hidalgo, Tesis de Maestría en Ciencias, 2012.

[17] Crerar, D. A,. "Geology and Geochemistry of Manganese", General Problems, Mineralogy, Geochemistry, Methods, Akadémiai Kiadó, Budapest, Vol. 1, 1980, pp. 293-334.

[18] Santos-Burgoa, C., Rios, C., Mercado, L. A., Arechiga-Serrano, R., Cano-Valle, F., Eden-Wynter, R. A., Montes, S., "Exposure to manganese: health effects on the general population, a pilot study in central Mexico." Environmental Research, Vol. 85, 2001, pp. 90-104.

[19] Jazcilevich A., Siebe C., Wellens A., Rojas I., Cortez M., "Finding sources of airborne manganese (Mn) in the Mining district of Molango, Mexico", Ponencia International Forum EcoHealth, 2008.

[20] Reimer PS, "Environmental effects of manganese and proposed freshwater guidelines to protect aquatic life in British Columbia [MSc thesis]", Vancouver, B.C., University of British Columbia, 1999.

GEOCHEMICAL TRENDS OF ARSENIC AND IRON IN A SMALL RESERVOIR THAT RECEIVES MINE DRAINAGE

Bravo América [1], Ramos Yann [1], Torres Esther [2], and Ayora Carlos [2]
[1]University of Guanajuato, Mexico, [2]Environmental Diagnostic Institute Water Studies CSIC, Spain.

ABSTRACT

This investigation is focused on detecting the spatial variability in chemical composition of sediments in a former reservoir that receives alkaline mine drainages since 1789. The reservoir has an original capacity of 500,000 cubic meters (m^3), great part of this volume (90 to 95 %) is occupied by terrigenous and chemical sediments. This reservoir is shallow, with a maximum depth of 5 m. In the water column a gradient in redox conditions is developed: at depth the aqueous concentration of ferrous, sulfur and manganese are higher than at the surface.

Four sediment samples were collected considering a longitudinal redox transect: near to the entrance predominantly oxidant conditions and at the curtain dam more reductantly. A sequential extraction methodology was adapted in order to know the distribution of arsenic and iron in the fractions: exchangeable-carbonates, oxides, oxidable (organic matter and sulphides) and residual as well.

Contents of arsenic and iron increases along the transect, suggesting a physical migration of suspended particles which it sediments at the barrier of the dam. Fraction associated to exchangeable-carbonates and sulphides phases increases from the entrance of the dam, suggesting a precipitation of arsenic and iron as pyrite and arsenopyrite. In contrary concentrations associated to oxides decreases.

Keywords: Redox Transect, Guanajuato, Alkaline Mine Drainage Sulphate-Reduction.

INTRODUCTION

Population water supply of good quality is essential for a healthy and correct social development. Mining activities, specifically waste disposal that produces mine drainages generates considerable pollution to water bodies that are subsequently used for human consumption. The extraction of ores and deposit of wastes facilitates the arrival of potentially toxic elements (PTE) to the sources of supply [1]. These PTE are transported as dissolved species or associated with suspended particles. PTE transforms depending on the geochemical conditions when species are into the mass water inside the dam. Redox gradients are developed inside the dam.

The dams are an ideal trap for the accumulation of sediments, which contains PTE associated to different mineralogical species [2]. Depending on the pH and redox conditions, the sediments act as a source or sink for PTEs [3]. The properties of the sediments provide information about the type of drainage that circulates in the feed channel. In the case of mine drainages, the periods of maximum release of PTE can be reflected, as well as the risks associated with the reception of water with these characteristics [4].

The main conditions that favor As are: redox potential and pH, as well as the underlying geology. In reducing conditions and with alkaline pH, its mobility and availability will increase.

MATERIALS AND METHODS

Study area

The Santana dam is located at the northwest of the city of Guanajuato, Mexico (Fig. 1). This reservoir receives the spills from the upstream dams Esperanza and Soledad when exceeds the storage volume. When was constructed in 1789, Santana dam had a storage capacity of 350,000 m^3. Currently this capacity is diminished due to terrigenous sediment transportation and accumulation, and secondary minerals precipitation as well. In a previous study the spatial and temporal variability on mass water chemistry was described from December 2014 to November 2015. Such work suggested that a sulphate-reduction process can be occurring. Arsenic is seen in higher concentration at inlet and at depth, the possible reason for this is the liberation from oxides under reductal conditions. The anion dominant is sulphate (average 219mg/L), electrical conductivity 665µS/cm, and pH 8.56 [5].

Fig 1 Study area. Santana dam

Sampling

The sampling strategy considers the longitudinal transect which shows redox gradient. As an illustration, sites of collected samples are showed in Fig. 1 and Table 1: EPB (before the entrance to the dam), L8 (entrance), L7 (oxic environment), L3 (reducing environment due to great of organic matter content, accord to Table 2).

Sequential Extractions

The sequential extractions provide information about elemental content in each mineralogical fractions and his potential mobility. This technique is based on the use consecutive of solutions of different degree of aggressiveness [6]. Collected samples were submitted to a modified protocol [7].

The concentration of Fe in the sediment samples were measured by Inductively Coupled Plasma Atomic Emission Spectrometry (ICP-AES). Arsenic was determined by Inductively Coupled Plasma Atomic Mass Spectroscopy (ICP-MS).

Table 1 Importance of sites where sediments samples were collected

Site	Prof [m]	Importance
L3	5.88	Deepest area of the dam. Reducted environment.
L7	2.11	Oxygen environment. Increment in the accumulation of sediments.
L8	1.5	Predominance of oxygenate environment. Entrance of the dam.
EPB	0.3	Before the dam, in the dry season mostly water from the mine.

Table 2 Properties of sediments

Sample	Texture	% Organic matter
EPB	Sand	9.81
L8	Sand	8.7
L7	Slime-clayey	45
L3	Slime-clayey	60

RESULTS

According to the data in the quantitative analysis it is noticeable that the arsenic enters predominantly associated with crystalline oxides, however, there is an evident tendency to decrease in this fraction as it advances in the body of the dam. As shown in Fig. 2. The increase in the elemental content of As in the fraction of amorphous oxides is also relevant, which suggests that due to the conditions inside due to the difference of environments a translocation of the metalloid will be taking place. Following this trend, the same behavior is observed in the exchangeable fraction and sulfides. Being a very small body, with little storage capacity, the reducing environment at point L3 is not related to the depth of the site, but rather due to the high oxygen consumption generated by the presence of organic matter (Table 2). Its elemental charge is practically constant, however, there is a greater presence at point L3.

In the case of iron (Fig. 3), an increase in the total concentration of this metal is observed in the samples collected along the transect (EPB <L8 <L7 <L3). This suggests that at point L3 exist geochemical conditions that give rise to a deposit (accumulation), originating a greater concentration and conditions that favor their presence and mobility.

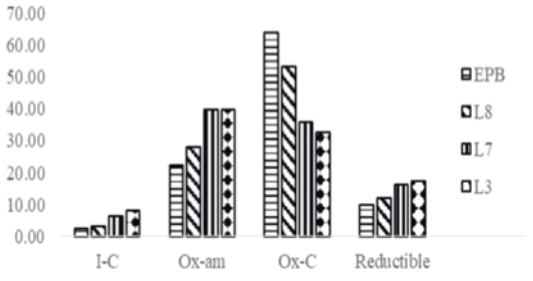

Fig. 2 Fractions of arsenic element, sediment samples

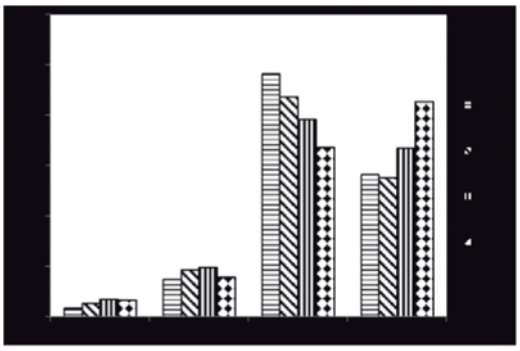

Fig. 3 Fractions of iron element, sediment samples

CONCLUSIONS

Thanks to the technical sequential extractions it was possible to determine trends and patterns in the mobility of the arsenic metalloid. This element enters the mass water as a particulate form associated with crystalline oxides, then relates preferably to the amorphous oxides and the exchangeable fraction. . The distinction between amorphous and crystalline oxides is important, because is in these phases where As is adsorbed and concentrated preferentially. The total concentrations of As are practically constant, unlike the point L3 where its presence is very high, while Fe in sediments increases from the entrance to the curtain of the dam. This suggests a mobility by migration associated with the suspended particles. The analysis of the sediments raises_scenarios of antiquity and behavior of the chemical species that are found in the solid matrix contained in the dam.

ACKNOWLEDGEMENTS

We appreciate greatly the support of: Universidad de Guanajuato, Environmental Diagnostic Institute Water Studies CSIC CSIC-IDAEA, Barcelona, Spain, and CONACYT.

REFERENCES

[1] Nordstrom, D.K., (2011) Hydrogeochemical processes governing the origin, transport and fate of major and trace elements from mine wastes and mineralized rock to surface waters. Applied Geochemistry 26, 1777-1791.

[2] Smedley, P.L., Kinniburgh, D.G., Macdonald, D.M.J., Nicolli, H.B., Barros, A.J., Tullio, J.O., Pearce, J. M. y Alonso, M.S., (2005). Arsenic associations in sediments from the loess aquifer of la Pampa, Argentina. Applied Geochemistry, 20, 989-1016.

[3] Hansen, A.M. (2012) Lake sediment cores as indicators of historical metal(oid) accumulation – A case study in Mexico. Applied Geochemistry 27, 1745-1752.

[4] Varol, M., (2013) Dissolved heavy metal concentrations of the Kralkizi, Dicle and Batman dam reservoirs in the Tigris River basin, Turkey, Chemosphere 93, 954-962.

[5] Bravo-Covarrubias A, Cano-Rodríguez I, Jofre-Melendez R, Gutiérrez-Valtierra M, Ramos-Arroyo Y "Mass balances in a dam that receives mine drainage", P. Earth and Planetary Science 17 (2017) 710 – 713.

[6] Rao, C.R.M., Sahuquillo, A., Lopez Sanchez, J.F. (2008). A review of the different methods applied in environmental geochemistry for single and sequential extraction of trace elements in soils and related materials. Water, Air & Soil Pollution, 189, 291-333.

[7] Torres-Sánchez, E. y Auleda, M., (2013). A sequential extraction procedure for sediments affected by mine drainage. J. Geochem. Expl. 128, 35-41.

DIATOMS IN MARINE SEDIMENTS CONTAMINATED BY POTENTIALLY TOXIC ELEMENTS FROM MINING ACTIVITIES

Martínez Yuriko Jocselin [1], Marmolejo-Rodríguez Ana J. [1] and Siqueiros Beltrones David A. [1]
[1]Centro Interdisciplinario de Ciencias Marinas, Instituto Politécnico Nacional, La Paz, BCS, México

ABSTRACT

Santa Rosalía is located to the northeast of the Baja California Sur, were a copper ore mine was exploited. Mining activities were closed in 1984 and returned in 2014. The wastes were discharged into the Gulf of California, however, eventually they back by currents to the beaches of this town. The objective of this study were 1) to determine the contents of potentially toxic elements (PTE) in beaches and harbor sediments of Santa Rosalía in 2016, 2) to compare their contents of PTE with respect to previous studies, 3) to analyze the assemblages of benthic diatoms. Results show average concentrations (mg kg^{-1}) that exceed the reference values for the earth's crust for Cu (3193), Zn (2393), Co (307), Pb (191), Cd (42) U (40). Species richness of live benthic diatoms appeared normal, and although they show deformities, these are not signifcant. It cannot be concluded if the mining wastes are unfavorable to the adjacent biota. Sediment obtained (2016) are equally concentrated than in previous studies, despite the reactivation of mining activities. Those contents exceed the mid-range effect (MRE) of sediments toxicity, which would be harmful to organisms in the area.

Keywords: Marine sediment, Metals, Contamination, Diatoms.

INTRODUCTION

Several studies have been conducted on marine sediments off Santa Rosalía, BCS, Mexico in different years, to evaluate the pollution that has, derived from mining waste [4]. Consequently, the beaches of Santa Rosalia have been assessed as contaminated [1].

In marine sediments different organisms live that could be affected by pollution, an example of these are benthic diatoms; microalgae that live in sediments, on seaweed and rocks. These organisms respond readily to disturbances in the environment. Therefore, the objective is to evaluate the PTE and determine the composition of diatom species in sediments.

MATERIALS AND METHODS

Sediment samples were collected during May 2015, January, and March 2016 from the port and north beach of Santa Rosalia, BCS. Five strategic sites were chosen in the port area. The collected sediments were oxidized, following the technique proposed for diatom cleaning and mounting [3]. Mounted diatoms were examined under an Olympus CH-2 microscope at 650× and 1000 ×. The pulverized sediment samples were analyzed with, acid digestion including HF, HClO4, HNO3 and HCl. The determination of the PTE was done with an inductively coupled mass spectrometer (ICP – MS). Certified reference standards (PACS-2 and MESS-3) of marine sediment were used for the validation of the technique.

RESULTS AND DISCUSSION

Overall 188 taxa were recorded within 61 genera. The most common diatom genera were *Psammodictyon, Navicula, Achnanthes, Halamphora, Stauroneis* and *Amphora.* The recorded species richness per sample was between 15 and 40 taxa, a common richness for diatoms (Fig. 1).

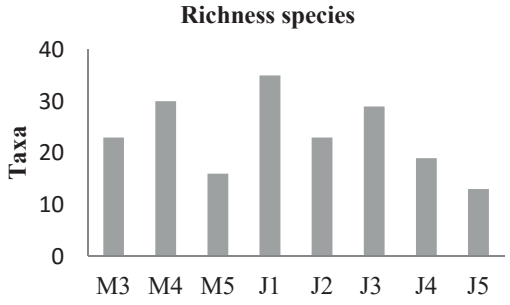

Fig. 1 Enrichment species diatoms in sediments. M=May, and J =January, # site

Results show concentrations (mg kg^{-1}) that exceed the reference values for the earth's crust [5]. And the toxicity criteria [2] Effect range low (ERL) and effect range medium (ERM). The elements concentrations of the sampling are equally concentrated than in previous studies despite the reactivation of mining activities (Table 1).

Table 1 Average concentration (mg kg^{-1}) of PTE

PTE	(This study) * 2015, 2016	[4] *2006	[5] **	[2] ** ERM
Cd	42.31	1.6	0.1	9.6
Cr	64.57	n.d.	35	370
Mn	8 071	31 500	527	n.d
Zn	2393	3500	52	410
As	8.98	n.d.	2	70
Ba	2 507	n.d.	668	n.d
Cu	3 193	3 940	14.3	270
Sr	2 410	n.d.	316	n.d
Pb	191.30	200	17	218
U	40.65	n.d.	2	n.d

*Sampling date, ** reference values, n.d. = no determinated

CONCLUSIONS

The sediments showed a composition of diatom species similar to uncontaminated environments and richness values similar to other environments. 10% of Diatoms show deformities of their valves. The EPT values have remained high since 2006 to date, therefore the sediments remain contaminated.

ACKNOWLEDGEMENTS

SIP 2016 0972 Geochemistry of major and trace elements in sediment influenced with ore mines. Alberto López Fuerte and Alejandro Aldana Moreno aided in field work.

REFERENCES

[1] Jonathan, M.P., E. Shumilin, , M.G. Rodríguez-Figueroa, P.F. Rodríguez-Espinoza, S.B. P. Sujitha. 2016. Potential toxicity of chemical elements in beach sediments near Santa Rosalía copper mine, Baja California Peninsula, Mexico. Estuarine, Coastal and Shelf Science. 180. 91-96.

[2] Long, E. R., D. D. Macdonald, S. L. Smith & F. D. Calder, 1995. Incidence of adverse biological effects within ranges of chemical concentrations in marine and estuarine sediments. Environmental Management 19:81-97.

[3] Siqueiros-Beltrones D. A. & D.Votolina. 2000. Grazing selectivity of red abalone (Haliotis rufescens) post-larvae on benthic diatom films under culture conditios. Journal World Aquatic Society. 31(2): 239-426.

[4] Shumilin, E, V. Gordeev, G. Rodríguez-Figueroa, L. Demina & K. Choumiline. 2011. Assessement of geochemical mobility of metals in surface sediments of the Santa Rosalía mining region, Western Gulf of California. Archives of Envirnomental Contamination and Toxicology, 60: 8-25.

[5] Wedepohl, K. h. 1995. The composition of the continental crust. Geochimica et Cosmochimica Acta 59:1217-1232.

MONITORED NATURAL ATTENUATION OF HEAVY METALS IN THE SONORA RIVER: THE WATER QUALITY

Ceniceros-Gómez Agueda E. [1], Gutiérrez Ruiz Margarita E. [1], Romero Francisco M. [2], Martínez-Jardines L. Gerardo [2] and Domínguez-Martínez Raquel [1]
[1]Faculty of Chemistry, [2]Geology Institute, Universidad Nacional Autónoma de México, México.

ABSTRACT

On August 6, 2014, approximately 40,000 m^3 of acidic solution from a hydrometallurgic process were released to the Tinajas stream (17.6 km), connected to the Bacanuchi and Sonora rivers in the state of Sonora, Mexico. The aims of this research is to elucidate the relevance of the role played by the industry for managing the spill, namely, the control of pH, the heavy metals ions and colloids removal, and secondly, estimate the importance of the natural phenomena involved. The following factors were considered: a) anthropogenic control measurements (construction of a barrier, lime neutralization of acidic solution and storage of the impacted materials in the tailings dam) b) heavy metal presence in sediments from natural sources and historical mining activities (Fe, Al, Si, Mn, Cu, Mn, Zn, As, Ni, Cd, Pb and Cr), c) extraordinary rainfalls linked with the Norberto and Odile hurricanes and d) natural attenuation processes related with pedogenic carbonates of sediments (pH increment and sorption).

The scientific results confirmed the successful synergy between nature and industrial actions but the public perception is still not in accordance, probably because the relationship between science, industry and society is weak and would be desirable to improve it.

Keywords: Natural Attenuation, Heavy metals, Water Quality, Sonora River

INTRODUCTION

On August 6, 2014, approximately 40.000 m^3 of acid solution containing ions and colloids of potentially toxic elements (ferro-Copper acid solution) were spilled, to “Las Tinajas” stream located on the municipality of Cananea, Sonora. The solution or acid liquor was stored in Las Tinajas dam, which is located in the facilities of the company Buenavista del Cobre (BVC) [1].

The acid liquor is the product of the copper leaching process and conforms the raw material of the solvent extraction process.

The chemical composition of the acid solution was determined by the CONAGUA on August 8, 2014. The main components identified and quantified were iron (Fe), aluminium (Al), copper (Cu) and Manganese (Mn). The rest of the detected elements present lower concentrations (Table 1). It is important to note that the concentrations of barium (Ba), antimony (Sb) and mercury (Hg) were lower than the limit of detection of the analysis technique and, even, to the permissible limits of water quality established by NOM-127-SSA1-1994 (Table 1).

According to information from the Secretaria del Medio Ambiente (SEMARNAT), the spill reached the following bodies of surface water: “Las Tinajas” stream (17.6 km), the Bacanuchi river (64 km) and the Sonora river (190 km); which, belong to the Sonora River basin.

The most important surface currents are the Sonora, San Miguel, El Zanjón and La Junta streams, which drain into the Ing. Rodolfo Félix Valdez (El Molinito) and Abelardo Rodríguez Luján dams.

Table 1 Chemical composition of the 40,000 m^3 spill of ferro-copper acidic solution from the "Tinajas 1" dam

Element	Concentration (mg/L)
Fe	1080
Al	461
Cu	114
Mn	98
Zn	51
As	43
Ni	1
Cd	7.8
Pb	2.5
Cr	1.5

STUDY AREA

The study area is constituted by the sub-basins of the Sonora River: 9Dd (Bacanuchi River), 9Dc (Sonora-Arizpe River) and 9Db (Sonora-Banámichi

River) that are part of the Sonora River Basin. There are in the northern and north-central portion of the state of Sonora. The zone partially covers the villages of Bacanuchi, Arizpe, San Felipe de Jesus, Sinoquipe, Banámichi, Huepac, Aconchi, Baviocora, Mazocahui and Ures.

The climate of the study area is predominantly dry and semi-dry with rainfall in summer. The annual rainfall varies between 513.9 and 338.2 mm, for a period of 32 years (1982-2013). According to the monthly data of the National Meteorological Service (SMN), the highest values of rain are registered in the months of July (125-145 mm) and August (102-110 mm). In the month of September, rainfall decreases to values between 45 and 55 mm. However, in 2014, anomalous values were recorded. Specifically, extraordinary rains occurred on September 5 to 9 due to Hurricane Norberto and from 17 to 18 due to Hurricane Odile. In September 2014, the meteorological stations of Cananea, Bacanuchi, Arizpe and Oregano recorded cumulative rainfall in mm of 232.0, 147.7 and 232.3, respectively.

GEOLOGY

The Sonora-Arizpe sub-basin, which is located in the north-central part of the Sonora River basin, was formed 25 million years ago and has been widely studied from the geological point of view [2].

Its volcanic and sedimentary fill of ~ 2.1 km thick, which dips towards the east, is assigned to the Báucarit formation. The most important mountain ranges that delimit the basin of the Sonora river are: (i) On the west flank from south to north: The Aconchi mountain range, the Locos mountain range, San Antonio mountain range, Los Azulitos mountain range and Elenita mountain range. (ii) On the east flank and from south to north: La Sierra Pinta, Sierra Las Palomas and Sierra Manzanal.

The mountain ranges of both flanks are characterized for containing numerous mineralizations of diverse types: copper porphyries, veins, skarns and epithermal systems. These deposits produce or have produced at different times economic mineralizations of: Cu, Mo, W, Pb, Zn, Au and Ag.

SEDIMENT GEOCHEMISTRY

The Mexican Geological Survey (SGM 1996 - 2000) conducted between 1996 and 2000 [3], analyzes of approximately 3,625 samples of stream sediments. The descriptive statistics of the geochemical data of the sediments of the Sonora River Basin are presented in Table 2. The results indicate that the total concentrations of the metals in the sediments decrease in the following order: Fe> Al> Mn> Zn> Cr ~ Cu> Pb> As ~ Ni> Sb> Cd, which is congruent with the concentrations of these elements in the rocks of this region [2].

Table 2 Mean, maximum and minimum values of metal concentrations in stream sediment samples in the Sonora river basin and surrounding areas (n = 3.625). (SGM 1996-2000)

Element (unit)	Mean	Minimum	Maximium
Fe (% wt)	3.65	0.89	18.33
Al (%wt)	2.41	0.26	6.58
Mn (mg/kg)	661.7	46	5319
Ba (mg(kg)	216.24	24	1436
Zn (mg/kg)	95.7	13	3502
Cr (mg(kg)	59.5	1	547
Cu (mg/kg)	54	1	6471
Pb (mg/kg)	47.7	2	17612
As (mg/kg)	18.4	0.32	2092
Ni (mg/kg)	14.8	0.9	838
Sb (mg/kg)	2.97	0.2	221
Cd (mg/kg)	0.88	0.04	61.6

Table 3 Chemical composition (% wt) of the rocks around Arizpe [1]

Rock Types	SiO_2	Al_2O_3	Fe_2O_3	MgO
El Toro Muerto Basalto (lower part)	51.9	16.59	9.78	4.24
El Toro Muerto Basalto (upper part)	51.37	17.33	8.66	3.51
Agua Caliente Basalto	53.08	15.61	8.52	2.79

ACTIVITIES CARRIED OUT IN THE EMERGENCY

In response to this environmental emergency BVC company carried out the following activities:

1) For the containment of the spilled solution, a containment board of 120 m in length, 80 m in width and 15 m in height was built over the bed of the Tinajas stream, approximately 8 km "downstream" from the spill point. Additionally, 250 tons of lime gravel was applied at different points of the Tinajas stream and the Bacanuchi river, as well as 30,000 L of lime slurry that was applied "downstream" of the containment board.

2) Extraction of 2,366,000 liters of the spilled solution contained in the containment board. The extracted solution was stored in dams within the company's facilities.

3) "Emergency cleaning" of the sediments visibly affected, in the bed of the water bodies through which the spilled solution flowed. A total of 6,096 m3 of visibly impacted sediments were collected and deposited in the accesses of the tailings dam of BVC company.

METHODOLOGY AND DATA GENERATED FROM THE SPILL

To evaluate the temporal and spatial evolution of the impact in the abiotic environment of the spill, the data generated between August 8 and October 21, 2014, by certified laboratories that have made periodic sampling and analysis of surface and groundwater, soil and sediments were analysed.

The location of the sampling sites is presented in Fig. 1 [1].

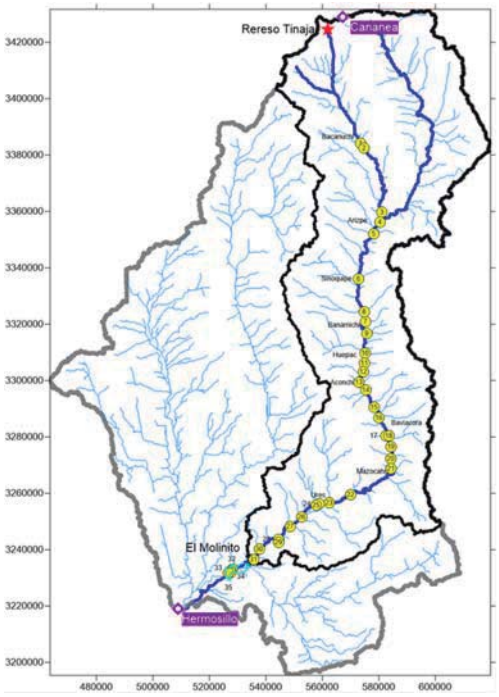

Fig. 1 Map indicating the location of sample sites

RESULTS AND DISCUSSION

The pH values in the surface water samples indicate that only in the first 8 days after the spill, acid values (pH = 2.6 - 3.7) were recorded in the upper-middle part of the sample basin. In the medium-low and low parts no significant pH change was observed, since throughout the contingency period it varied from slightly acidic to slightly basic (5.9 - 8.4). Since August 15, the surface water of the entire basin had already been neutralized, by the action of basic materials present naturally in water bodies, mainly soluble bicarbonates and carbonates; the addition of lime made by the company and the dilution produced by the heavy rains that occurred at that time.

About three months after the spill (October 21, 2014), the total concentrations of the metals analyzed in all surface and groundwater samples, except Al, Fe and Mn that form colloids, were less than permissible limits for water for human consumption [4]. The extraordinary rains from September 5 to 9 and from September 17 to 18, generated by hurricanes Odile and Norberto, respectively, generated a great dilution in the bodies of water of the Sonora river basin, the rapid increase in pH favored the precipitation of the metals that were deposited in the sediments (Fig. 2).

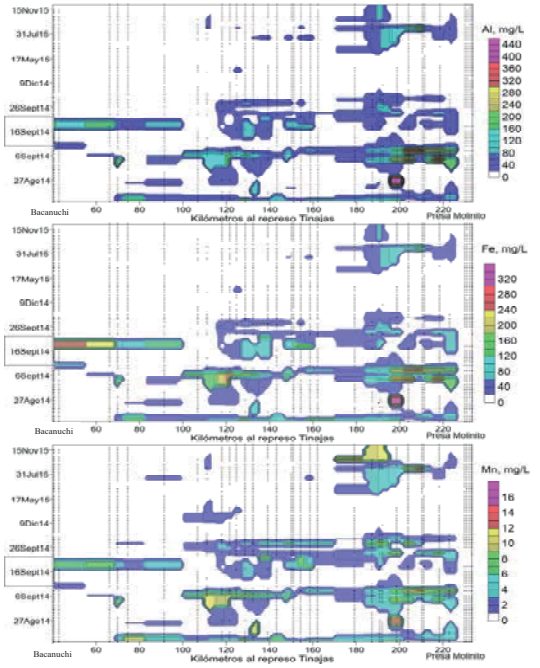

Fig. 2 Behavior of total surface water concentrations of metals associated with the spill. NOTE: The "Y" axis shows dates of the surface water sampling. On the "X" axis, the distance of the sampling sites from the Tinajas dam

However, the presence of Al, Fe and Mn in the superficial and underground bodies of water in concentrations above the limits for water for human consumption, which were determined 3 months after the spill, is a phenomenon related to the abundant sources natural elements of these elements. The main evidences of the natural origin of Fe, Al and Mn in the surface water are: a) the soils, sediments

and rocks of the region contain them in important concentrations (Tables 2 and 3).

The total amounts in certain water of Al, Fe and Mn, as well as those of Ba, which is not present in the acid leach, are similar to those reported by the Universidad Autónoma de Sonora [4], for the groundwater of the sub-basins Sonora-Arizpe, Sonora-Banámichi and Sonora-Ures-Topahue are analogous to those reported by the same authors in the groundwater of the neighboring sub-basins [5].

The total concentrations of the metals associated with the spill in the sediments of the riverbeds and in the soil of the potentially affected area indicate that they fall within the range of background values (Fig. 3) [6].

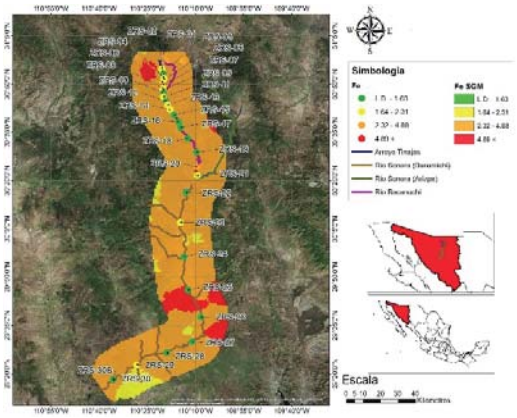

Fig. 3 Baseline for Fe concentration (%wt) in sediments of the area

The anomalies were also observed in the concentrations of major and minor elements of these metals in the sediments of the streams, reported by the Mexican Geological Survey, between 1996 and 2000.

CONCLUSIONS

The strong rainfall that occurred in the area was a determining factor for the rapid dispersion and dilution of the potentially toxic metals contained in the spilled acid solution.

In some areas of surface water bodies, the acidification of the water was observed only in the following 8 days after the accident, due to the dilution and dispersion of the rains and the retention and neutralization actions carried out by the mining company.

The presence of metals, except for Al, Fe and Mn, at 3 months their concentrations were lower than the limits indicated in NOM-127 for drinking water.

The concentrations of Al, Fe and Mn that exceed the limits for drinking water are similar to those reported for the bodies of water in the region before the accident. There is sufficient evidence to suggest that the presence of these metals is, for the most part, of natural origin and that they are found as colloids, although they could be soluble while the water was acidic.

The presence of potentially toxic metals (Fe, As, Mn, Pb and V) in some samples of sediments and soils in the middle of the basin, the area potentially affected by the spill, is strongly related to the natural anomalies identified on both sides. of the middle part of the basin, and / or with historical mining.

ACKNOWLEDGEMENTS

Authors thank Leticia Pérez Manzanera for her help doing maps and also to Reyna Roldan Armas and Karla Leiny López Hernández for their general assistance.

REFERENCES

[1] http://www.fideicomisoriosonora.gob.mx/docs/DPAAA%20INFORME%20DE%20RESULTADOS%20HASTA%20EL%2018092014%20v1.pdf.

[2] González-León CM, Valencia V, López M, Bellon H, Valencia Moreno MA, Calmus T, 2010, The Arizpe sub-basin: sedimentary and magmatic evolution of the Basin and Range in north-central Sonora, México: Revista Mexicana de Ciencias Geológicas, v. 27, p. 292-312.

[3] SGM (Servicio Geológico Mexicano), 1999 y 2006. Geoquímica de sedimentos de arroyo de las cartas (escala 1:50000) H12B54, H12B53, H12B52, H12B64, H12B63, H12B62, H12B74, H12B73, H12B72, H12B83, H12B82, H12D14, H12D13, H12D12, H12D23, H12D22, H12D32.

[4] Secretaría de Salud, 1999. Modificación a la Norma Oficial Mexicana NOM-127-SSA1-1994. Salud ambiental. Agua para uso y consumo humano. Límites permisibles de calidad y tratamientos a que debe someterse el agua para su potabilización.

[5] UNISON (Universidad de Sonora), 2005. Estudio geo-hidrológico de las sub-cuentas de los Ríos Sonora, Zanjón, San Miguel, Mesa del Seri–La victoria y Cuenca Bacoachi. Elaborado para la Comisión Estatal del Agua (CEA).

[6] SEMARNAT, 2007. Norma Oficial Mexicana NOM-147-SEMARNAT/SSA1-2004.

RETENTION OF METALS IN SECONDARY MINERALS IN SEDIMENTS OF A MINE DRAINAGE

Ramos Yann [1] and Ayora Carlos [2]
[1] Engineering Division, University of Guanajuato, Mexico; [2] IDÆA, CSIC, Spain

ABSTRACT

This paper presents an evaluation of the influence of secondary minerals in the quality of water that runs into La Esperanza basin (LEB) in Guanajuato, Mexico. Samples of mineral secondary phases that had formed in a deposit of mining residues were collected from which the mineralogy was determined and aqueous extracts were made to analyze certain elements. These secondary phases were observed in all of the water flowing into the basin and even more in the residues.

LEB contains a reservoir used for population water supply; it is divided into three sub-basins, one could have a risk of contamination. In this sub-basin, is possible find massive sulphides and a deposit of residues of 20,000 tons which liberates water with a pH less than 3 and high concentrations of sulfates (1,959 mg/L), iron (127 mg/L) and aluminum (140 mg/L). Minerals formed at the surface are alunogen, jarosite, hematite, goethite, syderotil, halotriquite, szomolnoquite, rozenite, and anhydrite.

Even though the percentage of the area of the sub-basin "El Durazno", is small (5.09%) of the total, a concentrated rain in this zone can not only wash away the salts accumulated but can cause problems changing the quality of the water in the reservoir.

Keywords: Guanajuato, Acid Mine Drainage, Washing of Secondary Minerals, Sulphides Oxidation

INTRODUCTION

Drinkable water should have minimal criteria of quality accord to official normativity. In the case of the supply to Guanajuato city, most of volume comes from extraction of groundwater from wells; nevertheless, 25% corresponds to reservoirs of surficial water.

La Esperanza basin (LEB) is located at north of Guanajuato city, in central Mexico (Fig. 1).

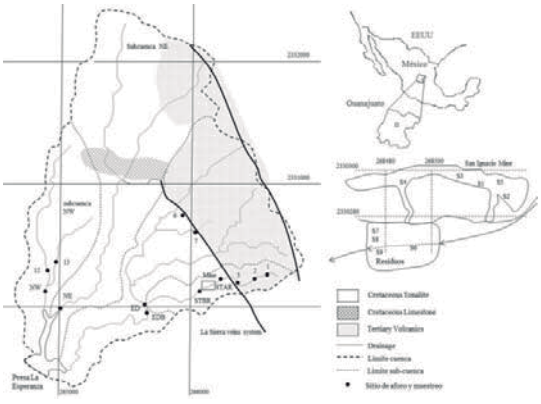

Fig. 1 Location of La Esperanza basin

Has an extension of 17.31 km^2, with an altitudinal gradient between 2,282 to 2,727 meters above sea level (masl). It is composed by three sub-basins: NW with 11.45% of total area, NE with 46.6 % and El Durazno (ED) with 41.9 % of total area. Climate is mild sub-humid with 85 % of rains during the summer, the average precipitation in last 100 years was of 880 mm with a wide variation, between 322 to 1,970 mm. Average temperature is 18º C with a range between 0 to 35 º C and an annual evaporation of 1,000 mm.

In 1890 the barrier of the "La Esperanza" reservoir was constructed to retain water for human consumption. Currently, the reservoir has a storage capacity of 910,000 m^3 with a daily extraction volume of 1,000 m^3 [1]. In the last 5 years, during the dry season (October to May) the reservoir had a volume equivalent to 20 % of his maximum capacity.

Lithology of LEB is diverse: the basement is composed by Jurassic rocks (diorite and tonalite) with minerals of low weathering rate as muscovite and quartz. Over these rocks, there are Tertiary volcanic rocks which main mineralogy is quartz and feldspar [2]. However, great extension of LEB (65 %) is cover by Cretaceous shales of Esperanza formation. In central zone of NE sub-basin outcrop limestones. There are two massive sulphides deposits emplaced at the shales. Particularly the "San Ignacio" mine in ED creek has a negative impact on water quality.

San Ignacio mine represents 1 million of tons of ore [3], was exploited 10 years ago and abandoned. Over the bank of ED creek, there is a deposit of mine wastes of 20,000 tons. At the surface of residues and near to the mine is possible to appreciate secondary minerals formation. Accumulation of these minerals (mainly sulfates) is

more appreciable during dry season and represents a risk factor due to a washing effect at the beginning of rainy season. This runoff produces local acidification by hydrolysis of iron and aluminum [4]. Other adverse effect is associated to the liberation of potentially toxic elements (PTE: Al, Cd and Cu). This effect of water quality affectation was documented in other mining districts around the world [5]-[6].

The objectives of this work are:

To identify the type of waters that drains over the basin analyzing main ions in representative samples and to describe the geochemical processes that control their composition.

To identify if exists affectation risks to water quality by dissolution of accumulated secondary phases.

METHODOLOGY

Sampling and quantification flow

Figure 1 A shows selected sites to quantify flow at the creeks and to collect water samples. Sites which samples were collected more than a one time was identified as the time series STAR and STBR over and under San Ignacio mine respectively. Other keys correspond to sites of sampling in the sub-basin NW, NE, ED and EDUM, for the point under El Durazno creek. Three sampling periods was developed in 2005 and 2006 and 33 water samples were collected. In January 2006 seven samples of secondary minerals were collected on the residues deposits of the San Ignacio mine. Flow was quantified at the channels by the volumetric method. When flows were greater than 1 l/s a flow-meter was used; for that, the channel was adapted for an appropriate dimension.

Each one of 33 collected samples was an aliquot of 1 L of a mix in a container of 20 l. Bottles used was of polyethylene, washed with HNO_3 to 10 % and two times with deionized water. Before the sampling, bottles were washed two times with the collected water. Field parameters as temperature, pH and electric conductivity were determined with an Oakton Waterproof 300 previously calibrated. Alkalinity was determined at field by volumetry with standardized 0.1 N sulfuric acid. For cations analyses 100 ml of each simple was filtrated with membranes of pore size of 0.45 μm and acidified with 1 ml of supra-pure concentrated nitric acid.

Chemical Analyses

Chlorides were quantified by volumetry (argentometry) and sulfates by turbidimetry. Cations (Al, Ca, Cd, Cu, Fe, K, Mg, Mn, Na, Si, and Zn) were analyzed by flame atomic absorption espectrophotometry at Guanajuato University. The values of water chemistry were interpreted and processed with AQUACHEM code (Waterloo Hydrogeologic) in order to describe water-rock interactions through Stiff and Piper diagrams.

PHREEQC code was used [7] to identify secondary phases that could be precipitate and to simulate mixing processes between different water types that drains over the basin. The database used for secondary minerals was complemented with previously reported data [8]-[9].

Solid samples were analyzed by X-ray Diffraction at Institute of Earth Sciences “Jaume Almera” in Barcelona, Spain. To this samples an aqueous extraction was applied, for that, 1 g of sample was dissolved with 60 ml of deionized water for 12 hours in polyethylene recipients. The resultant suspension was filtrated with Millipore membranes of 0.45 μm and the elements Al, Ca Cu, Fe, Mg, S and Zn were analyzed for ICP.

RESULTS

Hydrochemical trends

Measured pH values have a wide range of variation. The greater value, of 9.23, corresponds to the mass water of reservoir and the lower value, of 3.0, corresponds to mine wastes leachates. The greater values of electric conductivity (more than 2,000 μS/cm) correspond to samples of the time series over and under residues. It is related to the high sulfate concentrations, which has two possible origins: one is the sulphide oxidation (mainly pyrite) and other sulfates dissolution. Sulphides oxidation is favored by high porosity and the humidity of residues. Sulfates dissolution of the accumulated secondary minerals produces acidity by hydrolysis. Elevated iron concentrations of residues leachates (maximum values of 150.3 mg/L) and aluminum (maximum values of 183.7 mg/L), suggest that main source of acidity are dissolution and hydrolysis.

Concentrations of another metals as Cd, Cu y Zn are presents in higher concentrations at El Durazno creek and increase significantly in residue leachates, with maximum values of 0.8 mg/L for Cd, 20 mg/L for Cu and 68.1 for Zn. Accord Mexican Normativity, this values can have toxic effects.

The dominance of major ions are described and represented as type-waters trough Stiff diagrams in Fig. 2, for the samples collected in June 2005. All samples has a sulfated character, except for samples 1 and 2 which circulates over volcanic rocks having as dominant anion the bicarbonate. Figure 3 shows variation trough Stiff diagrams for four dates of the time series. When water circulates trough residues, diminish sodium and calcium concentrations and increase magnesium concentrations, this suggest that a cationic exchange process is present.

Fig. 2 Hydrochemical trends of LEB using Stiff Diagrams

Figure 3 shows the trends of waters trough a Piper diagram. Waters of El Durazno creek changes his condition from bicarbonate-sodic to sulphated-magnesic. Two samples in the mass water of reservoir has a condition of sulphated-magnesic, the other is sulphated-calcic. The character of mass water in the reservoir is a mix of the three different creeks and the sulphate reflects dominance of dissolution of secondary phases.

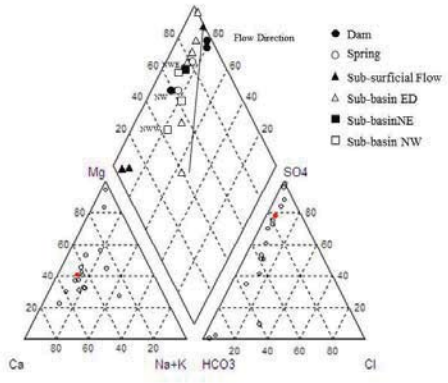

Fig. 3 Hydrochemical trends of water in June 2005

Secondary phases characterization

Five samples were collected at the interior of San Ignacio mine: one of the ore and four of secondary salts over the wall of the mine. Also, four samples were collected from mine waste deposits. These phases contain alunogen, $[Al_2(SO_4)_3{:}17H_2O]$; jarosite, $[KFe_3(OH)_6(SO_4)_2]$; hematite, (Fe_2O_3); goethite, $[FeO(OH)]$; siderotil, $[FeSO_4{:}5H_2O]$; halotriquite, $FeAl_2(SO_4)_4{:}22H_2O$; szomolnoquite, $FeSO_4{:}H_2O$, rozenite, $FeSO_4{:}4H_2O$ and anhidrite ($CaSO_4$).

The pH of aqueous extracts is acid (variation from 2.42 to 3.93) due to hydrolysis of aluminum and iron. Sulphate has concentrations between 1.6 to 423.4 mg/g; aluminum from 0.04 to 52.7 mg/g, copper from 0.01 to 55.4 mg/g and iron from 0.01 to 134.4 mg/g. Dissolution of these phases is responsible of acid pH.

CONCLUSIONS

Waters that enter to reservoir La Esperanza can represent a risk of cadmium pollution, iron and aluminum precipitates along the channel and seems that exist a natural attenuation processes related with oxides precipitation and neutralization of acidity.

Waters are sulfated due to accumulation of secondary minerals along the channel and mainly by the presence of mine wastes deposit of massive sulphides that liberates acidity and metals in solution.

Percentage of the basin which mine wastes is located represents only 5 % of total and in “normal” conditions a dilution of waters running from other sub-basins maintains good water quality. However in an extreme situation of a localized rain, a potential water affectation in quality is possible.

ACKNOWLEDGEMENTS

To the PROMEP Project “Caracterización geoquímica de suelos de la Cuenca del rio Guanajuato y su influencia en ñla calidad de las aguas superficiales y subterráneas” for economical support. To technical crew of Jaume Almera Institue by the support with mineralogical and chemical analyses.

REFERENCES

[1] SIMAPAG, 2006. Informe sobre el balance de la disponibilidad de agua potable para el Municipio de Guanajuato.

[2] Martínez-Reyes J, Mapa geológico de la Sierra de Guanajuato, escala 1:100,000, México, D.F., México, Instituto de Geología Universidad Nacional Autonóma de Mexico, 1992.

[3] Miranda-Gasca M, “The metallic ore-deposits of the Guerrero Terrane, western Mexico: an overview”, J. of South American Earth Sciences, Vol 13, 2000, pp- 403-413.

[4] Nordstrom D, Alpers C, 1999. Geochemistry of acid mine waters. In: Plumlee, G.S., Logson, M.J. (Eds.), The Environmental Geochemistry of Mineral Deposits, Rev. Econ. Geology, Vol. 6A. Soc. Econ. Geol. Inc., Littleton, pp. 33-160.

[5] Hammarstrom J, Seal R., Meier A, Kornfeld J, “Secondary sulfate minerals associated with acid drainage in the eastern US: recycling of

metals and acidity in surficial environments", Chemical Geology, 215, 2005, pp. 407-431.

[6] Olías M, Cánovas C, Nieto J, Sarmiento A, "Evaluation of the disolved contaminant load transported by the Tinto and Odiel rivers (South West Spain)" Applied Geochemistry, Vol 21, 2006, pp. 1733-1749.

[7] Parkhurst, D.L., Appelo, C.A.J., 1999. User´s guide to PHREEQC (version 2) a computer program for speciation, batch-reaction, one-dimensional transport, and inverse geochemical calculations. U.S. Department of the Interior, U.S. Geological Survey, Denver, Co., 326 pp.

[8] Hemingway B, Seal R, Chou I, "Thermodynamic data for modeling acid mine drainage problems: compilation and estimation of data for selected soluble iron-sulfate minerals", United States Geological Survey Open File Report 02-161, 2002.

[9] Tosca J, McLennan M, Clark C., Grotzinger J, Hurowitz A, Knoll H, Schröder C, Squayres W, "Geochemical modeling of evaporation processes on Mars: Insight from sedimentary record at Meridiani Planum", Earth and Planetary Science Letters, Vol 240, 2005, pp.122-148.

EVOLUTION OF THE QUALITY OF THE SEDIMENTS OF THE TODOS OS SANTOS BAY: ROLE OF BIOGEOCHEMICAL CONDITIONS AND ACTIONS OF MAIN STAKEHOLDERS

Tavares Tania M.[1,2], Silva Sonilda, M.T.[1], Oliva Sergio T.[1], Sant'Anna Jr[1], Nilson Lockwood David[1], Gutierrez-Ruiz Margarita[3], Queiróz-Vivanco Daniel[3] and Aguirre-Gomes Arturo[4]

[1] Chemistry Institute, Federal University of Bahia, Brazil, [2] School of Medicine, Federal University of Bahia, Brazil, [3]School of Chemistry, National Autonomous University of Mexico (UNAM), Mexico, [4]FES-Cuautitlán, National Autonomous University of Mexico (UNAM), Mexico

ABSTRACT

The Todos os Santos Bay is the second largest bay on the Brazilian coast. Its northeast shore is home to active oil processing, metallurgical and other activities, including a petrochemical complex. Salvador, capital of Bahia state, is on the peninsula that separates the bay from the Atlantic. The bay is shallow with an area-weighted depth of 9.8 meters. Mud occurs predominantly in the north and northeast of the bay and tends to adsorb inorganic and organic pollutants emitted by urban and industrial activities, transferring them to local seafood and to its consumers, primarily local fishermen of low socioeconomic status. In Brazil, environmental governance considers social, economic and environmental aspects in its decision making. Besides having Departments of the Environment at the state level, and a Federal Agency for the Environment, the country has a Brazilian Government Agency for Law Enforcement and Prosecution (MP, acronym in Portuguese), which is very active in the management and protection of the environment. This article will present the case study of Maré Island, where several industries had the intention of expanding the Aratú Port, creating a conflict with the local population and with the MP. Several technical studies were carried out and will be discussed.

Keywords: Industries, Contaminants, Health, Regulations, Case study

INTRODUCTION

The surface sediments of the Todos os Santos Bay (TSB) has a history of environmental quality to tell. Most of the surface sediment of this 1000 km^2 bay (the second largest coastal indentation of the Brazilian coast) is composed of mud or a sand/mud mixture. Only a small area of regressive fluvial sand can be found in the northeast of the bay and transgressive carbonate marine sand can be found at the entrance of the bay, in the south [1]. Industrial activities operate at the north and northeast of the bay which is the area of lowest energy, with surface sediments dominated by regressive bay mud. Fine grained sediments are efficient as adsorbents of several chemical substances, both inorganic and organic, and become a useful archive of the temporal evolution of pollutant inputs. Moreover, this muddy substrate presents high productivity of biota, mainly of mollusks and crustaceans, which serves as a source of income and the main food supply for artisanal fishermen. Several metals and toxic organic compounds are bioaccumulated and biomagnified along the food chain and, when consumed by humans, may cause harmful effects on their health.

The Portuguese colonization in Brazil was initiated around the Bay of All Saints, called Recôncavo. At its entrance, the first capital of the country was founded in 1549, Salvador, today with more than 2,5 million inhabitants. For 400 years, agropastoral activities dominated in their surroundings, particularly sugarcane. During the mid-twentieth century, crude oil was discovered for the first time in Brazil, resulting in rapid industrial growth. Today the TSB is home to an oil refinery, the largest petrochemical complex in the Southern Hemisphere, an industrial center with a major focus on the metallurgical and finished products industry, as well as animal, terrestrial and aquatic farming. Conflicts resulting from environmental deterioration are expected, with traditional communities being most affected, particularly artisanal fisheries.

Among the most impaired communities is the island of Maré, the second largest of the TSB. It is the closest island to the city of Salvador (14 nautical miles) located northeast of the TSB (Fig. 1). To the northwest of the island is the Landulfo Alves refinery (RLAM, acronym in Portuguese), with its port for inbound and outbound transport; to the northeast, the Aratu -Candeias Industrial Center (CIA, acronym in Portuguese), and to the east four ports, one belonging to the Brazilian Navy (ship repair), one for inbound

and outbound transport for the car industry, and two ports for inbound transport of raw materials and outbound transport of the products of the industrial center (Aratú-Candeias port) and of the Petrochemical Complex of Camaçari, which includes storage and loading of volatile organic compounds (Fig. 1). According to the last census of 2010, the population of Maré Island is 6,434, distributed in an area of 13.79 km^2, which results in a population density of 384.80 residents/km^2, distributed among several villages along the coast of the island. Sanitary drainage is done through septic tanks. The population earns their living by fishing, making and selling handcrafts (straw products and lace) and artisanal production of banana candy. Many residents work in the north part of Salvador and in other nearby towns and industrial areas on the mainland coast. Diesel-powered boats are used to transport residents and visitors.

Fig. 1 Main industrial activities around the Todos os Santos Bay, Bahia, Brazil

Brazil has a very good legal framework for environmental protection. Environmental governance considers social, economic and environmental aspects in its decision making. Besides having Departments of the Environment at the state level, and a Federal Agency for the Environment, the country has a Brazilian Government Agency for Law Enforcement and Prosecution (MP, acronym in Portuguese), which is independent and very active in the management and protection of the environment.

The aim of this work is to report the case study of Maré Island, where several industries, both from the Petrochemical Complex and the CIA have requested a license to expand the Aratú Port, creating a conflict with the local population and the local authorities.

METHODOLOGY

In December of 2016, the Department of Health of the State of Bahia, promoted a public presentation, with open discussions, of the Report of Quantitative Analysis of Risk to Human Health (AqR, acronym in Portuguese) [2] in Maré Island and its surroundings elaborated by the firm CETREL, and invited all local universities and colleges, as well as research groups and institutions dealing with the environment and health in the Recôncavo of Bahia and selected institutions in other states of Brazil. The idea was to get technical opinions from independent scientists on the study which had been undertaken.

The reason for this call to the scientific community was the disagreement between the results of previous studies, done by different academic researchers, the reports of the population of Maré Island and the results expected of the CETREL study.

In view of the numerous questions and discussions that took place after the presentation by CETREL, the Department of Health of the State of Bahia requested to the MP to obtain copies of other CETREL reports which were part of the group of studies which had been paid for by the industries, all references cited in the AqR report, which were not publicly available, as well as the copies of the reports of the chemical analyses of each sample of the AqR report which were done in different laboratories, including in labs abroad. It took a few months before the Department of Health received this material and made it available to the scientists which had participated in the presentation event and committed themselves to present a written expert opinion.

Several environmental and health researchers of the Federal University of Bahia (UFBA) agreed on preparing a single expert report and elected the first author of this paper to prepare the technical report.

All the material made available by the Health Department was examined thoroughly. All data produced in the last 20 years on the subject and published in peer reviewed scientific articles, in theses, in official reports and in books were reviewed and compared with the data of the AqR report. The final report was reviewed by five professors and researchers from different departments of UFBA.

For the elaboration of this paper, the main authors of the chemical pollution data on Maré Island, as well as some outside specialists on sediments were invited.

RESULTS AND DISCUSSION

History of the environmental licensing for expansion of the Aratú port

In 2010, when the license for the port expansion was requested, a term of technical cooperation was signed by several industries of the Petrochemical Complex and of the CIA and by some state government institutions as a result of a civil inquiry filed by the Brazilian Government Agency for Law Enforcement and Prosecution of the State of Bahia, representing the population of Maré Island, against the industries [3]. The population of the island was requesting from the industries an environmental study composed of an environmental assessment and monitoring program of the area of its influence, as well as identification of the pollution sources affecting the area of influence of the Maré Island and a proposal of mitigation measures. To fulfill its part of the agreement of technical cooperation, the industries contracted the firm CETREL, that belonged to the major shareholder (Odebrecht) of the Petrochemical Complex, which in turn, was predicted to be the greatest user of the requested extension of the port. CETREL has been the firm dedicated to the treatment of the liquid effluents and to air monitoring of the Petrochemical Complex since its implementation in the 1970's. By the end of last century, CETREL expanded its activities to selling its services to any institutions in the country, including the implementation and running of the atmospheric monitoring network of the Salvador municipality.

In August 2012, CETREL presented the final report on the assessment of environmental quality of the Maré Island, which was considered inadequate due to the complexity and diversification of the emission sources and the environmental receptor compartments (sediment, water, air and biota).

As a result, a new agreement was signed in December 2015, this time a Term of Conduct Adjustment (TAC - acronym in Portuguese) which included a study of Quantitative Analysis of the Risk to Human Health - AqR, of the population of Maré Island, in accordance with the methodology adopted by USEPA. This study includes risk of exposure from all environment compartments. CETREL was contracted to conduct the AqR.

In December 2016, CETREL presented its report on the health risk assessment. The levels of toxic metals and carcinogenic polycyclic aromatic hydrocarbons (PAHs) reported were much lower than values previously reported for sediments and seafood by other scientists. Conclusions of the AqR were that the risk of new cases of cancer due to exposure to carcinogenic pollutants was within the acceptable level of 1 new case during a lifetime in a population of 100,000 people), that levels of toxic non-carcinogenic metals were within acceptable levels or slightly above, and that those exceeding the reference levels could be managed appropriately.

Existing data on environment quality of Maré Island

For over 20 years, the residents of Maré Island have complained to the local authorities, particularly to the Department of Health of the State of Bahia, of fishery decline, which had always been the main source of food for the island population, and damage to their health, especially from odorous gases. The population attributed this environmental deterioration to the oil refinery with its several oil spills, and to its effluent and emissions releases, both to the sea and to the atmosphere, together with those of the CIA and of the port activities.

Several independent studies, mainly done by academic researchers, had proven that sediments and seafood from this island were contaminated with some heavy metals and with carcinogenic polycyclic aromatic hydrocarbons (PAHs) [4-8], Air measurements showed contamination of carcinogenic PAHs and arsenic and other toxic noncarcinogenic substances on the surroundings of this island. As example of existing data, Fig. 2 depicts the levels of chromium in sediments (dry basis) of the TSB, where levels of chromium in two sites of Maré Island exceed ISQG values, that is levels where probable effects occurs in marine life. Figure 3 presents the levels of PAHs in air, drinking water and edible molluscs, where PAHs values in Maré Island and surroundings are much higher than the rest of the bay. Figure 4 shows levels of Arsenic in atmospheric particles in the north and northeast of the bay exceeding limits established by European Union and increasing over time.

Main failures identified in the Quantitative Analysis of the Risk to Human Health - AqR

The following failures were listed in the report of UFBA experts on the AqR:

1. Failures in the term of reference and methodology adopted. A biomonitoring cohort study would have been much more effective for the purpose of population.
2. Inadequate selection of the substances and environmental compartments studied.
3. Lack of information on the experimental methodology adopted, such as sampling, chemical analyses, quality control.
4. Inadequacy of the criteria used for selecting the concentrations and reference doses used in the risk assessment.
5. Inadequacy of the data treatment methodology in assessing the risk of exposure to PAHs.

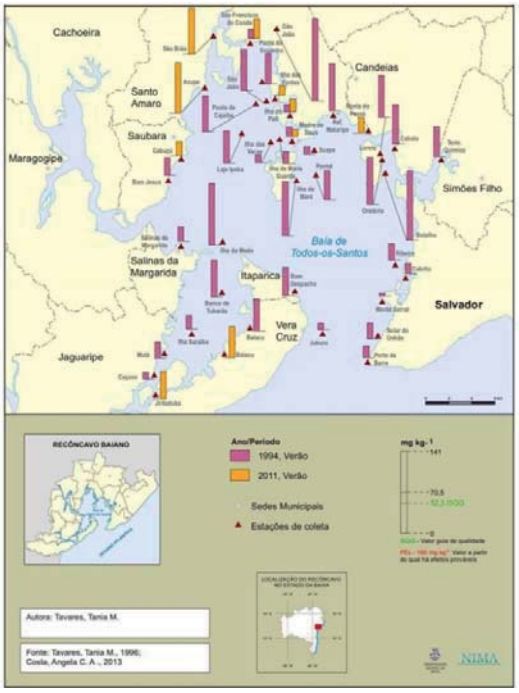

Fig.2 Evolution of Chromium (Cr) in the sediments of Todos os Santos Bay (TSB), Bahia, Brasil, 1994-2011

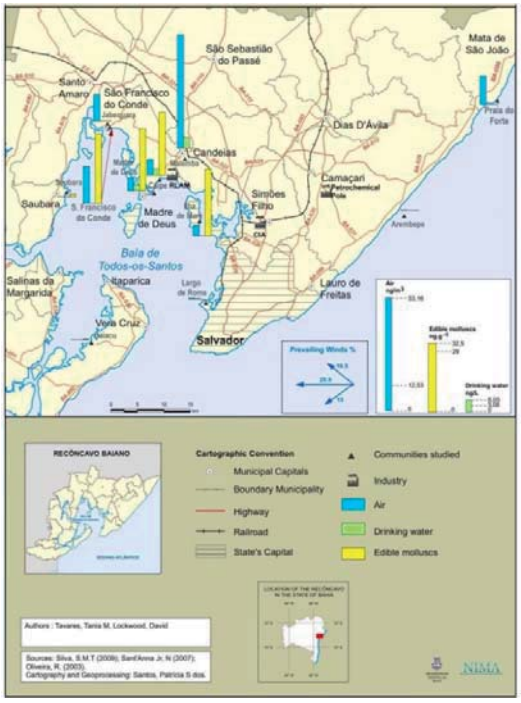

Fig. 3 Sum of the eight carcinogenic PAHs in air, edible molluscs and drinking water in different communities of the Recôncavo, Bahia, Brazil, 1994-2011

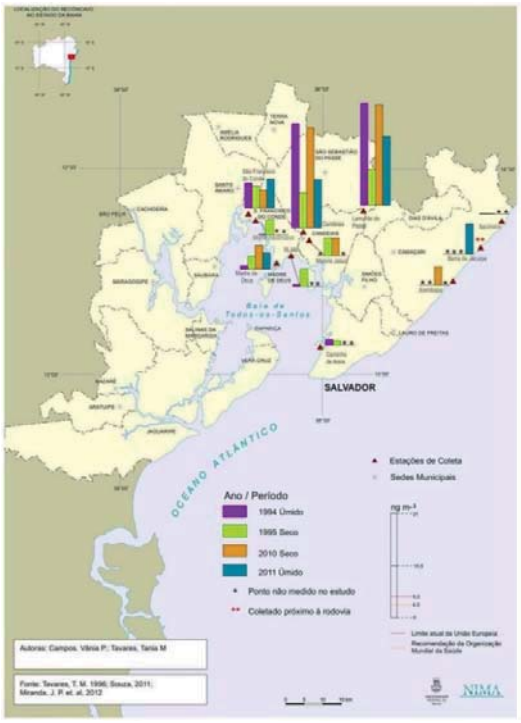

Fig. 4 Evolution of arsenic (As) in atmospheric particles in different communities of the Recôncavo, Bahia, Brazil, 1994-2011

6. Disregard for the nature and severity of the health effect involved; only the probability of the event occurring was taken into account.
7. Cancer caused by pollution is the result of a long exposure. A probabilistic risk assessment of new cases of cancer has to take into account past exposure values, and CETREL's study ignored existing historical values, and based the analysis only on its recent data.
8. A risk assessment study of new cases of cancer caused by HPA showed that the risk values of the shellfish-consuming Maré Island population were always higher (25 to 78 times) than the acceptable value in Brazil of 1 new case per 100,000 inhabitants [9], while the CETREL study concluded that all risk values were below this value.

CONCLUSIONS

The following conclusions can be drawn from the case study of Maré Island:

1. Lack of impartiality and independence of companies conducting studies

2. Lack of scientific and technical competence on complex pollution issues of all stakeholders of this case study.
3. Legal issues move too slowly in Brazil; the case study of Maré Island has been going on for over 20 years from which 8 years have gone by since the Brazilian Government Agency for Law Enforcement and Prosecution of the State of Bahia took the process over.
4. The population of Maré Island has not yet benefited from any measure so far.

ACKNOWLEDGEMENTS

We are indebted to the National Council for Scientific and Technological Development (CNPq), for the financial support, to the Coordination for the Improvement of Higher Level Education Personnel (CAPES) and the Foundation for Research Assistance of the State of Bahia (FAPESB) for research scholarships granted to some authors, and to the Department of Health of the State of Bahia, for promoting public discussions and making available all documents.

REFERENCES

[1] Lessa, GC. et al. A reevaluation of the late quaternary sedimentation in Todos os Santos Bay (BA), Brazil. An. Acad. Bras. Ciênc. [online]. 2000, vol 72, n.4, pp.573-590. Available from: http://dx.doi.org/10.1590/S0001-37652000000400008.

[2] CETREL.Análise Quantitativa de Risco à Saúde Humana- AqR em Ilha de Maré e seu Entrono. Relatório apresentado ao Ministério Públio Estadual da Bahia, 2016

[3] Ministério Público do Estado da Bahia (MPE), Termo de Ajuste de Conduta (TAC) celebrado entre o MPE, IBAMA, INEMA, CODEBA, COFIC, entre outros signatários referente ao inquérito Civil 003.0.12106/200m de 4 de dezembro de 2015.

[4] Tavares, Tania M., Nascimento, Dária M. C. Atlas Socioambiental do Recôncavo Baiano: Estado da Salvador: UFBA, 2014. 204 p

[5] CRA- CONSÓRCIO HYDROS/CH2MHILL, Análise Preliminar de Risco à Saúde Humana: Relatório Final. Volume I. Salvador, Bahia, 2004.

[6] Silva, Sonilda Maria Teixeira. Hidrocarbonetos policíclicos aromáticos associados ao PM_{10} na atmosfera do Recôncavo Baiano: variação sazonal, caracterização de fontes e avaliação de risco. 2009.152f. Tese (Doutorado em Química) – Instituto de Química, Universidade Federal da Bahia, Salvador, Bahia.

[7] Oliveira, Rui. Determinação de hidrocarbonetos policíclicos aromáticos em biota na Baía de Todos os Santos. 2003. 71 f. Dissertação (Mestrado em Química) – Instituto de Química, Universidade Federal da Bahia. Salvador

[8] Beretta, Magda. Adequação de protocolo analítico para hidrocarbonetos petrogênicos na atmosfera do Recôncavo Baiano.2000. 155f. Tese (Doutorado em Química) – Instituto de Química. Universidade Federal da Bahia.

[9] Lockwood, David. Hidrocarbonetos policíclicos aromáticos no Recôncavo baiano: contaminação ambiental e risco à saúde.2018. 152f. Tese (Doutorado em Química) – Instituto de Química, Universidade Federal da Bahia, Salvador, Bahia

MIGRATION OF POTENTIALLY TOXIC ELEMENTS IN CREEK SEDIMENTS FROM A SEMIARID COASTAL SYSTEM INFLUENCED BY THE ABANDONED GOLD MINING DISTRICT AT SAN ANTONIO - EL TRIUNFO

Romero Francisco[1], Gutiérrez-Ruiz Margarita[2], Martínez-Jardines Gerardo[1], Magdaleno-Rico Carlos[1], Espino-Ortega Violeta[1] and Hernández Cruz Griselda[1]
[1]Laboratorio de Geoquímica Ambiental. Instituto de Geología, Universidad Nacional Autónoma de México (UNAM), México.
[2]Grupo de Biogeoquímica Ambiental. Facultad de Química, Universidad Nacional Autónoma de México (UNAM), México.

ABSTRACT

A study was conducted in the "San Antonio – El Triunfo" mining district in the San Juan de los Planes basin in the southern region of Baja California Sur. The objective was evaluating the impact on soils and sediments of the historic mine wastes. Samples of 40 mining wastes and 128 superficial and sub-superficial soil and sediment, were collected. The total concentrations of heavy elements in the mining wastes samples analyzed by ICP-OES in mg/kg, were: As = 3,919, Pb = 4,223, Sb = 1,132, Ba=820, Ag = 105, Cr = 92 and Cd = 67.

The results showed that arsenic (As) is the main pollutant and only the superficial soils are contaminated since no vertical migration was detected. The sediment pollution was found up to approximately 12 km towards to the Bahía La Ventana. The particles greater than 2.0 mm of diameter contain the highest concentrations of As, but only runoff rates greater to 2.0 m/s can mobilize them. The As distribution in surface soils and sediments provided evidences that water is the one that transport those particles.

The hurricanes produce a seasonal migration of sediments through the creek during the summer and cause the overflow of this intermittent water-body dispersing the As and in lower concentration other toxic elements.

Keywords: Soil and sediment pollution, Arsenic sediment pollution, Mining wastes impact, Arsenic in soil, Arsenic in historical mining wastes

INTRODUCTION

San Antonio–El Triunfo mining district (SA-ET MD) is located 40 km southeast of La Paz, BCS, Mexico.

The climate is arid to semiarid with a mean annual temperature of 23°C. At the highest point (360 m asl), the annual precipitation is 400 mm, which is greater than at lower elevations (near to SA-ET MD) where the annual precipitation is 100–200 mm [1]. There are scarce tropical storms and sporadic hurricanes predominantly in summer. These sporadic events can be very strong. Three hydrogeological units compose the SA-ET MD: one part of the Carrizal catchment, Los Planes and La Muela–La Junta watersheds.

Zone drainage is efficient and the collecting water body is Los Planes creek. Currents are intermittent and usually infiltrate after reaching the floodplain. If rainfall volume is abnormally high, part of the runoff discharge westwards, to the sea [2].

According to Hernández Mendiola [3], " there are three different types of ore deposits in the SA-ET area: epithermal veins containing high concentrations of sulfide minerals associated with gold and silver (gold mostly associated with arsenopyrite), fault-related disseminated gold deposits in igneous rocks and one disseminated gold deposit in metamorphic rock (biotite- sillimanite schist).

Mineral deposits in the SA-ET area have been intermittently mined since 1700 when the gold beneficiation was mainly performed through leached heaps producing tons of leached material and low-grade ore; those residues were abandoned around the mines. It is estimated that 800,000 tons of this waste is scattered in the 400 km^2 of the SA-ET MD [4]. The recovery of metals by flotation procedures occurred less often, so a minor amount of tailing wastes was generated in the SA-ET area. Mineral refinement was performed in smelter plants where considerable amounts of by-products were generated inside chambers (mostly arsenolite). When the chambers filled up, they were periodically emptied out. However, once the mining operations were abandoned the chambers remained partially filled with those by-products.

METHODOLOGY

Composite samples were collected from tailings, waste low grade ores and historical metallurgical wastes (n=46, 2 kg each). Soils were collected from

San Antonio and El triunfo towns and from dry creeks (n=128, 2 kg), 12 from baseline sites, 57 surface (0-5 cm) and 59 subsurface depths (13 sites, every 50 cm on average). After air-drying, samples were sieved (2 mm), homogeneised and stored for further analysis. After reducing size for digestion (0.074 mm), chemical analysis, FRX and XRD diffraction was performed. Total concentrations of elements analysed included: As, Ba, Cr, Hg, Ag, Pb, Se, Cu, Zn, Ni, Co and V according to EPA 6200 method [6] through FRX (Niton XLT3 ThermoScientific).

Reference materials were used for validating the analysis and recovery quantification, every 10 samples as a routine: 2710 Montana soil, blank y TILL-4. Soluble fraction was extracted and analysed under the Mexican standard NOM-141-SEMARNAT-2003 [5], via ICP-OES (ThermoScientific, iCAP 6500 series). Acid-Base Accounting for Acid Mine Drainage measurement was done according to Laurence modified method, cited in NOM-141-SEMARNAT-2003. Wet chemical analysis for pH was done according to EPA 9045C [7] with a pH-meter (pH-ORP-ISE meter, HI98185). Electric conductivity on the same suspension was measured according to an international method (SSA-book series Number 5 part 3) using a portable conductimeter (Hanna HI99301).

RESULTS

The total mean concentrations of heavy elements in the historical mining metallurgic wastes analyzed by ICP-OES in mg/kg, were: As= 442,157, Sb= 25,178, Pb= 14,084, Ag= 350, Cr= 128, Ba=113, Cd= 63, Ca= 28,625, Fe= 65 949, K= 17 649, Mn= 537, Ni= 117, Ti= 3791, V= 145 and Zn=42. Carrillo and Drever [8] made a detailed mineralogical study of these types of wastes, and they show that the material from SA-ET plants is almost pure arsenolite (As2O3) with traces of Fe, Zn, Cu, Pb and S derived to the use of a different ore for gold and silver refinement. Confirmatory XRD analysis found arsenolite identified in these samples.

The total mean concentrations of heavy elements in tailings and waste low grade ores analyzed by ICP-OES in mg/kg, were: As=13,919, Pb= 4,223, Sb=1,132, Ba= 820, Ag=106, Cr= 92, Cd= 68, Ca= 10 503, Cu= 197, Fe= 86 760, K= 19273, Mn= 891, Ni=120, Ti= 3 487, V=130 and Zn=3 913

In the waste low grade ores, the pH varied between 3.3 y 8.73. In the historical wastes from furnaces between 3.09 y 5.68. The only sample of tailings that can produce acidity is practically neutral (6.36) and a electrical conductivity of 435 µS/cm.

The soluble fraction of heavy metals in all the mining wastes, with exception of metallurgic ashes (historical wastes of the sublimation chamber) are lower than the maximum permissible concentrations permitted by the environmental Mexican standards, also in acidic residues. This behavior probably is related with the high insolubility of the original ores and/or the precipitated minerals, or also the sorption of the heavy elements in compounds formed in acidic media, as jarosite $MFe3+3(OH)6(SO4)_2$.

This mineral was identified by DRX in the studied samples and several authors have reported the As retention by anionic substitution of sulfates by arsenates [9, 10, 11].

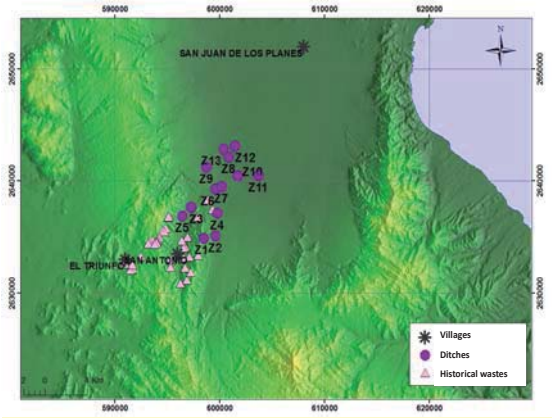

Fig. 1 Samples location

In order to evaluate the horizontal migration of mining wastes, samples of the ditches made in the dry streams, were taken from disposal sites to 30 km downstream up to the cost (La Ventana Bay) (Fig. 1). In the superficial samples the pH values varied from 5.7 and 9.0 with a median of 7.5 and the electrical conductivity (EC) from 9.2 to 761.5 µS/cm with a median of 64.7 µS/cm. The pH values are similar to the background values but the some of the EC are higher.

The total concentration ranges of the elements analyzed were in mg/kg: As (Non detected– 3,791), Cd (Non detected - 64), Hg (Non detected – 22 mg/kg), Pb (Non detected– 15,860), V (Non detected –216), Mn (111 – 1,407), Zn (Non detected– 6, 850) and Cu (Non detected– 324). The Fe range in % was 0.5 – 8.5. In the figure 2 is shown that the main heavy metals in the samples are Pb and As.

Sub-superficial samples of the ditches were analyzed to evaluate the vertical migration of the heavy metals. The pH varied from 6.1 to 9.0 with a median of 7.6. The EC varied from 4.1 5o 67.6 µS/cm, with a median of 31.1 µS/cm. The ranges of the As and Pb varied widely. The heavy metal total concentration ranges (mg/kg) are: As (Non detected – 720), Pb (Non detected– 681), V (Non detected – 192), Mn (157 – 683), Zn (19 – 152) and Cu (Non detected – 53).

The Fe range was 1.1 to 5.0 %. The individual values are shown in Table 1.

The length of the impact area of sediment considering the superficial and sub-superficial samples is approximately of 12 km towards to the Bahía La Ventana, and the concentration of heavy metals diminish with the distance of the wastes zone. Although the metallurgic wastes are the most important source of As (III), also there are natural sources of this element. According with the scanning electron microscope (SEM) results (not presented), the underlying rock contains As associated with Fe and S that correspond to arsenopyrite. The same behavior is observed with Pb and S, and probably is Galena. The As concentration in sediments and rocks are similar and, in both cases, higher than the background value. The Pb concentration is higher in rocks than in sediments and is far higher than the background value.

Relatively high concentrations (up to 18,948 mg/kg) of As were identified in nearby wells to the geological faults, that is a evidence of the dissolution of rocks rich in arsenopyrite. The dissolution magnitude increase with the ionic strength of the solution. The sea water intrusion can increase the dissolution up to 4 times more than actual.

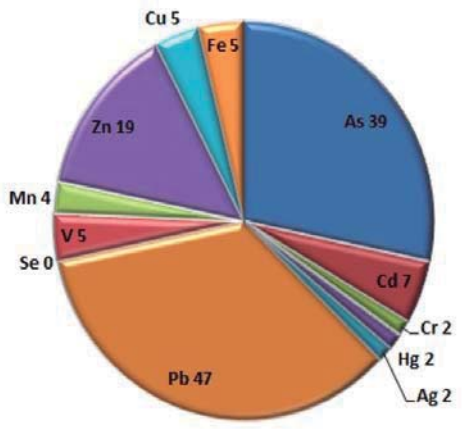

Fig. 2. Heavy metals detected in samples

Table 1. Values for As, Pb and Fe.

				As	Pb	Fe
Detection limit				14.5	3.7	0.01
Sample	Depth	pH	E.C.	As	Pb	Fe
	cm		µS/cm	mg/kg		%
ZSAT-01 5-50	-5	7.5	56.7	419	31	3.7
ZSAT-01 50-100	-50	8	47	397	18	4.1
ZSAT-01 100-150	-100	8.1	44.6	316	15	4.1
ZSAT-01 150-190	-150	8.3	47.7	380	24	4.3
ZSAT-01 190	-190	8.4	48.3	407	26	4.2
ZSAT-02 5-50	-5	8.1	44.5	414	25	2.8
ZSAT-02 50-100	-50	8.2	38.1	315	15	2.3
ZSAT-02 100-150	-100	8.8	39	231	14	2.1
ZSAT-02 150-190	-150	9	42.4	228	11	2.4
ZSAT-02 190	-190	9	38.9	222	14	2.3
ZSAT-03 5-50	-5	6.1	45.4	713	123	3.9
ZSAT-03 50-100	-50	6.7	39	720	160	3.6
ZSAT-03 100-150	-100	6.8	39.4	681	78	3.6
ZSAT-03 150-180	-180	7.3	47.5	351	71	2.9
ZSAT-04 5-50	-5	7.2	45.8	130	49	3.2
ZSAT-04 50-100	-50	7.6	52.7	96	36	2.7
ZSAT-04 100-150	-100	7.6	56.1	129	35	2.8
ZSAT-04 150-220	-150	8.1	56.2	121	34	3.5
ZSAT-04 220	-220	7.5	62.3	111	35	3.2
ZSAT-05 5-50	-5	7.9	58.5	36	16	3.1
ZSAT-05 50-100	-100	8	67.6	66	23	2.1
ZSAT-05 roca	-100	8.5	44.9	719	681	5
ZSAT-06 5-50	-5	8.2	19.5	283	31	1.9
ZSAT-06 50-100	-50	8.1	18.3	215	64	2.9
ZSAT-06 100-150	-100	8.3	16.9	109	44	2.9
ZSAT-06 150-200	-150	8.5	21.5	113	48	3.4
ZSAT-06 200	-200	8.2	14.2	75	16	3.3
ZSAT-07 5-50	-5	8.6	23.3	390	46	2.2
ZSAT-07 50-100	-50	8.6	24	399	70	2.9
ZSAT-07 100-150	-100	8.4	14.2	264	59	2.6
ZSAT-07 150-190	-190	8.7	19.6	126	102	3.7
ZSAT-08 5-50	-5	7.5	7	45	12	2.9
ZSAT-08 50-100	-50	7.4	4.1	37	< LOD	2.6
ZSAT-08 100-150	-100	7.3	4.5	64	< LOD	2.2
ZSAT-08 150-188	-188	7.1	4.2	31	11	1.9
ZSAT-09 5-50	-5	6.9	14.1	< LOD	11	1.2
ZSAT-09 50-100	-50	6.4	7.2	< LOD	12	1.2
ZSAT-09 100-150	-100	6.4	10.1	< LOD	14	1.8
ZSAT-09 150-200	-150	6.2	6	< LOD	11	1.4
ZSAT-09 200	-200	6.3	6.2	< LOD	11	1.3
ZSAT-10 5-50	-5	7.1	47.1	203	157	4.1
ZSAT-10 50-100	-50	7.2	42.6	92	40	3.6
ZSAT-10 100-150	-100	7.5	39.3	74	17	3.6
ZSAT-10 150-220	-150	7.4	48.1	73	14	3.5
ZSAT-10 220	-220	7.7	54.7	78	11	3.5
ZSAT-11 5-50	-5	7	8.1	< LOD	14	3.1
ZSAT-11 50-100	-50	6.7	5.3	19	14	2.1
ZSAT-11 100-150	-100	6.5	5.4	18	14	2.2
ZSAT-11 150-220	-150	6.5	5.9	17	13	2.7
ZSAT-11 220	-220	7.3	45.2	26	13	2.8
ZSAT-12 5-50	-5	6.7	13.1	35	10	2.6
ZSAT-12 50-100	-50	7	12.5	36	17	2.4
ZSAT-12 100-150	-100	7.1	37.6	53	11	2.5
ZSAT-12 150-220	-150	7.2	24.3	58	< LOD	3.1
ZSAT-12 220	-220	7.6	42.3	60	12	2.8
ZSAT-13 5-50	-5	7.3	28.9	20	9	1.1
ZSAT-13 50-100	-50	7.7	29.6	28	13	1.3
ZSAT-13 100-150	-100	7.9	27.1	41	13	1.2
ZSAT-13 150-180	-180	7.8	33.5	24	11	1.2
mean		7.6	31.3	194.5	44.6	2.8
median		7.5	37.6	111	16.5	2.8
Std. Dev.		0.7	18.4	195.6	91.2	0.9

CONCLUSIONS

Arsenic distribution in surface soils and sediments provided evidence that water is responsible for particle transport. Effective rainfall and the slope were used in the modelation runoff by Digital Elevation Models. Both the results of runoff simulations (in m3/s) and the Hjulström diagram were used to determine the particles that were transported (or deposited) and their sizes. In general, the results showed velocities over 3.0 m/s which can move particles of 0.001 to 100 mm, and velocities below 2.0 m/s that do not mobilize particles over 1.0 mm. Geochemical measurements in sediments of the area point out that the particles greater than 2.0 mm of diameter are associated with high concentrations of As (500-1,000 mg/kg). It was observed since the runoff rates of 2.0 m/s cannot mobilize these types of particles. Therefore, for runoff rates of 2.0 m/s we found deposition with high concentrations of As; conversely, when there are a runoff rate of 3.0 m/s (at least) natural values concentrations of arsenic are observed [12].

Based on the arsenic distribution in surface soils we can conclude that water is responsible for the particles (>2.0 mm diameter) mobilization, which are associated with high concentrations of arsenic. The hurricanes produce a seasonal migration of sediments through the creek during the summer and cause the overflow of this intermittent water-body dispersing the As and in lower concentration other toxic elements.

REFERENCES

[1] Nava-Sanchez EH (1992) Sedimentologia de la Cuenca San Juan de Los Planes, Baja California Sur, Mexico. M.S. Thesis, CICIMAR-IPN, Mexico.

[2]CONAGUA, 2009. Actualización de la disponibilidad media annual de agua subterránea, acuífero Los Planes, estado de Baja California Sur, Gerencia de Aguas Subterráneas, Subgerencia de Evaluación y Ordenamiento de Acuíferos, México D.F., México, 29 pp.

[3]Hernández-Mendiola, E., Romero, F. M., Gutiérrez-Ruiz, M., & Rico, C. A. M. (2016). Solid phases controlling the mobility of potentially toxic elements and the generation of acid drainage in abandoned mine gold wastes from San Antonio–El Triunfo mining district, Baja California Sur, México. Environmental Earth Sciences, 75(11), 969.

[4] Carrillo, A. Environmental geochemistry of the San Antonio-El Triunfo mining area, Baja California Peninsula, México. 1996. Tesis Doctoral. Ph. D. Thesis. Departament of Geology and Geophysics, University of Wyoming, USA. Unpublished, 193 pag.

[5]NOM, Norma Oficial Mexicana. 141-SEMARNAT-2003. Que establece el procedimiento para caracterizar los jales, así como las especificaciones y criterios para la caracterización y preparación del sitio, proyecto, construcción, operación y postoperación de presas de jales, publicada en el Diario Oficial de la Federación el, 2003, vol. 13.

[6] EPA, Environmental Protection Agency, Method 6200 and field portable X-ray fluorescence. In SACKETT, Donald; MARTIN, K. A presentation developed for the EPA Technology Innovation Office and On-Site In-Sights Workshops for innovative field characterization technologies. 1998.

[7] EPA Environmental Protection Agency (US–EPA), 1995, Method 9045C: Solid and waste pH, in SW–846, Test Methods for Evaluating Solid Waste, Physical/Chemical Methods: United States Environmental Protection Agency, 5 p.

[8]Carrillo, A., & Drever, J. I. (1998). Environmental assessment of the potential for arsenic leaching into groundwater from mine wastes in Baja California Sur, Mexico. Geofísica Internacional, 37(1), 0.

[9] Foster, A. L., Brown, G. E., Tingle, T. N., & Parks, G. A. (1998). Quantitative arsenic speciation in mine tailings using X-ray absorption spectroscopy. American Mineralogist, 83(5-6), 553-568.

[10]Paktunc, D., & Dutrizac, J. E. (2003). Characterization of arsenate-for-sulfate substitution in synthetic jarosite using X-ray diffraction and X-ray absorption spectroscopy. The Canadian Mineralogist, 41(4), 905-919.

[11]Asta, M. P., Cama, J., Martínez, M., & Giménez, J. (2009). Arsenic removal by goethite and jarosite in acidic conditions and its environmental implications. Journal of Hazardous Materials, 171(1-3), 965-972.

[12] Hernández Cruz, G. 2015. Evaluación de la dispersion hídrica de arsénico en el distrito minero de San Antonio- El Triunfo, Baja California Sur, México. PhD Thesis, National Autonomous University of Mexico. Earth Sciences Postgraduate Degree.

SOIL CLAY COMPONENTS AND TRACE METAL STABILIZATION

Bobadilla Ballesteros Martha Daniela[1], Tapia Sánchez Xóchitl[1], Millán Malo Beatriz Marcela[2], Fuentes Romero Elizabeth[1], García Calderón Norma Eugenia[1], Altuzar Coello Patricia Eugenia[3]
[1]UMDI-J, Facultad de Ciencias, México [2]Centro de Física Aplicada y Tecnología Avanzada, México
[3]Instituto de Energías Renovables, Universidad Nacional Autónoma de México, México

ABSTRACT

Soils from a toposequence were investigated in order to illustrate their functionality to stabilize heavy metals into their clay-mineral components in samples from weakly developed technogenic soils (located near a mine dumps) in transects from the lower part and their dissipation to the middle and upper steep-slope. To date the impact of layer alumino-silicates in Technosols from these regions have not been studied in detail. The aim of the present research was to examine the influence of clay minerals in soil profiles and their relationship between stabilization and storage of Zn, Cd, Pb, As and Cu in the mining area that were extracted and casting of sphalerite in Xichú, Guanajuato, México. Clay fractions were obtained from each soil horizon and analyzed using X-ray Diffractometry and Thermogravimetric analysis and Inductived coupled plasm. The profiles analyzed were previously identified as Technosol and Cambisol [3], results of their clay mineralogy indicate the presence of high calcite content in the upper part, and prevalence of Illite-Chlorite intergrades in the middle and lower part. Influence of the mine dumps is located in the topsoil of the lower part, decreasing from Zn>As>Pb>Cu>Cd, but mainly in the subsurface from 2-20 cm Zn>As>Pb>Cu~Cd of the total trace elements.

Keywords: Technosol, Illite-Chlorite, Mine-tailings

INTRODUCTION

In this work, clay mineral characteristics belonging to three soil profiles, located in the municipality of Xichu, Guanajuato[1] (Fig. 1) are studied as part of a research of dynamic soil components and their relation with the behaviour of clay fractions, in order to assess their influence in ecosystem regulation processes.

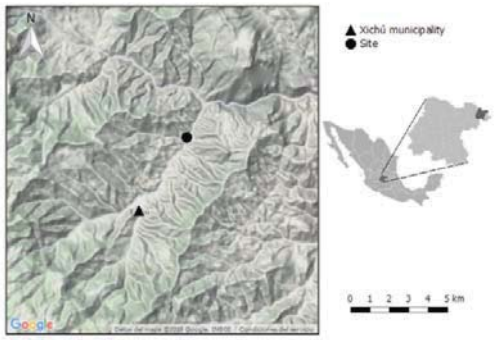

Fig. 1. Study area in Xichu, Guanajuato

MATERIAL AND METHODS

Geographic situation and soil samples

The samples under study were taken from three soil profiles located along a toposequence in altitudes ranging from 1103 to 1152 m asl. nearby an area of mine tailings deposition since the middle of the last century, in the municipality Xichu[2] with the following coordinates 100°03'37" W and 21°18'00" N. Each profile was sampled by horizons and previously classified as Technosols in the lower steep-slope (LSS), Cambisols (MSS) in the middle steep-slope and Regosols in the upper steep-slope (USS)[3] (Table 1).

Table 1. Main physics and chemical properties of the profiles from the toposequence

Site	Horizon	Depth cm	pH H2O	Clay g Kg^{-1}	Te	TOC g kg^{-1}
Regosol USS	A	0-3	8.1	8.0	L	12.8
	AC1	3-30	8.2	20.0	L	5.3
	AC2	30-56	8.3	13.0	L	5.3
Cambisol MSS	Ah	0-10	8.1	15.4	SiL	7.1
	Bw	10-40	8.1	14.4	L	8.2
	C1	40-48	8.1	7.0	LS	2.3
	C2	48-60	8.4	8.0	LS	4.7
Technosol LSS	Ap1	0-2	7.8	15.0	L	10.8
	Ap2	2-20	6.6	8.0	SL	2.86
	C2	20-40	7.6	16.0	L	8.20

TOC = total organic carbon, L= Loam; SiL= Silt Loam; LS= Loamy Sand; SL= Sandy Loam

Methodology

The sand, silt and clay fractions of the collected samples were separated by sedimentation after destruction of organic matter and dispersed using a Fisher mod. 150 for ultrasonic treatment (20 minutes

at 600 W for 250 ml of suspension). The <2 µm fraction was isolated by repeated siphoning of the dispersed material and centrifuged to concentrate the clay fractions.

The clay mineralogy diffraction diagrams (XRD) have been obtained in air dry conditions with a Rigaku Diffractometer, Ultima IV Model using Cu Kα radiation, with a scanning speed of 2°2θ per minute. Diagrams of oriented clay have been made, after saturating with magnesium, potassium and glycerin, at room temperature, 425°C and 525°C. As well as non-oriented aggregates of samples. To obtain the thermograms, the samples were stabilized, after saturation with magnesium, using a Thermogravimetric Analyzer TA Instruments Q500 with a heating rate of 10ºC per minute in an inert nitrogen atmosphere. The chemical analyzes were carried out by Inductively Coupled Plasm mass spectrometry (ICP-MS) with a Horiba Ultima 2.

RESULTS AND DISCUSSION

The qualitative range of clay mineral species in the toposequence shows the predominance of the Illite respect the chlorite (Table 2).

Table 2. Qualitative range of clay mineral

Profile	Depth cm	Illite	Chorite
Regosol USS	0-3	xxx	xx
	3-30	xxx	
	30-56	xxx	xx
Cambisol MSS	0-10	xxx	xx
	10-40	xxxx	xxx
	40-48	xxxx	xx
	48-60	xxxx	xx
Technosol LSS	0-2		
	2-20	xxx	xxx
	20-40	xxxx	xxxx

The diffractograms corresponding to the clay fraction of one of the samples of one Profiles shows the Chlorite, clearly identified by their spacings of 14 Å, 7 Å, 3.5 Å, 2.82 Å and 1.99 Å, which remain when the samples are heated till 425°C and change intensity in the diagrams obtained from the same treated samples at 525°C, especially the reflection of 7 Å, which manifests with greater intensity. Other spacing (9.8 Å, 4.92 Å, 3.3 Å and 1.99 Å) reveal the existence of Illite, in predominance proportion, compared to Chlorite. (Fig. 2).

The analysis by ICP-MS of the clay fraction is shown below, where it is observed that indeed the presence of heavy metals are assimilated into the structure of the clay, these being part of its structure and compostion. Influence of the mine dumps is located in the topsoil of the lower part, decreasing from Zn>As>Pb>Cu>Cd, but mainly in the subsurface from 2-20 cm Zn>As>Pb>Cu~Cd of the total trace elements. (Table 3)

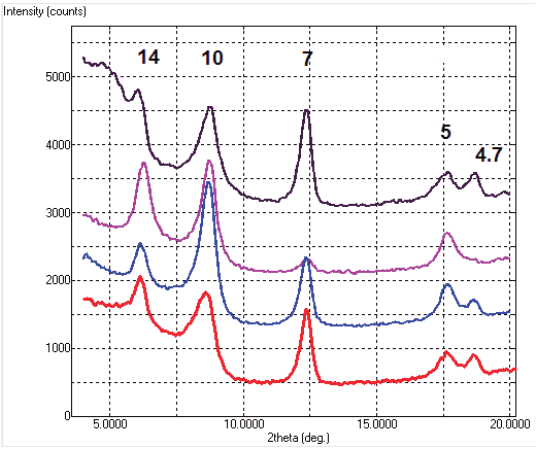

Fig. 2 X-ray diffracion of XG4 sample. Air-dried sample (red), glycolated (black), 425°C (blue) and 525°C (pink).

Table 3. Total trace elements concentration obtained from clay fraction

Site	cm	As	Cd	Cu	Pb	Zn
Reg.	0-3	46.23	2.7	26.51	67.3	154.1
USS	3-30	10.29	2.15	19.41	35.1	66.9
	30-56	8.36	1.96	17.33	34.3	58.0
Camb.	0-10	51.2	1.50	33.44	93.7	162.7
MSS	10-40	5.67	3.99	34.97	66.9	198.8
	40-48	25.80	5.21	148.51	184.1	357.8
	48-63	23.01	3.74	45.53	125.7	433.9
Tech.	0-2	1690	35.03	161.52	1375.8	3110.3
LSS	2-20	2713.9	38.52	38.52	2504.6	3288.1
	20-40	151.4	23.09	57.43	138.7	1790.4

It accompanies the mentioned minerals important amounts of calcite, quartz and gypsum, which have been clearly identified in the diagrams obtained in non-oriented aggregates, with the characteristic spacings of 3.03 Å, 3.34 Å and 4.28 Å, respectively.

The curves of thermogravimetric analysis of the clay fraction stabilized with potassium are similar, determining a first weight loss at low temperature (less than 50°C) product of adsorbed water and a second loss around 700°C, which indicate the presence of chlorite.

Based on the data obtained by X-ray diffraction in the material treated with potassium and heated to 525°C, the presence of Chlorite is confirmed by the permanent presence of both the reflection at 14 Å

and the reflection at 7 Å (Fig. 3). And on the basis of the Powder Diffraction File (PDF), Chlorite is identified as type IIb-4 with No. PDF: 01-075-8291 with Formula $Al_{12.78}$ $Fe_{0.94}$ H_{16} $Mg_{11.06}$ O_{36} $Si_{5.22}$ with crystalline system: Triclinic. The Illite is identified as Illite-2M2 with No. PDF: 00-024-0495 with Formula $A1_{2.1}$ H_2 $K_{0.7}$ O_{12} Si_4 and crystalline system: Monoclinic.

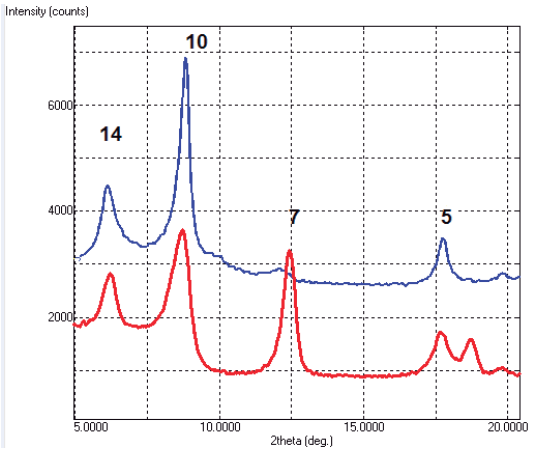

Fig. 3 Diffractograms of the clay fraction with potassium (red) and 525 ºC (blue).

The presence of chlorite in soils near mine tailings has been documented that resulted in the partial neutralization of very acidic tailings[5], it is thought that it is due to the interlayer hydroxide sheet reacting with the acid. And that as the pH increases, Fe and Al precipitate and act as a regulators for heavy metals in the environment in conjunction with the other clay minerals.

CONCLUSIONS

As a tool to obtain interpretations of soils environmental functions based on their clay mineralogy this research demostrates the presence of Chlorite, that could be arranged as interstratified Chlorite-Illite in soils derived from calcareous-lutite rocks in a toposequence as Cambisols and Technosols indicates that the alteration has taken place under conditions of moderate pressure and low temperature.

Likewise, the different contents in Illite and potassium content may correspond to the different proportions of biotite in the original rock [4].

The presence of Chlorite, correspond to pedogenesis processes under conditions of temperature and low pressure. We suggest that the presence of heavy metals were assimilated into the structure of the clay, these being part of its structure and composition.

ACKNOWLEDGEMENTS

I would like thank to appreciate José Campos, Oscar G. Daza, Gildardo Casarrubias for their technical support.

REFERENCES

[1]Instituto de información para el desarrollo de Guanajuato.

[2]http://sinat.semarnat.gob.mx/dgiraDocs/documentos/gto/estudios/2012/11GU2012M0030.

[3] Bobadilla Ballesteros, M.D., Tapia Sánchez, X., García Calderón, N.E., Fuentes Romero, E., "Memorias del XXI Congreso Latinoamericano de la Ciencia del suelo". División 1, 2016, pp.1072-1077.

[4] Deer, W.A., Howie, R.A., Zussmann, J., "Rock Forming Minerals", Vol.3 London Longmans Ed., 1963.

[5] Kohut, C.K. and Warren C. James, "Chlorites" Chap. 17 in: Dixon J.B. and Schulze G.D. (eds). Soil mineralogy with environmental applications, 2002, pp.531-553.

SPATIAL DISTRIBUTION OF ARSENIC AND LEAD IN STREAM SEDIMENTS IN A MICRO-BASIN WITH ANCIENT MINING ACTIVITIES

Montes-Avila I.[1], Cardona-Benavides A.[2], Lázaro-Báez I.[3] Razo-Soto I.[4] and Hernández-Ruiz S.[5]

[1,3] Instituto de Metalurgia, Universidad Autónoma de San Luis Potosí, San Luis Potosí; [2, 4] Área Ciencias de la Tierra, Facultad de Ingeniería, Universidad Autónoma de San Luis Potosí, San Luis Potosí; [5]Centro de Investigación y Estudios de Posgrado, Facultad de Ingeniería, Universidad Autónoma de San Luis Potosí, San Luis Potosí.

ABSTRACT

Extraction of mineral resources produces different types of residues; some of them are prone to the release of potentially toxic elements (PTEs) such as arsenic (As) and lead (Pb). This research analyzes the spatial distribution of As and Pb produced by their dispersion from ancient mining residues to sediments located within the Cerro de San Pedro micro-basin which is situated in a semi-arid region. Previous studies have shown that a pile of waste generated by ancient mining activities. The so-called Patio Victoria (RPV), which represent a contamination source, that is characterized by the content of sulfides that have led to, the generation of acid drainage [1],[2],[3]. However, its impact on stream sediments at the micro-basin level has not been evaluated in detail over a length of 12 km. The approach considered in the work includes the identification of three zones: i). Zone A, upstream of RPV, ii) Zone B adjacent to RPV and iii) Zone C, downstream of RPV. Results for total concentrations in the sediment samples taken along the main stream of the micro-basin, indicate that the lowest concentrations for Pb (399-689 mg/kg, median of 542 mg/kg) and As (76-200 mg/kg, median of 105 mg/kg) were identified in Zone A. While Zone B involves the most impacted sediments with high concentrations of Pb (858-7590 mg/kg, median of 4288 mg/kg) and As (140-1025 mg/kg, median of 409 mg/kg). The concentration values for Pb (1136-7317 mg/kg, median of 1469 mg/kg) and As (189-429 mg/kg, median of 296 mg/kg) in Zone C, represent dispersion of the contaminant source along the main stream. Considering Zone A as the reference, a trend in Pb is observed with an increase of 7.91 and 2.71 times for Zone B and Zone C respectively. In the case of As the increase in Zone B is 3.90 times and 2.83 times for zone C. There is a significant statistical correlation of As and Pb (r^2= 0.89), which are found in the sediments mainly as arsenopyrite and galena as primary minerals and jarosite, anglesite, cerusite and iron oxides as secondary minerals. Results from this investigation indicate there is a potential impact of these pollutants on superficial and groundwater quality.

Keywords: Sediments, potentially toxic elements, mine residues, dispersion.

INTRODUCTION

River streams are one of the most important environmental resources for a nation. Clean water is vital for all living organisms and plants and it is important for the economic development of the population. Because of this, there are several studies devoted to the characterization and control of streams and river flows [4], [5]. Mineral resources have brought economic, cultural and social development. Mexico is one of the countries located in a region with a significant diversity of minerals; in which, the mining tradition goes back to pre-Hispanic times; and it typically involves two stages: exploitation and benefit of metals [6].

However, the residues produced in mining operations are considered a significant source of pollution when they are not adequately handled. Among the problems that arise from the residues, there is the generation of acid mine drainage that promotes mobility of pollutants. Additionally, other sources of potential environmental impact are the increase in the levels of suspended solids in bodies of water and the contamination of soil and sediments with heavy metals [7], [8]. Sediments are an important receptor of pollutants and can act as filter that could either attenuate the effect of pollutants by stabilizing them or become a source of contamination of groundwater.

The impact of weathering together with torrential rains on abandoned residues in semi-arid zones cause oxidation and mobility of sulfides by different mechanisms (leaching and particle transport) and dispersed by gravitational transport and fluvial and atmospheric pathways [9], [1], [2]. The acidic conditions induce releases of pollutants, ie, Pb, As, Zn, Cu. [10]. The As and Pb are elements potentially toxic (PTE's).

As is a redox-sensitive element and occurs mainly in the inorganic forms of arsenate As(V), arsenite As(III), arsenic As (0) and arsine As(-III) [11],[12]. Under oxic conditions As adsorbs strongly on minerals such as Fe (hydr)oxides and to a lesser extent on manganese (Mn) oxides [13],[14]. Pb is mobilized by the oxidation of galena (PbS), but it is generally precipitated as a wide variety of secondary minerals, such as cerussite ($PbCO_3$), hydrocerussite [$Pb_3(CO_3)_2OH_2$] and anglesite ($PbSO_4$) [15], [16]. It is reported there is a close correlation between Pb and As mineralogy and therefore they are found associated with each in different mineral deposits, as well as in floodplain soils (the sink site). Hence an interaction between them during mobilization processes could be expected [17].

In México, historic mining activities have produced numerous sites with residues containing high concentration levels of As, Pb, Zn and Cu, in many cases associated to sulfides. In the particular case of the Cerro de San Pedro in San Luis Potosi, the ancient beneficiation process of Au and Ag resulted in abandoned residues that contain a variety of sulfides such as pyrite (FeS_2), arsenopyrite (FeAsS), galena (PbS) and iron-sphalerite [(Zn, Fe)S]. Some researchers have found high total concentrations of As and Pb in this study area known as Patio Victoria residues (RPV) [1]. The average results reported for the RPV were: total concentrations of 1,050 mg/Kg and 23,101 mg/kg for As and Pb, respectively [2], while for sediments in a longitude of 2.9 km of the San Pedro stream were of 602 mg/Kg of As and 4,615 mg/kg of Pb [3].

The environmental impacts of sediments is paramount and thus it is necessary to devote more studies to the evaluation of the nature of these materials in the different mining sites where they could represent a risk. In this work, the spatial distribution of arsenic and lead in sediments along the course of the San Pedro stream (intermittent) associated to ancient mining residues was investigated.

STUDY SITE

LOCATION

The study area is located in the eastern portion of the San Luis Potosí drainage basin, at 19.5 km approximately from San Luis Potosí City (Fig. 1). This district has an ancient mining history that begun in the late XVI century, where there have been intermittent activities associated to the exploitation of Pb-Ag and Au deposits.

GEOLOGY

The geological setting of the study area [18], [19], as presented in Fig. 1, is composed by outcrops of sedimentary rocks from Lower Cretaceous (limestones and shales) of the La Peña, Indidura and Cuesta del Cura formations; unconformably overlaid by continental sediments and volcanic rocks (Eocene-Oligocene), with variable composition from andesite to rhyolite. Basin fill sediments overlay volcanic rocks in the plain of the drainage basin; Quaternary alluvial deposits include sediments along intermittent streams.

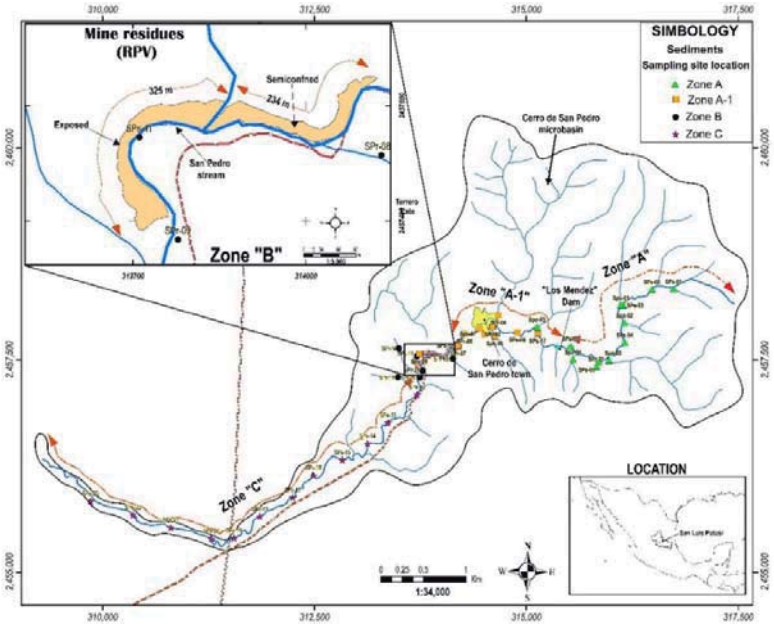

Fig. 1 Localization of the study area and sampling site

The economic mineralization is associated to a dioritic intrusive of Tertiary age with porphyritic alteration, tabular form, thickness from 15 to 500 m and intruding along fractures and stratification planes of Cuesta del Cura formation. This last, produces replacement ore bodies, and some cavity fillings that form layers and chimneys with disseminated mineralization present as stockworks, that are composed of calcite veinlet network with iron oxides (goethite) and deep sulphides zones (pyrite, sphalerite, tetrahedrite, arsenopyrite, chalcopyrite and acanthite).

HIDROLOGY

The study area has semiarid conditions (390 mm/annum, 1951-2010 period; [20] is drained by the San Pedro stream (Fig. 1), and located in the El Salado Hydrologic Region, it has an area of approximately 172 km2, with a dendritic pattern and an intermittent main stream length of 12 km. There is a small reservoir (<1000 m3) in the highlands of the basin. Mobility and dispersion of the sediments in the basin is usually produced by high intensity summer storms runoff.

CLIMATE

The predominant climate in the study area according to the Köppen classification, modified by Enriqueta García [9] corresponds to the group of climates type B (Dry) specifically BSokw, a temperate arid climate. The average annual temperature ranges between 12° to 18°C, temperatures in the coldest month are between -3°C to 18°C [10], and temperature of the hottest month is lower than 22°C. It has rain in summer and a percentage of winter rain from 5 to 10.2 % of the annual total; the average annual total precipitation in the 2005-2010 period was 311 mm [21].

HISTORICAL MINING ACTIVITY AND ANCIENT RESIDUES

In the Cerro San Pedro micro-basin, in a period of over more than 400 years (1592 to date) there have been different periods of mining activities and the elements of economic interest have been Au, Ag, Zn and Pb [22], [23], [24]. The present study is limited to historical mining residues from the Patio Victoria (RPV), which comes from the benefit of sulfides (pyrite, galena, arsenopyrite, among others), and which were located along the right bank of the San Pedro stream (currently the RPV has been relocated to a controlled site).

METHODS

In this section, the most important aspects related to the fieldwork and data analysis techniques used in this research are described.

Sampling design

Sampling was made using the methodology proposed by Salminem [25]. The strategy to monitor the spatial dispersion of the trace elements As and Pb in the microbasin consisted in three stages. i) identifying the main stream on the basis of its relationship with the main source of PTE's (RPV); ii) classifying the main stream zones where the samples were taken as A, B and C; iii) planning the collection of samples every 500 m on the main riverbed and in tributary streams of 1st and/or 2nd order.

Zone A are the upstream samples that are less likely to be impacted by PTE's from RPV. Nevertheless, this zone is affected by other residues from an area nearby to the San Pedro town labelled as A-1 (Fig. 1). Zone B are the samples adjacent to RPV. Zone C are the samples taken downstream RPV.

Collection of samples

They were collected along the active zone of the stream. Thus, the samples corresponded to the material deposited superficially (0-5 cm) on the bed of the stream. At each site, the sediments were collected with a stainless steel shovel, on a cross perpendicular to the flow of the stream, without including the area near the walls of the stream to avoid interferences. All the samples were sieved with a 2mm stainless steel mesh and quarter *in situ*. Approximately 1.0 kg of fine materials were collected in clean plastic bags. Geographic coordinates of sampling points were measured using a Global Positioning System (GPS) within ± 5 m accuracy, with the UTM map projection.

Chemical analysis.

The samples were dried at 35 °C and chemical analysis for As and Pb was made by digestion of the samples with aqua regia and analysis of the solutions generated by inductively coupled plasma-atomic emission spectrometry (ICP-AES). The accuracy of the analyses was determined through analysis of Montana Soil 2710a certified reference material (MCR), obtaining average recoveries of 109.4% of As and 98.1% of Pb.

Statistical and spatial data analysis.

Spatial correlation is clearly a natural phenomenon given the open nature of stream ecosystems and the complexity of process interactions occurring within and between the stream and the terrestrial environment [26]. However, the use of EDA-SDA technique using simple statistical tools provides more certainty of the results obtained since it allows relating the factors that can influence the distribution behavior.

The results are presented according with the different zones, where as a first step tables with

descriptive statistics (mean, median, standard deviation, maximum, minimum) that show the distribution of As and Pb in each segment of the stream were prepared. To provide more realistic values of central tendency and dispersion median values were used [27], [28], [29], [30]. Boxplot graphs allowed grouping the data by zones and characteristics and showed the differences or similarities between the different groups. Boxplots provide graphic information based on the inherent structure of the data regardless of their distribution and are unaffected by 15% of outliers in the data set [28], [31]. It is clear that a purely numerical method is not enough to make environmental decisions about both background values and geochemical anomalies. Since the results vary depending on the selected technique, a more detailed statistical analysis is necessary together with a spatial interpretation of the information and the results obtained. This last, can be achieved using the technique known as Exploratory Data Analysis (EDA), supported by the current techniques of geographic information systems (GIS), spatial analysis and geochemical distribution. The software used for the statistical analysis was Statistica 10 (Statsoft) that produced descriptive statistics, graphical analysis, correlations, boxplot and Excel database.

RESULTS AND DISCUSSION

Sampling

Four zones were classified for the sampling of stream sediments obtaining a total of 49 (Table 1), in length of 12 km. Collected every 500 m in the main riverbed and the intersection with a tributary of 1st and / or 2nd order (Fig. 1).

Table 1 Summary table of locations and characteristics of the sample

Location	Id	Characteristics	Num
Zone A	Sps-1 to Sps-6	main riverbed of the stream	6
	Spo-1 to SPo-5	1st or 2nd order tributary	5
	Spr-1	Tributary associated with residues.	1
Zone A-1	SPs-7 to Sps-10	Main stream riverbed. Town vicinity	4
	Spo-6 to Spo-8	1st or 2nd order tributary. Town vicinity	3
	Spr-3 to Spr-7	Tributary associated with residues. Town vicinity	4
Zone B	SPs-11	Main stream riverbed. RPV Adjacent	1
	Spr-8 to Spr-11	1st or 2nd order tributary. RPV Adjacent	4
	Spn-1	1st or 2nd order tributary	1
Zone C	Sps-12 to Sps-23	main riverbed of the stream	12

Num: Number of samples

Descriptive Statistics

Table 2 shows statistical results obtained for total concentrations of As and Pb from sediment samples along the main riverbed of the San Pedro stream. The median values seem high although there is not an established reference to compare with. Nevertheless, in comparing these results with reports of evaluations of sediments in sites under similar climatic conditions and with similar historic mining background it was found a comparable pattern. The Triunfo mining district in Baja California Sur, in a basin subjected to exploitation of Au and Ag for more than 300 years, the average total concentrations of As and Pb in stream sediments was of 207 mg/kg and 620 mg/ kg respectively [32]. These values were 0.73 and 3.3 orders higher than the results of As and Pb obtained for the San Pedro stream.

Table 2 Basic statistics total concentration (mg/Kg) of the sampling sediments

Parameters	As	Pb
N	49	49
Min	38	212
Max	1025	7590
Av	282	2066
Med	250	1428
DStd	194	1823

N: sample number, Min: Minimum, Max: Maximum, Av: Average, Med: Median, Dstd: Desviation standard

Exploratory data analysis (EDA) of the results

EDA boxplots were generated (Fig. 2) and a comparison of the medians show that in stream sediments the highest total concentrations occur in zone B (249 mg/Kg of As and 1427 mg/Kg of Pb). Zone A1 (As of 337 mg/Kg and 2978 mg/kg) and Zone C (296 mg/Kg of As and 1469 mg/Kg of Pb of the) showed intermediate values. While Zone A presented the lowest values (31 mg/Kg of As and 377 mg/kg of Pb) as it was expected.

Likewise, boxplots can show differences between the concentrations of elements according to different scenarios: the geological parental material (predominantly limestone rocks) as in the case of Zone A, land use (mining activities) case zone A-1 and B, as well as the hydrological (river stream) dispersion effect as in the case of zone C. These results suggest the possibility of associating the measured concentrations with natural values.

Results for total concentrations (Table 3) in the sediment samples taken along the main stream of the micro-basin, indicate that the lowest concentrations for Pb (399-689 mg/kg, median of 542 mg/kg) and As (76-200 mg/kg, median of 105 mg/kg) were identified in Zone A. While Zone B involves the most impacted

sediments with high concentrations of Pb (858-7590 mg/kg, median of 4288 mg/kg) and As (140-1025 mg/kg, median of 409 mg/kg). The Concentration values for Pb (1136-7317 mg/kg, median of 1469 mg/kg) and As (189-429 mg/kg, median of 296 mg/kg) in Zone C, represented dispersion in the microbasin through time caused by fluvial stream.

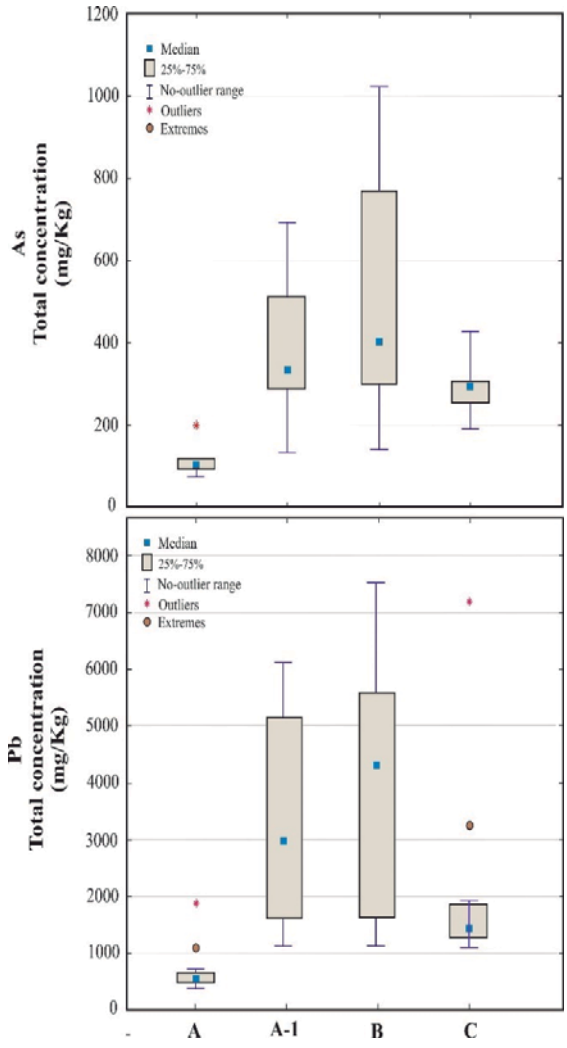

Fig. 2 Boxplot of As and Pb, the stream sediments by zone

DISTRIBUTION SPATIAL As AND Pb

The maps of the spatial distribution of As and Pb were generated with the results of EDA-SDA to pinpoint concentrations along the 12 km of the San Pedro stream evaluated (Fig. 3). The comparison of these maps shows the behavior through the main riverbed, demonstrating the use of numerical tools and spatial analysis.

Table 3 Descriptive statistics total concentration of As and Pb (mg/Kg) in sediments stream San Pedro by zone

Zone	Characteristics	n	Min	Max	Prom	Med	DStd
	As						
A	Upstream	12	76	200	110	105	31
A-1	Upstream town vicinity	11	135	694	401	337	165
B	RPV adjacent	5	140	1025	529	409	362
C	Downstream	12	189	429	293	296	69
	Pb						
A	Upstream	12	399	689	537	542	89
A-1	Upstream town vicinity	11	1094	6121	3169	2978	1729
B	RPV adjacent	5	858	7590	3984	4288	2786
C	Downstream	12	1136	7317	2100	1469	1741

n: sample size, Min: Minimum, Max: Maximum, Av: Average, Med: Median, DStd: Desviation standard

There is a significant statistical correlation of As and Pb (r^2= 0.89), which are found in the sediments mainly as arsenopyrite and galena as primary minerals and jarosite, anglesite, cerusite and iron oxides as secondary minerals. Results from this investigation indicate there is a potential impact of these pollutants on superficial and groundwater quality.

Considering Zone A as the reference, a trend in Pb is observed with an increase of 7.91 and 2.71 times (possible natural concentrations of the site) for Zone B and Zone C respectively. In the case of As the increase is 3.9 times and 2.83 times higher for zones B and C, respectively. This last, associated to the effect of the impact caused by the fluvial dispersion of the RPV material, coupled with the natural dilution of geological and soil substrates in the micro-basin (Fig. 2)

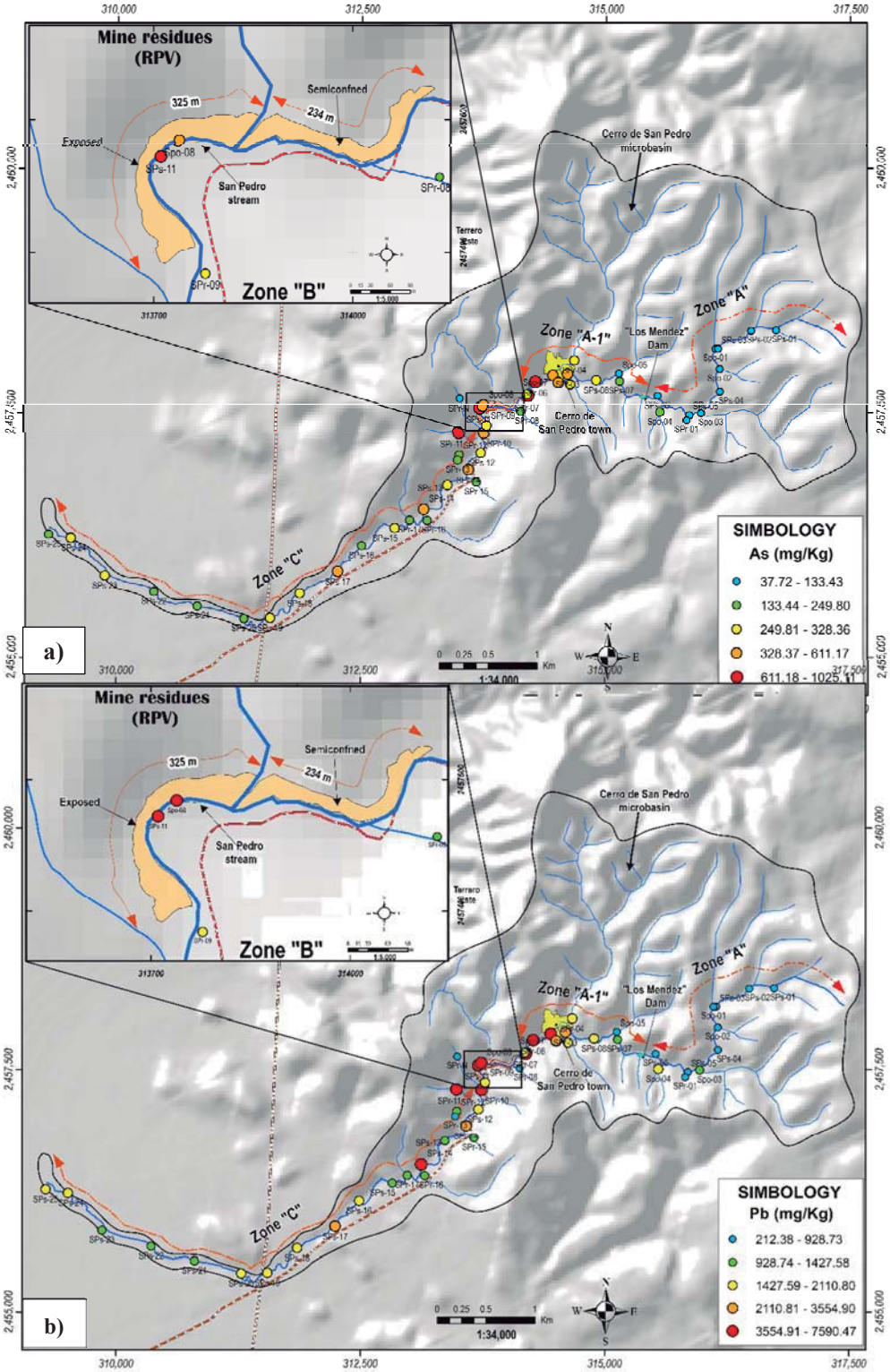

Fig. 3 Map of the spatial distribution of the sediments stream in Cerro de San Pedro microbasin, a) As and b) P

CONCLUSIONS

The spatial distribution of As and Pb in the Cerro de San Pedro micro-basin is clearly a result of the interaction of rocks-hydrology-mining residues along the San Pedro Creek. The behavior of the distribution of concentrations along the main stream for both As and Pb are low (Upstream, Zone A), high (RPV adjacent, zone A-1 and B) and low (zone C, downstream). This trend **r**epresents the effect of the impact caused by the fluvial dispersion of the RPV material, together with the natural dilution of geological and soil substrates in the microbasin. The use of EDA-SDA technique using simple statistical tools provides more certainty of the results obtained, since it allows relating the factors that can influence the distribution behavior. Correlation of the different processes that provoke the dispersion of As and Pb is complex. Complete analysis and comprehension of all these factors is beyond the scope of a geochemical and environmental study since it would be necessary to consider other variables that affect the dispersion of potentially toxic elements such as As and Pb (e.g. chemical mobility and wind). However, the use of EDA-SDA techniques through simple statistical tools coupled with knowledge of geology, hydrology, and geomorphology provides certainty to the results obtained. Further, it allows relating the factors that may influence the spatial distribution of chemical elements to the sediments stream and considers the spatial distribution of the elements of interest. The results of this investigation indicate that there is a possible impact of these pollutants on the quality of surface and underground water.

ACKNOWLEDGEMENTS

The present project had the financial support of the key fund FORDECYT 190966. We thank Dra. María Elena Garcia, Dr. Erik Espinosa and Ing. Miguel Cortina, from the analysis laboratory of the Geochemistry Laboratory of the UASLP Geology Institute, for its valuable support in the analysis of samples.

REFERENCES

[1] RAZO S., I.; Muñoz G., R.; Cepeda B., C.; Monroy F., M. (2007): Caracterización ambiental de residuos mineros históricos del distrito minero Cerro de San Pedro (San Luis Potosí, México). Memoria Convención minera AIMMGM. Tomo 1, No 27, pp. 352-357. (http://www.sgm.gob.mx/aimmgm/JspInforme.jsp)

[2] Vázquez, S. E. (2012). Caracterización de un depósito no controlado de residuos mineros y evaluación de su impacto en suelo superficial. Tesis de maestría de Geología Aplicada. Posgrado en Geología Aplicada. Universidad Autónoma de San Luis Potosí. San Luis Potosí, México. 131 p.

[3] Ortega Morales, N. B. (2012). Asociación entre la fracción bioaccesible y la bioacumulación en algunas especies vegetales que crecen en el cauce del arroyo de San Pedro.

[4] Torgersen, C. E., Gresswell, R. E., & Bateman, D. S. (2004). Pattern detection in stream networks: quantifying spatial variability in fish distribution. GIS/spatial analyses in fishery and aquatic sciences, 2, 405-420.

[5] Yuan, L. L. (2004). Using spatial interpolation to estimate stressor levels in unsampled streams. Environmental Monitoring and Assessment, 94(1-3), 23-38.

[6] Hernández Ruiz S., (2017). Estudio del transporte hídrico de plomo y arsénico en microcuencas del distrito minero Cerro de San Pedro, San Luis Potosí, México. Tesis de Tecnología y Gestión del Agua. Centro de Investigación y Estudios de Posgrado. Universidad Autónoma de San Luis Potosí. San Luis Potosí, México. 173 p.

[7] Romero, F. M., Armienta, M. A., Gutiérrez, M. E., & Villaseñor, G. (2008). Factores geológicos y climáticos que determinan la peligrosidad y el impacto ambiental de jales mineros. Revista internacional de contaminación ambiental, 24(2), 43-54.

[8] ELAW, 2010. Environmental Law Alliance Worldwide, 1st Edition July 2010. ISBN# 978-0-9821214-36, pp 110

[9] Davies, B. E. (1980). Applied soil trce elements (No. 631.82 D3).

[10] Singer, P. C., & Stumm, W. (1970). Acidic mine drainage: the rate-determining step. Science, 167(3921), 1121-1123.

[11] Masscheleyn, P.H., Delaune, R.D. & Patrick, W.H. 1991. Effect of redox potential and pH on As speciation and solubility in a contaminated soil. Environmental Science & Technology, 25, 1414–1418.

[12] Bissen, M., & Frimmel, F. H. (2003). Arsenic a review. Part I: occurrence, toxicity, speciation, mobility. CLEAN–Soil, Air, Water, 31(1), 9-18.

[13] Deschamps, E., Ciminelli, V.S.T., Weidler, P.G. & Ramos, A.Y. 2003. Arsenic sorption onto soils enriched in Mn and Fe minerals. Clays & Clay Minerals, 51, 197–204.

[14] Mitsunobu, S., Harada, T. & Takahashi, Y. 2006. Comparison of antimony behavior with that of arsenic under various soil redox conditions. *Environmental Science & Technology*, **40,** 7270–7276

[15] Davis, A., Ruby, M. V., & Bergstrom, P. D. (1992). Bioavailability of arsenic and lead in soils from the Butte, Montana, mining district.

Environmental Science & Technology, *26*(3), 461-468.

[16] Hudson-Edwards, K. A., Macklin, M. G., Curtis, C. D., & Vaughan, D. J. (1995). Processes of formation and distribution of Pb-, Zn-, Cd-, and Cu-bearing minerals in the Tyne Basin, northeast England: Implications for metal-contaminated river systems. *Environmental Science & Technology*, *30*(1), 72-80.

[17] Ackermann, J., Vetterlein, D., Kaiser, K., Mattusch, J. & Jahn, R. (2010). The bioavailability of arsenic in floodplain soils: a simulation of wáter saturation. *European Journal of Soil Science*, 61, 84–96.

[18] Labarthe-Hernández, G., Tristán-González, M., Aranda-Gómez, J.J., 1982, Revisión Estratigráfica del Cenozoico de la Parte Central del Estado de San Luis Potosí: Universidad Autónoma de San Luis Potosí, Instituto de Geología y Metalurgia, Folleto Técnico, 85, 205 p

[19] López Doncel, R. (2003). La Formación Tamabra del Cretácico medio en la porción central del margen occidental de la Plataforma Valles-San Luis Potosí, centro-noreste de México. Revista Mexicana de Ciencias Geológicas, 20(1).

[20] SMN, 2015. Servicio Meteorológico Nacional http://smn.cna.gob.mx/es/

[21] García Amaro, E. (2004). Modificaciones al sistema de clasificación climática de Köppen (No. C/551.6972 G3/2004).

[22] Salazar González, G. (2000). Las haciendas en el siglo XVII en la región minera de San Luis Potosí. San Luis Potosí, SLP, México: Universidad Autónoma de San Luis Potosí.

[23] Uribe, M. L. (2011). Doscientos años de Historia en San Luis Potosí: actores, prácticas e instituciones. Universidad Autónoma de San Luis Potosí, Facultad de Derecho. CENEJUS. San Luis Potosí, México

[24] Petersen, M. A., Libera, M. D., Jannas, R. R. Maynard, S. R. (2001). Geology of the Cerro San Pedro Porphyry-Related Gold-silver Deposit, San Luis Potosí, México. Society of Economic Geology. (8) 217-24

[25] Salminen, R., Tarvainen, T., Demetriades, A., Duris, M., Fordyce, F. M., Gregorauskiene, V., & Larson, J. (1998). FOREGS geochemical mapping field manual.

[26] Townsend, C. R. 1996. Concepts in riverecology: pattern and process in the catchment hierarchy. Archiv fur Hydrobiologie 113(Large Rivers Supplement):3–21.

[27] Salminen, R., & Tarvainen, T. (1997). The problem of defining geochemical baselines. A case study of selected elements and geological materials in Finland. Journal of geochemical exploration, 60(1), pp 91-98.

[28] Reimann, C., & Filzmoser, P. (2000). Normal and lognormal data distribution in geochemistry: death of a myth. Consequences for the statistical treatment of geochemical and environmental data. Environmental geology, 39(9), pp 1001-1014.

[29] Navas, A., & Machín, J. (2002). Spatial distribution of heavy metals and arsenic in soils of Aragon (northeast Spain): controlling factors and environmental implications. Applied Geochemistry, 17(8), pp 961-973.

[30] Chiprés, J. A., Salinas, J. C., Castro-Larragoitia, J., & Monroy, M. G. (2008). Geochemical mapping of major and trace elements in soils from the Altiplano Potosino, Mexico: a multi-scale comparison. Geochemistry: Exploration, Environment, Analysis, 8(3-4), pp 279-290.

[31] Bounessah, M., & Atkin, B. P. (2003). An application of exploratory data analysis (EDA) as a robust non-parametric technique for geochemical mapping in a semi-arid climate. Applied Geochemistry, 18(8), 1185-1195.

[32] Romero Guadarrama, J. A. (2011). Geoquímica de As, Hg, Pb y Zn y mineralogía en sedimentos superficiales de la Cuenca de drenaje del distrito minero El Triunfo, BCS, México.

9. Advances in sediment management

Session chairs: José Luis Arellano[1] and Silke Cram[2]
[1]Comisión Nacional del Agua Organismo de Cuenca Frontera Sur, México
[2]Departamento de Geografía Física, Instituto de Geografía de la UNAM, México

The soil erosion and sedimentation are processes related to hydrological processes and environmental degradation. The soil erosion-sediment relation affecting the environmental hydrological services. In tropical and subtropical regions, soil erosion and sedimentation processes are often associated with extreme rainfall and runoff events, soil conditions, steep land slopes, and management practices. All these factors are of very high importance in most Latin American countries. This thematic session includes measurement and evaluation of soil erosion, nutrimental losses in agricultural lands, sedimentation processes, and implementation of techniques of soil erosion and sedimentation control in watersheds, rivers, lakes, and wetlands.

PREVENTING LAND SUBSIDENCE: USING SEDIMENT AS A RESOURCE (USAR)

Verweij G.H.
Water Authority Schieland and the Krimpenerwaard, Rotterdam, Netherlands

ABSTRACT

The Regional Water Authority of Schieland and Krimpenerwaard (HHSK), The Netherlands will execute a pilot in 2018-2019 in which locally dredged sediment of high-organic composition will be upcycled, by blending it with other local waste products, e.g. green waste, animal manure and water purification deposits. This transforms the sediment into a valuable resource that can be used to elevate low-lying and sinking peatlands. Large areas of peatland in Dutch polders are compacting. This results in the last decades in sinking land elevation levels with big consequences for water management, bio diversity, economical and ecological utility, CO_2 emissions etc. HHSK dredges yearly approx. 150.000 m^3 from waterways at an average costs of €3.000.000. The HHSK pilot entails the first full-scale test of a promising concept, developed by Dutch engineers, called Topsurf [1]. The pilot investigates prevention of land subsidence of the low lying peatlands at risk of flooding as well as improvement of the soil quality with at the same time a positive effect on the reduction of sediment landfill, the costs of dredging, CO_2 output and disturbance for the environment (no/less transport needed).

Keywords: Sediment, Reuse, Land subsidence, GHG emissions, Nutrients

INTRODUCTION

Every year the Regional Water Authority of Schieland and the Krimpenerwaard remove about 150,000 m3 of sediment from their waterways. The annual costs for keeping the water household in good shape are around 3 million. We can save considerably on this if we use sediment as a useful resource and soil improvement of parcels in agricultural peat meadow areas.

We will demonstrate the applications of sediment as a resource during autumn of 2018 at three locations in the Krimpenerwaard. We process sediment with local manure and green waste into a soil improver, Topsurf. Research on behalf of the Dutch Ministry of Infrastructure & Environment has shown that the application is feasible [1]. Time for a first circular practical application in the Netherlands.

The three demonstration locations are fitted into the regular dredging works of Schieland and the Krimpenerwaard. Instead of removing sediment, manure and green waste at high costs, we will process this locally for soil improving and competing land subsidence due to oxidation of peat meadows. Direct cost savings for farmers and the Water Authority and in the longer term better for the environment.

The pilots are practical and concrete local projects, the knowledge and experience is widely applicable and applicable for projects worldwide. In the field of circular economy, prevention of subsidence, but certainly also in the area of flood protection.

METHODS

The approach to soil subsidence in peat meadow areas with an innovative product of dredging, manure and clippings requires cooperation in all directions. We investigate which composition the soil improver must meet. We do this Schieland and the Krimpenerwaard together with Topsurf-Netherlands (TSN) [2], knowledge institute Deltares, a number of dairy farmers from the Krimpenerwaard and interest groups.

For the pilot are 3 test locations available of 5-10 hectares each, which are private property. The total pilot are will consist of 25 hectares. The owners will make their land available for the project. On the test locations locally dredged sediment of high-organic composition will be upcycled, by blending it with other local waste products, e.g. green waste, animal manure and water purification deposits. This transforms the sediment into a valuable resource that can be used to elevate the low-lying and sinking peatlands as well as making a positive contribution to the manure problem, e.g. by the closing of the phosphate cycle. At the end of the pilot, the owner will continue using the areas (with Topsurf layer), of farm land and carry out the regular maintenance.

In the project we test the applicability and effects of Topsurf on soil conditions in different plots. With the use of renewable resources, we deliver an important contribution to a circular bio-based economy. This should result in measurable changes in the area of more efficient use of resources, reduced waste flows including volume of recycled

sediment and volume of saved primary raw materials.

In order to optimally measure the effect and various mixtures of Topsurf Land these compositions will be tested and compared.

The applications of sediment in this new mixture of Topsurf Land should measurably result in more efficiency in the use of resources (less volume of waste, volume of recycled sediment, volume of saved primary raw material). These changes are permanent. If the (local) partners will continue applying this circular approach as part of their regular way of working, it is to be expected that more similar results will be realised in the future.

RESULTS

The first results from the pilot are expected in the spring of 2019. The pilot in the Krimpenerwaard is the first circular application in which we process three waste streams - sediment, manure and green waste - into a locally applicable product. We reduce waste flows and we tackle the problem of soil subsidence in our peat meadow areas. Land subsidence that has major consequences for water management and use of the area. We focus on soil improvement and contribute significantly to the reduction of CO2 emissions.

Indirectly there are even more costs to save and benefits to mention. The application of Topsurf as soil improver should lead to less use of artificial fertilizer € 200 to 300/kg) and reduction of transport movements for waste disposal. Part of the pilot project is the development of the business case to value and further specify the direct and indirect effects of this new product.

Using the pilot project, we monitor the new application and develop business models and tools that water and area managers need to apply this circular approach in practice.

This pilot aims to contribute to the objective of HHSK: “dry feet and clean water” and besides we compensate land subsidence and are able to structurally improve the soil quality. Also, direct costs and time for dredging activities will reduce considerably as well as the indirect costs because of less transport and nuisance for the environment. Besides, the CO2 emission will be reduced conform the HHSK Corporate Social Responsibility policy.

DISCUSSION

Dredging is a never-ending obligation of water managers, as the deposit of sediments in waterways always continues. At present waterway managers are not yet investing in sediment upcycling, as these are new, unprecedented technologies. This USAR pilot “Blending organic sediments with green and agricultural waste for soil elevation and improvement”, is an essential step to break the ground for the wider uptake of this concept. This pilot will demonstrate the general feasibility and roll-out potential of sediment upcycling in real-life conditions to waterway managers

ACKNOWLEDGEMENTS

The project is a result of further development and innovation. For years we have been processing clean sediment as much as possible in our own area. In recent years, we have used geotextile tubes for the dewatering of sediment to use it for soil reinforcement and raising.

The pilot project is part of the international USAR project. Within USAR we work together with five partners from England, Belgium and France to develop new, smarter, cheaper and more sustainable applications for dredging sludge. With this, sediment must eventually end up in the circular economy and receive a positive value.

As lead partner, HHSK gratefully acknowledges the contributions of our USAR involved partners.

REFERENCES

[1] Agentschap NL (2010) Compensation ground decrease and guaranteeing water maintaining in peatland by applying Topsurf

[2] Deltares et al. (2013) *Feasibility Study Topsurf Krimpenerwaard*

THE EFFECT OF TREATED SEDIMENTS ON SELF-COMPACTING MORTARS PROPERTIES USING DESIGN OF EXPERIMENTS

Safhi Amine el Mahdi [1], Rivard Patrice [2], Benzerzour Mahfoud [3] and Abriak Nor-Edine [4]
[1, 3, 4] IMT Lille Douai, University of Lille, France; [1, 2, 4] University of Sherbrooke, Canada

ABSTRACT

A very significant quantity of sediments are dredged all over the world. Many previous studies demonstrate that this materials can be used as a cementitious supplementary material. In this paper, the raw sediments were dried, sieved, and thermally treated in order to eliminate organic matter and activate the minerals. The physical, chemical, and mineralogical properties were determined for the raw and treated sediments. Blended self-compacting mortars were formulated by substituting partial Portland cement with sediments. The compressive and bending strength, and dynamic modulus of elasticity were tested for different deadlines (7, 28, 60, and 90 days). The fresh properties of the pastes were investigated as well. The results shows that sediments can be used as a replacement of cement up to 12% of the volume of cement while maintaining the fresh compactibility properties.

Keywords: Sediments, Self-Compacting Mortars, Design of Experiments, Waste Management

INTRODUCTION

The accumulation of sediments at the bottom of harbors is natural phenomenon that causes impediments to marine works. A big quantities of sediments are dredged every year: nearly 300 m^3 in the United States [1], another 300 m^3 in Europe and around 50 m^3 just in France [2].

The evolution of the environmental regulations makes the dredging operations more and more complex. Recently, this material is no longer considered as a waste. Previous studies demonstrated the possibility of reusing this material in the field of civil engineering.

In the last decade, dredged sediments have been considered as a waste, but they are no longer stored or landfilled and they can be used as a commercial material in many cases. Several studies have investigated the use of dredged sediment as civil engineering materials : brick [3–5], lightweight aggregates [6,7], supplementary cementitious material for blended cement [8–10], Portland clinker [11], stabilized road-base [12–14], paving blocks [15,16], etc.

On the other hand, the Self-compacting concrete is recent generation of concrete which their use is continues to expand. The formulation of SCC is relatively expensive compared to the ordinary concrete. In order to reduce their price, many studies worked on reusing by-products in SCC like: rubber granules, clay and pozzolans, granite powder, glass powder [17], marble powder [18], and lightweight recycled aggregates [19].

The aim of this paper is to report a study where sediments were used as an admixtures in SCC, more precisely as a replacement of cement. The design of experiments was used to maximize the amount of the incorporated treated sediments.

MATERIALS CHARACTERISATION

Sediment sampling

The used sediments were extracted from the harbor of Dunkirk which located in north of France (Fig. 1). About 90% of the 6.5 million m^3 dredged sediments each year, is immersed directly in the sea.

Fig. 1 A view of the Harbor of Dunkirk (France)

The raw sediments contains a high amount of water, organic matter as well. In order activate the chemical elements and to eliminate in hazardous content, the sediments were dried in a stove of 105°C until a constant mass. Then crushed and sieved by using 120µm sieves. The outcome of this physical treatment were thermally treated at 850°C for one hour. Figure 2 shows the change of sediments after each step of the process.

Fig. 2 Process of sediments treatment

Physical characterization

Table 1 summarizes the main physical characteristics of the raw and the treated sediments. It shows that there is an increase in the specific density after the treatment generally due to the elimination of the organic content, and a high decrease of the specific area due to the agglomeration of the particles after the calcination.

Table 2 summarizes the physio-mechanical properties of the grey cement CEM I 52.5 N. The distribution of particles is given in Fig. 3. The median size D_{50} is equal to 15.9 µm for the cement, and went from 5.9 to 9.8 µm for the raw and treated sediments respectively.

Table 1 Physical properties of sediments

Characteristics	RS	TS
Water content (%)	100.2	0
Specific density (kg/m³)	2520	2851
Organic matter content 450°C -3h (%)	6.73	-
Organic matter content 550°C -2h (%)	9.85	1.50
Atterberg limit IP (%)	12.1	-
Value of blue of methylene (g /100g de MS)	1.18	-
Specific area BET (m²/kg)	3652	2335

Table 2 Physio-mechanical properties of cement

Characteristics	CEM I 52.5 N
Specific density (kg/m³)	3176
Apparent density (kg/m³)	1165
Specific area BET (m²/kg)	914
Normal consistency	27
Initial set (min)	193
Final set (min)	428
Compressive strength (MPa)	
7 days	52.5
28 days	64.8

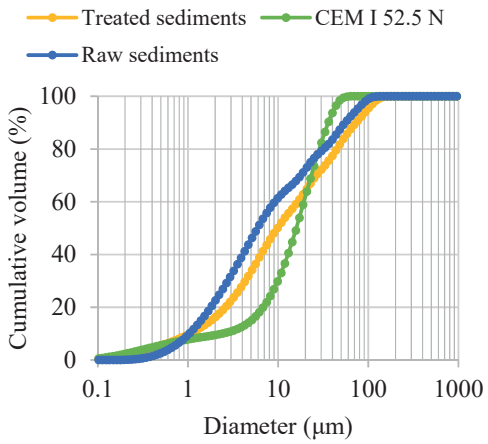

Fig. 3 Particle size distribution of cement, raw and treated sediments

Chemical and mineral characterization

Table 3 and Table 4 summarize the results of X-ray Fluorescence (XRF). It shows a huge presence of Oxygen, Silicon, Calcium, and Iron. Previous studies on the same material founded nearly the same results [20]. The change of the composition confirm the effect of the thermal treatment.

Table 3 Chemical elements of materials (%)

Elements	RS	TS	CEM
O	42.2	48.7	40.4
Na	1.7	1.3	0.5
Mg	1.5	1.4	0.7
Al	5.2	5.1	2.7
Si	16.6	15.8	7.6
P	0.2	0.2	0.2
S	2.1	1.5	1.7
Cl	1.6	1.1	0.1
K	1.3	1.5	0.6
Ca	18.1	14.5	42.3
Ti	0.3	0.3	0.2
Mn	0.1	0.1	Traces
Fe	8.7	8.1	2.7
Zn	0.1	0.1	0.1

Mineralogical analysis was performed on raw and treated sediments by using X-ray diffraction (XRD), the results are presented in Fig. 4. It shows a dominant presence of Quartz, Hematite, and Calcite which confirm a major crystalline modification.

The results of the thermogravimetric analysis (TGA) are presented in Fig. 5. It shows that after 700°C there is a decomposition of calcite carbonate

and a decrease in the TG percentage which confirms the choice of the calcination temperature.

Table 4 Oxide composition of materials (%)

Oxide	RS	TS	CEM
SiO_2	35.5	33.8	16.2
Al_2O_3	9.82	9.63	5.10
MgO	2.49	2.32	1.16
Fe_2O_3	12.4	11.6	3.86
CaO	25.3	20.3	59.2
Na_2O	2.29	1.75	0.67
K_2O	1.57	1.81	0.72
P_2O_5	0.46	0.46	0.46
SO_3	5.24	3.75	4.24
TiO_2	0.50	0.50	0.33
MnO	0.13	0.13	Traces
ZnO	0.12	0.12	0.12

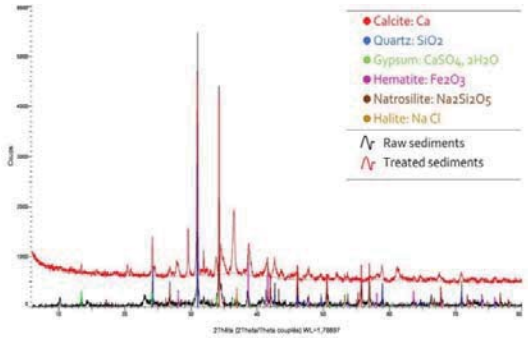

Fig. 4 XRD analysis on raw and treated sediments

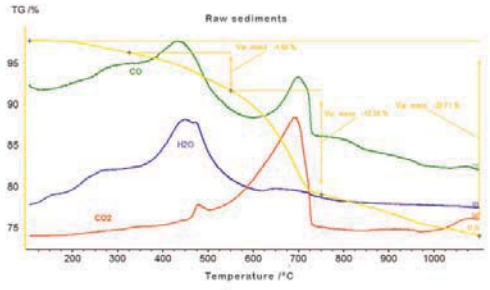

Fig. 5 TGA analysis on the raw sediments

MORTAR FABRICATION

Specimen preparation

More than ten self-compacting mortars formulations were prepared based on different percentages of treated sediments as replacement. In compliance with the provisions of EFNARC, the content of powder in the mixtures was 380 kg/m³. The amount of cement, treated sediments, treated sediments-to-cement-ratio (S/C), and water-to-binder-ratio (W/B) varied from 300 to 500 kg/m³, 0 to 250 kg/m³, 0 to 0.5 and 0.25 to 0.55, respectively. The content of the superplasticizer has been kept at 2% of the dry extract to the cement mass.

After the preparation of the mixtures, made according to NF EN 196-1 standard, the mini-slump flow and Marsh flow were measured on pastes. Then, all the specimens were cast in a prismatic mold and stored in a 90% R.H. room at an average temperature of 20 ±2°C. After 24 hours, the specimens were then removed from the mold and placed in water at 20 ±2°C. The hardened properties of the mortar specimens were determined at the end of 7th, 28th, 60th and 90th days.

Mixture design approach

The mixture design was based on three parameters. Since the aim is to substitute cement by sediments, the focus was on the water-to-binder-ratio, the sediments-to-cement-ratio, and the volume-of-binder-to-total-volume-ratio.

The used central composite design was based on a quadratic model:

$$y = \beta_0 + \sum_{i=1}^{k} \beta_i x_i + \sum_{i=1}^{k} \beta_{ii} {x_i}^2 + \sum_{i} \sum_{j} \beta_{ij} x_i x_j + \varepsilon$$

Where y is the material response (predicted), x_i and x_j are the coded values of the independent variables W/B and S/C respectively. i is the linear coefficient, j is the quadratic coefficient, β is the regression coefficient, k is the number of factors, and ε is the random residual error. The variables in RSM model and their range of variation are presented in Table 5.

Table 5 Variables and range of variation

Symbols	Range of variation		
Variables	-1	0	+1
W/B	0.25	0.40	0.55
S/C	0	0.25	0.50

RESULTS AND DISCUSSION

Fresh properties of SCC mortars

The effect of W/B and S/C on the mini-slump flow and Marsh flow are depicted in Fig. 6-7. The fluidity decreases with the presence of a low W/B ratio and vice-versa, compared to S/C ratio which has a less effect on the T_{flow}. The presence of sediments has no effect on the D_{flow}. The workability

increases depending only on the variation of W/B ratio. It is the main parameter.

Based on the results of previous studies as well as on the experimental tests on different combinations [cement-sediment] with a fixed percentage of S_P (2%), the acceptable minimum spreading diameter for the mini-slump flow is 165 mm, and 20 seconds for the Marsh-cone flow. The objective is to maximize D_{flow} and minimize T_{flow}.

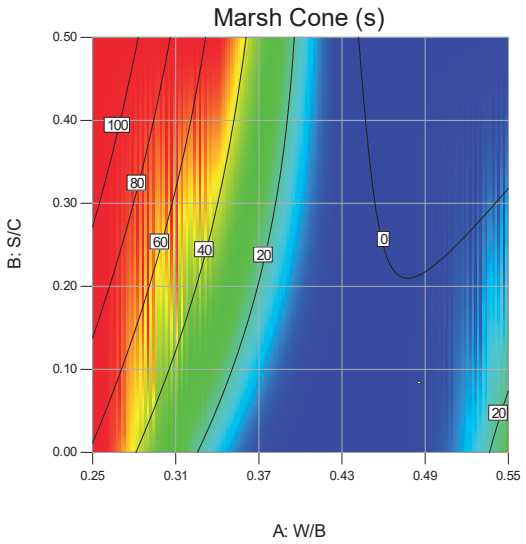

Fig. 6 Interaction effects of variables on the T_{flow}

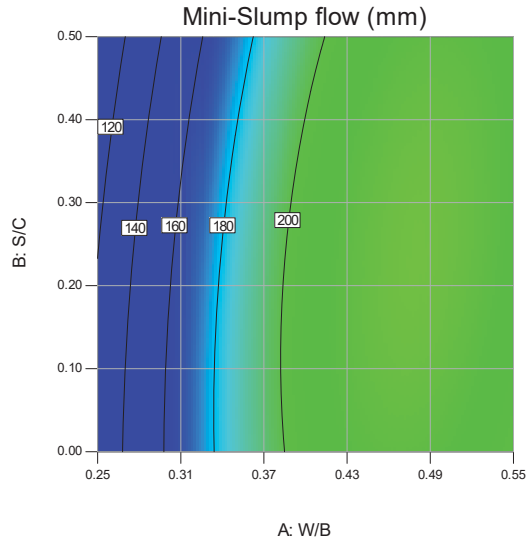

Fig. 7 Interaction effects of variables on the D_{flow}

Mechanical strength

Figure 8 and Fig. 9 were obtained using NCSS software for statistics and graphic analysis. It represents 3D Scatter Plots of the evolution of the bending and compressive strength over days. It shows that the amount of incorporated sediments decreased the mechanical strength. For a fixed W/B ratio, the compressive and bending strength decrease immediately with the growing of S/C ratio.

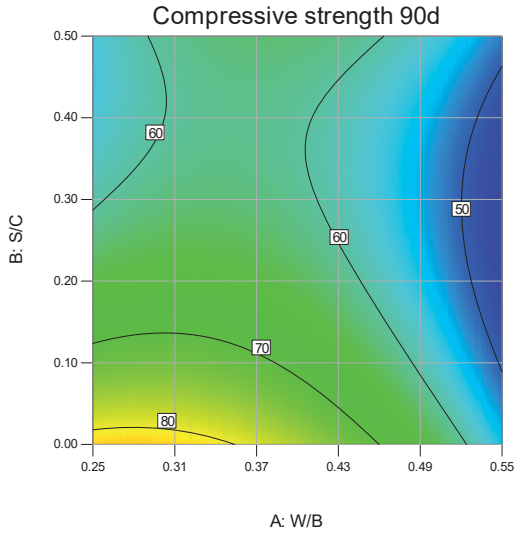

Fig. 8 Interaction effects of variables on the fc

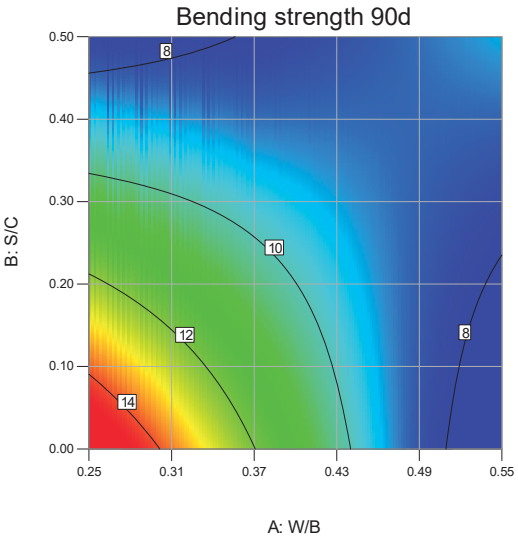

Fig. 9 Interaction effects of variables on the ft

Dynamic modulus of elasticity

Figure 10 shows the variation of E_{dyn} on the different mixtures; it shows that the incorporated sediments have a negative effect on E_{dyn}, as well as on the water-to-binder ratio. The addition of sediments decreased the E_{dyn} from 54 GPa to 47 GPa for S/C=0.5. The observations made for the mechanical strength are then confirmed.

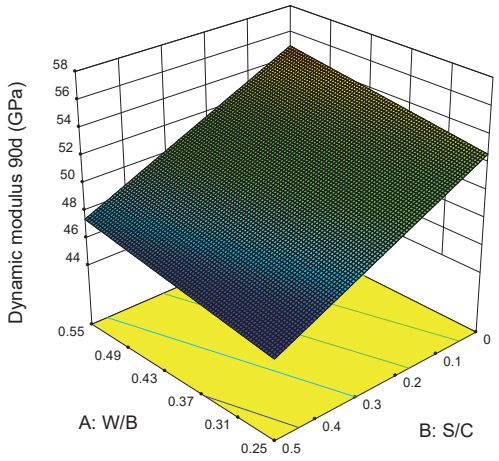

Fig. 10 3D plot for the interaction effects of variables on the E_{Dyn}

MIXTURE OPTIMISATION

Using Design-Expert software, and in order to optimize the mixtures, the overlay plot approach was used to simulate the optimization of one or more factors. The allowable goals are to keep a factor into a specific range, to maximize or minimize a factor, to target or to determine a specific value of factors. Each limits for any factor are related to a weight that determine the importance of the goal. A specific criterion for each variable and responses were chosen as in Fig. 11.

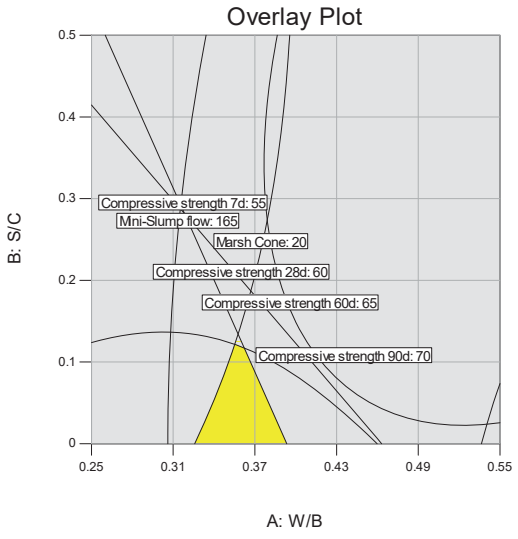

Fig. 11 Variation of desirability function for multi-objective optimization on W/B and S/C for a fixed binder dosage of 380 kg/m³

CONCLUSIONS

Facing the enormous quantity of dredged sediments around the world every year, and the increasing need of construction materials, this paper aimed to develop a SCC based on treated sediments as a replacement of part of the cement, which represent environmental and economic benefits. Through the carried out experiments, it was possible to identify the optimum dosage of treated sediments in a SCC.

The obtained results led to the following conclusions:

- The implementation of treated sediments in SCC as a substitute of cement can be used up to 12%.
- Treated sediments demonstrated their effectiveness as a supplementary cementing material, also they combine an important economic and mechanical performance ratio.
- The incorporation of the treated sediments doesn't have a significant effect on the fresh properties of the SCC pastes.

Furthermore, the replacement of a part of the cement by sediments will have a considered environmental and economic impact due to the high energy and costs of cement production.

ACKNOWLEDGEMENTS

This work was financed by the research funds of the IMT Lille Douai and the University of Sherbrooke through a PhD grant.

REFERENCES

[1] M. Benzerzour, M. Amar, N.-E. Abriak, New experimental approach of the reuse of dredged sediments in a cement matrix by physical and heat treatment, Constr. Build. Mater. 140 (2017) 432–444. doi:10.1016/j.conbuildmat.2017.02.142.

[2] M. Amar, M. Benzerzour, A.E.M. Safhi, N.-E. Abriak, Durability of a cementitious matrix based on treated sediments, Case Stud. Constr. Mater. (n.d.). doi:10.1016/j.cscm.2018.01.007.

[3] A. Mezencevova, N.N. Yeboah, S.E. Burns, L.F. Kahn, K.E. Kurtis, Utilization of Savannah Harbor river sediment as the primary raw material in production of fired brick, J. Environ. Manage. 113 (2012) 128–136. doi:10.1016/j.jenvman.2012.08.030.

[4] Y.-L. Wei, C.-Y. Lin, S.-H. Cheng, H.P. Wang, Recycling steel-manufacturing slag and harbor sediment into construction materials, J. Hazard. Mater. 265 (2014) 253–260. doi:10.1016/j.jhazmat.2013.11.049.

[5] Y. Xu, C. Yan, B. Xu, X. Ruan, Z. Wei, The use of urban river sediments as a primary raw material in the production of highly insulating brick, Ceram. Int. 40 (2014) 8833–8840. doi:10.1016/j.ceramint.2014.01.105.

[6] S. Brakni, N.E. Abriak, A. Hequette, Formulation of artificial aggregates from dredged harbour sediments for coastline stabilization, Environ. Technol. 30 (2009) 849–854. doi:10.1080/09593330902990154.

[7] H.-J. Chen, M.-D. Yang, C.-W. Tang, S.-Y. Wang, Producing synthetic lightweight aggregates from reservoir sediments, Constr. Build. Mater. 28 (2012) 387–394. doi:10.1016/j.conbuildmat.2011.08.051.

[8] M. Benzerzour, M. Amar, N.-E. Abriak, New experimental approach of the reuse of dredged sediments in a cement matrix by physical and heat treatment, Constr. Build. Mater. 140 (2017) 432–444. doi:10.1016/j.conbuildmat.2017.02.142.

[9] T.A. Dang, S. Kamali-Bernard, W.A. Prince, Design of new blended cement based on marine dredged sediment, Constr. Build. Mater. 41 (2013) 602–611. doi:10.1016/j.conbuildmat.2012.11.088.

[10] E. Rozière, M. Samara, A. Loukili, D. Damidot, Valorisation of sediments in self-consolidating concrete: Mix-design and microstructure, Constr. Build. Mater. 81 (2015) 1–10. doi:10.1016/j.conbuildmat.2015.01.080.

[11] G. Aouad, A. Laboudigue, N. Gineys, N.E. Abriak, Dredged sediments used as novel supply of raw material to produce Portland cement clinker, Cem. Concr. Compos. 34 (2012) 788–793. doi:10.1016/j.cemconcomp.2012.02.008.

[12] W. Maherzi, M. Benzerzour, Y. Mamindy-Pajany, E. van Veen, M. Boutouil, N.E. Abriak, Beneficial reuse of Brest-Harbor (France)-dredged sediment as alternative material in road building: laboratory investigations, Environ. Technol. (2017) 1–15. doi:10.1080/09593330.2017.1308440.

[13] W. Maherzi, F.B. Abdelghani, Dredged Marine Sediments Geotechnical Characterisation for Their Reuse in Road Construction, Eng. J. Eng J. 18 (2014) 27–37. doi:10.4186/ej.2014.18.4.27.

[14] M. Miraoui, R. Zentar, N.-E. Abriak, Road material basis in dredged sediment and basic oxygen furnace steel slag, Constr. Build. Mater. 30 (2012) 309–319. doi:10.1016/j.conbuildmat.2011.11.032.

[15] I. Said, A. Missaoui, Z. Lafhaj, Reuse of Tunisian marine sediments in paving blocks: factory scale experiment, J. Clean. Prod. 102 (2015) 66–77. doi:10.1016/j.jclepro.2015.04.138.

[16] L. Wang, T.L.K. Yeung, A.Y.T. Lau, D.C.W. Tsang, C.-S. Poon, Recycling contaminated sediment into eco-friendly paving blocks by a combination of binary cement and carbon dioxide curing, J. Clean. Prod. 164 (2017) 1279–1288. doi:10.1016/j.jclepro.2017.07.070.

[17] S. Nunes, A.M. Matos, T. Duarte, H. Figueiras, J. Sousa-Coutinho, Mixture design of self-compacting glass mortar, Cem. Concr. Compos. 43 (2013) 1–11. doi:10.1016/j.cemconcomp.2013.05.009.

[18] K.E. Alyamac, E. Ghafari, R. Ince, Development of eco-efficient self-compacting concrete with waste marble powder using the response surface method, J. Clean. Prod. 144 (2017) 192–202. doi:10.1016/j.jclepro.2016.12.156.

[19] A.A.A. Hassan, M.K. Ismail, J. Mayo, Mechanical properties of self-consolidating concrete containing lightweight recycled aggregate in different mixture compositions, J. Build. Eng. 4 (2015) 113–126. doi:10.1016/j.jobe.2015.09.005.

[20] H. Azrar, R. Zentar, N.-E. Abriak, The Effect of Granulation Time of the Pan Granulation on the Characteristics of the Aggregates Containing Dunkirk Sediments, Procedia Eng. 143 (2016) 10–17. doi:10.1016/j.proeng.2016.06.002.

ENVIRONMENTAL ASSESSMENT OF TWO SEDIMENTS REUSED IN ROAD ENGINEERING: FEEDBACK AFTER ONE YEAR OF MONITORING THROUGH THE SEDIMED PROJECT

USTACHE Aurélien [1], REBISCHUNG Flore [1], TESSIER Erwan [2] and PIETERS Alain [3]
[1]INERIS, France; [2]NEO-SUD, France, [3]ENVISAN, France

ABSTRACT

Road engineering is one way for sediments to be reused and enter the circular economy, instead of being stored in landfill. The so-called "Guide Setra" [1] constitutes the French framework for reusing alternative materials in road engineering, including three kinds of road structures: coated (with an impervious layer), covered (with at least 30 cm of natural material) or uncoated and uncovered.

The Sedimed project investigated those three options, settling lysimeters (uncoated and uncovered) and building experimental road (coated) and landforms (covered), incorporating two marine contaminated sediments from the Toulon bay, France (QN and QC). Leachates were collected and sampled on these three experimental structures, and the pollutants (12 metals – As, Ba, Cd, Cr, Cu, Hg, Mo, Ni, Pb, Sb, Se, Zn – 3 anions – Cl^-, F^-, SO_4^{2-} – 16 PAH and 3 emerging pollutants detected in the sediments – DBT, TBT and DEHP), were analyzed on every sample, enabling the determination of the total released quantity of each pollutant on a L/S basis (ratio between the volume of water that percolated through the structure and the mass of sediment in the structure).

The total content of organic pollutants of QN would normally disqualify this sediment for road engineering, according to the "Guide Setra". Yet, only considering the potential impact on groundwater, the released quantities of pollutants are far from very protecting limits.

For both QN and QC, the anions content (Cl^- and SO_4^{2-}) exceeded the "Guide Setra" limits for some structures, indicating that the control of these parameters and the reduction of their global content during the lagooning period might be triggering the reusing options for marine sediments.

Those new data and knowledge is a contribution to the definition of a specific framework for reusing sediments in road engineering.

Keywords: Sediments, Road engineering, Environmental monitoring, Lysimeters, Experimental road, Experimental landform, Emerging pollutants

INTRODUCTION

The Sedimed project was conducted between 2009 and 2016 and contributed to develop new solutions for sediment management and valorization. During the project a soil and sediment treatment centrum (CPEM) was constructed in the Toulon harbour at La Seyne-sur-Mer where a separate R&D platform was established on which the full scale test plots where installed and followed up. The R&D project was financially supported by the ADEME, Toulon Provence Méditerranée, l'Agence de l'eau, Marseille Provence Métropole, le Conseil Régional PACA and Ministère de la Transition Ecologique et Solidaire. The project was coordinated by Envisan and the other partners were INERIS, Armines, Cerema, ERG and Colas. The coordination of the scientific partners was led by Neo-Sud.

During this project, two sediments from the Toulon Bay (QN and QC) have been extensively studied, analysed [3][4][5] and tested for reusing in road engineering, from an environmental and a geotechnical point of view.

.

FRAMEWORK

The "Guide Setra" was published in 2011 and aims at regulating alternative materials reusing in road engineering. Therefore, it considers three kinds of road structures: coated with an impervious layer (1), covered with at least 30 cm of natural material (2) or uncoated and uncovered (3). Depending on their total and their leachable content in pollutants, alternative materials can or not be used in a road structure.

Figure 1 presents the flow chart defined by the "Guide Setra", with three levels of investigations: (1) total analysis and leaching test, (2) percolation test, and (3) lysimeters or pilot scale tests. A specific guidance document [2] covers this third level of investigations.

For the third investigation level, the "Guide Setra" provides two types of reference values.

The first one aims at preventing from a chronic pollution, and is to compare to the cumulated amount of released pollutants during the whole duration of the pilote test. Therefore, "initial limits" defined for the same list of pollutants as those

mentioned for leachate analysis at the first level – need to be converted into a specific limit for every pilot, with the equation 1:

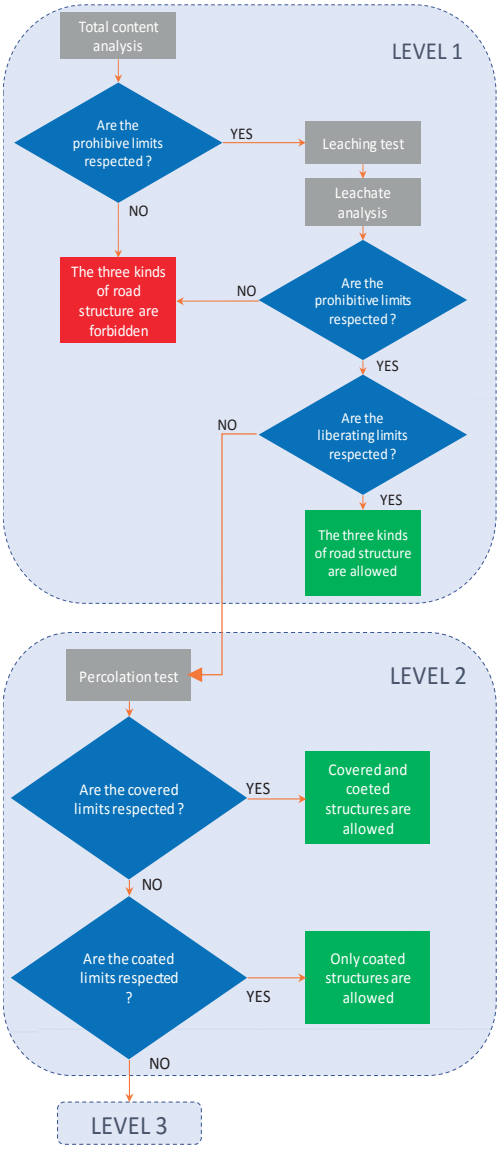

Fig. 1: « Guide Setra » flow chart for the reuse of alternative materials in road engineering

$$\textbf{\textit{specific limit}} = \textbf{\textit{initial limit}} * \min\left(d\,;\,\frac{P_{eff}}{P_{ref}}\right) \quad (1)$$

where :
- the specific limit is given in mg/m²
- the initial limit is given in mg/m²/y
- d is the duration of the experimentation and is given in y
- P_{eff} is the effective rainfall during the experimentation and is given in mm
- P_{ref} is the yearly reference effective rainfall, and equals 100 mm/y for a coated structure and 300 mm/y for a covered or an uncoated and uncovered structure.

The second one aims at preventing from an acute pollution, and is to compare to the highest concentration in pilot eluates.

The pollutants list defined by the "Guide Setra" is supposed to be completed for each material, depending on its specificities. Considering that sediments accumulate a huge variety of contaminants, defining an appropriate list of pollutants and their associated limits remains a major challenge.

In the Sedimed project, PAH and 3 emerging pollutants were analyzed at the third level. When possible, an initial limit was proposed for those contaminants, based on regulatory values for drinking water production, without considering any dilution factor that is a very conservative assumption.

MATERIAL AND METHODS

Investigated sediments

Two sediments from the Toulon Bay were chosen, representing two different types of materials with a different grain size distribution, organic matter and contamination content. The QN sediments are fine sediments extracted from a historically polluted zone whereas the coarser QC sediment was supposed to be cleaner. Both sediments were sieved and have been dewatered by lagooning before being incorporated in the experimental road and landform.

Organic pollutants scope

In addition to the "Guide Setra" pollutants, 16 PAH and 3 emerging contaminants were analyzed in the two sediments: DBT, TBT and DEHP. Those three pollutants were found both in total content and in sediments leachate.

Environmental characterization of sediments

Leaching tests were performed according to the NF EN 12457-2 standard.

Percolation tests were performed according to the NF CEN/TS 14405 standard.

Three lysimeters were set up in Aix-en-Provence (Fig 1). Their individual total surface was 5 m², but the inner section corresponding to the percolation area was 4.14 m². A collecting system was installed to retrieve the percolation and the run-off waters (from the inner and the outer parts of the lysimeters). Leachate collection and analysis started in June 2015 and was stopped in May 2016 (Table 1).

Table 1. Lysimeter technical data

Lysimeter parameters	Witness	QN	QC
Material	Sand	Alternative material	
Settled on...	24/03/2015	22/04/2015, 06/05/2015	12/06/2015
Mat. height in lys. (m)	1	0.96	1.06
Mat. weight (kg)	5909	5538	8177
Water content (%)	0	33.5	15.6
Dry matter weight (kg)	5909	3685	6900
Dry matter in the inner section (kg) (= « S »)	4893	3051	5714

Fig. 2. Three lysimeters and their percolate collecting system

Three experimental landforms were built on Envisan platform in La Seyne-sur-mer (Fig 2) in November 2015, and covered with a 30 cm layer of land. Leachate collection and analysis started in November 2015 and was stopped in September 2016 (Table 2).

Three experimental road sections were also built on the same place (Fig 3.) in October 2015, incorporating 30% of sediments in the base layer of the road. Leachate collection and analysis started in November 2015 and was stopped in September 2016.

Table 2. Land form technical data

Landform parameters	Witness	QN	QC
Material	Sand	Alternative material	
Mat. weight (kg)	120,320	108,000	130,00
Water content (%)	8.8	23.9	8.5
Dry matter weight (kg)	109,730	82,188	118,950
Landform surface (m^2)	91.17	99.95	105.72

Fig 3. Pilot landform and its percolation collecting system

RESULTS AND DISCUSSION

Level 1

For QC, the alternative material respects all the prohibitive limits from the “Guide Setra” first level, and even liberating limits, except for Cl^-, SO_4^{2-} and soluble fraction. However, anions levels might be reduced with a more efficient sediments preparation, that would allow QC to be used in any type of road engineering. Concerning the road material, pollutants leaching is globally reduced, because of the smaller amount of sediments in the

material (30%), apart from Ba, Cr, Cu, Mo, Pb – yet, their leaching levels stay under the Setra limits for any type of road engineering. Soluble fraction increases in road material, probably due to the lime and cement input (with an impact on pH too) and exceeds the prohibitive limit of 60,000 mg/kg.

For QN, level 1 results show exceedance of the limit for TPH, TOC, PAH and PCDD/F. Anions leaching is also problematic. According to the « Guide Setra », QN cannot be used in road engineering without any further treatment.

Level 2

For QC alternative material, all limits are respected, apart from Cd. Yet, the indicated value (<0.28 mg/kg DM) is calculated with the detection limits, and is probably not reached. All limits are also respected by the road material.

For QN alternative material, Cl^- and SO_4^{2-} stay beyond covered and/or coated limits, confirming the conclusions of the first level. Cd results presents the same artefact than QC. Concerning the road material, pollutants leaching increases for Ba, Cu, Mo, Ni and Pb, and exceeds the limits for the last three elements. This phenomenon might be linked to the pH increase, determining factor for some metal leaching and/or to a contribution from other components incorporated to the road material.

Level 3 – lysimeters

Exceedance of the limits are observed for Cd, Ni, Zn, Cl^- and SO_4^{2-}. The high quantification limits mainly contribute to the total release of cadmium. The high levels of Ni (Fig 4) might be attribute to the lysimeters steel corrosion and not to the sediment loading, as evidence by the evolution of Ni concentration in eluates after an anti-corrosion system was set up in February 2016.

No reason has been found to explain the high emission level of Zn in both QC and QN, that had not been noticed at the previous steps.

Cl- and SO42- remain a major issue for those two sediments, both from an acute and a chronic point of view. The TBT acute limit exceeding for the witness lysimètre can probably be attributed to an analytical mistake or a contamination.

Level 3 – landforms

In a covered scenario as landforms, only anions remain problematic for both QN and QC, even if the second level of the "Guide Setra" approach would have allowed to use QC in a covered system.

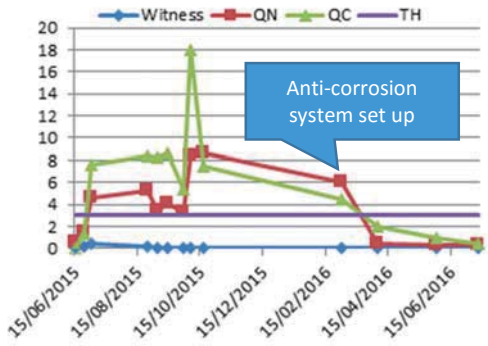

Fig. 4: Evolution of Ni concentration in lysimeters eluates

Level 3 – roads

In a coated scenario as roads, no exceeding is observed for QC, in coherence with the two first levels of the "Guide Setra" approach, with the exception of TBT, which is yet probably linked to an analytical mistake or a contamination, considering that the witness road also exceeds the chronic and acute limits for TBT.

For QN, the Cl^- content remains an issue even in this kind of structure.

Focus on organic pollutants

Apart from TBT, no organic pollutant exceeds the chosen limits, that were derived from regulatory values for drinking water production, without considering any dilution factor, that is a very conservative assumption.

CONCLUSION

All levels of the French current framework for environmental evaluation of alternative materials in road engineering have been applied on two contaminated marine sediments from the Toulon Bay. The main experienced difficulty in applying this approach was the lack of a methodology to determinate the organic pollutants to measure and the limits to associate. However, the results tend to show that the impact on groundwater is manageable for these contaminants.

Another limit of the "Guide Sétra" framework was the reference rainfall used for limits calculation, that was far from being reached after one year of monitoring in Aix-en-Provence and La Seyne-sur-mer. This led to consider very low limits at the third level. To avoid such a discordance, three solutions can be proposed: (1) simulate rainfalls on lysimeters, landforms and road structures, (2) make the monitoring last longer than a year, or (3) propose

new ways to calculate specific limits, adapted to the local climate.

Yet, for both QN and QC, the main concern remains anions emission, with Cl- and SO42-. Therefore, developing a framework for another way of valorization for marine sediments, where anions release would not be problematic, such as maritime works materials, could enhance marine sediments reuse.

From a scientific point of view, the constitution of a national database collecting and tracking the sites where alternative materials are used might be a way to ensure that other exposure scenario could be evaluated in the future, even after the end-of-life of those road engineering projects.

ACKNOWLEDGEMENTS

The R&D project was financially supported by the ADEME, Toulon Provence Méditerranée, l'Agence de l'eau, Marseille Provence Métropole, le Conseil Régional PACA and Ministère de la Transition Ecologique et Solidaire.

REFERENCES

[1] Acceptabilité de matériaux alternatifs en technique routière – Evaluation environnementale, Sétra, 2011

[2] Acceptabilité de matériaux alternatifs en technique routière – Aide à la mise en œuvre du niveau 3 de caractérisation environnementale – Volet N°1 : les essais lysimétriques et plots expérimentaux, Cerema, septembre 2015

[3] Etude sur les contaminants émergents dans les eaux françaises – Rapport de l'étude prospective sur les contaminants émergents dans les eaux littorales de la métropole et des DOM, IFREMER, octobre 2014

[4] Etude sur les contaminants émergents dans les eaux françaises - Résultats de l'étude prospective 2012 sur les contaminants émergents dans les eaux de surface continentales de la Métropole et des DOM, INERIS, Juin 2014, DRC-13-136939-12927A

[5] Diagnostic de la contamination sédimentaire par les métaux/métalloïdes dans la Rade de Toulon et mécanismes contrôlant leur mobilité, Thèse de chimie de l'environnement, E. TESSIER, mai 2012

SOME REASONS TO VALORIZE DREDGED SEDIMENTS

Semcha Abdélaziz [1], Marouf Hafida [2], Abbou Mohamed [1]
[1]Faculté des Sciences et de la Technologie, Université Ahmed Draia d'Adrar, Algérie
[2]Faculté des Sciences et de la Technologie, Université Abdelhamid Ben Badis de Mostaganem, Algérie

Abstract

The needs of building materials, in many countries are increasingly important for all infrastructures. The natural layers of the raw materials are not enough anymore, and we often witness over exploitations implying the fatal environmental repercussions. In another way, big volume of sediments results from dredging which are considered until now as wastes.

The valorization of dredged materials in the fields of the Civil Engineering, represents a true measure of assumption of repercussion responsibility related to the storage and the throwing away of these materials by decreasing constraints on other traditional materials.

The destiny of extracted matters by dredging was objective of many researches, but the real applications of the results remain limited. Our investigations are related to the treatment and the application of the sediments is also included in the processes design and building materials. However, we try to consider them as raw materials and not as waste. In this work, we try to present the essence to the understanding of valorization process of solid fine fraction of sediments.

Keywords: Sediment, Material, Reactivity, Brick, Cement, Mortar

INTRODUCTION

In Algeria, large projects of the construction industry have led to a strong aggregates demand over the period 2006-2009. The estimation of aggregates needs for this period is 445 MT (Million Tonnes) of which 159MT was composed of sand. The sand deficit is estimated at 60 MT. The demand of aggregates was in the same order in the new 2009-2013 program, and may be same in the new program. The shortage of natural aggregates and the increasing demand by the construction industry have encouraged the research of alternative sources. The new sources of materials can be the sea or/and dams dredged sediments, so new value can be added to sediments.

The destiny of extracted matters during dredging of the silted up works (ports, dams, channels…) was the object of many research, but the concrete applications of the results remain still weak

Our investigations during the last decade related to the treatment and the application of the sediments of Oran port taken in a basin accosting ships of strong tonnage where the depth must be maintained in spite of sedimentation.

Every year, big quantities of materials are extracted by dredging but their future use and storage cause problems that remain posed. In the same way, many dams built in Algeria with great cost to be used for storage and transfer of water, witnessed their lifetime being reduced by silting phenomena.

Our investigations on the sediments extracted by dredging were concretized by the use of these materials as raw materials in the processes of building materials, clothes and industry.

We present in what follows some reasons to valorize these new matters given by dredging and we try to give the essence to understand some processes of valorization of the fine solid fractions resulting particularly from dredging:

Fig. 1 Example of silted dam (Fergoug)

ALGERIAN WEATHER AND EROSION PHENOMENA

The north of Algeria in particular, and North Africa as all, have a semi-arid climate, characterized by seasonal raining in the form of short-time showers, where the concentration time rarely exceeds half an hour. The large volumes of showers dig the soil by tearing off the solid particles that will then be transported by the rivers (wadis).

Fig. 2 Example of silted dam (Fergoug: we see that the basin is silted)

Fig. 3 Exemple of rejection dredged sediments of Fergoug's dam

DEMOGRAPHY AND DEVELOPMENT IN ALGERIA

According to the highest population growth in the world, and the industrialization policy chosen by Algerian managers since independence, as well as the influence of new techniques of building materials, accentuated by the urgent need for housing, the Algerian government is currently forced to return to traditional materials and use all forms of raw material resources in the manufacture of building materials to meet a need as important as pressing.

The raw earth building materials that have existed since ancient times, and possess a wide variety of techniques, are expected to return as a solution to enrich the building sector.

The techniques of clay-based compressed clay bricks offer adaptation to the arid areas as desert environment. This meets the criteria of sustainability in these areas. Thus, all the means offered by local materials must be exploited knowing that the geographical situation of Algeria is among the regions most affected by erosion.

It is the phenomenon of erosion that impoverishes fertile lands.

According to [1], Algeria is among the countries most dangerously threatened by erosion and siltation of storage dams.

The Algerian reservoirs are mainly intended for the storage and regulation of water resources, are all the more vulnerable as they are disadvantaged in terms of the river regime related to rainfall in the form of showers of high intensity and short durations.

Despite the lack of studies on this particular phenomenon in the regions of North Africa, much effort has been made by the water services in the fight against siltation. It should be noted that Algeria is a pioneer in this problem and its singular experience in the world makes it a real referee to the experiences for other countries [2].

Historic of sedimentation and extracting sediments

Among the many control methods tested on Algerian dams, namely: the reforestation of watersheds, the elevation of dikes, the construction of settling dams and the use of the dam with hunting waves, dredging operations were also used and big quantities of sediments has been carried.

The most regions affected by the erosion and siltation of are the dams. Algeria is among the most disadvantaged countries. Some dams have been completely abandoned; others are currently causing great concern and will eventually perish if urgent action is not taken. Reference [1] gives for the year 2000 a cumulative volume of more than 650 million m3 of sediments found in 98 dams of Algeria. The author adds that the singular experience of Algeria places it at the forefront worldwide in the fight against siltation. Several control methods were used namely: the reforestation of watersheds, the elevation of dikes,

Today, the situation is not better, but the managers have taken mind that it is important to take seriously all the faces of the dredging problems. In this way some dams are cured and their sediments are storage in special managed areas in order to reuse the extracted sediments, in example more than 6 million cube meter of dredged sediments from Bouhanifia's dam located in west of Algeria, are stored in managed basins upstream the dam.

But the most question rest: how to do with all these materials? Now we answer that is really possible to transform these sediments from waste to raw materials.

Listing of some reasons to reuse the extracted matters,

We enumerate the most reasons to valorize the dredged sediments/

- The needs of building materials progresses year after year, because of the big progress of demography in Algeria.
- The exploitation of the "natural stratums" implies fatal repercussion in environment.
- The big quantities of dredged sediments are simply lost on the proximal environment
- Many mistakes are made when rejecting sediments downstream the dam
- The population of Algeria is young, and the needs to building houses and other works is a serious preoccupation of the managers and the political.
- The needs of water are big and it is important to build storage works as dams.
- Sediments are carried also from marine areas (ports and estuaries)

In other way we can list some ways of valorization sediments in order to preserve environment and to reduce the cost of dredging operations:

- As aggregates for concrete and mortars
- As fine mineral powders to use in cement manufacturing
- In road engineering
- In agriculture processes, as stabilization of sand soils
- To store water for agricular and farming processes
- In artisanal confections
- As ceramic manufacturing
- As traditional bricks to built

APPLICATION OF SEDIMENTS IN SOME PROCESSES

Activation by calcination

Pozzolanic activity:

The pozzolanic activity comprises all the physical and chemical reactions produced when water comes into contact with the lime, the silica or the alumina. These reactions pass through a preliminary solution, as it is accepted that the transfer of matter takes place in a dissolved state [4].

In fact the dissolution involves ionisation followed by diffusion of the ions in the aqueous phase, where the hydrates are going to form and develop.

The "reactivity" of the aqueous phase will be defined in these conditions as being the "quantity of material that is made into solution calculated per surface unit and time unit". The least stable clay structures are the most soluble, therefore the most reactive. This metastable crystalline structure is acquired by calcination.

The concept of substituting a certain amount of pozzolanic fired silt in Portland cement which hydration frees the lime (Candlot salt) allows binders to be obtained with similar or even better characteristics than those of Portland cement alone. In fact the free lime is fixed by the added artificial pozzolana.

On the face of it, the hydration of CEM I frees 20% to 25% of its weight in lime and the substitution of pozzolana or fired silt is envisaged in the same proportion [3].

Results and prospects of the pozzolanic process:

- The pozzolanic effect of the fired silt was thus confirmed.
- The 30% mixture of fired silt and 70% cement is doubly interesting: not only was the same resistance as that of the cement on its own achieved solely by storing it for longer time, but also the pozzolanic effect of the fired silt was confirmed.
- This study has been carried out on samples of mixed pastes binder. Similar studies can be proposed on mortar and concrete.
- The study of the durability of these products under harsh conditions should be permitted in order to characterise the domains of use for this composite based on cement and fired silt.
- Using silt given from dredging dam in any technologic process contribute to extend the life of the dam and contribute to protect the environment and not to look at silt as waste but as first matter.

Dredged Sediments as materials in tunnel construction

Tunnel lining structures can be exposed to the water infiltration and also to high temperatures. During heating, researchers agree that the dehydration of cement based materials causes shrinkage and that leads to crack initiation and propagation.The dehydration of components of the cement matrix occurs from 110°C up to approximately 550°C-600°C. Other studies on this topic have shown that the spelling can occur at temperatures between 190-300°C. The objective is to determine rheological, mechanical and durability properties of mortars made with Dredged Sediments.

Methodology of reuse dredged sediments: Dredged marine sediments have high salt levels, due to marine water content, that exceed salinity levels expected in cement based materials. The soil

leaching method and the natural decantation are considered economic methods to reduce the initial water and salts content of marine sediments: After 23 days of treatment, the water content of DS decreased to, a low value equal to about 7%. After this treatment, the chemical analysis was carried out and we note a decrease of the amount of chlorides (CL^-) and sulphates.

The following conclusions are given by results of this investigation [2].

The complete characterization of dredged sediments of the port of Oran unpolluted by heavy metals had shown the presence of hydrocarbon and salts. The methodology developed for the salts treatment and the dewatering of the DS is efficient in laboratory conditions. It was noted that in order to obtain the same consistency, the cement made with dredged sediment in partial substitution of raw sand, needed more water than this made with coarse sand. The unconfined compressive strength in mortars with sediments is similar to that normal mortar.

The addition of 20% or 25% of DS increases the ability of mortars to resist to the acid attacks which confirms the improvement of Rrc.

After heating, it can be seen that residual strengths of mortars (normal, and with sediments) are similar. Thus, we can conclude that the dredged of the port of Oran in the vicinity of the unpolluted zone by heavy metals can be substituted partially for the sand used in the manufacture of cement based materials. The addition of 20% or 25% of sediments increases the ability of mortars to resist to the acid attacks.

Hydrothermal Treatment of sediments

A new process in conception of a calcareous-silica brick, using the dredged sediment of bouhaifia's dam was made with cement or lime as activating product.

The main shedules of this process are:

-Braking and cleaning the sediment
-Dosage of the mixtures
-Mixing at dry and humid states
-Moulding and pressing of samples
-When samples aquiere suffisant stongly: we make them in autoclave (hydrothermal bath) sinse 6, 15 and 24 hours. After living in the hydrothermal bath (température 135°C and 330 Kpa of pressure), the samples were tested. The mechanical results were good, and we try to test the durability of these stones in agressive middle.

Self-compacting concrete based on dredged sediment

The concrete for self-compacting properties, needs a big quantity of fine materials to make the fresh concrete fluid. Our idea for conception this concrete was to use pozzolanic product. This product has been Bouhanifia's calcined sediment: So, in first the pozzolanic product give the fluid property and after hydration the pozzolanic reactions add more resistance for this concete. These experiments are very long and needs a biq number of formulations to find the better one. To reduce the number of experiments Belghomari, (2012). have used the « plans of experiments » methode for four factors: cement, artificial pozzolana, superplastifiant and watter.

At last, one matrix of only 40 experiments was made using the Nemrod logiciel and statistical methodes. A self compacting past was formilated using the Bouhanifia's calcined sediments.

CONCLUSION

The phenomena of silting basins or marine silting are natural phenomenon and the big quantities of solid matters change the bottoms of the sea or dams. So dredging works are used to restore the first activity of these works. The managers are confronted to the becoming of the big quantities of matters considered until now as wastes.

There is no way to take to use of these sediments when they are just lost in environment and the consequences are dramatics. The better way (and the alone way) to save the environment of future generations is to consider the sediments given by dredging as raw material and to looke for real and ecological applications witch existe realy. Just puting trust on researchers who propose many solutions.

REFERENCES

[1]. Remini B. 2002: «Quantification du transport solide dans le bassin versant d l'oued Isser. Application à l'envasement du barrage de Béni Amrane». 2ème CMEE Alger Oct. 2002

[2].Fatiha KAZI AOUAL et All: International Mechanical Engineering Congress "ASME 2013": DREDGED Sediments as Materials in Tunnel Construction", San-Diego USA.

[3].Abdélaziz SEMCHA et All : International Mechanical Engineering Congress "ASME 2013": "Reuse silt given from dredging dam in order to protect the environment", San-Diego USA.

[4].PERA J.: « Liants pouzzolaniques de synthèse » (Synthesising pozzolanic binders), interministerial programme, Laboratoire des matériaux minéraux (Mineral Laboratory), INSA Lyon (France) September 1988.

[5].Ilham BELGHOMARI, (2012) : « Conception d'un béton auto-plaçant à base de sédiments en utilisant les plans d'expérience » thèse de magister, ENPOran (ex ENSET), 2018

VALORISATION OF FINE DUNE SAND IN ASPHALT CONCRETE

Akacem Mustapha[1], Mekerta Belkacem[1], Zester Rachid[2], Moulay Omar Hassan[1] and Abbou Mohamed[1]
[1] Faculté de la Technologie, Université Ahmed Draïa Adrar, Algérie; [2] IMT Lille Douai, France

ABSTRACT

The south region of Algeria is characterized by a wide surface, a scattered population and a very small ratio of road length per habitant. To allow the development of agricultural, industrial and touristic activities between different cities in the south of Algeria, it is necessary to maintain and to develop the road infrastructure. However the development of these infrastructures necessitates the use of huge amount of certified aggregates from quarries which is not available in the vicinity of the need. For these raisons, in the framework of sustainable development, a strategy which consists in using local materials like fine sediments (dune sand) and other types of material is engaged.

In this paper the main concern is about the development of a material including fine dune sand for wearing layer in the road construction.

The semi grained bituminous concrete BBSG intended for wearing layers, known by the name BB 0/14, generally is prepared by mixing two components: aggregates and bitumen. The design of this material considers several criteria related to one hand to the aggregates, namely mechanical characteristics, shape, and cleanliness of stones, the blue value of the fine, the particle size of the mixture (% passing through), the choice of the bitumen grade and mechanical performance as well the water resistance of asphalt concrete 0/14.

The present work aims to study the influence of the substitution of the fraction 0/3 mm of the crushed sand (usually used in this type of materials) by fine dune sand, on the mechanical performance including Duriez and Marshall Stability and water resistance.

Keywords: Sand Dunes, Formulation, Mechanical Performance, Duriez and Marshall Stability, Water Resistance.

INTRODUCTION

The aggregates used in the wearing courses in regions of the great south of Algeria, have resistance to shocks or attrition far exceeding the values required by the specifications in force [1], [2].

A preliminary experimental study carried out on aggregates from the Adrar and Ghardaïa region showed that the values of LA; MDE are just at the recommended thresholds for wearing courses [2], [3].

Subsequently, formulation trials of asphalt concrete with aggregates (classes: 0/3 - 3/8 - 8/15) will be carried out without the addition of dune sand to compare their mechanical performance (Durièz and Marshall saturation) to those obtained with bituminous mixes from formulations containing sand dune levels.

This procedure is very useful in order to highlight the possibility of the exploitation of sand dunes in the Saharan road construction.

The study highlights an optimal value of adding dune sand.

CHARACTERISTICS OF MATERIALS

Gravels

For gravel, it is the classes 3/8 and 8/15 used in Algeria for semi-grinded bituminous concretes that are studied. The percent flattening (AP), Los Angeles (LA), Dicro Deval in the presence of water (MDE), cleanliness, and absolute density values are shown in Table 1.

Table 1 Characteristics of the aggregates – classes 3/8 and 8/15

Aggregates	LA (%)	MDE (%)	AP (%)	P (%)	Density (kN/m3)
3/8	21	22	10	1,1	2,65
8/15	19	21	9	0,7	2,67

The values of the intrinsic characteristics of the two classes of gravel used in the preparation of semi-gritted bituminous concrete (BBSG) 0/14 are acceptable with regard to the Algerian specifications [2] which respectively recommend a threshold of 25 and 20% for the results of Los Angeles (LA) and Micro Deval (MDE) trial in the presence of water. The manufacturing characteristics - flattening coefficient and cleanliness also revealed acceptable values: AP $\leq$ 20%; P $\leq$ 2% [2]. The summary chemical analysis of the gravel used is provided in Table 2.

Table 2 Chemical compositions of the aggregates and crushed sand

Minerals	CaCo3	NaCl	SO3	Insoluble	Others
%	93	0,03	0,01	1,3	5,66

According to the chemical composition, the aggregates have a high carbonate content.

Sands

For sands, class 0/3 crushed sand and dune sands are considered. The values of absolute density, sand equivalent and fines are given in Table 3.

Table 3 Characteristics of the crushed sand and sand from dunes

	Density (kN/m3)	E.S.	% < 0.08 (mm)
Crushed sand 0/3	26.9	81	22
Sand from dunes 0/0.4	27.1	85	4

The crushed sand has an ES much greater than 60 and contains an acceptable fine level [2], [4].The sand of the dunes has a narrow grain size (0 / 0.4) and the percentage of fines shows a poverty of fine elements <0.08 mm. Figure 1 shows the particle size curves of the gravel used (classes 3/8 and 8/15) and the sands (crushed sand 0/3 - dune sand 0 / 0.4).

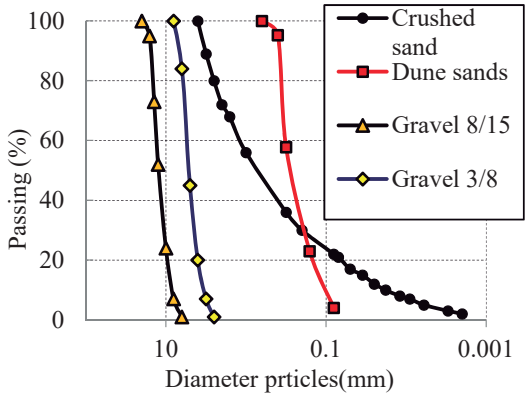

Fig. 1 Particle size curves of gravel and sand used

Binder

The binder used is a 40/50 bitumen. The bitumen used is brought back from the NAFTAL unit (Ghardaïa in south of Algeria).

STUDY OF THE MIXTURE

Granular composition

On the basis of the particle size obtained from the different fractions studied, a mixture was prepared in such a way that it was inscribed in the reference zone 0/14 [2], [4]. The percentages retained are the following:
- 45% of the 0/3 class;
- 25% of class 3/8;
- 30% of the class 8/15.

The Particle size curve of the mixture of the three classes 0/3 - 3/8 and 8/15 without the addition of dune sands is given in Fig. 2.

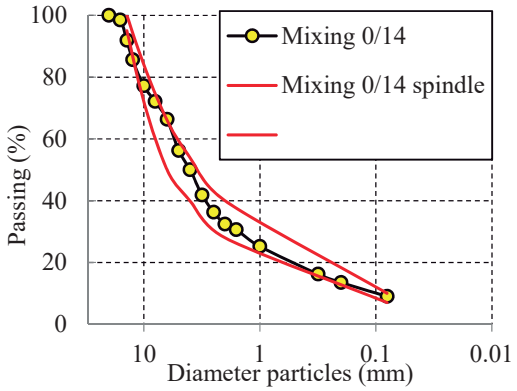

Fig. 2 Particle size curve 0/14 without adding dune sands

Binding dosage calculation

The bitumen content represents the ratio of the mass of binder to the mass of dry aggregates expressed as a percentage, for which the following formula is used [4]:

$$\text{Content bitumen (\%)} = K.\ \alpha.\ (\Sigma)^{1/5} \quad (1)$$

Σ: conventional surface area:

$$\Sigma = 0.25G + 2.3S + 12s + 135f \quad (m^2 / kg) \quad (2)$$

With:
G: proportion of elements greater than 6.3 mm;
S: proportion of the elements between 6.3 and 0.315;
s: proportion of the elements between 0.315 and 0.08;
f: proportion of elements less than 0.08 mm;
K: richness module that characterizes the average thickness of the film around the aggregates;
α: coefficient intended to take into account the real density of the aggregates (MVRg), if this differs from 2,65 KN / m3, one uses the following formula:

$$\alpha = 2.65 / MVRg \quad (3)$$

The binder dosage is calculated with three wealth modules, so we will have three formulations. For each formulation, the real density of the bituminous mix is calculated from the densities of the components by the following formula [2]:

$$MVR = 100 / [(\% G1 / \rho 1) + (\% G2 / \rho 2) + (\% G3 / \rho 3) + ... + (Pb / Db)] \quad (4)$$

% Gi: percentages of granular fractions;
Pb: percentage by weight of the bitumen;
ρi: densities of aggregates;
Db: density of the bitumen.

TESTS ON MIXTURES

In order to verify the mechanical properties of the mixes, blends were made in the laboratory and subjected to the following tests:

- DURIEZ test (Normal for BB0 / 14);
- MARSHALL test with 50 shots.

Duriez Test

This test makes it possible to evaluate the water resistance of an asphalt mixture by measuring the drop in compressive strength, after a 7-days immersion period.

In our case, for a bituminous concrete 0/14, and in accordance with the standard (NF P 98-251-1) [5], 12 cylindrical specimens of diameter 80 mm, 1000 grs are manufactured for each specimen, statically compacted with a force of 6KN (Fig. 3);

Fig. 3 Static compaction: 6 KN

- 2 test pieces for the measurement of bulk density by hydrostatic weighing (Fig. 4);
- 5 specimens for preservation without immersion at 18 ° C,
- 5 test pieces intended for immersion preservation at 18 ° C (Fig. 5);

Fig. 4 Preparation for hydrostatic weighing

Fig. 5 Conservation after demolding

After 7 days of storage, the simple compression test is carried out (Fig. 6)

Fig. 6 Static compaction: 6 KN

The average compressive strength of the five specimens kept in the air is measured: R,

The average compressive strength of the test pieces preserved with water is measured:

- We calculate the ratio r / R.

Marshall Test

The test consists in making test pieces of hydrocarbon mixtures by impact compactor according to a determined process [6].

The specimens of bituminous mixes of cylindrical shape with a diameter of 101.6 mm and a target height of 63.5 mm are molded using impact compactor.

The standardized compaction lady is constituted of a sliding mass on a guide rod and falling freely on the foot of the lady in direct contact with one of the faces of the mixture contained in the mold. The number of strokes per side (compaction energy) is generally taken as 50 (Fig. 7). The minimum number of test pieces per tested formula is 4.

Fig. 7 Compaction (50 shots per side)

After compaction and before demolding, the test pieces must be kept at least 4 hours at room temperature, then, the apparent density of each specimen is determined.

After having immersed the test pieces in water at 60 ° C for 40 minutes (Fig. 8), the diameter compression test is carried out using a constant compression deformation press 50 mm / min, equipped with a device to measure the effort during the test (Fig. 9).

The results of the test are as follows:

Marshall S stability which corresponds to the maximum resistance of the specimen expressed in (KN),

Creep F, which represents the sagging of the test piece according to its vertical diameter at the moment of rupture, expressed in (mm),

The Marshall quotient which represents the S / F ratio between the stability S and the creep F expressed in (KN / mm).

Fig. 8 Immersion for 40 min at 60 °C

Fig. 9 Diameter compression crushing

Test Results

Three mixtures with different binder dosages for the hot mix grade (BB 0/14) were made.

The results obtained for Duriez and Marshall tests are summarized in Tables 4 and 5. The formulation retained is given in Table 6.

Table 4 Duriez test performance

Reference asphalt mix (without dune sands)		Algerian specifications
Dry compressive stress (Mpa) R	8.84	> 7 MPa
Compressive stress after immersion (Mpa) r	7.54	
r/R	0.85	> 0.75

Table 5 Marshall test performance

Reference asphalt mix (without dune sands)		Algerian specifications
Stabilité value (kN)	13.88	> 10.5
Flow value (mm)	1.35	< 4

Table 6 Formulation of the asphalt mix (in %)

Sand 0/3 (%)	Gravel (%) 3/8	Gravel (%) 8/15	Bitumen 40/50 (%)	Density (kN/m³)
45	25	30	6	22.1

STUDY OF MIXTURES WITH SAND DUNES

The study of the effect of sand dune incorporation in the formulation of asphalt concrete 0/14 for the wearing course is done by partial substitution of crushed sand with increasing rates of sand dune ranging from 10% up to 40% .

For each dune sand addition rate (10, 20, 30 and 40%), three mixtures were studied in the laboratory with different bitumen contents in order to choose the formulation that gives the best performance. Table 7 groups the stopped formulations.

Table 7 Asphalt mixes with various percentage of sand from dunes (in%)

Dune sands (%)	Sand 0/3 (%)	Gravel (%) 3/8	Gravel (%) 8/15	Bitumen 40/50 (%)	Density (kN/m³)
10	38	20	32	5.9	22.3
20	28	20	32	5.8	22.6
30	15	20	35	5.7	23.0
40	10	20	30	5.6	23.3

For each of the formulations stopped, Table 8 gives the compressive strengths of the test specimens after one week of storage in air and water as well as the values of the ratio (r / R) reflecting the water resistance of bituminous mix.

Table 8 Results of Duriez test on asphalt mixes with various percentages of dune sands

Dune sands (%)	0	10	20	30	40
Dry compressive stress (Mpa) R	8.84	9.10	9.10	9.10	8.84
Compressive Stress after immersion (Mpa) r	7.54	8.32	8.58	7.80	7.02
r/R	0.85	0.91	0.94	0.86	0.79

Note: R> 7 Mpa; r/R > 0.75 (according to Algerian specifications).

The Marshall stability values as well as the creep - of the Marshall test carried out on specimens of each optimal formulation - are presented in Table 9

Table 9 Results of Marshall test on asphalt mixes with various percentages of dune sands

Dune sands (%)	0	10	20	30	40
Stability Value (kN)	13.5	14.0	13.6	11.1	9.3
Flow value (mm)	1.35	1.36	1.38	1.42	1.44

Note: Flow value < 4 mm (according to Algerian specifications).

DISCUSSION

Firstly, classical mechanical tests for the characterization of asphalt mixes (Marshall, Duriez) showed that the addition of dune sand modified the performance levels while remaining in conformity with the Algerian normative requirements.

Referring to Table 7, it can be seen that the incorporation of dune sand up to a rate of 30% improves the compressive strength (stability Duriez), and that for both modes of conservation: dry and in immersion (respectively 3 and 12%), Fig. 10.

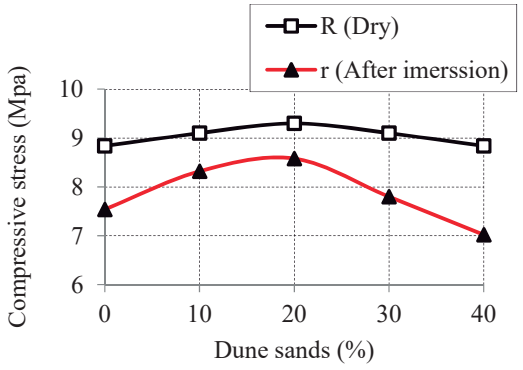

Fig. 10 Evolution of the stability Duriez according to the % sand dunes

Similarly, for the water resistance characterized by the immersion / compression ratio, it shows an encouraging improvement of up to 20% in the addition of sand dunes, Fig. 11.

This is explained by the fact that the addition of sand up to at these rates contributes to the decrease of the voids while increasing the compactness and the actual density of the bituminous mix.

Beyond this value, the effect becomes negative and the mechanical performances tend to degrade.

Regarding Marshall stability, and despite the fact that the latter is decreasing as we add dune sand to the formulation of 0/14 bituminous concrete, we see that it remains in the standards (≥ 10.5 kN) to a dune sands percentage of 20%, Fig. 12.

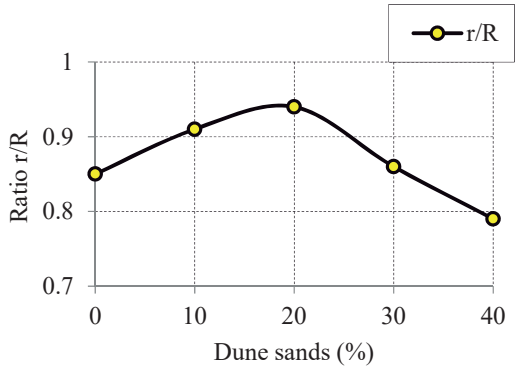

Fig. 11 Effect of adding dune sands on the water resistance of asphalt mix

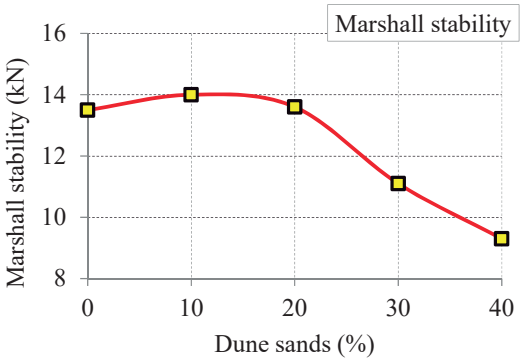

Fig. 12 Influence of adding dune sands on Marshall stability

CONCLUSION

Asphalt mix production always aims to choose the optimal formulation that ensures good mechanical performance.

Several factors influence the final result of a formulation, namely the particle size of the mixture and the different mechanical characteristics, intrinsic and manufacturing characteristics of the aggregates on the one hand, and the choice of the bitumen class and its content.

In this work, we have chosen to study the influence of the incorporation of dune sand into the granular composition of bituminous mix by replacing crushed sand (class 0/3) with dune sands and this in a gradual way.

Taking into account the results of this study in terms of mechanical performance, and in order to valorize this local material available in abundance in the south of Algeria, one can retain for formulation of the 0/14 bituminous concrete a formulation containing a rate of dune sands up to 20%.

ACKNOWLEDGEMENTS

This work was done in two laboratories: Central Laboratory of Public Works (LCTP) at Algiers and the Laboratory of Public Works in the South (LTPS) at Ghardaïa.

I would like to express my sincere thanks to the administrative and technical managers for the help provided during the trial period, as well as the mobilization of technicians and equipment for the smooth running of the work.

REFERENCES

[1] M.H. Ben Dhia (1998), Quelques particularités de l'utilisation du sable de dune en construction routière en milieu Saharien, Bulletin des laboratoires des ponts et chaussées - 213 - Janvier-février 1998 - réf. 4159 - PP. 33-42

[2] CTTP, Alger (2004). Recommandations sur l'utilisation des bitumes et des enrobés bitumineux à chaud, fascicule2 (La formulation), 37 p.

[3] M.N. Fatani, A.M. Khan, (1990), Improvement of Dune Sand Asphalt Mixes for Pavement Bases. Eng. Sci.. Vol. 2, pp. 35-47.

[4] SETRA – LCPC (1984). Mémento des specifications de chaussées. Lyon, 67p.

[5] NF P98-251-1 Septembre 2002 Essais relatifs aux chaussées - Essais statiques sur mélanges hydrocarbonés - Partie 1 : essai Duriez sur mélanges hydrocarbonés à chaud.

[6] EN 12697–34, bituminous mixtures – test methods for hot mix asphalt – Part 34: Marshall test, 2012

THE RELATIONSHIP BETWEEN ORGANIC MATTER CONTENT AND THE IMMEDIATE BEARING INDEX OF DREDGED SEDIMENTS

HAMOUCHE Fawzi and ZENTAR Rachid
Department of civil engineering, Institute Mines Telecom Lille Douai, France

ABSTRACT

Dredged sediment listed as waste according to European classification and available in important quantities. The valorisation of dredged sediments for road construction could constitute an interesting solution. However, in the road construction sector, the material engineering characteristics needed vary and depend on the road category, the layer of the road structure and the type and amount of binders used. Dredged sediments consist of a mineral phase; an organic phase (in various forms) and a liquid phase generally water. The presence of organic matter (OM) in sediment, even in low amounts, can affect the physical, chemical and mechanical behavior.

This paper investigates the relationship between the organic matter content and the immediate bearing index (IBI) of dredged sediments. For this purpose, a specific methodology to reconstitute samples with different amounts of organic matter content is proposed. The IBI measured on the compacted specimens in the CBR mould using the normal Proctor test and modified Proctor test.

Keywords: Sediment, Organic Matter, Relationship, Immediate Bearing index, Mechanical behavior.

INTRODUCTION

The practice of dredging generates large volumes of sediments, which in some cases may contain contaminants. In France each year about 50 million m^3 of sediment are dredged [1]. These dredged sediment volumes are traditionally dumped at sea, a few kilometers from the coast, in controlled areas. However, due to the harmful induced by dumping at sea, new management solutions are explored over the world.

The civil engineering uses over 400 million tons of material (aggregates, sand, cement) of which 96% are of natural origin [2]. The materials reserves are becoming unusable or inaccessible for various reasons: too expensive operation, risk of impact on the environment, integrated with urban areas or located in classified or protected sites. In this context, the dredged sediment, listed as waste according to European classification, could constitute a new resource in the context of sustainable development.

In France, the road construction sector is a greatest consumer, with a yearly consumption of about 200 million tons of material per year. Hence, the valorisation of dredged sediments for road construction could constitute an interesting solution. However, in the road construction sector, the material engineering characteristics (IBI) needed vary and depend on the road category, the layer of the road structure and the type and amount of binders used. On the other hand, the dredged sediment generally consists of a mineral phase, an organic phase (in various forms) and a liquid phase (water). It generally agreed that the presence of organic matter (OM) in sediment, even in small amounts, acts to the detriment of their engineering qualities [3]–[9].

In road applications, under different practice guidelines developed in different countries, the use of organic materials is limited to organic matter content between 2% to 4% for road pavement material and between 5% and 7% for use as embankment materials. The argument used for the limitation of the amount of organic materials is generally linked to the evolution of organic matter with time, which was supposed to increase the void ratio and hence the compressibility of the material. In this context, as a first step in the valuation of dredged sediments in road construction, it was considered important to explore to what extent organic matter affects the mechanical parameters and to some extent predict the relative evolution of the parameters in the used material.

This paper investigates the relationship between the organic matter content and the immediate bearing index (IBI) of dredged sediments. For this purpose, a specific methodology to reconstitute samples with different amounts of organic matter content is proposed. The IBI measured on the compacted specimens in the CBR mould using the normal Proctor test and modified Proctor test.

MATERIALS AND METHODS

In this study, the sediments are dredged from Dunkirk Harbour, which is the third most important French harbour. By its location, it is ranked as the seventh port on the northern European side, extending from Le Havre to Hamburg. The dredged sediments were stored in barrels at the laboratory after a period of natural dewatering on site (Fig. 1). In the laboratory, samples from different barrels are mixed to constitute a representative sample.

Fig. 1 Samples preparation of the dredged sediment

The organic material used for specimen enrichment was an industrial compost (C) with high organic matter content (Fig. 2). Prior to mixing with sediment for enrichment, a specific procedure of preparation was developed in order to ease the mixes.

Fig. 2 Samples preparation of the organic material

Prior to the preparation of the different samples, dredged sediment and the organic material were first oven dried at low temperature to eliminate water in the materials. The organic material was pulverized in a blender to reduce the size of its constituents, and then the obtained material was sieved at 400 µm to remove coarse particles (Fig. 2). The sediment with an initial organic matter content of 5.6 % was mixed with the compost (with an organic matter content of 42 %) in the required proportions to prepare samples with organic matter content ranging from 7.5% to 15%, with a step of 2.5%. The choice of theses ranges of values will also make it possible to analyse whether the limits set in terms of organic matter content in road works material is correlated to a significant change in the engineering properties.

The experimental program undertaken in the framework of this research enclose physical properties determination of raw materials as the reconstituted samples used in the study. The physical properties consists in the determination of grain size distribution curves, the organic matter content, the specific gravity for each material. The tests are undertaken according respectively to the test standards (ISO 13320, 2009; XP P94-047, 1998; NF P94-054, 1991). To assess the impacts of organic matter content on the immediate bearing index, the experimental program enclose compaction tests according to test standard (NF P94-093, 2014) and the measurement of immediate Bearing Index (IBI) following to test standard (NF P94-078, 1997).

RESULTS AND DISCUSSION

The physical properties of the raw dredged sediment, the reconstituted samples (S7.5%, S10%, S12.5%, S15%) and the organic material (C) are evaluated. Figure 3 illustrates the grain size distribution tests results of the different samples. The addition of organic material to the dredged sediment drives the grain size distribution curves to the right. This result is predictable as the grain size distribution of the organic material is coarser than that of the dredged sediment.

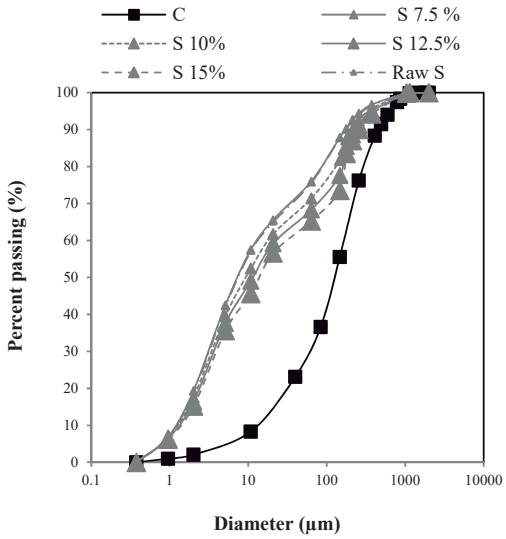

Fig. 3 Grains size distribution of the reconstituted samples

From the obtained results (Fig. 3 and Table 1), the material classification according to the French soil classification system dedicated to road works [10], all reconstituted dredged sediments belong to F class grouping organic soils. Three from experimented dredged sediments are classified as F_{11} subclass for low organic soils (Raw S, S7.5%, S10%) and two to F_{12} subclass for high organic materials (S12.5%, S15%). From grain size distribution point of view, overall sediments are classified as fine soils, called class A, characterised by a maximum grain size (Dmax) less than 50 mm

and fine percentage greater than 35 %. Subclass is then determined by clay activity (MBV) and sediment plastic nature (PI). Thereby, all reconstituted dredged sediments belong to A_1 subclass.

Table 1 Physical properties of the reconstituted samples

Parameters	Raw S	C	S7.5 %	S10 %	S12.5 %	S15 %
OMC (%)	5,6	42.2	7.5	10	12.5	15
Gs	2.57	1.92	2.55	2.51	2.45	2.52
IP (%)	12	-	11	14	12	12
MBV (g/cm^3)	0.93	-	1.09	1.39	1.38	1.49

The IBI is conventionally defined to evaluate the suitability of a soil or a man-made material to withstand heavy machinery moving over it. The Fig. 4 shows the IBI results of compacted samples according to the normal Proctor test. It can be observed that the IBI curves are shifted down. Similar trend is observed for the IBI curves for the compacted samples using modified Proctor test (Fig. 5). The Fig. 6 shows the IBI results at optimum Proctor compaction for the studied samples, it can be seen that when the organic matter range increase from 5 to 15%, the highest organic matter sample loses about 60% of its bearing capacity relative to that of the raw specimen compacted in the CBR mould, according to the Proctor test with standard effort. For the specimens compacted in the CBR mould, according to the modified Proctor test, a dramatic decline of the bearing capacity of the highest organic matter sample around 80 % compared to that of the raw dredged sediment.

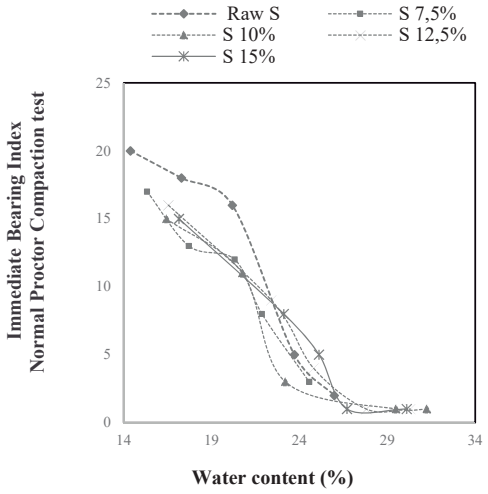

Fig. 4 IBI curves of the reconstituted samples using the normal Proctor test

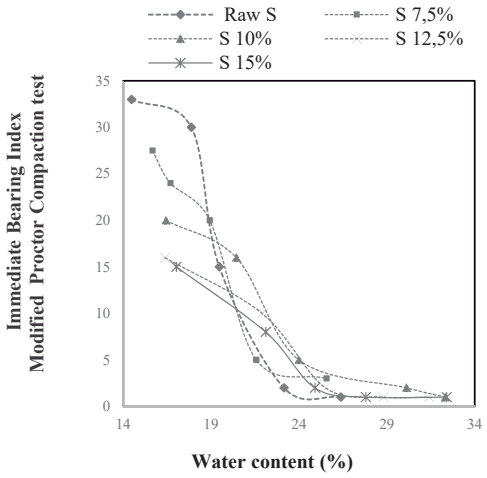

Fig. 5 IBI curves of the reconstituted samples using the modified Proctor test

The organic material with lower specific gravity (1.92 g/cm^3) once added to the raw dredged sediment makes change the rearrangement of particles of the mixture below compaction energy and consequently, its bearing capacity.

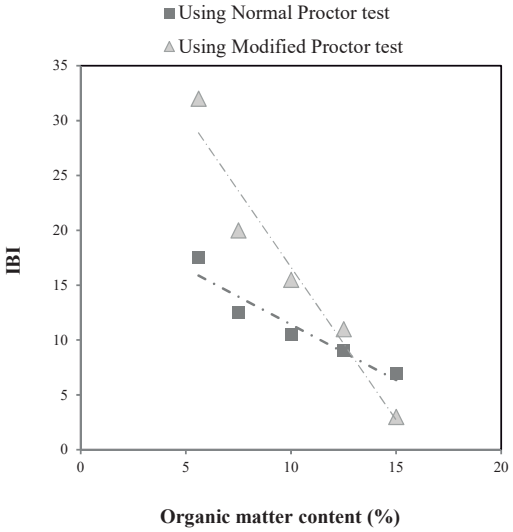

Fig. 6 IBI values versus Organic Matter Content

In fact, from the observation of the Table 2, it can be said that there exists a strong relationship between IBI and the organic matter content. The coefficient of determination R^2 is equal to 0.90 for the compacted samples according to the normal Proctor test and 0.94 according to the modified Proctor test, which means regression line fits very well with the data obtained from the test.

Table 2 Correlation equations of relationship between The IBI and the organic matter content

Parameters	Correlation equations	R^2
Using Normal Proctor test	IBI=-1.01 OM+21.5	0.90
Using modified Proctor test	IBI=-2.78 OM +44.4	0.94

CONCLUSIONS

The effect of organic content on the immediate bearing index of the dredged sediments has been investigated. The tests results indicate that the organic content significantly alter the geotechnical properties of the dredged sediments. The IBI values reduced with increasing organic matter content.

It can be concluded from the results that organic matter have negative effect on engineering properties of dredged sediment for road construction purposes even in small amounts. However, even the effect of organic matter on IBI values, the materials studied can still be used as embankments according to the French soil classification system dedicated to road works [10].

ACKNOWLEDGEMENTS

The authors are grateful to les HAUTS DE FRANCE region for their financial support to the action 3: Impacts of organic matter in the framework of industrial chair ECOSED.

REFERENCES

[1] Cerema, Enquête dragage 2011 ; synthèse des données, Cetmef. Margny Lès Compiègne: Cerema, 2015.

[2] J. Foucher, 'Valorisation des déblais sableux de dragage portuaire en France', CETMEF Brest, Ifremer Brest, PFE, 2005.

[3] M. A. Rashid and J. D. Brown, 'Influence of marine organic compounds on the engineering properties of a remoulded sediment', Eng. Geol., vol. 9, no. 2, pp. 141–154, 1975.

[4] G. H. Keller, 'Organic matter and the geotechnical properties of submarine sediments', Geo-Mar. Lett., vol. 2, no. 3–4, pp. 191–198, 1982.

[5] A. I. H. Malkawi, A. S. Alawneh, and O. T. Abu-Safaqah, 'Effects of organic matter on the physical and the physicochemical properties of an illitic soil', Appl. Clay Sci., vol. 14, no. 5–6, pp. 257–278, 1999.

[6] R. Zentar, N.-E. Abriak, and V. Dubois, 'Effects of salts and organic matter on Atterberg limits of dredged marine sediments', Appl. Clay Sci., vol. 42, no. 3, pp. 391–397, Jan. 2009.

[7] F. Hamouche and R. Zentar, 'Caractérisation des Matières Organiques dans les sédiments de dragage par méthodes thermiques et chimiques en vue d'une valorisation dans le domaine des travaux routiers', presented at the 35èmes Rencontres de l'AUGC, Nantes, 2017, pp. 1–4.

[8] I. Develioglu and H. F. Pulat, 'Geotechnical Properties and Compressibility Behavior of Organic Dredged Soils', World Acad. Sci. Eng. Technol. Int. J. Environ. Chem. Ecol. Geol. Geophys. Eng., vol. 11, no. 2, pp. 194–198, 2017.

[9] A. Al-Kifae and M. A. Hamad, 'Inspecting the Effects of Organic Content on Compaction and Consolidation Characteristics of Organic Soil Models', Am. Sci. Res. J. Eng. Technol. Sci. ASRJETS, vol. 31, no. 1, pp. 109–123, 2017.

[10] LCPC and SETRA, 'Réalisation des remblais de couches de forme, Fascicule I, Principes Généraux', SETRA, France, Technical guide, 2000.

10. Radioisotope dating and chronological characterization of sediments

Session chairs: Vinicio Macías[1] and Maria de los Ángeles Calixto Romo[2]
[1]Instituto de Investigaciones Oceanológicas, Universidad Autónoma de Baja California, México
[2]Colegio de la Frontera Sur, México

Sediment cores obtained under conditions such as fine-grained sediments, non-disturbed by physical or biological perturbations, are excellent candidates to determine historical pollutant deposition and accumulation in water bodies such as lakes and reservoirs. The use of radiometric dating of sediment cores are useful tools to describe chronological sediment accumulation. Pollutants are typically transported from their sources to water bodies in high-altitude or latitude regions due to the grasshopper effect. Here they accumulate in sediments or ice that act as destination for many contaminants. No permanent sediments monitoring programs have been implemented in most countries, and there are therefore no formal inventories of pollutants or evaluation of their exposure risks. Therefore, sediments cores are excellent matrices for the reconstruction of historical contamination through the sampling and chronological and chemical characterization. The analyses of these matrices represent a powerful tool to reconstruct historical changes in contaminants concentrations. Papers addressing such issues are very welcome for this session.

CHRONOLOGICAL STUDY OF METALS IN A SEDIMENT CORE FROM THE ALVARADO LAGOON SYSTEM (SLA), VERACRUZ, MEXICO

Velandia AL[1], Villanueva FS[2] and Botello AV[2]
[1]Posgrado en Ciencias de la Tierra, Universidad Nacional Autónoma de México, México; [2] Instituto de Ciencias del Mar y Limnología, Universidad Nacional Autónoma de México, México

ABSTRACT

This study was part of the "Environmental Diagnosis of the Laguna Alvarado System (SLA), Veracruz, Mexico" Project. A sedimentary core was analyzed by calculating the sediment accumulation rate by ^{210}Pb to determine the contamination tendency of Al, Cd, Cr, Cu, Hg, Ni, Pb, and V. The activities of total Pb and supported Pb were 83.1 and 29.5 Bq kg^{-1} respectively, estimated average accumulation rate was 0.48 ± 0.09 cm^{2}year^{-1}. The organic matter showed a linear behavior in the core, (< 2.5%). The metals presented the following order concentration: Al> V> Cr> Ni> Cu> Pb> Hg> Cd. The changes in the concentrations of Cr, Ni, Pb and V that occurred in the 1950s are related to meteorological phenomena that affected the state of Veracruz in 1955. The calculation of the enrichment factors and the geoaccumulation index of the metals showed moderate enrichments for Cr, Cu, Hg, Ni and V, and Category 2 classification (moderately contaminated). Metal fluxes were calculated and showed a tendency to increase over time. The concentrations of Cr, Cu, Ni and Hg exceeded the values of the ERL index and only the Ni exceeded the ERM value and is considered toxic concentration values for the benthonic organisms.

Keywords: Metals, Sediments, Core, Enrichment Factor, Geo-accumulation Index

INTRODUCTION

The richness and diversity of resources present in the coastal zones entail the corresponding concentration of activities and human settlements along the littorals and estuaries throughout the world. Thus, the increase in human activities within the Coastal Zone is the main driver of changes in ecosystems and water quality in coastal aquatic systems. This increase is directly related to a rapid urban growth, alterations in the hydrological and nutrient cycles, as well as the contribution of pollutants from terrestrial sources, the destruction of estuarine and marine habitats, the loss of fishing resources and the recreational and economic values of the coastal zone [1].

The Alvarado Lagoon System (SLA) is one of the most productive ecosystems in the Gulf of Mexico, composed of three large lagoons and more than two hundred interior lagoons. It is a space that flows along great rivers, such as the Papaloapan and the Blanco River, and it has great economic and ecological importance due to fisheries as it serves as a shelter, feeding and reproduction area for the numerous fish and crustacean populations that inhabit it. In 2004, it was declared a RAMSAR site [2]. The Alvarado wetland stands out as the second largest mangrove area in the Gulf of Mexico. The ecological and productive importance of this ecosystem is evident for local people who depend directly and/or indirectly from him.

Within the environmental problems associated with the SLA, 15 natural environmental units have been identified. These homogeneous units present nine environmental problems and only one with direct social impact, of which there are six urban zones and three agricultural zones that occupy a considerable area, which could alter their environmental stability and put at risk the permanence of the coastal ecosystems of the SLA Among the environmental problems presented by the SLA are the contamination of aquatic bodies and sediments as reservoirs that make up this system, mainly due to the change in land use and the degradation of vegetation as the most relevant.

On the other hand, the sediments can be used to reconstruct the environmental conditions that prevailed at the time of deposit, provided they are not altered or mixed so that it is possible to establish a reliable time frame. The most widely used method for dating sediments is to analyze certain radioactive isotopes that are sedimentological tracers such as ^{14}C and ^{210}Pb [3]. If we know the half-life of the radionuclide, its activity in the present and the activity that reigns in the sedimentary layers, we can estimate the age of the sediments using the law of radioactive decay and, therefore, estimate the accumulation rates of the sediments and flows of pollutants. When this information is combined with

historical data, sedimentary records are of great interest because they offer the possibility of retrospective studies on the factors that caused environmental changes, well above the time scale of any existing monitoring program.

Most of the metals used in the various industrial activities manifest their presence in the coastal regions of the Gulf of Mexico, especially in the vicinity of oil refineries, fertilizer production, mining and metallurgy and of course in the surrounding areas of coastal cities with a large number of inhabitants. Similarly, untreated domestic discharges provide large volumes of sludge enriched with metals such as Pb, Zn, Cd and Cr among others, whose final destination are rivers and lagoons or are directly discharged into the sea [4].

The objective of this study was to perform the analysis of a sedimentary core dated with ^{210}Pb to determine the trend of metals contamination over time, as well as to determine the enrichment factors, the geo-accumulation index and the flows of metals to establish the gradients of distribution of the metals in the sedimentary core and contamination level.

MATERIAL AND METHODS

Study area

It is located in the South Coastal Plain of the Gulf of Mexico (Fig. 1), between the coordinates 18º 44 '00 "and 18 ° 52' 15" of latitude N and 95º 44 '00 "and 95º 57' 00" of longitude O. The type of climate is warm humid with temperatures higher than 18° C, with few thermal oscillations and with an annual average of 25.23° C, and rainfall regime. Because the SLA is connected to the Gulf of Mexico, it has a great influence on the coastal, Lazo and littoral currents between Punta Morro and Alvarado, presenting a significant response to the intensity and direction of the wind, at low frequency and to the propagation of the tidal wave, in the diurnal and semidiurnal bands. It is 17 km long parallel to the coastline and with a maximum width of 4.5 km. The communication with the sea is made through a bar 0.4 km wide [5]. Selection of the sampling site was based on the guidelines stated in Regional Project Manual RLA/7/012/ (IAEA 2009), which considers lagoon geomorphology, fluvial and tidal influence, settlements along the margins, and sediment grain size [6].

Radiochronology using ^{210}Pb

The total Lead-210 activity ($^{210}Pb_{total}$) was determined through the analysis of its descendent Polonium-210 (^{210}Po, assuming a secular equilibrium between the two) using alpha spectrometry (Ortec – Ametek system with model 576A cells). The procedures described in the [*ICMyL*] Academic Dating Service (SAF) standard technique were followed [7], which utilize ^{209}Po as an internal standard. A 0.5 g sample was taken from the dried and ground sediment and digested in a mix of concentrated acids (HF+HNO_3+HCl) on a heating slab at a temperature of 150°C for 6 hours. Po isotopes were isolated using the spontaneous deposition method on silver discs. Two core samples were also analyzed by gamma spectrometry, to determine the ^{214}Pb activity to estimate the ^{226}Ra activity (that is, the activity of supported ^{210}Pb assuming secular equilibrium among them. To this end, 4 g of dried and ground sediment were placed into polypropylene vials with screw caps, which were then sealed with Teflon tape to reduce the possibility of any ^{222}Rn leakage. The samples were housed for 21 days prior to analysis to allow production of ^{222}Rn and were then analyzed for 72 h in an Ortec - Ametek well detector. Analysis quality control was evaluated through the analysis of replicas taken from certified reference IAEA-300 “Radionuclides in Baltic Sea”. The ^{210}Pb value (concentration interval 273.6 - 361.0 Bq kg^{-1}) was found to be within the certified limits of uncertainty [7].

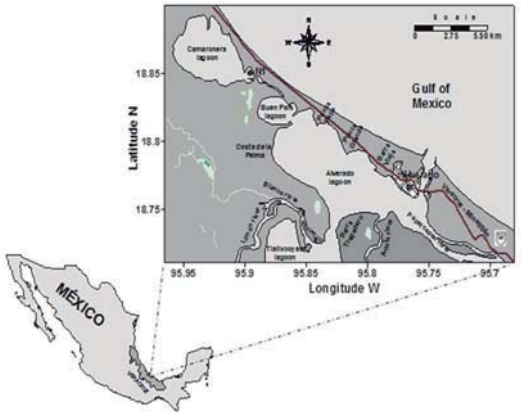

Fig. 1 Location and sampling site of ALS sedimentary core, Veracruz

Metals

The technique described by Suwandana et al. [8] was used to quantify the Al, Cd, Cr, Cu, Hg, Ni, Pb and V. The procedure involves digestion in a microwave (CEM Mars5x microwave) at 120 psi for 20 minutes, using 3 mL of HF, 5 ultrapure ml of HNO3, and 10 mL of type 1 water. Samples were quantified in an Inductively Coupled Plasma – Mass Spectrophotometer (ICP-MS 7500c). The quality control of analysis was performed using certified standards for each metal, which are in certified reference material for marine sediment (IAEA-433). The recovery percentages were: 98% for Al, 90% Cd,

Cr 90%, Cu 92%, Hg 88%, Ni 90%, Pb 98% and V 89%. The blank solution was analyzed 10 times. Detection limits for each metal were: Al 0.093 µg g^{-1}, Cd 0.0026 µg g^{-1}, Cr 0.0226µg g^{-1}, Cu 0.0247 µg g^{-1}, Hg 0.0344 µg g^{-1}, Ni 0.0201 µg g^{-1}, Pb 0.0170 µg g^{-1} and V 0.0213 µg g^{-1} [9].

Enrichment Factor (EF)

A common approach to estimate how much the sediment is impacted (naturally and anthropogenically) with metals is to calculate the Enrichment Factor (EF) for metal concentrations above contaminated background levels [10][11]. Pollution will be measured as the amount or ratio of the sample metal enrichment above the concentration present in the basal sediment. The EF method normalizes the measured heavy metal content with respect to a samples reference such as Fe, Al or Zn. The EF of a metal in sediment can be calculated with the Eq. (1) and used elements concentrations (in ppm) in the Upper Continental Crust [11] with background concentrations.

$$EF = \frac{M_{sediment}/Al_{sediment}}{M_{earth\ Crust}/Al_{earth\ crust}} \quad (1)$$

Where $M_{sediment}$ is the concentration of the metal examined in sediments, $Al_{sediment}$ is the concentration of the Al in the sediments examined and $M_{earth\ crust}$ and $Al_{earth\ crust}$ are concentrations the metal and Al in the earth's crust respectively .

Values of EF between 0.5 and 1.5 were interpreted as indicative of crustal material or natural weathering processes. Values of EF greater than 1.5 were concluded to have arisen from non-crustal sources, i.e. anthropogenic pollution.

Index of Geo-accumulation (Igeo)

The Index of Geo-accumulation (Igeo) has been used widely to evaluate the degree of metal contamination or pollution in terrestrial, aquatic and marine environment. The Igeo categorizes the degree of contamination of sediments from uncontaminated to heavily polluted (on a scale of 0 to 7 respectively). The Igeo of a metal in sediment can be calculated with the Eq. (2) [10] [11] [12]. Where $M_{sediment}$ is the concentration of the element examined and $M_{earthcrust}$ the geochemical concentration of the metal in the earth's crust. The factor 1.5 was introduced to minimize the effect of possible variations in the background values which might be attributed to lithologic variations in the sediments.

$$I_{Geo} = log_2 \left[\frac{M_{sediment}}{1.5\ M_{earth\ crust}}\right] \quad (2)$$

Metals fluxes

Metals fluxes are based on the metal concentration results and were calculated by multiplying of the metal concentration and mass accumulation rate (derived from the ^{210}Pb dating method) [13][14] according to with the Eq. (3):

$$F_M = C_M S \quad (3)$$

Where F_M is metal flux the interval of a layer ($mgcm^2Kg^{-1}y^{-1}$), S the average sedimentation rate estimated for this core as the accumulation rate derived ^{210}Pb method (cm^2y^{-1}) and C_M is metal concentration ($mgKg^{-1}$) the interval of a layer.

RESULTS AND DISCUSSION

The profile of the activities of the total ^{210}Pb with respect to the depth, showed an exponential type decay, reason why the nucleus was apt to be dated; however, it was not possible to calculate the rate of mass accumulation (TAM), which allows to compensating the natural variations of compaction in each stratum, instead the sedimentary accumulation rate (TAS) was used to estimate the apparent age values for each section of the nucleus and thus determine in what year the different types of pollutants were deposited. The activities of total Pb and Pb supported in the samples were 83.1 and 29.5 Bq kg^{-1} respectively, while the activity of excess Pb was estimated from the difference of the activities of total Pb and supported Pb obtaining 53.6 Bq kg^{-1} (Fig. 2a).

Calculation of sedimentation rate (SR)

The sedimentation rate in cm yr^{-1} was estimated following the Constant Flux Constant Sedimentation (CFCS) model, which is based on the supposition that both the ^{210}Pb and the sediment fluxes have remained constant throughout the formation of sedimentary layers. When both suppositions are true, a linear relationship between the natural logarithm of $^{210}Pb_{exc}$ and depth is observed [7] [15]. Figure 2b shows the $ln^{210}Pb_{exc}$ profile according to core depth. That relation is described by the exponential regression equation also shown in Fig. 2b, from which the slope used to calculate the SR (SR= λ/slope) was obtained. The average sedimentation rate (S) estimated for this core was 0.48 ± 0.09 cm $year^{-1}$.

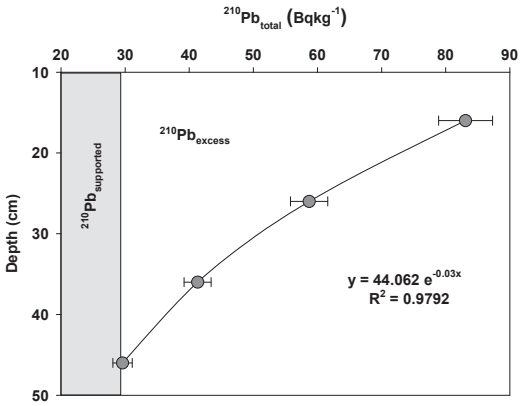

Fig. 2(a) ^{210}Pbtotal and $^{210}Pb_{excess}$ activity profiles

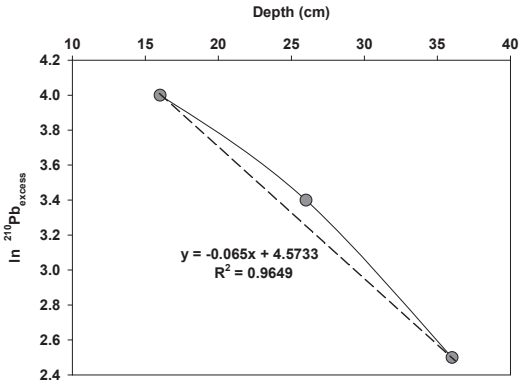

Fig. 2(b) ln ^{210}Pbexcess related to depth

Calculation of ages

According to the law of radioactive decay, the TAS was used to estimate the apparent ages for each stratum of the nucleus. The values of the variables of depth and concentration in the exponential decay equation were substituted and the maximum apparent age determined for said nucleus involved a formation period of 85.5 ± 16.9 years corresponding to the sediments of 46 cm depth.

Figure 3 shows the concentrations of the analyzed metals, as well as their ERL and ERM sediment quality index values. It was there in observed that Cr, Cu, Ni and Hg exceeded the ERL index values, where there are occasional events that affect the communities that inhabit the bottom. Only the Ni concentrations exceeded the ERM value, where events posing a toxicological threat to the organisms inhabiting the sediments frequently take place. Pb and Cd did not exceed any of the limits [16].

The results of the calculation of the EF and Igeo are shown in the Tables 1 and 2 respectively, for the calculations the values of the crustal abundance data of Wendepohl (1995) were used [11].

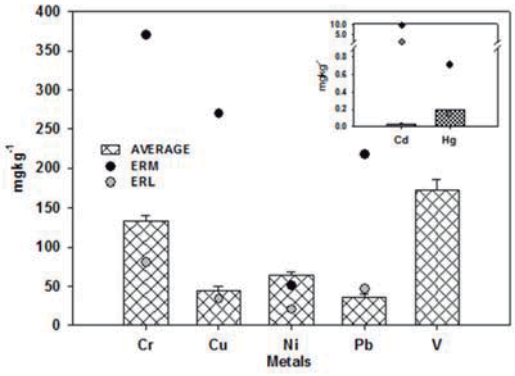

Fig. 3 Sediment quality indices for metals in core, average concentrations in the four strata

Table 1 Results of the calculation of the EF

Cd	Cr	Cu	Hg	Ni	V	Pb
0.2	5.6	4.0	4.8	4.8	4.5	3.2
0.3	5.0	3.6	4.0	4.3	3.9	2.6
0.4	4.9	4.4	4.4	4.3	3.8	2.6
0.6	5.7	5.4	5.4	5.4	4.0	3.5

The metals Cr, Cu, Hg, Ni and V had EF values of 3 to 5, so it is considered that there is a moderate enrichment in all the strata of the core of these metallic elements, the Cd did not present enrichment and the Pb showed a minor enrichment. As for the Igeo of the sediments of all the strata of the nucleus, they were classified as Category 2 (moderately contaminated) for the metals Cr, Cu, Hg, Ni and V.

Table 2 Results of the calculation of the I_{geo}

Cd	Cr	Cu	Hg	Ni	V	Pb
-3.3	1.4	0.9	1.2	1.2	1.1	0.6
-2.6	1.3	0.9	1.0	1.2	1.0	0.4
-2.3	1.2	1.1	1.1	1.1	0.9	0.3
-1.9	1.4	1.3	1.3	1.3	0.9	0.7

The concentration intervals of the metals detected in the four sedimentary strata were: Cd 0.016–0.0417 mg kg^{-1}, Cr 123.97–140.07 mg kg^{-1}, Cu 40.06–52.59 mg kg^{-1}, Hg 0.17–0.21 mg kg^{-1}, Ni 58.0 –0.69.27 mg kg^{-1}, Pb 31.86–40.35 mg kg^{-1} and V 161.07–190.73 mg kg^{-1}. This makes it possible to determine the potential ecotoxicological threat to the organisms that inhabit sediments [9].

The Cu and Cd concentrations obtained in the historical profile showed a negative linear trend from 1929 to 1971, with values of 52.59 to 40.06 mg kg^{-1} for Cu, showing a slight increase of

41.14 mg kg^{-1} in 1998, and that is about above the ERL index of 34 mg kg^{-1}. The Ni values were detected in a range of 58.04 to 69.27 $mgkg^{-1}$, above the ERM index of 51.6 $mgkg^{-1}$, with the highest value in 1929 around 70 mg kg^{-1}, to decrease in the 50's where the lowest value was presented to increase until 1998 close to 65 mg kg^{-1}. Pb levels ranged from 31.86 to 40.36 mg kg^{-1}, with values below the ERL index of 46.7 mg kg^{-1} [15]. The concentrations of V detected presented a range of 161.07 to 190.73 $mgkg^{-1}$, this metal showed a pattern of accumulation similar to Cr, Ni and Pb where the highest value was presented in 1929, to decrease in 1950, and increasing in 1998 to around 175 $mgkg^{-1}$ (Fig. 4).

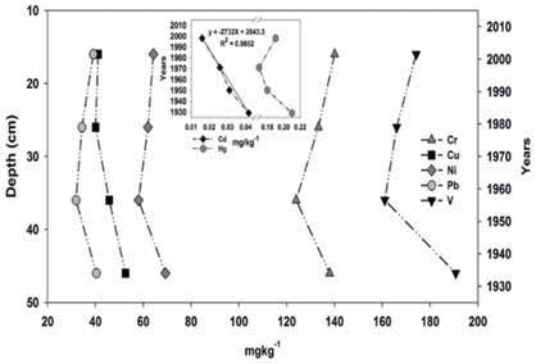

Fig. 4 Vertical distribution of Cd, Cr, Cu, Hg, Ni, Pb and V metals in ASL sedimentary core.

The contributions of the metals through the Blanco and Papaloapan rivers, can occur in particulate form and be quickly incorporated into organometallic compounds or some mineral phases, which are fixed in the sediments by the clays, hydrated oxides of Fe, Mn and Al, carbonates and MO, to be retained in the sediments when horizontal transport ceases and then establish the accumulation patterns observed in the historical profile (Fig. 5).

The changes observed in the concentrations of the Cr, Ni, Pb and V metals that correspond to the 1950 stratum are related to a critical season in the state of Veracruz and Tamaulipas, since three meteorological phenomena that affected the region were presented. Hurricanes Gladys, Hilda and Janet in September 1955. The consequences of these events caused flooding and overflowing of the rivers, which caused damages to the crops, the infrastructure, alteration to the marine and continental biotic elements, for what could be one of the causes of the change in the rate of accumulation of metals, as well as the change of the concentrations that were observed in the metals analyzed, in the study area.

The flows of metals show similar behavior except for the Cd that their concentrations throughout the cores were negligible as a result of the affinity of this metal to form complexes with the Cl^{-1} ions present in the water column of this saline lagoon.

The flows of metals show similar behavior except for the Cd that their concentrations throughout the cores were negligible as a result of the affinity of this metal to form complexes with the Cl^{-1} ions present in the water column of this saline lagoon.

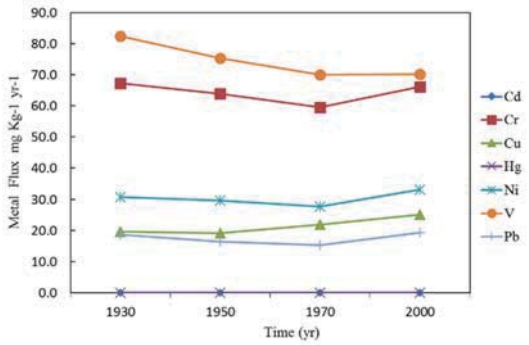

Fig. 5 Metal flux of Cd, Cr, Cu, Hg, Ni, V and Pb.

As for metals Cr, Cu, Hg, Ni, Pb and V, an inflection was observed in the concentrations in the 1950s when the state of Veracruz presented extreme meteorological phenomena that caused an increase in river flows and overflow of the lagoons and with this, disturbances in the processes of sedimentation of the area, which are reflected in the concentrations of metals Fig. 5. The tendency of the metals flows is with slight increases for more recent years.

The increase of the flow of metals towards the sediments of the lagoon are the result of the intensification of the erosive processes of the continental zone by the meteorological events as well as by the change of land use and the growth of the urban area [15].

CONCLUSIONS

The metal concentrations showed the following decreasing order V> Cr> Ni> Cu> Pb> Hg> Cd. Only the Ni exceeded the ERM index where adverse conditions are frequently observed to the organisms that inhabit the benthos, Cr values, Cu, Pb and Hg, presented slightly above the ERL index. In the Cd, a negative linear tendency was observed that is related to its capacity to form soluble complexes with the chlorine ions present in the water column of this saline lagoon.

The changes in the concentrations of Cr, Ni, Pb and V that occurred in the 1950s are related to the meteorological phenomena that struck the states of Veracruz and Tamaulipas in 1955. The contributions

of V, Ni and Hg deposited in SLA sediments come from anthropogenic and lithogenic sources. In calculating the EFs, moderate enrichment of the Cr, Cu, Hg, Ni metals was observed in the sediments of the whole core, while the IGeo classified them as moderately contaminated for the same metals. The intensification of the erosive processes of the continental zone by the meteorological events as well as by the change of land use and the growth of the urban area increase the sedimentation rates in the lagoon and with this contribution of metals.

REFERENCES

[1] UNESCO, Intergovernmental Oceanographic Commission. The Final Design Plan for the HOTO Module of GOOS. GOOS Report No.99. 2002. Paris, Francia. 45p.

[2] CONABIO. Technical Sheet for the Evaluation of Priority Sites for the Conservation of the Coastal and Oceanic Environments of Mexico. 2003. "Alvarado Lagoon System".

[3] Valette Silver, N.J. (1993). The use of sediment cores to reconstruct historical trends in contamination of estuarine and coastal sediments. Estuaries 16 (3B) 577-588.

[4] Veerasingam S., Vethamony P., Mani Murali R. and Fernandes B. (2015). Depositional record of trace metals and degree of contamination in core sediments from the Mandovi estuarine mangrove ecosystem, west coast of India. Mar. Pollut. Bull., vol. 91(1): 362-367.

[5] Secretaria de Marina (SEMAR) 2015 Alvarado, Veracruz; Consultado en línea el 17-05-2016 http://digaohm. semar.gob.mx/cuestionarios/cnarioAlvarado.pdf

[6] International Atomic Energy Agency (IAEA) (2009) Aplicación de técnicas nucleares en la solución de problemas específicos del manejo integrado de zonas costeras en el Gran Caribe. Manual del Proyecto Regional RLA/7/012/2009

[7] Sanchez-Cabeza JA, Ruiz-Fernandez AC (2012) 210Pb sediment radiochronology: An integrated formulation and classification of dationg models. Geochimica et Cosmochimica Acta 82: 183-200.

[8] Suwandana E, Kawamura K, Soeyanto E (2011) Assessment of the heavy metals and nutrients status in the seawater, sediments and seagrass in Banten Bay, Indonesia and their distributional patterns. Journal of Fisheries International 6 (1): 18-25

[9] Botello AV, Villanueva FS, Rivera RF, Velandia AL, de la Lanza GE (2018) Analysis and tendencies of metals and POPs in a sediment core from the Alvarado Lagoon System (ALS), Veracruz, Mexico. Archives of Environmental Contamination and Toxocilogy. Https://dol.org/10.1007/s00244-018-0516-z

[10] Sutherland, R.A. (2000). Bed sediment-associated trace metals in an urban stream, Oahu, Hawaii. Environmental Geology 39: 611 – 37.

[11] Wedepohl, K.H. (1995). The composition of the continental crust. Geochim. Cosmochim. Acta 59, 1217–1232.

[12] Muller, G. (1979). Schwermetalle in den sediments des Rheins-Veran-derungen seitt 1971. Umschan 79, 778–783

[13] Martínez V. Vammen K., Sanchez Cabeza J. A., Alonso Hernández C. A., Quejido Cabezas A. (2014). Flujo Cronológico de Metales en sedimentos y la Sedimentación en la Bahía de Bluefields, Nicaragua. Revista Agua y Conocimiento. Vol 1:1. http://revistacira.unan.edu.ni/

[14] Huu, H. H., Rudy S. and An Van Damme (2010). Distribution and contamination status of heavy metals in estuarine sediments near Cau Ong harbor, Ha Long Bay, Vietnam. Geology Belgica 13(1-2): 37 – 47.

[15] Ruiz Fernández A.C., Maanan M., Sánchez Cabeza J. A., Hascibe L., Pérez Bernal L.H., López Mendoza P., Limoges A., 2014. Cronología de la sedimentación reciente y caracterización geoquímica de los sedimentos de la laguna de Alvarado, Veracruz (suroeste del golfo de México) Ciencias Marinas 40(4): 291–303

[16] Long ER, Macdonald DD, Smith SL, Calder FD (1995). Incidence of adverse effects within ranges of chemical concentrations in marine and estuarine sediments. Environmental Management 19(1): 81-97.

ANTHROPOGENIC INFLUENCE ON THE SEDIMENT CHEMISTRY OF BALAMTETIK LAKE, CHIAPAS, MEXICO

Caballero Margarita [1], Mora Lucy [2], Muñoz Esperanza [2], Escolero Oscar[2], Bonifaz Roberto[1], Prado Blanca[2]
[1]Instituto de Geofísica, UNAM, México; [2]Instituto de Geología, UNAM, México

ABSTRACT

Balamtetik is the first of a series of lakes at Montebello National Park, Chiapas, México, and it is the receiving body of the Rio Grande, the main river of the Comitán-Lagos de Montebello watershed. Multi-elemental and 137-Cs analyses in a 75 cm sediment core were used to reconstruct the historical fluxes of C, N, Mg, and heavy metals to the lake during the last 130 years. Sedimentation rates in the Montebello lakes are high (> 6 mm/year). The tendency of C, Fe, Al, Mn concentrations together with the variation of the C/N relationship along time, allows identifying the effects of land use change (deforestation), wastewater inflow to the lake as well as the changes in the redox conditions in the water/sediment interface. The set of results show high human activity in the area the last 60 years, causing a strong arrival of pollutants in the lake.

Keywords: Deforestation, Wastewater, Erosion,

INTRODUCTION

The substances that reach the lakes from the basin, in dissolved or particulate form, tend to accumulate in the sediments. The sediment profile constitutes a historical record of the temporal changes of events that occur on the surface, for example, fires, deforestation, etc. [1]. In the particular case of the arrival of urban and agricultural wastewater, the high concentration of nutrients causes anthropogenic eutrophication of a lake, which results in a decrease in dissolved oxygen in the water column, constituting one of the main environmental problems in the aquatic ecosystems. In addition, the nutrient exchange can occur between the water column and the sediments mediated by the trophic state [2]. In this way, the sediments are a file that can provide information on the evolution of the flow of nutrients in the water column.

The anthropogenic activity in the Comitán river basin, Chiapas, generates wastes that are discharged into the river and this last discharge into Balamtetik lake. The analysis of the historical content of nutrients and trace elements in the sediments of the receiving lake, together with the dating and sedimentation rate, allow the reconstruction of the anthropogenic activities in the watershed. This work presents the analysis of a sediment core of Balantetik lake as a direct receiving body of the discharge of the Río Grande de Comitán. Specifically, an analysis of the historical nutrients concentration, the relationships between them and the content of trace elements, in order to evaluate the role of anthropogenic activities in the water quality of the lake.

METHODS

The studied site

The basin of the Rio Grande,is a semiendoreic basin of 810 km^2 of karstic origin. The geological materials are associated with the Cantelha Group, Jolpabuchil and Cintalapa[3], composed mainly of partially or totally dolomitized limestones. The Rio Grande originates in Lake Juznajab, crossing the municipalities of Comitán de Domínguez, La Trinitaria, Las Margaritas and La Independencia, to end in the lake complex known as the "Lagunas de Montebello". This National Park is located in the southeast of the state of Chiapas, Mexico, on the border with Guatemala, in the Chiapas Macizo Central (Fig. 1) [4,5].The hydrological system of the park consists of a lacustrine complex of karstic origin of varied morphologies that extends through the southeastern part of the State of Chiapas to Guatemala. The waters that feed this system are mainly ground water [6] are cataloged within the National Hydrological Region No. 30 [7]. The surface water flow is carried out through the Rio Grande, and the first lake that receives its discharges is Balamtetik, which evidenced loss of depth and changes in the color of the water [8].

Sediment sampling

In July 2013, three short sedimentary sequences were recovered from Balamtetic Lake, using a UWITEC gravity corer (Margarita Caballero and Felipe Franco Gaviria) that recovered the sediment in transparent PVC pipes of 8.6 cm in diameter. The

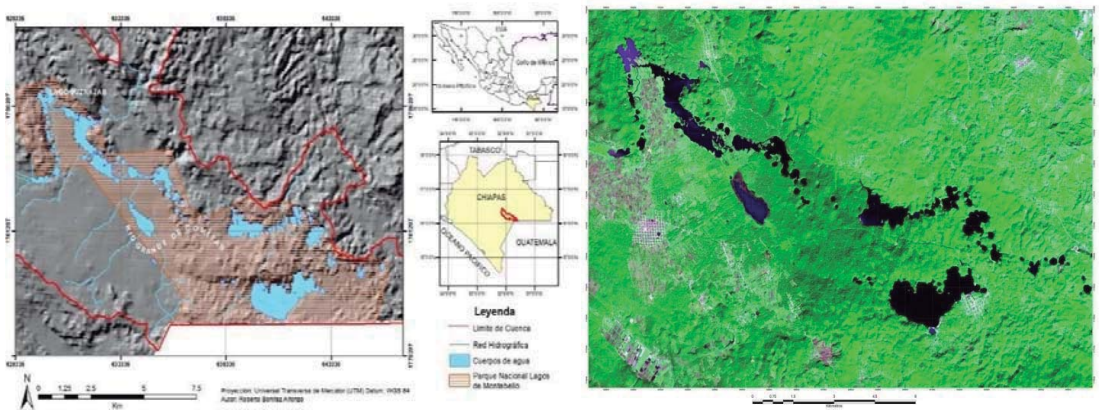

Fig. 1 Regional location of the Lagunas de Montebello National Park, Chiapas (left). Change in the color of the water from crystal clear (pristine) to yellowish-green (deteriorated) of the first lakes, Lake Balamtetik (SPOT satellite image, right) [8].

recovered sequences (Balam13-GI to GIII) had a maximum length of 75 cm and were sampled by pushing the sediment with a piston and continuously recovering 1 cm in thick slices. During sampling, physical characteristics such as color and texture were described.

Analytical methods

Dry sediment samples were analyzed for total C and N by dry combustion in a Perkin Elmer 2400, while the organic carbon fraction was analyzed in a TOC Shimazud. Sediment samples were freeze-dried and crushed, aqua regia digestion (HCl/HNO_3 1/3 v/v ratio) was performed to assess the pseudo total amount of metals (Al, Ca, Fe, Mn, Pb, Si, and P), using an Anton Paar microwave (EPA method 3051A). The concentration of major and trace elements was determined by ICP-OE Perkin Elmer 8600, with a relative analytical error for each sample (from triplicate measurements) lower than 10 %.

^{137}Cs fallout

^{137}Cs is a man-made radionuclide with an~30 years half-life which production is related to the nuclear tests performed since 1945 [10]. By 1950, the number of nuclear tests was high enough to atmospherically disperse the ^{137}Cs around the whole globe [11,12].This radionuclide fallout to the Earth´s surface and its strong attach to clay particles[13], make it possible to consider ^{137}Cs as good tracer for studying depositional processes in sedimentary environments since 1950 up to recent days.

Additionally, ^{137}Cs production has changed since 1950 making it possible to use its concentration at different depths in an unaltered sedimentary sequence to identify some specific years and periods of globally high production. These are: (1) the period between 1950 and 1963, that corresponds to the time of maximum nuclear bomb testing [14], (2) the breakdown of the Chernobyl nuclear plant in 1986[15], and (3) the accident in the Fukushima nuclear plant in 2011[16].

The analysis of ^{137}Cs was made in a Gamma Beta Spectrometer (ATOMEX AT1315)

RESULTS AND DISCUSSION

The estimated sedimentation rate from ^{137}Cs data was 6.45 mm/year (Fig. 2).Considering the characteristics of this radionuclide, this sedimentation rate was assigned to the period from 1950 to 2013.To calculate the sedimentation rate before 1950, the Si peaks that account for the eruptions of the Santa Maria volcano in 1902 were used. The approximate sedimentation rate estimated for this period was 3.9 mm/year. The higher sedimentation rate since 1950 can be the related to the agrarian reform that happen in Mexico starting in the 1940. This reform result in the agriculture expansion substituting pasture lands generating a high rate of soil loss. The extracted core gives us information from 1876 to 2013. Along the core, the sediments had a clayey silt texture; the only variation between them was color, varying between gray, dark gray and black.

The variation of total nutrients concentration over time shows a cyclic behavior of increase and decrease at different times. There are four moments on which it is possible to observe important increases: 1909, 1945, 1993 and 2003. The greatest increase in nutrients occurred in 1909, it is very likely that this is the result of a deforestation event, where a large surface of native forest were transformed into pastureland. The arrival of large amounts of nutrients in the lake is associated with the surface horizon of the soil, which is highly enriched with organic matter, impacted by deforestation.In 1945, a new arrival of nutrients is

observed, which coincides with the agrarian reform period, at the time, there was a distribution of the territory from large haciendas to small farmers, the last under the traditional agriculture that favors the loss of soil. In more recent years, 1993 and 2003, a new change in the use of the land occurred in the basin, there was an increase in agricultural production of vegetables mainly tomato, promoted by the large transnational corporations of agriculture.

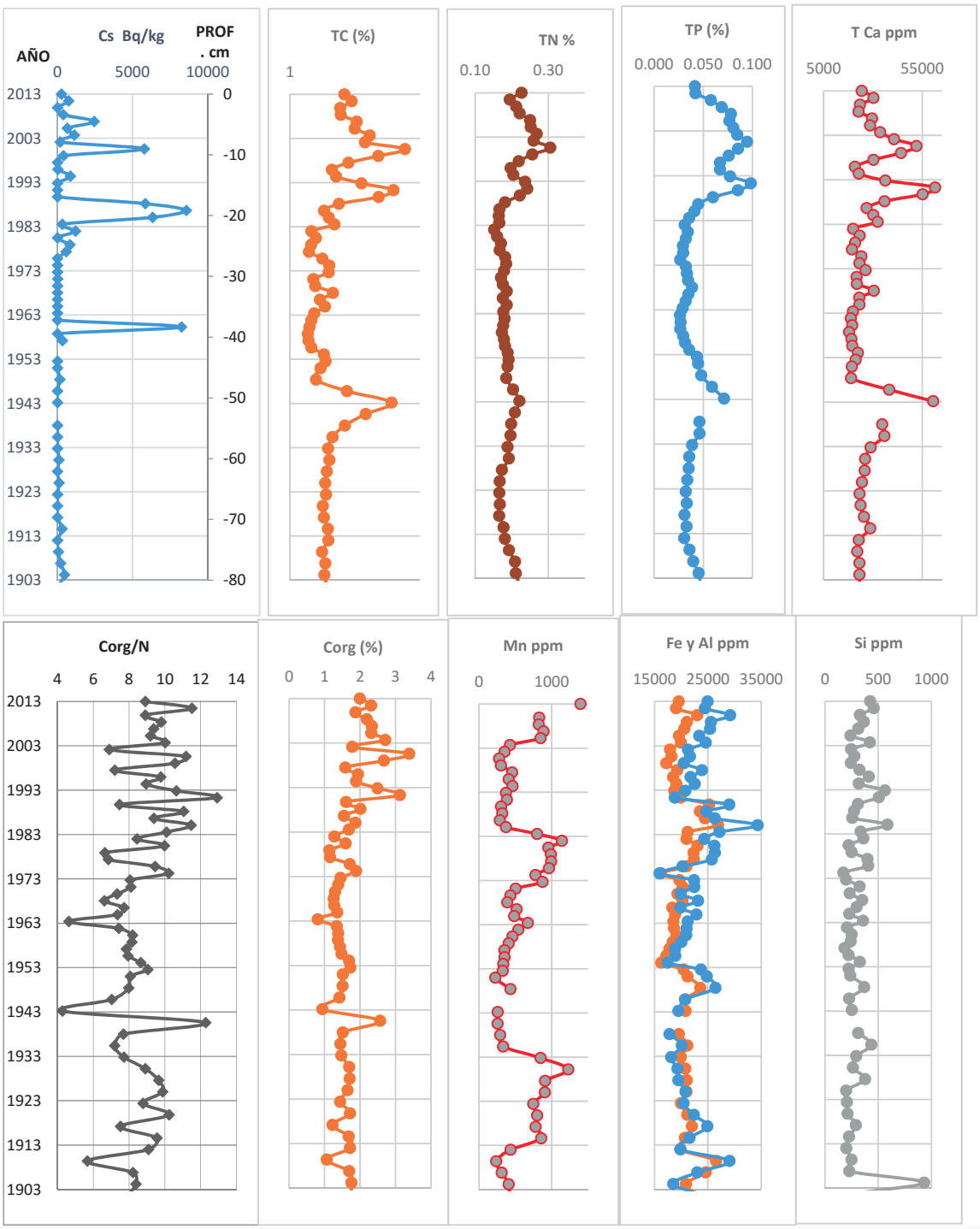

Fig. 2 ^{137}Cs, C, N, P, Ca, Mn, Fe and Si profiles from sediment core

Regarding the nature of the carbon, in Fig. 2, it is observed that in the last century, the lake received more organic carbon than inorganic carbon. This is due, probably, to the increase in the erosion processes in the basin due to the change in land use. When more organic matter arrives, the intensity of the mineralization increases, increasing the oxygen consumption. The above can explain the decrease of Mn in certain moments. Mn concentration variations indicates variations in oxygen content, which may be due to low levels of the water column that imply higher oxygenation or, low carbon levels in sediments, which implies less oxygen consumption for its degradation. The slight peaks of Mn correspond to stages of low carbon concentration, the last, together with the little variation of the concentration of Mn in the sediments (concentration varies around 250 ppm along the profile), the Mn concentration can then be an indicator of an invariable content of oxygen dissolved in the water at the bottom of the lake.

The variation of the TOC concentration is an indicator of the variation of the carbon flow that reaches the lake [18]. The carbon content in sediments may have two origins, from soil erosion, mainly from the organic horizon due to changes in land use causing carbon losses, for example from forest use to agricultural use, in this case the sedimentation rate should be correlated with the increase in organic C; the second origin is the arrival of wastewater to the lake, in this case there is not, necessarily, a correlation between the sedimentation rate with organic C content. Thus, the increase in organic C observed in 1993 is associated with the arrival of sediments, which could be related, as mentioned before, to erosion resulting from deforestation. While the increase in organic C observed in 2003 can be attributed to the arrival of wastewater in the lake. To corroborate this, there is the fact that the tendency of the carbon concentration follows an inverse behavior to that observed in the Fe, if we consider the latter as an indicator of terrestrial contributions, the opposite trend indicates that the increase in the contribution of organic carbon over time can be associated with the arrival of water with a high carbon content due to anthropogenic reasons.

In almost all the sediment profile the C/N ratio oscillates between 8 and 12, with peaks of up to 15 at specific times: 1925, 1955 and 1988. Guilizzoni et al. [18], associate an increase in the C/N ratio in the sediment profiles with periods in which the sediments receive a high proportion of terrestrial organic matter. According to Spycher et al. [19], the organic matter in the soil (organic matter associated with mineral surfaces) has a C/N ration smaller than 20.

Variations in Si concentrations in the sediments are associated with the arrival of volcanic materials. The study area received ash fall from the Santa María Volcano in Guatemala during the first years of the century. The above coincides with the increase of Fe and Al associated with volcanic materials. Similarly, at the end of 1982 the eruption of El Chichón volcano occurred in the north of Chiapas, the deposition of ash to the region is observed in the sediments of the lake enriched with Si, Fe and Al. The increase in Fe and Al, but not in silica content, around the year 1943, is associated to the process of soil erosion, consequence of the change of use by the agrarian reform. Iron and aluminum concentration profiles show similar trends. The foregoing indicates that Fe has a predominantly terrigenous origin, since both Fe and Al are the major constituents of a large variety of minerals [20]. This result evidences the arrival of sediments from the basin to the lake, and also by air during the volcanoes eruptions.

CONCLUSIONS

The work evaluates the pattern of accumulation of nutrients and heavy metals in the sediments of Balamtetik lake, the receiving lake of the Rio Grande Basin, in Chiapas. The first 70 cm of depth were evaluated, which represent the last 130 years approximately, time in which the study area was subject to strong changes due to human activity. The sedimentation rate was higher the last 60 years than the time before 1950, deforestation due to government policies to convert forest areas into agricultural areas may explain this result. The arrival of soil by erosion becomes evident with the variations of the C/N ratio and the similar tendencies observed in the Al and Fe profiles. The accumulation of metals comparing with C behavior, show the arrival of domestic wastewater.

ACKNOWLEDGEMENTS

This research was funded by the Fondo Sectorial de Investigación y Desarrollo Sobre el Agua (Sectorial Fund for Water Research and Development) (CONAGUA-CONACYT) through the project Estudio hidrológico y de Calidad del Agua del sistema Lagunar de Montebello, en el estado de Chiapas. The authors thank Kumiko Shimada and Javier Tadeo, LANGEM, for their help with the chemical analysis.

REFERENCES

[1] Mulligan, C.N., Yong, R.N. and Gibbs, B.F., 2001. An overview of technology for heavy metal remediation of dredged sediments. J. Hazardous Materials 85, 145-163

[2] Alaoui-Mhamdi, M., Dhib, A., Bouhaddioui, A., Ziadi, B., Turki, S., Aleya, T., 2014. Assessment of nitrogen and phosphate balance and the roles of bacteria and viruses at the water-sediment interface in the Allal El Fassi reservoir (Morocco). Environmental Monitoring and Assessment, 186 (9), 5817-5829

[3] Quezada- Meñetón, J. M. 1987. El Cretàcico Medio Superior, y el límite Cretàcico superior Terciario Inferior de la Sierra de Chiapas: Boletìn de la Asociación Mexicana de Geólogos Petroleros, 34 (1), 3-97.

[4] Comisión Nacional de Áreas Naturales Protegidas y Secretaría del Medio Ambiente y Recursos Naturales (CONANP-SEMARNAT), 2007, "Programa de Conservación y Manejo Parque Nacional Lagunas de Montebello, México", *disponible en* <http://www.conanp.gob.mx/ que_hacemos/pdf/programas_manejo/ Final_Montebello.pdf>

[5] Durán CL, Escolero OF, Muñoz EFM, Castillo MCS, Rodríguez GSR, Cartografía geomorfológica a escala 1:50000 del Parque Nacional Lagunas de Montebello, Chiapas (México), Boletín de la Sociedad Geológica Mexicana Vol. 66, Nr. 2, 2014, pp. 263–277

[6] Vázquez, M.A., Méndez, E., 1994, Aspectos generales de la región: Lagos de Montebello, Reporte del trabajo para el curso de conservación de naturaleza y recursos naturales, Maestría en Ciencias: Recursos Naturales y Desarrollo Rural, ECOSUR Chiapas**.**

[7] Alcocer J, LA Oseguera, G Sánchez, CG González, JR Martínez, R González, Bathymetric and morphometric surveys of the Montebello lakes, Chiapas, Journal of Limnology, Vol. 75, 2016, pp. 56-65.

[8] Mora L, R Bonifaz, R. López-Martínez, Unidades geomorfológicas de la cuenca del Río Grande de Comitán, Lagos de Montebello, Chiapas-México, Boletín de la Sociedad Geológica Mexicana, Vol. 68, Nr. 3, 2016, pp. 377-394.

[9] Ritchie JC, McHenry R (1975) Fallout Cs-137: a tool in conservation research. Journal of Soil and Water Conservation 30: 283-286.

[10] Horn HG, Bonka H, Maqua M (1987) Measured particle bound activity size-distribution, deposition velocity, and activity concentration in rainwater after the Chernobyl accident. Journal of Aerosol Science 18: 681-684.

[11] Chino M, Nakayama H, Nagai H, Terada, H., Katata G, Yamazawa H (2011) Preliminary estimation of release amounts of I-131 and Cs-137 accidentally discharged from the Fukushima Daiichi Nuclear Power Plant to the atmosphere. Journal of Nuclear Science Technology 48: 1129-1134.

[12] Ritchie JC, McHenry R (1990) Application of Radioactive Fallout Cesium-137 for Measuring Soil Erosion and Sediment Accumulation Rates and Patterns: A Review. Journal of Environmental Quality 19: 215-233.

[13] Walling DE, Bradley SB (1988) The use of caesium-137 measurements to investigate sediment delivery from cultivated areas in Devon, UK. Sediment budgets (Proceedings of the Porto Alegre Symposium). IAHS Publication 174: 325-335.

[14] Pöllänen R, Valkama I, Toivonen H (1997) Transport of radioactive particles from the Chernobyl accident. Atmospheric Environment 31: 3575-3590.

[15] Wei L, Kinouchi T, Yoshimura K, Velleux ML (2017) Modelling watershed-scale 137Cs transport in a forested catchment affected by the Fukushima Dai-ichi Nuclear Power Plant accident. Journal of Environmental Radioactivity 171: 21-33.

[16] Olvera-Viascán, V., L. Bravo-Inclán, J. Sánchez-Chávez. Aquatic ecology and management assessment in Valle de Bravo reservoir and its watershed. Aquatic Ecosystem Health and Management 1 (1998) 277–290.

[17] Guilizzoni, R., A. Marchetto, A. Lami, N. G. Cameron, R G. Appleby, N. L. Rose,

[18] O. A. Schnell, C. A. Belis, A. Giorgis I & L. Guzzi. The environmental history of a mountain lake (Lago Paione Superiore, Central Alps, Italy) for the last c. 100 years: a multidisciplinary, palaeolimnological study. *Journal of Paleolimnology*15: 245-264, 1996.

[19] Sovcher G. Sollins P. and Rose S. L. (1983) Carbon and and Nitrogen in the light fraction of a forest soil: vertical distribution and seasonal patterns. *Soil Science 135,79-87.*

[20] Bortleson, G.C. and G.F. Lee. 1972. Recent sedimentary history of Lake Mendota, Wis. Environ. Sci. Tech. 9:799

IMPORTANCE OF SURFACE SEDIMENTS FOR RELIABLE 210Pb DATING

Yang Handong, Lencioni Lucia and Patmore Ian[1]
[1]Environmental Change Research Centre, University College London, UK

ABSTRACT

Lead-210, ^{137}Cs and ^{241}Am dating techniques have been extensively used in the dating of recent sediments. However, collection of an intact core is the first essential step towards having reliable ^{210}Pb chronologies for the sediments. We collected short gravity cores from Loch Morar, a deep (310 m max. depth), steep-sided lake in Scotland. Lead-210 chronologies for one of the cores did not match with the ^{137}Cs and ^{241}Am records, and the radionuclide data indicate that surface sediments in this core were likely missing. Therefore, sediment chronologies and accumulation rates calculated from unsupported ^{210}Pb activities in the core were deemed unreliable, as confirmed by another core from the same lake. Dating of the cores suggests that sediment dating not only depends on accurate counting of radionuclide activities, but also on the integrity of the cores, in turn determined by sampling location. Importantly, however ^{210}Pb, ^{137}Cs and ^{241}Am data can be carefully assessed to determine the integrity of sediment cores.

Keywords: Sediment dating, Pb-210, Cs-137, Intact sediment core, Reliable chronology

INTRODUCTION

^{210}Pb (half-life 22.3 years) is a naturally-produced radionuclide, derived from atmospheric fallout (termed unsupported ^{210}Pb). Cesium (half-life 30 years) and ^{241}Am are artificially-produced radionuclides, introduced to the environment by atmospheric fallout from nuclear weapons testing and nuclear reactor accidents. They have been extensively used in the dating of recent sediments to establish the timing of ecological or environmental changes, especially in lakes for which long-term limnological data are lacking.

For calculating sediment chronologies based on unsupported ^{210}Pb activities, several models have been developed, including the Constant Rate of ^{210}Pb Supply (CRS) model and the Constant Initial Concentration (CIC) model [1]. Where possible, independent assessments of a 1963 date are also used, derived from the peak activities of ^{137}Cs and ^{241}Am stratigraphic records. These represent a global peak in fall-out prior to the Partial Nuclear Test Ban Treaty in that year. In regions where it is detectable, a second peak in ^{137}Cs occurs in 1986 due to the Chernobyl nuclear reactor accident in Ukraine. In general, ^{210}Pb chronologies need to be validated by independent time markers such as ^{137}Cs and ^{241}Am peaks.

While the CRS model is suitable in most cases, the CIC model may provide a valid alternative if primary sedimentation rates have been constant. In many cases, one or other of these simple models is valid for use. In complex situations, it may be necessary to apply them in a 'piece-wise' way to different sections of the sediment sequence.

However, all of these assumptions are based on collection of an intact core. If surface sediments are missing from a core, as can occur through in-lake sediment slumping events prior to sampling or during sample collection, the real age of the surface in the collected core is unknown. In this case, ^{210}Pb dating is problematic, and the chronologies are difficult to match with the ^{137}Cs and ^{241}Am dates. Conversely, it may suggest changes in ^{210}Pb deposition or sedimentation, or even lack of surface sediments.

This study provides an example to show the importance of surface sediments for ^{210}Pb dating, and how to examine ^{137}Cs, ^{241}Am and ^{210}Pb activities in sediment core to assess if the surface sediments are missing.

METHODS

Study Site

Loch Morar is a freshwater loch, lying in a glacial trough, orientated on an east-west axis and dammed by a natural rock threshold, in Lochaber, Highlands, Scotland (Fig. 1). It is the fifth-largest loch by surface area in Scotland, at 26.7 km², and the deepest freshwater body in the British Isles, with a maximum depth of 310 m. The loch was created by glacial action around 10,000 years ago, and has a surface elevation of 9 metres above sea level. The loch is designated as Site of Special Scientific Interest (SSSI) for its clear, oligotrophic waters and has a low catchment to lake ratio (6.3), with a minimal intake of nutrients.

Fig. 1 Sampling locations of the sediment cores (MORAR1 and MORAR2) at Loch Morar, Scotland, UK

Sample Collection and Gamma Dating

Two sediment cores were taken in February 2015, MORAR1 and MORAR2, at depths of 310m and 285m respectively, using an HTH Renberg gravity corer [2]. The sediment cores were sampled at 0.25 cm intervals throughout the cores using the HTH extrusion device [2]. Sediment wet density measurements were conducted using a $2cm^3$ container. Moisture content and organic matter (as loss-on-ignition) were measured according to standard methods [3], samples were then freeze-dried.

Dried sediment samples from the cores were analysed for ^{210}Pb, ^{226}Ra, ^{137}Cs and ^{241}Am by direct gamma assay in the Environmental Radiometric Facility at University College London, using ORTEC HPGe GWL series well-type coaxial low background intrinsic germanium detector. Lead-210 was determined via its gamma emissions at 46.5 keV, and ^{226}Ra by the 295 keV and 352 keV gamma rays emitted by its daughter isotope ^{214}Pb following 3 weeks storage in sealed containers to allow radioactive equilibration. Cesium-137 and ^{241}Am were measured by their emissions at 662 keV and 59.5 keV [4]. The absolute efficiencies of the detector were determined using calibrated sources and sediment samples of known activity. Corrections were made for the effect of self-absorption of low energy gamma rays within the sample [5].

RESULTS AND DISSCUSION

Core MORAR1

Lead-210 Activity

The base of the core has not reached equilibrium depth of total ^{210}Pb activity with supported ^{210}Pb activity. Unsupported ^{210}Pb activities, calculated by subtracting supported ^{210}Pb activity from total ^{210}Pb activity, decline with depth more or less following an exponential trend with some small departures (Fig. 2b; Table1), suggesting relatively stable sedimentation rates with small changes.

Table 1 ^{210}Pb concentrations in core MORAR1 taken from Loch Morar, Scotland

Depth	Dry Mass	Pb-210			
		Total		Unsupported	
cm	g cm^{-2}	Bq Kg^{-1}	±	Bq Kg^{-1}	±
0.75	0.0283	2815.55	155.49	2719.35	157.57
2.75	0.1796	2338.25	73.19	2261.93	74.18
4	0.2845	2441.88	121.75	2392.41	123.29
5.13	0.3932	1557.29	80.58	1527.82	81.71
6.5	0.5311	1084.52	92.35	992.13	94.44
7.5	0.6336	1630.72	80.55	1561.09	82.29
8.38	0.7168	1557.31	38.18	1512.71	38.6
9.25	0.8002	968.33	85.08	878.63	88.63
11.13	0.9878	856.29	27.24	810.35	27.6
12.13	1.0835	598.03	25.34	550.86	25.78
14.38	1.3071	506.86	41.72	400.15	43.07
15.38	1.4125	479.68	20.81	430.29	21.19
16.13	1.492	572.06	14.72	521.87	14.96
17.25	1.6084	454.93	19.22	416.16	19.59

Artificial Fallout Radionuclides

The ^{137}Cs activity versus depth profile (Fig. 2c; Table 2) shows two peaks at 5.13 and 8.38 cm, which are likely to be derived from fallout of 1986 Chernobyl accident and the atmospheric testing of nuclear weapons with maximum fallout in 1963, respectively. Notable ^{241}Am activities between 5.13 and 12.13 cm sediments confirm nuclear weapon testing fallout.

Table 2 Artificial fallout radionuclide activities in core MORAR1

Depth	Cs-137		Am-241	
cm	Bq Kg^{-1}	±	Bq Kg^{-1}	±
0.75	149.91	19.62	0	0
2.75	361.52	13.99	0	0
4	426.19	24.6	0	0
5.13	479.6	19.39	13.25	4.37
6.5	378.1	22.9	13.29	6.99
7.5	475.48	18.86	0	0
8.38	481.51	9.55	18.74	2.32
9.25	414.33	20.14	0	0
11.13	343.49	6.86	21.78	2.01
12.13	208.19	5.96	12.9	1.94
14.38	75.73	7.33	0	0
15.38	78.62	3.52	0	0
16.13	70.92	2.32	0	0
17.25	54.24	3.24	0	0

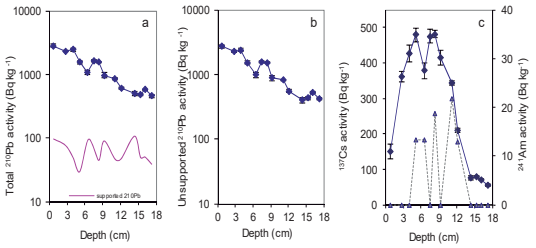

Fig. 2 Fallout radionuclide concentrations in core MORAR1, showing (a) total ^{210}Pb, (b) unsupported ^{210}Pb, and (c) ^{137}Cs and ^{241}Am concentrations versus depth

Core Chronology and Sedimentation Rates

The simple CRS and CIC models all place 1963 at around 12.13 cm, which is considerably deeper than the 1963 depth suggested by the ^{137}Cs record, while the CRS model puts 1986 depth at 7.5 cm, also deeper than the ^{137}Cs peak at 5.13 cm (Fig. 3). In addition, both models suggest a relatively uniform sedimentation rate with a mean value of 0.023 ± 0.003 g cm^{-2} yr^{-1}. If we assume that the sediments at 8.4 cm was formed in 1963/4, with a mean sedimentation rate of 0.023 g cm^{-2} yr^{-1}, the surface of the core can be assigned to 1995. All of these suggest that the real surface sediments of the core might be missing.

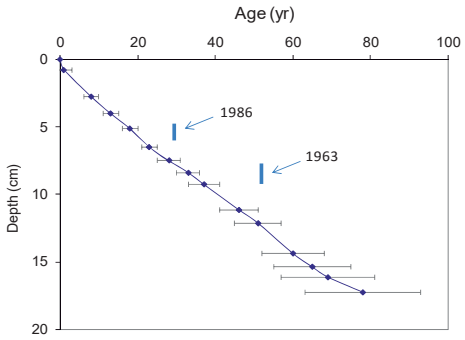

Fig 3 Radiometric chronology of core MORAR1 taken from Loch Morar, Scotland, showing the CRS model ^{210}Pb dates and the ^{137}Cs and ^{241}Am time markers

Core MORAR2

Lead-210 Activity

Similar to MORAR1, unsupported ^{210}Pb activities in MORAR2 also decline more or less exponentially with depth. However, there is little net decline in unsupported ^{210}Pb activities in the top 4 cm (Fig. 4b; Table 3), suggesting possible increase in sedimentation rates towards the sediment surface. There are some small fluctuations in unsupported ^{210}Pb activities at different depths such as at 12 cm and 26 cm, which also suggest possible changes in sedimentation rates. Overall, the more or less exponential decline would suggest that changes in sedimentation rates are relatively small.

Table 3 ^{210}Pb concentrations in core MORAR2 taken from Loch Morar, Scotland

Depth	Dry Mass	Pb-210			
		Total		Unsupported	
cm	g cm^{-2}	Bq Kg^{-1}	±	Bq Kg^{-1}	±
0.13	0.0051	3047.33	103.04	2957.5	104.28
1.38	0.067	2957.65	89.8	2892.36	90.81
2.38	0.1235	3095.23	97.13	3046.02	97.87
3.88	0.2176	2921.98	79.08	2876.44	79.58
4.63	0.2669	2596	66.1	2538.01	66.54
5.38	0.3213	2330.34	69.74	2272.17	70.32
6.13	0.3866	1974.62	65.88	1931.42	66.49
7.13	0.472	1894.95	62.8	1854.19	63.36
8.63	0.5967	1628.99	42.4	1582.94	42.8
9.88	0.6958	1281.72	36.58	1235.44	36.97
10.63	0.7621	1077.74	32.5	1021.84	32.86
11.88	0.8808	1061.52	45.51	993.45	46.04
12.88	0.9746	1091.49	44.08	1041.36	44.53
13.88	1.0665	1062.74	45.78	1021.64	46.32
14.88	1.1603	875.27	43.28	821.3	43.8
15.88	1.2561	861.91	42.54	806.12	43.03
16.88	1.356	691.74	25.96	642.42	26.32
17.88	1.4586	655.19	42.22	613	42.84
18.88	1.5658	594.58	25.22	538.72	25.64
20.13	1.6981	484.47	22.27	429.19	22.76
22.13	1.9124	388.73	23.81	341.88	24.47
24.13	2.1335	312.52	18.91	258.98	19.36
26.13	2.3657	312.9	21.8	255.56	22.36
28.13	2.6085	198.52	16.98	141.71	17.54
30.13	2.8624	135.46	15.33	82.84	15.89
32.13	3.1332	109.51	11.81	57.46	12.2

Artificial Fallout Radionuclides

The ^{137}Cs activity versus depth profile (Fig. 4c; Table 4) also shows two peaks: The peak at around 13 -15 cm derived from maximum fallout of the atmospheric testing of nuclear weapons in 1963, and the peak at 8.5 – 10 cm from the 1986 Chernobyl accident fallout. The ^{241}Am profile of the core also shows a good peak at around 15.88 cm, confirming that the ^{137}Cs peak at around 13 – 15 cm was derived from the atmospheric testing of nuclear weapons.

Table 4 Artificial fallout radionuclide concentrations in core MORAR2

Depth	Cs-137		Am-241	
cm	Bq Kg^{-1}	±	Bq Kg^{-1}	±
0.13	251.17	13.59	0	0
1.38	224.99	12.25	0	0
2.38	265.03	14.67	0	0
3.88	379.39	12.98	0	0
4.63	393.02	11.36	0	0
5.38	453.44	13.72	10.47	3.66
6.13	520.92	14.61	5.51	3.45
7.13	555.38	14.34	12.17	3.43
8.63	578.91	10.48	9.38	2.4
9.88	565.48	9.7	9.21	2.36
10.63	488.82	8.46	13.07	2.08
11.88	487.58	11.91	13.68	3.13
12.88	496.55	11.53	23.24	3.07
13.88	548.68	12.9	25.73	3.56
14.88	548.43	12.85	31.43	3.42
15.88	437.16	11.08	34.79	3.31
16.88	268.54	6.08	21.11	2
17.88	176.52	8.91	7.63	2.97
18.88	131.23	4.88	4.28	1.86
20.13	90.57	3.71	0	0
22.13	67.76	4.02	0	0
24.13	42.96	3.08	0	0
26.13	32.5	2.87	0	0
28.13	30.55	2.53	0	0
30.13	16.52	2.06	0	0
32.13	11.45	1.43	0	0

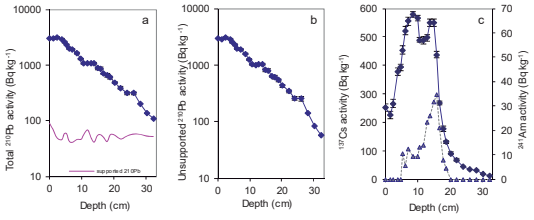

Fig. 4 Fallout radionuclide concentrations in core MORAR2, showing (a) total ^{210}Pb, (b) unsupported ^{210}Pb, and (c) ^{137}Cs and ^{241}Am concentrations versus depth

Core Chronology

Use of the CIC model was precluded by the non-monotonic features in the unsupported ^{210}Pb profile. Lead-210 dates were calculated using the CRS model [3]. The simple CRS dating model places 1963 and 1986 at c. 16.5 and c. 10 cm, respectively, which are in reasonable agreement with the ^{137}Cs and ^{241}Am records. Sediment accumulations calculated using ^{210}Pb data in the core are given in Table 5 and shown in Fig. 5. Overall, sedimentation rates were relatively stable over the last one and half centuries or so, with a mean at 0.022 g cm^{-2} yr^{-1}.

Table 5 ^{210}Pb chronology of core MORAR2 taken from Loch Morar, Scotland

Depth	Dry mass	Chronology			Sedimentation Rate		
		Date	Age				
cm	g cm^{-2}	AD	yr	±	g cm^{-2} yr^{-1}	cm yr^{-1}	± %
0	0	2015	0				
0.13	0.0051	2015	0	2	0.0283	0.582	3.8
1.38	0.067	2013	2	2	0.027	0.512	3.5
2.38	0.1235	2010	5	2	0.0239	0.396	3.6
3.88	0.2176	2006	9	2	0.0223	0.349	3.2
4.63	0.2669	2004	11	2	0.0236	0.341	3.2
5.38	0.3213	2002	13	2	0.0246	0.308	3.6
6.13	0.3866	1999	16	2	0.0267	0.31	3.9
7.13	0.472	1996	19	2	0.0251	0.299	4
8.63	0.5967	1991	24	2	0.0252	0.31	3.5
9.88	0.6958	1987	28	2	0.0288	0.348	3.8
10.63	0.7621	1985	30	2	0.0325	0.352	4
11.88	0.8808	1981	34	2	0.0297	0.315	5.3
12.88	0.9746	1978	37	2	0.0255	0.275	5.1
13.88	1.0665	1974	41	2	0.0231	0.249	5.5
14.88	1.1603	1970	45	2	0.0255	0.269	6.3
15.88	1.2561	1966	49	2	0.0229	0.234	6.5
16.88	1.356	1962	53	2	0.0253	0.25	5.8
17.88	1.4586	1958	57	2	0.0232	0.221	8.3
18.88	1.5658	1953	62	2	0.0229	0.215	7
20.13	1.6981	1948	67	2	0.0241	0.226	8
22.13	1.9124	1939	76	3	0.0227	0.209	10.3
24.13	2.1335	1929	86	3	0.0221	0.195	12.2
26.13	2.3657	1916	99	5	0.0151	0.127	16.1
28.13	2.6085	1901	114	7	0.0169	0.136	24.1
30.13	2.8624	1886	129	10	0.0184	0.14	36.5
32.13	3.1332	1871	144	16	0.0164	0.123	45.6

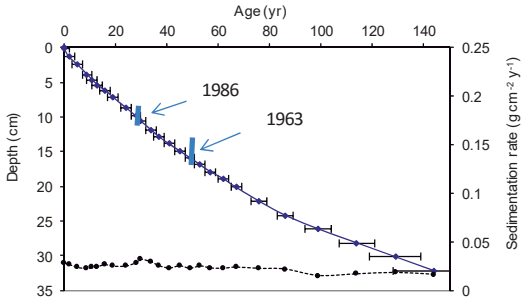

Fig. 5 Radiometric chronology of core MORAR2 taken from Loch Morar, Scotland, showing the CRS model ^{210}Pb dates, ^{137}Cs time markers, and sedimentation rates. The solid line shows age while the dashed line indicates sedimentation rate.

Lead-210 chronologies in MORAR2 match the dates suggested by the ^{137}Cs and ^{241}Am records of the core, while there are considerable discrepancies between ^{210}Pb and ^{137}Cs ages in MORAR1. Although unsupported 210Pb activities in the surface sediments of MORAR2 only slightly higher than that in MORAR1, they show a clear relatively uniform in the top 4 cm, while MORAR1 does not show this feature. Comparison of MORAR1 and MORAR2 would also suggest that the real surface sediments in MORAR1 are likely to be missing.

This study shows that having an intact sediment core is important for ^{210}Pb dating, and that lack of surface sediments could result in inaccurate chronologies. Sediment ^{210}Pb chronologies need to be validated by independent time markers. By examining sediment ^{210}Pb, ^{137}Cs and ^{241}Am data, the integrity of sediment cores can be assessed.

ACKNOWLEDGEMENTS

This study was funded by Scottish Natural Heritage and fieldwork assistance provided by Nutopia Ltd. Assistance with sampling design was provided by Prof. Helen Bennion and Dr. Carl Sayer, Environmental Change Research Centre, University College London. Dr. Carl Sayer gave comments on an early proof of this article.

REFERENCES

[1] Appleby PG, Chronostratigraphic techniques in recent sediments, Tracking Environmental Change Using Lake Sediments. Last and Smol, Ed. Vol. 1, Basin Analysis, Coring, and Chronological Techniques. Kluwer Academic Publishers, Dordrecht, 2001, pp. 171-203.

[2] Renberg I, Hansson H. The HTH sediment corer, J. Paleolimnol., Vol. 44, 2008, pp. 655-659.

[3] Heiri O, Lotter AF, Lemcke G, Loss on ignition as a method for estimating organic and carbonate content in sediments: reproducibility and comparability of results, J. Paleolimnol., Vol. 25, 2001, pp. 101-110.

[4] Appleby PG, Nolan PJ, Gifford DW, Godfrey MJ, Oldfield F, Anderson NJ, Battarbee RW, 210Pb dating by low background gamma counting, Hydrobiologia, Vol. 141, 1986, pp. 21-27.

[5] Appleby PG, Richardson N, Nolan PJ, Self-absorption corrections for well-type germanium detectors, Nucl. Inst. & Methods B, Vol. 71, 1992, pp. 228-233.

TEMPORAL VARIATION OF METAL ENRICHMENT IN COASTAL MARINE SEDIMENTS OFF BAJA CALIFORNIA, MEXICO

Macías-Zamora J.V.[1], Ramírez-Álvarez N.[1], Álvarez-Aguilar A.[1] and Hernández-Guzmán F.A.[1]
[1]Instituto de Investigaciones Oceanológicas, Universidad Autónoma de Baja California, México.

ABSTRACT

In four regional sampling events: 1998, 2003, 2008, and 2013, 60-79 marine sediment samples were analyzed per year. The metal concentrations (Cd, Co, Cr, Cu, Fe, Ni, Pb, Mn, and Zn) were measured along the southern end of the Southern California Bight (SCB) in Baja California coast. The concentrations of metals were similar for the first three years. In the last one, most metals showed a tendency to decrease, which was probably related to a regional change in the pattern of distribution of fine grain sediment in the area (%< 63 μm) and a larger accumulation of organic carbon (%) in the deepest stations. The metal enrichment was evaluated using iron as a reference element. Most of the metals were correlated with iron, the exception was Cd since its distribution appears related to other mechanisms such as upwelling events in the area. For the period 1998-2008, the percentage of enriched sites in at least one metal were 45-51%, while in 2013 it decreased to 35%. These sites were located mainly in zones of deposition nearby the 200 m isobath and close to natural and wastewater plants discharges. The distribution, changes in concentration and enrichment of metals appear to be partially related to regional weather conditions (El Niño-Southern Oscillation and a recent drought event) along with local anthropogenic discharges of wastewater treatment plants in the area.

Keywords: Trace metals, Marine sediment, Wastewater plants, ENSO, Drought

INTRODUCTION

Trace metal on surface sediments resulting on coastal pollution appears to be most frequently the result of coastal development as it has been shown to be directly associated to economic development [1]. However, originated by the natural presence of trace metals derived from physicochemical processes such as rocks and soil intemperism and their transport to the coastal zones, results is the need to separate one source (anthropogenic) from natural origins. Elements such as aluminum, iron or lithium would be more or less unchanged by anthropogenic influences and they would only increase in number and reinforce the data base for better estimation of those sites with enrichment by more anthropic elements. We have however, observed what we suggest may be significant changes for iron, element that has been previously selected for South California Bight (SCB) as a good normalizing element [2]-[3].

We propose that some of these metals may be useful predictor of cyclic processes if one is to look carefully to their behavior. Not only the concentration of iron varies along the time of the study, but also as we have shown previously [4] it varies, depending on the latitude, along the coast of Baja California.

MATERIALS AND METHODS

Study area

The Southern part of the SCB extends from the international border between the political border of California and Baja California and extends south to Point Colonet (about 190 Km). Our work has been limited to the most populated region in Mexico, from the border to Punta Banda (100 km) (Fig.1). This is the area where most development has occurred along the coast. To the north of the area, there are three cities that may be point sources, those are San Diego, CA on the US side of the border; Tijuana, Baja California and Rosarito Baja California on the Mexican side. In the study area from north to south the main discharges of wastewater plants are: Binational, Punta Bandera, El Sauzal, El Gallo and El Naranjo. The northern and center part of the study area also have the most permanent rivers, respectively the Tijuana River and La Mision River.

Data collection

In four regional sampling years: 1998, 2003, 2008 and 2013, 60-79 sediment samples were collected per year, using a Van Veen grab of 0.1m^2.

The study area was subdivided into three zones using an stratified random sampling (Fig.1), based mainly on the human population distribution: The northern zone includes the cities of Tijuana and Rosarito; the center zone with a reduced population and lack of important discharges of wastewaters and; the south zone which include the city of Ensenada, the second largest city on the coast of Baja California.

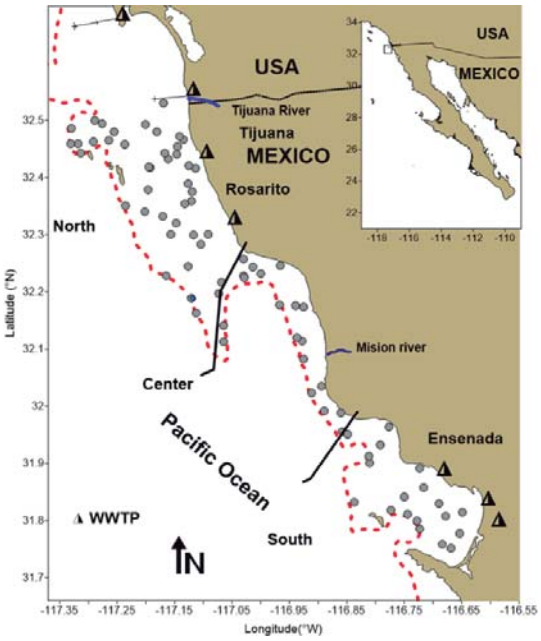

Fig. 1 Study area. The isobath of 200 m is indicated in dotted line. WWTP = waste water plant

Sample treatment

Sediment grain size (%< 63 μm) was determined using a Horiba (model LA-910) laser/tungsten particle size analyzer according to the methodology described by [5]. The determination of the percentage of organic carbon (%OC) in the sediment samples was done using a LECO (model CHNS-932) elemental analyzer.

The following metal concentrations were measured in surface sediments: Cd, Co, Cr, Cu, Fe, Ni, Pb, Mn, and Zn. The methods for measurements of trace metal concentrations have been described by [4]. Quantification was made using an Agilent 240FS AA fast sequential atomic absorption spectrometer.

The enrichment of metals was evaluated using iron as a reference element [1, 6].

RESULTS AND DISCUSSION

Grain Size

From 1998 to 2008, the average percentage of fine sediment was similar (34-38%) but in 2013 this value decreased to around 24%. The distribution of fine fraction was similar from 1998 to 2008. The north zone was characterized by sandy sediments (<10% fine fraction) in shallow stations (<50 m of depth); for the center zone, the percentage of fine fraction between 10 to 99%, with highest values in the deepest station (~200 m); and the south zone, fine sediments showed values between 10-50% in shallow stations, and 50-90% in deepest stations.

This change was originated by a decrease of fine sediments (<10%) in the center and south zones of the study area in relation with to previous sampling years.

Organic Carbon

The average percentage of organic carbon (OC %) was similar from 1998 to 2003 (~0.5%) while in 2008 increased to 1% mainly attributed an increase of %OC in the deepest stations of the study area. Finally the average of %OC in 2013 decreased again to about 0.5%. The correlation between fine sediment fraction and %OC was low (r^2 = 0.15) in sampling years except in 2003 year, when the correlation was moderate (r^2 = 0.69).

Concentration of Metals

Most metal concentrations could be measured in all sampling years, except for Co (in 1998); and Cd (in 2003 and 2008) when their concentrations were below the detection limit. The concentrations of metals were similar for the first three years of sampling (1998-2008) but in 2013 there was a tendency of decrease, most notorious in Cr and Mn (Fig.2).

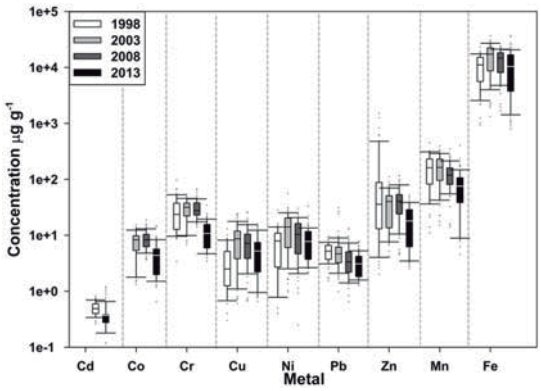

Fig. 2 Box plots for metals concentration

Metals enrichment

In all sampling years most of the metals were correlated with iron ($r^2 > 0.5$) the exception was Cd with a low correlation ($r^2 < 0.4$). The distribution of Cd appears related to other mechanisms such as upwelling events in the area [7]-[8].

In the period 1998-2008, the percentage of enriched sites in at least one metal were 45-51%, while in 2013 it decreased to 35% (Fig.3).

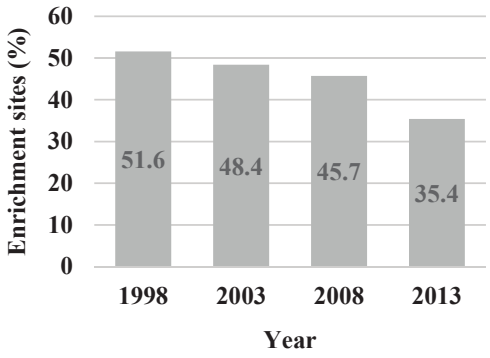

Fig. 3 Percent of stations enrichment in at least one metal by year

These sites were located mainly in deposition zones nearby of the 200 m isobath and close to natural and wastewater plants discharges (Fig. 4).

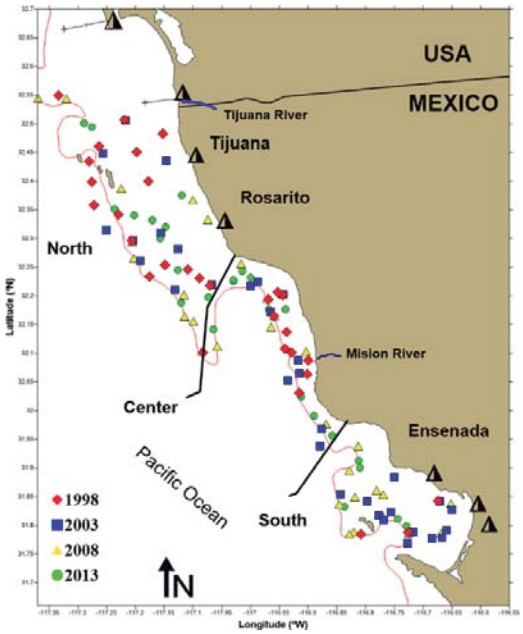

Fig. 4 Localization of enriched sites with at least one metal

The temporal changes in the percentage and distribution of % <63 μm and %OC along with the enrichment metal sites, could be relate with the local effects of the discharges of waste water plants and natural discharges in the area. However in a regional aspect we considered a probable effect by weather.

Our samplings were realized in different El Niño conditions from 1998 to 2008 and under drought conditions in 2013 (Table 1).

Table 1 Weather conditions in the study area during sampling years

Condition	Intensity	Years
El Niño	Very Strong	1997-1998
El Niño	Moderate	2002-2003
La Niña	Weak	2008-2009
Drought	Abnormal	2012-2014

Note: based on Oceanic Niño Index (ONI) source: http://ggweather.com/enso/oni.htm

A higher intensity of El Niño, increases the probability of an above average precipitation [9]. In 1998 the precipitation in the area was around 500 mm/yr while in 2003 and 2008 was almost half (250 mm/yr) and finally in 2013, the precipitation fell to less than 200 mm/yr (Fig.5) cataloged as the most severe drought condition in the last century in the region (from 2012-2014) [10].

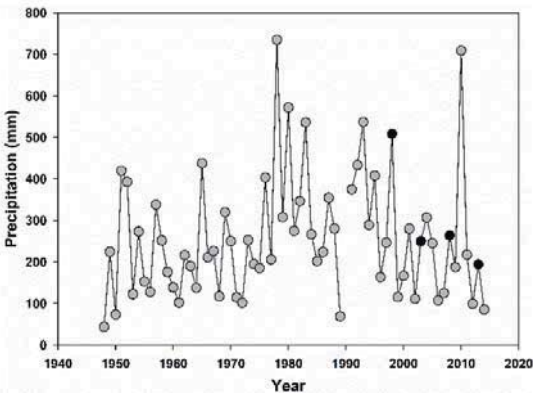

Fig. 5 Annual precipitation in Baja California. The dark points are the sampling years. Meteorological Station Santo Tomas. Source: http://clicom-mex.cicese.mx and https://smn.cna.gob.mx

The relation in the intensity of El Niño with the precipitation may be related with the variability in the terrigenous discharges to the ocean.

This is consistent with the decrease of enrichment stations for any metal from 1998-2013 in the area and with variation in the pattern of distribution of fine fraction %< 63 μm and OC%. Although at the moment we just hypothesized this relation, a longer time series could give a better understanding.

CONCLUSION

The distribution, changes in concentration and enrichment of metals appeared to be related to regional weather conditions (El Niño-Southern Oscillation and a recent drought event) along with local anthropogenic discharges of wastewater treatment plants in the area. Some trace metals maybe sensitive to this condition.

ACKNOWLEDGEMENTS

We would like to thank Algalita Marine Research Institute and SEMAR for providing ship support.

The Autonomous University of Baja California partially financed this work with the internal project from 17th call contract #629. Thanks are also given to CONACYT for providing doctoral scholarships to AAA and FAHG.

REFERENCES

[1] Gao, X., Zhou, F., & Chen, C. T. A, "Pollution status of the Bohai Sea: An overview of the environmental quality assessment related trace metals", Environment International¨ Vol. 62, 2014, pp. 12-30.

[2] Schiff, K. C., & Weisberg, S. B, "Iron as a reference element for determining trace metal enrichment in Southern California coastal shelf sediments", Marine Environmental Research, Vol. 48(2), 1999, pp.161–176.

[3] Huu Hieu Ho, Rudy Swennen, Valérie Cappuyns, Elvira Vassilieva, Tan Van Tran. "Necessity of normalization to aluminum to assess the contamination by heavy metals and arsenic in sediments near Haiphong Harbor, Vietnam", Journal of Asian Earth Science, 56, 2012, pp. 229-239.

[4] Macías-Zamora, J. V., Sánchez-Osorio, J. L., Ríos-Mendoza, L. M., Ramírez-Álvarez, N., Huerta-Díaz, M. A., & López-Sánchez, D., "Trace metals in sediments and Zostera marina of San Ignacio and Ojo de Liebre lagoons in the central pacific coast of Baja California, Mexico", Archives of Environmental Contamination and Toxicology, Vol 55(2), 2008, pp. 218–228.

[5] Daesslé, L. W., Ramos, S. E., Carriquiry, J. D., & Camacho-Ibar, V. F. "Clay dispersal and the geochemistry of manganese in the Northern Gulf of California". Continental Shelf Research, Vol. 22(9) 2002, pp. 1311–1323.

[6] Windom, H. L., Schropp, S. J., Calder, F. D., Ryan, J. D., Smith Jr., R. G., Burney, L. C., Rawlinson, C. H. "Natural trace metal concentrations in estuarine and coastal marine sediments of the southeastern United States", Environmental Science & Technology, Vol. 23(3). 1989, pp. 314-320

[7] Sañudo-Wilhelmy, S. A., & Flegal, A. R, "Trace Metal Concentrations in the Surf Zone and in Coastal Waters off Baja California, Mexico", Environmental Science & Technology, Vol. 30(5), 1996, pp. 1575–1580.

[8] Delgadillo-Hinojosa, F, et al, "Seasonal behavior of dissolved cadmium and Cd/PO4 ratio in Todos Santos Bay: A retention site of upwelled waters in the Baja California peninsula, Mexico", Marine Chemistry, Vol. 168, 2015, pp. 37–48.

[9] Hoell, A, et al, "Does El Niño intensity matter for California precipitation?" Geophysical Research Letters, Vol. 43(2), 2016, pp. 819–825.

[10] Griffin, D, & Anchukaitis, K. J., "How unusual is the 2012 – 2014 California drought ?" Geophysical Research Letters, Vol. 41, 2014, pp. 9017–9023.

11. Contamination of sediments by oil spills: current situation, management strategies and regulations

Session chairs: Alfonso Botello[1] and Teresa Álvarez[2]
[1]Instituto de Ciencias del Mar y Limnología (ICMyL), Universidad Nacional Autónoma de México
[2]Colegio de la Frontera Sur, México

The oil spills, ships accidents, ruptures in transport lines, natural seeps and discharges from urban waters, introduce an important quantity of petroleum into marine and coastal areas, whose final destination are the surrounding sediments. The more conspicuous examples are the spills of Ixtoc-I well (Bay of Campeche) and the Macondo well (Lousiana) both occurred in waters of the Gulf of Mexico. Once the oil is trapped in sediments, it remains there for long periods of time, being a risk for benthic and marine organisms interacting with them, and affecting local fisheries. In others big spills around the world (Alaska, USA: Spain, Saudi Arabia) the spilled oil had the same destination but different behavior. Regarding the management and regulations in different countries, these are very variable and depend on the enforcement of national laws and perhaps regional agreements, but actually there is a lack of action in this matter. Finally, it seems to be an excellent matter of discussion for this session.

AQUIFER AND AGRICULTURAL SOIL CONTAMINATION ORIGINATING FROM CLANDESTINE DRILLING IN PIPELINES TRANSPORTING HYDROCARBONS

Suárez-Arriaga Mario-César [1]
[1]Asociación Geotérmica Mexicana & International Geothermal Association, México

ABSTRACT

The pipelines transporting hydrocarbons in the Mexican territory are located close to highways and near secondary ways in rural areas with sedimentary soils. Diesel and gasoline are transported from production centers to the pumping and distribution stations using these pipelines. Despite both military and police surveillance, there is a constant illegal activity extracting distillate petroleum products through clandestine perforations made by powerful mafias in hundreds of country sites. These actions impact the ecological environment damaging agricultural sedimentary soils. The problem becomes more serious if the affected soil is linked to a shallow aquifer. Based on real data measured at different contaminated sites, a mathematical, numerical and computational model in 3D was created and used in this problem. The processes of molecular and hydrodynamic solute dispersion in soils made of sediments were numerically simulated in several cases. The model is based on the properties and physical parameters of the affected soil, of the groundwater system, and of the hydrocarbons. It was possible to predict the solute transport in the sedimentary aquifer materials from the moment at which the spill started. The mathematical and numerical tool developed helps to estimate approximately the horizontal extension and the vertical depth of the underground hydrocarbon spread behavior. The mathematical model, the data, and the results in graphical form are discussed in the paper.

Keywords: Soil contamination, sedimentary aquifer materials, dispersion, mathematical model, finite elements

INTRODUCTION: THE MODEL

Diffusion is a common molecular phenomenon in sedimentary aquifer materials, in soils and in porous rocks that occurs because of the presence of different concentrations of a solute substance in the fluid filling up the pores. Diffusion is the mechanism by which particles of a fluid mixture are transported from regions of high concentration to regions of lower concentration of the solute. Diffusion is the macroscopic effect of a molecular random motion that depends mainly on temperature [1]. In the aquifers herein studied, the solvent is the underground water and the solute is the diesel or the gasoline leaked. For diffusion in soils and in sedimentary aquifer materials, the transport equation is modified to consider the presence of both, the pores and the solid grains. The first form of Fick's law in porous media is a steady state equation [2]:

$$\vec{q}_D = -\varphi\,\mathbf{D}\cdot\vec{\nabla}C(x,y,z,t) = \\ = -\varphi\left(D_x\frac{\partial C}{\partial x} + D_y\frac{\partial C}{\partial y} + D_z\frac{\partial C}{\partial z}\right) \qquad (1)$$

Where $\boldsymbol{q}_D$ is the diffusion flux; $\mathbf{D}$ is diffusivity tensor; φ is effective porosity; C ($\mathbf{x}$, t) represents the molecular concentration of the solute in [mol/m^3], however, other units can be used such as [kg/m^3] or ppm.

Diffusion is quite different from the movement of molecules when a fluid is flowing. In this case, movement is not random; all molecules are moving together and in the same direction. The non-steady-state of Fick's law considers the change in concentration of the substance with respect to time. Combining Fick's law with the principle of conservation of mass for the spreading molecules, we obtain the following partial differential equation:

$$-\vec{\nabla}\cdot\vec{q}_D = \frac{\partial C(\vec{x},t)}{\partial t} = \vec{\nabla}\cdot(\mathbf{D}\cdot\vec{\nabla}C) \qquad (2)$$

Where ∇ is the spatial gradient and t means time.

Fick's Law with Convection and Dispersion

The general solute flux in sediments with fluid movement is made up of three components: diffusion, convection and mechanical dispersion. Convection occurs because the groundwater natural movement transport the solutes. Dispersion occurs because there is a mixing process produced by local velocity variations, which is macroscopically similar to molecular diffusion. This generalization of Fick's Law is expressed as follows:

$$\vec{\nabla}\cdot\left(\mathbf{D}\cdot\vec{\nabla}C\right)-\vec{\nabla}\cdot(C\vec{v}_f)=\frac{\partial C}{\partial t}+\frac{C_S q_V}{\varphi}$$

$$\mathbf{D}=\begin{pmatrix} D_x & 0 & 0 \\ 0 & D_y & 0 \\ 0 & 0 & D_z \end{pmatrix} \tag{3}$$

The scalar function C (x, y, z, t) is the solute concentration in moles/m^3, the matrix of coefficients D_x, D_y, D_z (m^2/s) are the principal values of the diffusion tensor $\mathbf{D}$, $\boldsymbol{v}_f$ is Darcy's velocity, C_S is the solute concentration in the source fluid and q_V [m^3/s/m^3] is the volumetric flow rate per unit volume of the source or sink in the aquifer.

Darcy's law is an expression of conservation of momentum, when the kinetic energy of the fluid is neglected. In two and three dimensions, gravity must be accounted for, because the vertical pressure drops because of gravity affecting the flow. In this case Darcy's law for a single phase fluid in an anisotropic porous medium of permeability tensor $\mathbf{K}$ is:

$$\vec{v}_f=-\frac{\mathbf{K}}{\mu_f}\left(\vec{\nabla}p-\rho_f\,\vec{\mathrm{g}}\right)=\begin{pmatrix} v_x \\ v_y \\ v_z \end{pmatrix}= \\ =\frac{-1}{\mu_f}\begin{pmatrix} k_x & 0 & 0 \\ 0 & k_y & 0 \\ 0 & 0 & k_z \end{pmatrix}\cdot\begin{pmatrix} \partial_x p \\ \partial_y p \\ \partial_z p-\rho_f g \end{pmatrix} \tag{4}$$

Where $\boldsymbol{v}_f$, μ_f, ρ_f, p, $\mathbf{K}$ and $\boldsymbol{g}$ are velocity, dynamic viscosity, density, pressure of the fluid, permeability tensor and gravity acceleration respectively. Darcy's law for a single phase fluid in an anisotropic porous medium of hydraulic conductivity tensor $\mathbf{K}_H$ is:

$$\vec{\nabla}\cdot\left(\mathbf{K}_H\cdot\vec{\nabla}h\right)=S_S\frac{\partial h}{\partial t}+q_V$$

$$\mathbf{K}_H=\begin{pmatrix} K_X & 0 & 0 \\ 0 & K_Y & 0 \\ 0 & 0 & K_Z \end{pmatrix}=\frac{\rho_f g}{\mu_f}\mathbf{K} \tag{5}$$

Where h (x, y, z, t) is hydraulic head in meters, S_S [m^{-1}] is the specific storage coefficient; the matrix coefficients K_X, K_Y, K_Z (m/s) are the principal values of the hydraulic conductivity tensor $\mathbf{K}_H$. The Principle of Conservation of Mass for the fluid in any porous medium is given by:

Equation (6) combined with Eq. (4) or (5) form a single coupled equation called the fundamental groundwater flow equation. Equation (3) is coupled to Eq. (4) via the flow velocity; this coupling allows computing the solute transport in both soil and aquifer.

$$\frac{\partial\left(\varphi\rho_f\right)}{\partial t}+\vec{\nabla}\cdot\left(\varphi\rho_f\vec{v}_f\right)=0 \tag{6}$$

Hydrodynamic Dispersion

This type of dispersion can be represented by two empirical coefficients (α_L, α_T), which quantify the amount of contaminant that is separated from the trajectory of the underground flow carrying the solute. Some portion of the solute could remain behind or ahead of this flow originating a longitudinal dispersivity α_L. Another part of the contaminant can be separated from the flow causing the transverse dispersivity α_T. Dispersivity is also affected by the permeability heterogeneity of the aquifer, and therefore by the hydraulic conductivity (see Eq. (4)). A portion of the fluid can follow a preferential path in one direction and another portion, follow a different path. This mechanism explains why contaminants can disperse irregularly in groundwater flow.

Dispersion represents the diffusion of solute by molecular diffusion and mechanical mixing. The components of the diffusion tensor $\mathbf{D}$ for any anisotropic medium can be calculated as follows:

$$\varphi D_{ii}=\alpha_L\frac{v_i^2}{\left\|\vec{v}_f\right\|}+\alpha_T\frac{v_j^2}{\left\|\vec{v}_f\right\|}+D_0; \\ \varphi D_{ij}=\varphi D_{ji}=\left(\alpha_L-\alpha_T\right)\frac{v_i v_j}{\left\|\vec{v}_f\right\|}+D_0 \\ \left\|\vec{v}_f\right\|=\sqrt{v_x^2+v_y^2+v_z^2}=\sqrt{v_i v_i} \tag{7}$$

Where v_i and v_j are the cartesian components of fluid velocity in Darcy's Law, and D_0 is the effective molecular diffusion coefficient.

BOUNDARY CONDITIONS AND MODEL PARAMETERS

The mathematical model boundary conditions for the solute concentration in the fluid flow are:

1). Dirichlet condition for solute concentration: C (x, y, z, t) = 0. This occurs at the lateral borders and at the bottom of the region where the solute does not arrive. The same condition is valid at the upper open boundary; this zone only receives rainwater, except in the area defined by the initial spill located in the sites where the discharge of the contaminant occurred. H_0 is the initial hydraulic head along this boundary.

2). Neumann condition at the area A_i occupied by the initial spill:

$$\vec{n}\cdot\left(\varphi\mathbf{D}\cdot\vec{\nabla}C - C\vec{v}_f\right) = C_0 R, \text{ if } 0 < t \le t_d$$
$$\vec{n}\cdot\left(\varphi\mathbf{D}\cdot\vec{\nabla}C - C\vec{v}_f\right) = 0, \text{ if } t > t_d \quad (8)$$

Where t_d is the total time of the hydrocarbon spill through the escaping point; n is a boundary normal vector, C_0 is the initial solute concentration, R is the recharge.

3). Neumann condition with advective flux at the open boundaries:

$$\vec{n}\cdot\left(\varphi\,\mathbf{D}\cdot\vec{\nabla}C\right) = 0 \quad (9)$$

This last boundary condition (Eq. (9)) allows the natural recharge from rainwater and the hydrodynamic dispersion of the contaminant in the same direction (Fig. 1, illustration adapted from COMSOL-Multiphysics, 2009, [3]).

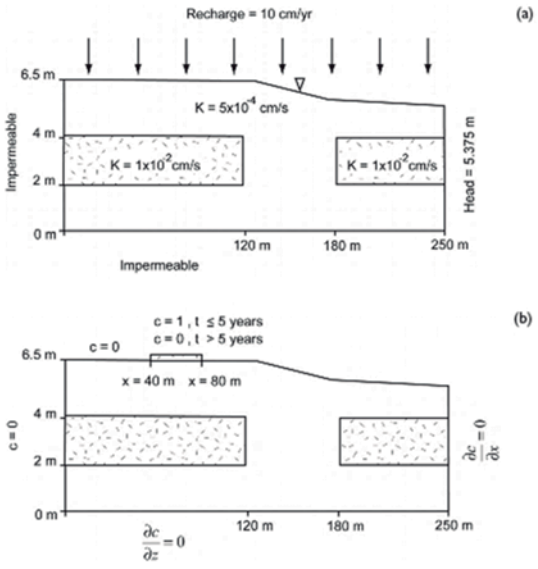

Fig. 1 Two-dimensional illustration of the solute transport, including rainwater recharge and boundary conditions [3]

a) Underground water flow is stationary. The soil is for agricultural use-type, formed by fine grain sediments in three layers with different hydraulic conductivity each one, named K_1, K_2, K_3. Two more coarse grain blocks are included to simulate heterogeneity. Rainwater is represented by a vertical recharge R [cm/year]. The X axis is the length of the zone. The height in this example, is equal to 6.5 m at the left side (Y axis), the height on the right side is 5 m. The water level is an unknown free surface in contact with the atmosphere. The base of the aquifer has very low permeability, and it is assumed equal to zero.

b) Starting at time $t = 0$, the water in the aquifer is clean and free of contaminants. The initial concentration of the solute is zero $C(0) = 0$. During the time interval t_d the solute infiltrates into the soil through a region of horizontal coordinates $[x_1, x_2]$ m. The concentration of the contaminant has a constant value $C(x, y, t) = C_0$ [kg/m^3] and only penetrates the soil through the spill area [$x_1 \le x \le x_2$].

This initial value C_0 is an important variable setting for the numerical simulation, because it will determine the evolution and distribution of the solute during the entire simulation time lapse. The concentration allows modeling the effect of the volume and weight of the solute while infiltrating at each site during a maximum time t_d of the spill. At the end of time t_d, the concentration at the source becomes zero ($C = 0$), because the source of the contaminant disappears. The contaminant moves by advection and dispersion into the soil reaching the aquifer. We assume typical values of longitudinal and transverse dispersivity $\alpha_L = 0.5$ m, $\alpha_T = 0.005$ m respectively. The effective molecular diffusion coefficient is equal to $D_0 = 1.87\times10^{-9}$ m^2/s, which corresponds to a prototypical value for hydrocarbons [1]. Porosity is uniform and homogeneous but has different values at each stratum. A technique to calculate porosity and permeability of the subsoil, based on its hydraulic conductivity, is developed in the next section.

Computing Porosity and Permeability of the Site

To approximate the value of porosity at each contaminated site, an inverted form of the 1976 Pearson's formula for permeability was used [1]:

$$k(\varphi) = 0.987\left(10^{(13.614\,\varphi - 1.8126)}\right)\times10^{-15} \Leftrightarrow$$
$$\varphi(k) = A\cdot\mathrm{Log}\left[6.580863\times10^{16}k\right] \quad (10)$$

Where $A = 0.03190058$ is an empirical coefficient. Relating permeability in Eq. (10) and hydraulic conductivity using Eq. (5):

$$K_H = \frac{\rho_f\, g}{\mu_f}k \Leftrightarrow k = \frac{\mu_f\, K_H}{\rho_f\, g} \quad (11)$$

This inversion formula makes possible to compute porosity as an approximated function of tensor $\mathbf{K}_H$:

$$\varphi(k) = A \cdot \mathrm{Log}\left[6.580863 \times 10^{16} \frac{\mu_f \, K_H}{\rho_f \, g} \right] \qquad (12)$$

The Numerical Model and the Parameters

The first part of the numerical model consists of the set of Eq. 3 to 7, plus the boundary conditions described in previous section. The second part is formed by the algorithms of the finite element method used to numerically solve these equations. The third part of the model is obtaining the corresponding numerical results in graphical form. A specialized software was used to solve the equations in the third part of the model [3].

From studies of soil mechanics, the necessary parameters were obtained. These parameters are: hydraulic conductivity, densities of sediments and of hydrocarbons, dynamic viscosities, compressibility of fluids and of soil, average temperature at the site and in the underground, initial solute concentration, initial volume of hydrocarbons on site, geometry and characteristics of the damaged zone, initial volume of affected soil, vertical penetration and superficial extension of the initial solute.

From laboratory data other correlations were estimated such as initial soil porosity and permeability, hydrocarbons diffusion coefficients and longitudinal dispersivity α_L and transverse dispersivity α_T.

NUMERICAL SIMULATION AND DATA

There are six layers in the subsoil with different geologic and physical characteristics. The altitude is 1762 meters above sea level (masl). There is a rain recharge of R = 70.81 cm/year = 2.25 × 10^{-8} m/s, which affects the flow. The natural underground flow direction is NE-SW. An aquifer is located 2 m depth. The horizontal geometry of the site and the points (P_1, P_2, P_3, P_4, P_F) of measured initial contamination are shown in Fig. 2. Table 1 contains the parameters needed in the simulation for a point-site called P_F. Permeability and hydraulic conductivity were measured in a soil mechanics laboratory.

Porosity was estimated using the inverted Pearson's formula (Eq. (12)). Water properties were computed using the equation of state for water IAPWS-95 [4]. Table 2 contains the physical coefficients of three main layers of this site.

Table 1 Parameters of the contaminated site

Parameter	Value	Units
altitude	1762	m
P_0	0.8188	bar
T_0	21.2	°C
R	70.81	cm/year
C_0	312.45	kg/m^3
V_0	575.0	m^3
A_S	400.0	m^2
V_S	1360	m^3
H_S	3.5	m
M_S	424.925	10^3 kg

Note: P_0 = atmospheric pressure, T_0 = average temperature, R = rain recharge, C_0 = initial solute concentration, V_0 = initial solute volume, A_S = soil area (contaminated), V_S = contaminated soil volume, H_S = contaminated soil depth, M_S = contaminated soil mass.

Table 2 Physical coefficients of the three layers

Coefficient	1st Layer	2nd Layer	3rd Layer
Depth (m)	0.5	0.8	2.1
ρ_S (kg/m^3)	1785.0	1760.6	1798.3
φ (%)	28.3	28.5	29.8
K_H (cm/s)	8.69×10^{-5}	1.16×10^{-4}	2.2×10^{-4}
k (m^2)	1.09×10^{-13}	1.15×10^{-13}	1.8×10^{-13}
ρ (kg/m^3)	739	739	739
δ (m^2/s)	1.9×10^{-9}	1.9×10^{-9}	1.9×10^{-9}
α_L (m)	0.5	0.5	0.5
α_T (m)	5.0×10^{-3}	5.0×10^{-3}	5.0×10^{-3}
ρ_{H2O} (kg/m^3)	999.5	997.9	995.6
μ_{H2O} (Pa.s)	12.3×10^{-4}	9.73×10^{-4}	7.9×10^{-4}
C_{H2O} (bar^{-1})	4.73×10^{-5}	4.57×10^{-5}	4.5×10^{-5}

Note: ρ_S = soil density, φ = porosity, K_H = hydraulic conductivity, k = absolute permeability, ρ = solute density, δ = diffusion, α_L = longitudinal dispersion α_T = transverse dispersion, ρ_{H2O} = water density, μ_{H2O} = water viscosity, and C_{H2O} = water compressibility.

Location of one contaminated site

The numerical simulations presented in this paper correspond to a site located in an agricultural region in the central part of Mexico. Figure 2 shows the geographical location of the contaminated site. Because of obvious (security) reasons, it is not possible to publish more detailed data about the site.

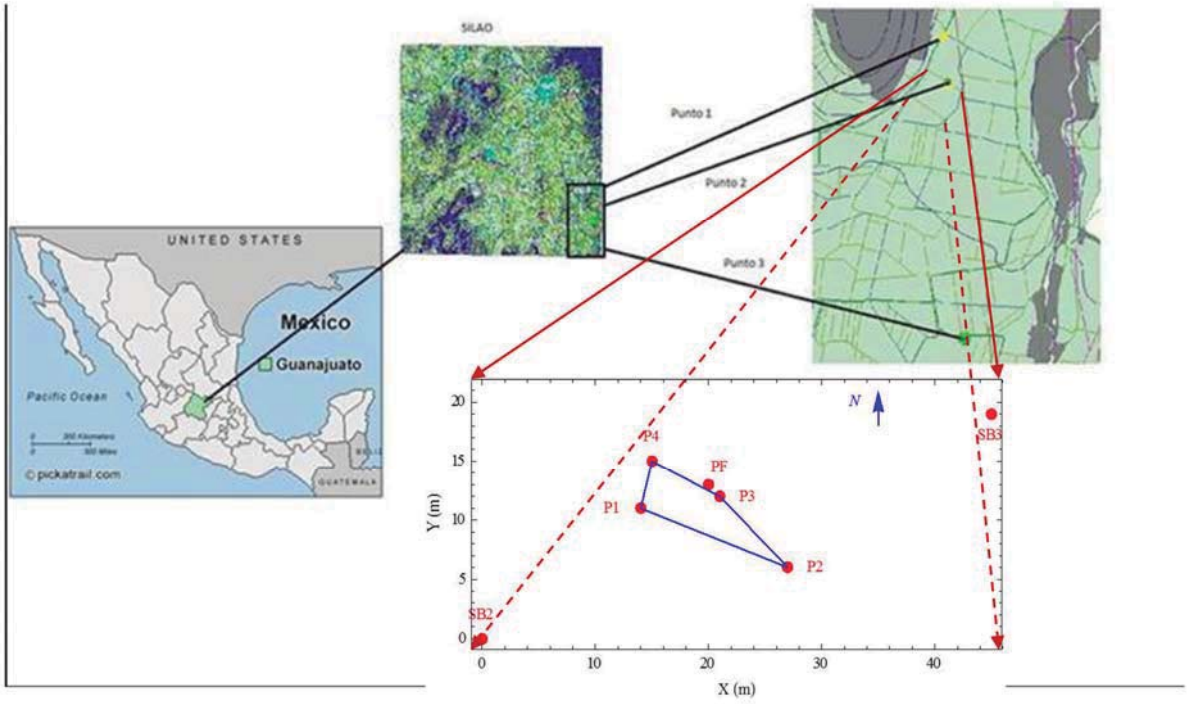

Fig. 2 Location of a contaminated site near the city of Silao, state of Guanajuato, Mexico

Mesh for the numerical simulation

The geometry of the contaminated zone is illustrated at the bottom of previous Fig. 2. This simplified geometry needs to be represented within the numerical frame of the finite element method in the form of a computational mesh formed by very simple geometrical objects, triangles in this case. Figure 3 shows the constructed mesh for this problem at the top of the contaminated area.

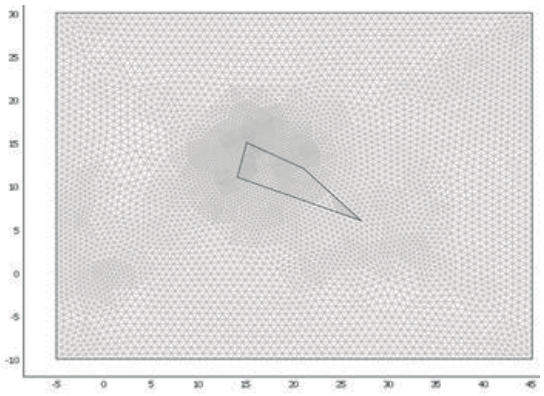

Fig. 3 Computational mesh of the site. It contains 10,960 triangular finite elements and 44,298 degrees of freedom. This size mesh was enough to attain desired precision

Transformation of field units

The practical units used in the laboratory for the solute concentration are ppm (1 ppm = 1 mg/kg, parts per million). The units in the model herein introduced and, in the software used [3] are [kg/m^3]. The practical conversion formulas, which include soil porosity are:

$$\rho_C = \frac{M_C}{V_C} = (1-\varphi)\rho_{soil} + \varphi\,\rho_{Solute}$$
$$1\ ppm = 1\frac{mg_{Solute}}{kg_{solvent}} = 10^{-6}\frac{kg_{Solute}}{kg_{solvent}} \qquad (13)$$

Where sub index *C* means contaminated. Thus, to convert [ppm] into [kg/m^3] and vice versa, the following equations are useful:

$$\boxed{C\left(\frac{kg}{m^3}\right) = \left((1-\varphi)\rho_{soil} + \varphi\,\rho_{Solute}\right)\frac{C\,(ppm)}{10^6}} \qquad (14)$$

$$\boxed{C\,(ppm) = \frac{10^6\ C\left(kg/m^3\right)}{(1-\varphi)\rho_{soil} + \varphi\,\rho_{Solute}}} \qquad (15)$$

Equations (14) and (15) were incorporated within the model equations described in the Introduction,

using the mesh shown in Fig. 3, the numerical model was programmed and solved with the Finite Element Method [3].

DISCUSSION OF GRAPHICAL RESULTS

Initial state

The contamination initial state was obtained from measurements of the solute concentration made *in situ* and analyzed in the laboratory with specific techniques. Figure 4 shows the computed initial state, which corresponds to time $t = 0$.

Numerical simulations at different times

The transport and distribution of refined hydrocarbons, essentially gasoline and diesel in Mexico, are made using pipelines which are located underground, parallel to highways and to secondary ways in agricultural areas, such as the site described in previous sections. Despite both military and police surveillance, there is a constant illegal activity of extracting these products through clandestine perforations made directly in the pipelines. These actions damage the agricultural soils and have a serious impact in shallow aquifers when they are present. The oil company must confront this situation and is responsible for its remediation.

In Mexico, the maximum solute concentration allowed in agricultural soils, established by a federal law, is 200 ppm or 0.3 kg/m^3, which is called Federal Norm Number 138 (NOM-138).

First of all, it is necessary to estimate the total contaminated soil volume and forecast the underground diffusion of the solute at different times, for six, twelve and eighteen months. Figures 5 and 6 illustrate the evolution and distribution of hydrocarbons within an interval of 11 m depth during 18 months of numerical simulation. Figure 6 shows the vertical distribution of the solute transported after 18 months of underground solute dispersion.

After 18 months of contaminant diffusion, the solute attains a maximum concentration of 1732 ppm (2.57 kg/m^3) at 8 m depth (Fig. 6). Numerical calculations allow to estimate the area and the soil volume affected by the hydrocarbon. The maximum area and volume contaminated were estimated to be 900 m^2 and 1848.5 m^3 respectively, the most affected depth is located between 3 and 9 m below the soil surface. With the help of these results, practical and cheap remediation actions could be executed with good precision.

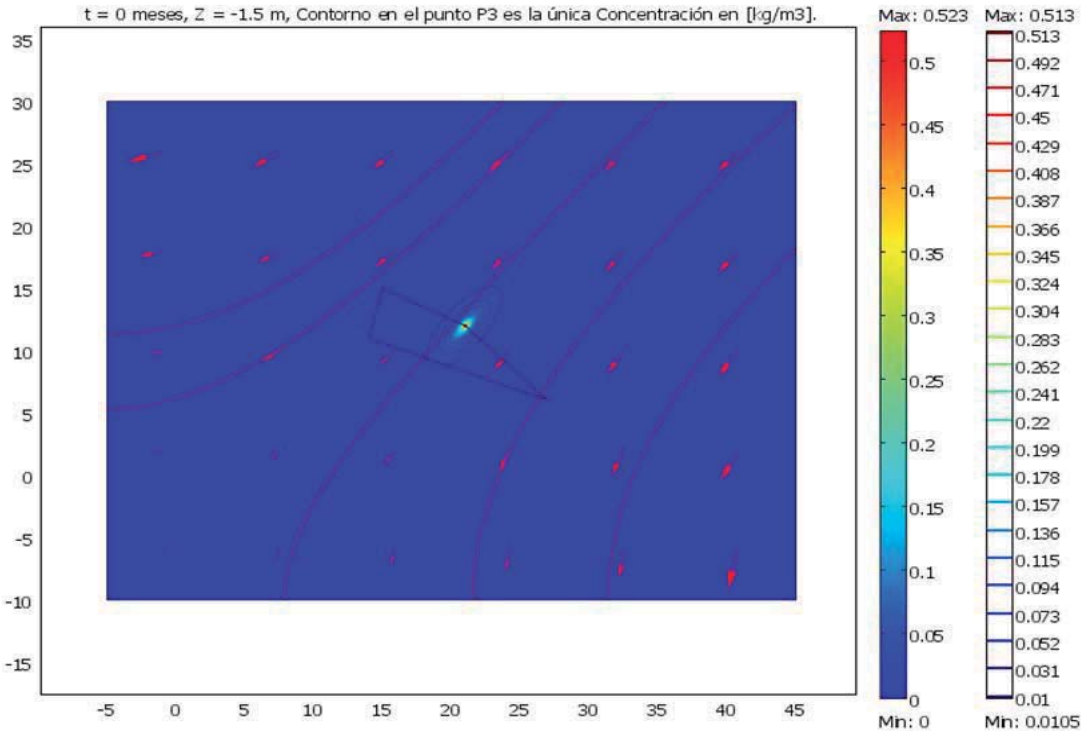

Fig. 4 Initial state of the contaminated site, at time $t = 0$ months, depth = 1.5 m. In all figures, the blue-light contours are iso-concentrations of the hydrocarbon in site. The red lines correspond to the underground flow of rain water; arrows indicate flow direction. The spill started at the point P_3 shown in Fig. 2

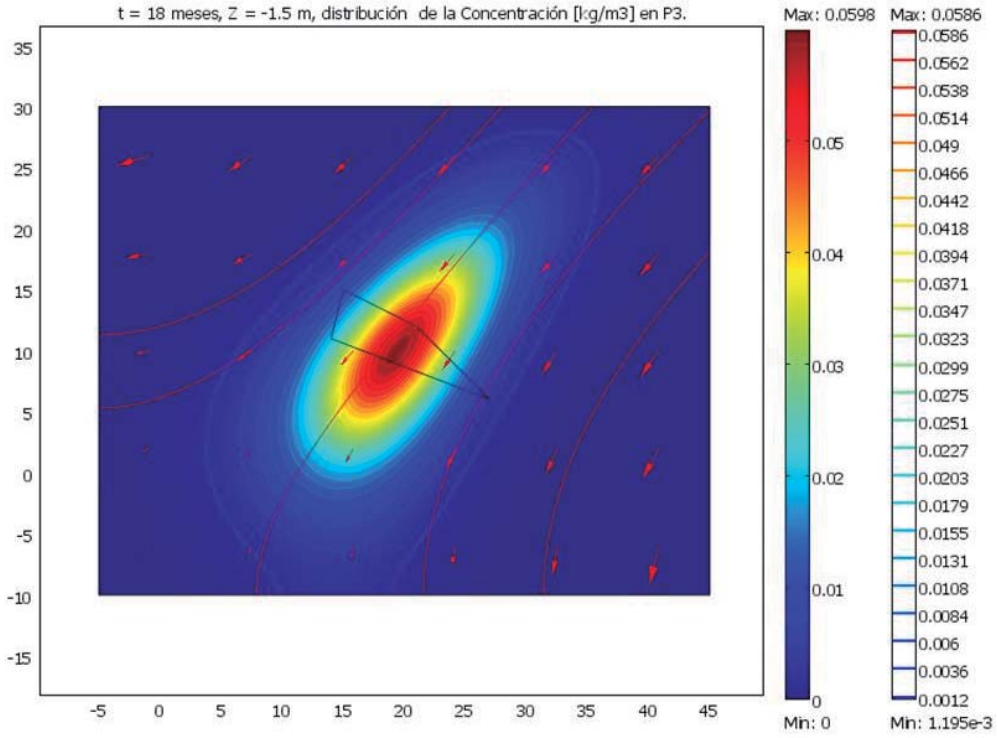

Fig. 5 State of the contaminated site, at time t = 18 months, depth = 1.5 m. The units are kg/m^3

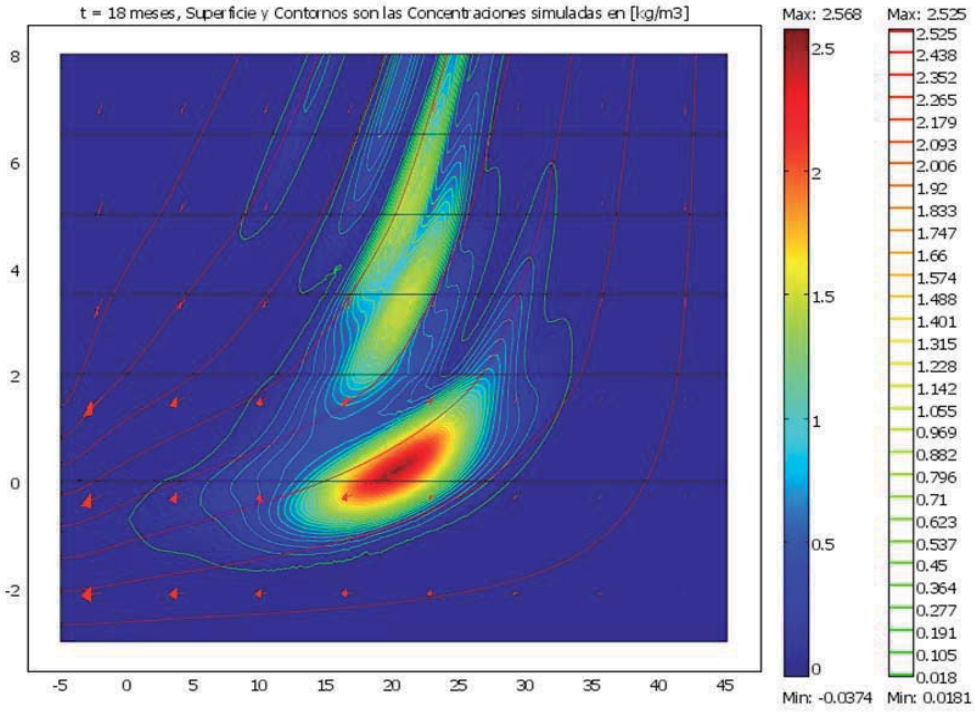

Fig. 6 State of the contaminated site, at time t = 18 months, the graphic shows the vertical distribution of the solute. The contours are hydrocarbon iso-concentrations. The units in the right bar are kg/m^3. The maximum concentration was 1732 ppm at 8 m depth. The total depth shown in this figure is 11 m

CONCLUSIONS

The hydrocarbon contamination of an agricultural soil made of sedimentary materials, linked to a shallow aquifer, was described. The mathematical model, data, and graphical results of the dispersion problem were presented and discussed in this paper.

The environmental problem originates from the fact that diesel and gasoline are transported from production zones to the distribution centers using federal pipelines. In Mexico there is a constant illegal activity of extracting those distillate petroleum products through clandestine perforations. These actions impact the ecological environment damaging agricultural soils affecting shallow aquifers subject to rain recharge.

Based on real data measured at different contaminated sites, a mathematical, numerical and computational model in 3D was created and used in one of the contaminated sites. The processes of molecular and hydrodynamic solute dispersion were numerically simulated at this site. In this way, it was possible to predict the hydrocarbons transport in the soil-aquifer system, estimating approximately the horizontal and vertical extension of the underground hydrocarbon dispersion.

Between one and six months after the hydrocarbon leakage, new measurements of the solute concentration were done at different parts of the site, verifying that the numerical results were successful and in good agreement compared with the real data.

The solute follows a complex preferential vertical path with lateral and longitudinal hydrodynamic diffusion because of the influence of the natural rain recharge. After 18 months of dispersion, the solute attains a maximum concentration of 1732 ppm (2.57 kg/m^3) at 8 m depth. The maxima contaminated area and volume were estimated equal to 900 m^2 and 1848.5 m^3 respectively, the affected depth is located between 3 and 9 m below the surface. With the help of these figures, remediation actions could be executed.

REFERENCES

[1] Bundschuh J, Suárez-Arriaga MC. Introduction to the Numerical Modeling of Groundwater and Geothermal Systems – Fundamentals of mass, energy and solute transport in poroelastic rocks. The Netherlands: Multiphysics Modeling Series Vol. 2, CRC Press/Balkema – Taylor & Francis Group, 2010, ch.4, pp. 115-128.

[2] Batu V. Applied flow and solute transport modeling in aquifers—Fundamental principles and analytical and numerical methods. Boca Raton, FL: CRC Press/Taylor & Francis, 2006, ch.2, pp. 11-33.

[3] COMSOL-Multiphysics software. “User’s guide version 3.5a”, COMSOL AB, 2009 Stockholm, Sweden.

[4] Wagner W and Pruss A. “The IAPWS Formulation 1995 for the Thermodynamic Properties of Ordinary Water Substance for General and Scientific Use”. J. Phys. Chem. Ref. Data, Vol. 31/2, 2002, pp. 395-478.

METALS IN SEDIMENTS OF THE NW OF THE GULF OF MEXICO, LITHOGENIC *vs* ANTHROPOGENIC. POSSIBLE GEOCHEMICAL DISTURBANCE DUE TO THE SPILL OF THE DEEPWATER HORIZON

Reyes-Yedra Claudia [1], Ponce-Vélez Guadalupe [2] and Vázquez-Botello Alfonso [2]
[1]Postgraduate course in marine sciences and limnology, National Autonomous University of Mexico, Mexico; [2]Institute of Marine Sciences and Limnology, National Autonomous University of Mexico, Mexico

ABSTRACT

The continental shelf and slope facing Tamaulipas state in the NW Gulf of Mexico is highly impacted by activities related to industry, agriculture and urban waste [1]. The important physical factors in the region are, the Loop Current, the high rainfall and the coastal circulation to the north in summer, while in winter the "nortes" and the coastal circulation to the south [2]; the presence of the Laguna Madre, and the contributions of the Bravo, San Fernando, Soto la Marina and Panuco rivers have a fundamental influence on the sedimentological composition of the area, prevailing silt-clayey sediments. In april 2010 the spill of the "Macondo" well to the north of the Gulf of Mexico, caused the interest to know the affectations in the national coasts, conforming a large geochemical data base derived from three oceanographic cruises carried out in summer 2010 and winter 2011 and 2012, collecting information on metals, organic matter and granulometry, combining a universe of 93 analyzed sites [3]. The objective of this work is to make a robust, exhaustive statistical analysis of the concentrations of Co, Cr, Ni and V in this Mexican region to know its dominant source and the main factors that define its spatial and temporal distribution. Most of the metals and sites evaluated were classified as lithogenic except for V and there were significant differences between the pattern observed in summer with respect to that recorded for both winters as well as between the inner continental shelf and the slope and latitudinally between the northern region under the influence of Rio Bravo and the central and southern area of the study area.

Keywords: Metals. Marine sediments. Lithogenic vs Anthropogenic

INTRODUCTION

Coastal and marine sediments are the final site for contaminants that are produced by human activities both in the continent and in the ocean. These pollutants carry in their composition heavy metals that are transported by the runoff of the rivers, via underground and atmospheric. In this way they can alter the natural concentrations of metals in sediments, and represent a threat to life because of their persistence in the environment, bioaccumulation and high toxicity [4] – [6]. So, the sediments are not just working as an anthropic metal sink but also as a source of pollutants in aquatic environments [7], and therefore of high importance to evaluate the environmental quality of aquatic systems.

The NW Gulf of Mexico (GoM) continental slope and platform area are highly impacted by activities related to agriculture, urban waste, and trade and oil industry in both continent and ocean. This area in its coastline has the mouth of rivers that go through different cities where there is still no control of both urban and industrial waste. In the ocean, side the recent explosion of the Macondo well in April 2010 caused the spilling of thousands of tons of oil causing the uncertainty of the impact on the national coasts. This led to the initiation of an environmental monitoring for which three oceanographic cruises were carried out: in summer of 2010, and winter of 2011 and 2012. It´s of paramount importance to know the main source of the metals in sediments, as well as the factors that intervene in their distribution to contribute to the development of strategies and control of pollutants in coastal zones [8], [9].

This work has as objectives i) to distinguish the geogenic source *vs* anthropogenic, of metals Co, Cr, Ni and V through the use of the estimators of Enrichment Factor (FE) and the Index of Geoaccumulation (Igeo), ii) identify the spatial and/or temporal distribution patterns of these metals in the NW of the GoM

Study Area

The continental shelf in front of the state of Tamaulipas is narrow (100 km) and terrigenous [10]. Recent studies on the origin of terrigenous sediments in the GoM have said that are derived from andesitic and basaltic rocks located along the coastal areas of the region. These are igneous mafic rocks that

present high concentrations of transition ferro-magnesian elements such as Cr, Sc, Ni, Co and V [11]-[14]. The state of Tamaulipas in its coastal line has the largest lagoon in Mexico The Madre lagoon, with the mouth of the Rio Bravo to the north, and the rivers Pánuco, San Fernando and Soto la Marina to the south. The winds that prevail in winter are towards the south as a result of the penetration of polar air masses to the GoM. These winds called "Nortes", produce a flow on the continental shelf of Tamaulipas-Veracruz directed towards the south, while from April to August (Spring-Summer) the flow is northward [15]. It has been pointed out that due to the action of the "Nortes", large amounts of sand are dragged towards the ocean, and sometimes the sea adopts a brown tone in a strip covering 1 Km of the sea in the beach line [16]. The circulation of GoM is dominated by the loop current that penetrates through the Yucatan channel and goes out through the strait of Florida, with its highest levels in spring and summer, and the minimums in winter [17]. In its intrusion the loop current has a westward direction forming anticyclonic whirlpools that are detached from it [18]. When the turns are in front of the coast of Tamaulipas, they begin to elongate in the form of ellipses and to dissipate to form cyclonic whirlpools [19]. It is an area highly impacted by cyclones and hurricanes occurring between May and December, its maximums are recorded mainly in mid-August and late October [20].

MATERIALS AND METHOD

The sampling area was located Northwest of the GoM, within the latitudes 22.5 ° – 25.9 ° N and lengths 96.7 ° – 97.0 ° W (Fig. 1). Three oceanographic cruises were conducted in two climatic seasons M-I in Summer (2010) and M-II and M-III in Winter (2011 and 2012 respectively). The sampling network of stations understood seven (2010), five (2011) and six (2012) transects perpendicular to the coast which had the influence of various river discharges: Rio Bravo (TI and TII), Río San Fernando (TIII and TIV), Río Soto la Marina (TV), Pánuco River (TVII); TVI received the effect of both the Soto la Marina and the Pánuco at different times of the year; five stations were established in each one at depths of 50, 100, 200, 500 and 1500 m, with 93 sediment samples total. Metals included Co, Cr, Ni and V, the technique used was that described by [21] consisting of a digestion in a microwave oven (CEM Mars5x) with HF, reagent water and super-pure HNO_3 and use an ICP-MS (ICP7500c); analytical quality was controlled using blanks, approved standards, reference material and recuperation percentages were 89% Cr, 102% Ni and 97% V; detection limits were, Cr 0.0226, Ni 0.021 and V 0.0213 $\mu g g^{-1}$. Organic carbon determination in sediments was based on the method of [22] for oxidation with K_2CrO_7 and concentrated H_2SO_4 followed by titration of the excess dichromate with 0.5 N $Fe(NH_4)2(SO_4)6H^2O$. Granulometric analysis was conducted with the aid of a Beckman Coulter LS230 laser diffraction particle size analyzer adjusted for samples with a range size of 0.04 y 2000 mm [23].

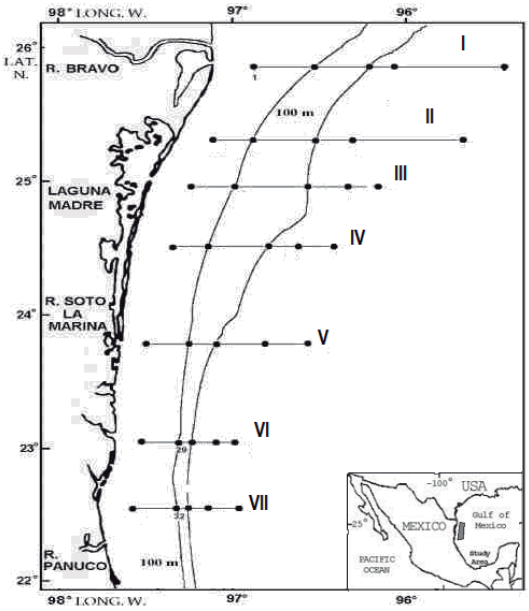

Fig. 1 Map of the study area and sampling sites in the NW of Gulf of Mexico

Evaluation of pollution in sediments

In this study two different indices were used to evaluate the degree of contamination by metals in sediments.

Enrichment Factor (FE)

Normally it is used to evaluate the source and degree of contamination by metals in sediments [24], by the following equation

$$\boldsymbol{FE} = \left[\left(\frac{\boldsymbol{M}}{\boldsymbol{Fe}}\right)\boldsymbol{sample}\right] / \left[\left(\frac{\boldsymbol{M}}{\boldsymbol{Fe}}\right)\boldsymbol{cortex}\right] \quad (1)$$

This equation considers the relationship between the concentration of a metal (M) and the Fe present in the sample and the same relationship in the terrestrial cortex (natural background level) [25]. There is no classification system for pollution or categorization of the degree of pollution based on the FE methodology that has been accepted. Two Categories of pollution have been proposed for the FE: < 2 is considered as lithogenic origin, ≥ 2 is due to anthropogenic source [26].

Index of Geoaccumulation (Igeo)

This index allows to evaluate the level of contamination of the metals in sediments by comparing the current concentrations with the preindustrial ones by means of the following equation

$$Igeo = log_2\left(\frac{Cn}{1.5*Bn}\right) \quad (2)$$

where Cn is the measured concentration of the metal analyzed "n" in the sediment and Bn is the background geochemical concentration [27], [28].

[29] defined seven classes of this level of pollution: 1 (0 < Igeo < 1) of No Contaminated (NC) to Moderately Contaminated (MC); 2 (1 < Igeo < 2) Moderately Contaminated (MC), 3 (2 < Igeo < 3) of Moderate (MC) to Highly Contaminated (HC), 4 (3 < Igeo < 4), Highly Contaminated (HC), 5 (4 < Igeo < 5) from Highly Contaminated (HC), to Extremely contaminated (EC) and 6 (Igeo > 5) Extremely Contaminated (EC).

RESULTS AND DISCUSSION

The calculations of FE and Igeo were realized for Co, Cr, Ni and V concentrations of each of the three cruise stations (n = 93). A comparison was made between cruises, depth and transects both in a general way and in detail fashion, in order to detect some effect by season, depht, or latitude in the FE and in Igeo of these metals. To calculate both indices, background levels of [30] were used. To evaluate the value of FE the classification of [26] and for Igeo that of [29] were used.

The estimated results of FE for Co, Cr and Ni, both general (average) and detailed (specific sites) of the three cruises made, indicated to be lithogenic as those of V for the oceanographic campaigns of summer 2010 and Winter 2011 (FE < 2). In the case of the results of V for Winter 2012, 63.6% of the stations analyzed, had a FE corresponding to anthropogenic sources (FE ≥ 2) (Fig. 2); the observed north-south latitudinal distribution of sites with an anthropogenic V was between 80 and 100% in transects I and II with the influence of the Rio Bravo, of 50-80% in the TIII and TIV, and between 20 and 50% in TV and TVI; when considering the depth it was observed that in the sediments obtained from the continental shelf at < 200 m, 61.1% had V anthropic whereas those from the continental slope were divided into those collected at ~ 500 m depth with 33.3% of V-type anthropogenic and deeper areas (> 500 m) registered 88.8% of the sediments with vanadium of human origin.

However, in order to be conclusive about the origin of the metals, particularly of the V, it is important to consider all the geological information possible of the place of study. Recent research on the origins of terrigenous sediments in the GoM highlight that are derived from andesitic and basaltic rocks located along the coastal areas of the region; these rocks present high concentrations of transition ferro-magnesia elements as Cr, Ni and V [31]; these data can contribute to clarify the high concentrations of this metal in this marine region where they can dominate in winter by the action of the "Nortes" due to the sand intrusion into the sea [16].

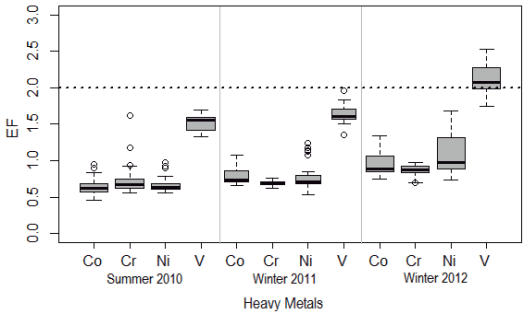

Fig. 2 FE of metals Co, Cr, Ni and V in surface sediments of platform and continental slope of NW Gulf of Mexico. Oceanographic Cruises: Summer 2010, Winter 2011 and 2012

The results of Igeo for the average concentrations of Co, Cr, Ni and V indicated that the sediments were classified as NC (Class 1) by these elements (Igeo < 0) (Fig. 3).

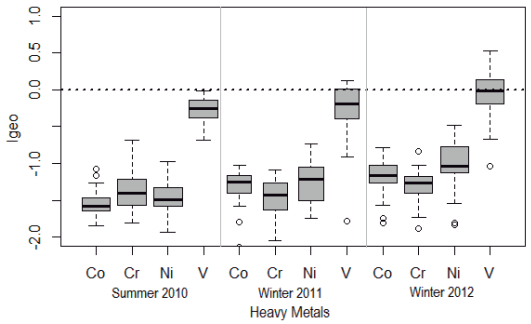

Fig. 3 Igeo Co, Cr, Ni and V In surface sediments of platform and continental slope Of NW of Gulf of Mexico. Oceanographic Cruises: Summer 2010, Winter 2011 and 2012

However, the specific data of the IgEo for V pointed out that different sediments were classified as type 2, i.e. between NC and MC for winter sampling 2011 (28% of the stations) and winter 2012 (42.4% of the sites). Considering the depth of the winter samplings, the sites of the continental shelf ≤ 200 m, they had between 26 and 44% of type 2 sediments for their values of Igeo; for the

continental slope, the collection stations with depths of ~ 500m, presented between 50-60% of NC-MC sediments and those sites located > 500 m, only had 33% in this category for the winter of 2012. The latitudinal distribution of V type 2 (not contaminated to moderately contaminated) observed for the 2011 winter collection showed an interval of 60 to 20% of sediments in this category of Igeo, between the TII transect and the TIV, i.e. between the southern part of the Río Bravo and the Soto la Marina; in contrast, by the winter of 2012, the interval was from 20 to 75% vanadium sedimentary Class 2, where the lowest value had the area of TVI, intermediate zone between the rivers Soto la Marina and Pánuco and the highest corresponded to the region of influence of the Bravo (Fig. 1).

The FE and Igeo had congruent results, on the one hand evidence that Co, Cr and Ni were lithogenic and they probably derive from the basalt geological component that prevails in the region and on the other, by indicating that the concentrations of V can have a contribution of human sources (FE > 2) giving as a result a degree of pollution from incipient to moderate (IgEo > 0 < 1), mainly in the winter of 2012. The continental contribution is important in this region of the Gulf of Mexico due to the large flows that carry a considerable amount of suspended materials, mainly terrigenous sediments, that drain and flood the continental shelf and part of the slope with them from the northern border with the undeniable influence of the Rio Bravo to the adjacent Mexican state of Veracruz where the Pánuco River can affect the coastal circulation and the distribution of all the content that contributes to GoM.

As a complementary it was studied the interaction between metals and the main sedimentologic characteristics such as type of sediment and organic carbon content through a principal component analysis (Fig. 4). A close relationship between Ni and Co was observed with a tendency to associate with clays, while Cr showed greater affinity for organic carbon and silts; the V did not have a clear pattern of correlating with the type of grain or with the organic carbon showing a small tendency towards Cr, probably as a result of the anthropogenic component.

CONCLUSIONS

The results of FE and Igeo confirm the factors involved in the presence and distribution of the metals studied in superficial sediments of the NW of the Gulf of Mexico. According to the values of the considered estimators, concentrations of Co, Cr, Ni are of a geogenic nature, while for the V was of anthropogenic; however, we should not rule out that the lithological characteristics of the region and the action of the dominant winds participate in the composition of sedimentary metals present in the marine zone. In addition, it is essential to include the origin and contamination level estimators in order to be able to correctly diagnose whether the data obtained from the environmental studies that include metals represent a risk to the ecosystems or are part of the natural habitat conditions under the which the biological communities have evolved together.

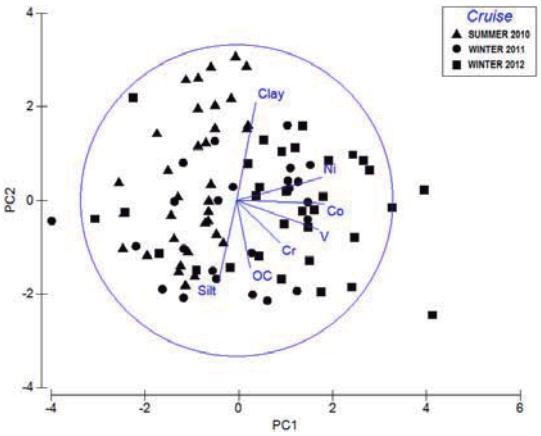

Fig. 4 Principal component analysis (PCA) of the data of surface sediment of NW of Gulf of Mexico

ACKNOWLEDGEMENTS

This work was part of the research project "Environmental framework of oceanographic conditions in the NW Sector of Mexico's ZEE in the Gulf of Mexico (MARZEE)", funded by the CONABIO, SEMARNAT and UNAM. In the same way, we appreciate the support granted by the Postgraduate course in marine sciences and limnology of UNAM for the development of the master thesis work of the first author.

REFERENCES

[1] Ponce-Vélez G *et al*., "Organic and inorganic pollutants in marine sediments from northern and southern continental shelf of the Gulf of Mexico", Int. J. Environment and Pollution, Vol. 26, 2006, pp. 295-311.

[2] Figueroa-Espinoza B *et al*., "On the wind power potential in the northwest of the Yucatan Peninsula in Mexico", Atmósfera, Vol. 27(1), 2014, pp. 77-89.

[3] Botello AV *et al*., "Baseline for PAHs and metals in NW Gulf of Mexico related to the Deepwater Horizon oil spill", Estuarine, Coastal and Shelf Science, Vol. 156, 2015, pp. 124-133.

[4] Tam NF, Wong YS, "Spatial variation of heavy metals in surface sediments of Hong Kong

mangrove swamps", Environ Pollut., Vol. 110(2), Nov. 2000, pp.195-205.
[5] Haruna A *et al*., "Chemical fractionation of trace metals in sewage water-irrigated soils", Int. J. Environ. Res., Vol. 5, 2011, pp. 733-744.
[6] Ghaderi AA *et al*., "Evaluating the effects of fertiliziers on bioavailable metallic pollution of soils, case study of Sistan farms, Iran", Int. J. Environ. Res., Vol. 6(2), 2012, pp. 565-570.
[7] Singh KP *et al*., "Studies on distribution and fractionation of heavy metals in Gomti river sediments – A tributary of the Ganges, India", J. Hydrology, Vol. 312, 2005, pp. 14-27.
[8] Long ER *et al*., "Incidence of adverse biological effects within ranges of chemical concentrations in marine and estuarine sediments", Environmental Management, Vol. 19(1), 1995, pp. 81-97.
[9] SEPA (State Environmental Protection Administration of China). Marine sediment quality GB18668-2002. Standars Press of China, Beijing, 2002.
[10] Ward CH, Tunnell JW, "Habitats and biota of the Gulf of Mexico: An overview", Habitats and Biota of the Gulf of Mexico: Before the Deepwater Horizon Oil Spill, Vol. 1, Ed. C. Herb Ward: Springer Open, 2016, pp. 7-9.
[11] Cullers RL *et al.*, "Rare earths in size fractions and sedimentary rocks of Pennsylvanian-Permian age from the mid-continent of the USA", Geochim Cosmochim. Acta 43, 1979, pp. 1285-1302.
[12] Armstrong-Altrin JS *et al.*, "Geochemistry of the Jurassic and upper Cretaceous shales from the Molango Region, Hidalgo, Eastern Mexico: implications of source-area weathering, provenance, and tectonic setting", CR Geosci., Vol. 345, 2013, pp. 185-202.
[13] Armstrong-Altrin JS, Natalhy-Pineda O, "Microtextures of detrital sand grains from the Tecolutla, Nautla, and Veracruz beaches, western Gulf of Mexico, Mexico: implications for depositional environmental and palaeoclimate", Arab J Geosci, Vol. 7, 2014, pp. 4321-4333.
[14] Armstrong-Altrin JS *et al*., "Petrography and geochemistry of sands from the Chachalacas and Veracruz beach areas, western Gulf of Mexico, Mexico: constrains of provenance and tectonic setting", J. S. Am. Earth Sci., Vol. 64, 2015, pp. 199-216.
[15] Zavala-Hidalgo J *et al.*, "Seasonal circulation on the western shelf of the Gulf of Mexico using a high-resolution numerical model", J. Geophys. Res., Vol. 108, 2003.
[16] CIFSA, Estudio regional de la laguna Madre de Tamaulipas. Estudio preliminar para la rehabilitación de la laguna madre de Tamaulipas, México, 1967.
[17] Molinari RL, Morrison J, "The separation of the Yucatan Current from the Campeche Bank and the intrusion of the loop current into the Gulf of Mexico", Journal of Geophysical Research, Vol. 93, 1988, pp. 10645-10654.
[18] Vukovich FM, Loop Current boundary variations, J Geophys. Res., Vol. 93, 2007, pp. 15585-15591.
[19] Merrell WJ, Morrison JM, "On the Circulation of Western Gulf of Mexico with Observations from April 1978", Journal of Geophys., 1981, pp. 4181-4185.
[20] NHC, National Hurricane Center. 2012
[21] Suwandana E, Kawamura K, Soeyanto E, "Assessment of the Heavy Metals and nutrients in the Seawater, Sediment and Seagrass in Banten Bay, Indonesia and Their Distributional Patterns" , J of Fisheries International, Vol. 6, 2011, pp. 18-25.
[22] Ortiz ML, Sánchez E, Gutiérrez ME, "Análisis de suelos, fundamentos y técnicas Parte 1", Cuernavaca. Universidad Autónoma del Estado de Morelos, México, 1993. 104p.
[23] Solleiro-Rebolledo E *et al*., "Fluvial processes and paleopedogenesis in the Teotihuacan Valley, Mexico: Responses to late Quaternary environmental changes", Quaternary International", Vol. 76/77, 2011, pp. 231-240.
[24] Zhang J, Lui CL, "Riverine composition and estuarine geochemistry of particulate metals in China - Weathering features, antropogenic impact and chemical fluxes", Estuar. Coast. Shelf, Vol. 54, 2002, pp. 1051-1070.
[25] Alomary AA, Belhadj S, "Determination of heavy metals (Cd, Cr, Cu, Fe, Ni, Pb, Zn) by ICP-OES and their speciation in Algerian Mediterranean Sea sediments after a five-stage sequential extraction procedure", Environmental Monitoring and Assessment, Vol. 135, 2007, pp. 265-280.
[26] Grousset FE *et al.,* "Anthropogenic *vs*. lithogenic origins of trace elements (As, Cd, Pb, Rb, Sb, Sc, Sn, Zn) in water column particles northwestern Mediterranean Sea", Mar Chem, Vol. 48, 1995, pp. 291-310.
[27] Yin H, Gao Y, Fan C, "Distribution, sources and ecological risk assessment of heavy metals in surface sediments from Lake Taihu, China", Environ. Res. Lett., Vol. 6, 2011, pp. 1-11.
[28] Marchand C, Allenbach M, Lallier-Vergès E, "Relationships between heavy metals distribution and organic matter cycling in mangrove sediments (Conception Bay, New Caledonia)", Geoderma, Vol. 160, Jan. 2011, pp. 444-456.
[29] Müller G, "Die Schwermetallbelastung der Sedimente des Neckars und seiner Nebenflusse: Eine Bestandsaufnahme", Chem-Ztg, Vol. 105, 1981, pp. 157-164.
[30] Wedepohl KS, "The composition of the continental crust", Geochimica et Cosmochimica Acta, Vol. 59, 1995, pp. 1217-1232.
[31] Armstrong-Altrin JS, Machain-Castillo ML, "Mineralogy, geochemistry, and radiocarbon ages of deep sea sediments from the Gulf of Mexico, Mexico". J. of South American Earth Science, Vol. 71, 2016, pp. 182-200.

EVALUATION OF AN HYDROCARBON POLLUTED SOIL AFTER BEING REMEDIATED

Lara Guzmán Uriel [1], Castillo Román José [1], Sánchez Hernández Andrés [2], and Teutli León Margarita[1]
[1]Facultad de Ingeniería, [2]Facultad de Arquitectura, Benemérita Universidad Autónoma de Puebla, Mexico

ABSTRACT

An evaluation of restoration achievements for a hydrocarbon polluted soil is conducted through geotechnical and physicochemical analysis of soil quality. It is known that hydrocarbon polluted soil remediation can be enhanced by adding microbial population from either wastewater sludge, compost, manure, oxidant metals or plants [1-5]. This study was done for a soil, which three years ago, was impacted by an hydrocarbon spill, at that time a tomography was performed; actual soil quality was assessed by in-situ performing a new tomography, and soil agricultural quality is assessed by soil sampling at three parcels: the impacted one, a nearby one and a clean one. Samples were collected at top soils and for critical points it was done a vertical sampling at 0.3, 0.6 and 0.9 m; all samples were analyzed for 23 physicochemical parameters, and with the information it was estimated the SAR and ESP parameters, also to assess the interdependence of the chemical parameters a Pearson correlation was done. Results have provided evidence that the impacted soil has reached a good recovery and now is suitable for landfarming activities.

Keywords: Hydrocarbon pollution, Soil remediation, Tomography, Physicochemical analysis

INTRODUCTION

It is widely accepted that there is a remarkable proportion of Hydrophobic Organic Compounds (HOCs) that once entering into the soil matrix will tightly associate with aggregates and persist in it. It has been reported that presence of Polycyclic Aromatic Hydrocarbons (PAHs) in soils is dependent of surface area and bulk chemical composition of the organic matter in humic substances [1]. However, when artificially organic compounds are added to soil samples, these spiked samples behave different from real soils. It is reported that topsoil samples amended with poultry manure, allowed for hydrocarbon removals of up to 40% with a 25% amendment [2]. Environmental factors can affect biodegradation of organic contaminants in soil, examples of these factors are content of organic matter, clay minerals, temperature, water content, pH, salinity, ionic content having presence of Na^{+}, Cl^{-}, CO_3^{-2}, SO_4^{-2}, particle and pore size distribution, supply of oxygen, C/N ratio and bioavailability of inorganic nutrients; also, it has been reported that while salinity inhibits microbial activity impeding rapid removal of hydrocarbons, addition of wastewater sludge might alter soil characteristics providing nutrients and microorganisms to accelerate their dissipation. In two soils amended with wastewater sludge and polyacrylamide, it was observed a faster removal of anthracene and phenanthrene [3].

Pollutants either as particulate or liquid films, can be adsorbed, absorbed, dissolved in the intersticial pore water, or present as solid phases in the soil pores. It is known that pollutant availability and mobility can be assessed from the water soluble fraction analysis. A report about nanotechnologies applied to soil remediation refers the onsite use of zero valent iron nanoparticles (nZVI), which in combination with bioremediation produces a synergistic effect where iron acts as strong reducing agent, while use of compost ensures the nutrients and organic matter for microorganisms and for having a proper C/N ratio (recommended value is 10) [4]. The effectiveness of plant-bacteria partnerships depends largely on the survival and metabolic activities of exogenous bacteria carrying degradation genes required for the enzymatic degradation of organic pollutants, then HOCs and PAHs can be degraded if there is a plant-bacteria association; usually it is recommended using bacteria having both pollutant degrading and plant growth promoting activities, the most beneficial bacteria are those living in the root zone [5].

In this work it is reported an evaluation of soil quality for a land impacted by a hydrocarbon spill that happened three years ago.

METHODOLOGY

The study area is described in UTM coordinates, it corresponds to the polygon generated from point A (630112 E, 2097414 N) to point B (630457 E, 2097213 N), an aerial view is shown in Figure 1. This area comprise three nearby parcels with different characteristics which are designated as A= parcel contaminated and under natural attenuation process (12 samples), B= non contaminated parcel (12 samples), C= parcel contaminated and bioremediated (22 samples).

Fig. 1 Aerial view of the studied zone at Acatzingo, Puebla, México.

Sample collection and analysis was done according to the Mexican Norm NOM 021 RECNAT 2000 specifications for fertility, salinity and soil classification. Studies, sampling and analysis [6]. Top soil samples (20-30 cm depth) were collected, properly labeled and transported to the laboratory. Samples were dried at room temperature, and later on a soluble fraction was obtained by preparing an analytical sample (1:2 soil:water ratio), filtration was done with a #2 Whatmann paper, and filtered solution was used for determining pH with a conductronic potentiometer, electrical conductivity (EC, □S cm^{-1}) with a CL8 conductronic tester; anions like SO_4, NO_3, NO_2, PO_4 and the chemical oxygen demand (COD) were determined with HACH reagents and the 2500 DR HACH spectrophotometer; gravimetric methods were applied for chloride (Cl), phenolphthalein and methyl orange alkalinity (Alkf, AlkT), Total Hardness (TH) and Organic Matter (OM); metals like Cr, Na, K, Ca, Fe, Mn, Pb, Ni, Cu, Cd, Zn , were determined with the GBC932 Atomic Absorption spectrophotometer.

In order to discriminate contributions, the MINITAB17 software was used to generate a Pearson correlation analysis involving all chemical parameters. Additionally surface plots were generate for each parameter using the surfer program version # 1.

RESULTS AND DISCUSSION

Results will be presented as follows: physicochemical data first, Pearson's correlation interpretation second, and tomography correlation last.

Physicochemical parameters

In this section discussion is restricted to the most relevant parameters which are: pH, EC, CO_3, PO_4, OM, COD, SAR and ESP.

pH

The three parcels A, B, C registered values above the slightly alkaline range and .few samples from parcel A and B overcome the strongly alkaline values. Results are shown in Figure 2

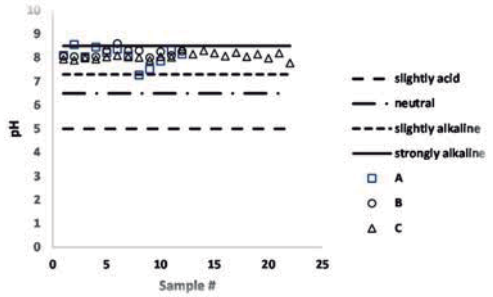

Fig 2. pH results for parcels A, B and C

Electrical Conductivity (EC)

This parameter represents a salinity risk condition, and in this sense it is observed that parcel A exhibits an irregular pattern with about 30% in the slight salinity and 60% above the moderate salinity; for parcel B samples are closer to the moderate salinity threshold value being 42% below and 58% above; finally the parcel C all samples are below the low salinity threshold value. Although none of the samples in any parcel A, B, C exceed the 4 dS m^{-1}, threshold value which combined with a ESP>15% will classify the soil as a sodic saline one. Results are shown in Figure 3.

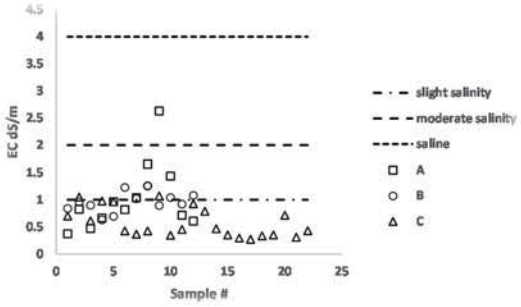

Fig 3. Electrical conductivity (EC) results for parcels A, B and C

Carbonate (CO_3)

This parameter can modify the micronutrients availability, for parcel A all samples have very low content; in parcel B some samples have very low content, but also 25% of the samples are above the medium content threshold value; finally in parcel C

carbonate content falls between medium and high content values. Which implies that natural attenuation has led the conditions to a non calcareous soil in parcel A. While the bioremediation has produce an alkaline effect on parcel C. Results are shown in Figure 4.

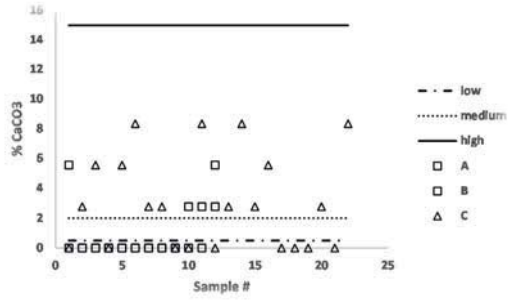

Fig 4. Carbonate results for parcels A, B and C

Phosphate (PO_4)

Soil fertility requires a phosphate content which according to the NOM 021 can be classified as low (<5 mg Kg^{-1}), medium (5<PO_4<11 mg Kg^{-1}) and high (>11 mg Kg^{-1}). Findings are as follow: parcel A has irregular content since 58% are low, 25% are medium and 17% are high; parcel B has values around the medium threshold values being 70% above medium and 30% below. Otherwise for parcel C all samples are in the low content range. Results are shown in Figure 5.

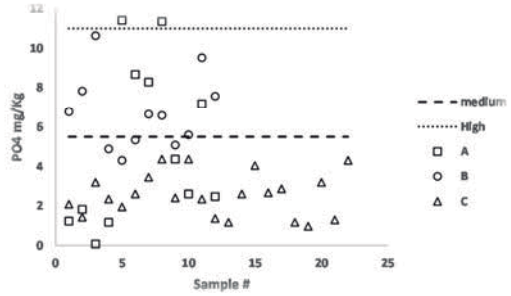

Fig 5. Phosphate results for parcels A, B and C

Organic Matter (OM)

Samples from parcel A exceed the very high content threshold value, while parcel B even though it has values above high content these are lower than the ones found for A, and parcel C has its values between medium and high content. Results are shown in Figure 6.

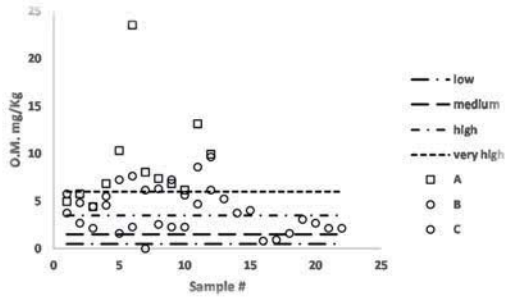

Fig 6. Organic Matter (OM) results for parcels A, B and C

Chemical Oxygen Demand (COD)

This parameter can be used to estimate the amount of oxygen demanding pollutants, and even though it is not referred in the NOM 021 it is worthy to point out that parcel B has the higher values since 30% of samples are above 1000 mg Kg^{-1}; parcel C can be considered of medium toxicity since most of its COD values are under 600 mg Kg^{-1}, and parcel A is the least contaminated since most of its values are under 200 mg Kg^{-1}, in this sense it is worthy to point out that natural attenuation (parcel A) has produced better conditions than the bioremediated one (parcel C) and the one that it was not impacted (parcel B) should be examined under other parameters oxygen demanding. Results are shown in Figure 7.

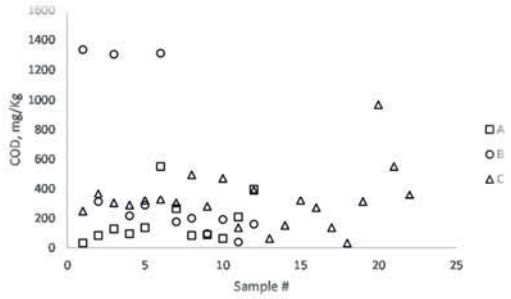

Fig 7. Chemical Oxygen Demand (COD) results for parcels A, B and C

Sodium Adsorption Ratio (SAR)

This parameter is useful to estimate the salinity risk as a function of the balance between Na^{+}, Ca^{+2} and Mg^{+2}, medium risk threshold value is 10, but all parcels (A, B and C) have values below 5, these means that there is not risk at all. Results are shown in Figure 8.

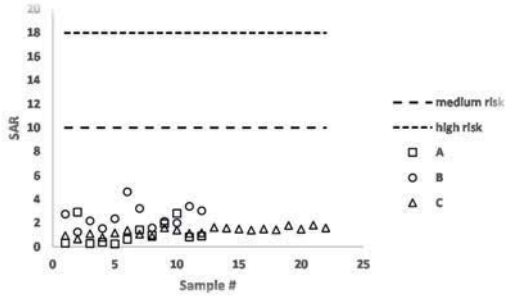

Fig 8. Sodium Adsorption ratio (SAR) results for parcels A, B and C

Exchangeable Sodium Percentage (ESP)

This parameter reflects the possible structural affectation of soil matrix due to its ionic content, structural matrix modifications can be referred as dispersion, (ESP<5), Tactoid repulsion (ESP>10), expansion (ESP>25) and total rupture (ESP>50). For its calculation is required to know concentrations for Cl^-, SO_4^{-2}, NO_3^-. Estimated values for parcel A show an irregular pattern in the values since 33% are above dispersion, 34% are above tactoid repulsion and 33% are above expansion; for parcel B all points are above expansion and 1 value reach the total rupture condition; otherwise parcel C values are nearby the expansion threshold value being 50% below and 50% above. Results are shown in Figure 9.

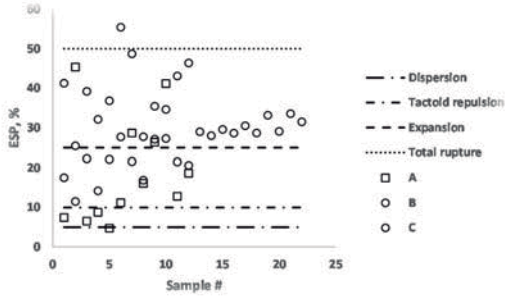

Fig 9. Exchangeable Sodium Percentage (ESP) results for parcels A, B and C

Pearson's statistical analysis

A Pearson correlation was run for the 23 physicochemical parameters for each parcel; from obtained results are chosen those pairs exhibiting positive correlations with values above 0.6, combinations are reported in Table 1. As it can be observed there are some parameters in which the 3 parcels (A, B, C) agreed, there are combinations where only two parcels agreed. Otherwise in strong negative correlation it was not possible to find agreement between parcels. The natural attenuated parcel A exhibit a negative strong correlation between pH with EC, NO_3 and Mn; also between Mn with Alkf and AlkT; and finally TH correlates with Fe. The bioremediated parcel C exhibits negative strong correlation between metals in combination Cr-K, Cr-Ca, Cr-Mn, K-Cu, K-Cd, K-Zn, Ca-Mn, Ca-Ni, Ca-Cu and TH with Cu; finally as it was evidenced in Figure 7, parcel B exhibits a negative strong correlation between the chemical oxygen demand (COD) exhibit strong negative correlation with Cr, Ca, Cu, Cd, Zn, and Mn; as well as K with Mn, and Alkf with Ca.

Table 1 Pearson Correlation values >+ 0.6

Items	A	B	C
NO_2-Fe	X	X	X
EC-Cl	X	X	X
Cr-Cu	X	X	X
Cr-Zn	X	X	X
Cu-Cd	X	X	X
Cu-Zn	X	X	X
Ni-Cu		X	X
Ni-Cd		X	X
Ni-Zn		X	X
Cd-Zn		X	X
EC-SO_4	X	X	
SO_4-Cl	X	X	
TH-Ca	X		X

Vertical sampling

After analyzing all the physicochemical data it was determined the necessity of doing a vertical sampling at the points with most critical values in the parameters. Samples were collected at 0.3, 0.6 and 0.9 m depth for specific points in parcel A and, in general all data agree with the ones from top soil sampling, and attending to the COD parameter, for parcel A (natural attenuation) it was observed that the 0.3 m samples have the lower COD, the 0. 6 m have the highest ones, and the medium values belong to the 0.9 m, which could mean that aerobic processes allow for hydrocarbon degradation. Otherwise vertical sampling at parcel B indicates a decreasing trend since the 0.3 m has the highest value, medium values at 0.6 m, and very low values at the 0.9 m sample, also taking as 1.0 the B top soil samples with highest COD, it happened that 0.3 m has about 1/3, 0.6 m is about 1/6 and 0.9 m is about 1/12 in reference to top soil, this behavior could indicate that parcel B has received the COD demanding substances after the spill.

Tomography results

The tomography obtained at the time when the spill happened clearly indicated the direction in which the hydrocarbons plume had run, the new tomography performed last year indicated that the hydrocarbon pollution has been overcome.

CONCLUSIONS

From the obtained chemical characterization it can be affirmed that applied bioremediation in parcel C provided a soil with a lower salinity risk, but the one with lowest toxicity is parcel A, the one left to natural attenuation; and the one with highest toxicity is the parcel B which is the one unaffected by the spill.

From the statistical analysis is worthy to point out that choosing pairs exhibiting a positive correlation >0.6 there are 6 pairs common to the 3 parcels being NO_2-Fe, EC-Cl, Cr-Cu, Cr-Zn, Cu-Zn and Cu-Cd; there are 4 pairs common to B and C involving Ni, Cu, Cd, Zn; there are two pairs common to A and B involving SO_4 with EC or Cl, and a pair common between A and C involves total hardness (TH –Ca).

From the vertical sampling and tomography it is confirmed that the natural attenuation has provided better soil conditioning, and it is assumed that parcel B has been polluted in recent times because higher COD was found at top soil and it decreases significantly from top soil to depth.

REFERENCES

[1]. Chen, Weixiao, y otros. Association of 16 priority polyciclic aromatic hydrocarbons with humic acid and humin fractions in a peat soil and implications for their long term retention. *Environmental pollution*, 2017: 882-890.

[2]. Ezene, G. I., O A Nwoke, D E Ezikpe, S E Obalum, y B O Ugwishiwuo. Use of poultry droppings for remediation of crude-oil-polluted soils: effects of application rate on total and poly-aromatic hydrocarbon concentration . *International Biodeterioration and Biodegradation*, 2014: 57-65.

[3]. Fernández-Luqueño, Fabián, Fernando López-Valdez, Luc Dendooven, Silvia Luna-Suárez, y Juan M Ceballos-Ramírez. Why wastewater sludge stimulates and accelerates removal of PAHs in polluted soils. *Applied Soil Ecology*, 2016: 1-4.

[4]. Galdames, A, y otros. Development of new remediation technologies for contaminated soil based on the application of zero-valent iron nanoparticles and bioremediation with compost. *Resource-efficient rtechnologies*, 2017: 166-176.

[5]. Khan, Sumia, Muhammad Afzal, Samina Iqbal, y Qaiser M Khan. Plant-bacteria partnershipsfor the remediation of hydrocarbon polluted soils. *Chemosphere*, 2013: 1317-1332.

[6]. Gobernación, Secretaria de. «NOM 021 RECNAT-2000.» *diario oficial de la federación.* 09 de 03 de 2011. dof.gob.mx/nota_detalle.php?codigo=717582&fecha=09/03/2011 (último acceso: 28 de 12 de 2017)